A Novel Role for Thiols in the Regulation of Platelet Function

A thesis submitted to Dublin City University for the award of PhD.

By

Emily C. Reddy, B.Sc. (Hons)

School of Chemical Sciences,
Dublin City University,
Glasnevin,
Dublin 9.

September 2013

Supervisors:

Prof. Robert J Forster (DCU)

Dr. Sarah O'Neill (RCSI)

Prof. Tia E. Keyes (DCU)

Table of Contents

Acknowledgements

First and foremost, I would like to extend a huge thank you to my supervisor in RCSI, Sarah. From day one, we hit it off and you have been so kind, encouraging, optimistic and, above all, a great support to me all along. I'm sure, at times, you regretted your open-door policy when I constantly popped in to wreck your head, but our chats and your advice have been invaluable. You have played a major role not only in my professional but also my personal development throughout the last four years and have been as much of a Mammy to me as a supervisor! Thank you!

Thank you to my supervisor in DCU, Robert, and to Tia, for your help and advice and for giving me the opportunity to undertake this PhD. Thank you to all the other members, past and present, of our research group in DCU who were always on hand to offer assistance whenever I needed it. To Chuck and Tib for all the help from the start with the Raman spectroscopy, it wasn't easy! To Una for all your help with the SEM imaging and for always being a 'willing' blood donor! A special thank you to Roisin, not only for all your help with the confocal imaging, cell work and the unenviable task of reading endless chapters of my thesis but also for all the 'quick' chats and your friendship over the years. Also, thanks to the National Biophotonics and Imaging Platform in Ireland (NBIPI) for funding the project and to the NBIPI staff for their support.

Thank you to all the staff of RCSI and, in particular, the staff in the Molecular and Cellular Therapeutics department. Thank you to Kay and Olwen for all the chats (and abuse!), you were always very patient and helpful whenever I came

down to annoy you! Thanks to all the blood donors and the phlebotomists, especially Helen and Una. Thank you to Stephen and Joanna for your help and contributions to the bile acid project. A very special thank you to Des, I have missed you a lot over the last year, lab meetings just haven't been the same! Your knowledge and advice was always top notch and was greatly appreciated. Thank you to Niamh for all your help, no matter how busy you were, you always had time for me whenever I dropped in. Thank you to Maria for the entertainment and late night chats when we were the only crazy people still hanging around in the office! To everybody working in lab. 5, from sharing your donors to having the banter over tea/lunch/pints, you were all great! To everybody in lab. 4, I thoroughly enjoyed working with you all; there was never a dull moment! Thank you especially to all the lads for the fun times and friendships we've made, it was great to know one of you would always be on hand for a quick cup of tea! Seamus, 'joke of the day' was the best invention ever; Kalyan, you're the wildest Indian I know; Jonny, the endless Father Ted/Simpsons quotes always gave me a laugh; Annachiara, baby, sure you know yourself, my Italian has never been better; Tony, the 'sensible' one, our tea and lunch breaks got out of control when you left us and Thea, for all the banter and endless science conversations (you big brain!). Thank you to Ciaran, for all the tea and chocolate breaks, the adventures of tag rugby, and for all your advice, encouragement and friendship. Thank you to Naadiya, for the never-ending craic and banter, for all the chats, both serious and, mainly, not so serious, for always having time to listen to me ranting on at length about some experiment or other, for distracting me to no end but somehow always ensuring

I wasn’t slacking off either, for just being a Betty and most of all for being such a great friend.

Thank you to all the girls, for constantly being there, even if I was disastrous at keeping in contact at times! It was great to know you would always be at the end of the phone if I was in need of anything. Thanks to women in the bakery and the lads in the butchers, who were always good for a laugh and kept me in touch with reality just in case I got any fancy ideas while I was away in ‘The Big Smoke’! Unfortunately, you won’t be able to slag me off for ‘being in school for over 20 years’ any more now!

And last but certainly not least, a huge thank you to my parents, Trish and Eddie, and to my brother, Paul. You have been an amazing support to me throughout the years and have always strongly encouraged me in everything I have undertaken. You have been full of praise and guidance and have constantly shown a keen interest in my work (even if secretly you still have no clue what I actually do!). Thank you for keeping me in the loop with all the gossip from home and making me laugh about the latest antics of all the crazy pets! Above all, thank you for just being there for me.

Thank you all so much for everything.

Summary

Platelets are small, megakaryocyte-derived cell fragments that play a key role in haemostasis. Platelet receptors, in particular integrins, contain high numbers of reactive cysteines making them prime targets for thiol modifications. The plasma redox environment is controlled by low-molecular-weight thiol couples along with reactive oxygen/nitrogen species (RONS) and their respective scavengers. 'Stress' arises when an imbalance occurs within this tightly regulated redox system. The aim of this thesis is to investigate the role of thiol signalling in platelet function and examine the modulation of this signalling by the external redox environment. Previous work in our laboratory has demonstrated thiol/disulphide exchange to be critical to integrin $\alpha_{IIb}\beta_3$ function.

In this study, a significant increase in purified integrin $\alpha_{IIb}\beta_3$ free thiols was observed upon activation. Integrin activation was inhibited in a reducing redox environment. Subsequently, it was found that platelet surface thiol population was increased upon stimulation with collagen only. Platelet activation by collagen was exclusively inhibited by a reducing external redox environment, with a concomitant modulation of the platelet surface thiol population. These results pointed to an exquisitely redox sensitive element of the collagen activation pathway, namely integrin $\alpha_2\beta_1$. Furthermore, the phosphorylation state of VASP (vasodilator-stimulated phosphoprotein), a protein found downstream of integrin $\alpha_2\beta_1$, was found to be affected by an external reducing redox environment in collagen stimulated platelets only. These results indicate modification of the receptor by the external environment can also impact on downstream, intra-platelet signalling events. These findings suggest a potential

novel therapeutic target for diseases with a characteristic imbalanced redox environment in which thromboembolic events are common, such an inflammatory bowel disease.

Publications

Reddy E.C., Murphy D. Keyes T.E., Moran N., Forster R.J. and O'Neill S. The redox modulation of the platelet surface thiol population. *Platelets* June 2012; 23(4): 322–330. (Abstract for UK Platelet Group Meeting, 2011)

Reddy, E.C., Blackledge, C., Moran, N., Keyes, T.E., Forster, R.J., O'Neill, S. Whole Platelet Analysis by Raman Spectroscopy. *Irish Journal of Medical Science.* 2010; 179 (7): S301. (Abstract for Royal Academy of Medicine in Ireland Meeting, 2010)

Murphy D, **Reddy E**, Forster R, O'Neill S. Platelet reactivity to collagen is diminished in an external reducing environment. *Platelets*. August 2010; 21(5): 411. (Abstract for UK Platelet Group Meeting, 2010)

Currently under review

Murphy, D.D., **Reddy, E.C.**, Moran, N. and O'Neill, S. Regulation of platelet activity in a changing redox environment. (Forum Review article: Antioxidants and Redox Signaling (ARS))

Manuscripts in preparation

Reddy, E.C., Murphy, D.D. and O'Neill, S. Regulation of platelet surface thiol populations by the external redox environment. (*J Biol Chem*)

Murphy, D.D., **Reddy, E.C.** and O'Neill, S. Reductive stress decreases collagen-induced platelet activation. (*J Biol Chem*)

Murphy, D.D. **Reddy, E.C**. and O'Neill, S. Redox mediated *S*-glutathionylation of reactive cysteine residues within the platelet $\alpha_2\beta_1$ collagen receptor. (*Biochemistry*)

Conferences

Oral Presentations:

- RCSI Research Day, March 2013 - Internal: *When is an 'activated' platelet activated?*
- BSHT (British Society for Haemostasis and Thrombosis) / UK Platelet Group Joint Meeting, October 2012 - International: *When is an 'activated' platelet activated?*
- Young Life Scientists in Ireland (YLSI) Symposium, November 2011 - International: *Thiol signalling in platelets*
- UK Platelet Group Meeting, September 2011 - International: *The redox modulation of the platelet surface thiol population*

Poster Presentations:

- RCSI Research Day, April 2012 - Internal: *Platelet function is regulated by a changing redox environment*
- Irish Platelet Symposium, November 2011 - National: *Using Raman spectroscopy to evaluate platelet activation*
- RCSI Research Day, April 2011 - Internal: *Using Raman spectroscopy to evaluate platelet activation*
- National Imaging and Biophotonics Platform in Ireland (NBIPI) BioPic conference, October 2010 - International: *Using Raman spectroscopy to evaluate platelet activation*
- Royal Academy of Medicine in Ireland (RAMI) Meeting, June 2010 - National: *Whole platelet analysis by Raman spectroscopy*

- RCSI Research Day, April 2010 - Internal: *Whole platelet analysis by Raman spectroscopy*
- NBIPI Biophotonics and Imaging Graduate Summer School (BIGSS), September 2009 - International: *Imaging platelet function*

Abbreviations

5-HT	Serotonin
AU	Arbitrary units
AA	Arachidonic acid
ACD	Acid-Citrate-Dextrose
ADMIDAS	Adjacent to MIDAS
ADP	Adenosine diphosphate
ATP	Adenosine triphosphate
BAM	Bile acid malabsorption
BSA	Bovine serum albumin
Ca^{2+}	Calcium ion
$CaCl_2$	Calcium chloride
cAMP	Cyclic adenosine monophosphate
cGMP	Cyclic guanosine monophosphate
COX	Cyclooxygenase
CRP	Collagen related peptide
Cvx	Convulxin
Cys	Cysteine
CySS	Cystine
DMSO	Dimethylsulfoxide
DTNB	5, 5'-Dithiobis (2-nitrobenzoic acid)
DTT	Dithiothreitol
ECM	Extra-cellular matrix
eNOS	Endothelial nitric oxide synthase

ERP5	Endoplasmic reticulum protein 5
FcR	Fc (Fragment, crystallizable) receptor
FDA	Fisher's discriminant analysis
FITC	Fluorescein isothiocyanate
GCL	Glutamate-cysteine ligase
GFOGER	Gly-Phe-Hyp-Gly-Glu-Arg
GFP	Gel-filtered platelets
GP	Glycoprotein
GPCR	G-protein-coupled receptor
GPO	Gly-Pro-Hyp
GPx	Glutathione peroxidase
GR	Glutathione reductase
GRx	Glutaredoxin
GS	Glutathione synthase
GSH	Glutathione (reduced)
GSSG	Glutathione (oxidised)
GST	Glutathione *S*-transferases
H_2O_2	Hydrogen peroxide
HCl	Hydrochloric acid
HEPES	N-(2-hydroyethyl) piperazine-N'-(2-ethanesulfonic acid)
$HO_2^{\bullet}$	Hydroperoxyl radical
HRP	Horse radish peroxidase
HSP	Heat shock protein
IBD	Inflammatory bowel disease
Ig	Immunoglobulin

IP_3	Inisitol-1, 4, 5-trisphosphate
ITAM	Immunoreceptor tyrosine-based activation motif
KCl	Potassium chloride
kDa	Kilodaltons
LDA	Linear discriminant analysis
LIMBS	Ligand induced metal binding site
Mg^{2+}	Magnesium ion
MHBP	Modified Hepes-based platelet buffer
MIDAS	Metal ion-dependent adhesion site
MTT	3-(4,5-Dimethylthiazol-2-yl)-2,5-diphenyltetrazolium bromide
NaCl	Sodium chloride
NAD(P)H	Nicotinamide adenenine dinucleotide phosphate
NEM	N-ethyl maleimide
NO	Nitric oxide
NTB	2-nitro-5-benzoic acid
$O_2^{\bullet-}$	Superoxide radical
OCS	Open canalicular system
$OH^{\bullet}$	Hydroxyl radical
$ONOO^{\bullet-}$	Peroxynitrite radical
PAF	Platelet-activating factor
PAR	Protease activated receptor
PCA	Principal component analysis
pCMBS	*para*-chloromercuribenzene sulphonate
pCMPS	*para*-chloro-mercuriphenyl sulphonate

PDI	Protein disulphide isomerase
PE	Phycoerythrin
PF4	Platelet factor-4
PGE_1	Prostaglandin E_1
PGI_2	Prostaglandin I_2/Prostacyclin
PK	Protein kinase
PKA	cAMP-dependent protein kinase
PKG	cGMP-dependent protein kinase
PLA	Platelet-leukocyte aggregates
PLCy2	Phospholipase Cγ2
pNPP	*para*-nitrophenyl phosphate
PP2	4-amino-5-(4-chlorophenyl)-7-(*t*-butyl)pyrazolo[3,4-*d*]pyrimidine
PPP	Platelet poor plasma
PRP	Platelet rich plasma
PSGL-1	P-selectin gycoprotein ligand-1
PTP	Protein tyrosine phosphatase
PVDF	Polyvinyl difluoride
qBBr	Thiolyte monobromotrimethyl-ammoniobimane
RGD	Arg-Gly-Asp
RNS	Reactive nitrogen species
$RO_2^{\bullet}$	Peroxyl radical
RONS	Reactive nitrogen and oxygen species
ROS	Reactive oxygen species
RS	Raman spectroscopy

RTK	Receptor tyrosine kinase
SDS	Sodium dodecyl sulphate
SDS-PAGE	Sodium dodecyl sulphate polyacrylamide gel lectrophoresis
SEM[1]	Scanning electron microscopy
SEM[2]	Standard error of the mean
SERT	Serotonin 5-HT transporter
SOD	Superoxide dismutase
TBS	Tris buffered saline
TCEP	Tris(2-carboxyethyl)phosphine
Trx	Thioredoxin
TxA_2	Thromboxane A_2
UC	Ulcerative colitis
VASP	Vasodilator-stimulated phosphoprotein
VWF	von Willebrand factor
WP	Washed platelets
X/XO	Xanthine/Xanthine oxidase
γ-GT	γ-Glutamyl-transpeptidase

Chapter 1

Introduction

1.1 Haemostasis and platelets

Haemostasis is a complex biological process which stops bleeding caused by injury or damage to blood vessels. It is a term that essentially encompasses all the processes through which a clot is formed. This includes events involving the coagulation cascade along with platelet plug formation, the eventual removal of this clot, through fibrinolysis, and vascular remodelling. Platelets are cell fragments, derived from megakaryocytes in the bone marrow, which play a key role in haemostasis. They are small in size, approximately 3.0 μm x 0.5 μm, with a mean volume of 7 – 11 fL and are anucleated (Watson, 2005). Platelets form through the rearrangement of the cytoskeleton of mature megakaryocytes leading to the development of long, thin cytoplasmic extensions called proplatelets (De Botton et al, 2002). The platelets are subsequently released into the blood stream and the megakaryocytes undergo cell death by apoptosis.

Under normal conditions, discoid shaped platelets circulate in blood in a quiescent or unactivated state, and are only activated in response to endothelial damage. The average lifespan of a platelet is 7 - 10 days and the normal concentration of platelets in blood is approximately 1.5 – 4.0 X 10^8/ml. When an injury to a blood vessel occurs, endothelial cells lining the vessel are damaged leading to the exposure of the platelet activating agent collagen in the subendothelium. Von Willebrand factor (vWF) is a large multimeric glycoprotein found circulating in the plasma that becomes immobilised by binding to collagen through its A3 domain. VWF then assists in capturing and tethering platelets to the site of vascular injury under high shear rates (> 600 s^{-1}). The interaction of platelets with these agents is via receptors on the platelet surface. GP Ib-IX-V

complex along with integrin $\alpha_{IIb}\beta_3$ interact with vWF, while glycoprotein VI (GPVI) and integrin $\alpha_2\beta_1$ interact with collagen. These interactions promote the adhesion of platelets to the site of injury. Platelets subsequently undergo major morphological changes with dramatic spreading and the development of filopodia. This, in turn, results in the activation of signalling and secretion pathways within the platelet. These events lead to recruitment of additional platelets and, ultimately, the formation of platelet aggregates via the cross-linking of platelets through the interaction of the plasma protein fibrinogen with its receptor integrin $\alpha_{IIb}\beta_3$ on the platelet surface. All of these processes work together in association with the blood coagulation cascade. Ultimately, a blood clot or thrombus is formed. This prevents further blood loss from the damaged blood vessel by 'plugging' the damaged endothelium (Zucker & Nachmias, 1985).

1.2 General platelet biology

1.2.1 Platelet structure

Unactivated platelets circulate in the blood as small discs. Their surface is smooth and predominantly featureless except for some membrane invaginations or pits. These invaginations are entrances into the open canalicular system (OCS), a complex system of internal membranes organised into a network of tubules which run through the platelet (Hartwig & DeSisto, 1991). The OCS provides a large surface area for the platelets and becomes exposed when the platelets spread during the activation process. The invaginations allow the entry of some small particles but restrict the entry of

larger particles, i.e. they are semi-selective. They also facilitate the discharge of granule contents during secretion (White & Escolar, 1991).

A multifaceted cytoskeletal system is present in unactivated platelets which aids in maintaining their discoid shape when they encounter high shear stress whilst in circulation. The cytoskeletal system consists of three components: a spectrin-based cytoskeleton, a microtubule coil and a rigid actin network. The cytoplasmic space of platelets is predominantly filled by the rigid actin network. Actin is the most abundant platelet protein with approximately 2 million copies per platelet (Nachmias, 1988). Around 30 - 40 % of actin in unactivated platelets is in the form of filaments (F-actin). This number increases greatly with activation (Hartwig & DeSisto, 1991). These filaments are assembled to form linear actin polymers, interconnecting at various points to form the rigid actin cytoplasmic network. This is evident from the presence of high concentrations of actin-crosslinking proteins such as filamin and α-actinin (Rosenberg & Stracher, 1982; Rosenberg et al, 1981a; Rosenberg et al, 1981b)

The cytoplasm of platelets contains secretory organelles such as alpha (α) and dense granules, lysosomes, mitochondria and a dense membrane system. There may also be some other organelles or structures such as glycosomes, electron-dense chains and clusters or tubular inclusions (White, 1999; White, 2002; White, 2004). The secretory granules contain proteins and other substances which are released upon platelet activation.

1.2.2 Platelet activation

1.2.2.1 Platelet adhesion

Adhesion is the first event to occur physiologically when platelets come in contact with the site of injury in the blood vessel wall. Adhesion is a complex process mediated by the platelet surface glycoprotein (GP) Ib-IX-V complex which binds von Willebrand factor (vWF). Members of the integrin family also play a role in the process, particularly integrin $\alpha_2\beta_1$, which binds collagen. When platelets come in contact with damaged endothelium they initially bind to vWF, through the receptor GP Ibα, initiating platelet adhesion. The A1-domain of vWF interacts with GP Ibα (Ruggeri & Ware, 1993) reducing the velocity of platelets in contact with the surface under high flow conditions, thereby prolonging the time available for the occurrence of other interactions (Savage et al, 1996). This binding also generates a signal which causes activation of integrin $\alpha_{IIb}\beta_3$, which in turn leads to stability of adhesion, platelet spreading and further platelets being recruited to the site forming aggregates via the interaction of fibrinogen with integrin $\alpha_{IIb}\beta_3$ (Ikeda et al, 1991).

1.2.2.2 Platelet shape change

Upon activation, platelets undergo significant structural changes. The processes by which shape change occurs are complex in nature. Platelet activation leads to increased levels of intracellular calcium. This triggers membrane reorganisation, with phosphatidylserine (PS) exposure, and rearrangement of the platelet's cytoskeleton. The development of new actin filaments is necessary for cytoskeletal restructuring. A number of proteins are involved in the control of the actin architecture and dynamics during activation. Proteins

involved in the regulation of the actin polymerisation and rearrangement include heat shock protein 27 (HSP27), talin-1, kindlin-2, kindlin-3 and vasodilator-stimulated phosphoprotein (VASP) (Butt et al, 2001; Montanez et al, 2008; Moser et al, 2008).

The first change in the structure of platelets upon activation is they become more spherical and lose their discoid shape. Finger-like projections, known as filopodia, develop and grow from the cells periphery (Figure 1.1). The platelets become flattened and all the organelles are forced into the centre of the platelets giving them a distinct 'fried-egg-like' appearance (Figure 1.2). Membrane ruffles begin to form and retract inwards and novel filopodia are extended from the centre of the platelet and rotate around the cell periphery. New actin filaments are formed and fill the space created by the spreading of the cells (Figure 1.3).

Figure 1.1 A platelet in the early stage of spreading. Finger-like projections known as filopodia develop. The central body of the platelet is still visible but is flattening out and gradually disappearing as the cytoplasm spreads and fills the spaces between the filopodia. Image is taken by a scanning-electron microscope (SEM), magnification X 11,000 (White, 2007)).

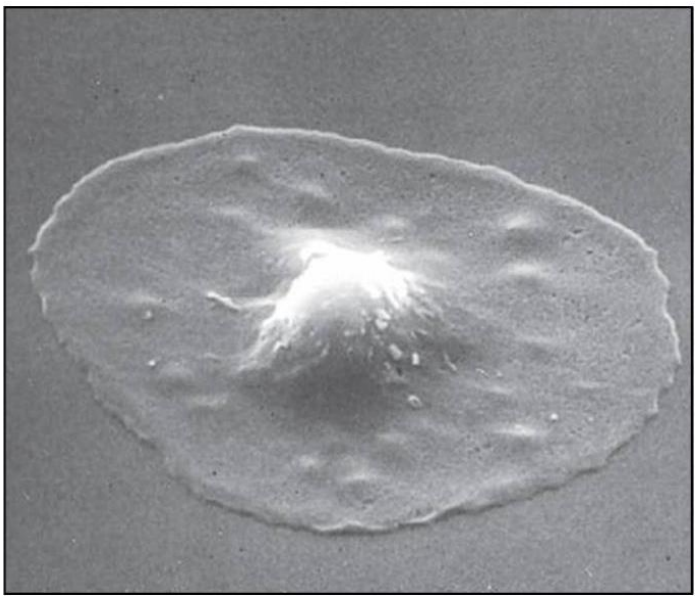

Figure 1.2 A fully spread platelet. The platelet has lost its discoid shape and become flattened. The organelles have been forced into the centre of the platelet, giving it a distinct 'fried-egg-like' appearance. Image is taken by scanning-electron microscope (SEM), magnification X 9,000 (White, 2007).

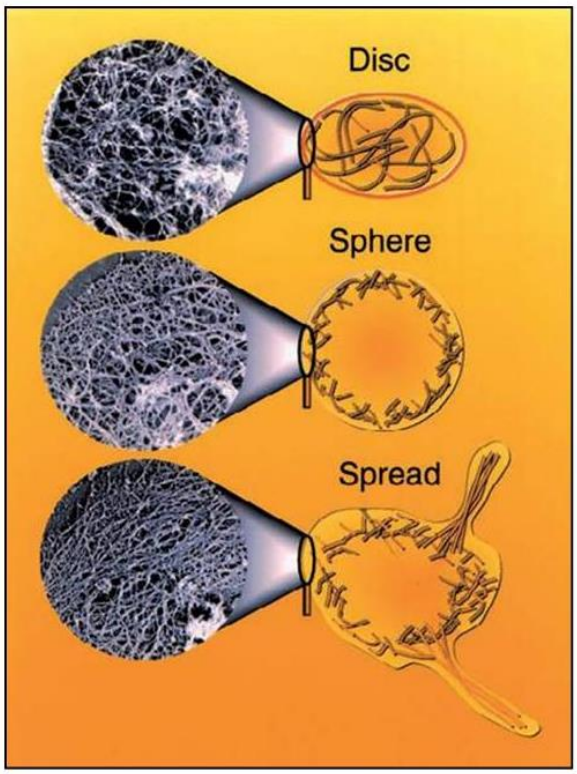

Figure 1.3 Actin rearrangement and formation in spreading platelets. When platelets are activated, they are transformed from a disc shape to a spread form, a process which involves remodelling of the cytoskeleton. Initially, as the platelet changes from a disc to a more spherical shape, long actin filaments are severed into many short filaments. In order to spread, new filaments are then formed from the barbed end of these short filaments (Hartwig, 2007)

1.2.2.3 Platelet secretion

Platelets contain three types of secretory organelles: lysosomes, alpha (α) granules and dense granules. Secretion, or degranulation, is a process that occurs when platelets are activated and involves granules releasing their contents extracellularly. α-granules are the most abundant granules present in platelets, with approximately 40 - 80 per platelet (Sixma et al, 1989). They are oval in shape and measure approximately 200 - 500 nm in diameter. The interior is divided into a number of zones: the submembrane, peripheral and

central zones. The submembrane zone contains vWF arranged into tube-like structures (White, 1968). The peripheral zone contains many proteins, including coagulation factor V, thrombospondin, P-selectin, and vWF in addition to proteins synthesised in other cells and taken up by platelets, such as fibrinogen. The central zone is similar in composition to the peripheral zone but is denser in nature.

Dense granules are fewer in number, with only approximately 3 - 8 per platelet (Israels et al, 1990; White, 1969). They are small in size and relatively opaque in appearance. Dense granules are rich in adenine nucleotides such as adenosine triphosphate (ATP) and adenosine diphosphate (ADP). They also contain serotonin, pyrophosphate, calcium and magnesium.

Platelets contain a small number of lysosomes. There can be up to three while some platelets may not possess any. Lysosomes are spherical organelles and are slightly smaller than α-granules. They contain approximately 13 acid hydrolases. The process by which lysosomes secrete their contents is uncertain, but it is known that they require a much stronger stimulus than the α- or dense granules. The functional role of lysosomes in platelets is not fully understood but the fact that platelets do not exhibit phagocytic behaviour like other cells which contain lysosomes indicates that they may not have a significant role in platelet function (White, 2005).

Secretion occurs through a process known as exocytosis. Exocytosis involves the rearrangement of the actin cytoskeleton, movement of the granules to the

membrane surface, fusion of the granules to the membrane and eventually, due to an increase in intracellular calcium, a release of the intracellular contents from the platelet into the extracellular space (Flaumenhaft et al, 2005; White, 1974). It is a SNARE-dependent mechanism. SNARES (**SNA**p (Soluble NSF (N-ethylmaleimide sensitive factor) Attachment Protein) **Re**ceptors) are a group of structurally similar proteins. Platelets contain the SNARE proteins syntaxin 2, syntaxin 4, SNAP-23, SNAP-25, SNAP-29, VAMP 3, and VAMP 8. SNAREs form tight, stable *trans* complexes, through a motif of approximately 60 amino acids, which are sufficient to catalyse membrane fusion (Weber et al, 1998).

1.2.2.4 Platelet aggregation

Platelet aggregation is an event which occurs following the adhesion and activation of platelets at the site of injury. It involves the recruitment of more platelets to the site. Platelet aggregation is mediated by the integrin $\alpha_{IIb}\beta_3$, a platelet specific receptor. It is also known as glycoprotein (GP) IIbIIIa (Plow & Byzova, 1999). Integrin $\alpha_{IIb}\beta_3$ is a member of the integrin family, a large group of adhesive and signalling molecules present on most cell types. They mediate cell-cell and cell-extracellular matrix (ECM) adhesions, acting as bi-directional signalling molecules that provide a link between the ECM and cytoskeleton of a cell.

Integrin $\alpha_{IIb}\beta_3$ is the major integral plasma membrane protein on platelets. It can bind several adhesive glycoproteins including vWF, fibronectin and vitronectin, all RGD-containing ligands. Fibrinogen is the main ligand of integrin $\alpha_{IIb}\beta_3$. In unactivated platelets, integrin $\alpha_{IIb}\beta_3$ is found in an inactive conformation which has low affinity for its ligands. This allows platelets to circulate freely in the

blood without interacting with these ligands. When platelet agonists activate platelets through their specific receptors, intracellular pathways are stimulated, leading to the generation of inside-out signals through the integrins' cytoplasmic tails. Inside-out signalling leads to a change in the conformation of integrin $\alpha_{IIb}\beta_3$ and this 'switch' mechanism is essential for the integrins cellular function (Yan & Smith, 2001). The integrin is converted from a bent-over conformation to a straightened, extended conformation upon activation (Humphries et al, 2003). Inside-out signalling also causes clustering of integrins into oligomers within the plane of the membrane, which has been shown to enhance platelet adhesion (Bazzoni & Hemler, 1998). These conformational changes in the integrin, convert it to an 'active' state and cause increased binding affinity for its ligand fibrinogen. Human fibrinogen exists as a dimer with each half molecule composed of three different polypeptide chains (Aα, Bβ and γ) (Blomback, 2001). It is this dimeric conformation that leads to the cross-linkage of platelets, resulting in platelet aggregation. Fibrinogen binding to the ectodomains of integrin $\alpha_{IIb}\beta_3$ initiates outside-in signalling (Leisner et al, 1999). This outside-in signalling induces further conformational changes in the receptor and although not fully understood, may lead to cytoskeletal reorganisation and further receptor clustering. The complementary functions of inside-out and outside-in signalling, i.e. bi-directional transmembrane signalling, in integrin $\alpha_{IIb}\beta_3$ are crucial for platelet adhesion, aggregation and, ultimately, thrombus formation.

1.2.3 Platelet receptors

A number of receptors are found on the platelet surface, which regulate platelet function through complex interactions with their respective ligands. A defect or lack of a specific receptor can lead to loss of platelet function and, ultimately, a disorder or disease state in the subject. Glanzmann's thrombasthenia, which is characterised by the absence or dysfunction of integrin $\alpha_{IIb}\beta_3$ on platelets, is an example of such a bleeding disorder. Platelet receptors are critical to a platelets identity and normal function and, therefore, a huge amount of research has been dedicated to platelet receptors, their ligands and their role in platelet function.

1.2.3.1 Integrins

Integrins are a large family of transmembrane receptors that mediate cell adhesion and signalling between intracellular and extracellular environments (Humphries, 2000). They consist of heterodimers of alpha (α-) and beta (β-) subunits, associated in a 1:1 ratio. Both α- and β-subunits are non-covalently associated, type I transmembrane proteins with large extracellular domains (700 - 1100 residues) and short cytoplasmic tails (30 - 50 residues) (Humphries, 2000). Integrins exist in a number of forms; ranging from a bent low affinity state to an extended high affinity ligand binding state which is formed following cytoplasmic signalling at the tails of the subunits (Hynes, 2002) (Figure 1.5). Eighteen α-subunits and eight β-subunits have been identified to date, forming at least twenty-four heterodimers (Bennett et al, 2009; Shimaoka & Springer, 2003). Platelets possess three families of integrins (β_1, β_2 and β_3) and have six different integrins in total: $\alpha_2\beta_1$, $\alpha_5\beta_1$, $\alpha_6\beta_1$, $\alpha_L\beta_2$, $\alpha_V\beta_3$ and $\alpha_{IIb}\beta_3$. In all

α-subunits the N-terminal contains seven tandem repeats with internal homology that can be folded into a seven-bladed β-propeller structure (Springer, 1997). The β-propeller contains three to four calcium co-ordination sites. Some α-subunits also contain an inserted I-domain. The I-domain folds into five parallel and one antiparallel β-strand surrounded by seven α-helices including a metal coordination site. In the β-subunit the N-terminal domain has a sequence that is similar to I-domains and metal-ion dependent adhesion sites (MIDAS) and is thought to be folded into a related structure.

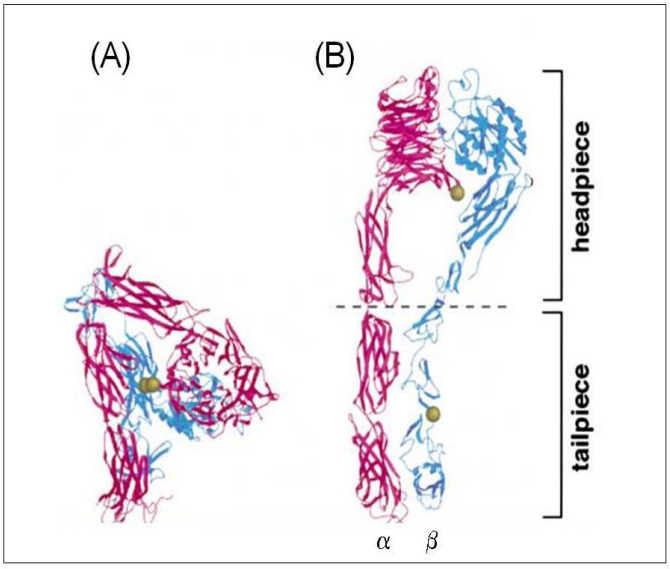

Figure 1.4 Ribbon diagrams of the extracellular segment of integrin. (A) A bent-over (unactivated) conformation. (B) A straightened, extended (active) conformation. The pink colour represents the α-subunit, while the blue colour represents the β-subunit. The model of the extended conformation was created by breaking the bent form at the junction between the thigh and calf-1 domains in α– and I-EGF1 and 2 in β– (dashed line) into the headpiece and tailpiece, and moving the headpiece relative to the tailpiece. Illustration is a model of $\alpha_V\beta_3$ but is representative of general integrin conformational changes as a result of activation (Takagi et al, 2002).

Integrin $\alpha_5\beta_1$ (fibronectin receptor) and $\alpha_6\beta_1$ (laminin receptor) are minor integrins on platelets and their functions are not fully understood. It is thought they have supplementary roles in platelet adhesion (Piotrowicz et al, 1988). Similarly, little is known about integrin $\alpha_V\beta_3$ in platelet function. Only several hundred copies are found on platelets. It is found on many other cell types, including endothelial cells (Cheresh, 1992), where it is a receptor for vitronectin, an adhesive protein that can also bind to integrin $\alpha_{IIb}\beta_3$. There is also limited knowledge about integrin $\alpha_L\beta_2$ on platelets. It is found only on the surface of activated platelets, which suggests it may be expressed on platelet granule membranes (Philippeaux et al, 1996).

Integrin $\alpha_2\beta_1$, also known as GPIa-IIa, is the second most abundant integrin on platelets, with around 2000 – 4000 copies per platelet. It is the main receptor for collagen on platelets. Similar to other integrins, the α-subunit contains a seven-bladed β-propeller structure containing three to four calcium binding sites and, unlike integrin $\alpha_{IIb}\beta_3$, an inserted (I)-domain. The I-domain consists of around 200 amino acids folded into five parallel and one antiparallel β-strands, surrounded by seven α-helices and a conserved cation binding site, a metal ion-dependent adhesion site (MIDAS), for magnesium cations (Mg^{2+}). It is this I-domain that controls collagen binding (Depraetere et al, 1997). Integrin $\alpha_2\beta_1$ can bind GFOGER (glycine-phenylalanine-hydroxyproline-glycine-glutamate-arginine) peptides, a collagen derived sequence, with high affinity (Knight et al, 2000). Additionally, studies have shown that binding of the GFOGER peptide to the α_2 I-domain was mediated by Mg^{2+}, suggesting collagen may bind the integrin in a similar Mg^{2+} dependent manner (Emsley et al, 2000). In addition,

calcium binding outside the I-domain, is another requirement for integrin $\alpha_2\beta_1$ function (Onley et al, 2000). The β-subunit of $\alpha_2\beta_1$ contains a sequence similar to a MIDAS, called an I-like domain, at its N-terminal. As with other integrins, $\alpha_2\beta_1$ works through both outside-in signalling and inside-out signalling. Collagen interacting with the extracellular domains of integrin $\alpha_2\beta_1$ can lead to conformation changes in the integrin and trigger inside-out signalling. This inside-out signalling occurs through the binding of cytoskeletal proteins, such as talin-1 (Nieswandt et al, 2007), kindlin-2 (Montanez et al, 2008) and kindlin-3 (Moser et al, 2008), to the cytoplasmic tails of the β-subunit. Further conformational changes in the integrin are induced by this binding and more collagen binding sites exposed. Intracellular signalling and cross-talk may lead to inside-out signalling to integrin $\alpha_{IIb}\beta_3$ also, subsequently resulting in platelet aggregation.

Integrin $\alpha_{IIb}\beta_3$ is the most abundant integrin on platelets. It makes up 3 % of the total protein in platelets and there are approximately 80,000 - 100,000 copies per platelet (Wagner et al, 1996). Both subunits of integrin $\alpha_{IIb}\beta_3$ are synthesised as single glycosylated polypeptide chains. The α_{IIb}-subunit is cleaved proteolytically to form a heavy and a light chain which are connected by a disulphide bond. The α_{IIb}-subunit is composed of 1008 amino acids while the β_3-subunit is composed of 762 amino acids (Poncz et al, 1987; Zimrin et al, 1990). Unlike other α-subunits, the α_{IIb}-subunit does not contain an I-domain (Humphries, 2000). Integrin $\alpha_{IIb}\beta_3$ is calcium-dependent, with calcium binding sites in both the α- and β-subunits. There are a number of ligands for integrin

$\alpha_{IIb}\beta_3$, including fibronectin, vitronectin, thrombospondin-1 and vWF. However, fibrinogen is the main ligand and the key player in platelet aggregation though integrin $\alpha_{IIb}\beta_3$. All of these ligands contain an RGD sequence which acts as a recognition motif for integrin $\alpha_{IIb}\beta_3$ and other integrins. Fibrinogen also contains a second binding site, a dodecapeptide (HHLGGAKQAGDV) found on the C-terminus of the γ-chain which binds to integrin $\alpha_{IIb}\beta_3$ (Kloczewiak et al, 1984). In fact, this site may primarily mediate fibrinogen binding integrin $\alpha_{IIb}\beta_3$, rather than either of its two RGD sequences in its Aα-chain. To date, two major ligand binding sites have been identified within integrin $\alpha_{IIb}\beta_3$: the putative β-propeller site within the α_{IIb}-subunit and the I-like domain within the β_3-subunit. There are two types of signalling which are associated with integrin $\alpha_{IIb}\beta_3$ activation, namely inside-out and outside-in signalling. It is these signalling pathways that determine the conformational state and ligand binding ability of integrins. Inside-out signalling is initiated upon stimulation of platelets by agonists such as collagen or vWF. These agonists interact with their respective receptors, triggering downstream intracellular signalling, culminating in an elevated calcium level. The cytoplasmic tails play a significant role in the conversion of integrin to an activated conformation through inside-out signalling, though the exact mechanism remains unclear. It is known, however, that a number of proteins are implicated in the process. Talin, a cytoskeletal protein that binds to the β_3 cytoplasmic tails, is thought to be one of the main players in the event and a final common pathway in the integrin activation process (Tadokoro et al, 2003). Both kindlin-2 and kindlin-3 are also implicated in the process (Montanez et al, 2008; Moser et al, 2008). When the cytoplasmic tails of the integrin are converted into the activated form, parallel conformational changes in the

extracellular domain of the integrin occur. These conformational changes and subsequent clustering of the subunits are necessary for full outside-in signalling to occur. When the extracellular domain is in the activated conformation, ligands can then bind to the integrin, initially reversibly, then progressively irreversible. This promotes further clustering of integrins and also further conformational changes that are transmitted to the cytoplasmic tails (Shatill, 2004). Interactions between the cytoplasmic tails and intracellular proteins trigger signalling cascades which are responsible for major platelet responses such as aggregation and secretion.

1.2.3.2 Glycoprotein Ib-IX-V

Glycoprotein Ib-IX-V, a receptor exclusively expressed in megakaryocytes and platelets, is the second most abundant receptor on platelets with approximately 50,000 copies per platelet. It is a receptor complex composed of four membrane spanning polypeptides: GPIbα, GPIbβ, GPIX and GPV (Lopez et al, 1992; Modderman et al, 1992). The complex is formed through the non-covalent linkage of GPIbα - GPIbβ (disulphide bonded to each other) to GPIX and GPV (Andrews et al, 1997; Berndt et al, 2001). Owing to its vast array of ligands, GPIb-IX-V is involved in a range of platelet functions. The first to be uncovered and the main ligand for GPIb-IX-V is the adhesive ligand vWF (von Willebrand Factor). While vWF is found circulating in plasma, it can also be secreted from α-granules in activated platelets, and released from damaged endothelial cells. vWF binds to GPIb-IX-V and plays a key role in the initial adhesion of platelets to the site of injury under shear. VWF binds to GPIbα through its A1-domain and collagen through its A3-domain, thereby indirectly implicating GPIb-IX-V in collagen adhesion (Nieswandt, 2003). It has been long assumed that the main

function of the interaction between vWF and GPIbα was to slow down platelets and enable the interaction of collagen with its platelet receptors, eventually leading to activation of integrin $\alpha_{IIb}\beta_3$ and platelet aggregation. More recent studies, have suggested that activation of GPIb-IX-V may induce intracellular signalling that is capable of activating integrin $\alpha_{IIb}\beta_3$ and inducing platelet aggregation alone (Ozaki et al, 2005). However, this intracellular signalling pathway, involving Src family kinases activating phospholipase C γ2 (PLCγ2), has yet to be fully elucidated.

1.2.3.3 Glycoprotein VI (GPVI)

Glycoprotein VI (GPVI) is another collagen receptor, in addition to integrin $\alpha_2\beta_1$, found on platelets. GPVI is a 62 kDa glycoprotein, and a member of the immunoglobulin (Ig) super family. It is found in a complex with the Fc receptor (FcR) γ-chain, consisting of two GPVI molecules and one FcR γ-chain dimer (Moroi & Jung, 2004). The FcR γ-chain contains an immunoreceptor tyrosine-based activation motif (ITAM) which becomes phosphorylated upon platelet activation by collagen. SH2 domains of another protein, Syk, bind to the phosphorylated tyrosine residues in the ITAM, which in turn leads to activation of Syk and the production of activation signals to other proteins. These intracellular, or inside-out signals, then activate and convert integrins into their high affinity conformation. These intracellular signals also induce the release of second-wave platelet agonists such as ADP and thromboxane A_2 (TxA_2). The integrins $\alpha_2\beta_1$ and $\alpha_{IIb}\beta_3$, through ligation by vWF, then initiate firm adhesion, which strengthens the GPVI-collagen interaction and leads to further signalling and activation of the platelet (Nieswandt et al, 2001a; Nieswandt, 2003). Others

still argue that the primary interaction with collagen is through integrin $\alpha_2\beta_1$, inducing intracellular signalling leading to activation of GPVI, a lower affinity co-receptor, which then triggers its cascade of downstream signalling events (Barnes et al, 1998; Santoro, 1999).

1.2.3.4 Protease activated receptors (PARs)

Protease activated receptors (PARs) have seven transmembrane domains and are G protein-coupled receptors (GPCRs) activated by a proteolytic cleavage at a specific site in the N-terminal extracellular domain. This is unlike most other GPCRs which signal through a standard ligand/receptor interaction. To date, there are four known PARs, numbered 1-4. PAR-2 is expressed in a number of human tissues including the gastrointestinal tract, neurons and astrocytes in the central nervous system (CNS) and also in the skin but is not found on platelets (D'Andrea et al, 1998). PAR-1 and PAR-4 are expressed on human platelets. A third PAR, the PAR-3 receptor, was identified by Ishihara et al (Ishihara et al, 1997). However, a study by Kahn et al suggests PAR-3 plays little or no role in human platelets (Kahn et al, 1999). This conclusion is confounded by the fact that PAR-3 is present on human platelets in very small numbers, 150 - 200 (Cupit et al, 1999), compared to approximately 1500 - 2000 copies of PAR-1 (Brass et al, 1992; Norton et al, 1993). The coagulation protein α-thrombin, also known as coagulation factor II, is the ligand for PARs on platelets. Thrombin, a trypsin-like serine protease, cleaves the peptide bond in PARs between receptor residues Arg 41 and Ser 42. This unmasks a new N-terminus, beginning with the sequence SFLLRN that functions as a tethered ligand,

docking intramolecularly with the body of the receptor to effect transmembrane signalling (Coughlin, 2000).

Thrombin is a potent platelet activator and plays a critical role in promoting thrombus formation (McNicol & Gerrard, 1993). It initiates platelet degranulation, aggregation and indirectly activates the integrin $\alpha_{IIb}\beta_3$ through the activation of a number of signalling cascades. Thrombin also plays a role in the shape change of platelets during activation. Activation of platelets with thrombin leads to the complexing of gelsolin to actin within seconds (Kurth & Bryan, 1984; Lind et al, 1982). Gelsolin is a calcium-dependent protein associated with remodelling of the cytoskeleton during activation. Thrombin is also involved in the coagulation cascade where it converts soluble fibrinogen into insoluble fibrin. It also catalyses and potentiates many other reactions by activating Factors V, VIII, XI and XIII.

In humans, PAR-1 is necessary for responses to both high (30 nM) and low concentrations (1 nM) of thrombin, but it plays a particularly important role in platelet activation at low concentrations of thrombin. PAR-4 appears to mediate platelet responses at high concentrations of thrombin only. Interestingly, a PAR-1 antagonist only becomes effective at blocking platelet activation by high concentrations of thrombin when PAR-4 is blocked simultaneously (Kahn et al, 1999). This also suggests some crosstalk between PAR-1 and PAR-4, with PAR-1 being the primary mediator and PAR-4 taking on a ‘back-up’ role.

1.2.3.5 P2-purinergic receptors

Three P2-purinergic receptors are found on platelets. $P2Y_1$ and $P2Y_{12}$ are the receptors for ADP on platelets (Jin et al, 1998; Savi et al, 2001). ADP is a weak, but important, primary platelet agonist. It also plays a key role in enhancing platelet activation levels and recruiting further platelets when secreted from dense granules upon platelet activation by other agonists (Packham & Mustard, 2005). Both $P2Y_1$ and $P2Y_{12}$ are seven transmembrane G-protein-coupled receptors. The ATP receptor, $P2X_1$, is a ligand-gated ion channel, activation of which leads to a short-lived influx of calcium insufficient to induce platelet activation alone but it may work in synergy with the ADP receptors (Rolf & Mahaut-Smith, 2002; Vial et al, 2002).

1.2.3.6 Other platelet receptors

There are a number of other receptors present on the surface of platelets, not addressed in detail in this thesis but which are equally important in terms of normal platelet function. The prostaglandin receptors found on platelets include the thromboxane TXA_2/PGH_2, prostacyclin (PGI_2), PGD_2 and PGE_2 receptors. Receptors for serotonin (5-HT2A), dopamine (D3, D5), epinephrine (β2-adrenergic receptor), adenosine ($A2_a$-adenosine receptor), vasopressin (V_{1a} receptor), platelet activating factor (PAF receptor), along with toll-like receptors are also found on platelets and are involved in various activating and inhibitory processes.

1.3 Redox and thiol signalling in platelets

1.3.1 Thiols and disulphides

Sulphur is a vital element for living organisms. It is present in cells in a number of forms, namely sulphide, sulphate or as sulphydryl (thiol) (-SH) and disulphide (SS) groups. Thiols undergo many chemical reactions and are therefore of great interest in biological processes. Thiols can be readily converted to disulphide groups and vice versa in the chemical reactions reduction, oxidation and thiol/disulphide exchange. Figure 1.5 illustrates the reactions involving thiol and disulphide groups, and their respective reducing and oxidising agents, in proteins.

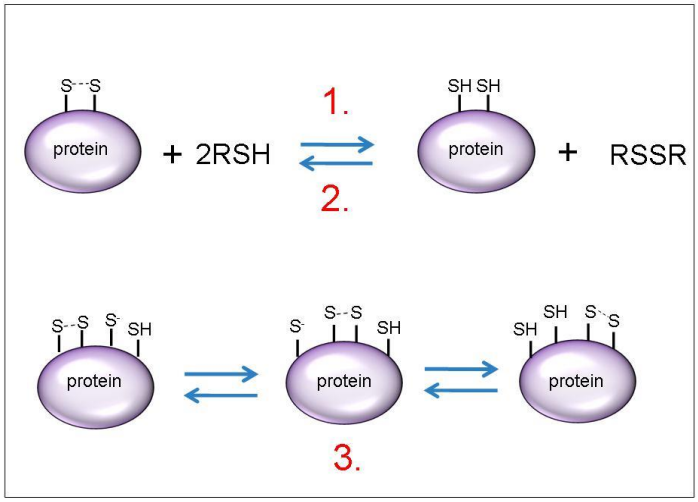

Figure 1.5 The formation of thiol/disulphide bonds in proteins. 1. Reduction: Disulphide bonds (SS) are reduced to form 2 thiol groups (-SH) in the presence of a reducing agent (RSH), resulting in the reducing agent itself becoming oxidised (RSSR). 2. Oxidation: In the presence of an oxidising agent (RSSR), thiols (-SH) become oxidised resulting in the formation of a disulphide bond (SS), the oxidising agent is itself reduced. 3. Thiol/disulphide exchange: A thiolate anion (S^-), formed from the deprotonation of a thiol, attacks a disulphide bond, displacing one of the sulphur atoms. This leads to the formation of a mixed-disulphide bond. The remaining thiolate anion then attacks and resolves the mixed-disulphide bond. The end result of the thiol/disulphide exchange mechanism is the reduction of the original disulphide bond and oxidation of the original free thiol groups. (Exchange mechanism adapted from (Sevier & Kaiser, 2002)).

A number of free thiol containing proteins have been identified to be associated with platelets (Essex & Li, 2006). Some known thiol containing platelet proteins include: protein disulphide isomerase (PDI), glycoprotein Ibα (GPIbα) (Burgess, 2000) and $P2Y_{12}$, the ADP receptor (Ding, 2003). Thiol/disulphide groups have also been found to be a crucial component of the platelet integrins $\alpha_{IIb}\beta_3$ (O'Neill et al, 2000; Yan & Smith, 2000) and $\alpha_2\beta_1$ (Gofer-Dadosh, 1997).

Thiol and disulphide groups play a critical role in integrin function, owing to the large number of cysteine residues present in their structure. The α_{IIb}-subunit of integrin $\alpha_{IIb}\beta_3$ contains 18 cysteine residues, while there are 56 cysteine residues found in the β-subunit, which are highly conserved across all integrin β-subunits. Studies examining the effects of the reducing agent dithiothreitol (DTT) on platelet function found DTT caused platelet aggregation in the presence of fibrinogen, (MacIntyre, 1974; Zucker & Masiello, 1984). These studies suggested that disruption of disulphide bonds in integrin $\alpha_{IIb}\beta_3$ by a reducing agent modulated the activity of the integrin and thereby induced platelet aggregation. Studies by Yan and Smith uncovered a redox site involved in integrin $\alpha_{IIb}\beta_3$ activation (Yan & Smith, 2000). They found integrin $\alpha_{IIb}\beta_3$ in the unactivated conformation contained 2 - 3 free thiols, with an increase to 4 - 5 free thiols in the activated conformation, an overall net reduction of one disulphide bond upon activation. They suggest that while DTT may not be capable of recapitulating all of the steps involved in physiological activation of the integrin, it does cause re-shuffling of disulphide bonds which may be an element of the physiological activation mechanism. They further explored the mechanism of integrin activation and observed that DTT reduces two disulphide bonds within the cysteine-rich domain of integrin $\alpha_{IIb}\beta_3$, leading to global conformational changes in both subunits and thereby exposing the fibrinogen binding sites (Yan & Smith, 2001). More recent investigations have confirmed that DTT induces platelet aggregation and suggest that these results may be caused not only by reduction of disulphide bonds in integrin $\alpha_{IIb}\beta_3$ but also in a series of other surface proteins including $P2Y_{12}$ and GPVI (Margaritis, 2011). It

has also been revealed that vicinal (closely spaced thiols that interconvert between thiol and disulphide) thiols in integrin $\alpha_{IIb}\beta_3$ may be a contributing factor in its redox sensitivity (Manickam et al, 2011). A number of studies show thiol blocking agents, such as N-ethylmaleimide (NEM), *para*-chloro-mercuriphenyl sulphonate acid (pCMPS) and *para*-chloromercuribenzene sulphonate (pCMBS), decrease platelet aggregation responses, again underlining the importance of thiol groups in normal platelet function (Lahav et al, 2000; Manickam et al, 2008; Margaritis, 2011).

Previous work carried out in our laboratory uncovered a role for thiol/disulphide exchange in integrin $\alpha_{IIb}\beta_3$ activity along with endogenous thiol isomerase activity (O'Neill et al, 2000; Walsh et al, 2004). The reactivity of thiol groups, and the importance of this feature in integrin function, has also been demonstrated by our laboratory using Raman spectroscopy, to examine the S-nitrosylation of thiols present in purified integrin $\alpha_{IIb}\beta_3$ (Walsh et al, 2007).

While not as well established as integrin $\alpha_{IIb}\beta_3$, redox sensitivity and a role for thiol/disulphide groups have also been demonstrated in integrin $\alpha_2\beta_1$. Gofer-Dadosh *et al* have shown that binding of collagen to integrin $\alpha_2\beta_1$ results in the increased affinity of the receptor for its ligand with a suggestion of the presence of intra-receptor disulphide bond linkages in integrin $\alpha_2\beta_1$. The suggestion was supported by the fact that type I collagen does not contain any cysteines within its structure. Therefore, the linkage between collagen and integrin $\alpha_2\beta_1$ was mediated through a conformational change in the integrin rather than a direct physical interaction with the collagen (Gofer-Dadosh, 1997).

Furthermore, it has been shown that blocking protein disulphide isomerase activity on platelets inhibits adhesion to collagen (Lahav et al, 2000). In addition adhesion to the $\alpha_2\beta_1$-specific peptide, GFOGER, is disulphide-exchange dependent and protein-disulphide isomerase mediated (Lahav et al, 2003).

1.3.2 Redox environments: Cysteine and glutathione

One of the major pathways for signalling in cells involves modifications of the thiol status of proteins induced by alterations in the redox environment. The redox environment of a cell, biological fluid or tissue is a reflection of the state of the redox couples present (Schafer & Buettner, 2001). The redox state of a couple refers to the ratio of absolute concentrations of reduced to oxidised forms of the couple. Some examples of redox couples are NAD^+/NADH, and $NADP^+$/NADPH. Glutathione (GSH/GSSG) and cysteine (Cys/CySS) are the major low-molecular-weight redox couples present in human plasma. The redox state of a couple may be quantified by its redox potential, which measures the reducing capacity of the couple. Redox potential (E_h) is calculated using the Nernst equation and is expressed in terms of millivolts (mV) (Schafer & Buettner, 2001). A negative redox potential is indicative of a reducing environment whereas a positive value indicates an oxidising environment. A study of the redox environment of human plasma in 740 subjects analysed over 2 years found the redox potential in plasma for glutathione (GSH/GSSG) ranges from -198.8 to -55.1 mV and cysteine (Cys/CySS) ranges between -112.4 and -24.2 mV (Go & Jones, 2005). In addition, changes in the redox state of the cysteine couple do not impact on the redox state of the glutathione

couple, i.e. the redox couples are maintained independently (Go & Jones, 2005; Jones et al, 2004).

Cysteine (Cys), along with its disulphide form cystine (CySS), is the major redox couple in human plasma (Jones et al, 2000). In fact, due to its abundance, the redox potential of the plasma is largely dependent on that of the Cys/CySS couple. Cysteine can undergo rapid auto-oxidisation to form cystine. Likewise, cystine can be reduced back to cysteine. However, the oxidation process is more likely to occur. The conversion between cysteine and cystine is shown in the half cell reactions:

$$2Cys \longrightarrow CySS + 2e^- + 2H^+$$

$$CySS + 2e^- + 2H^+ \longrightarrow 2Cys$$

Cysteine is a semi-essential amino acid, indicating that it can be synthesised in the body. However, the majority of cysteine is derived from the diet and through protein degradation within the body (Lu, 2009). Cysteine biosynthesis occurs in the liver through methionine metabolism. This metabolic pathway is referred to as the trans-sulfuration or cystathione pathway and was first described by Tarver and Schmidt (Tarver & Schmidt, 1939). There are a number of enzymes involved in the conversion of methionine to cysteine, two of which are unique to the trans-sulfuration pathway, namely cystathionine-β-synthase and γ–cystathionase (Finkelstein & Martin, 2000). Methionine is initially converted to S-adenosylmethionine (SAMe) in a rapid reaction catalysed by methionine adenosyltransferase. S-adenosylhomocysteine (SAH) is then generated as a

result of trans-methylation of SAMe, in a reaction catalysed by methyltransferases. Hydrolysis of SAH, catalysed by SAH hydrolase, leads to the formation of homocysteine (Hcy) and adenosine. At this stage Hcy can either be remethylated and recycled, or it can be converted to cysteine. The conversion to cysteine is a two-step process in which Hcy is converted to cystathionine, catalysed by cystathionine-β-synthase, and finally cysteine is formed from cystathionine in a reaction catalysed by γ-cystathionase (Finkelstein, 1990; Finkelstein & Martin, 2000; Lu, 2009). Both cystathione-β-synthase and γ-cystathionase require vitamin B_6 as a cofactor. The synthesis of cysteine through the trans-sulfuration pathway is illustrated in Figure 1.6. The resulting free cysteine is used in the synthesis of glutathione (GSH).

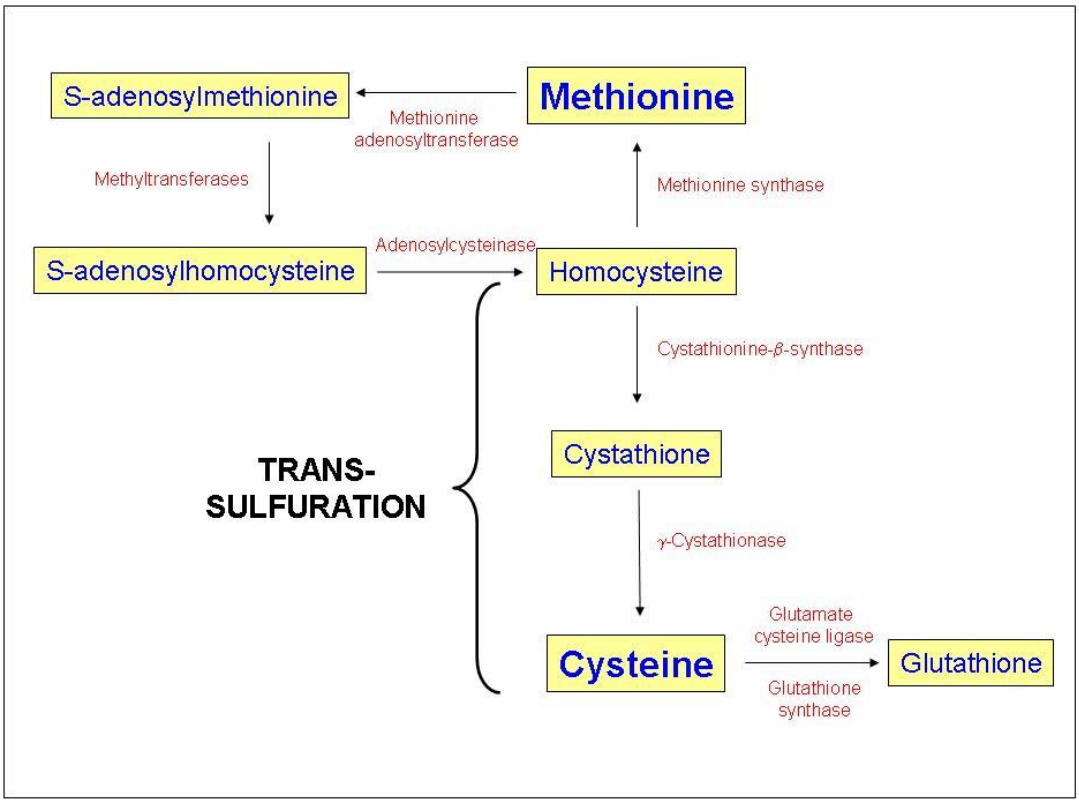

Figure 1.6 The biosynthesis of cysteine through methionine metabolism. The biosynthesis of cysteine occurs in the hepatic cells in the body. Methionine is catabolised to S-adenosylmethionine (SAMe), in a reaction catalysed by methionine adenosyltransferase. SAMe is subsequently transmethylated to form S-adenosylhomocysteine, which is in turn converted to homocysteine (Hcy), catalysed be adenosylcysteinase. Hcy may at this stage be remethylated and converted back to methionine or broken down into cysteine in a two-step process. Hcy is firstly converted to cystathione, catalsysed by cystathione-β-synthase, and finally cystathione is converted to cysteine, a process catalysed by γ-cystathionase. Cysteine may then be utilised in the synthesis of glutathione. (The cysteine synthesis pathway is adapted from (Finkelstein & Martin, 2000; Lu, 2009)).

Glutathione (GSH) is one of the most abundant non-protein cellular thiols present in the body. GSH molecules can readily react together to form the oxidised, disulphide form of glutathione: GSSG. The conversion between reduced and oxidised glutathione is shown in the half cell reactions:

$$2GSH \rightarrow GSSG + 2e^- + 2H^+$$

$$GSSG + 2e^- + 2H^+ \rightarrow 2GSH$$

GSH is a tripeptide composed of the three amino acids: glutamic acid (Glu), cysteine (Cys) and glycine (Gly). The structure of glutathione is illustrated in Figure 1.7. Glutathione is synthesised in all mammalian cells and its synthesis is of particular importance in organs, such as the liver, where there is increased exposure to toxins (Kretzschmar, 1996). Decreased circulating GSH, including supply to plasma, has been shown to occur in hepatic cirrhosis, due to decreased hepatic function (Chawla et al, 1984).

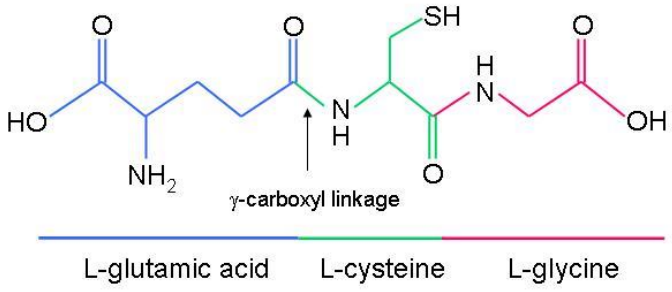

Figure 1.7 The chemical structure of glutathione (GSH). Glutathione (GSH) is a tripeptide composed of the three amino acids: glutamic acid, cysteine and glycine. Glutamic acid and cysteine are bonded via an unusual γ-carboxyl linkage between the amine group of cysteine and the carboxyl group of glutamic acid. Cysteine and glycine are linked through a normal peptide linkage. (GSH structure adapted from (Lu, 2009)).

Approximately 85 % of GSH is synthesised in the cytosol of cells, with a small percentage also produced by the mitochondria and the endoplasmic reticulum (Hwang et al, 1992; Meredith & Reed, 1982).

The synthesis of GSH is a two-step process catalysed by two ATP-dependent enzymes as follows:

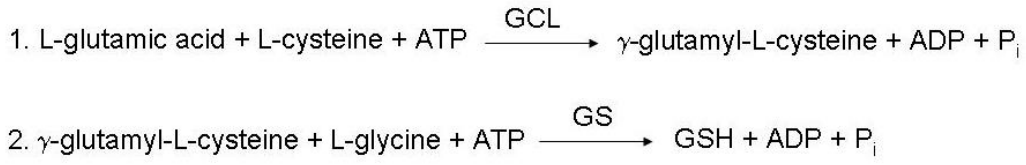

The synthesis is preceded by the trans-sulfuration pathway in which cysteine is produced as described in Figure 1.6. Cysteine is one of the limiting factors in the synthesis of glutathione. In the initial step, glutamic acid (Glu) and cysteine (Cys) are converted to γ-glutamyl-L-cysteine (γ-GluCys), in a reaction catalysed by glutamate cysteine ligase (GCL, formerly known as γ-glutamylcysteine synthetase (γ-GCS)). This is then converted to GSH by glutathione synthase (GS) (Griffith, 1999; Griffith & Mulcahy, 1999). GCL is the rate limiting enzyme for GSH synthesis, with the regulation and expression of the enzyme playing a key role in maintaining GSH homeostasis. The synthesis is also regulated, not only by the availability of cysteine, but also by the concentration of GSH itself, which works through a negative feedback mechanism to inhibit GCL activity (Lu, 2009). GSH can also be regenerated from GSSG by a flavoenzyme, glutathione reductase (Gred), using NADPH as a reductant (Argyrou & Blanchard, 2004). GSH is metabolised, only extracellularly, by γ-glutamyltranspeptidases (GGTs), which catalyse the cleavage of the γ-glutamyl amide bond to Cys and transfer

the Glu residue to another amino acid. CysGly and γ-Glu-CySS (γ-Glu-cystine) are the resulting products of this reaction. CysGly is then broken down into Cys and Gly by extracellular dipeptidases and transported back into the cell, while γ-Glu-CySS is also transported back to the cell where it is reduced to γ-GluCys. It may then be converted back to GSH again. It is this cycle which maintains a balanced GSH pool, both intra- and extra-cellularly. This cycle also serves as a continuous source of cysteine, which by its nature is extremely unstable and is rapidly auto-oxidised to cystine (Meister, 1988). The biologically active site of glutathione corresponds to the thiol group of the cysteine residue within its structure. It is the high nucleophilicity of this thiol group that provides glutathione with its characteristic antioxidant properties. Glutathione can directly scavenge free radicals, along with assisting in the regeneration of other antioxidants and acting as a cofactor for glutathione peroxidase (GPx) and glutathione S-transferase (GST) in the degradation of hydrogen peroxide (H_2O_2) and other toxic peroxides. These functions of GSH are critical in the defence against oxidative stress.

1.3.3 Oxidative and reductive stress

Oxidative stress has attracted much attention in recent years and is well documented to be a major factor contributing to the process of aging (Beckman & Ames, 1998). It has also been implicated in the development and progression of a wide range of diseases such as diabetes (Baynes & Thorpe, 1999; Ceriello, 2000), neurodegenerative diseases (Coyle & Puttfarcken, 1993), various cancers (Reuter et al, 2010; Toyokuni et al, 1995) and CVD such as stroke and atherosclerosis (Bennett, 2001; Harrison et al, 2003). Oxidative stress can be

brought about by exposure of biological macromolecules to reactive oxygen (ROS) or nitrogen species (RNS) resulting in alterations of their fundamental physical and chemical properties. Oxidative stress induces conformational modifications, through the targeting of critical cysteine thiols, ultimately, leading to a change or loss of function of the macromolecule in question. RONS is a term encompassing both ROS and RNS. RONS can cause a broad spectrum of damage through attacking lipids, proteins and DNA, inducing membrane damage, enzyme deactivation and DNA disruption.

A free radical is defined as a cluster of atoms with one or more unpaired electrons in the outer shell. This is an extremely unstable conformation and is the basis for the radical's high reactivity status. ROS refers collectively to oxygen radicals and certain non-radical oxidising agents that can be readily converted to radicals (Halliwell, 1989). ROS are generated during the process of aerobic energy metabolism. The metabolites of molecular oxygen (O_2), an essential component of the process, are referred to as ROS. Aerobic cellular metabolism involves a process in which the oxidoreduction energy of mitochondrial electron transport is converted to the high-energy phosphate bond of ATP. O_2 acts as the final electron acceptor for cytochrome-*c*-oxidase, an enzyme which catalyses the four-electron reduction of O_2 to H_2O. This reaction leads to the formation of partially reduced and highly reactive metabolites such as superoxide ($O_2^{\bullet -}$), hydroxyl ($OH^{\bullet}$) (a radical formed in the presence of transition metals (Fe/Cu)), peroxyl ($RO_2^{\bullet}$), and hydroperoxyl ($HO_2^{\bullet}$) (Thannickal & Fanburg, 2000) radicals. Additionally, other non-radical

substances may be formed namely hydrogen peroxide (H_20_2), hypochlorous acid (HOCl) and ozone (O_3) (Table 1.1).

Similar to ROS, RNS are physiologically necessary but also potentially toxic and destructive. RNS are reactive species derived primarily from nitric oxide (NO). NO, originally recognised as a vaso-relaxing agent, is also now well described as an important cell-signalling and antioxidant molecule. Nitric oxide itself is formed through the enzymatic action of nitric oxide synthases: neuronal NO synthase (nNOS), endothelial NO synthase (eNOS) and inducible NO synthase (iNOS). A by-product of this enzymatic reaction can be $O_2^{\bullet-}$. A rapid reaction occurs between NO and $O_2^{\bullet-}$ leading to the formation of peroxynitrite ($ONOO^{\bullet-}$). $ONOO^{\bullet-}$ has the potential to react with all major biological molecules thereby rendering it capable of mediating cytotoxicity independently of both NO and $O_2^{\bullet-}$. Other NO-derived radicals are listed in Table 1.1. The most potent effects of RNS appear to be thiol modifications that may affect the function of signalling systems or result in the production of tissue-derived donors of NO. RNS readily react with GSH and protein thiols resulting in their oxidation or formation of nitrosylated thiols (Dalle-Donne et al, 2005). Indeed, studies in our laboratory have shown the S-nitrosylation of free thiols in platelet integrin $\alpha_{IIb}\beta_3$ impacts on the integrin's activity (Walsh et al, 2007).

Table 1.1 Reactive oxygen species (ROS) and reactive nitrogen species (RNS), known collectively as RONS. These radicals are produced during normal metabolism in cells and tissues of the body and but can be potentially destructive (adapted from (Dalle-Donne et al, 2005)).

Reactive Oxygen Species (ROS)		Reactive Nitrogen Species (RNS)	
Superoxide	$O_2^{\bullet}$	Nitric oxide	$^{\bullet}NO$
Hydroxyl	$OH^{\bullet}$	Nitrogen dioxide	$^{\bullet}NO_2$
Peroxyl	$RO_2^{\bullet}$	Nitrous acid	HNO_2
Alkoxyl	$RO^{\bullet}$	Nitrosyl cation	NO^+
Hydroperoxyl	$HO_2^{\bullet}$	Nitrosyl anion	NO^-
Hydrogen peroxide	H_2O_2	Dinitrogen tetroxide	N_2O_4
Hypochlorous acid	HOCl	Dinitrogen trioxide	N_2O_3
Hypobromous acid	HOBr	Peroxynitrite	$ONOO^-$
Ozone	O_3	Peroxynitrous acid	ONOOH
Singlet oxygen	$^1O_2$	Alkyl peroxynitrites	ROONO
-	-	Nitronium cation	NO_2^+
-	-	Nitryl chloride	NO_2Cl

As RONS are produced during normal metabolism, they play a role in a number of normal biological processes, including enzymatic reactions, mitochondrial electron transport, signal transduction and gene expression (Bayir, 2005). The redox environment and the levels of RONS are tightly regulated by the action of antioxidants and RONS scavengers such as superoxide dismutase (SOD), catalase, glutathione peroxidase (GPx), glutathione, ascorbic acid (vitamin C), α-tocopherol (vitamin E) and thioredoxin. All of these substances display protective properties. Problems arise when the level of RONS exceeds that of the antioxidants, i.e. the redox balance is upset.

Oxidative stress can also arise as a result of an imbalance in low-molecular-weight thiol couples GSH/GSSG and Cys/CySS. If the concentration of the oxidised form (GSSG/CySS) of the couple increases, this leads to a more positive redox potential and an oxidising redox environment. A number of studies have analysed the redox potentials of these couples in plasma in order to establish a link between a change in plasma redox potentials and an onset of a disease state within the body. It has been determined that the redox state of plasma is more oxidised in smokers and patients with type 2 diabetes or cardiovascular disease (Duman et al, 2003; Harrison et al, 2003; Moriarty et al, 2003). Variations in these values may be an indication of the onset of atherosclerosis (Go & Jones, 2005). Additionally, more recent studies have shown that oxidised Cys/CySS redox potentials are associated with not only increasing age and smoking but also obesity and alcohol abuse, all of which are high risk factors for cardiovascular events (Go & Jones, 2011).

While oxidative stress is the most commonly known type of ‘stress’ related to an imbalance in redox couples, reductive stress can also occur if the balance is tipped in favour of the reducing form. An increase in the reducing element (GSH or Cys) of the couple, results in a more negative redox potential and subsequently a reducing redox environment. Reductive stress may indeed be as common and clinically significant as oxidative stress (Ghyczy & Boros, 2001). Reductive stress has been linked to corruption of growth factor signalling leading to abrogated coronary collateral growth, an adaptation of the myocardium to minimise the effects of ischemia within an area of the heart (Rocic et al, 2007). A study in mice also has found that reductive stress caused

by elevated levels of GSH may be implicated in cardiomyopathies (Rajasekaran & al., 2007). Additionally, the mice in this study were found to have increased expression of heat shock proteins. Further studies have shown that over expression of heat shock protein 27 (HSP27) in transgenic mice resulted in an increased GSH/GSSG ratio along with decreased levels of ROS. These mice were found to suffer from cardiac hypertrophy, dysfunction and reduced life span (Zhang et al, 2010).

In recent years, research focussing on redox states and their regulatory role on various different cell types has become increasingly popular. Yet, the amount of work carried out to examine the interaction between platelets and redox is limited. As mentioned in section 1.2.3.1, platelet receptors and in particular integrins, contain high numbers of cysteines within their structure. These cysteines are potentially prime targets for thiol modifications either by oxidation or reduction of their intramolecular bonds by the redox couples or alternatively through S-glutathionylation or S-cysteinylation of these free thiols. Such interactions could potentially result in compromised function of the platelet receptors and, ultimately, impact on platelet activity.

1.4 Platelets and inflammation

The primary function of platelets is in the complex processes of haemostasis and thrombosis. The significance of platelets appears to have been underestimated in the past, mainly due to the notable absence of a nucleus in platelets. However, an expanding body of evidence shows platelets are involved in a number of other biological responses including inflammation.

Atherosclerosis and rheumatoid arthritis are prime examples of inflammatory conditions in which inflammation and the coagulation cascade are intricately linked. The involvement of platelets in the inflammation process stems from the interaction between platelets and endothelial cells at a site of injury. As mentioned previously, platelets tether and adhere to the exposed subendothelium, leading to platelet activation, recruitment of further platelets and eventually the formation of a platelet plug. Upon platelet activation, signalling cascades within the platelet are initiated inducing the release not only of secondary platelet activators but also pro-inflammatory cytokines such as CD40 ligand (CD40L) (Henn et al, 1998) and interleukin-1β (IL-1β) (Lindemann et al, 2001). CD40L is a transmembrane protein related to the cytokine TNF-α, and becomes expressed on the surface of platelets within seconds of activation (Henn et al, 1998). CD40L induces the secretion of chemokines from endothelial cells, which are involved in the recruitment of leukocytes to the site of injury. Lindemann *et al* have shown that platelets are capable of synthesising IL-1β from messenger RNA (mRNA) located within the platelet and production of IL-1β is regulated by engagement of β_3 integrins. Activated platelets also secrete the chemokines CCL5 (RANTES) and CXCL4 (platelet factor 4) (von Hundelshausen et al, 2001). These pro-inflammatory chemokines are deposited on the microvasculature, aortic endothelium and monocytes. This in turn may lead to activation of monocytes and integrins with further recruitment of monocytes to the site of injury. The promotion of leukocyte adhesion and activation induces firm attachment of the leukocytes to the vessel wall and may eventually lead to transmigration of these leukocytes into the subendothelial

tissue. These examples of platelet derived chemokines demonstrate platelets as key players in mediating the inflammatory response at a site of injury.

Inflammatory bowel disease (IBD) is another example of a clinical inflammatory condition in which a role for platelets has been implicated, yet the mechanism of this interaction remains to be fully understood (Yoshida & Granger, 2009). Subclinical thrombosis is common in IBD and is a major source of morbidity in approximately 25% of IBD deaths (Tabibian & Roth, 2009). Furthermore, thromboembolic events are 3-fold more likely in IBD patients compared to controls, with a particularly high risk of thromboembolic events during active disease states (Zitomersky et al, 2011). Circulating platelets in IBD patients have been found to be in an active-like state with an increased expression of activation-dependent surface antigens such as P-selectin and GP53 (Collins et al, 1994). Plasma levels of CD40L and platelet factor 4 are increased in patients with IBD (Collins & Rampton, 1997; Danese et al, 2003b). Additionally, *in vitro* studies of platelets from patients suffering with both active and quiescent IBD display hypersensitivity to stimulation of platelets with collagen and ADP along with spontaneous platelet aggregation (Mori et al, 1980; Webberley et al, 1993). Although the etiology of IBD remains poorly understood, immunoregulatory factors are hypothesised to be the main dysfunctional players in the process. The redox environment is thought to be one such dysfunctional immunoregulatory system. An abnormally high level of ROS production has been associated with IBD patients (Rezaie et al, 2007). Interestingly, a number of studies have also shown not only an increase in ROS, but also a dramatic change in the levels of antioxidants present in these IBD patients. A study of

knockout mice lacking glutathione peroxidase genes found these mice developed a destructive colitis similar to ulcerative colitis (UC) as early as 11 days old (Esworthy et al, 2001). Further studies investigating the redox status of glutathione in human IBD cases found not only a significant increase in the oxidised form of glutathione (GSSG) in the colonic mucosa, which was positively correlated to the disease severity (Holmes et al, 1998), but also a concomitant decrease in reduced glutathione (GSH) levels leading to an overall oxidising environment (Tsunada et al, 2003). There exists an ongoing argument as to whether oxidative stress is a cause or a consequence of IBD. Due to the phenomenon of oxidising agents inducing IBD like symptoms (Bilotta & Waye, 1989; Meyer et al, 1981) and mice lacking the antioxidant Gpx developing colitis with a pathology similar to that seen in IBD, it seems oxidative stress may indeed be a cause.

1.5 Aims

The mechanisms of platelet activation remain to be fully elucidated despite in-depth research. Integrins, in particular, play a major role in the process of platelet activation and are, therefore, a major focus of current platelet research. There is overwhelming evidence to suggest cysteine residues and thiol/disulphide bonds are critical players in the complex conformational changes associated with integrin activation. However, the precise role of thiols in these molecular mechanisms, whereby integrins are converted from an unactivated state to an active, ligand-binding state, remains to be indentified. Similarly, it has been suggested thiols are an important structural component of other platelet receptors. The principle aim of this thesis, therefore, is to examine

changes in the surface thiol population of platelets in various activating scenarios in conjunction with alterations of integrin thiols.

The external redox environment of platelets is tightly controlled by the balance of the major low-molecular-weight redox couples, glutathione and cysteine. Alterations in the balance of this redox environment may result in the development of oxidative or reductive stress. Oxidative stress, in particular, has been implicated in a range of disease states, which interestingly, are associated with an increased risk of thromboembolic events. The effects of redox-related stress are mainly brought about by thiol modifications of proteins leading to conformational changes in proteins resulting in the alteration or loss of protein function. The presence of thiol-containing proteins on platelets makes them potential prime targets for post-translational redox modifications. I will investigate the effects of an altered external redox environment on the platelet surface thiol population. Additionally, I will examine the impact of the modification of platelet surface thiols on downstream, intra-platelet signalling events and, ultimately, the effects of such modifications on platelet function.

Chapter 2

Materials and Methods

2.1 Materials

5,5'-dithiobis-(2-nitrobenzoic acid) (DTNB); glutathione (free acid), reduced and oxidised, were obtained from Merck Chemicals Ltd., Nottingham, UK.

Alexa Fluor® 488 Phalloidin was obtained from Invitrogen Corporation, Carlsbad, CA, USA.

Chinese hamster ovarian-K1 (CHO-K1) cells expressing integrin $\alpha_{IIb}\beta_3$ were a kind gift from Professor Niamh Moran, RCSI, and were kindly cultured and passaged by Dr. Roisin Moriarty, DCU.

Collagen related peptide (CRP) was a kind gift from Professor Richard Farndale, Department of Biochemistry, Cambridge University, UK.

Collagen, lyophilised preparation of soluble calf skin (type 1) and siliconised, flat-bottom aggregation tubes (7.25 X 55 mm) were obtained from Bio/Data Corporation, Horsham, PA, USA.

CD62P-PE, CD41a-FITC and PAC-1-FITC, antibodies and Falcon™ tubes, (polystyrene, round bottom), were obtained from Becton-Dickinson, Oxford, UK.

Convulxin, lyophilised, ≥ 90 % (SDS-PAGE), (50 μg), was obtained from Enzo Life Sciences (UK) Ltd., Exeter, UK.

Econo-Pac chromatography columns, Protein DC assay kit and P6 spin columns were obtained from Bio-Rad Laboratories Ltd., Hertfordshire, UK.

Flat bottom, 96-well microplates (clear) and Immulon 2HB, flat bottom, 96-well plates were obtained from Fisher Scientific Ireland, Ballycoolin, Dublin, Ireland.

Fluorescent mounting medium was obtained from Dako, CA, USA.

Platelet membrane GPIIbIIIa (integrin $\alpha_{IIb}\beta_3$) (isolated from human platelets), and Amicon® Ultra centrifugal filters (0.5 ml, 30K MWCO) were obtained from Merck Millipore, Billerica, MA, USA.

Poly-L-lysine adhesion slides, and glass cover slips (rectangular: 22 X 50 mm, round: diameter (Ø) 16 mm) were obtained from VWR International Ltd., Ballycoolin, Dublin, Ireland.

Sepharose® 2B-300, prostaglandin E_1 (minimum 98 % (HPLC) synthetic) (PGE_1), thrombin from bovine plasma: lyophilised powder, 600 - 2,000 NIH units/mg protein (biuret); manganese chloride tetrahydrate ($MnCl_2.4H_2O$); DL-Dithiothreitol (DTT); tris(2-carboxyethyl)phosphine (TCEP), hydrochloride salt; L-cysteine and L-cystine, non-animal source; collagen from calf skin (Bornstein and Traub Type I); fibrinogen from human plasma (50 - 70% protein (≥ 80 % of protein is clottable)), albumin from bovine serum (≥ 98 % (agarose gel electrophoresis), lyophilised powder); calcium chloride; glycine; Hepes; potassium chloride; magnesium chloride; potassium phosphate; sodium

bicarbonate; sodium chloride; sodium citrate, sodium dodecyl sulphate (SDS), for electrophoresis, > 98.5% (GC); 30 % bis-acrylamide, 0.2 μm filtered; ammonium persulfate (APS) for electrophoresis, >=98 %; tetramethylethylenediamine (TEMED), approximately 90 %; bromophenol blue; sodium fluoride; sodium pyrophosphate; sodium orthovanadate; Triton-X-100; trizma-base, > 99.9 % titration; dextrose (D-glucose); citric acid; Tween-20; polyvinyl difluoride (PVDF) membrane; Ponceau S, practical grade; acetic acid; Brilliant Blue G250 (Coomassie); hydrochloric acid (HCl); dimethyl sulfoxide (DMSO), puriss.,absolute, over molecular sieves; methanol; ethanol, deoxycholic acid (DCA), sodium taurodeoxycholate hydrate (taurodeoxycholic acid (TDCA)) and Atto 655-maleimide were obtained from Sigma Aldrich Ltd, Tallaght, Dublin, Ireland.

Supersignal® West Pico chemiluminescent substrate; Halt protease inhibitor (100X), and *p*NPP (*p*-Nitrophenyl phosphate) were obtained from Thermo Fisher Scientific, Rockford, IL, USA.

Thiostar, thiol detection substrate, was obtained from BioQuote Ltd., York, UK.

Ursodeoxycholic acid (sodium salt) was obtained from Santa Cruz Biotechnology, Leopardstown, Dublin, Ireland.

VASP (A290), phospho-VASP (Ser157) and phospho-VASP (Ser239) were obtained from Cell Signaling Technology, Beverly, MA, USA.

2.2 Methods

2.2.1 Isolation of platelets from whole blood

Venous whole blood was drawn from healthy volunteers, free from aspirin and other drugs that may affect platelet function for 7 - 10 days. Blood was drawn from the antecubital vein using a Butterfly® 19 gauge needle by a qualified phlebotomist. Ethical approval was granted by Royal College of Surgeons in Ireland Research Ethics Committee. Blood was anti-coagulated with 15 % (v/v) Acid-Citrate-Dextrose (ACD) (38 mM Citric Acid (Anhydrous), 75 mM Sodium Citrate, 124 mM Dextrose) (stored at 4 ºC and brought to room temperature before use) i.e. 4.5 ml of ACD drawn into a syringe and blood drawn to the 30 ml mark, with gentle mixing. Blood was divided into 5 ml aliquots in 15 ml tubes and centrifuged for 12 minutes at 150 x g (no brake) at room temperature (RT). This centrifugation step separated whole blood into two fractions. The top two thirds of the top fraction, referred to as platelet rich plasma (PRP), were carefully transferred to a 50 ml tube with a plastic transfer pipette. The remaining blood portion was discarded. The pH of the PRP was adjusted to pH 6.5 using ACD. Prostaglandin E_1 (PGE_1) was added at a final concentration of 1 µM. The PRP was centrifuged for 10 minutes at 720 x g (no brake) at RT to pellet platelets. The supernatant was carefully removed and the platelets were resuspended in 1 ml (per 30 ml blood, i.e. resuspend platelets in 2 ml platelet buffer if 60 ml of blood was drawn) of a modified Hepes platelet buffer (MHPB) (6 mM Dextrose, 130 mM NaCl, 9 mM $NaHCO_3$, 10 mM Sodium Citrate, 10 mM Hepes, 3 mM KCl, 0.81 mM KH_2PO_4, 0.9 mM $MgCl_2.6H_2O$, pH 7.35).

2.2.1.1 Preparation of gel-filtered platelets

Gel-filtration is an example of size-exclusion chromatography. It is a method commonly used to separate particles in an aqueous solution based on the particle size. The concept on which the technique is based is one in which beads of a specific size are packed together in a column to form a matrix with specific spacing between the beads and a solution is placed on top. The smaller particles in the solution can pass into the beads, while the larger particles do not. The end result is that the larger particles, therefore, pass through the matrix quickly, whereas the smaller particles pass through at a slower rate and can be collected at a later time point. In this case, gel-filtration was employed to ensure platelets used in the study were in a purified system, with all plasma proteins and other cells and cellular fragments removed.

The column for gel-filtration of platelets was prepared by rinsing a plastic column (height 15 cm, diameter 1.5 cm) with deionised water. A dilute slurry of sepharose 2B-300 beads was prepared with deionised water using 10 ml sepharose 2B-300 with 10 ml deionised water. The sepharose 2B-300 slurry was layered into the plastic column and allowed to pack without drying out. The packed column height was directly related to the volume of suspended platelets to be filtered, namely 5 – 6ml packed sepharose 2B per 1 ml of platelets. The sepharose column was rinsed with deionised water, using 10 - 20 times column volume. The rinsed column was equilibrated with 3 - 4 times column volume of platelet buffer (MHPB). Once equilibrated, all platelet buffer was allowed to pass into the gel column before layering the platelets onto it. When all platelets

had passed into the column, approximately 1 ml platelet buffer (MHPB) was layered onto the top of the column. Gel-filtered platelets were collected in 0.5 ml fractions, platelets were counted using a Sysmex KX-21 haematology analyser and the most concentrated fractions were pooled together. The final platelet count was adjusted to a count of 2.5 – 3.0 × 10^8/ml, which is within the normal physiological range, by addition of platelet buffer (MHPB). Platelets were allowed to rest for approximately 30 minutes. $CaCl_2$ was added at a final concentration of 1.8 mM immediately prior to platelets being used in experiments.

2.2.1.2 Preparation of washed platelets

Following the removal of PRP after the second centrifugation step in section 2.2.1, 0.5 ml platelet buffer (MHPB) was gently added on top of the platelet pellet, whilst ensuring the pellet was not disturbed. This platelet buffer was then removed. This step was repeated twice. While the washed platelet preparation is not as rigorous as the gel-filtered platelet preparation, this step ensured that the majority of plasma proteins were removed. The platelet pellet was then resuspended in 1 ml platelet buffer (MHPB) (per 30 ml blood, i.e. resuspended in 2 ml platelet buffer if 60 ml blood was used) and the platelets were counted using the Sysmex KX-21 haematology analyser. The platelet count was adjusted to 2.5 – 3.0 × 10^8/ml by addition of platelet buffer (MHPB). Platelets were allowed to rest for approximately 30 minutes. $CaCl_2$ was added at a final concentration of 1.8 mM immediately prior to platelets being used in experiments. In the case of washed platelets being used in the platelet adhesion assays, platelets were supplemented with 2 mM $MgCl_2$ as an alternative to $CaCl_2$. This is due to the dependency of the collagen receptor

integrin $\alpha_2\beta_1$ on Mg^{2+} ions. This step is particularly important due to the presence of the chelating agent, sodium citrate, in the anticoagulant (ACD) into which the blood is originally drawn. It has been shown that in the absence of Mg^{2+} ions, receptors other than integrin $\alpha_2\beta_1$, such as integrin $\alpha_{IIb}\beta_3$ or GPVI may become involved in the adhesion of platelets to collagen (de Groot & Sixma, 1997).

2.2.2 Platelet aggregation studies

Percentage platelet aggregation is determined by the percentage of light transmission through a sample of platelets in solution. As platelet aggregates are formed, they fall to the bottom of the tube thereby increasing the level of light transmission through the sample (Figure 2.1). A 100 % percentage aggregation baseline is set in the aggregometer by measuring the level of light transmission through a platelet poor sample. In the case of gel-filtered platelets this baseline is acquired using the platelet buffer (MHPB). This technique is based on the principles and technique first described by Born (Born, 1962).

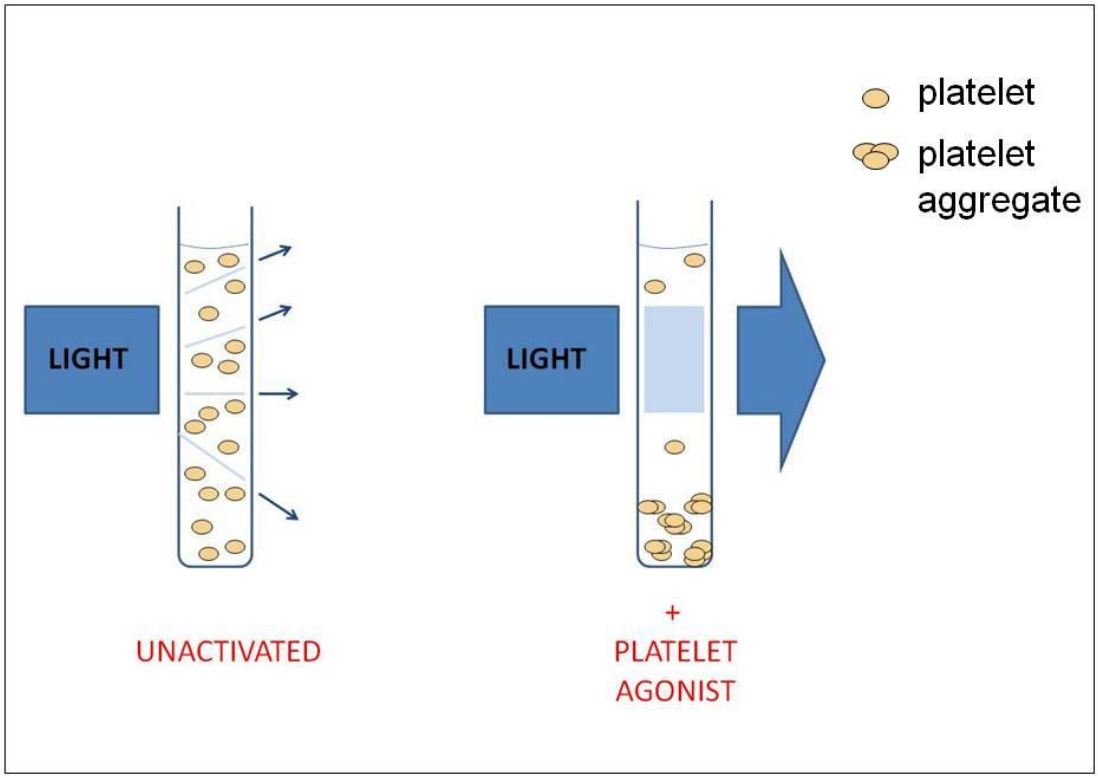

Figure 2.1 A schematic illustrating platelet aggregometry. Unactivated platelets in solution form a cloudy suspension allowing little or no light to pass through. Upon stimulation with a platelet agonist, the platelets aggregate and the resulting platelet aggregates fall to the bottom of the tube. This results in a greater amount of light passing through the sample, i.e. the percentage light transmission through the sample is directly proportional to the level of platelet aggregation.

2.2.2.1 Assessing the levels of platelet aggregation induced by manganese chloride ($MnCl_2$), dithiothreitol (DTT) and thrombin

Gel-filtered platelets were prepared as described in section 2.2.1.1. The platelet count was adjusted to 2.5 – 3.0 × 10^8/ml. Platelets were stimulated with either 1 mM, 3 mM or 5 mM manganese chloride ($MnCl_2$) or dithiothreitol (DTT) or 1U/ml thrombin in a BioData Corporation PAP4 aggregometer at 37 °C with constant stirring at 1100 revolutions per minute (rpm) for 10 minutes. The levels of platelet aggregation were observed at 0, 5 and an endpoint of 10 minutes after

addition of the activator to determine incubation times that would be useful in subsequent experiments.

2.2.2.2 Assessing the effects of an altered external redox environment on platelet aggregation

Gel-filtered platelets were prepared as described in section 2.2.1.1. Platelets were activated with 0.1U/ml thrombin, 50 ng/ml convulxin and 38 μg/ml collagen, in the presence of a reducing or oxidising external environment. A reducing environment was generated with 45 μM reduced glutathione (GSH), *tris*(2-carboxyethyl)phosphine (TCEP) or dithiothreitol (DTT). An oxidising environment was generated with 45 μM oxidised glutathione (GSSG), cystine (CySS) or 5,5'-dithiobis-(2-nitrobenzoic acid) (DTNB). Platelet aggregations were carried out in a Biodata Corporation PAP4 aggregometer at 37 °C with constant stirring at 1100 rpm. Aggregations were followed for 10 minutes.

2.2.2.3 Assessing the effects of bile acids on platelet aggregation

Gel-filtered platelets were prepared as described in section 2.2.1.1. Platelets were incubated with ursodeoxycholic acid (UDCA), deoxycholic acid (DCA) or taurodeoxycholic acid (TDCA) at concentrations of 10 μM, 100 μM or 500 μM for 10 minutes at 37 °C with constant stirring at 1100 rpm. Platelets were left unactivated or were activated with either 0.1U/ml thrombin, 50 ng/ml convulxin or 38 μg/ml collagen. Platelet aggregations were followed for 10 minutes at 37 °C with constant stirring at 1100 rpm in a Biodata Corporation PAP4 aggregometer.

2.2.2.4 Assessing the effects of protein kinase inhibitors on platelet aggregation

Gel-filtered platelets were prepared as described in section 2.2.1.1. Platelets were incubated with either 5 μM BAY 61-3606 or 25 μM PP2 for 10 or 15 minutes, respectively, at 37 °C with constant stirring at 1100 rpm. Platelets were left unactivated or were activated with either 0.1U/ml thrombin, 50 ng/ml convulxin or 38 μg/ml collagen. Platelet aggregations were followed for 10 minutes at 37 °C with constant stirring at 1100 rpm in a Biodata Corporation PAP4 aggregometer.

2.2.3 Measurement of the level of activation of the platelet specific integrin $\alpha_{IIb}\beta_3$

Flow cytometry is a technique that can be used to analyse particles, usually cells, based on their physical characteristics, namely particle size and relative granularity. These properties are measured when the injected sample is formed into a stream of single cells, which pass through the path of a laser beam. As the cells pass through the laser beam, they deflect the light resulting in light scattering. The physical properties of the cells can be determined by analysing the scattered light. There are two types of scattered light: forward scatter (FSC) and side scatter (SSC). Forward scatter is proportional to cell size while side scatter is proportional to the granularity or internal complexity of the cell (Figure 2.2 (a)). The two types of scattered light are collected by their respective detectors and translated into electrical signals (voltages), which are detected by photodetectors. The voltages are amplified and assigned a digital value by the

Analog-to-Digital Convertor (ADC), which converts a voltage pulse to a channel value. This signal is transmitted to a computer where the light signal is displayed on a data plot, represented as either a contour plot or a dot plot (Figure 2.2 (b)).

In addition to measuring scattered light, flow cytometry can also measure fluorescence. A cell surface marker can be specifically targeted with a probe such as an antibody conjugated to a fluorophore. When this fluorophore passes through the laser beam, it absorbs light energy causing its electrons to move to a higher energy state. The electrons are highly unstable in this excited state and quickly return to ground state, causing the release of excess energy in the form of a photon of light. This released energy is referred to as fluorescence. This fluorescence can be collected by detectors, which sort it according to the emission wavelength (Figure 2.3 (a)). For example, the FITC fluorophore has peak emission fluorescence at 525 nm and is detected by the FL-1 detector in the flow cytometer. A change in fluorescence associated with a sample population is displayed in a histogram. An increase or decrease in the level of fluorescence detected is illustrated as a shift in the histogram along the x-axis to the right or left, respectively (Figure 2.3 (b)).

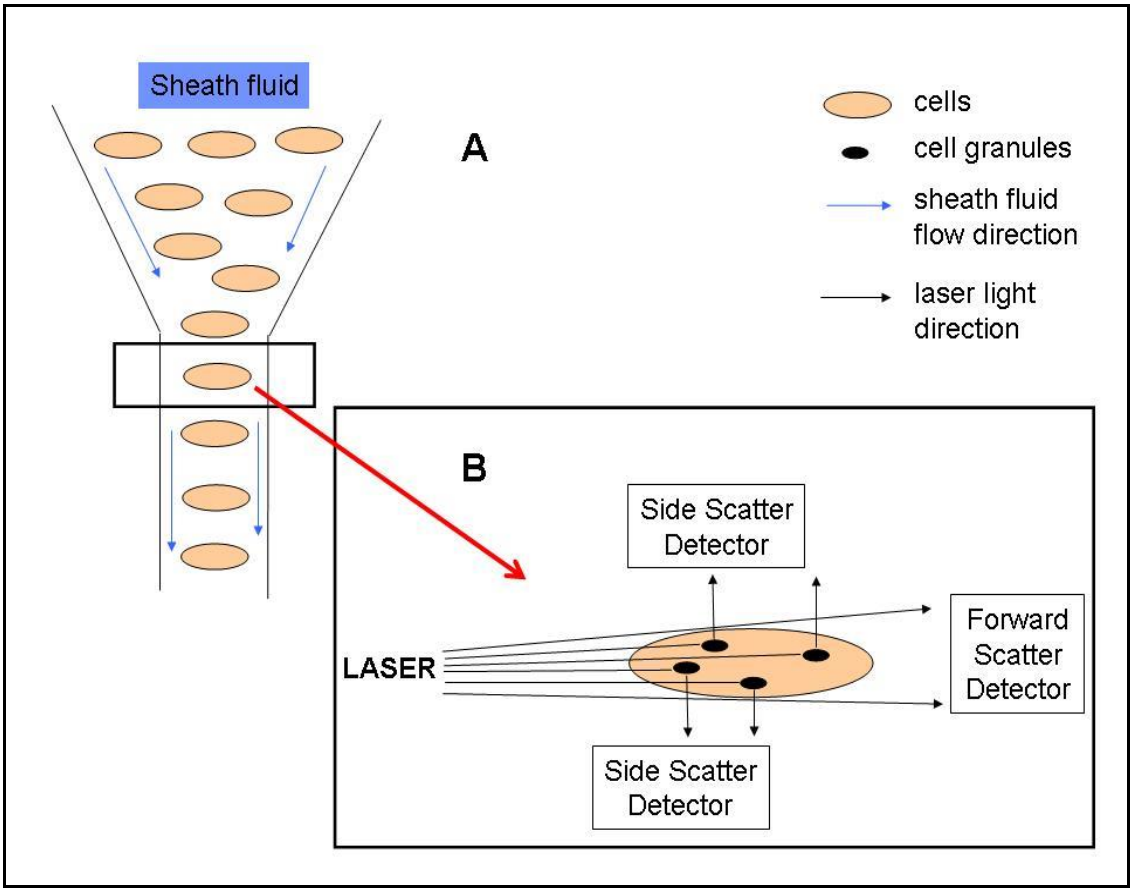

Figure 2.2 (a) A schematic illustrating the principle of light scattering by cells in flow cytometry. (A) The sample containing the cells to be analysed is injected into the flow cytometer and focussed into a stream of single cells in sheath fluid through a pressurised flow system. (B) A laser beam is focussed across the path of the cells. As the cells intercept the path of the laser beam, a scattering of light occurs. Light that is scattered along the same axis as the laser is referred to as forward scatter (FSC) and is detected by a forward scatter detector. FSC is proportional to cell size. Light that is scattered at 90° to the axis of the laser is referred to as side scatter (SSC) and is detected by a side scatter detector. Side scatter is a measure of the cells granularity or internal complexity.

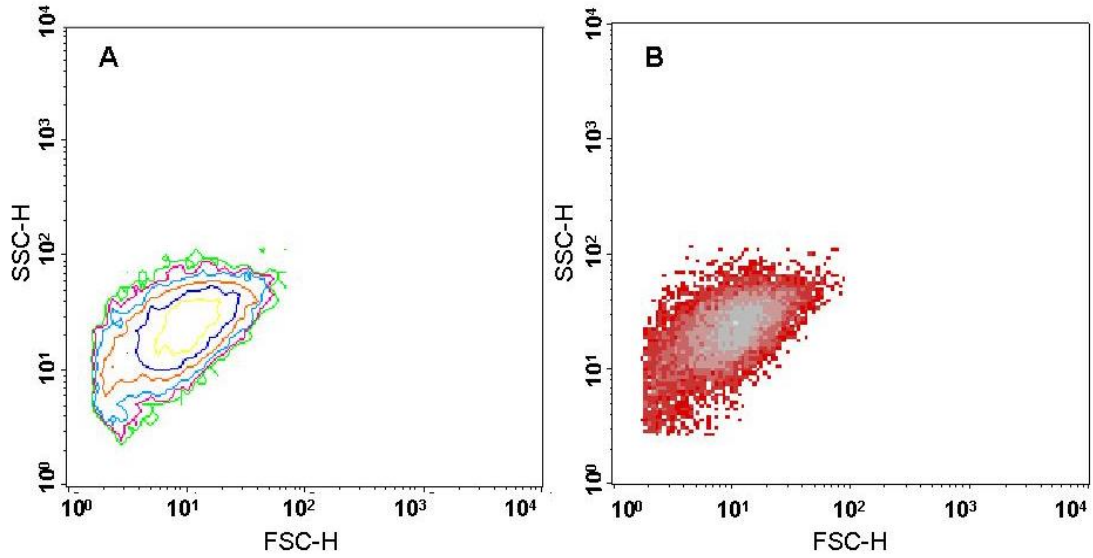

Figure 2.2 (b) Example of a contour plot (A) and a dot plot (B) of a sample of unactivated gel-filtered platelets in flow cytometry. Forward scatter (FSC-H) is shown on the x-axis, the intensity of which is representative of the particle size, in this instance the platelets. Side scatter is on the y-axis, the intensity of this scattering is indicative of the granularity of the particles. The location of the population in the bottom left hand corner of the plots indicates the small size of resting platelets (2 - 4 μm) and also the relatively low granular content of platelets. A threshold has been set on the FSC-H axis to eliminate any events from particles or debris smaller than the platelets that may be present in the sample. (A) The lines, or contours, in the contour map connect fields with the same number of events. (B) Each dot on the density plot represents an individual platelet that has passed through the flow cytometer; the grey colour indicates large numbers of events at this particular point.

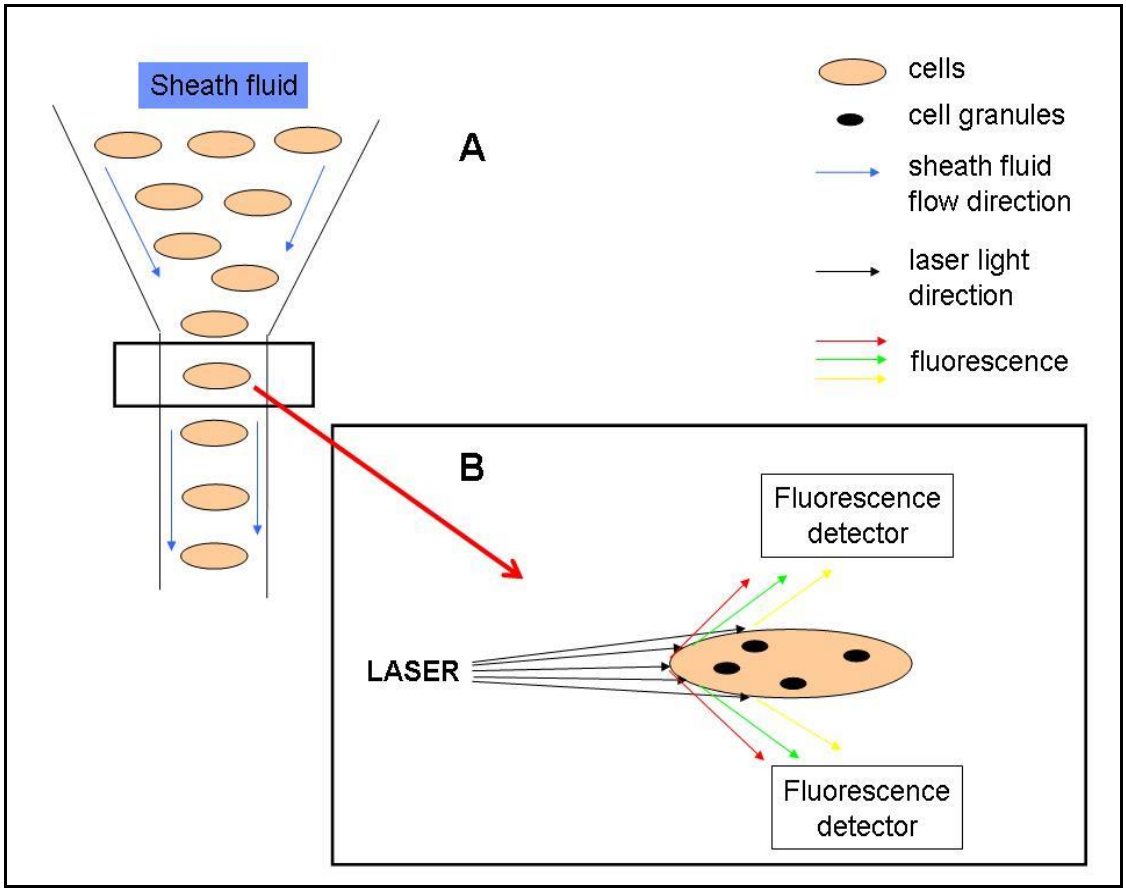

Figure 2.3 (a) A schematic illustrating the generation of fluorescence in flow cytometry. (A) The sample containing the cells to be analysed is injected into the flow cytometer and focussed into a stream of single cells in sheath fluid through a pressurised flow system. (B) The cells have been labelled with fluorescent compound, for example a specific cell surface marker can be probed with an antibody conjugated to a fluorophore. A laser beam is focussed across the path of the cells. When the fluorophore comes in contact with the laser, it absorbs light and moves into an excited state. However, this excited state is very unstable and the fluorophore quickly returns to the ground state. The excess energy is emitted in the form of a photon and is referred to as fluorescence. The fluorescence is detected by fluorescence detectors.

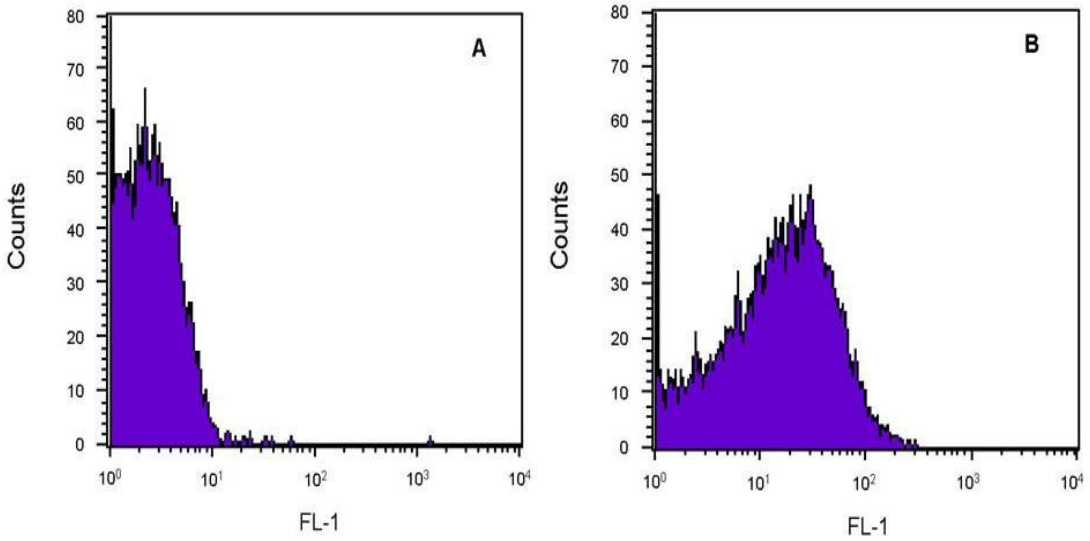

Figure 2.3 (b) Example of a histogram, demonstrating an increase in fluorescence is illustrated as a shift in the histogram from left to right. A cell surface marker can be specifically targeted with a probe such as an antibody conjugated to a fluorophore. When this fluorophore passes through the laser beam, it absorbs light energy causing its electrons to move to a higher energy state. The electrons are highly unstable in this excited state and quickly return to ground state, causing the release of excess energy as fluorescence. A change in fluorescence associated with a sample population is displayed in the form of a histogram. An increase or decrease in the level of fluorescence detected is illustrated as a shift in the histogram along the x-axis to the right or left, respectively. These histograms demonstrate an example of increased fluorescence detected in B, compared to that detected in A.

PAC-1 antibody is used to examine the activation state of the platelet specific integrin $\alpha_{IIb}\beta_3$. It is a monoclonal antibody which binds only to the activated conformation of integrin $\alpha_{IIb}\beta_3$. In this case, it is conjugated to the fluorophore fluorescein isothiocyanate (FITC). Therefore, the amount of fluorescence emitted from the fluorophore after its excitation by laser (488 nm argon-ion laser) is directly proportional to the quantity of activated integrin $\alpha_{IIb}\beta_3$ on the

platelet surface. PAC-1 was originally developed by fusing a murine myeloma cell line with splenic lymphocytes from a mouse which had been immunised with platelets from a Glanzmann's patient (Shattil et al, 1985).

Gel-filtered platelets were prepared as described in section 2.2.1.1. The platelet count was adjusted to 2.5 - 3 X 10^8/ml. Platelets were activated with either 1U/ml thrombin, 3 mM DTT or 3 mM $MnCl_2$ for 10 minutes, with 10 µl of PAC-1 antibody present. All incubations were carried out at 37 °C without stirring. These times for incubation were obtained from the analysis of the platelet aggregation studies described above.

After the 10 minute incubation, samples were diluted in 2 ml platelet buffer (MHPB) in 5 ml Falcon™ tubes. Samples were analysed on a Becton Dickinson FACSCalibur™ flow cytometer using CellQuest Pro software. The platelet population was gated, and 10,000 events were analysed.

2.2.4 Assessment of platelet degranulation

Flow cytometry was also used to assess the level of platelet degranulation or secretion, a process associated with platelet activation. P-selectin is released from α-granules upon platelet activation and is expressed on the platelet surface (Jurk & Kehrel, 2005). CD62P is a monoclonal antibody, which selectively binds P-selectin. In this case, the antibody is conjugated to the fluorophore phycoerythrin (PE). PE has a peak emission fluorescence at 578 nm and is detected by the FL-2 detector in the flow cytometer. The amount of fluorescence is indicative of the quantity of P-selectin on the surface of the

platelets, and hence, an indicator of the platelet activation state induced by the various platelet activators.

Gel-filtered platelets were prepared as described in section 2.2.1.1. The platelet count was adjusted to 2.5 - 3 X 10^8/ml. Platelets were activated with either 1U/ml thrombin, 3 mM DTT or 3 mM $MnCl_2$ for 10 minutes. All incubations were at 37 °C without stirring. 10µl CD62P antibody was present during the incubations.

Samples were then diluted in 2 ml platelet buffer (MHPB) in 5 ml Falcon™ tubes and analysed on a Becton Dickinson FACSCalibur™ flow cytometer using CellQuest Pro software. The platelet population was gated, and 10,000 events were analysed.

2.2.5 Raman Spectroscopy: Analysis of intact platelets

Raman spectroscopy (RS) is an optical technique used in the determination of molecular structure. Monochromatic light, usually a laser, is focussed onto a sample and interacts with the bonds in the molecules of the sample. Upon interaction with the light or photons, the molecules are transformed into oscillating or induced dipoles. This occurs when a molecule is placed in an electric field (laser) causing a distortion, whereby the positively charged nuclei are attracted to the negative pole and the negatively charged electrons are attracted to the positive pole (Ferraro, 2003). The scattering of photons by a molecule is dependent on the molecules polarisability. The polarisability of a molecule is defined as the ability of an applied electric field to induce a dipole

moment in an atom or molecule (Ball, 2001). These induced dipoles have the potential to emit or scatter light at three different frequencies. The three types of scattering are known as Rayleigh, Stokes and anti-Stokes scattering.

Rayleigh scattering is an elastic scattering which occurs in molecules which contain no Raman-active modes. When the molecule is excited, it returns back to the same vibrational state and emits photons at the same frequency as the excitation source, i.e. the light does not gain or lose energy during the scattering (Figure 2.4).

If there are Raman-active modes present in the molecules, the frequency of the photons emitted from the molecules is shifted up or down compared to the frequency of the original monochromatic light. It is this molecular inelastic scattering of light upon which the principle of Raman spectroscopy is based. Stokes scattering is a Raman effect which occurs when a photon is absorbed by a Raman-active molecule which at the time of interaction is in the basic vibrational state. Part of the photon's energy is transferred to the Raman-active mode and, therefore, the frequency of scattered photon is reduced. Anti-stokes scattering is essentially the opposite of Stokes scattering. It occurs when a photon interacts with a Raman-active molecule which is already in an excited state. The molecule releases this excess energy, which results in the molecule returning to a basic vibrational state while the frequency of the resulting scattered photons is increased (Figure 2.4). It is important to highlight that the energy difference is due to the energy difference in vibrational states of the molecule and is not related to the absolute energy of the photon. When

obtaining a Raman spectrum from a sample, approximately 99.999 % of incidence photons will undergo Rayleigh scattering with only about 0.001 % producing inelastic Raman signals.

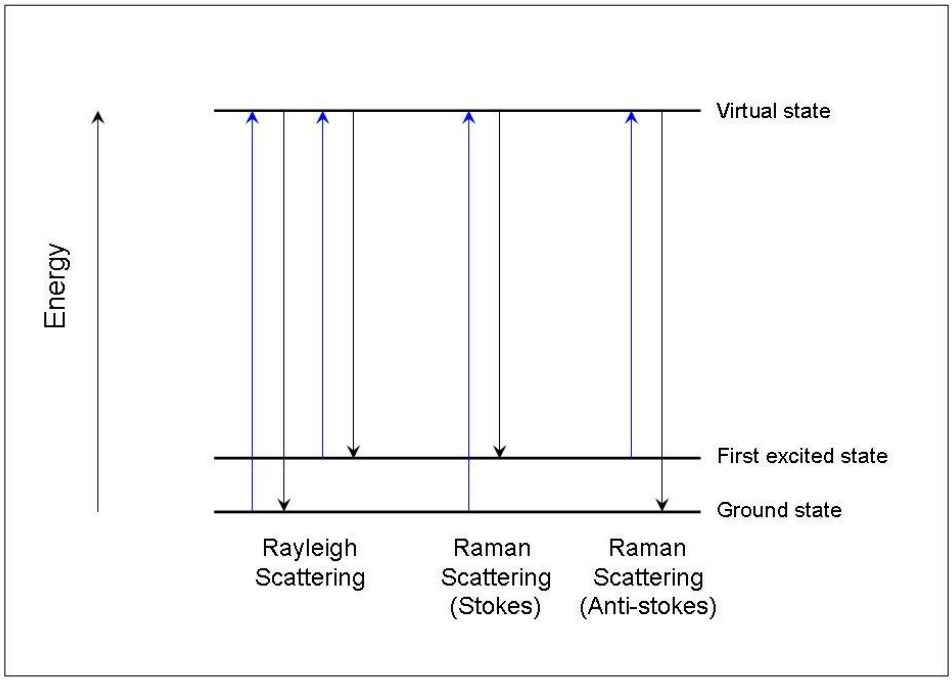

Figure 2.4 A diagram illustrating Rayleigh and Raman scattering. The blue arrows represent the excitation light, while the black arrows represent scattered light. Rayleigh scattering involves photons being absorbed by molecules and re-emitted at the same frequency as the excitation light; elastic scattering. Raman scattering, both Stokes and anti-Stokes, is inelastic scattering. Stokes scattering occurs when photons interact with molecules in a ground state which causes some of the photons energy to be transferred to the Raman-active mode in the molecule, thereby reducing the frequency of the scattered photons. Anti-stokes scattering occurs when the excitation photons interact with molecules already in an excited state, the molecule releases the excess energy causing an increase in the frequency of the resulting scattered photons.

Due to the low levels of Raman scattering, all scattered light is collected by a lens and is filtered to separate the strong Rayleigh scattering from the weaker

Raman scattering. The Raman scattered light is then dispersed on to a detector by a diffraction grating and a spectrum is generated (Figure 2.5).

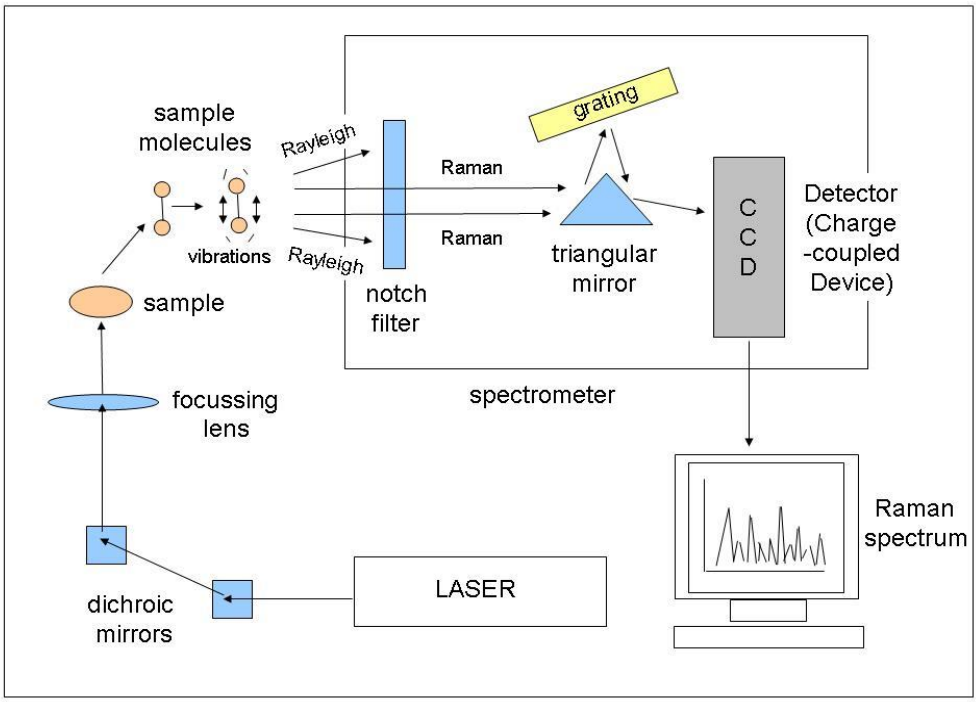

Figure 2.5 A schematic illustrating the basic Raman spectroscopy set up. A laser is focussed on the sample of interest. The photons of the excitation laser interact with the molecules of the sample and scattering of the photons occurs. Strong Rayleigh scattering is separated from the weaker Raman scattering by a filter. The light is then dispersed onto a detector by diffraction grating. This detector in turn sends a signal to the connected computer and a Raman spectrum providing information about the molecular structure of the sample is generated by the Raman analysis software.

Gel-filtered platelets were prepared as described in section 2.2.1.1. The platelet count was adjusted to approximately 1.0×10^9/ml. This higher platelet count ensured a high Raman signal. Platelets were incubated with 1U/ml thrombin, 3 mM $MnCl_2$ or 3 mM DTT for 10 minutes. All incubations were carried out at 37 °C, without stirring. Platelets were then fixed in 1 % formaldehyde. Initially,

1 µl of sample was pipetted on to a glass cover slip and allowed to dry for approximately 10 minutes. This method was changed after it was found that centrifuging the samples in a microcentrifuge for 2 minutes at 9,300 x g, removing the supernatant and placing the platelet pellet on the glass cover slip gave a much larger signal. Raman Spectra were recorded on a Horiba/Jobin Yvon LabRam HR spectrometer. The laser line of 473 nm was employed, focussed through a 200 µm hole with a 100X objective. A grating of 600 grooves/nm was used. The instrument was calibrated using a silicon chip. Power at the sample level was 1 mW. All spectra were analysed using LabSpec software.

Alternative substrates to glass cover slips were tested to minimise background signal. These were poly-L-lysine slides and quartz slides. Surface Enhanced Raman Spectroscopy (SERS) was also carried out. SERS is a technique which enhances the weak Raman scattering signal when substances are adsorbed onto roughened metal surfaces (nano scale: 10 - 100 nm), most commonly gold, silver or copper (Campion, 1998). SERS is expected to enhance Raman signal from molecules by a factor of 10^6 or more. The surfaces that we used for SERS were a glass slide coated with fluorine-doped tin oxide (FDTO) onto which gold nanoparticles were electrodeposited (Sheridan, 2007) and also an aluminium oxide plate coated with gold which contained nanocavities (3 - 4 µm diameter) (Jose et al, 2009). Other SERS substrates tested included aluminium oxide plates coated with gold or silver.

2.2.6 Principal component analysis (PCA)

Principal component analysis (PCA) was carried out on the data collected from the whole platelet analysis by Raman spectroscopy as described in section 2.2.5. PCA is a multivariate statistical analysis technique used for finding patterns in data of high dimension. It allows the data to be expressed in a way in which differences or similarities in the data are highlighted. Each Raman spectrum consists of 1681 channels, not all of which contain useful information. PCA defines a new dimensional space in which the major variance in the original data can be defined by a small number of principal components (PC). This allows the identification of the most important channels where the most differences are detected. The data was baseline subtracted and normalised with Origin® software. It was then imported into The Unscrambler® software where the data was transposed and PCA was performed.

2.2.7 Preparation of redox reagents

Reduced and oxidised species of glutathione, GSH and GSSG respectively, and reduced cysteine (Cys) and oxidised cystine (CySS) were combined in different ratios to generate various redox potentials using the Nernst equation (Schafer & Buettner, 2001). Redox potential is a measure of the reducing capacity of the redox couple and is expressed in terms of millivolts (mV). A very negative redox potential value indicates a highly reducing environment, while a less negative, or more positive, value indicates an oxidising environment.

$$\text{Nernst equation: } E_h = E^\circ - RT/nF \log [Red]^2/[Ox]$$

where E_h is electromotive force, E° is standard electrode potential (-264 mV for GSH/GSSG, -250 mV for CyS/CySS), R is the ideal gas constant (8.314 J K^{-1} mol^{-1}), T is absolute temperature (K), n is the number of electrons transferred, F is the Faraday constant, [Red] and [Ox] are the molar concentrations of the reduced and oxidised species, respectively. Redox potentials were set at mean plasma values (-130 mV for GSH/GSSG and -82 mV for CyS/CySS) ± 6 standard deviations. These mean plasma values were obtained from a study by Go and Jones (Go & Jones, 2005) in which the range of plasma redox potentials for both GSH/GSSG and Cys/CySS were determined from a group of over 700 randomly selected individuals. The mean plasma value plus 6 standard deviations yields an oxidising redox environment, whereas the mean plasma value minus 6 standard deviations gives a reducing redox environment. The reducing, mean and oxidising redox potentials for the GSH/GSSG and Cys/CySS redox couples, as used here, were determined as shown in Table 2.1. The concentrations of redox reagents used to generate these redox potentials are shown in Table 2.2.

Table 2.1 The reducing, mean and oxidising potentials generated by combining various ratios of GSH/GSSG and CyS/CySS using the Nernst equation.

Redox Potential	GSH/GSSG	CyS/CySS
Reducing	-264 mV	-148 mV
Mean	-130 mV	-82 mV
Oxidising	-10 mV	+4 mV

Table 2.2 The concentrations of GSH, GSSG, Cys and CySS used to generate the reducing, mean and oxidising redox potentials using the Nernst equation.

Redox potential	[GSH]	[GSSG]	[CyS]	[CySS]
-264 mV	45 μM	2 nM	-	-
-130 mV	3.02 μM	0.302 μM	-	-
-10 mV	0.25 μM	25 μM	-	-
-148 mV	-	-	60.44 μM	9.8 μM
-82 mV	-	-	14.22 μM	93.33 μM
+4 mV	-	-	0.5 μM	100.44 μM

Redox reagents, GSH, GSSG, Cys and CySS, were prepared as stock solutions at a concentration of 200 mM in 0.1 M hydrochloric acid (HCl). The reduced form of the reagents, in particular, has a tendency to become oxidised, therefore preparation of the reagents in concentrated HCl ensures the reagents remain in their correct forms. Reagents were diluted to the required working stocks in platelet buffer and thus the concentration of HCl to which the platelets were exposed was minimal (μM).

2.2.8 Measuring the number of thiols (-SH) on platelet surface

2.2.8.1 Measuring free thiols on platelet surface using DTNB (5,5'-dithiobis-(2-nitrobenzoic acid) on platelets in solution

The DTNB assay (also known as Ellman's Test (Ellman, 1959)) is a standard test used for the quantification of thiols. DTNB is a water-soluble compound that reacts with a thiol group to form a mixed disulphide and 2-nitro-5-thiobenzoic

acid (NTB) (Figure 2.6). NTB has a yellow colour and has a relatively intense absorbance at 412 nm. The stoichiometry of NTB to free thiols is in a 1:1 ratio. Therefore, measuring NTB formation allows us to determine the number of thiols present. As DTNB is cell impermeable, it was used to assess the number of platelet surface thiols.

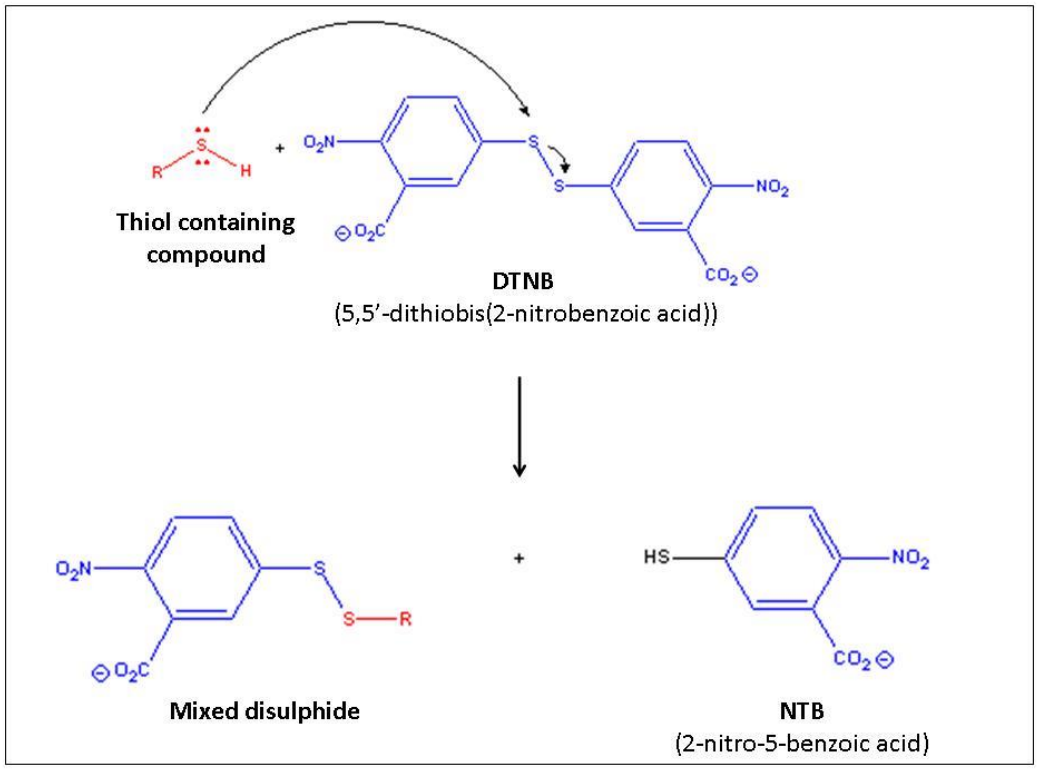

Figure 2.6 The chemical reaction between a thiol containing compound and DTNB (5,5'-dithiobis(2-nitrobenzoic acid). The thiol group of the thiol containing compound (RSH) reacts with DTNB causing its cleavage to form a mixed disulphide and NTB (2-nitro-5-benzoic acid). NTB is a coloured species, the absorbance of which can be measured at 412 nm and used to calculate the number of thiol groups in the original compound. (This schematic is adapted from UCDAVIS BioWiki: Structure and Properties of Amino Acids)

Gel-filtered platelets were prepared as described in section 2.2.1.1. Platelets were incubated with various GSH/GSSG or CyS/CySS redox conditions, as

described in section 2.2.7. Platelets were subsequently activated with either 0.1U/ml thrombin, 50 ng/ml convulxin or 38 μg/ml collagen for 10 minutes at 37 °C, without stirring. 100 μM DTNB (5,5'-dithiobis-(2-nitrobenzoic acid) was added to the samples and incubated for 1 minute at room temperature. Samples were centrifuged in a microcentrifuge for 30 seconds at 13,400 x g. The supernatant was removed and transferred to a clear, flat-bottom 96-well plate. Absorbance was measured, using a Wallac plate reader at 405 nm (as this was the closest filter to 412 nm available).

A standard curve was generated using known concentrations of cysteine (Cys), a thiol containing compound. Cysteine, at concentrations ranging from 0 - 15 μM, was incubated with DTNB (100 μM), in triplicate, for 1 minute at room temperature. The absorbance of the samples was read in a clear, flat bottom 96-well plate at 405 nm in the Wallac plate reader. Results were plotted and the equation of the line was generated using GraphPad Prism® 5 software. Platelet surface thiol populations were estimated from this standard curve.

2.2.8.2 Measuring free thiols on platelet surface using DTNB (5,5'-dithiobis-(2-nitrobenzoic acid) on adhered platelets

Clear, flat bottom, 96-well plates were coated with 100 μl per well of either 1 % bovine serum albumin (BSA) in Tris buffered saline (TBS: 150 mM NaCl, 50 mM Tris (base), pH7.4), 20 μg/ml fibrinogen in TBS or 1 μg/ml CRP in TBS overnight at 4 °C. Plates were coated with 10 μg/ml collagen overnight at room temperature. Excess substrate was removed and plates were then blocked with 5 % BSA in TBS for 1 hour at 37 °C. Excess BSA was removed and plates were washed once with TBS, once with 0.1 % BSA in TBS and once with 0.1 % BSA

in TBS supplemented with 1.8 mM $CaCl_2$ (BSA, fibrinogen and CRP wells) or 2 mM $MgCl_2$ (collagen wells). Washed platelets (prepared as described in section 2.1.1.2) were incubated with GSH/GSSG redox potentials for 10 minutes at 37 °C. 50 μl of redox treated washed platelets were added per well and plates were incubated for 45 minutes at 37 °C. All experiments were carried out in triplicate. Following incubation, non-adhered platelets were removed. Plates were washed twice with platelet buffer (MHPB). 100 μl of 100 μM DTNB (5,5'-dithiobis-(2-nitrobenzoic acid), was added to each well and incubated for 1 minute at room temperature. Absorbance was read on the Wallac plate reader at 405 nm.

2.2.9 Platelet static adhesion assay

Clear, flat bottom, 96-well plates were coated with 100 μl per well, of either 1 % bovine serum albumin (BSA) in Tris buffered saline (TBS: 150 mM NaCl, 50 mM Tris (base), pH7.4), 20 μg/ml fibrinogen in TBS or 1 μg/ml CRP in TBS overnight at 4 °C. Plates were coated with 10 μg/ml collagen overnight at room temperature. Excess substrate was removed and plates were blocked with 5 % BSA in TBS for 1 hour at 37 °C. Excess BSA was removed and wells were washed once with TBS, once with 0.1 % BSA in TBS and once with 0.1 % BSA supplemented with 1.8 mM $CaCl_2$ for those wells coated with either BSA, fibrinogen or CRP; or 0.1 % BSA in TBS supplemented with 2 mM $MgCl_2$ for those wells coated with collagen. 50 μl of washed platelets were added per well, and incubated for 45 minutes at 37 °C. Each condition was performed in triplicate. Following incubation, non-adhered platelets were removed. Plates

were washed twice with platelet buffer (MHPB). 100 μl of lysis buffer (70 mM sodium citrate, 30 mM citric acid, 0.1% (v/v) Triton-X-100) containing 5 mM *p*NPP (*para*-nitrophenyl phosphate) was added to each well and incubated for 1 hour at room temperature. The reaction was stopped by adding 100 μl of 2 M NaOH, per well. *p*NPP is a chromogenic substrate for most phosphatases including alkaline, acid, protein tyrosine and serine/threonine. The reaction yields *para*-nitrophenol, which becomes an intense yellow soluble product under alkaline conditions, hence the addition of NaOH. The absorbance was read on the Wallac plate reader at 405 nm. The absorbance is directly proportional to the amount of phosphatases present and, therefore, is an indirect measure of the total number of adhered platelets.

2.2.10 Purified integrin $\alpha_{IIb}\beta_3$: Buffer exchange and concentration

Purified integrin $\alpha_{IIb}\beta_3$ was purchased from Merck Millipore and stored at -80 °C until ready for use in experiments. The concentration of the purified integrin $\alpha_{IIb}\beta_3$ was approximately 1.3 mg/ml, according to the manufacturer. As the protein was required at a high concentration, the purified integrin was concentrated as follows: 0.5 ml purified integrin was centrifuged through centrifugal filters for 5 minutes at 14,000 x g at 4 °C in a microcentrifuge, as recommended in the manufacturer's instructions. This step was repeated a number of times, checking the volume of integrin after each centrifugation step. After 40 minutes, the volume of integrin present had decreased. Therefore, the purified protein was now anticipated to be more concentrated than the original stock.

Upon purchase, the purified integrin is in the following buffer: 100 mM NaCl, 20 mM Tris-HCl, 1 mM $CaCl_2$, 50 % glycerol, 0.1 % (v/v) Triton-X-100 and ≤ 0.1 % sodium azide, pH 7.4). In order to ensure all glycerol was removed from the system, a buffer exchange step was required. A volume of buffer A (100 mM NaCl, 1 mM $CaCl_2$, 20 mM Tris-HCl, 0.1 % (v/v) Triton-X-100, pH 7.4), was added to the centrifugal filter to make the volume back up the original stock volume before the integrin was concentrated. The integrin was then centrifuged for 10 minutes at 14,000 x g at 4 °C. The filtrate was discarded and the filter device was removed, inverted and placed in a new, clean tube. It was then centrifuged for 2 minutes at 1000 x g at 4 °C to recover all purified integrin $\alpha_{IIb}\beta_3$.

A protein quantitation assay (section 2.2.11) was performed to calculate the concentration of purified integrin $\alpha_{IIb}\beta_3$. Note: the protein quantitation assay was not performed before the buffer exchange step as high concentrations of glycerol are known to interfere with this assay. The purified integrin $\alpha_{IIb}\beta_3$ was subsequently found to be at a final concentration of 5 mg/ml.

2.2.11 Protein quantitation assay

The protein quantitation assay is a colorimetric assay used to determine protein concentration of a solution. It was carried out using the Bio-Rad DC (detergent compatible) Protein Assay kit. The principal of this particular assay is similar to that described by Lowry (Lowry et al, 1951). The concept on which it is based is a reaction of protein with an alkaline copper tartrate solution and Folin reagent. It is a two-step reaction where the protein initially reacts with copper in an

alkaline medium, and the Folin reagent is then reduced by the copper-treated protein resulting in a subsequent colour change. A standard curve is generated using concentrations of BSA (Bovine serum albumin prepared in the buffer in which the protein sample of interest is diluted) ranging from 0 – 1.5 mg/ml (0, 0.2, 0.4, 0.6, 0.8, 1.0, and 1.5 mg/ml). The exact contents of the solutions are not specified by the manufacturer and are referred to as solution S and reagents A and B. Solution A' was prepared by adding 20 μl solution S to 1 ml reagent A. 20 μl of solution A' was added to each required well in a clear, 96-well plate. Following this, 5 μl of either BSA or the protein of interest was added to the wells. 200 μl reagent B was then added and incubated for 15 minutes at room temperature. The assay was carried out with each sample in triplicate. The absorbance of the samples was read on the Wallac plate reader at 690 nm. A standard curve was generated using GraphPad Prism® 5 software (Figure 2.7) and the concentration of the protein of interest was calculated from the equation of the line. Note the protein of interest may be diluted if it is thought to be very concentrated. If so, it was important to remember this dilution factor when calculating the final concentration of protein.

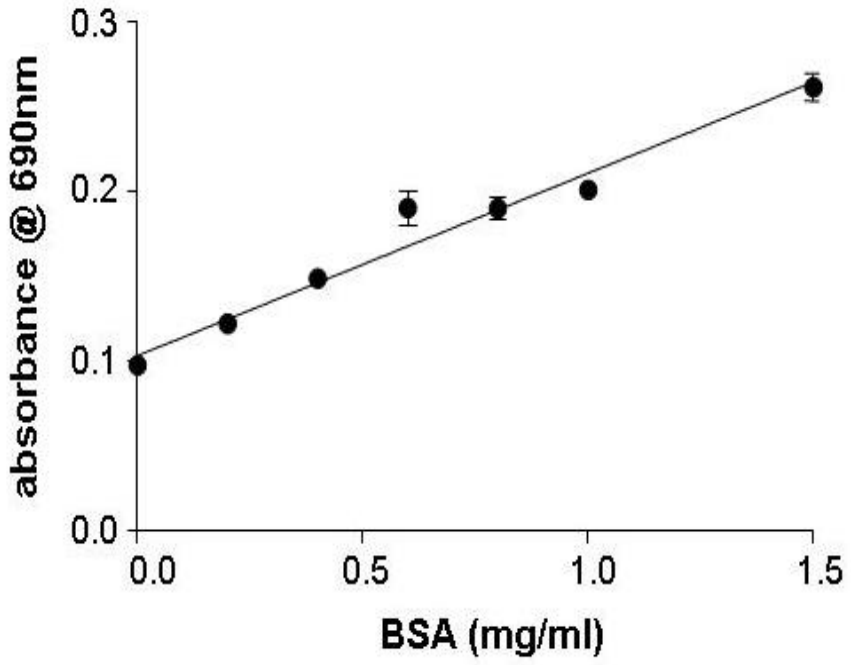

Figure 2.7 A representative BSA standard curve generated using the BioRad DC Protein assay. Known concentrations of BSA ranging from 0 – 1.5 mg/ml (5 μl per sample, in triplicate) were incubated with 20 μl Solution A' and 200 μl reagent B for 15 minutes at room temperature. The absorbance was read on the Wallac plate reader at 690 nm. A standard curve was generated by plotting the absorbance (at 690 nm) versus concentration of protein (mg/ml) using GraphPad Prism® 5 software. The concentration of unknown protein samples was calculated from the equation of the line: $y = 0.1072x + 0.1033$, $r^2 = 0.9367$.

2.2.12 Determining the free thiol population of purified integrin $\alpha_{IIb}\beta_3$

The thiol population of purified integrin $\alpha_{IIb}\beta_3$ was determined using a thiol detection reagent known as Thiostar®. This reagent was used as an alternative to DTNB, which was used in the platelet thiol population, due to its higher sensitivity and ability to measure low concentrations of thiols on proteins. Thiostar® is a commercial product, the exact chemical mechanism of which is not available. However, it is known to be converted to a brightly fluorescent

product upon reaction with thiols. This fluorescence can be measured at a wavelength between 475 nm and 570 nm, with an excitation wavelength of 350 – 410 nm.

Purified integrin $\alpha_{IIb}\beta_3$ was incubated with GSH/GSSG redox potentials for 10 minutes at 37 °C. The excess, unreacted redox reagents were then removed from the system using P6 Bio-Spin columns. This step was carried out in order to ensure the excess reduced glutathione (GSH) did not interfere with the assay. The P6 spin columns were prepacked with polyacrylamide size exclusion gel which allowed the integrin to pass through and left the contaminating redox reagents behind in the column. The columns were pre-hydrated with 10 mM Tris buffer which needed to be exchanged for buffer A (100 mM NaCl, 1 mM $CaCl_2$, 20 mM Tris-HCl, 0.1 % (v/v) Triton-X-100, pH 7.4). The original buffer was allowed to drain out by gravity initially, then 500 μl buffer A was added to the column and centrifuged for 1 minute at 1000 x g at room temperature. This step was repeated four times ensuring ≥ 99.9 % buffer exchange according to the manufacturer's instructions.

Following incubation with the GSH/GSSG redox potentials, the integrin was centrifuged in the P6 spin columns, equilibrated with buffer A, for 4 minutes at 1000 x g at room temperature. The integrin was recovered and incubated with 1 mM, 3 mM or 5 mM manganese chloride ($MnCl_2$) for 10 minutes at 37 °C. It was found that 3 mM $MnCl_2$ caused a significant increase in integrin thiols and all subsequent experiments were carried out using 3 mM $MnCl_2$ to activate integrin $\alpha_{IIb}\beta_3$. The resting or activated integrin (10 μg/ml), in the absence or

presence of GSH/GSSG redox potentials, was incubated with Thiostar® (2.5 μg/ml) for 5 minutes, at room temperature, in a black, clear bottom 96-well plate. The fluorescence was measured using the Wallac plate reader at 355/535 nm.

2.2.13 Chinese hamster ovarian-K1 (CHO-K1) cell culture

Chinese hamster ovarian-K1 (CHO-K1) cells expressing platelet integrin $\alpha_{IIb}\beta_3$, as previously described by Aylward et al (Aylward et al, 2006) were used in these studies. Two cell lines were employed: a mock transfected CHO-K1 cell line and a CHO-K1 cell line expressing integrin $\alpha_{IIb}\beta_3$ with a KVGFFKR sequence in the α_{IIb}-subunit (referred to as FF cells). FF cells express integrin $\alpha_{IIb}\beta_3$ in a native, resting conformation. All cell lines were grown in Nutrient Mixture F-12 (HAM) and Dulbecco's Modified Eagle Media (DMEM) supplemented with 10 % bovine calf serum, 375 μg/ml Geneticin and 250 μg/ml Zeocin. Cells were grown to 80 - 90 % confluency and either used in experiments or passaged (split), for further culturing. 0.025 % Accutase® solution was used during cell splitting as an alternative to trypsin in order to ensure the integrin expressed in the CHO-K1 cells remained intact.

2.2.14 Assessment of Chinese hamster ovarian-K1 (CHO-K1) cells by flow cytometry

2.2.14.1 Assessment of levels of integrin $\alpha_{IIb}\beta_3$ activation in Chinese hamster ovarian-K1 (CHO-K1) cells

The Chinese hamster ovarian-K1 (CHO-K1) cells employed in this study were a mock transfected CHO-K1 cell line and a cell line expressing integrin $\alpha_{IIb}\beta_3$ in a resting conformation (FF cells). When cells reached a confluency of 80 - 90 %, they were deemed suitable for use in experiments. Cells were removed from the cell culture flasks and transferred to a 50 ml plastic tube. Cells were centrifuged for 3 minutes at 1200 x g to pellet them. Cell culture media was removed and cells were resuspended in TBS (150 mM NaCl, 50 mM Tris (base), pH7.4).The cell count for all cell lines was adjusted, by addition of TBS, so that they were all at a similar concentration of approximately 3.0 X 10^6/ml. The levels of integrin expression in the CHO-K1 cells were checked using the monoclonal antibody CD41a, which binds to the α_{IIb}-subunit of integrin, conjugated to a FITC fluorophore. Cells were incubated with 10 µl CD41a-FITC for 10 minutes at 37 °C. The reaction was stopped by adding 1 ml TBS in 5 ml Falcon™ tubes. Samples were analysed on a Becton Dickinson FACSCalibur™ flow cytometer using CellQuest Pro software. The CHO-K1 cell population was gated, and 3,000 events were analysed.

The activation state of the integrin $\alpha_{IIb}\beta_3$ expressed in the FF cells was assessed using the FITC-conjugated monoclonal antibody PAC-1. PAC-1 binds specifically to the active conformation of the integrin. FF cells were incubated with $MnCl_2$ at final concentrations of 1 mM, 3 mM, and 5 mM for 10 minutes at

37 °C in the presence of 10 μl PAC-1 antibody. The reaction was stopped by adding 1 ml TBS in 5 ml Falcon™ tubes. Samples were analysed on a Becton Dickinson FACSCalibur™ flow cytometer using CellQuest Pro software. The CHO-K1 cell population was gated, and 3,000 events were analysed.

It was found 3 mM $MnCl_2$ induced a significant increase in the level of PAC-1 binding to FF cells, compared to untreated FF cells, therefore 3 mM $MnCl_2$ was chosen as the optimal concentration and used in all subsequent experiments.

2.2.14.2 Assessment of the effect of an altered external redox environment on integrin $\alpha_{IIb}\beta_3$ activation in Chinese hamster ovarian-K1 (CHO-K1) cells

CHO-K1 cells were prepared as described in section 2.2.14.1 and the cell count adjusted to 3 X 10^6/ml by addition of TBS. FF cells were incubated with GSH/GSSG redox potentials (reducing (-264 mV), mean (-130 mV) and oxidising (-10 mV)) (section 2.2.7) for 10 minutes at 37 °C. FF cells were subsequently incubated with 3 mM $MnCl_2$ for 10 minutes at 37 °C before stopping the reaction by adding 1 ml TBS in 5 ml Falcon™ tubes. Samples were analysed on a Becton Dickinson FACSCalibur™ flow cytometer using CellQuest Pro software. The CHO-K1 cell population was gated, and 3,000 events were analysed.

2.2.15 Assessment of platelet adhesion and spreading using confocal microscopy

Confocal microscopy is an imaging technique pioneered by Marvin Minsky in 1955 (Minsky, 1988). The main principle upon which confocal microscopy is based, and what makes it superior to conventional microscopy, is that it focuses a point of light on a specimen and excludes most of the scattered light from the specimen that is not directly from the focal point. This ensures the majority of unwanted light is not collected, producing a sharper, better resolved image with enhanced contrast compared to that produced by conventional microscopy. The majority of modern confocal microscopy employs fluorescent imaging, whereby a specimen is stained or labelled with a fluorescent dye. The fluorescence emitted from the fluorophore when excited by a laser, at its specific wavelength, is filtered, collected and an image is generated (Figure 2.8). A pinhole is used to exclude the out of focus, unwanted light. The smaller the pin hole the more unwanted light is excluded. However, reducing the size of the pinhole too much can also limit the amount of light of interest from the sample. This problem may be addressed by increasing the excitation laser intensity, although this can, in turn, lead to problems, such as damage to the sample. Therefore, a balance needs to be struck between pinhole size and excitation laser intensity.

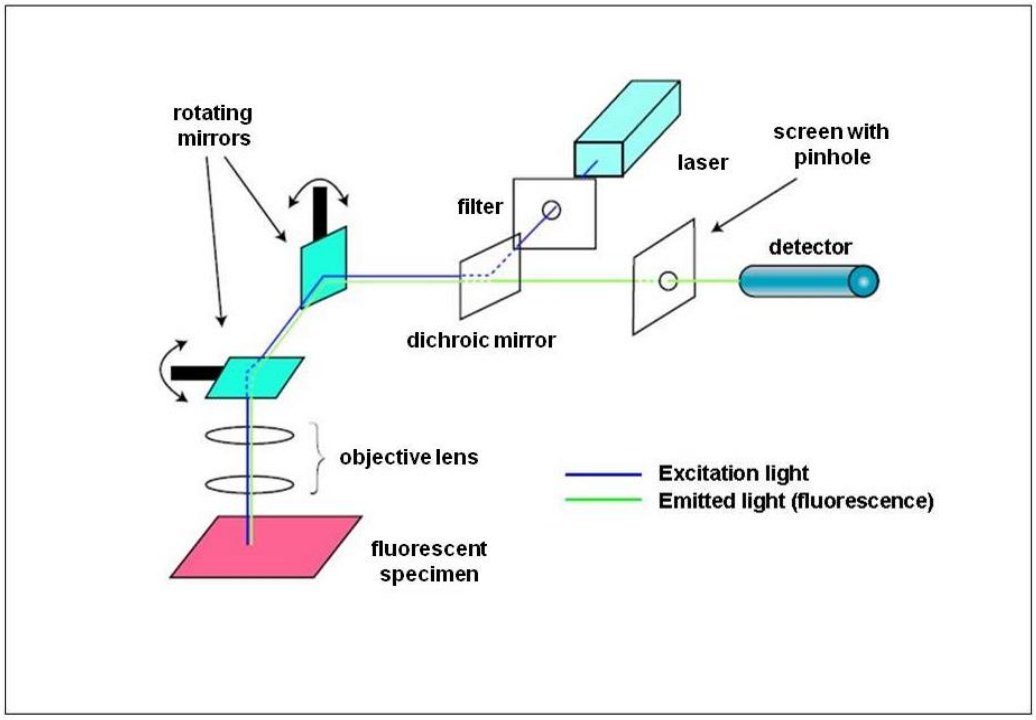

Figure 2.8 A schematic illustrating the basic set up of a confocal microscope. A specimen of interest is labelled, or stained, with a fluorescent dye. An excitatory laser light is focussed on the specimen through the microscopes objective lens. The fluorophore molecules absorb the light and its electrons are moved from ground state to a higher excited state. However, they are unstable in this excited state and quickly fall back to a ground state, releasing excess energy in the form of photons or fluorescence. This emitted light, or fluorescence, passes back through the objective lens, the dichroic mirror and the pinhole to the detector. The detector then sends the signal to a computer and an image, representing a thin cross-section of the specimen, is generated. (Image adapted from (Semwogerere, 2005)).

Poly-L-lysine coated glass slides were cleaned with ethanol. The slides were coated with 1 % bovine serum albumin (BSA) in Tris buffered saline (TBS: 150 mM NaCl, 50 mM Tris (base), pH7.4), 20 μg/ml fibrinogen in TBS, or 1 μg/ml collagen related peptide (CRP) in TBS, overnight at 4 °C. Slides were coated with 10 μg/ml collagen overnight at room temperature. The slides were gently washed twice with TBS and then blocked with 1 % BSA in TBS for 1 hour at 37 °C. Slides were washed gently with 0.1 % BSA in TBS, followed by another

wash with 0.1 % BSA supplemented with 1.8 mM $CaCl_2$ for the BSA, fibrinogen and CRP coated slides or 2 mM $MgCl_2$ for the collagen coated slides. The platelet count of washed platelets (prepared as described in section 2.1.1.2) was adjusted to 3.0 X 10^7/μl. Washed platelets were incubated with GSH/GSSG redox potentials (reducing (-264 mV), mean (-130 mV) or oxidising (-10 mV)) for 10 minutes at 37 °C. Platelets were placed onto the slides and incubated for 45 minutes at 37 °C. The slides were then gently washed twice with platelet buffer (MHPB) to remove non-adhered platelets. Samples were fixed with 1 % formaldehyde for 10 minutes at room temperature and gently washed twice with platelet buffer (MHPB). Platelets were permeabilised with 0.1 % (v/v) Triton-X-100 for 10 minutes at room temperature. Slides were washed gently three times with platelet buffer (MHPB). Platelets were then stained with Alexa Fluor® 488 phalloidin, in platelet buffer at a 1 in 100 dilution of the original stock, for 20 minutes at room temperature. Slides were gently washed three times with platelet buffer (MHPB). Glass cover slips were carefully cleaned and a drop of mounting media was placed onto a coverslip. The coverslip was carefully placed on the slide, at an angle in order to avoid any air bubbles being created. The slides were left at room temperature for 1 hour to allow the mounting media to dry, and then imaged immediately or stored at 4 °C for imaging at a later date. Confocal microscopy was carried out using a Zeiss LSM510 Meta confocal microscope. A 488 nm laser, at 1 % intensity was employed for the analysis of platelets stained with Alexa Fluor® 488 phalloidin. A 63X oil-immersion objective was used when obtaining confocal images. A bandpass (BP) 505-550 filter was used, along with a pinhole of 90 μm.

2.2.16 Examination of platelet thiol population by confocal microscopy

Poly-L-lysine slides were coated as described in section 2.2.16. Washed platelets were prepared as outlined in section 2.2.1.2. The platelet count was adjusted to 3.0 X 10^7/μl. Platelets were placed onto the slides and incubated for 45 minutes at 37 °C. The slides were gently washed twice with platelet buffer (MHPB) to remove non-adhered platelets. Samples were stained with 100 nM Atto 655 maleimide for 10 minutes at room temperature. Slides were washed gently three times with platelet buffer (MHPB). Samples were fixed with 1 % formaldehyde for 10 minutes at room temperature and then gently washed twice with platelet buffer. Glass cover slips were carefully cleaned and a drop of mounting media was placed onto a coverslip. The coverslip was then carefully placed on the slide, at an angle, in order to avoid any air bubbles being created. The slides were left at room temperature for 1 hour to allow the mounting media to dry, imaged immediately or stored at 4 °C for imaging at a later date. Confocal microscopy was carried out using a Zeiss LSM510 Meta confocal microscope. A 633 nm laser, at 30 % intensity was employed for the analysis of platelets stained with Atto 655 maleimide. A 63X oil-immersion objective was used when obtaining confocal images. A long pass (LP) 650 filter was used, with a pinhole of 122 μm.

2.2.17 Analysis of platelet spreading by scanning electron microscopy (SEM)

Scanning electron microscopy (SEM) is a powerful technique which uses electrons to generate an image of a specimen, in contrast to most imaging

techniques that use light. SEM has a number of advantages over traditional light microscopy including having a greater depth of field, higher resolution and more control of the degree of magnification. The basic principle upon which SEM works is a beam of electrons, the incident beam, is focussed on a sample under high vacuum. When the beam hits the specimen electrons and x-rays are emitted, collected by a detector and an image is generated. The incident beam of electrons is produced by an electron gun, accelerated to a high voltage and focussed into a thin beam of electrons towards the specimen by electromagnetic lenses. Upon interaction with the specimen an energy exchange occurs between the incident electrons and the electrons of the specimen. This results in the release of elastically scattered high-energy electrons, secondary electrons by inelastic scattering and electromagnetic radiation. These signals can be amplified and collected by specialised detectors. These detectors transmit the signal to a computer where the image of the specimen is generated. The preparation of specimens, in particular biological samples, for SEM is very important. Since the chamber in the SEM is under high vacuum, samples should be fixed and all water must be removed. All non-metals also require coating with a conductive metal such as gold. This process is known as sputter coating. It involves placing the specimen in the vacuum chamber filled with argon gas and gold foil. An electric field causes an electron to be removed from the argon, leaving it with a positive charge which is attracted to the negatively charged gold. The argon ions then knock gold atoms from the surface of the gold foil which fall and settle on the specimen forming a thin gold coating on the surface. This advanced technology allows SEM to

generate clear, detailed and striking images superior to those produced by conventional microscopy.

Round, glass coverslips (diameter (Ø) 16 mm) were pre-coated with poly-L-lysine. A 1 in 10 dilution of the original stock solution (in dH_20) was placed on the cover slips for 5 minutes at room temperature, excess was removed and the cover slips were allowed to dry for 2 hours at 37 °C. Cover slips were coated with 1 % BSA, 20 μg/ml fibrinogen, 10 μg/ml collagen or 1 μg/ml CRP as described in section 2.2.16. Washed platelets were prepared as outlined in section 2.2.1.2. The platelet count was adjusted to 3.0 X 10^7/μl. Platelets were placed onto the coverslips and incubated for 45 minutes at 37 °C. The coverslips were gently washed twice with platelet buffer (MHPB) to remove non-adhered platelets. Samples were fixed with 1 % formaldehyde for 10 minutes at room temperature. Samples were gently washed twice with platelet buffer and stored in platelet buffer until the dehydration process was carried out. Samples were dehydrated and washed in a series of acetone concentrations (30 %, 50 %, 75 %, 80 %, 85 %, 90 %, 95 % and 100 %) for 15 minutes at room temperature. Samples were sputter coated with approximately 20 nm gold, using an Emitech sputter coater, and mounted for SEM imaging. Images were obtained using a Hitachi S3400n SEM operating at 5 kV.

2.2.18 Western blotting

Western blotting is a technique widely used to identify proteins in a sample or identify post-translational modifications of a protein, such as phosphorylation.

Firstly, proteins are separated according to their apparent molecular weight by sodium dodecyl sulphate polyacrylamide gel electrophoresis (SDS-PAGE). Once separated the proteins are transferred from the polyacrylamide gel to a nitrocellulose or polyvinyl difluoride (PVDF) membrane, which is more stable and easier to handle for subsequent steps than the polyacrylamide gel. The membrane is blocked to ensure a uniform protein surface, preventing unwanted non-specific binding, and is subsequently probed with a specific antibody to the protein of interest. The membrane is then probed with a secondary antibody which binds specifically to the primary antibody. The secondary antibody is conjugated to a reporter enzyme, such as horse radish peroxidase (HRP), which plays a key role in the enhancement of the signal during the blot development through a chemiluminescence detection technique.

2.2.18.1 Preparation of platelet lysates

Gel-filtered platelets were prepared as outlined in section 2.2.1.1. The platelet count was adjusted to approximately 8 X 10^8/ml. This high platelet count was used to ensure a sufficient concentration of protein was generated for subsequent Western blotting. Platelets were unactivated or activated with either 0.1U/ml thrombin, 50 ng/ml convulxin or 38 μg/ml collagen, in the presence of GSH/GSSG redox potentials, prepared as outlined in section 2.2.7. The samples for gel electrophoresis were prepared using a platelet aggregation assay. The platelet aggregations were carried out in a Biodata Corporation PAP4 aggregometer at 37 °C with constant stirring at 1100 rpm and followed for 10 minutes. At the 10 minute time point, 10X radioimmunoprecipitation assay (RIPA) platelet lysis buffer (0.5 M NaCl, 10 mM sodium orthovanadate (Na_3VO_4), 200 mM tetra sodium pyrophosphate ($Na_4P_2O_7.10H_2O$), 500 mM

sodium fluoride (NaF), 10 % (v/v) Triton X-100, and 100 mM Tris pH 7.4) containing 10X protease inhibitor cocktail (100X protease inhibitor cocktail: 100 mM AEBSF.HCl, 80 µM Aprotinin, 5 mM Bestatin, 1.5 mM E-64, 1 mM EDTA, 2 mM Leupeptin, 1 mM Pepstatin A, in 95 % DMSO) was added to the aggregation tubes. RIPA lysis buffer was at a final concentration of 1X in the platelet lysate samples. Lysates were vortexed, and kept on ice for 1 hour with regular vortexing, approximately every 10 minutes. Platelet lysates were either used immediately or divided into aliquots and stored at -20 °C.

2.2.18.2 Sodium dodecyl sulphate polyacrylamide gel electrophoresis (SDS-PAGE)

Sodium dodecyl sulphate polyacrilamide gel electrophoresis (SDS-PAGE) is a method used to separate proteins. SDS is an anionic detergent which means its molecules carry a net negative charge when dissolved in an aquatic solution. Polypeptide chains bind to SDS and the negative charge of the SDS, along with heating or reducing of the samples causes the denaturation of the proteins to their primary amino acid sequences. The SDS also negates any positive charges on the protein, thereby, rendering the protein completely negative in charge and linearised. These negatively charged proteins will all migrate towards a positive charge (anode) at the same rate when a constant electrical field is applied to the gel. However, in a polyacrylamide gel, large molecules will migrate at a slower rate than smaller molecules, due to the size of the pores in the gel. Smaller proteins pass through the pores with ease while the bigger proteins will experience some resistance and take longer for them to pass through. Therefore, combining SDS with a polyacrylamide gel, allows us so separate proteins according to their size, or relative molecular mass, only.

2.2.18.2.1 Preparation of SDS-PAGE gels

SDS-PAGE mini gels, 10 %, were prepared in sealed 1.0 mm Bio-rad glass plates. The 10 % resolving gel solution was prepared, in a final volume of 14 ml (sufficient for two mini gels), by mixing 3.5 ml resolving buffer (1.5 M Tris, pH 8.8, 0.4 % sodium dodecyl sulphate (SDS)), 5.8 ml 30 % acrylamide and 4.7 ml dH_2O. This solution was incubated for 5 minutes at 37 °C. Immediately before pouring the gel, 82 µl 10 % (w/v) ammonium persulfate (APS) and 7.8 µl tetramethylethylenediamine (TEMED) were added to the solution. The resolving gel was poured to approximately 2.5 cm from the top of the glass plate. Approximately 3 ml dH_2O was carefully placed on top of the gel. The gel was allowed to polymerise for 1 hour at room temperature. The stacking gel (4.5 %) was prepared by mixing 3.75 ml stacking buffer (0.5 M Tris, pH6.8, 0.4 % SDS), 2.25 ml 30 % acrylamide and 9 ml dH_2O. The gel solution was incubated for 5 minutes at 37 °C. Immediately before pouring the stacking gel, 110 µl 10 % (w/v) APS and 15 µl TEMED were added to the solution. The dH_2O was carefully removed from the top of the resolving gel. The stacking gel was gently poured on top of the resolving gel and a 10 lane (1.0 mm) comb was carefully inserted, at an angle in order to avoid forming air bubbles. The gel was left to polymerise for 1 hour at room temperature.

2.2.18.2.2 Preparation of samples and SDS-PAGE

A protein assay, as described in section 2.2.11, was performed to measure the protein concentration in the platelet lysates. The assay was carried out using the Bio-Rad DC Protein Assay kit. In brief, a stock solution of 15 mg/ml bovine serum albumin (BSA) was prepared in 1X RIPA lysis buffer. BSA at

concentrations ranging from 0 – 1.5 mg/ml (5 μl per sample, in triplicate) were incubated with 20 μl Solution A' (1 ml reagent A + 20 μl solution S) and 200 μl reagent B for 15 minutes at room temperature. The absorbance was read on the Wallac plate reader at 690 nm. A standard curve was generated by plotting the absorbance (at 690 nm) versus concentration of protein (mg/ml) using GraphPad Prism® 5 software. The concentration of the unknown platelet lysates was calculated from the equation of the line.

Having found the concentration of protein present in the platelet lysates, the volume required for an equal loading of 20 μg of protein per lane was calculated. This volume of platelet lysate was incubated with 5X reducing sample buffer (312.5 mM Tris, 5 % (w/v) SDS, 20 % (v/v) glycerol, 0.25 % (w/v) bromophenol blue, 2 % (w/v) dithiothreitol (DTT)), such that the final concentration of sample buffer was 1X, for 5 minutes at 95 °C. Samples were loaded in their respective lanes, along with 10 μl molecular weight marker in lane 1. Any empty lanes were loaded with sample buffer in order to keep the gel balanced while running. Gels were set up in the electrophoresis rig with running buffer (192 mM glycine, 25 mM Tris, 0.1 % (w/v) SDS) and run at a constant voltage of 100 V for approximately 1 hour.

2.2.18.3 Coomassie Blue staining of SDS-PAGE gel

Following electrophoresis, gels were stained to visualise the protein in the samples and examine them for any degradation or differences in protein loading between samples. Gels were stained with a sensitive Coomassie Blue solution (10 % (v/v) phosphoric acid, 10 % (w/v) ammonium sulphate, 0.12 % (w/v) Coomassie Blue Brilliant, 20 % (v/v) methanol) overnight at room temperature

with gentle rocking (Candiano et al, 2004). A destain step was subsequently carried out to remove the stain from the gel so the blue stained protein bands could be visualised more clearly. This was carried out by placing the stained gel into a destain solution A (40 % (v/v) methanol, 7 % (v/v) acetic acid) overnight at room temperature with gentle rocking. The gel was then placed in a destain solution B (5 % (v/v) methanol, 7 % (v/v) acetic acid) for three hours at room temperature with gentle rocking. The gel was stored in dH_2O and imaged.

2.2.18.4 Protein transfer

Following SDS-PAGE, the gel, containing the now separated protein bands was equilibrated in transfer buffer (192 mM glycine, 25 mM Tris, 20 % (v/v) methanol). The equilibrated gel was next placed in a cassette in a 'sandwich' as illustrated in Figure 2.9. The sponges, filter paper and membrane were all equilibrated in transfer buffer. The polyvinyl difluoride (PVDF) membrane was pre-activated for 1 minute in 100 % methanol before equilibration in transfer buffer. The cassette was placed in the transfer rig in transfer buffer, with an ice pack to prevent the generation of Joule heating. The transfer was carried out for 1 hour at a constant voltage of 100 V at room temperature. Alternatively, the transfer could be carried out overnight at 4 °C at a constant voltage of 30 V.

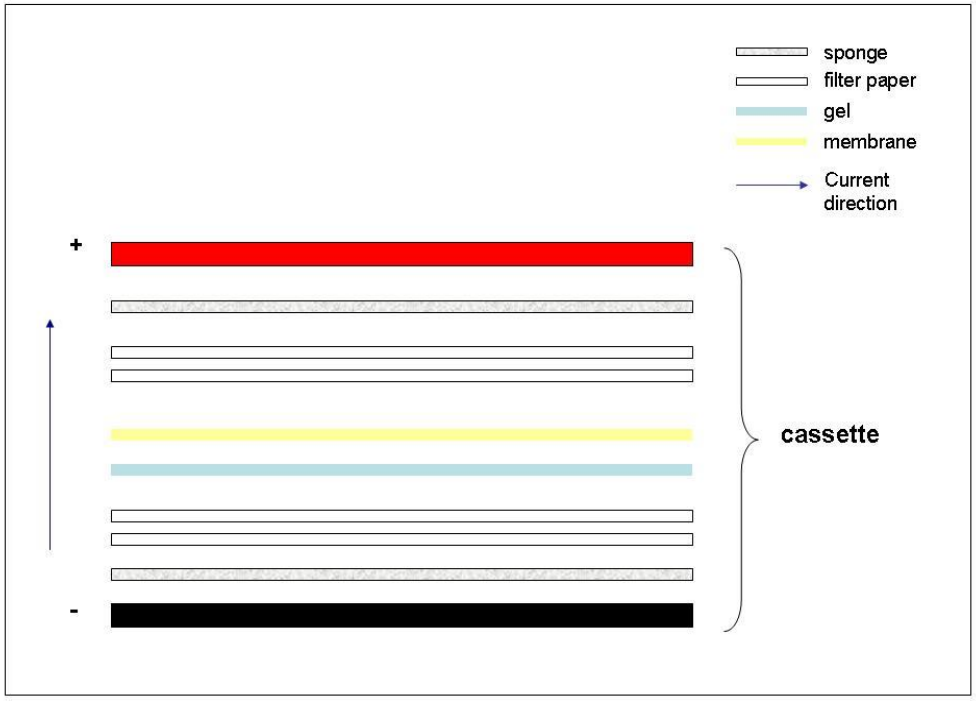

Figure 2.9 A schematic illustrating the set-up of the transfer cassette 'sandwich'. A transfer cassette (BioRad) was opened and a sponge was placed on the black side (negative side), followed by two pieces of filter paper, all equilibrated in transfer buffer. The gel was carefully removed from the glass plates in which the SDS-PAGE was carried out, equilibrated in transfer buffer and then placed on top of the filter paper. A piece of PVDF membrane, activated for 1 minute in 100 % methanol and equilibrated in transfer buffer, was placed on top of the gel. Any air bubbles that may have been trapped between the gel and membrane were rolled out. Two more pieces of filter paper were placed on the membrane, followed by another sponge; again all were equilibrated in transfer buffer. The cassette was then closed and placed in the transfer rig, ensuring that the black side of the cassette was towards the black side of the rig, indicating the transfer of proteins in a negative to positive direction.

2.2.18.5 Probing with vasodilator stimulated phosphoprotein (VASP) antibodies

Following the protein transfer, the membrane (which now contains the immobilised proteins) can be stained with Ponceau S to check if the proteins transferred correctly from the SDS-PAGE gel. If this step was carried out, the

membrane was stained with Ponceau S solution (0.1 % (w/v) Ponceau S in 5 % (v/v) acetic acid) for 5 minutes at room temperature with gentle rocking. The protein bands were stained a red colour if the transfer worked correctly. The membrane was then washed with TBS for 10 minutes at room temperature. This step was repeated with fresh TBS until all red staining was removed.

The membrane was then blocked in 3 % BSA (in TBS-T: TBS with 0.1 % (v/v) Tween-20) for 1 hour at room temperature with gentle rocking. The membrane was probed with the primary antibody (VASP A290 (total VASP), phospho-VASP (Ser157) or phospho-VASP (Ser239) antibody). All of the VASP antibodies were polyclonal antibodies produced by rabbits. In all cases, the primary antibody was made at a 1:1000 dilution in 3 % BSA (in TBS-T). The membrane was incubated with the primary antibody, in a sealed plastic bag, on a rotator, overnight at 4 °C.

Following incubation with the primary antibody the membrane was washed three times for 5 minutes with TBS-T. The secondary anti-rabbit antibody (conjugated to horse radish peroxidase (HRP)) was prepared at a dilution of 1:10,000 in 3 % BSA (in TBS-T). The membrane was then incubated with the secondary antibody for 2 hours at room temperature, with gentle rocking. After two hours the membrane was washed for 3 X 5 minutes with TBS-T. This was followed by washing by 3 X 5 minutes with dH_2O.

2.2.18.6 Developing the Western blots

The blot was developed using SuperSignal West Pico Chemiluminescent Substrate. This is a luminol based substrate which emits light in the form of luminescence in the presence of the HRP conjugated to the secondary antibody. There are also chemical enhancers present in this particular substrate which intensify the light emission. This is referred to as enhanced chemiluminescence (ECL). There are two reagents present in the kit, a luminol/enhancer and a stable peroxide buffer. 1 ml of each reagent was mixed together and incubated with the membrane for 2 – 5 minutes. The excess solution was removed from the membrane and the membrane was placed in the AutoChemi™ UVP Bioimaging system. The system was set to take 30 images over a 40 minute period and a final image of all 30 combined was then generated.

2.2.19 Statistics

Statistical analyses were performed using GraphPad Prism® 5 software. One-way Anova, repeated measures tests with a Bonferroni post-hoc analysis were performed on the data, unless otherwise stated. Data was expressed as the mean ± SEM and a value of $p < 0.05$ was considered statistically significant. Principal component analysis (PCA) was used for the analysis of the Raman spectroscopy data (as described in section 2.2.6).

Chapter 3

The role of thiols in integrin activation

3.1 Introduction

Integrins are a family of adhesion molecules which comprise a large portion of platelet surface receptors and are available to mediate interactions between platelets and their extracellular environment. Platelets possess three families of integrins, with a total of six different integrins present in total, namely $\alpha_2\beta_1$, $\alpha_5\beta_1$, $\alpha_6\beta_1$, $\alpha_L\beta_2$, $\alpha_V\beta_3$ and $\alpha_{IIb}\beta_3$. Integrin $\alpha_{IIb}\beta_3$ is one of the major integrins present on platelets, with approximately 80,000 – 100,000 copies per platelet. As integrin $\alpha_{IIb}\beta_3$ is the critical player in platelet aggregation, through its interaction with the plasma protein fibrinogen, extensive research has been conducted to reveal the intricacies of integrin activation. The vast number and highly conserved nature of cysteine residues present in integrins' subunits structure is indicative of the significant role of thiol groups have in integrins' function. Indeed, the pairing of these residues to form disulphide bonds has been shown to be essential for the structural integrity of the receptor (Calvete, 1999; Calvete et al, 1991; O'Neill et al, 2000). In a study in 2000, Yan and Smith investigated the on/off switch commonly associated with integrin $\alpha_{IIb}\beta_3$ activation. They uncovered a redox site in a domain of approximately 200 residues that essentially encompassed the cysteine-rich domain of the β_3-subunit. Free, unpaired cysteines were located within this region. They also showed there was an overall net reduction of one disulphide bond associated with a change in the activation state of the integrin (Yan & Smith, 2000). Furthermore, in 2001 they demonstrated that DTT reduces two disulphide bonds leading to global conformational changes in both integrin subunits. Selective mutation of critical cysteine residues within integrin $\alpha_{IIb}\beta_3$ has been demonstrated to induce a

constitutively active conformation of the integrin, particularly the long-range thiol bond between Cys^{5} and Cys^{435} (Sun et al, 2002).

Previous studies in our laboratory used purified integrin $\alpha_{IIb}\beta_3$, in a cell-free system, to investigate the relationship between thiol/disulphide groups and the activation state of integrin $\alpha_{IIb}\beta_3$. It was demonstrated that both integrin $\alpha_{IIb}\beta_3$ and $\alpha_v\beta_3$ have endogenous thiol isomerase activity, due to the presence of nine CXXC motifs within the β-subunit. The function of this thiol isomerase activity is still not clear. However, inhibition of its activity with the pharmacological inhibitor bacitracin, led to disruption of both integrin activation and platelet aggregation (O'Neill et al, 2000). This endogenous thiol isomerase activity, and consequently integrin activation, could be induced by manganese chloride ($MnCl_2$) and modulated by nitric oxide (NO) and glutathione (GSH) (Walsh et al, 2004). Subsequently, a direct interaction between thiols in integrin $\alpha_{IIb}\beta_3$ and NO, termed S-nitrosylation, was revealed to induce thiol/disulphide shuffling. This reinforces the importance of thiol groups in the regulation of both the activation and deactivation of integrin $\alpha_{IIb}\beta_3$ (Walsh et al, 2007).

In this chapter, I will further investigate the role of thiol groups in purified integrin $\alpha_{IIb}\beta_3$ in a cell-free system and explore the impact of an altered redox environment on this thiol population. I will use Chinese hamster ovarian-K1 (CHO-K1) cells expressing integrin $\alpha_{IIb}\beta_3$ as a model cell system to study the activation status of the integrin and the impact of the external redox environment in the regulation of integrin activation. The CHO-K1 cell line used in the study is as described previously by Aylward et al (Aylward et al, 2006).

Briefly, a mock transfected CHO-K1 cell line was used along with the CHO-K1 cell line expressing integrin $\alpha_{IIb}\beta_3$. These cells express integrin in a constitutively resting conformation, thereby making it possible to observe the effects of treatment with $MnCl_2$ and the effect of the presence of redox potentials on the integrin activation state. Subsequently, I will examine the effects of $MnCl_2$, dithiothreitol (DTT) and thrombin on platelet activity using platelet function tests. Additionally, I will investigate the impact of these activators on platelet structure at a molecular level using Raman spectroscopy. $MnCl_2$ and DTT are both well established integrin $\alpha_{IIb}\beta_3$ moderators, while thrombin is a potent platelet agonist. The potency of thrombin will be useful in this study, as platelet activity induced by $MnCl_2$ and DTT can be measured relative to the level of platelet activity brought about by thrombin stimulation.

(α)-thrombin, also known as coagulation factor II, is a coagulation protein. It is a trypsin-like serine protease that converts soluble fibrinogen into insoluble fibrin. It also catalyses and potentiates many other reactions in the coagulation cascade by activating Factors V, VIII, XI and XIII. Thrombin is formed through the cleavage of two sites on the vitamin K-dependent zymogen prothrombin. This cleavage is performed through the action of a prothrombinase complex, which is composed of activated Factor X bound to Factor V. Thrombin is composed of 2 chains, an A and a B chain. The A chain is composed of 36 residues and is non-essential for proteolytic activities, while the three active site amino acids of thrombin are found amongst the 259 residues of the B chain.

Thrombin is a potent platelet activator and plays a critical role in promoting thrombus formation (McNicol & Gerrard, 1993). It initiates platelet degranulation, aggregation and indirectly activates the integrin $\alpha_{IIb}\beta_3$ through the activation of a number of signalling cascades. Thrombin is also involved in the process of platelet shape change upon activation. Thrombin activates platelets predominantly through the G-protein-coupled protease-activated receptors (PARs) PAR-1 and PAR-4, and through the GPIb-IX-V complex. PARs are seven transmembrane domain receptors which are activated by a proteolytic cleavage at a specific site in the N-terminal extracellular domain.

The GPIb-IX-V complex on the platelet surface also has a high affinity binding site for thrombin located at the N-terminal region of the GPIbα subunit. It is well established that patients suffering from Bernard-Soulier syndrome, which lack GPIb-IX-V, have impaired responses to thrombin (Clemetson & Clemetson, 1994). However, the involvement of the GPIb-IX-V complex in thrombin activation is controversial. While it has been found that GPIbα has a key role in platelet activation by thrombin, particularly at low doses, the exact nature of the interaction remains unclear (Dormann et al, 2000). Elucidation of the crystal structure of the GPIα-thrombin complex also further reconciles the important role of this interaction in platelet activation and in particular in the process of platelet aggregation (Dumas et al, 2003).

Dithiothreitol (DTT), also known as Cleland's reagent, is a strong reducing agent, due to its low redox potential of -330 mV at pH 7.0. It is a small, water-soluble molecule that readily crosses biological membranes. Due to its

potent reducing powers DTT is often used to reduce disulphide bonds in proteins or peptides. The reduction of a typical disulphide bond is shown in Figure 1.5.

Although DTT induces platelet aggregation, little is known about the mechanisms involved in activation of platelets by DTT. It is hypothesised that DTT is not capable of initiating full integrin activation (Yan & Smith, 2000). However, it does induce conformational changes in integrin $\alpha_{IIb}\beta_3$, and potentially other platelet receptors, resulting in platelet aggregation (MacIntyre, 1974; Margaritis, 2011; Zucker & Masiello, 1984).

Manganese chloride ($MnCl_2$) is the universal integrin activator, the exact mechanism of which is yet to be fully elucidated. In general, integrins exhibit low ligand affinity and require activation in order to interact with their respective ligands (Hynes, 1992). It is believed conformational changes accompany integrins transition to a high affinity binding state. Studies indicate the I-domain of integrins is likely to be involved in the conformational changes observed in the activation of integrins (Landis et al, 1994; McDowall et al, 1998). The presence of a conserved divalent cation binding site in the I-domain suggests a role for divalent cations such as Mg^{2+} and Mn^{2+}. The determination of the crystal structure of integrins led to major advances in understanding the mechanism of ligand binding to integrins and the role of the cation binding sites. These cation binding sites have been termed as metal ion-dependent adhesion sites or MIDAS (Humphries et al, 2003). However, the relationship between cation binding, integrin ligand binding and integrin conformation remains unclear.

Studies of integrin $\alpha_{IIb}\beta_3$, specifically, have shown that Mn^{2+} does indeed induce an active-like conformation, which in turn increases ligand binding. Previous studies in our laboratory have found that Mn^{2+} induces key conformational changes in integrin $\alpha_{IIb}\beta_3$ (Walsh et al, 2007). Raman spectroscopic analysis revealed that Mn^{2+} treatment of purified integrin $\alpha_{IIb}\beta_3$ leads to a shift in the amide I feature to a lower frequency in the spectrum and also a shift in the disulphide stretch envelope to a higher frequency, indicating a reduction in strain in cysteine sites. These findings confirm the importance of divalent cations in integrin activity. Mn^{2+} cations can also induce the endogenous thiol isomerase activity of integrin $\alpha_{IIb}\beta_3$ (Walsh et al, 2004).

Raman spectroscopy (RS) is one of few techniques that can unambiguously detect the presence of thiols and disulphide bonds in proteins (Pelton & McLean, 2000). This makes Raman an ideal tool to analyse thiol/disulphide events occurring on the surface of platelets in response to stimulation with platelet activators

RS is an optical technique used in the determination of molecular structure. It was discovered in 1928 by Sir Chandrasekhra Venkata Raman (Raman, 1928). It is based on the analysis of the frequency of scattered light from the interaction of monochromatic light with a sample. The data generated yields vibrational information that is specific for each chemical bond within the molecule.

A Raman spectrum is generated by plotting the intensity versus the frequency of the shifted light. The frequency shift is measured by wavenumber and is

expressed as an inverse unit of length, i.e. cm^{-1}. The spectrum is usually plotted so that the Rayleigh scattering occurs at 0 cm^{-1}. The Raman spectrum can then be analysed to determine the molecular composition in this case, of platelets. The energy required to excite the molecular vibrations depends on the molecular mass and the type of chemical bonds within the molecule (Krafft, 2003). Therefore, the position and relative intensity of peaks in the spectra correspond to different chemical bonds (Table 3.1).

Table 3.1 Peak position and assignment of main Raman vibrational modes (Lyng et al, 2007)

Peak position (cm^{-1})	**Assignment**
622	C-C twisting
724	CH_2 deformation
746	CH_2 rocking
754	Symmetric ring breathing
779	Ring vibration
832	CCH deformation aliphatic
853	CCH deformation aromatic
873	CC stretch
922	C-C stretching
1004	CC aromatic ring breathing
1034	C-C stretching
1065	C-N stretch
1096	C-C chain stretching

1098	CC stretch
1102	CC stretch
1124	CC skeletal stretch *trans*
1214	CC stretch backbone carbon phenyl ring
1236	CN stretch, NH bending amide III band
1240	CN stretch, NH bending amide III band
1314	CH deformation
1337	CH_2 deformation
1335	CH_2 deformation
1366	CH_2 bending
1440	CH_2 scissoring
1484	CH_2 deformation
1548	NH deformation; CN stretch amide II band
1578	C=C olefinic stretch
1585	C=C stretching
1602	CO stretching
1660-1665	C=O stretch amide I α-helix
2930	CH_2 stretching
2932	CH_3 symmetric stretch

RS has been traditionally used for the analysis of chemical samples and their composition. However, using RS as a tool to study biological and cellular samples is becoming increasingly popular. Platelet activation leads to structural modifications and, ultimately, conformational changes in platelet proteins. Along

with thiol/disulphide groups, other features of interest when analysing the Raman spectra of platelets include amide I (1630 -1700 cm^{-1}) and amide III (1230 -1310 cm^{-1}) (amide II has a very weak Raman signal). Additionally, the α-helix and β-sheet content of the proteins can be examined as changes in the relative abundance of each structure type may be detected by RS. Amide III is particularly sensitive to structural changes and is a promising region by which to estimate secondary structure.

The objective of this aspect of the study is to obtain signature Raman spectra of unactivated platelets and platelets stimulated with various activators. Any changes that are observed in the spectra upon analysis may be attributed to a change in the molecular structure of the platelet membrane as a result of platelet activation. It is anticipated these studies will not only further our knowledge of key structural components of platelets but may also potentially uncover a platelet surface biomarker or a number of biomarkers associated with platelet activation that can be exploited in the development of Raman spectroscopy as a novel technique for the assessment of platelet activation states.

3.2 Results

3.2.1 The effects of protein concentration and buffer exchange on purified integrin $\alpha_{IIb}\beta_3$

Commercially available purified integrin $\alpha_{IIb}\beta_3$ was used in these studies. Initially, the purified integrin was concentrated using micro-centrifugal filters and subsequently a buffer exchange step was carried out in order to remove

glycerol from the system. These manipulations of the integrin did not impact on the integrity of the protein. This was confirmed by running 20 μg of purified integrin on a 7.5 % polyacrylamide gel and staining it with a sensitive Coomassie Blue stain. Bands corresponding to the α_{IIb}- and β_3-subunits were stained and there was an absence of any other low-molecular weight bands which could be indicative of degradation of the protein (Figure 3.1 (a)). Additionally, a Western blot analysis of the integrin was also performed. The integrin was transferred from the polyacrylamide gel to a polyvinyl diflouride (PVDF) membrane and probed with SZ.22, an antibody specific for the α_{IIb}-subunit of the integrin. It was demonstrated that the α_{IIb}-subunit was indeed present and intact (Figure 3.1 (b)).

3.2.2 The effect of manganese chloride ($MnCl_2$) on the thiol population of integrin $\alpha_{IIb}\beta_3$

The concentration of purified integrin was determined using a protein quantitation assay. The thiol population of the integrin was measured in an assay using the commercially available fluorescent thiol detection reagent Thiostar®. It was established that integrin at a concentration of 10 μg/ml was the minimal concentration of integrin which contained a significant, detectable number of thiols in this particular assay (n=4, *$p < 0.05$, **$p < 0.01$) (Figure 3.2). Therefore, all subsequent purified integrin studies used an integrin concentration of 10 μg/ml.

Manganese chloride ($MnCl_2$), an established universal integrin activator, was used to examine the effects of integrin activation on the thiol population of integrin $\alpha_{IIb}\beta_3$. Treatment with 3 mM $MnCl_2$ induced a significant increase in the number of free thiols present in the integrin, compared to unactivated integrin (n=5, *$p < 0.05$) (Figure 3.3).

3.2.3 The effect of GSH/GSSG redox potentials on the thiol population of integrin $\alpha_{IIb}\beta_3$

The redox environment of integrin $\alpha_{IIb}\beta_3$ was altered by glutathione (GSH/GSSG) redox potentials. These redox potentials were generated by combining reduced (GSH) and oxidised (GSSG) in various ratios according to the Nernst equation and as outlined in Tables 2.1 and 2.2. The effects of a reducing (-264 mV), mean (-130 mV) and oxidising (-10 mV) redox environment were investigated. There was no significant effect of any of the redox potentials on the thiol population of unactivated integrin $\alpha_{IIb}\beta_3$. Interestingly, the oxidising and mean redox potentials reduced the increase in the thiol population induced by treatment with 3 mM $MnCl_2$ while the reducing redox potential completely abolished this increase (n=5) (Figure 3.4).

3.2.4 The effect of manganese chloride ($MnCl_2$) on integrin $\alpha_{IIb}\beta_3$ expressed in Chinese hamster ovarian (CHO)-K1 cells

Chinese hamster ovarian (CHO)-K1 cells expressing integrin $\alpha_{IIb}\beta_3$ were used as a model cell system to further investigate the mechanisms of integrin activation. Two cell lines were employed in the study: a mock transfected

CHO-K1 cell line and CHO-K1 cells expressing native integrin $\alpha_{IIb}\beta_3$, termed FF cells. The expression of integrin $\alpha_{IIb}\beta_3$ in the FF cell line was confirmed by flow cytometry using CD41a, an antibody specific for the α_{IIb}-subunit of the integrin. There was a significant increase in integrin expression on FF CHO-K1 cells compared to mock CHO-K1 cells (n=3, **p < 0.01) (Figure 3.5). Furthermore, it was confirmed that the FF CHO-K1 cell line does indeed express integrin in an unactivated conformation using the monoclonal antibody PAC-1, which binds only to integrin $\alpha_{IIb}\beta_3$ in an activated conformation (n=3) (Figure 3.6).

A concentration-response study investigating the effect of $MnCl_2$ on the activation status of integrin $\alpha_{IIb}\beta_3$ in FF CHO-K1 cells was carried out. There was a significant increase in PAC-1 binding to FF cells upon stimulation with 3 mM and 5 mM $MnCl_2$ compared to untreated FF cells (n=3, **p < 0.01 and ***p < 0.001 respectively) (Figure 3.7). Thereby, confirming $MnCl_2$ as an integrin $\alpha_{IIb}\beta_3$ activator.

3.2.5 The effect of GSH/GSSG redox potentials on integrin $\alpha_{IIb}\beta_3$ expressed in Chinese hamster ovarian (CHO)-K1 cells

The external redox environment of FF CHO-K1 cells was altered by glutathione (GSH/GSSG) redox potentials. These redox potentials were generated by combining reduced (GSH) and oxidised (GSSG) in various ratios according to the Nernst equation and as outlined in Tables 2.1 and 2.2. The effects of a reducing (-264 mV), mean (-130 mV) and oxidising (-10 mV), environment on integrin $\alpha_{IIb}\beta_3$ expressed in CHO-K1 cells were investigated. FF cells were incubated with the GSH/GSSG redox potentials, and subsequently treated with

3 mM $MnCl_2$. The activation state of integrin $\alpha_{IIb}\beta_3$ expressed by the FF cells was assessed with the monoclonal antibody PAC-1 using flow cytometry. An oxidising redox environment had no significant effect on the level of PAC-1 binding to FF cells activated by 3 mM $MnCl_2$. A mean redox environment decreased PAC-1 binding, while a reducing redox environment almost completely inhibited PAC-1 binding induced by 3 mM $MnCl_2$ (n=3, *p < 0.05, **p < 0.01 respectively) (Figure 3.8).

3.2.6 The effects of manganese chloride ($MnCl_2$), dithiothreitol (DTT) and thrombin on platelet function

Platelet aggregation studies to generate concentration-response curves for manganese chloride ($MnCl_2$) and dithiothreitol (DTT) were carried out with the following concentrations: 0 mM (unactivated platelets), 1 mM, 3 mM and 5 mM.

Platelet aggregation of approximately 10 % and 40 % was induced by 3 mM $MnCl_2$ and 3 mM DTT, respectively. It indicated 3 mM was the lowest concentration of each activator to induce a significant level of platelet aggregation compared to unactivated platelets (n=4, **p < 0.01 and *p < 0.5 respectively) (Figure 3.9). Therefore, 3 mM was the concentration of both $MnCl_2$ and DTT chosen for further studies. Platelets did not aggregate in the absence of an activator. In additional studies gel-filtered platelets activated with either 1U/ml thrombin, 3 mM $MnCl_2$ or 3 mM DTT induced platelet aggregation to levels of approximately 80 %, 7 % and 40 % respectively (n=9) (Figure 3.10).

Using flow cytometry, the levels of PAC-1 binding to unactivated gel-filtered platelets or platelets treated with either 1U/ml thrombin, 3 mM $MnCl_2$ and 3 mM

DTT were assessed. Levels of binding were expressed as percentage gated relative to an arbitrary 2 % gate placed on unactivated platelets. Platelets activated with 1U/ml thrombin, 3 mM $MnCl_2$ and 3 mM DTT resulted in activation of integrin $\alpha_{IIb}\beta_3$ as indicated by PAC-1 binding at levels of approximately 70 %, 15 % and 30 % respectively (Figure 3.11).

Platelet activation results in secretion of P-selectin from α-granules, which is then expressed on the platelet surface, thereby acting as a surface marker for platelet activation. Platelet secretion induced by 1U/ml thrombin, 3 mM $MnCl_2$ and 3 mM DTT was assessed by using the monoclonal antibody CD62P to measure the levels of P-selectin expressed on the surface of platelets. Levels of CD62P binding were expressed as percentage gated relative to an arbitrary 2 % gate placed on unactivated platelets. A significant level of CD62P binding was observed in platelets activated with thrombin, compared to unactivated platelets ($n=4$, $^{***}p < 0.001$). $MnCl_2$ and DTT did not induce any P-selection secretion as there was no statistically significant difference in the levels of CD62P binding to platelets treated with $MnCl_2$ and DTT compared to unactivated platelets ($n=4$) (Figure 3.12).

The data for PAC-1 and CD62P binding to gel-filtered platelets treated with 1U/ml thrombin, 3 mM $MnCl_2$ or 3 mM DTT is summarised in Table 3.1.

3.2.7 The optimal conditions for obtaining Raman spectra of gel-filtered platelets

Before the Raman spectroscopic analysis of platelets treated with various activators was carried out, a number of factors needed to be taken into consideration in order to ensure optimal conditions for the study. One such

condition was the acquisition time, i.e. the total time required to collect a Raman spectrum. Initially, I employed a relatively long acquisition time of 200 seconds which caused bleaching of major peaks, especially the carotenoid peaks. This implied that the platelet sample being exposed to the laser for long periods of time induced photochemical damage. To avoid this, a shorter acquisition time of 25 seconds was employed for all subsequent experiments (Figure 3.13).

A number of substrates on which to place the platelets when acquiring Raman spectra were tested. Glass coverslips were chosen as they do not have a large Raman signal and therefore, background signal was minimal. While glass is a known activator of platelets, this was not considered to be an issue due to the platelets being fixed before being placed on the glass. Other substrates which were considered included poly-L-lysine coated slides and Surface Enhanced Raman Spectroscopy (SERS) surfaces. SERS was carried out on flourine-doped tin oxide (FDTO) coated glass slides upon which gold nanoparticles were immobilised (Sheridan, 2007), or on slides with gold nanocavities which were formed by electrodepositing gold around polystyrene spheres, then removing the spheres (Jose et al, 2009). The nanocavities were approximately the same size as platelets, 3 - 4 µm in diameter (Figure 3.14), while the nanoparticles were smaller in size (< 100 nm). Neither of these surfaces gave a significant enhancement of the Raman signal of the platelets compared to platelets on glass cover slips and it was therefore decided to continue using glass cover slips (Figure 3.15).

3.2.8 The effects of thrombin, manganese chloride ($MnCl_2$) and dithiothreitol (DTT) on platelet molecular structure assessed by Raman spectroscopy

Platelets remained unactivated or activated with either 1U/ml thrombin, 3 mM $MnCl_2$ or 3 mM DTT and Raman spectra were obtained. Upon inspection of the data, small spectral differences between the platelet samples can be observed. However, these differences are not clearly distinguishable from each other. This is an obstacle which is seen across the board with Raman analysis of biological samples due to their complexity. Therefore, principal component analysis (PCA) was carried out on the data in order to determine if unactivated platelets could be differentiated from activated platelets and also to analyse any molecular differences between platelets treated with the various activators. PCA is a multivariate statistical technique which employs mathematical formulae to describe major trends in data of high dimensions. The spectra were baseline subtracted and normalised using Origin® software before PCA analysis. All spectra were normalised to a lipid peak at approximately 3000 cm^{-1}. This peak was chosen as there was very little variation in this peak regardless of the platelet activation state.

A full signature, or ‘finger print’, Raman spectrum of platelets treated with each activator was obtained by averaging 3 - 5 spectra from each spectra sample from all donors together (n=4) (Figure 3.16 (a)).

PCA was carried out on all of the spectra. There was clear separation of the platelets samples based on the platelet activator (Figure 3.16 (b)). The principal components used to construct this scatter plot are illustrated in Figure 3.16 (c).

The principal component loadings represent the correlation between the principal components and the original data. Plotting the loadings of the principal components as a function of the wave number gives an indication of the position at which the variation between samples arises within the original spectra. This analysis encompassed the full platelet spectrum. However, what this analysis does not tell us is where exactly, in terms of molecular structure, the differences between platelet samples arise. In an attempt to answer this question, the regions in which I anticipated molecular modifications to occur were examined in more detail. The regions focused on were: thiol (2550 - 2600 cm^{-1}) (Figures 3.17 (a-c)); disulphide (470-530 cm^{-1}) (Figures 3.18 (a-c)); amide I (1630 - 1700 cm^{-1}) (Figures 3.19 (a-c))) and amide III (1230 - 1310 cm^{-1}) (Figures 3.20 (a-c)) stretches. The regions of interest were extracted from the full spectrum and PCA was performed specifically on these data.

The thiol region of the platelet Raman spectrum stretches from approximately 2550 - 2600 cm^{-1} (Figure 3.17 (a)). The PCA analysis of this region separated the platelet samples into well-defined clusters based on the platelet activation state (Figure 3.17 (b)). As shown in Figure 3.17 (a), there is a lot of background noise associated with this region. When the PCA results were examined, it was found that PC-1 accounted for a lot of this noise, therefore, the lower components PC-2 and PC-3 were used to generate the score plot. The loadings of PC-2 and PC-3 are shown in Figure 3.17 (c).

Based on the distinct clustering in the thiol region, I anticipated complementary results in the disulphide region because of the strong relationship between thiol and disulphide groups. The disulphide region is located at approximately 470 - 530 cm^{-1} in the Raman spectrum. As this region is quite narrow, I therefore, chose a slightly larger region to analyse (Figure 3.18 (a)). The Raman signal in this region is relatively low while the noise in the region is quite high. Despite this and although the samples are all located close together, there is an obvious clustering of samples based on the platelet activation state (Figure 3.18 (b)). Figure 3.18 (c) demonstrates the loading of the principal components plotted in the score plot.

The amide I and III regions were focussed on due to the potential protein structural information that may be found therein. The amide I region extends from 1630 - 1700 cm^{-1} in the Raman spectrum (Figure 3.19 (a)). Again, there is noticeable clustering of samples based on the activator used to activate the platelets (Figure 3.19 (b)). The loadings of PC-1 and PC-2 are shown in Figure 3.19 (c).

Amide III is present in the Raman spectrum at 1230 – 1310 cm^{-1} (Figure 3.20 (a)). Similar to the results of the PCA analysis of the amide I region, it was found that the samples clustered together based on the platelet activator (Figure 3.20 (b)). The loadings of the principal components PC-1 and PC-5 are shown in Figure 3.20 (c).

Furthermore, having examined the PCA of the regions in which structural differences between platelets in various states of activation were anticipated, the full platelet spectrum (200 – 3500 cm^{-1}) was divided into regions to examine each in greater detail. This analysis was performed in order to ensure that we did not unintentionally overlook any area of the spectrum which may contain crucial information. The spectrum was divided into 6 regions, each 700 cm^{-1} in length except for the last region, region 6, which was 800 cm^{-1} in length. Each region overlapped the previous region by 200 cm^{-1} and they were designated as follows:

- Region 1: 200 – 900 cm^{-1}
- Region 2: 700 – 1400 cm^{-1}
- Region 3: 1200 – 1900 cm^{-1}
- Region 4: 1700 – 2400 cm^{-1}
- Region 5: 2200 – 2900 cm^{-1}
- Region 6: 2700 – 3500 cm^{-1}

PCA was performed specifically on each of these regions. It was found the regions of greatest separation between the platelet samples were: 700 - 1400 cm^{-1} (Figures 3.21 (a-c)); 1200 – 1900 cm^{-1} (Figures 3.22 (a-c)); 2200 – 2900 cm^{-1} (Figures 3.23 (a-c)) and 2700 – 3500 cm^{-1} (Figures 3.24 (a-c)).

The region of the Raman spectra of all samples stretching from 700 – 1400 cm^{-1} is shown in Figure 3.21 (a). PCA analysis of this region reveals the Raman

spectra separated into obvious clusters corresponding to the platelet activator (Figure 3.21 (b)). The loadings of the principal components PC-1 and PC-2 which account for most of the variance within this data set are shown in Figure 3.21 (c).

The Raman spectra of each platelet sample in the region stretching from 1200 - 1900 cm^{-1} is plotted in Figure 3.22 (a). The results of the PCA analysis are illustrated in Figure 3.22 (b), where clustering of the Raman spectra into groups corresponding to the same platelet activator is obvious. The loadings of the principal components used to plot the scores graph are shown in Figure 3.22 (c).

The region of the Raman spectra stretching from 2200 – 2900 cm^{-1} is plotted in Figure 3.23 (a). The PCA results of the data from this region are in Figure 3.23 (b). The Raman spectra are clearly discriminated as a result of the platelet activator used to activate the platelets. The loadings of the first two principal components, PC-1 and PC-2, used to plot the scores scatter plot are illustrated in Figure 3.23 (c).

Figure 3.24 (a) illustrates the Raman spectra in the region stretching from 2700 - 3500 cm^{-1}. A scatter plot of PC-1 versus PC-2 is shown in Figure 3.24 (b). The loading of these principal components as a function of wave number is plotted in Figure 3.24 (c).

Upon examination of these regions, namely 700 – 1400 cm^{-1}, 1200 – 1900 cm^{-1}, 2200 – 2900 cm^{-1} and 2700 – 3500 cm^{-1}, in which there is evident clustering of the Raman spectra corresponding to the platelet activator, it was found that each of these regions contain a peak or peaks associated with lipid structure. Further examination of the PCA results of the full spectrum (Figure 3.16) again demonstrate the significance of the carotenoid and lipid profile of the platelets as the higher principal components, PC-1 and PC-2, pick out the peaks associated with lipids as being the regions with the highest variability.

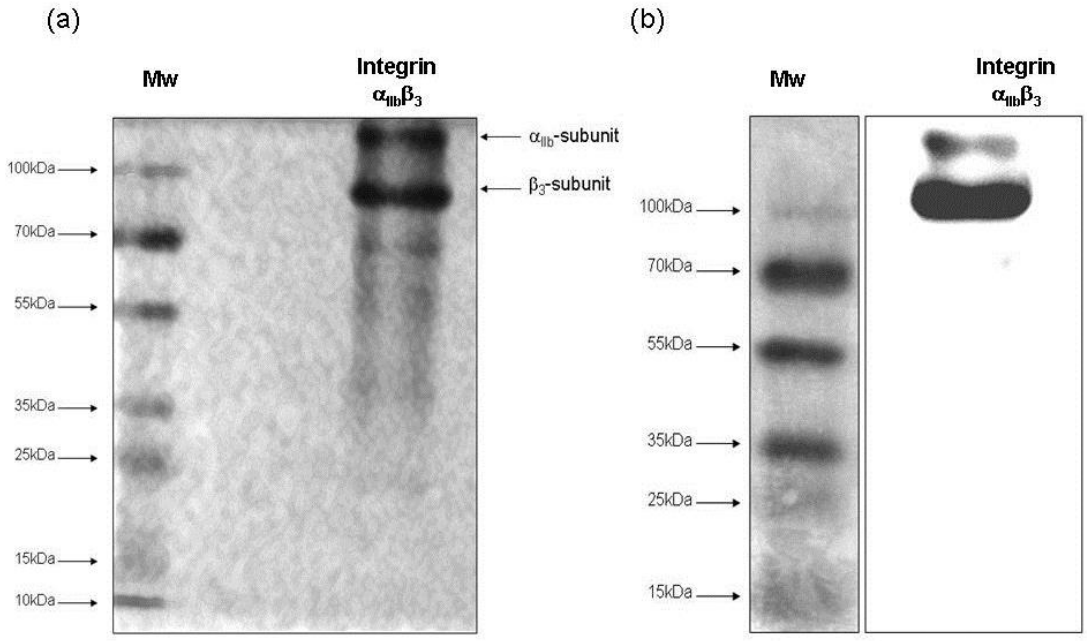

Figure 3.1 Concentration and buffer exchange of purified integrin $\alpha_{IIb}\beta_3$ does not lead to degradation of the protein: (a) Coomassie Blue stain, (b) Western blot. 20μg of purified integrin $\alpha_{IIb}\beta_3$ was run on a 7.5 % polyacrylamide gel. (a) Gel was stained with a sensitive Coomassie Blue solution overnight at room temperature with gentle rocking. Gels were destained and imaged. The purified integrin was found to be intact with prominent bands at ~120 kDa and ~90 kDa for both α- and β-subunits, respectively. (b) The protein was transferred from the gel to polyvinyl difluoride (PVDF) membrane, blocked and probed with SZ.22, an antibody that is specific for integrin α_{IIb}-subunit. The α-subunit was found to be intact with a strong band present at ~120 kDa. The band present at a higher molecular weight of ~240 kDa suggests the presence of a potential dimer of α_{IIb}-subunit.

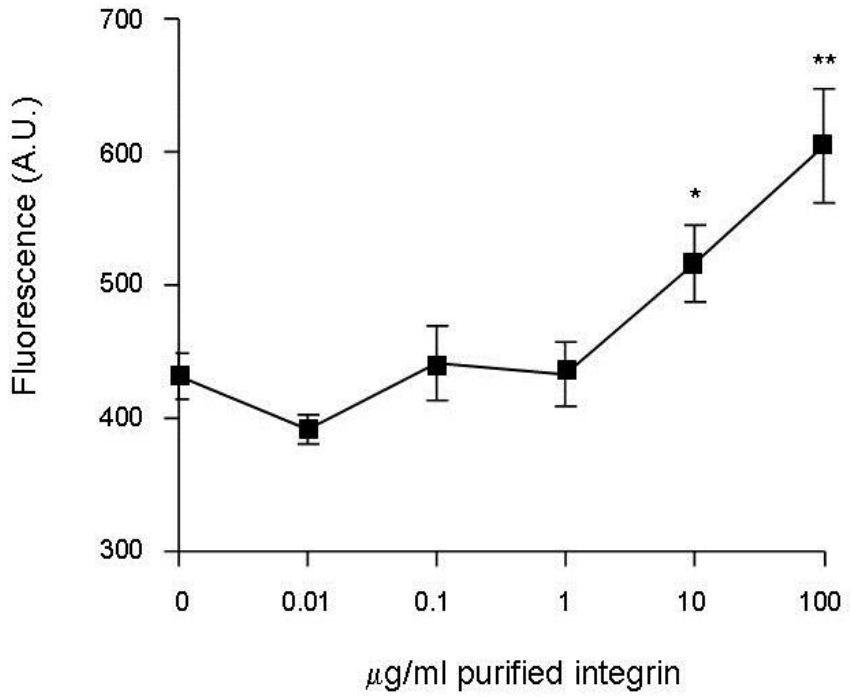

Figure 3.2 Concentration curve demonstrating a measurable number of free thiols present in purified integrin $\alpha_{IIb}\beta_3$. Purified integrin $\alpha_{IIb}\beta_3$, at concentrations ranging from 0 – 100 μg/ml was incubated with Thiostar® (2.5 μg/ml) for 5 minutes at room temperature, in a black, clear bottom 96-well plate. The fluorescence was measured using a Wallac plate reader. Thiols were found to be detectable at a concentration of at least 10 μg/ml. Data is presented as the mean ± SEM, n=4 independent experiments, *$p < 0.05$, **$p < 0.01$.

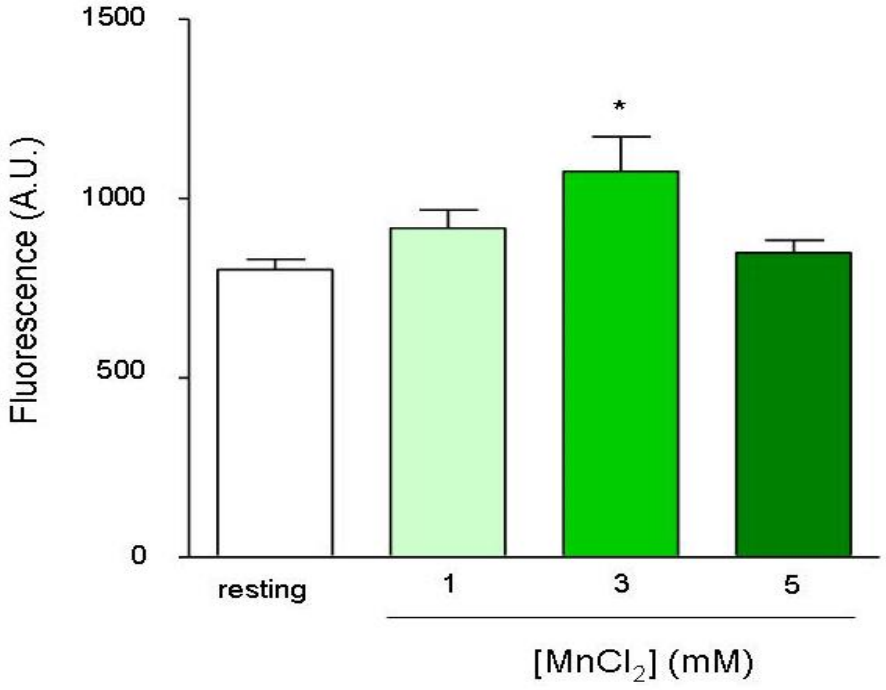

Figure 3.3 Activation of purified integrin $\alpha_{IIb}\beta_3$ by 3 mM $MnCl_2$ causes a significant increase in the integrin free thiol population. Purified integrin $\alpha_{IIb}\beta_3$ was activated with 1 mM, 3 mM or 5 mM $MnCl_2$ for 10 minutes at 37 °C. It was then incubated with Thiostar® (2.5 μg/ml) for 5 minutes at room temperature. The fluorescence was measured using a Wallac plate reader. Data is presented as the mean ± SEM, n=5 independent experiments, *$p < 0.05$.

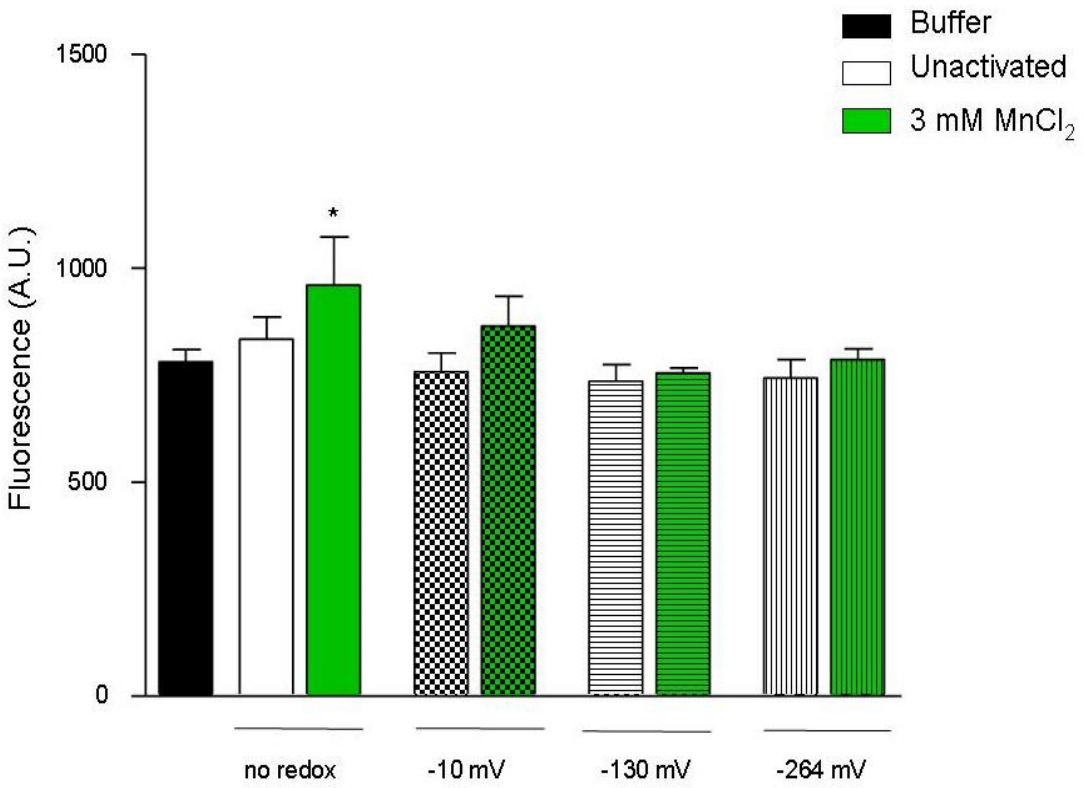

Figure 3.4 The significant increase in the free thiol population of activated integrin $\alpha_{IIb}\beta_3$ is decreased in the presence of reducing GSH/GSSG redox potentials. Purified integrin $\alpha_{IIb}\beta_3$ was incubated with GSH/GSSG redox potentials (-10mV, -130 mV or -264 mV) for 10 minutes at 37 °C. Excess, unreacted GSH/GSSG was removed from the system. Integrin was recovered and activated with 3 mM $MnCl_2$ for 10 minutes at 37 °C, then incubated with Thiostar® (2.5 μg/ml) for 5 minutes at room temperature. The fluorescence was measured using a Wallac plate reader. Altering the redox environment had no impact on the thiol population of the unactivated integrin. Data is presented as the mean ± SEM, n=5 independent experiments, *$p < 0.05$.

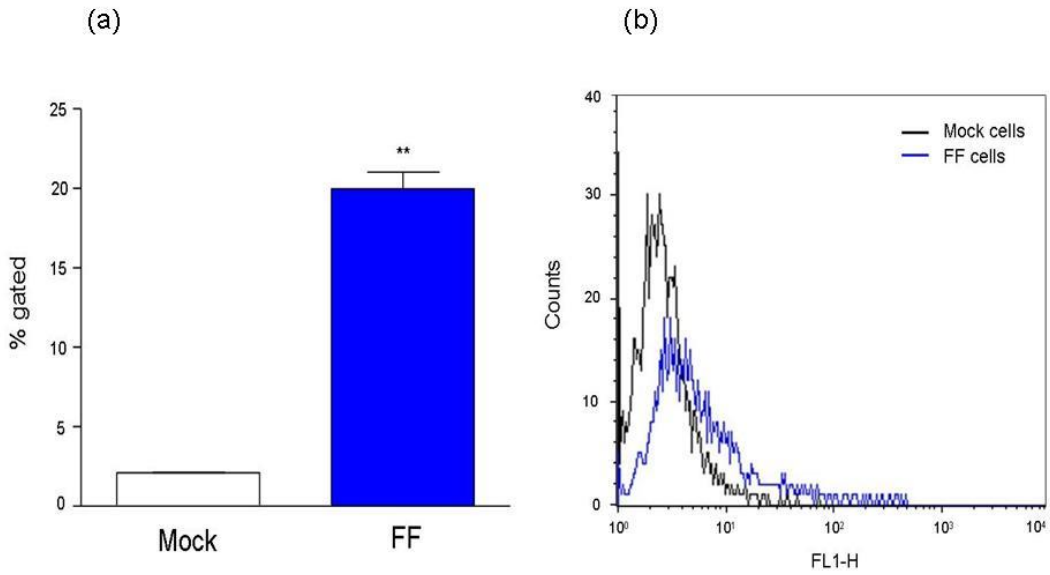

Figure 3.5 The 'FF' Chinese hamster ovarian-K1 (CHO-K1) cell line expresses intact integrin $\alpha_{IIb}\beta_3$. (a) The level of integrin $\alpha_{IIb}\beta_3$ expression was significantly greater in the FF cells when compared to mock transfected CHO-K1 cells when measured by flow cytometry using the α_{IIb}-subunit specific monoclonal antibody, CD41a. Data is presented as the mean ± SEM, n=3 independent experiments, **p < 0.01. (b) A histogram illustrating the increase in integrin $\alpha_{IIb}\beta_3$ expression levels in FF CHO-K1 cells compared to mock transfected CHO-K1 cells, representative of n=3 independent experiments.

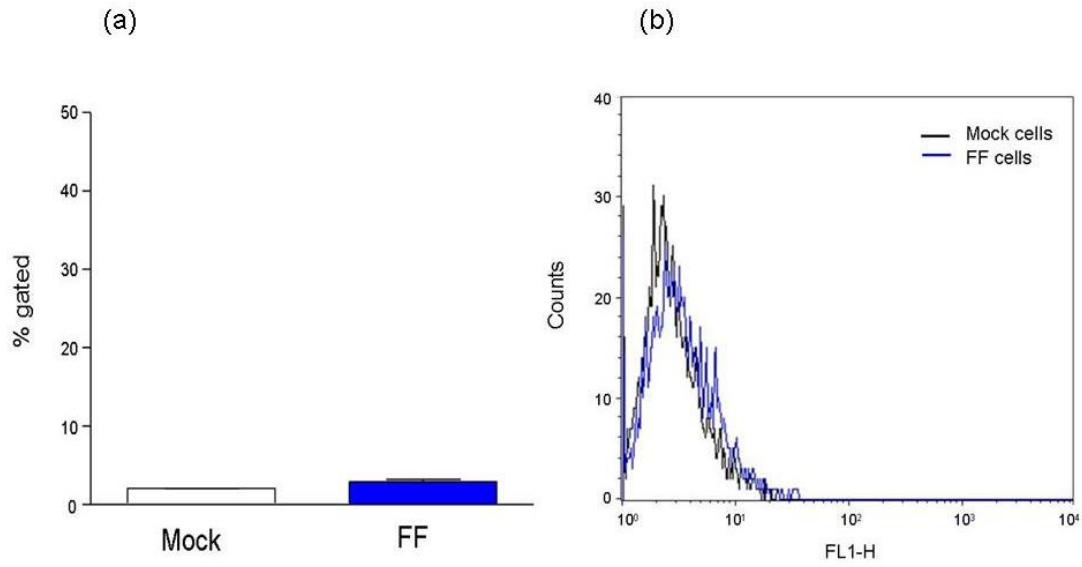

Figure 3.6 The 'FF' Chinese hamster ovarian-K1 (CHO-K1) cell line expresses integrin $\alpha_{IIb}\beta_3$ in a resting conformation. (a) There was no significant difference between the levels of PAC-1 binding to mock transfected CHO-K1 cells and to FF cells, as measured by flow cytometry. Data is presented as the mean ± SEM, n=3 independent experiments. (b) A histogram illustrating that there was no change in the level of PAC-1 binding between FF CHO-K1 cells and mock transfected CHO-K1 cells, representative of n=3 independent experiments.

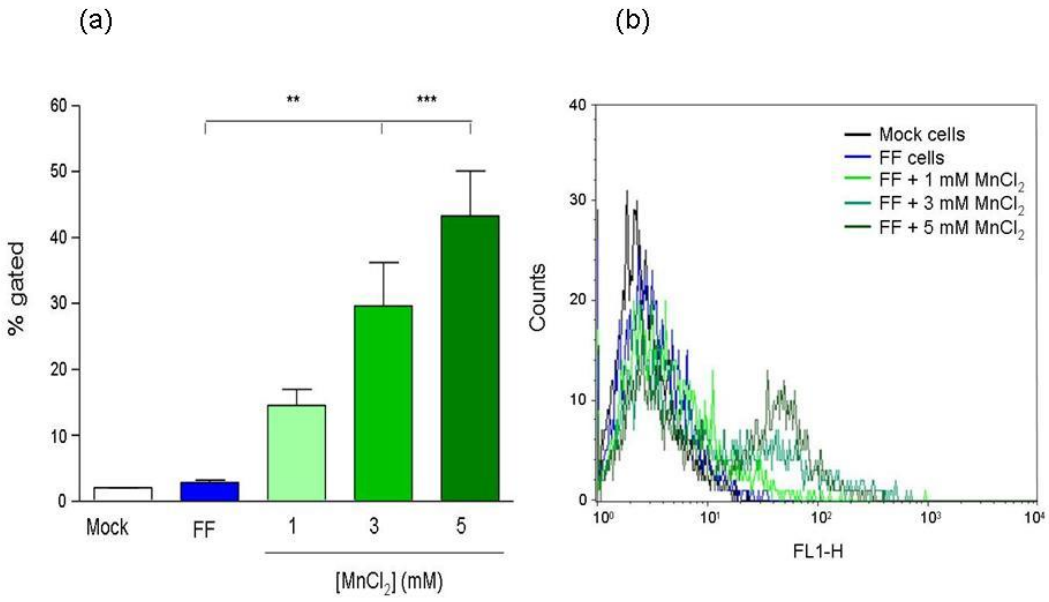

Figure 3.7 Manganese chloride ($MnCl_2$) treatment of FF CHO-K1 cells induces PAC-1 binding to integrin $\alpha_{IIb}\beta_3$. (a) PAC-1 is a monoclonal antibody that binds only the activate conformation of integrin $\alpha_{IIb}\beta_3$. The levels of PAC-1 binding to FF CHO-K1 cells increased with increasing concentrations of $MnCl_2$, thereby indicating $MnCl_2$ induced an active conformation of integrin $\alpha_{IIb}\beta_3$, as measured by flow cytometry. Data is presented as the mean ± SEM, n=3 independent experiments, **p < 0.01, ***p < 0.001. (b) A histogram illustrating the increase in PAC-1 binding to FF CHO-K1 cells upon stimulation with increasing concentrations of $MnCl_2$, representative of n=3 independent experiments.

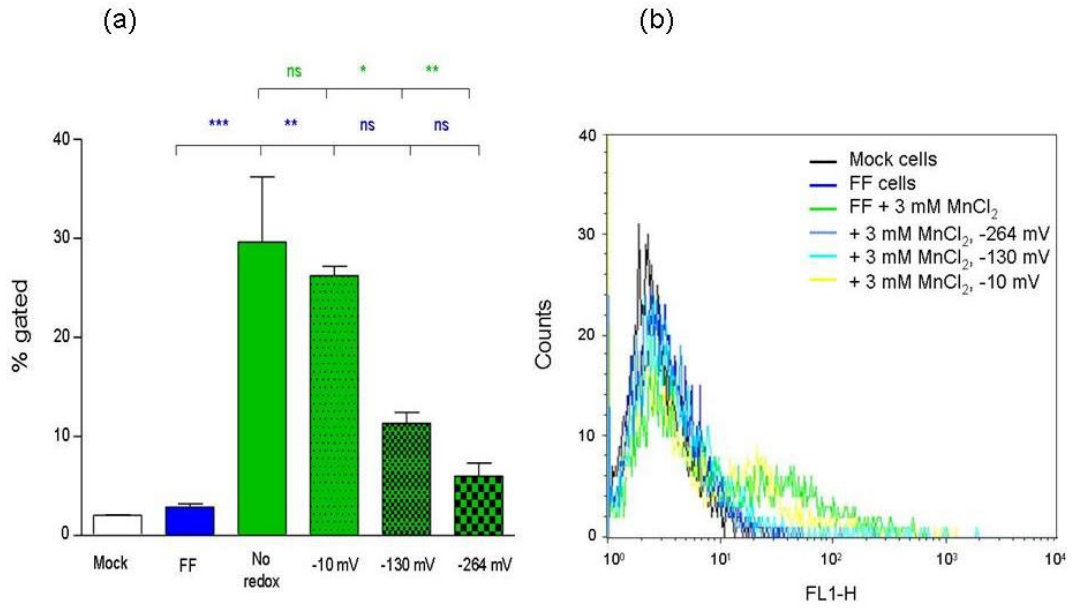

Figure 3.8 PAC-1 binding to FF CHO-K1 cells induced by 3 mM $MnCl_2$ is inhibited by more reducing GSH/GSSG redox potentials. (a) FF cells were incubated with GSH/GSSG redox potentials (-10 mV, -130 mV and -264 mV) for 10 minutes at 37 °C and were subsequently stimulated with 3 mM $MnCl_2$ for 10 minutes at 37 °C in the presence of PAC-1 antibody. PAC-1 binding to activated integrin $\alpha_{IIb}\beta_3$ expressed on FF CHO-K1 cells was measured using flow cytometry. Data is presented as the mean ± SEM, n=3 independent experiments, *$p < 0.05$, **$p < 0.01$, ***$p < 0.001$. (b) A histogram illustrating the inhibition of PAC-1 binding to CHO-K1 cells upon stimulation by 3 mM $MnCl_2$ as the GSH/GSSG redox environment became more reducing, representative of n=3 independent experiments.

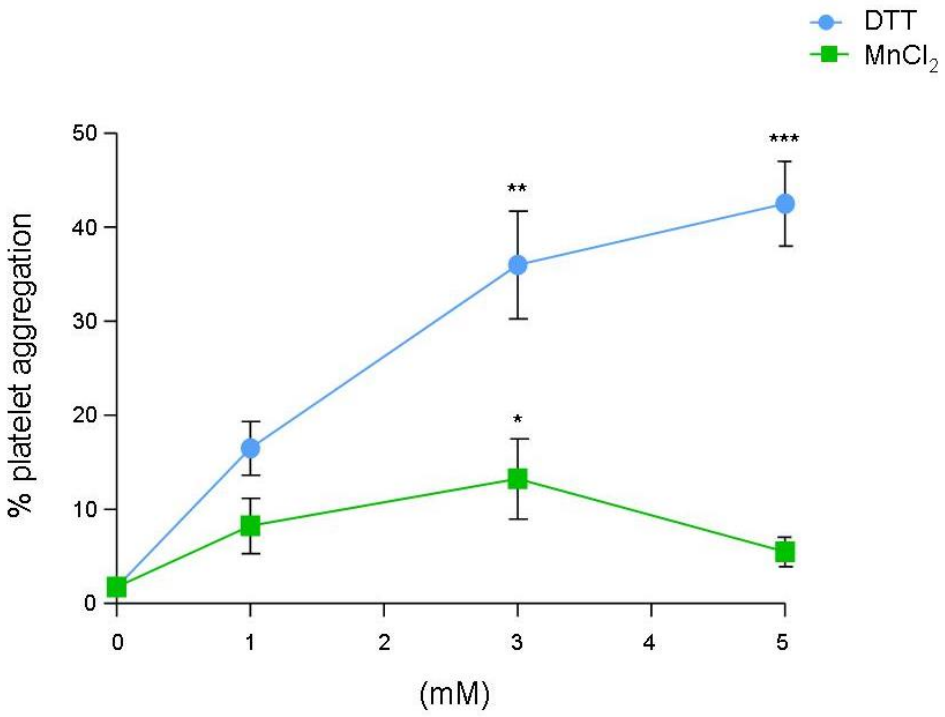

Figure 3.9 A significant level of platelet aggregation is induced by dithiothreitol (DTT) and manganese chloride ($MnCl_2$). Gel-filtered platelet were either unactivated or activated with 1 mM, 3 mM or 5 mM DTT or $MnCl_2$ for 10 minutes at 37 °C with constant stirring at 1100 rpm. Data is presented as the mean ± SEM, n=4 independent experiments, *p < 0.05, **p < 0.01, ***p < 0.001.

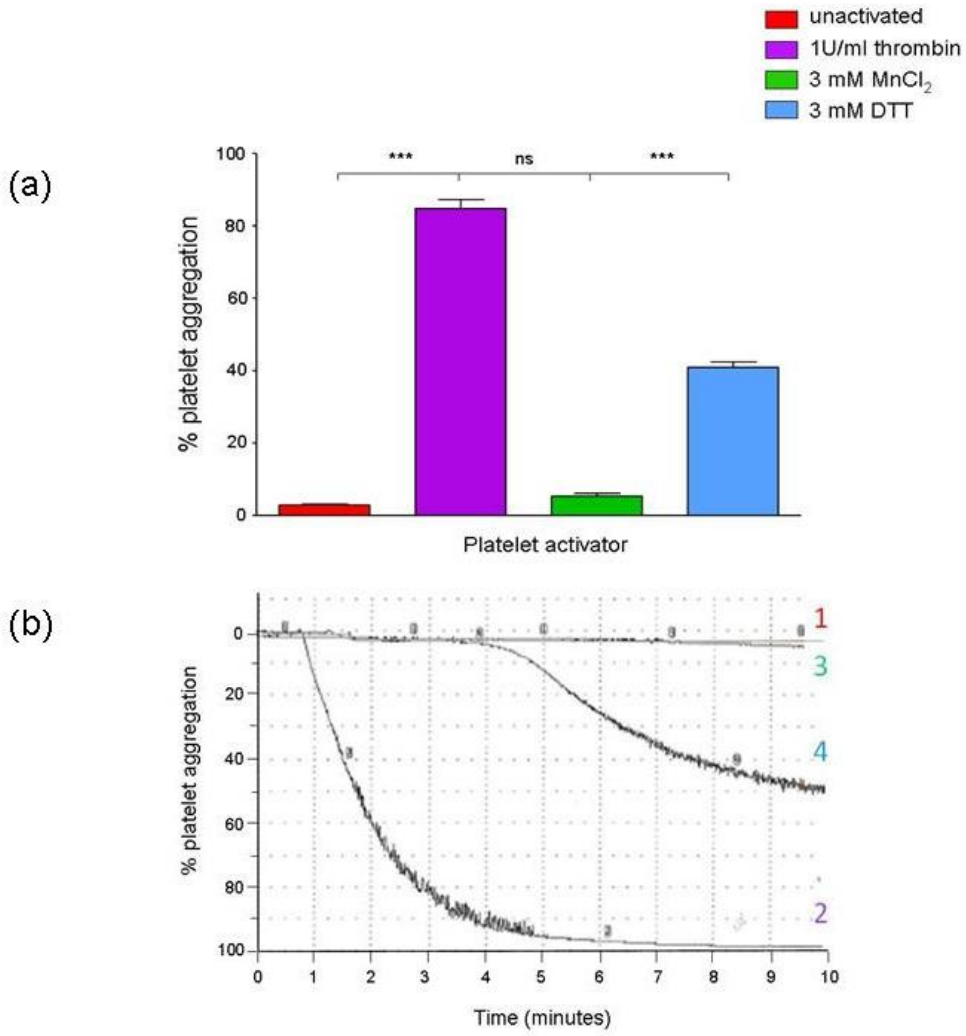

Figure 3.10 Platelet aggregation is induced, at varying levels, by 1U/ml thrombin, 3 mM $MnCl_2$ and 3 mM DTT. (a) Gel-filtered platelets remained unactivated or were activated with either 1U/ml thrombin, 3 mM $MnCl_2$ or 3 mM DTT for 10 minutes at 37 °C with constant stirring at 1100 rpm. Data is presented as the mean ± SEM, n=9 independent experiments, ***$p < 0.001$. (b) A platelet aggregation tracing illustrating the levels of platelet aggregation of (1) unactivated gel-filtered platelets, (2) gel-filtered platelets activated with 1U/ml thrombin, (3) gel-filtered platelets activated with 3 mM $MnCl_2$, (4) gel-filtered platelets activated with 3 mM DTT. Aggregation tracing is representative of n=9 independent experiments.

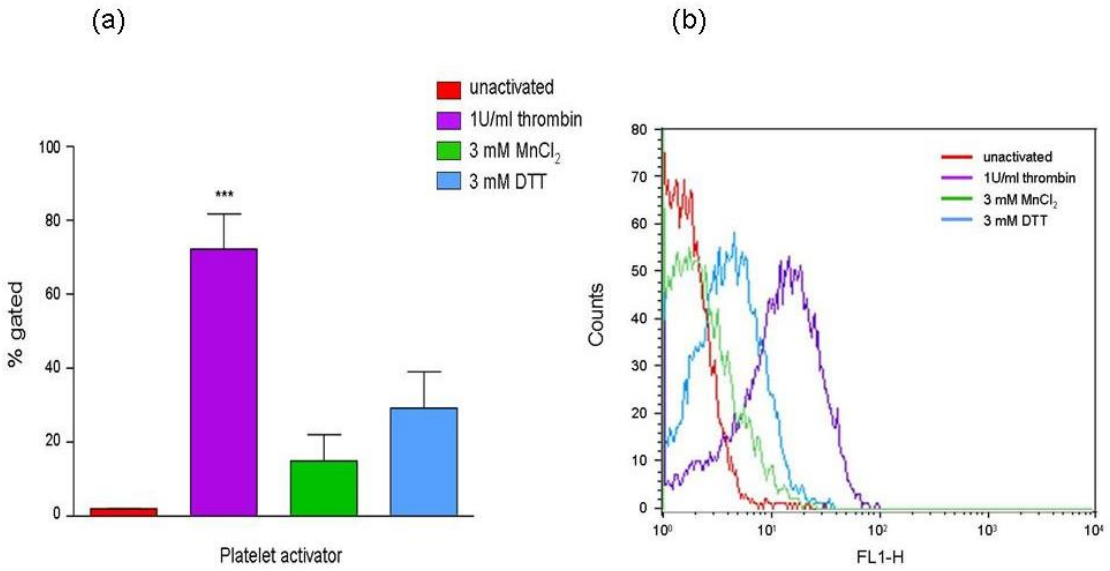

Figure 3.11 The level of PAC-1 binding to platelets varies between platelets activated by 1U/ml thrombin, 3 mM $MnCl_2$ and 3 mM DTT (a) Gel-filtered platelets were activated with 1U/ml thrombin, 3 mM $MnCl_2$ or 3 mM DTT, in the presence PAC-1 antibody for 10 minutes at 37 °C. PAC-1 binding to platelets was measured by flow cytometry. Data is presented as the mean ± SEM, n=5 independent experiments, ***p < 0.001. (b) A histogram illustrating the increase in PAC-1 binding to platelets following treatment with 1U/ml thrombin, 3 mM $MnCl_2$ or 3 mM DTT compared to unactivated platelets, representative of n=5 independent experiments.

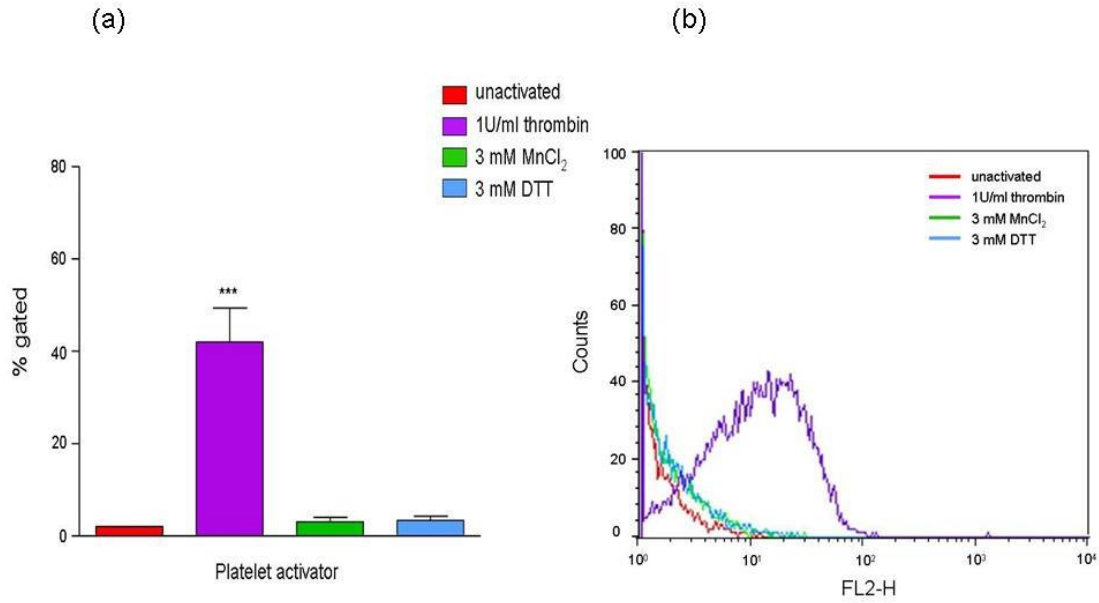

Figure 3.12 Platelet secretion is induced by 1U/ml thrombin but not 3 mM $MnCl_2$ or 3 mM DTT. (a) Gel-filtered platelets were unactivated or activated with either 1U/ml thrombin, 3 mM $MnCl_2$ or 3 mM DTT in the presence of CD62P for 10 minutes at 37 °C. The level of CD62P binding indicating P-selectin expression on the surface of platelets as a result of platelet activation was measured by flow cytometry. Data is presented as the mean ± SEM, n=4 independent experiments, ***p < 0.001. (b) A histogram illustrating CD62P binding to platelets following activation with either 1U/ml thrombin, 3 mM $MnCl_2$ or 3 mM DTT. Data is representative of n=4 independent experiments.

Table 3.1 A summary of PAC-1 and CD62P binding to unactivated platelets or platelets activated with either 1U/ml thrombin, 3 mm $MnCl_2$ or 3 mM DTT. Gel-filtered platelets were incubated with 1U/ml thrombin, 3 mM $MnCl_2$ or 3 mM DTT in the presence of PAC-1 or CD62P antibodies for 10 minutes at 37 °C. The levels of antibody binding to platelets were measured using flow cytometry. The values are expressed as mean percentage gated ± SEM; PAC-1 n=5, CD62P n=4 independent experiments.

	PAC-1 (% gated ± SEM)	**CD62P** (% gated ± SEM)
Unactivated	2.016 ± 0.03311	2.005 ± 0.03227
1U/ml thrombin	72.33 ± 9.387	42.01 ± 7.386
3 mM $MnCl_2$	14.98 ± 7.088	3.115 ± 0.8866
3 mM DTT	29.23 ± 9.838	3.335 ± 0.9489

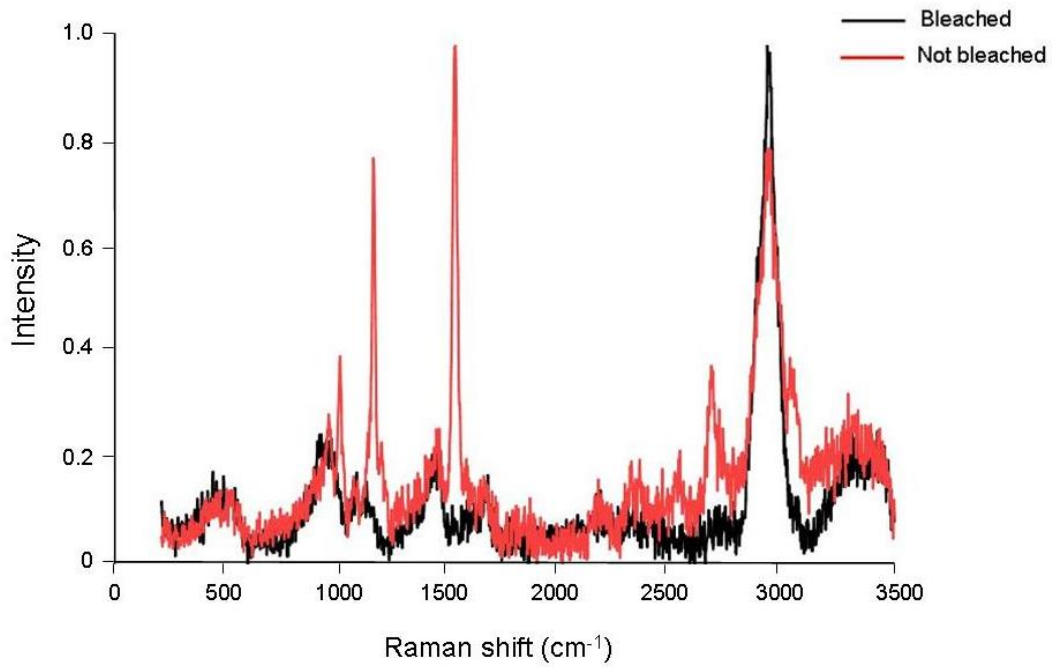

Figure 3.13 An increased acquisition time for platelet Raman spectra caused photo-bleaching of prominent peaks in the spectra. Unactivated gel-filtered platelets were fixed with 1 % formaldehyde, centrifuged, supernatant removed and the platelet pellet was used for Raman analysis. Raman spectra were recorded, with a laser line of 473 nm, on a Horiba/Jobin Yvon LabRam HR spectrometer. Spectra were acquired for 25 seconds (not bleached) or 200 seconds (bleached). Spectra were initially analysed using Lab Spec software; baseline subtraction and normalisation were then performed using Origin® software.

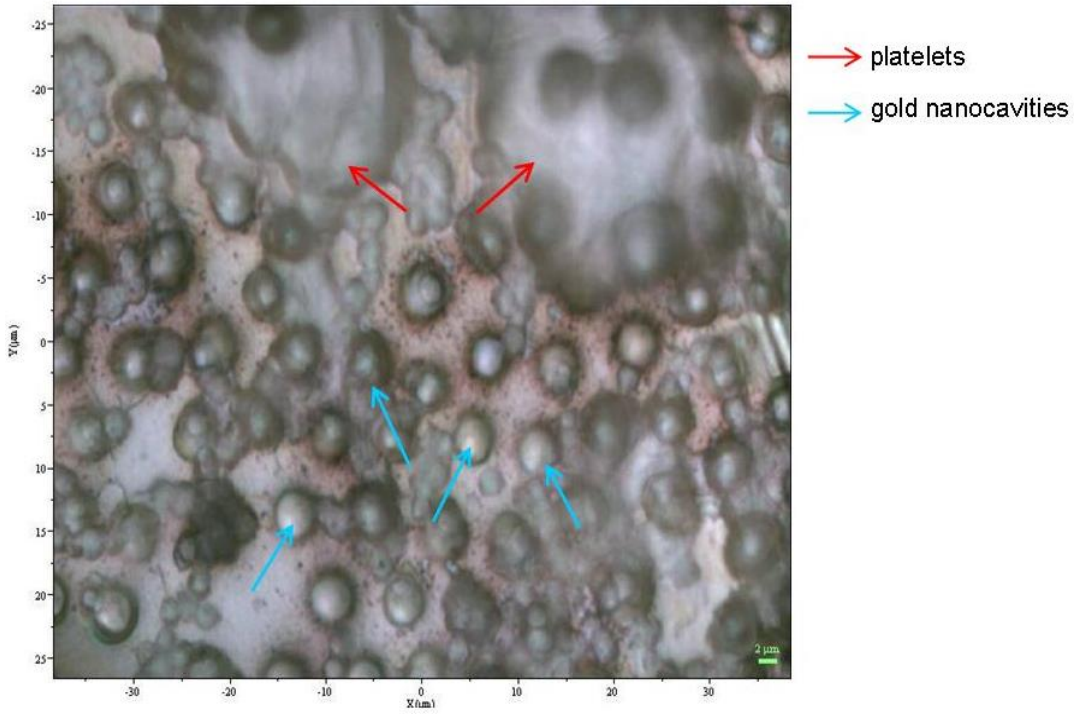

Figure 3.14 Gel filtered platelets on a gold nanocavity surface for Surface Enhanced Raman spectroscopy (SERS). Unactivated gel-filtered platelets were fixed in 1 % formaldehyde, centrifuged, supernatant removed. The resulting platelet pellet was placed on the gold nanocavity surface and images were obtained using the upright microscope attached to the Horiba/Jobin Yvon LabRam HR spectrometer, magnification X 100.

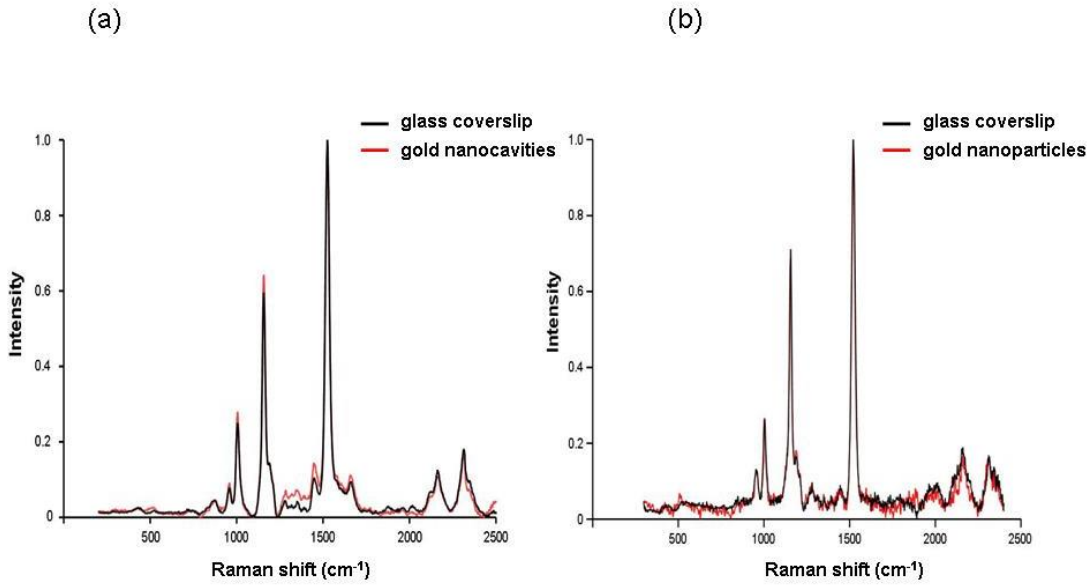

Figure 3.15 Surfaced enhanced Raman spectroscopy (SERS) on either gold nanocavity or gold nanoparticle covered surfaces did not enhance platelet Raman spectra. Fixed, unactivated, gel-filtered platelets were placed on glass coverslips for comparison with platelets placed on either (a) gold nanocavity or (b) gold nanoparticle covered surfaces. Raman spectra were obtained, with a laser line of 473 nm, on a Horiba/Jobin Yvon LabRam spectrometer. Baseline subtraction and normalisation were performed using Origin® software.

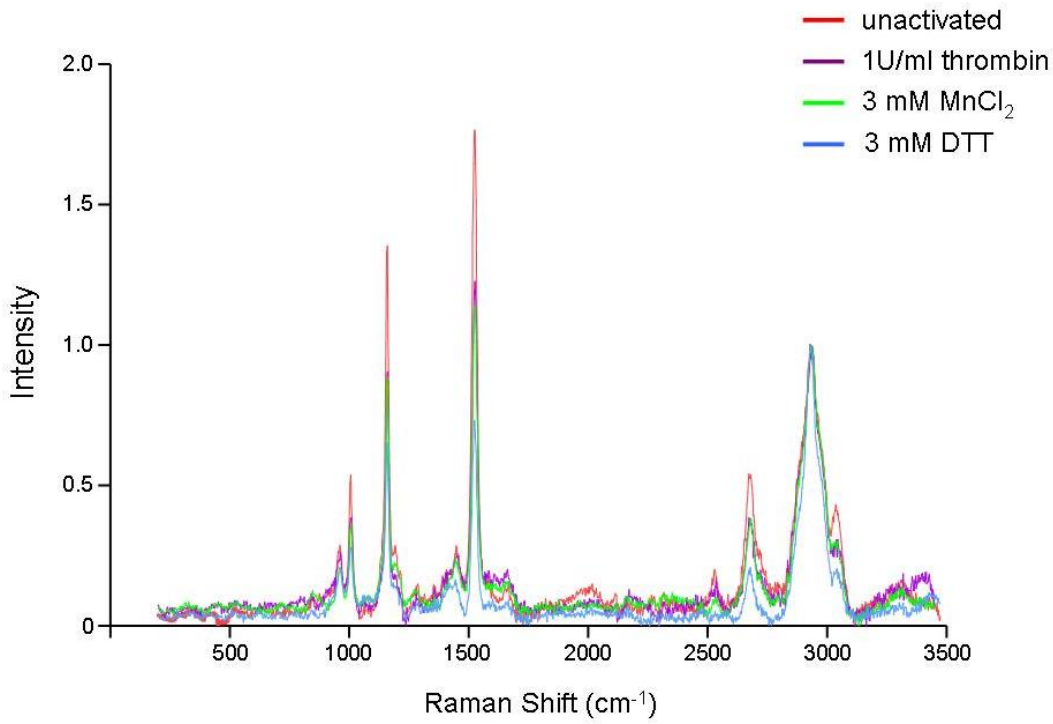

Figure 3.16 (a) Signature Raman spectra of unactivated platelets and platelets activated with either 1U/ml thrombin, 3 mM $MnCl_2$ or 3 mM DTT. Gel-filtered platelets were fixed with 1 % formaldehyde, centrifuged and supernatant removed. Raman spectra were obtained from the resulting platelet pellet. Spectra were baseline subtracted and normalised to the lipid peak at approximately 3000 cm^{-1}. Spectra shown are the average spectra of n=4 independent experiments with 3 - 5 spectra from each experiment.

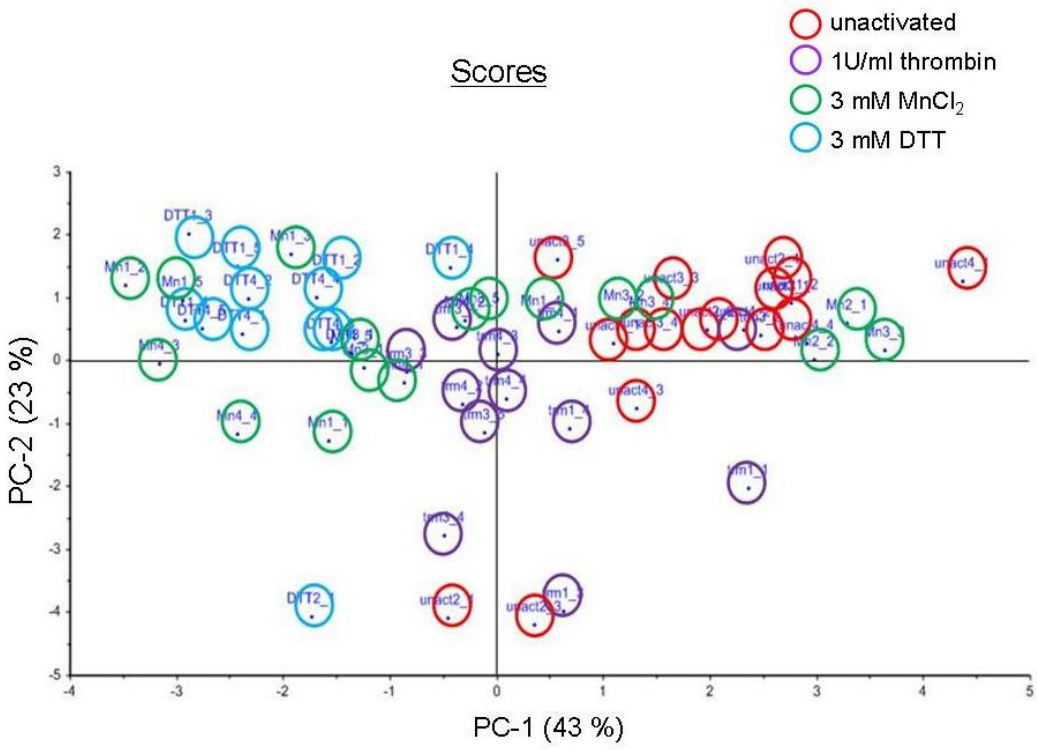

Figure 3.16 (b) Principal component analysis (PCA) showing distinct clustering of each of the platelet activators (full spectrum). PCA analysis was performed on the Raman spectra of gel-filtered platelets which were unactivated or activated with either 1U/ml thrombin, 3 mM $MnCl_2$ or 3 mM DTT. The numbers on each sample refer to the donor number and spectrum number for that particular donor, for example unact1_2 refers to unactivated platelets, donor number 1 and spectrum number 2. The graph is a scatter plot of the first principal component (PC-1) versus the second principal component (PC-2). PCA analysis was carried out using The Unscrambler® software. Data shown is 3 - 5 spectra from n=4 independent experiments.

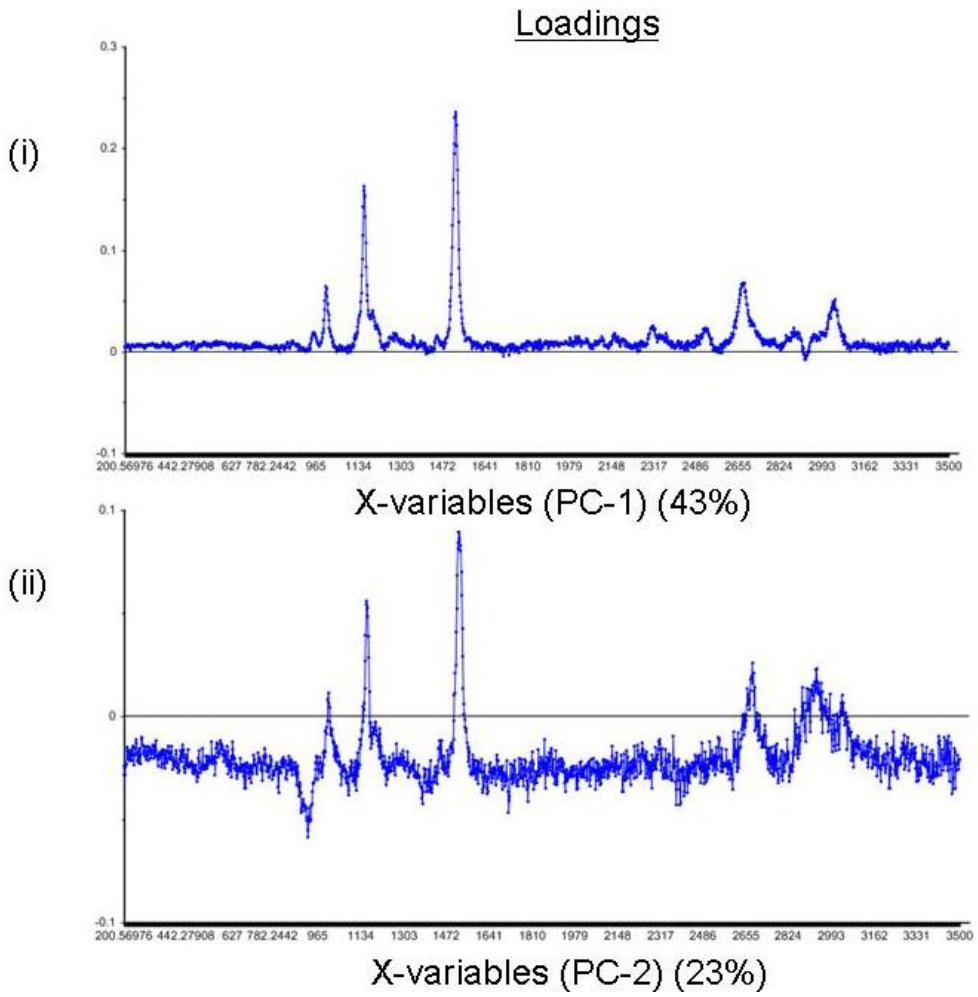

Figure 3.16 (c) The loadings of the two principal components used in the Principal component analysis (PCA) scatter plot of the full spectrum of all samples: (i) Principal component-1 (PC-1) and (ii) Principal component-2 (PC-2). The components are numbered according to the amount of variance they account for, i.e. PC-1 accounts for most of the variance found between the platelet samples. PCA analysis was carried out on the baseline subtracted and normalised Raman data of all samples using The Unscrambler® software.

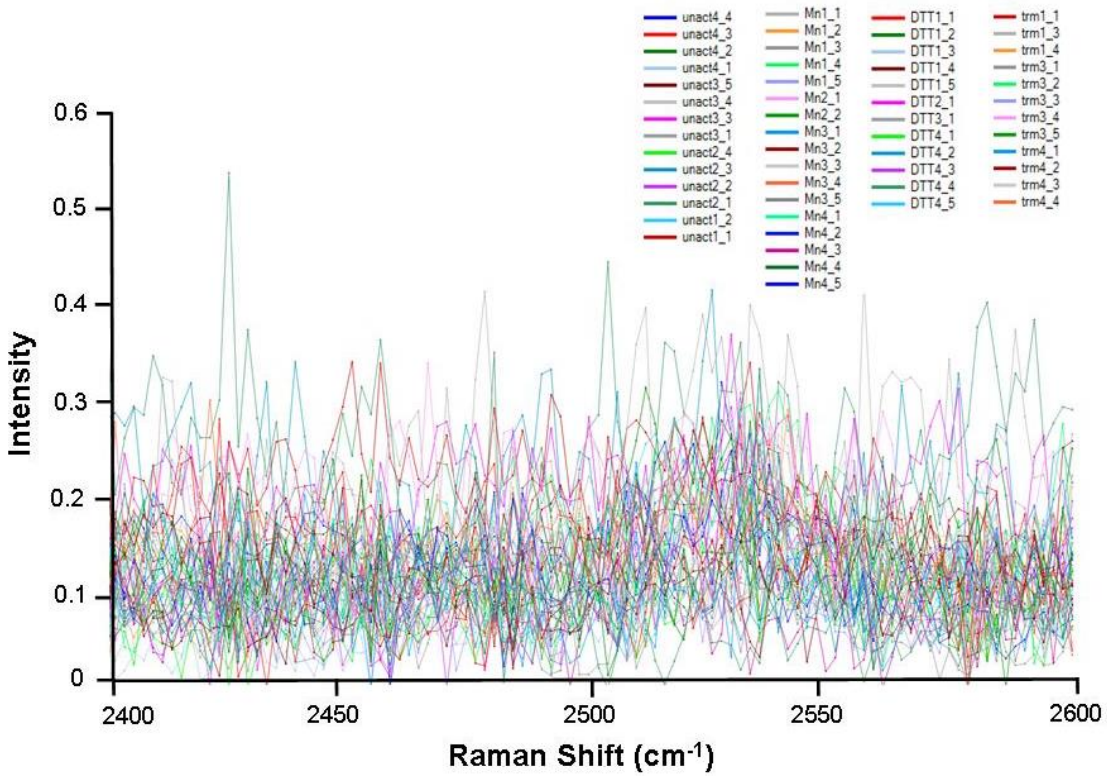

Figure 3.17 (a) The thiol region of the Raman spectra for all unactivated platelet samples or platelet samples activated with either 1U/ml thrombin, 3 mM $MnCl_2$ or 3 mM DTT. Gel-filtered platelets were fixed with 1 % formaldehyde, centrifuged and supernatant removed. Raman spectra were obtained from the resulting platelet pellet. Spectra were baseline subtracted and normalised to the lipid peak at approximately 3000 cm^{-1}. Data shown is 3 - 5 spectra from n=4 independent experiments.

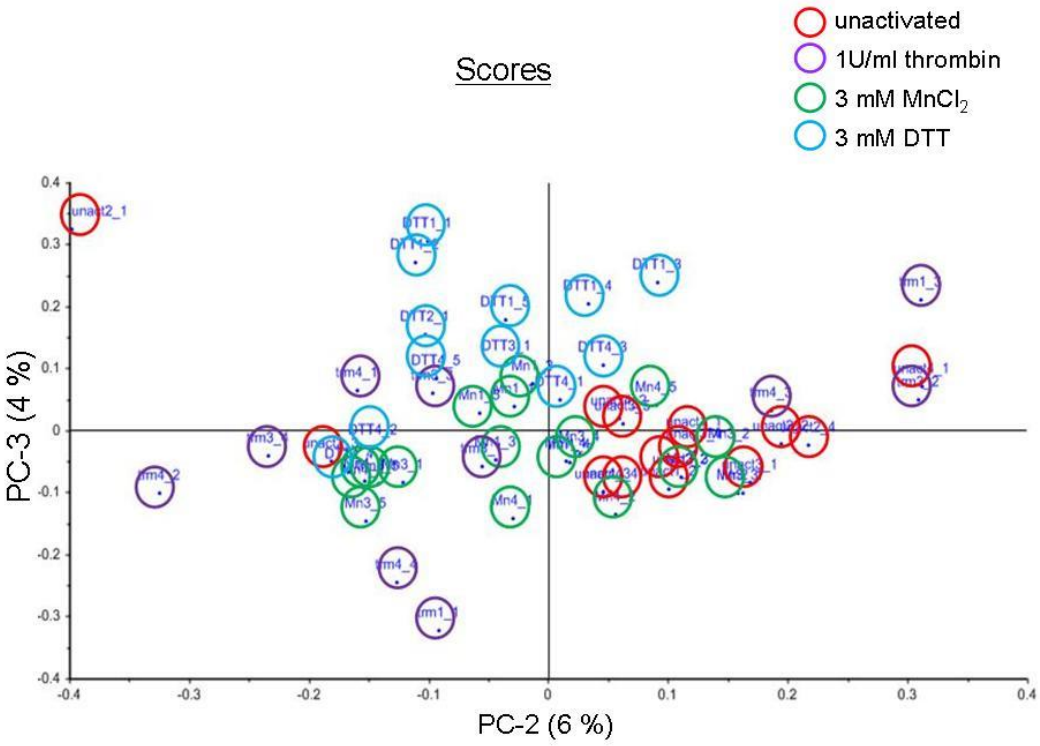

Figure 3.17 (b) Principal component analysis (PCA) of the thiol region showing distinct clustering of samples based on the platelet activator. PCA analysis was performed on the Raman spectra of gel-filtered platelets which were unactivated or activated with either 1U/ml thrombin, 3 mM $MnCl_2$ or 3 mM DTT. The numbers on each sample refer to the donor number and spectrum number for that particular donor, for example unact1_2 refers to unactivated platelets, donor number 1 and spectrum number 2. The graph is a scatter plot of the second principal component (PC-2) versus the third principal component (PC-3). PCA analysis was carried out using The Unscrambler® software. Data shown is 3 - 5 spectra from n=4 independent experiments.

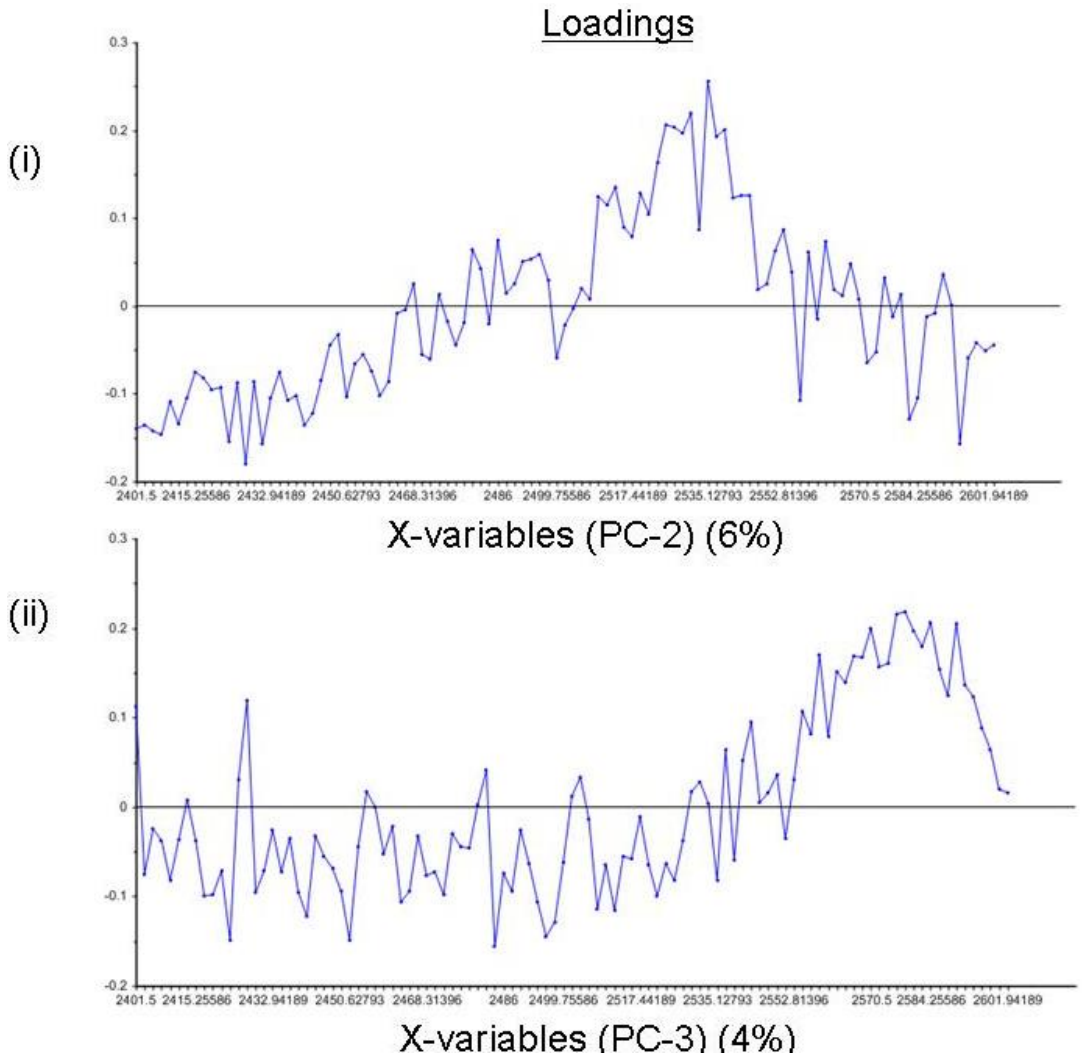

Figure 3.17 (c) The loadings of the two principal components used in the Principal component analysis (PCA) scatter plot of the thiol containing region only: (i) Principal component-2 (PC-2) and (ii) Principal component-3 (PC-3). The components are numbered according to the amount of variance they account for. PCA analysis was carried out on the baseline subtracted and normalised Raman data of all samples, in the thiol containing region 2400 – 2600 cm^{-1} only, using The Unscrambler® software.

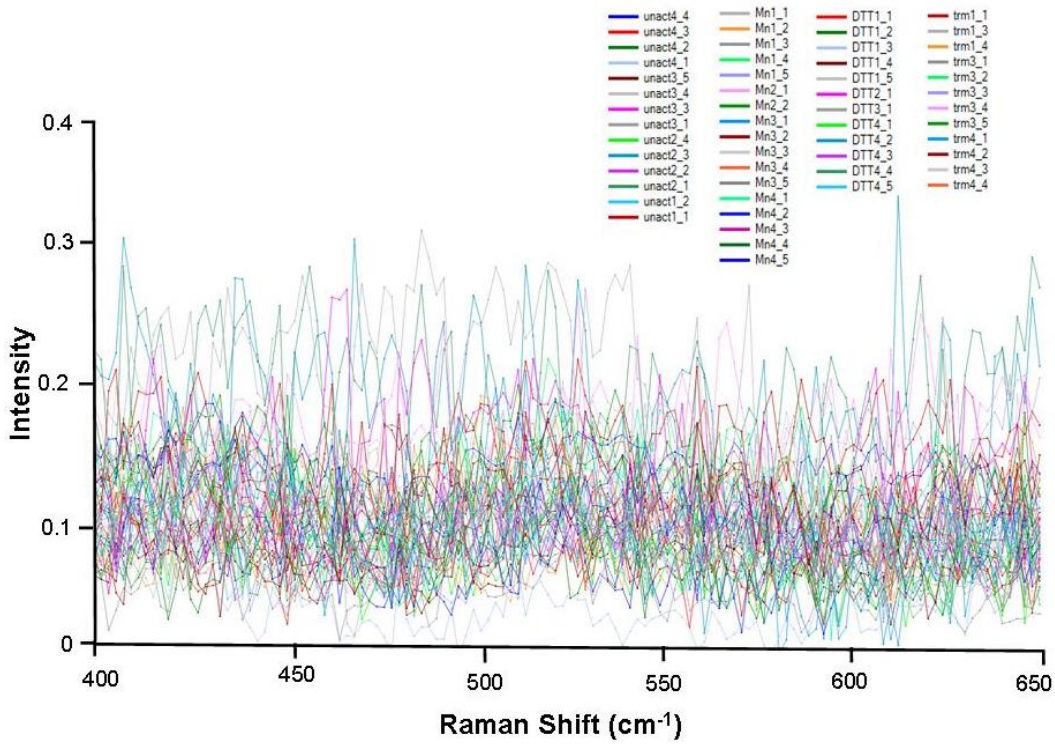

Figure 3.18 (a) The disulphide region of the Raman spectra for unactivated platelet samples or platelet samples activated with either 1U/ml thrombin, 3 mM $MnCl_2$ or 3 mM DTT. Gel-filtered platelets were fixed with 1 % formaldehyde, centrifuged and supernatant removed. Raman spectra were obtained from the resulting platelet pellet. Spectra were baseline subtracted and normalised to the lipid peak at approximately 3000 cm^{-1}. Data shown is 3 – 5 spectra from n=4 independent experiments.

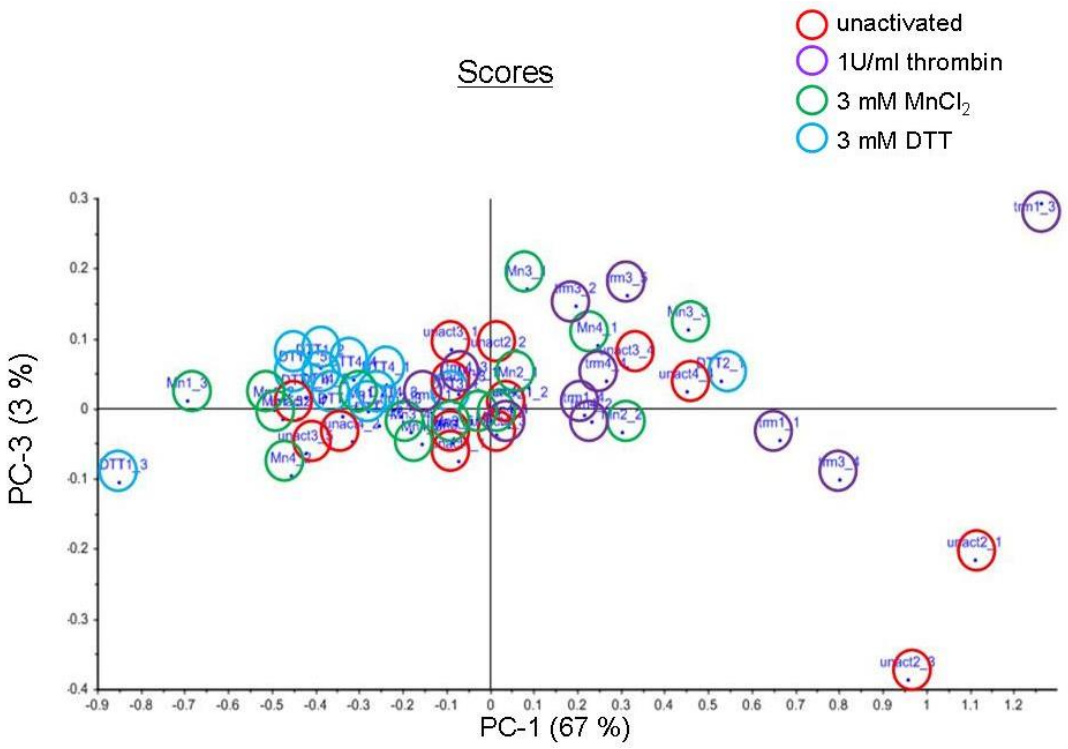

Figure 3.18 (b) Principal component analysis (PCA) of the disulphide region showing distinct clustering of samples based on the platelet activator. PCA analysis was performed on the Raman spectra of gel-filtered platelets which were unactivated or activated with either 1U/ml thrombin, 3 mM $MnCl_2$ or 3 mM DTT. The numbers on each sample refer to the donor number and spectrum number for that particular donor, for example unact1_2 refers to unactivated platelets, donor number 1 and spectrum number 2. This is a scatter plot of the first principal component (PC-1) versus the third principal component (PC-3). Data shown is 3 - 5 spectra from n=4 independent experiments.

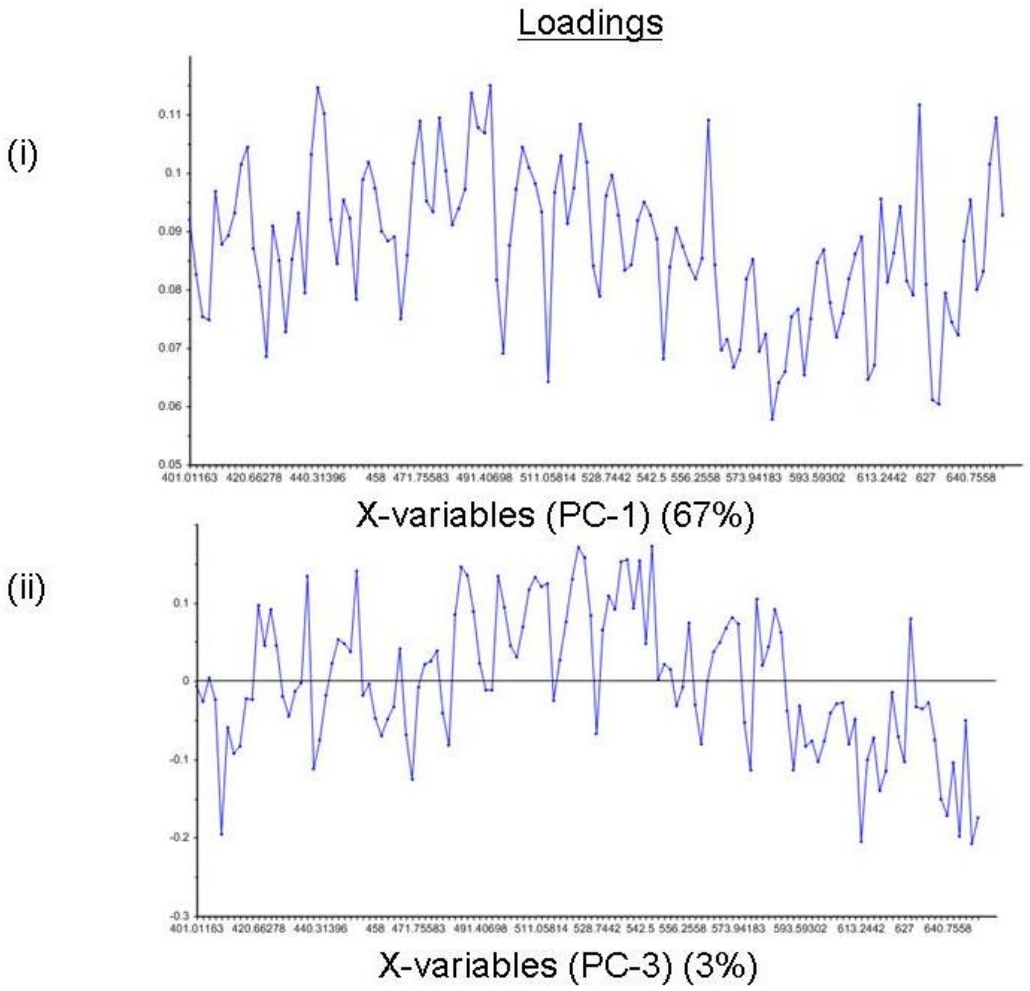

Figure 3.18 (c) The loadings of the two principal components used in the Principal component analysis (PCA) scatter plot of the disulphide containing region only: (i) Principal component-1 (PC-1) and (ii) Principal component-3 (PC-3). The components are numbered according to the amount of variance they account for. PCA analysis was carried out on the baseline subtracted and normalised Raman data of all samples, in the disulphide containing region 400 – 650 cm^{-1} only, using The Unscrambler® software.

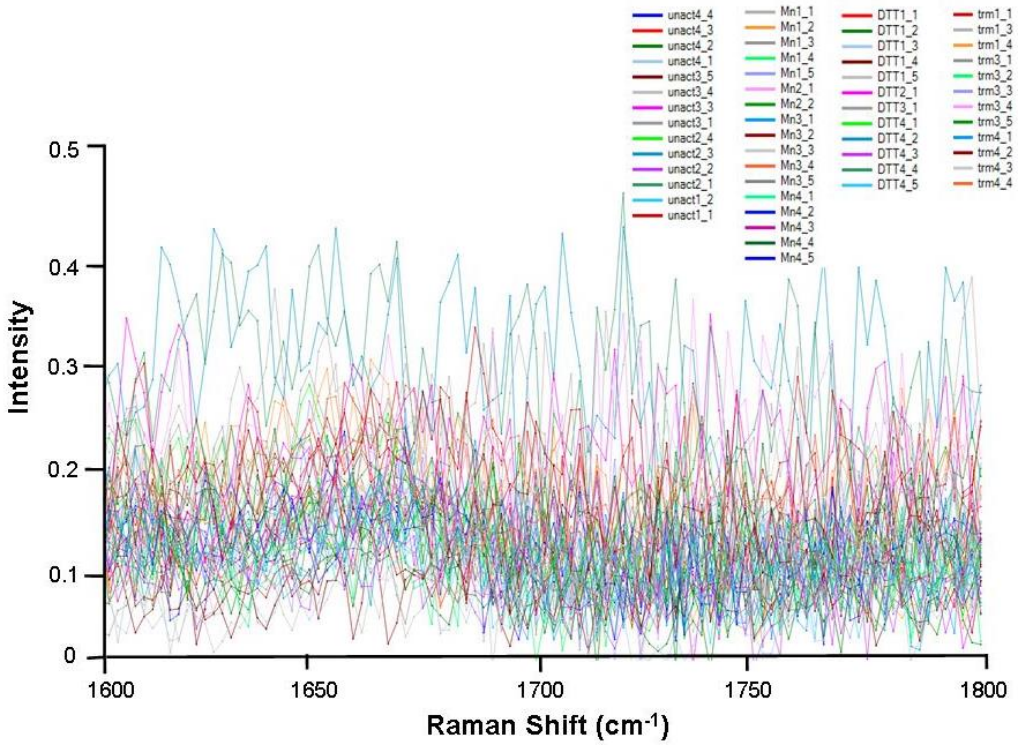

Figure 3.19 (a) The amide I region of the Raman spectra for unactivated platelet samples or platelet samples activated with either 1U/ml thrombin, 3 mM $MnCl_2$ or 3 mM DTT. Gel-filtered platelets were fixed with 1 % formaldehyde, centrifuged and supernatant removed. Raman spectra were obtained from the resulting platelet pellet. Spectra were baseline subtracted and normalised to the lipid peak at approximately 3000 cm^{-1}. Data shown is 3 – 5 spectra from n=4 independent experiments.

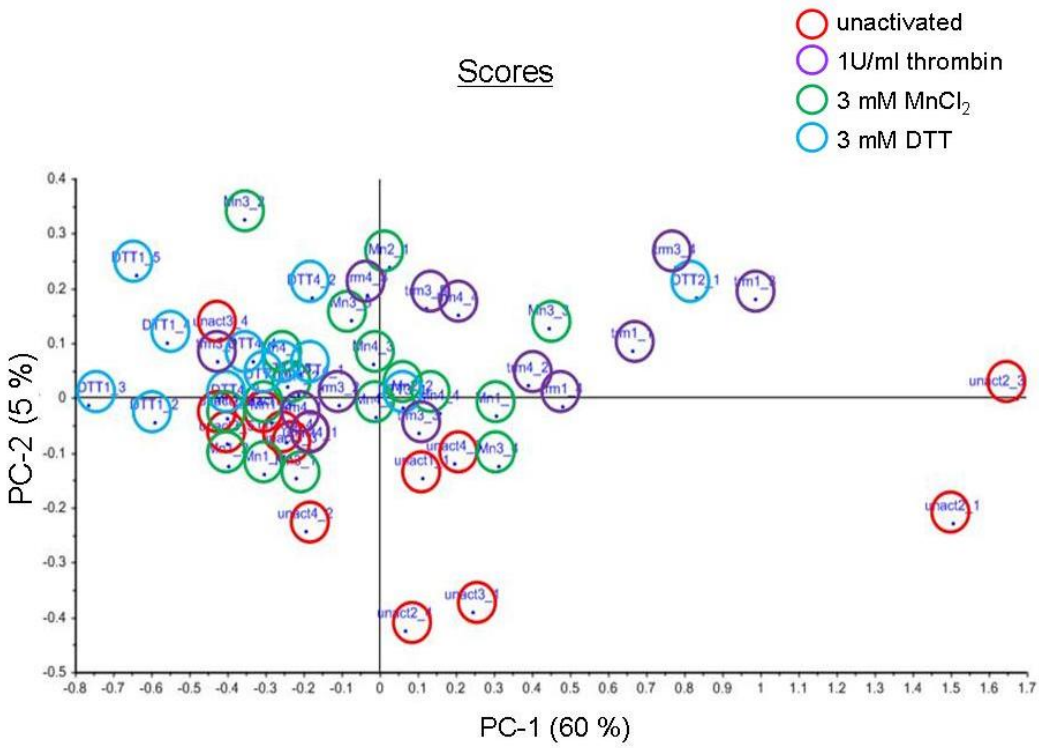

Figure 3.19 (b) Principal component analysis (PCA) of the amide I region showing distinct clustering of samples based on the platelet activator. PCA analysis was performed on the Raman spectra of gel-filtered platelets which were unactivated or activated with either 1U/ml thrombin, 3 mM $MnCl_2$ or 3 mM DTT. The numbers on each sample refer to the donor number and spectrum number for that particular donor, for example unact1_2 refers to unactivated platelets, donor number 1 and spectrum number 2. The graph is a scatter plot of the first principal component (PC-1) versus the second principal component (PC-2). Data shown is 3 - 5 spectra from n=4 independent experiments.

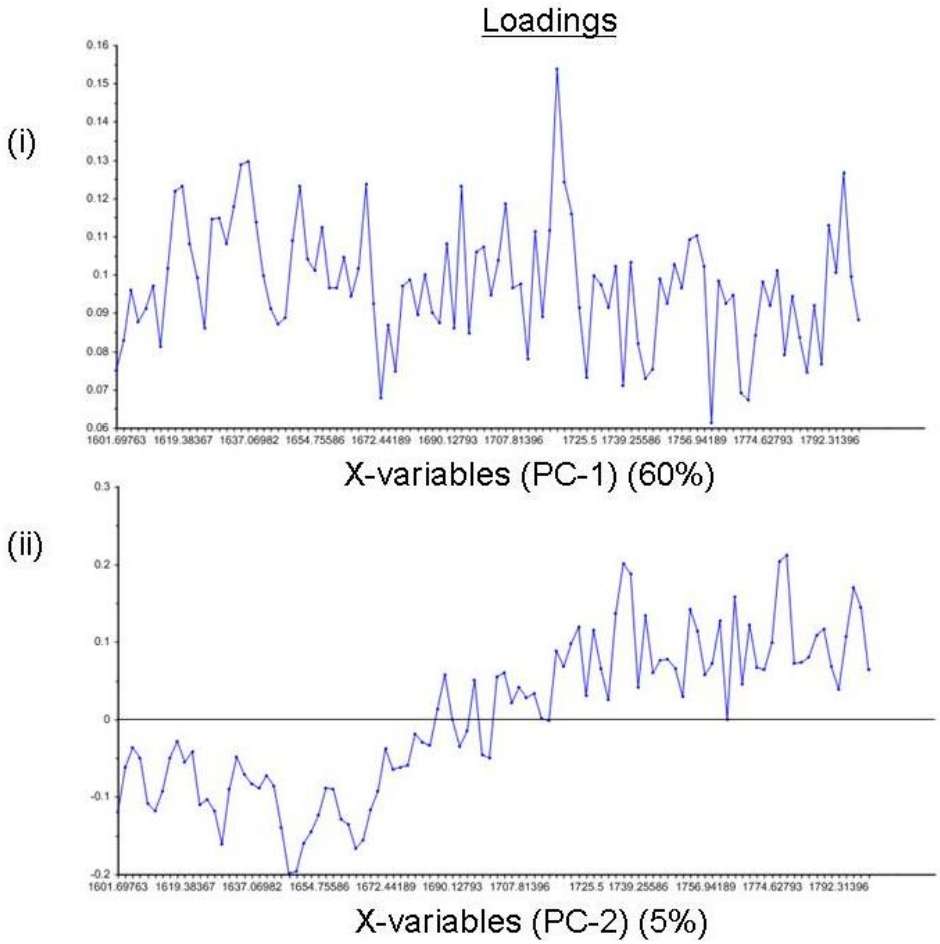

Figure 3.19 (c) The loadings of the two principal components used in the Principal component analysis (PCA) scatter plot of the amide I containing region only: (i) Principal component-1 (PC-1) and (ii) Principal component 2 (PC-2). The components are numbered according to the amount of variance they account for. PCA analysis was carried out on the baseline subtracted and normalised Raman data of all samples, in the amide I containing region 1600 – 1800 cm^{-1} only, using The Unscrambler® software.

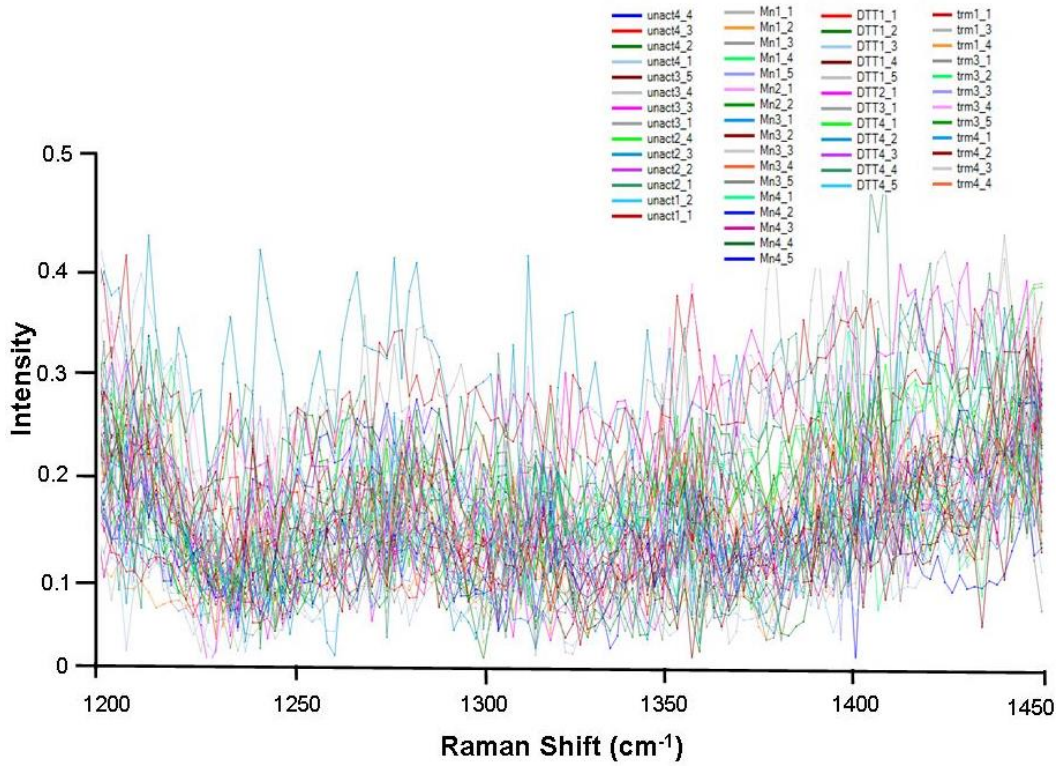

Figure 3.20 (a) The amide III region of the Raman spectra for unactivated platelet samples or platelet samples activated with either 1U/ml thrombin, 3 mM $MnCl_2$ or 3 mM DTT. Gel-filtered platelets were fixed with 1 % formaldehyde, centrifuged and supernatant removed. Raman spectra were obtained from the resulting platelet pellet. Spectra were baseline subtracted and normalised to the lipid peak at approximately 3000 cm^{-1}. Data shown is 3 – 5 spectra from n=4 independent experiments.

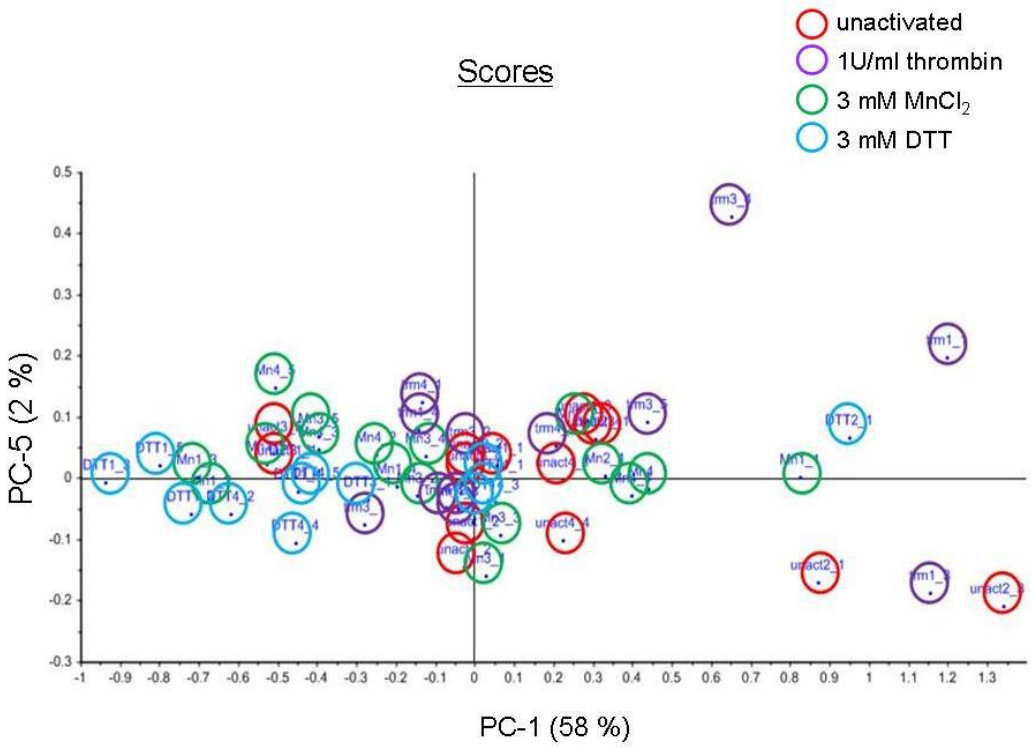

Figure 3.20 (b) Principal component analysis (PCA) of the amide III region showing distinct clustering of samples based on the platelet treatment activator. PCA analysis was performed on the Raman spectra of gel-filtered platelets which were unactivated or activated with either 1U/ml thrombin, 3 mM $MnCl_2$ or 3 mM DTT. The numbers on each sample refer to the donor number and spectrum number for that particular donor, for example unact1_2 refers to unactivated platelets, donor number 1 and spectrum number 2. The graph is a scatter plot of the first principal component (PC-1) versus the fifth principal component (PC-5). Data shown is 3 - 5 spectra from n=4 independent experiments.

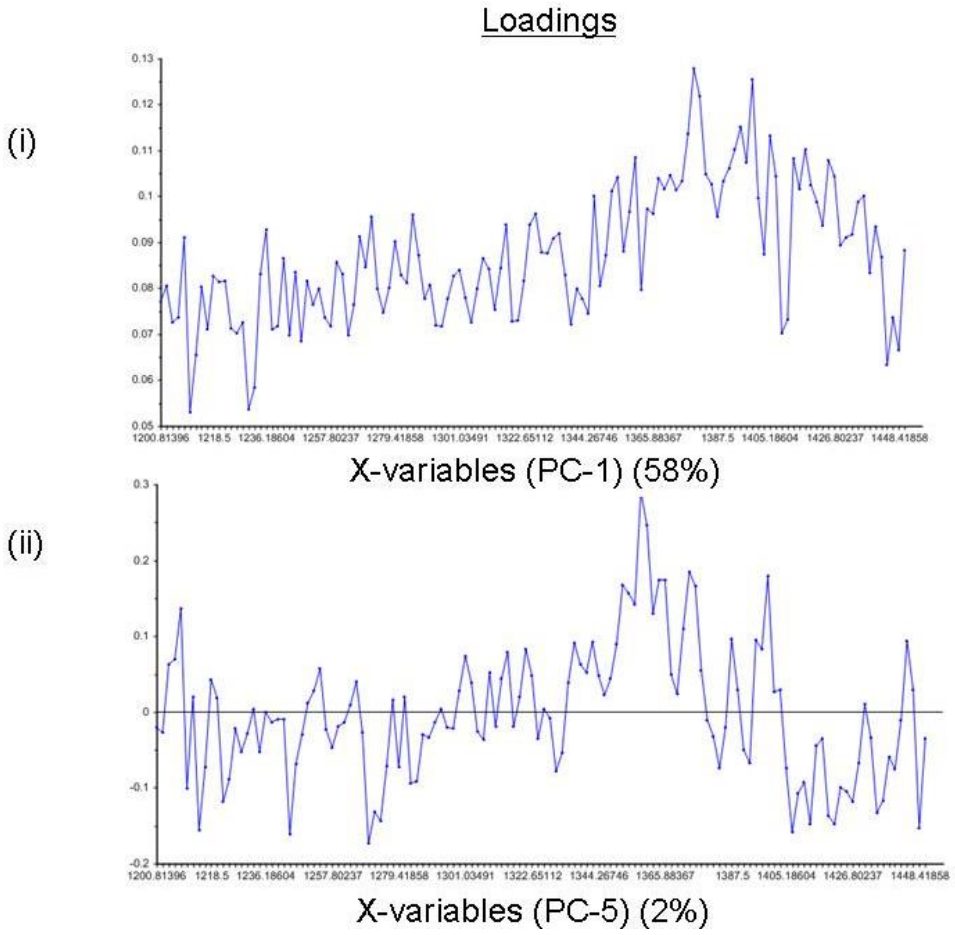

Figure 3.20 (c) The loadings of the two principal components used in the Principal component analysis (PCA) scatter plot of the amide III containing region only: (i) Principal component-1 (PC-1) and (ii) Principal component-2 (PC-2). The components are numbered according to the amount of variance they account for. PCA analysis was carried out on the baseline subtracted and normalised Raman data of all samples, in the amide III containing region 1200 – 1450 cm^{-1} only, using The Unscrambler® software.

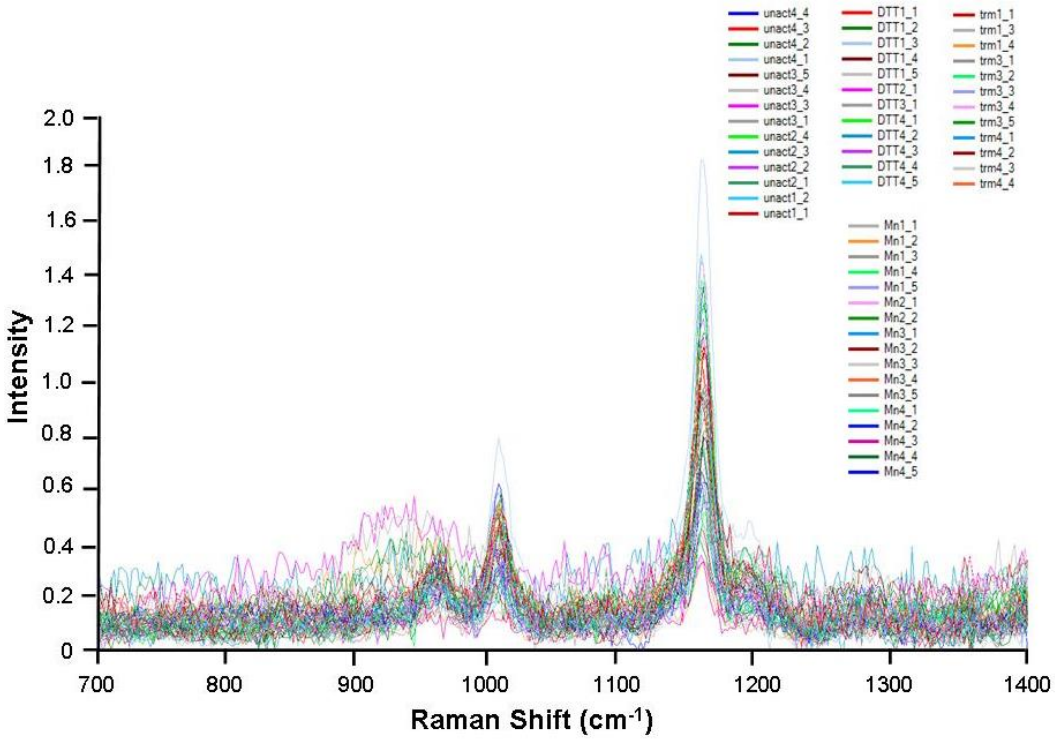

Figure 3.21 (a) The 700 – 1400 cm^{-1} region of the Raman spectra for all unactivated platelet samples or platelet samples activated with either 1U/ml thrombin, 3 mM $MnCl_2$ or 3 mM DTT. Gel-filtered platelets were fixed with 1 % formaldehyde, centrifuged and supernatant removed. Raman spectra were obtained from the resulting platelet pellet. Spectra were baseline subtracted and normalised to the lipid peak at approximately 3000 cm^{-1}. Data shown is 3 – 5 spectra from n=4 independent experiments.

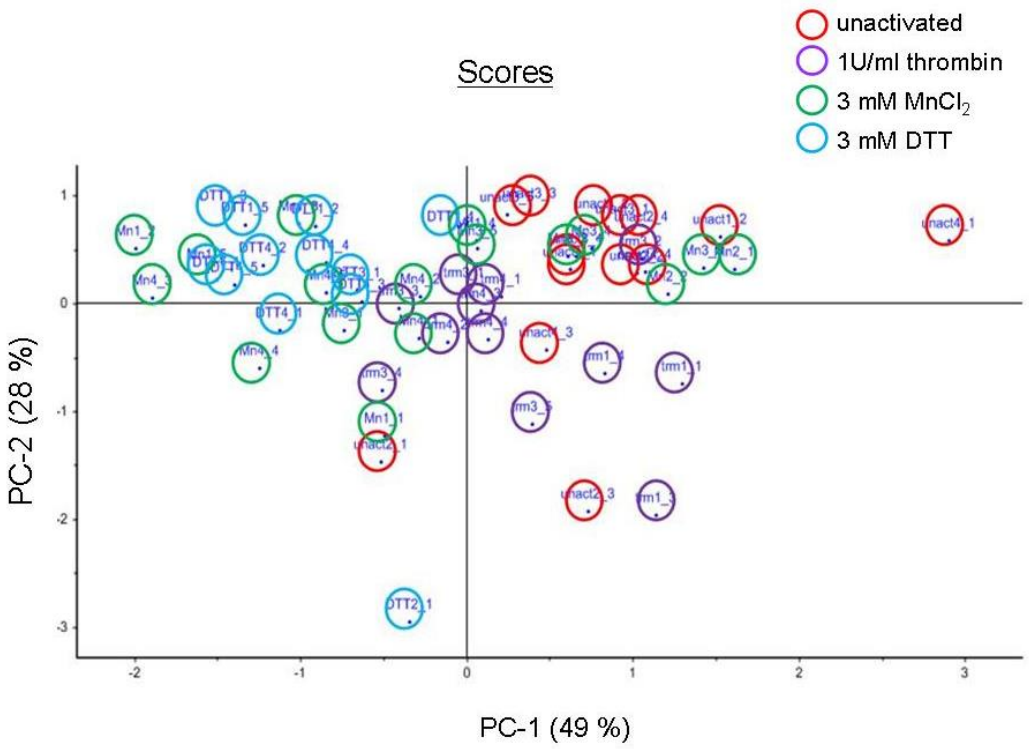

Figure 3.21 (b) Principal component analysis (PCA) of the 700 – 1400 cm^{-1} region showing distinct clustering of samples based on the platelet treatment activator. PCA analysis was performed on the Raman spectra of gel-filtered platelets which were unactivated or activated with either 1U/ml thrombin, 3 mM $MnCl_2$ and 3 mM DTT. The numbers on each sample refer to the donor number and spectrum number for that particular donor, for example unact1_2 refers to unactivated platelets, donor number 1 and spectrum number 2. The graph is a scatter plot of the first principal component (PC-1) versus the second principal component (PC-2). Data shown is 3 - 5 spectra from n=4 independent experiments.

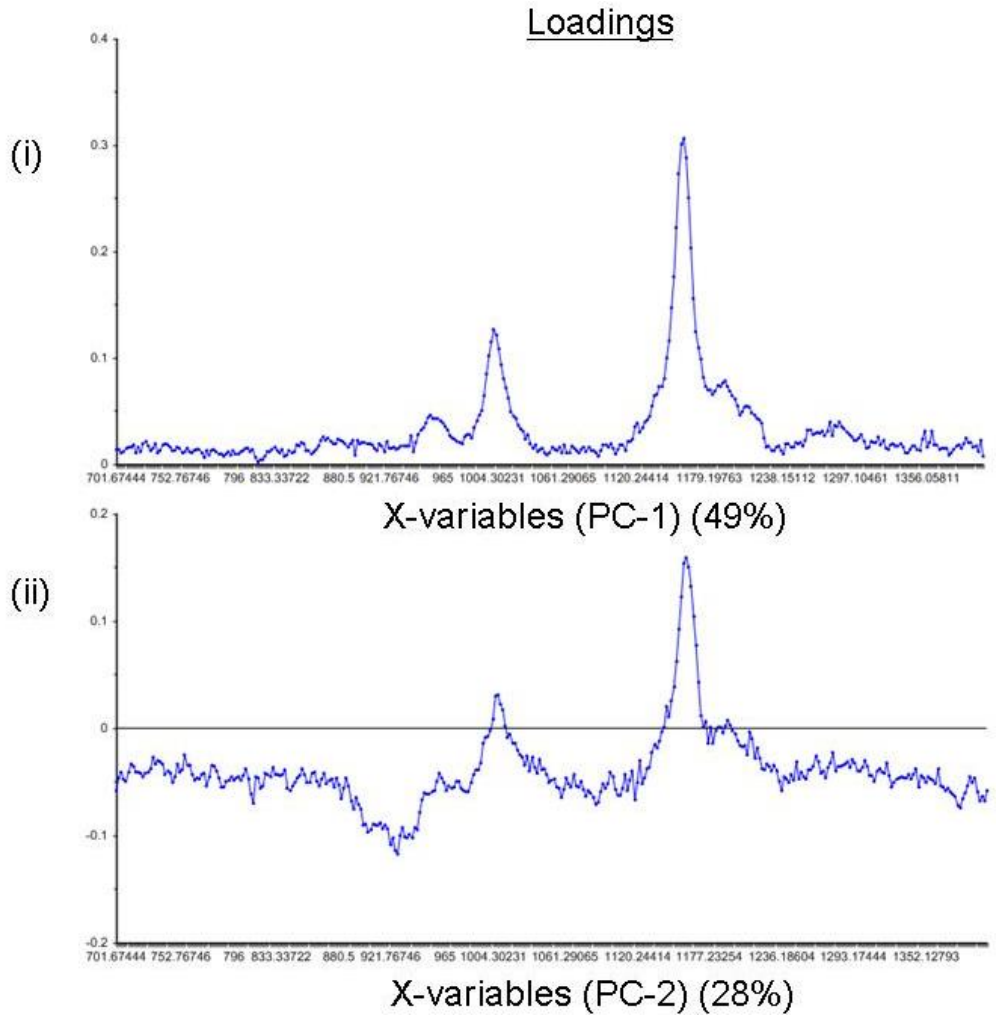

Figure 3.21 (c) The loadings of the two principal components used in the Principal component analysis (PCA) scatter plot of the 700 – 1400 cm^{-1} region only: (i) Principal component-1 (PC-1) and (ii) Principal component-2 (PC-2). The components are numbered according to the amount of variance they account for. PCA analysis was carried out on the baseline subtracted and normalised Raman data of all samples, the 700 – 1400 cm^{-1} region only, using The Unscrambler® software.

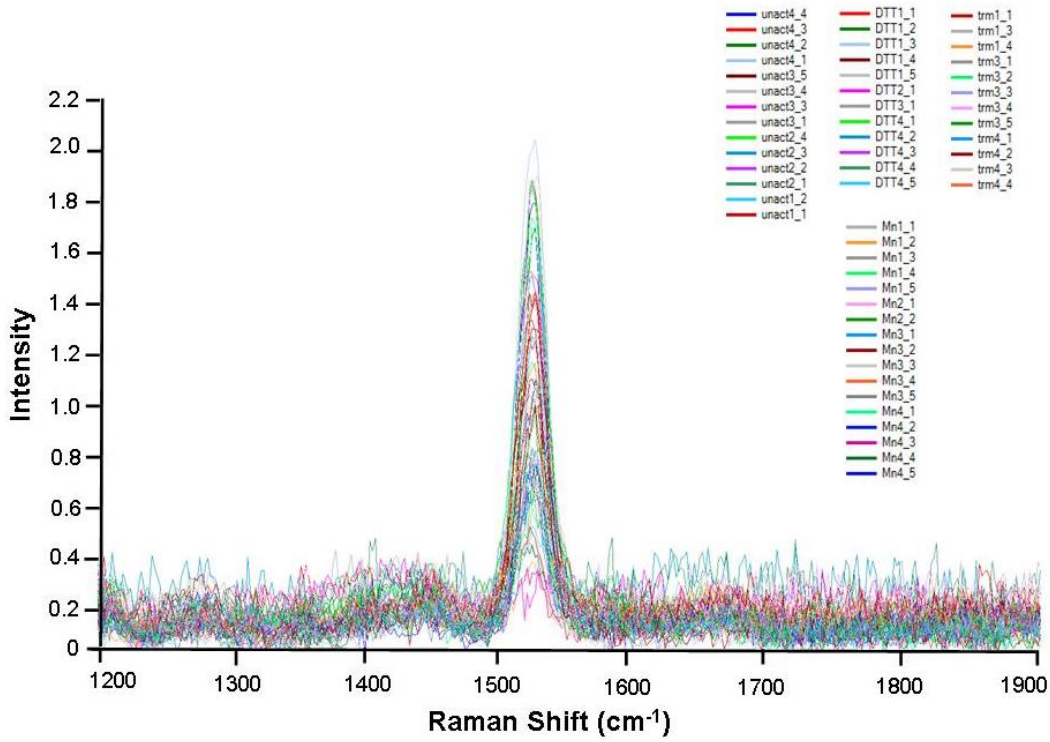

Figure 3.22 (a) The 1200 – 1900 cm^{-1} region of the Raman spectra for all unactivated platelet samples or platelet samples activated with either 1U/ml thrombin, 3 mM $MnCl_2$ or 3 mM DTT. Gel-filtered platelets were fixed with 1 % formaldehyde, centrifuged and supernatant removed. Raman spectra were obtained from the resulting platelet pellet. Spectra were baseline subtracted and normalised to the lipid peak at approximately 3000 cm^{-1}. Data shown is 3 – 5 spectra from n=4 independent experiments.

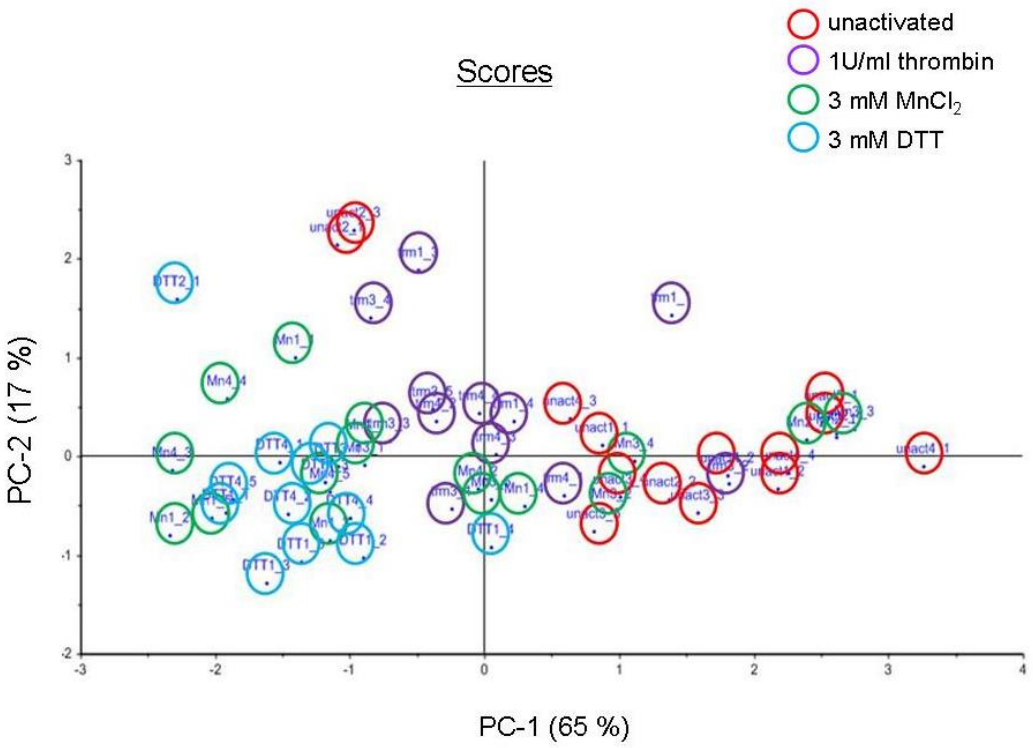

Figure 3.22 (b) Principal component analysis (PCA) of the 1200 – 1900 cm^{-1} region showing distinct clustering of samples based on the platelet activator. PCA analysis was performed on the Raman spectra of gel-filtered platelets which were unactivated or activated with either 1U/ml thrombin, 3 mM $MnCl_2$ and 3 mM DTT. The numbers on each sample refer to the donor number and spectrum number for that particular donor, for example unact1_2 refers to unactivated platelets, donor number 1 and spectrum number 2. The graph is a scatter plot of the first principal component (PC-1) versus the second principal component (PC-2). Data shown is 3 - 5 spectra from n=4 independent experiments.

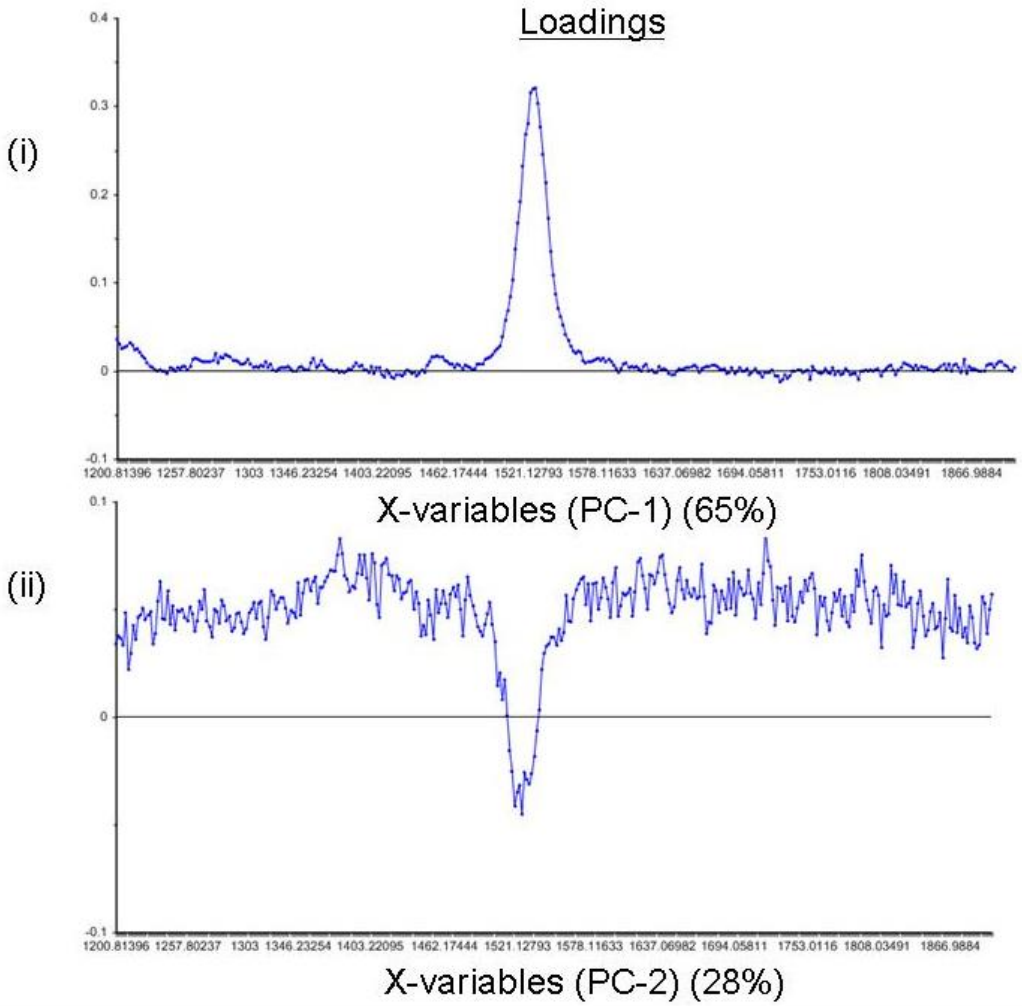

Figure 3.22 (c) The loadings of the two principal components used in the Principal component analysis (PCA) scatter plot of the 1200 – 1900 cm^{-1} region only: (i) Principal component-1 (PC-1) and (ii) Principal component (PC-2). The components are numbered according to the amount of variance they account for. PCA analysis was carried out on the baseline subtracted and normalised Raman data of all samples, the 1200 – 1900 cm^{-1} region only, using The Unscrambler® software.

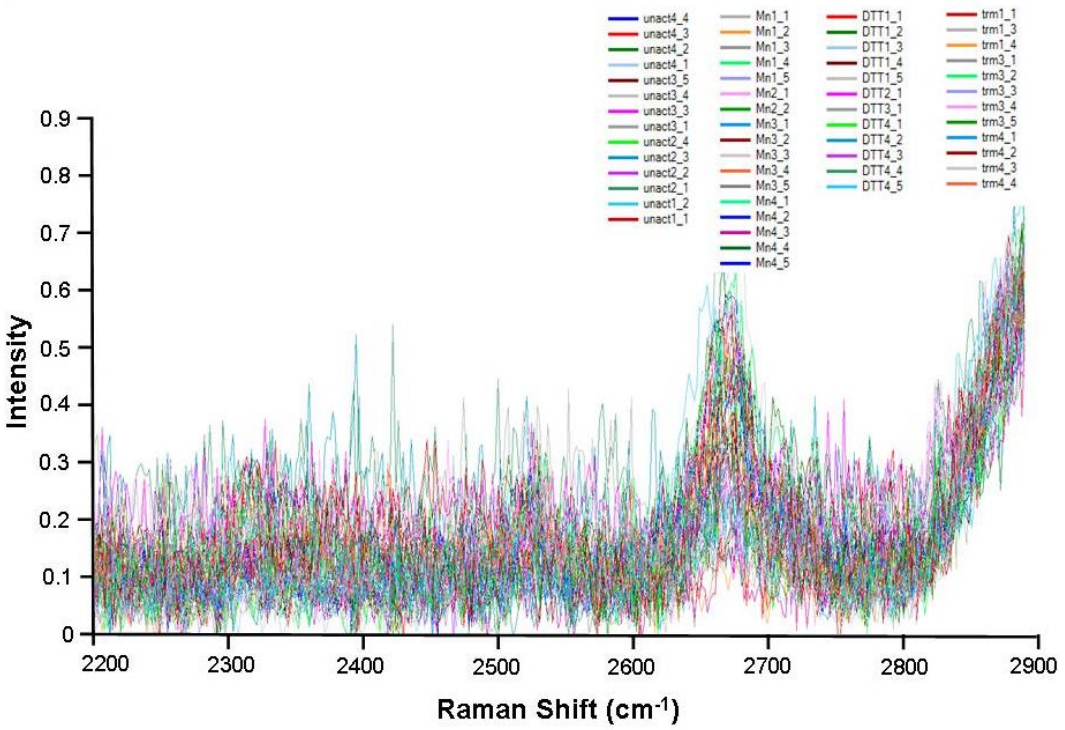

Figure 3.23 (a) The 2200 – 2900 cm^{-1} region of the Raman spectra for all unactivated platelet samples or platelet samples activated with either 1U/ml thrombin, 3 mM $MnCl_2$ or 3 mM DTT. Gel-filtered platelets were fixed with 1 % formaldehyde, centrifuged and supernatant removed. Raman spectra were obtained from the resulting platelet pellet. Spectra were baseline subtracted and normalised to the lipid peak at approximately 3000 cm^{-1}. Data shown is 3 – 5 spectra from n=4 independent experiments.

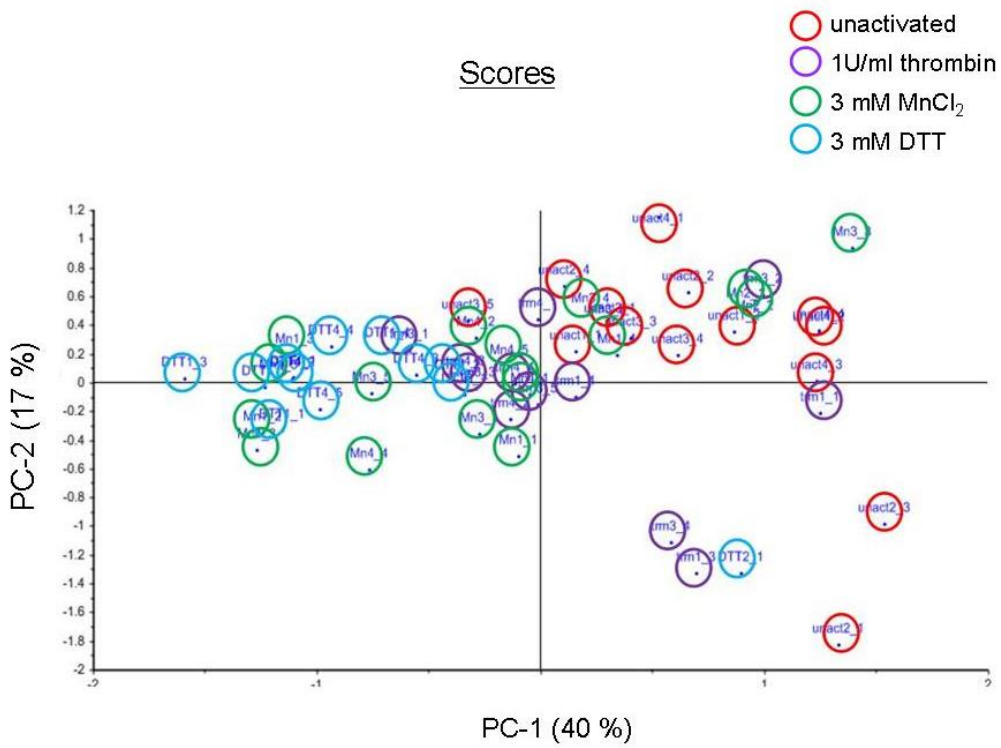

Figure 3.23 (b) Principal component analysis (PCA) of the 2200 – 2900 cm^{-1} region showing distinct clustering of samples based on the platelet activator. PCA analysis was performed on the Raman spectra of gel-filtered platelets which were unactivated or activated with either 1U/ml thrombin, 3 mM $MnCl_2$ and 3 mM DTT. The numbers on each sample refer to the donor number and spectrum number for that particular donor, for example unact1_2 refers to unactivated platelets, donor number 1 and spectrum number 2. The graph is a scatter plot of the first principal component (PC-1) versus the second principal component (PC-2). Data shown is 3 - 5 spectra from n=4 independent experiments.

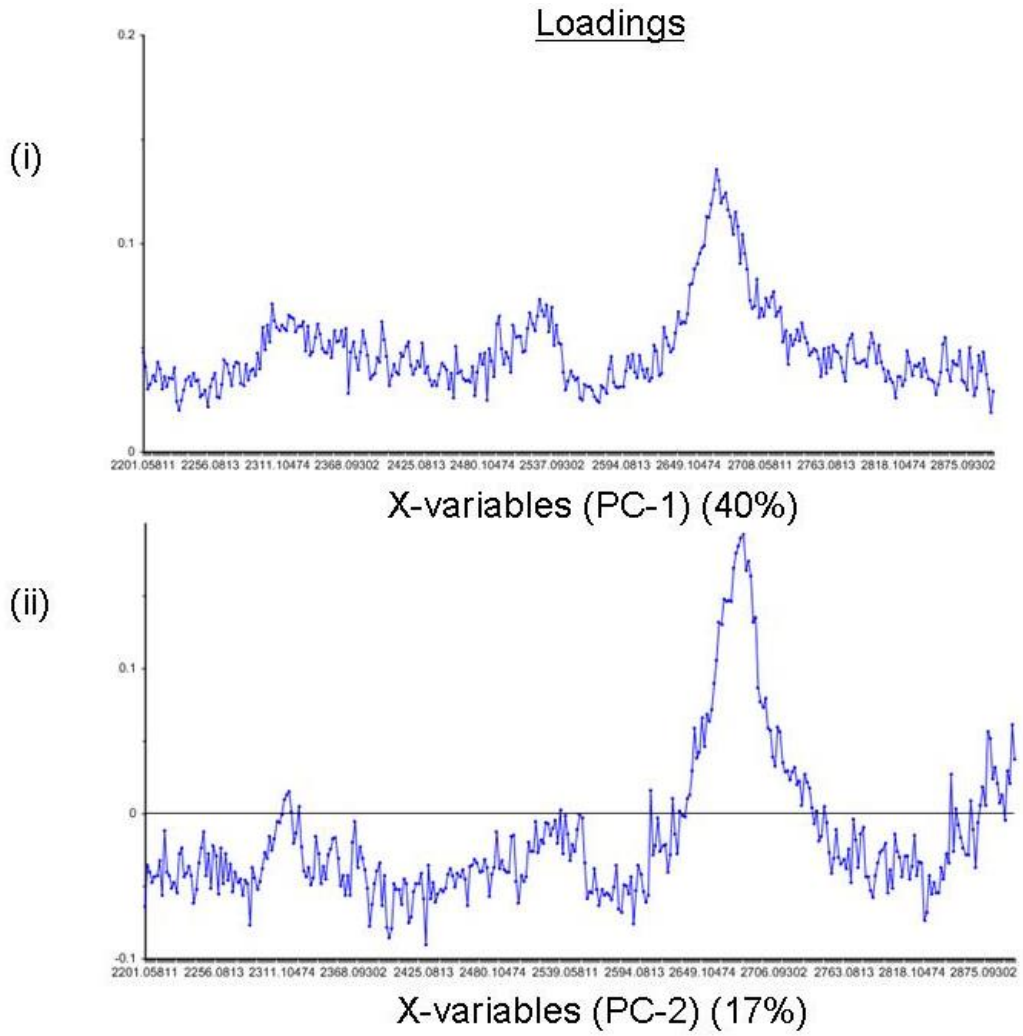

Figure 3.23 (c) The loadings of the two principal components used in the Principal component analysis (PCA) scatter plot of the 2200 – 2900 cm^{-1} region only: (i) Principal component-1 (PC-1) and (ii) Principal component (PC-2). The components are numbered according to the amount of variance they account for. PCA analysis was carried out on the baseline subtracted and normalised Raman data of all samples, the 2200 – 2900 cm^{-1} region only, using The Unscrambler® software.

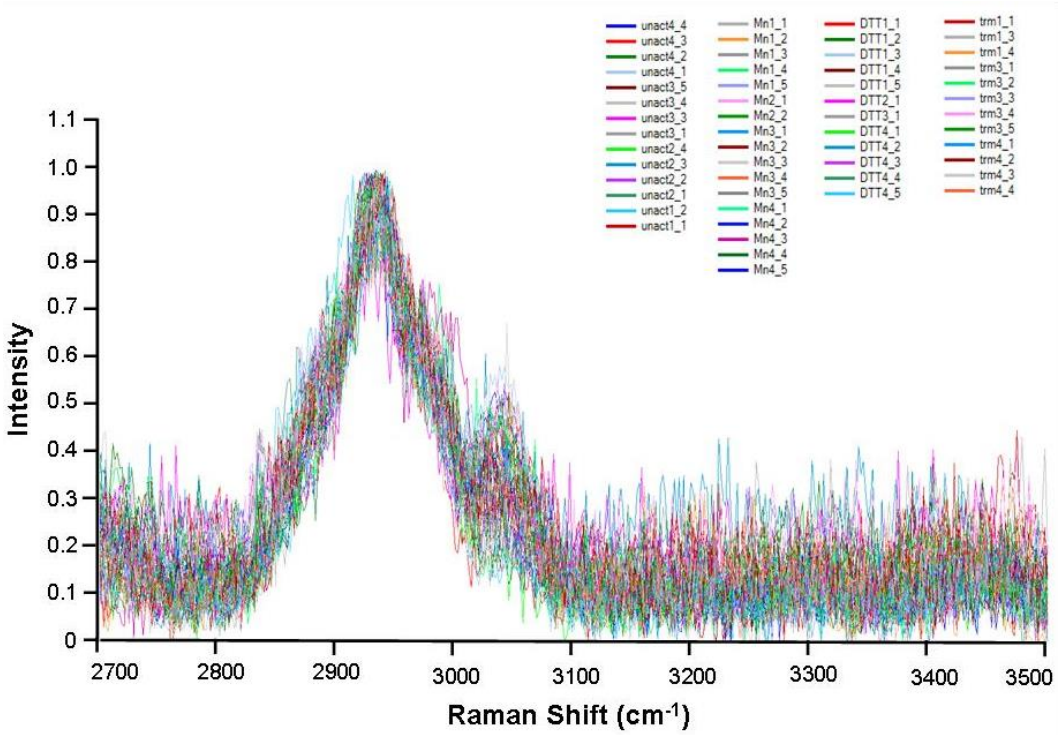

Figure 3.24 (a) The 2700 – 3500 cm^{-1} region of the Raman spectra for all unactivated platelet samples or platelet samples activated with either 1U/ml thrombin, 3 mM $MnCl_2$ or 3 mM DTT. Gel-filtered platelets were fixed with 1 % formaldehyde, centrifuged, supernatant removed. Raman spectra were obtained from the resulting platelet pellet. Spectra were baseline subtracted and normalised to the lipid peak at approximately 3000 cm^{-1}. Data shown is 3 – 5 spectra from n=4 independent experiments.

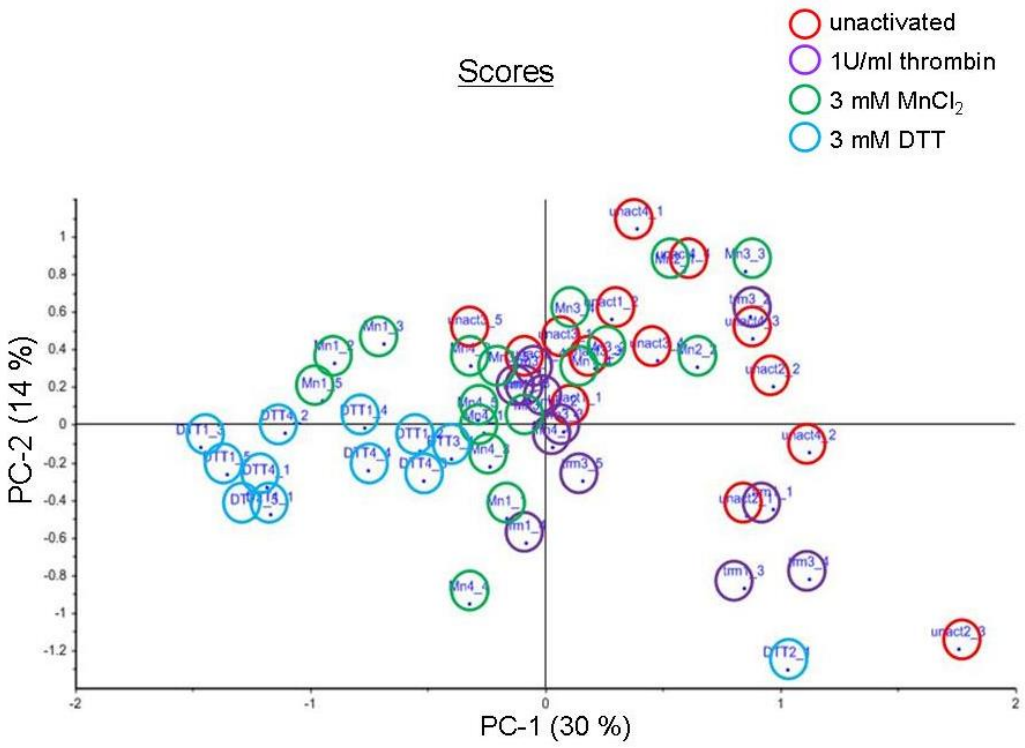

Figure 3.24 (b) Principal component analysis (PCA) of the 2700 – 3500 cm^{-1} region showing distinct clustering of samples based on the platelet activator. PCA analysis was performed on the Raman spectra of gel-filtered platelets which were unactivated or activated with either 1U/ml thrombin, 3 mM $MnCl_2$ or 3 mM DTT. The numbers on each sample refer to the donor number and spectrum number for that particular donor, for example unact1_2 refers to unactivated platelets, donor number 1 and spectrum number 2. The graph is a scatter plot of the first principal component (PC-1) versus the second principal component (PC-2). Data shown is 3 - 5 spectra from n=4 independent experiments.

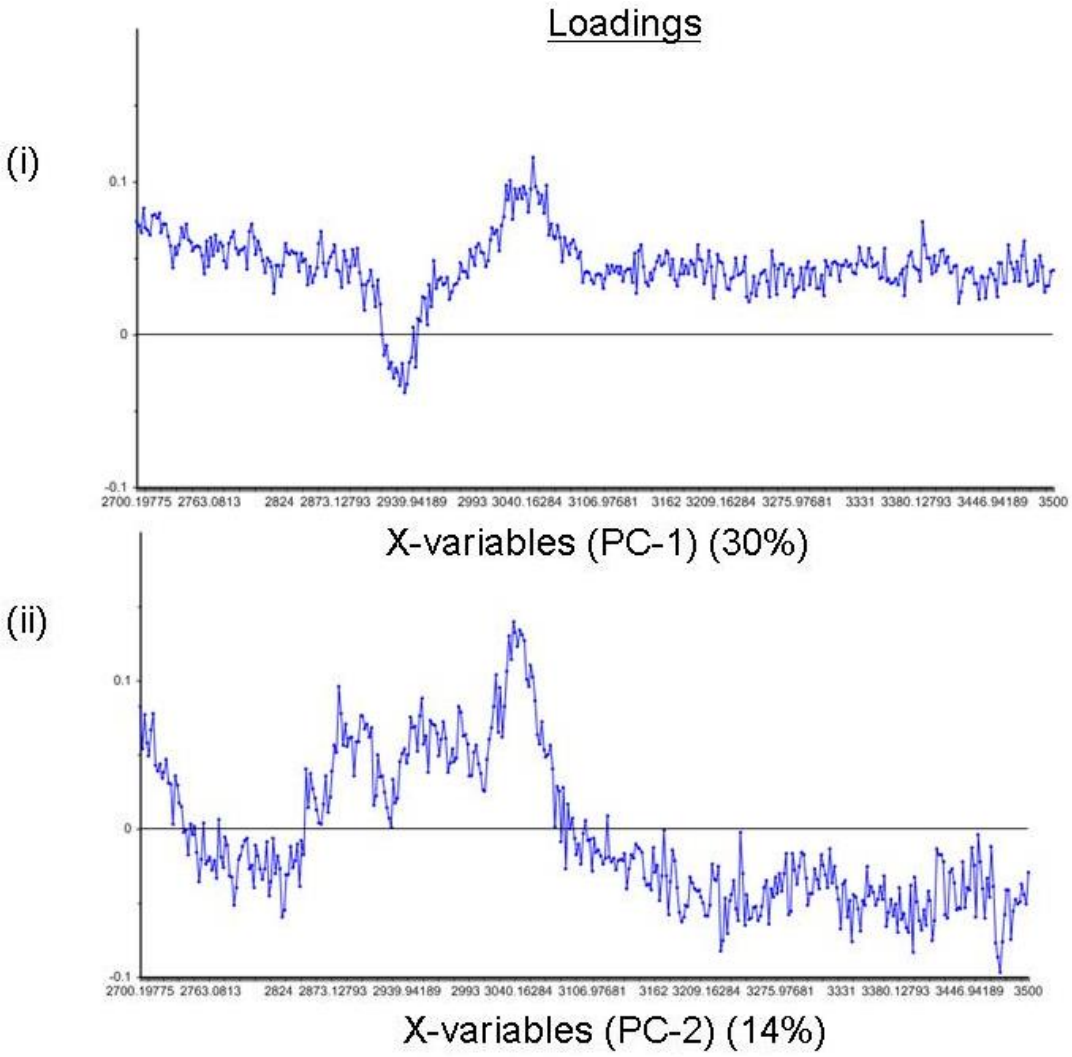

Figure 3.24 (c) The loadings of the two principal components used in the Principal component analysis (PCA) scatter plot of the 2700 – 3500 cm^{-1} region only: (i) Principal component-1 PC-1 and (ii) Principal component-2 (PC-2). The components are numbered according to the amount of variance they account for. PCA analysis was carried out on the baseline subtracted and normalised Raman data of all samples, the 2700 – 3500 cm^{-1} region only, using The Unscrambler® software.

3.3 Discussion

Extensive research investigating the significance of thiols in integrin $\alpha_{IIb}\beta_3$ has been carried out. Platelet activation leads to reduction of disulphide bonds, with a concomitant increase in free thiols, within the cysteine rich repeats of integrin $\alpha_{IIb}\beta_3$. This causes conformational changes of the integrin and exposure of ligand binding sites (Yan & Smith, 2000). In my studies, I have confirmed that in a purified, cell-free system $MnCl_2$ does indeed cause an increase in the free thiol population of integrin $\alpha_{IIb}\beta_3$ which is associated with an activated conformation of the integrin. Modification of thiol/disulphide groups in integrin $\alpha_{IIb}\beta_3$ by thiol blockers or reducing reagents can impact on its function (Essex et al, 2001; Lahav et al, 2000; Manickam et al, 2008; Margaritis, 2011; Yan & Smith, 2001). However, the impact of an altered redox environment employing low-molecular-weight thiols, such as glutathione, at various redox potentials on the function of integrin $\alpha_{IIb}\beta_3$ has yet to be explored in detail until now.

Reduced (GSH) and oxidised glutathione (GSSG) were combined, in ratios determined by the Nernst equation and outlined in Tables 2.1 and 2.2, to generate reducing (-264 mV), mean (-130 mV) and oxidising (-10 mV) redox environments. The increase in free thiols in integrin upon activation by $MnCl_2$ persisted in an oxidising redox environment. This indicates the generation of this thiol population is a robust event. Interestingly, it was found that a reducing redox environment completely abolished the increase in the free thiol population induced by $MnCl_2$ in purified integrin $\alpha_{IIb}\beta_3$. An investigation into the impact of GSH/GSSG redox potentials on the activation state of integrin $\alpha_{IIb}\beta_3$ expressed

on FF CHO-K1 cells demonstrated that a reducing redox environment inhibited activation of the integrin induced by $MnCl_2$. It has been previously demonstrated in our laboratory that GSH (3 mM) could decrease $MnCl_2$ induced integrin $\alpha_{IIb}\beta_3$ activation in platelets (Walsh et al, 2004). Of particular interest in this study here, however, is the concentration of GSH used to generate the redox potential of -264 mV, which was only 45 μM, more than a 60 fold decrease in concentration. This demonstrates a sensitivity of the receptor to the external redox environment. This finding indicates a rearrangement or shuffling of thiol/disulphide groups rather than simply a reduction of disulphide bonds. It may also be potentially as a result of a direct modification of the thiol groups in a process known as S-glutathionylation. S-glutathionylation is a reversible process in which mixed disulphide bonds are formed between the thiol group of the protein itself and glutathione (Dalle-Donne et al, 2007). It is a potential mechanism for the post-translational regulation of proteins. This thiol modification is associated with the reactivity of the cysteine residues in the protein, integrin $\alpha_{IIb}\beta_3$ in this case. Reactivity of a cysteine is determined by its pK_a value which can be variable, depending on electrostatic interactions with adjacent amino acids. A reactive cysteine can form a thiolate in redox-sensitive proteins. A cysteine thiolate anion (S^-) (i.e., an 'active cysteine'), can react to form a mixed disulfide with GSH or a protein disulfide (Rhee et al, 2000). The formation of a thiolate anion is favoured by the presence of basic amino acids (histidine (H), lysine (K) or arginine (R)) in the vicinity of the cysteine. The β_3-subunit of integrin $\alpha_{IIb}\beta_3$ contains 56 cysteine residues. An examination of the protein sequence and, specifically, cysteine residues of the β_3-subunit by my colleague, Dr. Desmond Murphy (personal communication), found there are 10

cysteine residues adjacent to a single basic amino acid present. This gives rise to a redox sensitivity within the integrin, thus supporting the theory of S-glutathionylation of critical cysteine residues involved in the activation mechanism of integrin $\alpha_{IIb}\beta_3$.

The platelet aggregation and flow cytometry studies demonstrated thrombin, $MnCl_2$ and DTT activate platelets to different extents. Thrombin is a potent physiological platelet agonist. Therefore, as anticipated, it activated platelets to a large extent as opposed to DTT and $MnCl_2$ which are not physiological platelet agonists. The potency of thrombin as a platelet activator was confirmed with platelet aggregation levels of approximately 80 %, PAC-1 binding of 70 % and CD62P binding of 42 %. DTT is a strong reducing agent and induces platelet aggregation by reducing disulphide bonds on the platelets surface and causing the activation of integrins in particular. The reduction of disulphide bonds within the cysteine-rich domain in integrin $\alpha_{IIb}\beta_3$ leads to an active conformation of the integrin (Walsh et al., 2004). This was confirmed in this study as platelets in the presence of DTT had approximately 40 % PAC-1 binding, compared to 2 % with unactivated platelets. DTT also induced approximately 40 % platelet aggregation. From the CD62P data it can be seen that there is no platelet degranulation or secretion associated with DTT activation. $MnCl_2$ is a known universal integrin activator. Integrins are known to bind their ligands in a divalent cation-dependent manner and manganese promotes this binding (Humphries et al, 2003). The flow cytometry studies show that $MnCl_2$ increases PAC-1 binding (approximately 20 %), in comparison to unactivated platelets (approximately 2 %), therefore, indicating the presence of

an active conformation of integrin $\alpha_{IIb}\beta_3$. $MnCl_2$ also induces approximately 10 % platelet aggregation. There is no CD62P binding associated with platelets activated by $MnCl_2$ which indicates that no platelet degranulation has occurred. In the case of both DTT and $MnCl_2$, the lack of platelet secretion implies that neither of these platelet activators is potent enough to induce further intra-platelet signalling and, consequently, complete platelet activation. The results of the platelet aggregation studies, levels of PAC-1 binding and levels of secretion indicated by CD62P binding, confirm each of the platelet activators acts on the platelets in a different manner. It was anticipated that the differences observed in these platelet function assays between platelets activated with the various activators, would be reflected by differences in platelet membrane structure and revealed in the analysis of platelets by Raman spectroscopy (RS).

A number of successful studies have been carried out using RS and the spectral analysis method of principal component analysis (PCA) in the evaluation of biological samples in recent years. Crow *et al* showed that Raman can be used as a method to distinguish between benign and malignant bladder and prostate cancers with an accuracy of 84 % and 86 % respectively (Crow et al, 2005). These numbers are compared to standard histological and classification by a uropathologist prior to Raman analysis. This study demonstrates the high level of accuracy of RS analysis *in vitro* and paves the way for the introduction of RS to a clinical *in vivo* setting. In a separate study of renal cancer, RS could differentiate normal and tumoural renal tissue, high and low-grade renal cell carcinoma (RCC) along with histological subtypes of RCC (Bensalah et al, 2010). This study highlights the sensitivity of RS, not only can it

distinguish between normal and tumoural tissue but it can be used to differentiate various grades of tumoural tissue. Similarly, a study investigating the potential of RS as a cervical cancer diagnosis tool found that RS was highly sensitive to biochemical changes in tissue allowing them to discriminate between normal cervical tissue, cervical intraepithelial neoplasia (CIN) and invasive carcinoma (Lyng et al, 2007). The results showed high sensitivity and specificity with accuracy between 98 – 100 %. These numbers were based on the comparison of Raman results to the prior classification of samples by a consultant pathologist. A very small number of samples were incorrectly classified but importantly no abnormal samples were classified as normal.

All of these studies have focussed on the diagnosis of tissue states. It is important also to understand the spectral features of the tissue components, i.e. the individual cells and their subcellular components. There is a growing interest in the use of RS to study cells alone as opposed to studying tissue samples in which there are a variety of cells present. The morphology and biochemical composition of cells are commonly studied using electron microscopy or fluorescent spectroscopy. These methods require extensive preparation, which may compromise the integrity of the sample, and also staining or markers need to be decided on in advance. Potentially, RS can overcome these limiting issues. While it may be advantageous in some cases, RS does not specifically require staining or labelling in general. The inelastic scattering of light by Raman-active vibrational modes, upon which the principle of RS is based, ensures the molecular specificity of RS. These properties, combined with immediate results, make RS a valuable analytical tool in the characterisation of

cellular processes. In a study examining the sensitivity of RS as a tool for studying single cells Krafft *et al* found that upon analysis of individual spectra combined with Raman mapping data of a variety of cells they could identify individual bands corresponding to proteins, lipids and nucleic acids. They also found that the relative intensities of these bands was dependent on the specific location of the components within the cells (Krafft, 2003). To date, Raman has not been used routinely as a tool to examine platelet activation processes. However, studies have been carried out using RS to investigate the effects of activation on the molecular structure of other cell types. One such study found clear differences in the spectra of eosinophils in an unactivated state compared to the spectra of those stimulated with interleukin-5 (IL-5) (Puppels, 1995). They found that activation of eosinophils leads to the secretion of granule contents so that little or no eosinophil peroxidase (EPO) remains in the cells. A decrease in the intensity of the EPO peak along with a shift in the mid peak value from 1352 cm^{-1} in unactivated eosinophils to 1369 cm^{-1} in activated eosinophils illustrated this finding. This peak shift was also indicative of a change in the iron oxidation state of EPO from 3^+ to 2^+. These were significant observations with regard to elucidating the activation mechanism of eosinophils.

Based on the interesting results from the purified integrin $\alpha_{IIb}\beta_3$ assays, in addition to the flow cytometry and platelet aggregation studies in which the levels of PAC-1 binding to activated integrin and the levels of platelet aggregation varied depending on the platelet activator, it was anticipated changes in the spectra, particularly in the regions of thiols and disulphides, of platelets would be evident. Any change in the thiol region should correspond to

a similar, complementary shift in the disulphide region. PCA analysis of both the thiol and disulphide regions of the platelet Raman spectra show that these regions do, indeed, contribute to the separation of the platelet spectra into distinct clusters based on the platelet activator. In the thiol region, the score plot of PC-2 versus PC-3 shows the most obvious clustering of the platelet samples (Figure 3.17 (b)). When I examined the loadings of these principal components, the peaks present corresponded to the thiol (-SH) stretch. In the case of complex biological samples such as platelets, it can prove difficult to attribute differences in the region to specific events. However, any differences in this region can be indicative of not only a change in the absolute number of thiol groups present but may also indicate shuffling or rearrangement of the bonds or changes in the strain on the cysteine bonds.

The score plot in the analysis of the disulphide stretch demonstrates that when PC-1 is plotted against PC-3, the Raman spectra can be discriminated from each other according to the platelet activator. The separation of the Raman spectra here is not as clean as in other regions as there tends to be higher noise levels in the region. However, there is a definite trend towards the clustering of the Raman spectra according to the platelet activator. Changes in this region may be due to shuffling or rearrangement, along with reduction of disulphide bonds, which would be consistent with the results we have found in the thiol region of the spectrum. This result also strengthens the model of thiol/disulphide exchange mechanisms involved in platelet activation (Essex & Li, 1999; Walsh et al, 2004).

It was also predicted there would be a change in the amide I (1630 – 1700 cm^{-1}) and amide III (1230 – 1310 cm^{-1}) regions, whereby platelet activation may cause a change in the secondary protein structure. Based on this prediction, these two regions were focussed on, in a similar manner to the thiol and disulphide stretches. As anticipated, in both amides I and III regions Raman spectra could be separated according to the platelet activator. The score plots for both cases do not show as good discrimination as expected but there is a clear trend present. Changes in these amide stretches indicate alterations in the α-helix and β-sheet content of proteins. The amide I mode is described as a CO stretching mode with some mixture of CCN deformation (Chen et al, 1994). Using the amide I band for structural analysis is known to be difficult, necessitating a combination of experiments with classical and quantum methods for advanced interpretation (Petersen & Nielsen, 2009). The amide III is a CN stretch and NH in-plane bending mode with $C(C)H_3$ symmetric bending and CO in plane bending contributions (Jordan & Spiro, 1994). From my current data, it is not possible to determine what exact modifications in protein secondary structure are occurring due to platelet activation or how each activator is actually inducing these modifications.

The score plot is a projection of data onto subspace used to interpret relations amongst observations. PCA of each of the regions extracted from the full spectrum all platelet samples invariably demonstrated a visible trend in their location within the score scatter plots. The consistency in these results gave increased confidence in the data analysis. This ensured there was no bias when stating platelet activation states could be discriminated in a region of particular

interest such as the thiol/disulphide region. Clustering or grouping of samples within PCA score plots indicates similarities between the samples. Conversely, the platelet samples in this study were clearly distinct and separate from each other demonstrating obvious differences. In order to convey absolute confidence in the analysis, further multivariate analysis of the data such as linear discriminant analysis (LDA) or Fisher's discriminant analysis (FDA) or the development of an appropriate mathematical algorithm would be required. In this case, PCA was a sufficient analysis indicating platelets do indeed express structural differences upon activation and these differences in fact are also dependent on the platelet activator in question.

Following the analysis of specific regions within the platelet Raman spectrum in which we expected to find differences, a comprehensive analysis was performed in order to ensure important information was not overlooked. Further examination revealed the presence of a prominent carotenoid or lipid peak in each of these stretches in unactivated and activated platelets. The 700 - 1400 cm^{-1} stretch contains very strong Raman peaks at 968 cm^{-1}, 1006 cm^{-1} and 1160 cm^{-1}. The region from 1200 – 1900 cm^{-1} also contains a major peak at 1525 cm^{-1}. All of these peaks are characteristic spectral features of carotenoids. Carotenoids are a group of organic pigments, lipid in nature, which are found in most cell membranes including platelets (Stefanini et al, 1957). The exact role of carotenoids in cell membranes has yet to be fully elucidated but the antioxidant properties of carotenoids are particularly interesting with regard to their potential role in platelets (Di Mascio et al, 1989).

In summary, it has been found that Raman spectroscopy, combined with the multivariate statistical analysis technique PCA, may be employed as a novel tool to investigate the activation state of platelets. The structural components of platelets which have emerged as crucial in the discrimination of platelets in various states of activation are the lipids, carotenoids, thiols, disulphides, along with both amide I and III. The discovery that the thiol and disulphide regions of the platelet Raman spectrum contribute to the discrimination of platelet activation states is a particularly exciting result. These observations, combined with the potential antioxidant function of carotenoids further compound the importance of thiol populations, the redox environment and oxidative/reductive stress on platelet function. In Chapter 4, I will further investigate the role of thiols and redox in platelets.

Chapter 4

The external redox environment regulates platelet function through modulating the platelet surface thiol population

4.1 Introduction

The redox environment of a cell, biological fluid or tissue is defined by the state of the low-molecular-weight redox couples present, along with reactive oxygen and nitrogen species (RONS) and their respective scavengers. Studies relating to redox environments have become increasingly popular in recent times due to the expanding number of disease states in which oxidative stress has been implicated. The redox homeostasis within biological systems is emerging as a critical regulatory factor as disturbances in this balance can have profound effects.

RONS are readily generated during normal energy metabolism, and are typically scavenged and recycled. However, in the event of an imbalance in the system whereby there is an over-production of RONS or a depletion of scavengers or antioxidants, oxidative stress can arise. Furthermore, a disparity in the low-molecular-weight thiol couples, such as glutathione (GSH/GSSG) or cysteine (Cys/CySS), in which the concentration of the oxidising form of the couple becomes greater than that of the reducing form, can also lead to the development of oxidative stress. Oxidative stress can disrupt the fundamental structure of proteins and lipids, ultimately, resulting in alterations of their physical and chemical properties.

Conversely, the phenomenon of reductive stress can also occur. Reductive stress arises upon a shift in the balance of the redox couple in favour of the reducing species. While it is less well known and researched, the implications of reductive stress may indeed be just as significant as those associated with oxidative stress. The modification of biological molecules during

oxidative/reductive stress is primarily due to the targeting of critical cysteine residues within their structure.

It has been established that there are a number of cysteine, or thiol, containing proteins associated with platelets (Essex & Li, 2006). This makes platelets prime targets for modifications as a result of oxidative/reductive stress. It, therefore, emphasises the importance of the extracellular redox environment in the regulation of platelet function.

Amongst these platelet thiol containing proteins are protein disulphide isomerase (PDI), glycoprotein Ibα (GPIbα) (Burgess, 2000) and $P2Y_{12}$, the ADP receptor (Ding, 2003). Thiol/disulphide groups have been shown to be intrinsic players in the regulation and modulation of the activity of platelet integrin $\alpha_{IIb}\beta_3$ (Manickam et al, 2011; Manickam et al, 2008; O'Neill et al, 2000; Yan & Smith, 2000; Yan & Smith, 2001) and this has been substantiated by the findings in Chapter 3.

Similarly, integrin $\alpha_2\beta_1$ also exhibits functional properties related to the presence of thiol/disulphide groups within its structure (Gofer-Dadosh, 1997; Lahav et al, 2000; Lahav et al, 2003). Integrin $\alpha_2\beta_1$ is one of the major collagen receptors on platelets. The other main collagen receptor is glycoprotein VI (GPVI). While information about the exact role of the collagen receptors in haemostasis and thrombosis is crucial to the development of clinical therapies, the individual role of these two receptors in the adhesion of platelets to collagen is not well defined as of yet. It remains unclear if there is a physical interaction or signalling events which occur between the receptors, or indeed if there is any interaction at all.

Some argue that GPVI is the central collagen receptor and that platelet adhesion to collagen initially requires GPVI-collagen interactions to initiate platelet activation. It is suggested that collagen binding initiates signalling from GPVI, inducing a conformational change in integrin $\alpha_2\beta_1$ allowing it to bind collagen, thereby increasing the strength of the adhesion.

However, the role of integrin $\alpha_2\beta_1$ may be underestimated, as the integrin itself can generate intracellular signals. Indeed, it has been demonstrated that patients deficient in integrin $\alpha_2\beta_1$ have more severe bleeding disorders than those deficient in GPVI. Reduced expression of integrin $\alpha_2\beta_1$ is associated with prolonged bleeding times, chronic mucocutaneous bleeding and reduced platelet adhesion to collagen (Nieuwenhuis et al, 1985). Additionally, over expression of integrin $\alpha_2\beta_1$ has been linked to an increased risk for the development of cardiovascular disease (Carlsson et al, 1999; Moshfegh et al, 1999; Samaha et al, 2005). On the other hand, mice deficient in the GPVI-FcR γ-chain have only minor effects with mildly increased bleeding times (Nieswandt et al, 2001b). Interestingly, a recent study suggests integrin $\alpha_2\beta_1$ can bind collagen, under shear, without receptor pre-activation (Nissinen et al, 2012). This further supports integrin $\alpha_2\beta_1$ as an independent collagen receptor capable of functioning without the need for inside-out signals. In the study, the authors suggest the initial low-affinity interaction between integrin $\alpha_2\beta_1$ and collagen induces signals to promote integrin activation. This leads to a high-affinity conformation of the integrin for its ligand resulting in firm adhesion (Nissinen et al, 2012). Furthermore, it has been demonstrated that a thiol/disulphide exchange mechanism is required for platelet adhesion to collagen via integrin

$\alpha_2\beta_1$, which is independent of GPVI and may be enzymatically catalysed by PDI (Lahav et al, 2003).

Previous work carried out in our laboratory has shown that altering the external redox environment impacts on platelets ability to function in response to collagen (Murphy et al, 2010). These findings, along with those of Lahav et al, are key to the studies carried out in this chapter.

In Chapter 3, an examination of platelets by Raman spectroscopy, combined with the multivariate statistical analysis technique, principle component analysis (PCA), revealed the importance of thiols and disulphides in the structure of platelet membranes. PCA analysis revealed that both thiol and disulphide groups were modified upon stimulation with the platelet activators. These modifications were unique to the platelet activator, as an analysis of the thiol (2550 – 2600 cm^{-1}) and disulphide (470 – 530 cm^{-1}) regions uncovered clustering of the Raman spectra based on the platelet activator (Figures 3.17 (a-c) and 3.18 (a-c)). Interestingly, the characteristic carotenoid profile of platelets also appeared to play a significant role in the discrimination of platelet Raman spectra. Based on these findings, an assessment of platelets activated with more physiologically relevant agonists using Raman spectroscopy was carried out. Subsequently, the free thiol population on the surface of platelets was examined in greater detail and the impact of altering the external redox environment on this thiol population was investigated.

A number of platelet agonists were used in the study, namely, thrombin, convulxin and collagen. As previously described, thrombin is a coagulation protein and a known potent physiological platelet activator. Collagen is the

major insoluble fibrous structural protein in the extracellular matrix and in connective tissue. It is the most thrombogenic component of the subendothelium (Baumgartner & Haudenschild, 1972). Upon vascular damage, collagen becomes exposed to circulating platelets. It acts as both a substrate for adhesion of platelets and also as a platelet activator through interactions with the receptors integrin $\alpha_2\beta_1$ and GPVI. Twenty-eight types of collagen, composed of 46 distinct polypeptide chains have been identified (Brinckmann, 2005). However, 80 – 90 % of all collagen in the body is either type I, II or III. Collagen has a triple helical structure formed by three parallel polypeptide strands in a left-handed, polyproline II-type (PPII) helical conformation. These polypeptides coil around each other with a one-residue stagger to form a right-handed 'coiled coil' or triple helix. The tight packing of the PPII helices dictates that every third amino acid in the sequence is a glycine (Gly, G). This results in a repeated sequence of XYGly, where X and Y are any amino acid. The amino acids seen most frequently at the X and Y position are proline (Pro, P) and 4-hydroxyproline (Hyp, O), with ProHypGly being the most abundant triplet in collagen (Ramshaw et al, 1998). Type I collagen is used in this study due to its tendency to favour binding to integrin $\alpha_2\beta_1$. It possesses a high affinity binding motif, a hexapeptide GFOGER (glycine, phenylalanine, hydroxyproline, glycine, glutamic acid, arginine), in its triple helix which was found co-crystallised with the I-domain of the α_2-subunit (Emsley et al, 2000; Knight et al, 1998; Knight et al, 2000).

Convulxin is a snake venom protein from a tropical rattlesnake *Crotalus durissus terrificus*. It is a C-type lectin composed of two subunits, α and β, which are cross-linked by disulphide bonds to form a hexamer: $\alpha_3\beta_3$. Convulxin

is a well-known, potent platelet activator which acts through specific binding to the collagen receptor GPVI (Niedergang et al, 2000). Therefore, this makes convulxin a useful tool in studies examining the interaction between collagen and its receptors. Similarly, in the platelet adhesion studies, collagen related peptide (CRP) was used due to its specificity for the GPVI receptor. CRP consists of a backbone of GPO (GlyProHyp) sequences which has the ability to spontaneously form the helical structure of collagen. CRP is recognised by and is a potent platelet activator specifically through GPVI (Knight et al, 1999). (This peptide sequence is also recognised by integrin $\alpha_2\beta_1$, however, there is no platelet reactivity associated with the interaction (Knight et al, 1999)).

The effects of both the glutathione redox couple and the cysteine redox couple on platelets were examined, as Go and Jones have shown that the redox couples do not exert any effect on each other (Go & Jones, 2005; Jones et al, 2004).

Other reducing and oxidising agents are also used in order to determine if the effects on platelet function observed with the addition of GSH/GSSG and Cys/CySS redox potentials were unique to these physiological redox couples. These include dithiothreitol (DTT) and tris(2-carboxyethyl)phosphine (TCEP), both of which are well-known reducing agents, and also reduced glutathione (GSH) alone. Oxidising environments are generated using DTNB (5,5'-dithiobis-(2-nitrobenzoic acid)), a thiol blocker, and also using the oxidising component of the redox couples alone, i.e. GSSG or CySS.

A number of assays will be performed in order to assess the thiol population on the surface of whole platelets under various redox conditions and activation

states. It is anticipated that changes in the surface thiol population will be detected, and any variations in this population may be attributed to a specific receptor or signalling pathway of platelets allowing us to further elucidate the role of thiols in platelet function.

.

4.2 Results

4.2.1 The effects of thrombin, collagen and convulxin on platelet molecular structure assessed by Raman spectroscopy

Platelets were unactivated or activated with either 0.1U/ml thrombin, 38 μg/ml collagen or 50 ng/ml convulxin and Raman spectra were obtained. Three to four spectra were obtained per platelet sample and an average spectrum for each condition per donor was generated (Figure 4.1 (a) (i)). Similarly, a signature or 'finger print' Raman spectrum for unactivated platelets and platelets activated with each agonist was generated by averaging the spectra from all donors in each condition (Figure 4.1 (a) (ii)).

Upon initial visual inspection of the Raman spectra in Figure 4.1 (a), any clear variation between unactivated and activated platelets was difficult to pinpoint. As mentioned in Chapter 3, to overcome this problem commonly experienced when analysing biological samples, principal component analysis (PCA) was performed on the platelet Raman data. Prior to carrying out PCA, all of the spectra were baseline subtracted and normalised to a peak at 3000 cm^{-1} using Origin® software. Normalisation of the data to one specific peak within the spectrum eliminates the differences in absolute signal intensity, which is influenced by environmental factors, and thereby ensures consistency across the data set. Initially, PCA was carried out on the full Raman spectra of all 10 independent donors and it was found that the majority of samples clustered quite close together, while others were scattered randomly. This made it difficult to establish a clear pattern between unactivated and activated platelets (Figure 4.1 (b) (i)). PCA was then performed on the average or signature

platelet Raman spectra and the PCA scatter plot was plotted. Although the samples were located in close proximity, they could be distinguished from each other (Figure 4.1 (b) (ii)). Subsequently, when the PCA scatter plot was zoomed in on and graphed on a larger scale, it demonstrated that the samples could be easily discriminated from each other based on the platelet activator (Figure 4.1 (b) (iii)). The loadings of the principal components used to construct the PCA scatter plots for all the individual donors are illustrated in Figure 4.1 (c), while the principal components for the signature spectra are illustrated in Figure 4.1 (d). The principal components highlight the areas which account for the most variance between samples. In order to further investigate the molecular differences between spectra, a number of important structural components were focussed on: thiol (2550 – 2600 cm^{-1}), disulphide (470 – 530 cm^{-1}), amide I (1630 – 1700 cm^{-1}) and amide III (1230 – 1310 cm^{-1}) regions. Due to the narrow spectral range of these structural components a slightly larger region was analysed.

A region stretching from 2400 – 2600 cm^{-1} encompassing the thiol region was extracted from the full Raman spectra of platelets and analysed. An analysis of the data through PCA of the signature spectra showed the samples could be separated based on the platelet activator (Figure 4.2 (a-c)).

Similarly, upon extraction of the disulphide containing region (400 – 650 cm^{-1}), despite the poor signal to noise ratio in this stretch, the platelet samples could be clearly discriminated according to the platelet activator upon PCA of the signature Raman spectra (Figure 4.3 (a-c)).

To investigate the potential protein structural rearrangement as a result of platelet activation the amide I (1600 – 1700 cm^{-1}) and amide III (1200 - 1400 cm^{-1}) stretches of the platelet Raman spectra were examined. Again, it was demonstrated that PCA could discriminate the samples according to the platelet activator (Figures 4.4 and 4.5).

For each of the thiol, disulphide and amide regions, the unactivated and the thrombin activated platelet sample were almost always found in close proximity to each other; whereas the collagen and convulxin activated platelet samples were almost frequently 'far away' from both the unactivated and thrombin samples and from each other. This was an interesting observation and due to the consistency of the trend from region to region it indicates a correlation between collagen and convulxin compared to either with unactivated or thrombin.

Furthermore, the spectra were subsequently divided into a number of regions, each one encompassing 700 cm^{-1} of the spectrum, overlapping the previous by 200 cm^{-1}. This in depth and rigorous analysis of the data ensured no potentially valuable data went undetected. The regions examined were as follows:

- Region 1: 200 – 900 cm^{-1}
- Region 2: 700 – 1400 cm^{-1}
- Region 3: 1200 – 1900 cm^{-1}

- Region 4: 1700 – 2400 cm^{-1}
- Region 5: 2200 – 2900 cm^{-1}
- Region 6: 2700 – 3500 cm^{-1}

Regions 2, 3, 5 and 6 proved to be of most significance and interest. As was demonstrated previously in Chapter 3, these regions were found to contain at least one peak, corresponding to a carotenoid or lipid group, which accounted for the most variance across the data set (Figures 4.6 – 4.10). These findings suggested the carotenoid profile plays a significant role in the separation of the platelet Raman spectra. Therefore, further examination of the impact of these carotenoid peaks on platelet activation was necessitated. The characteristic carotenoid profile is labelled in the signature Raman spectra of unactivated and activated platelets (Figure 4.10 (a)).

The intensity of characteristic carotenoid peaks at 968 cm^{-1}, 1006 cm^{-1}, 1160 cm^{-1} and 1525 cm^{-1} in the Raman spectra of all platelet samples was measured. The fold increase in the peak intensity at each of the four carotenoid peaks was calculated relative to that of unactivated platelets. While statistically not significant, it was interesting to note a trend towards an increase in the intensity of all of the carotenoids peaks in platelets activated with either thrombin, collagen or convulxin when compared to unactivated platelets (Figure 4.10 (b)).

4.2.2 The effects of an altered external redox environment on platelet aggregation

Thrombin, collagen and convulxin at concentrations of 0.1U/ml, 38 μg/ml and 50 ng/ml, respectively, induced comparable levels of platelet aggregation. Unactivated platelets did not aggregate while all activated platelets aggregated to levels of approximately 80 % (n=4, ***p < 0.001) (Figure 4.11).

The redox reagents glutathione, both reduced (GSH) and oxidised (GSSG), and cysteine (Cys) and cystine (CySS) were prepared as stock solutions in 0.1 M hydrochloric acid (HCl) in order to reduce their tendency to convert to the alternative reduced or oxidised species of the redox couple. Prior to carrying out any experiments with the redox reagents, the impact of 1 mM HCl alone on platelet function was examined. It had no significant impact on the levels of platelet aggregation induced by 0.1U/ml thrombin, 38 μg/ml collagen or 50 ng/ml convulxin nor did it induce any platelet aggregation in unactivated platelets (n=4) (Figure 4.12). In fact, the maximum concentration of HCl to which the platelets were exposed was in the micromolar (μM) range, and therefore any ‘interference’ from HCl on the activity of the platelets in these experiments was ruled out.

In previous work carried out by my colleague, Dr. Desmond Murphy (Murphy et al, 2010), redox potentials were generated by combining reduced (GSH) and oxidised (GSSG) or cysteine (Cys) and cystine (CySS) in various ratios according to the Nernst equation and their impact on platelet aggregation was

examined. It was shown that neither the GSH/GSSG or Cys/CySS redox potentials (oxidising, mean or reducing) had any effect on the platelet aggregation response of unactivated platelets (n=6) (Figure 4.13). Additionally, it was demonstrated platelet aggregation to collagen was completely inhibited in the presence of a reducing external redox environment (GSH/GSSG: -264 mV and Cys/CySS: -148 mV). As the external redox environment was altered by mean (GSH/GSSG: -130 mV, Cys/CySS: -82 mV) and oxidising (GSH/GSSG: -10 mV, CyS/CySS: +4 mV) redox potentials, the platelet aggregation response to collagen was restored to levels observed in platelets in which the external redox environment was not altered. In contrast, platelet aggregation induced by thrombin or convulxin was not affected by either a reducing, mean or oxidising external environment generated by GSH/GSSG or Cys/CySS redox potentials (n=6, ***$p < 0.001$) (Figure 4.14).

In order to further investigate this phenomenon, the effect of alternative reducing or oxidising agents on the levels of platelet aggregation of unactivated platelets and platelets activated with 0.1U/ml thrombin, 38 μg/ml collagen and 50 ng/ml convulxin were examined. The effects of the well-known reducing agents dithiothreitol (DTT) and *tris*(2-carboxyethyl)phosphine (TCEP), along with reduced glutathione (GSH) alone, on platelet aggregation were investigated. Platelet aggregation induced by collagen was inhibited by 45 μM DTT, 45 μM TCEP and 45 μM GSH. There was no effect on the level of platelet aggregation induced by thrombin or convulxin in the presence of any of the reducing agents (n=4, ***$p < 0.001$) (Figure 4.15 (a)).

The effects of oxidising agents on the platelet aggregation response to 0.1U/ml thrombin, 38 μg/ml collagen and 50 ng/ml convulxin were also investigated. Oxidised glutathione (GSSG) alone, cystine, (CySS) alone and 5, 5'-Dithio-bis-(2-nitrobenzoic acid) (DTNB), at a concentration of 45 μM, were chosen as oxidising agents. It was found that none of these agents had any significant effect on platelet aggregation in unactivated platelets or platelets activated with thrombin, collagen or convulxin (n=4) (Figure 4.15 (b)). This was a result consistent to that seen with platelets in the presence of oxidising redox environments generated by GSH/GSSG and Cys/CySS redox potentials (Figure 4.14).

4.2.3 Investigation into the signalling pathway of type I collagen

Throughout this study, type I collagen was used based on the assumption that it was signalling primarily through integrin $\alpha_2\beta_1$, as opposed to glycoprotein VI (GPVI). As a control, convulxin, a GPVI specific agonist was used. However, due to the interesting results observed thus far with altered redox environments and their impact specifically on the activation of platelets by collagen, it was deemed essential to clarify that the type I collagen used was indeed interacting with integrin $\alpha_2\beta_1$.

A broad Src family kinase inhibitor, PP2 (25 μM), inhibited platelet aggregation to both 38 μg/ml collagen and 50 ng/ml convulxin. PP2 had no effect on the platelet aggregation response of unactivated platelets or platelets activated with 0.1U/ml thrombin. (n=4, ***$p < 0.001$) (Figure 4.16 (a)).

Bay 61-3606 (5 μM), a specific Syk kinase inhibitor, inhibited platelet aggregation induced by 50 ng/ml convulxin. Bay 61-3606 had no significant impact on the level of platelet aggregation of unactivated platelets or platelets activated with 38 μg/ml collagen or 0.1U/ml thrombin (n=4, ***$p < 0.001$) (Figure 4.16 (b)).

4.2.4 Examination of the surface thiol population of platelets in suspension

The surface thiol population of platelets, in suspension, was examined using the well-known Ellman's test (Ellman, 1959), a colourimetric assay which employs Ellman's reagent, also known as 5, 5'-Dithio-bis-(2-nitrobenzoic acid) (DTNB). In the presence of a thiol group, DTNB is cleaved to form a mixed disulphide group and 2-nitro-5-benzoic acid (NTB). The ratio of thiol groups to NTB is 1:1. Therefore, measuring the concentration of NTB gives a direct measure of the numbers of free thiol groups present in a sample. NTB has an intense yellow colour, the absorbance of which was measured by a Wallac plate reader at a wave length of 405 nm.

In order to calculate the concentration of thiol groups detected on the surface of platelets, a standard curve was first generated with the thiol containing compound: cysteine (0 - 15 μM), in the presence of 100 μM DTNB (Figure 4.17). The standard curve was found to have an r^2 value of 0.989 and the equation of the line to determine the platelet thiol population (μM) was calculated: $y = 0.007x + 0.059$.

The surface thiol population of unactivated platelets and platelets activated with 0.1U/ml thrombin, 38 μg/ml collagen or 50 ng/ml convulxin was measured. Activation of platelets by collagen was found to induce a significant increase in the platelet surface thiol population, compared to unactivated platelets and platelets activated with thrombin or convulxin. The surface thiol population of unactivated platelets and platelets activated with thrombin or convulxin was comparable (n=6, ***$p < 0.001$) (Figure 4.18 (a)).

The external redox environment was altered by the introduction of glutathione or cysteine redox potentials. These redox potentials were generated by combining various ratios of the reduced (GSH, Cys) and oxidised (GSSG, CySS) forms of these low molecular weight thiols according to the Nernst equation and Tables 2.1 and 2.2.

In the presence of an oxidising (GSH/GSSG: -10 mV, Cys/CySS: +4 mV) external redox environment, there was also a significant increase in the surface thiol population of platelets activated with collagen, compared to unactivated platelets. Again, the thiol population of unactivated platelets was similar to that of platelets activated with thrombin and those activated with convulxin (n=6, ***$p < 0.001$) (Figure 4.18 (b)). There was a similar trend, though not statistically significant, of increased thiols on the surface of collagen activated platelets compared to unactivated platelets in the presence of a mean (GSH/GSSG: -130 mV, Cys/CySS: -82 mV) redox environment. There was no change in the thiol population of platelets activated by thrombin or convulxin (n=6) (Figure 4.18 (c)).

However, in the presence of a reducing (GSH/GSSG: -264 mV, Cys/CySS: -148 mV) external redox environment, the generation of free thiols on the surface of platelets activated with collagen was inhibited. There was also no effect on the surface thiol population of unactivated platelets or platelets activated with thrombin or convulxin (n=6) (Figure 4.18 (d)).

The fold increase in the surface thiol population of platelets activated with either thrombin, collagen or convulxin compared to unactivated platelets in the presence of each external redox environment is shown in Figures 4.19 (a) and (b). These graphs illustrate very clearly the dramatic, (approximately 8-fold), increase in the thiol population of platelets activated with collagen, compared to unactivated platelets and platelets activated with thrombin or convulxin. This thiol population increase noticeably diminishes as the external redox environment becomes more reducing. Furthermore, there is no change in the thiol population of platelets activated with thrombin or convulxin, compared to unactivated platelets in the presence of any of the redox environments (n=6, *$p < 0.05$, **$p < 0.01$) (Figure 4.15). While the trend of the results is similar in the presence of both GSH/GSSG and Cys/CySS redox potentials; it is interesting to note the different kinetics between the two redox couples. This may be due to differing reactivity between the thiol groups of each redox couple, with Cys/CySS appearing the more reactive. The pK_a ionisation constants for the thiol groups of GSH and Cys are 8.8 and 8.3, respectively (Winterbourn & Metodiewa, 1999).

From the graphs in Figure 4.19 (a) – (d), there is a considerable difference in the thiol concentrations of platelets in the absence of an altered external redox environment, compared to in the presence of a reducing external redox. This is due to the presence of excess thiol containing redox reagents themselves (GSH or Cys) reacting with DTNB and thus creating a background. Subtraction of this background was performed. However, subtraction of the background signal resulted in negative values. This may be due to platelet thiol/disulphide groups themselves reacting with the redox reagents.

The average number of moles of thiol per platelet in each of the activation states and redox environments were calculated and are shown in Tables 4.1 (a) and (b). Again, these figures very clearly demonstrate the significant increase in the average number of moles of thiol found on the surface of collagen activated platelets. This diminishes as the redox environment becomes more reducing in nature. It is important to note the figures for the average number of moles of thiols in the presence of the redox environments, again, do not take the background of excess redox reagents into consideration. Nonetheless, it is fair to make a comparison of the platelets activated with each agonist in the same external redox environment, for example, the number of moles of thiol on unactivated platelets in the presence of an oxidising environment can be compared to that of platelets activated with collagen, convulxin or thrombin in an oxidising environment but not to platelets in a mean or reducing redox environment.

4.2.5 Examination of the surface thiol population of statically adhered platelets

The levels of platelet adhesion to a number of substrates were investigated using the chromogenic substrate *para*-nitrophenyl phosphate (*p*NPP). *p*NPP reacts with phosphatases to form *para*-nitrophenol which has an intense yellow colour in the presence of alkaline conditions. The absorbance of *para*-nitrophenol, read at 405 nm with a Wallac plate reader, is directly proportional to the quantity of phosphatases present and therefore an indirect measurement of the number of adhered platelets.

Under static conditions, unactivated platelets adhered to 20 μg/ml fibrinogen, 10 μg/ml collagen and 1 μg/ml collagen related peptide (CRP) at comparable levels. Platelet adhesion to 1 % bovine serum albumin (BSA) was used as a negative control for the adhesion assay (n=6, ***$p < 0.001$) (Figure 4.20).

The thiol population of platelets adhered to BSA (1 %), fibrinogen (20 μg/ml), collagen (10 μg/ml) and CRP (1 μg/ml) was assessed using Ellman's test with 5, 5'-Dithio-bis-(2-nitrobenzoic acid) (DTNB). While not quite reaching statistical significance, there was an increase in the thiol population of platelets adhered to collagen compared to platelets adhered to fibrinogen or CRP. Interestingly, there was also a trend towards an increase in the thiol population of platelets adhered to fibrinogen, compared with platelets adhered to CRP (n=6) (Figure 4.21).

The impact of an altered redox environment on the levels of platelet adhesion to 1 % BSA, 20 μg/ml fibrinogen, 10 μg/ml collagen and 1 μg/ml collagen related peptide (CRP) was also examined. This study was carried out by determining the numbers of platelets adhered to each substrate as observed by confocal microscopy. Adhered platelets were stained with Alex Fluor® 488 phalloidin, imaged and counted using ImageJ software.

There was a significant decrease in the number of platelets adhered to collagen in the presence of a reducing (GSH/GSSG: -264 mV) external redox environment, compared to the level of platelet adhesion to collagen in the absence of an altered redox environment. In a mean (GSH/GSSG: -130 mV) or oxidising (GSH/GSSG: -10 mV) external redox environment no significant impact on platelet adhesion to collagen was observed. Platelets adhered to BSA, fibrinogen or CRP were not altered by an altered external redox environment ($n=4$, $*p < 0.05$) (Figures 4.22 (a - e)).

The impact of an altered external redox environment on the thiol population of adhered platelets was also investigated. Platelets were incubated with GSH/GSSG redox potentials: oxidising (-10 mV), mean (-130 mV) and reducing (-264 mV) then adhered to 1 % BSA, 20 μg/ml fibrinogen, 10 μg/ml collagen and 1 μg/ml CRP. The thiol population of adhered platelets was assessed using Ellman's test with 5, 5'-Dithio-bis-(2-nitrobenzoic acid) (DTNB).

There was an indication of a decrease in the thiol population of platelets adhered to collagen in the presence of a reducing external redox environment, compared to the thiol population of platelets adhered to collagen in the absence of an altered external redox environment. However, this did not reach statistical

significance. In an oxidising or mean external redox environment no impact on the thiol population of platelets adhered to collagen was observed. The surface thiol population of platelets adhered to BSA, fibrinogen or CRP remained unchanged regardless of the external redox environment (n=3) (Figure 4.23).

The thiol population of platelets adhered to BSA, fibrinogen, collagen and CRP was also examined with confocal microscopy. Platelets adhered to each of the substrates were stained with a fluorescently labelled, thiol reactive probe: Atto 655 maleimide. Similar to the results obtained from the DTNB adhesion studies, there was increased binding of Atto 655 maleimide to platelets adhered to collagen and fibrinogen compared to platelets adhered to BSA or CRP. This is indicative of an increased surface free thiol population on platelets adhered to collagen or fibrinogen. There was a degree of binding of Atto 655 maleimide to platelets adhered to CRP. However, the fluorescence was found to be associated with the outer regions and lamellipodia of the platelets, in contrast to platelets adhered to collagen and fibrinogen, whereby the fluorescence was concentrated in the centre region of the spread platelets (n=4) (Figure 4.24).

(i)

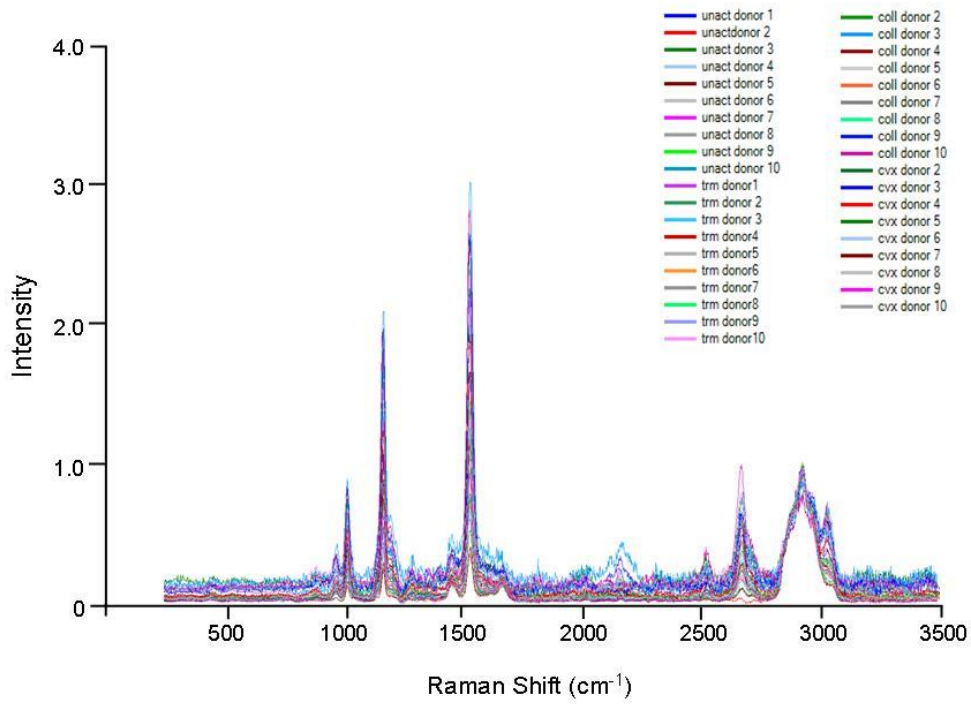
unact donor 1
unactdonor 2
unact donor 3
unact donor 4
unact donor 5
unact donor 6
unact donor 7
unact donor 8
unact donor 9
unact donor 10
trm donor1
trm donor 2
trm donor 3
trm donor4
trm donor5
trm donor6
trm donor7
trm donor8
trm donor9
trm donor10
coll donor 2
coll donor 3
coll donor 4
coll donor 5
coll donor 6
coll donor 7
coll donor 8
coll donor 9
coll donor 10
cvx donor 2
cvx donor 3
cvx donor 4
cvx donor 5
cvx donor 6
cvx donor 7
cvx donor 8
cvx donor 9
cvx donor 10
Intensity
4.0
3.0
2.0
1.0
0
500
1000
1500
2000
2500
3000
3500
Raman Shift (cm-1)

(ii)

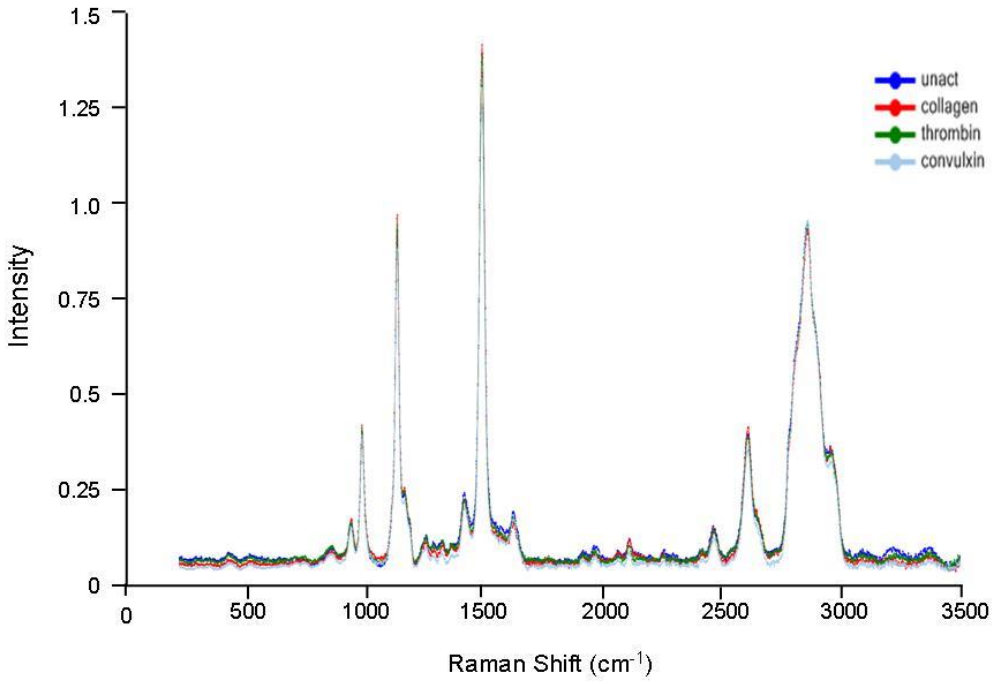
unact
collagen
thrombin
convulxin
Intensity
1.5
1.25
1.0
0.75
0.5
0.25
0
0
500
1000
1500
2000
2500
3000
3500
Raman Shift (cm-1)

Figure 4.1 (a) Raman spectra of unactivated platelets and platelets activated with either 0.1U/ml thrombin, 38 μg/ml collagen or 50 ng/ml convulxin. Gel-filtered platelets were fixed with 1 % formaldehyde, centrifuged and supernatant removed. Raman spectra were obtained from the resulting platelet pellet. Spectra were baseline subtracted and normalised to the lipid peak at approximately 3000 cm^{-1}. (i) Three or four spectra were taken for each platelet activator and averaged, to give one spectrum per activator per donor. (ii) Signature Raman spectra of platelets generated by averaging spectra for each platelet activator from all n=10 donors.

(i)

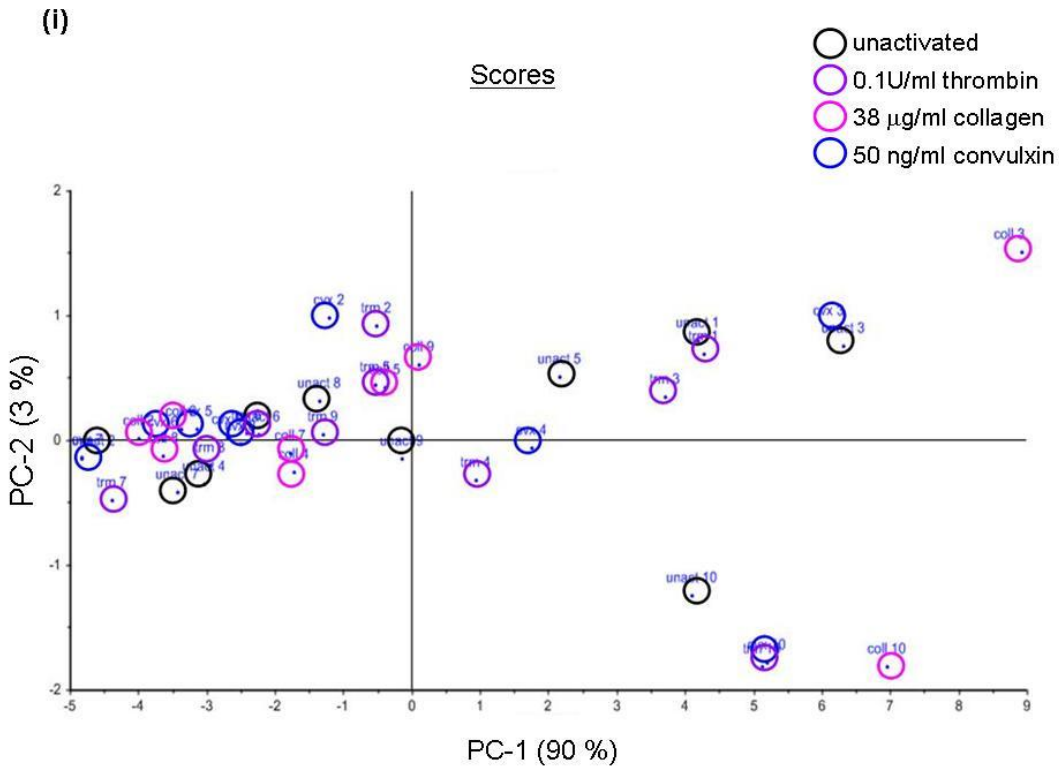
Scores
unactivated
0.1U/ml thrombin
38 μg/ml collagen
50 ng/ml convulxin
PC-2 (3 %)
PC-1 (90 %)

(ii)

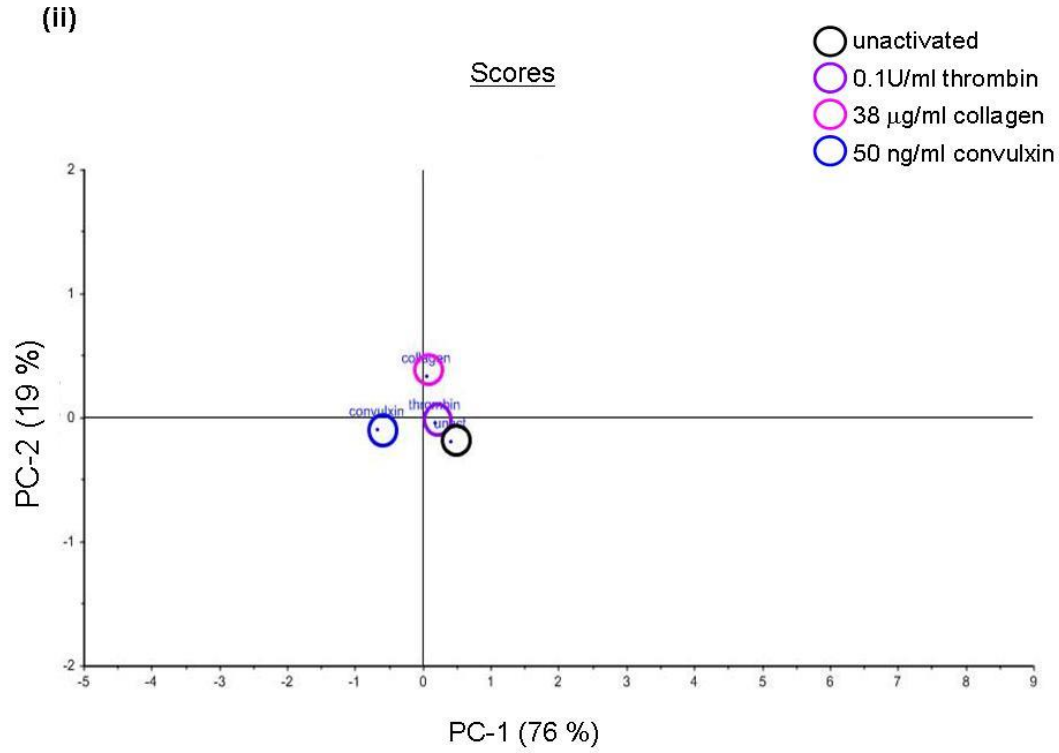
Scores
unactivated
0.1U/ml thrombin
38 μg/ml collagen
50 ng/ml convulxin
PC-2 (19 %)
PC-1 (76 %)
collagen
thrombin
convulxin

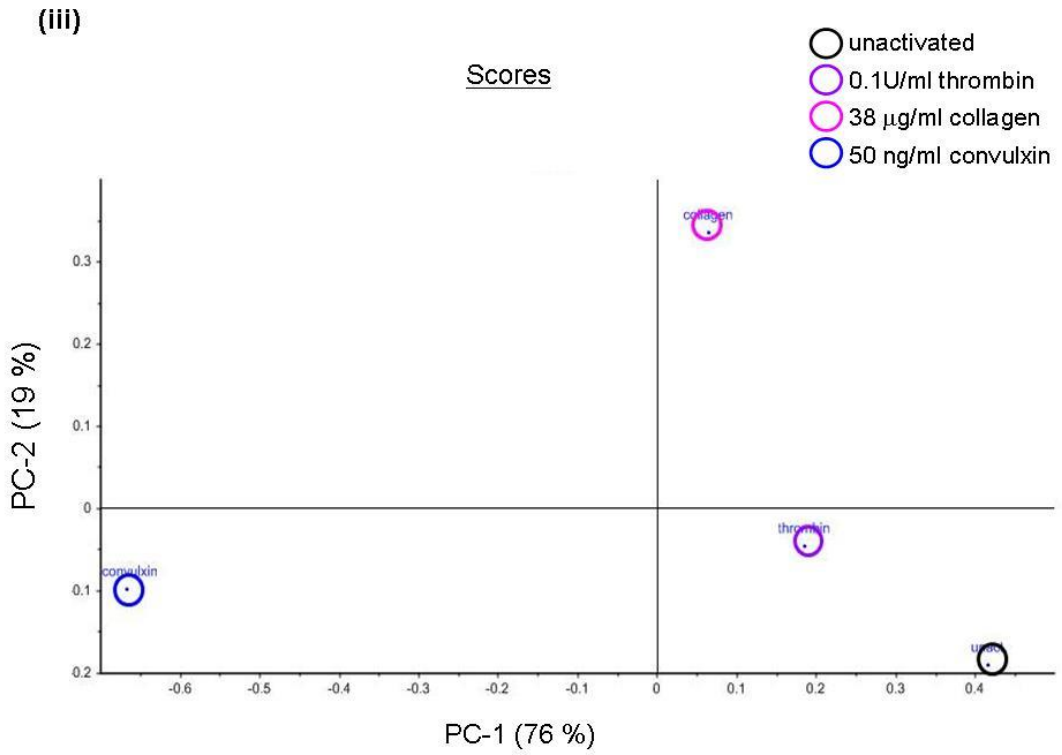

Figure 4.1 (b) Principal component analysis (PCA) of full Raman spectra of unactivated platelets and platelets activated with either 0.1U/ml thrombin, 38 μg/ml collagen or 50 ng/ml convulxin. (i) PCA of all spectra of all donors. (ii) PCA of average spectra, graphed on same scale as (i). (iii) PCA of signature, average spectra on a smaller scale illustrating that the samples can be differentiated according to the platelet activator. Data shown is from n=10 independent experiments.

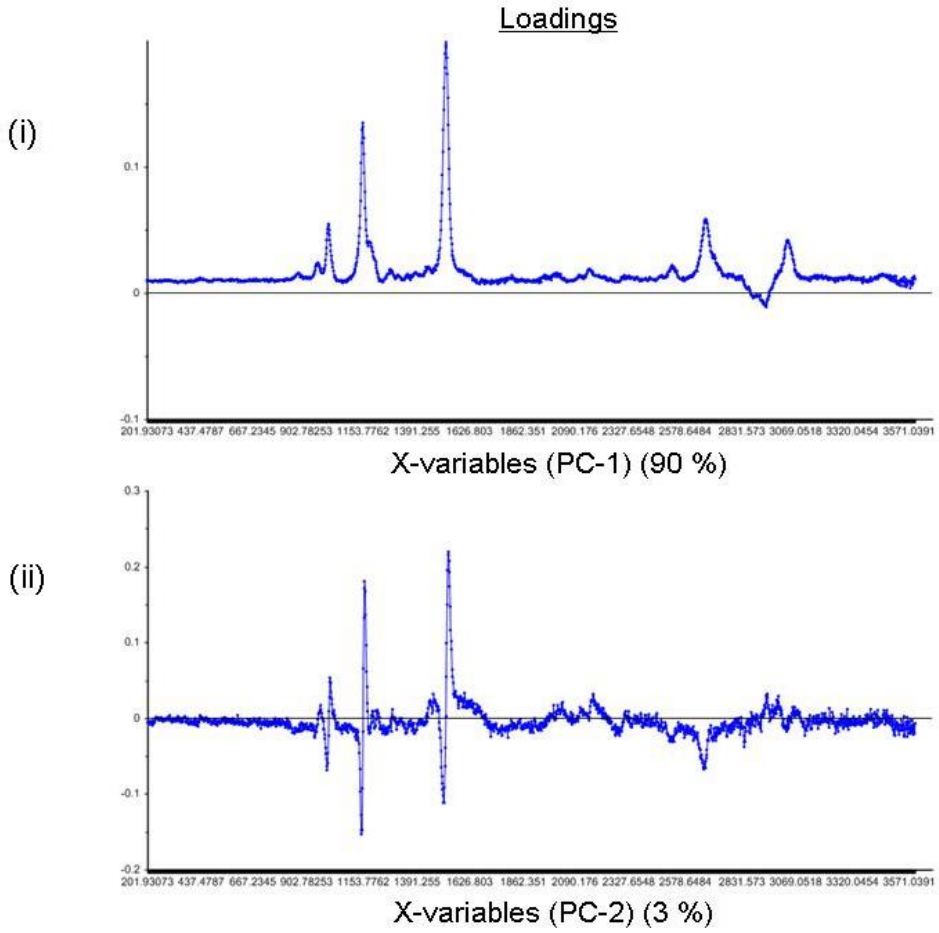

Figure 4.1 (c) The loadings of the principal components used in the Principal component analysis (PCA) scatter plot of the full spectrum of all the platelet Raman spectra. (i) Principal component-1 (PC-1) and (ii) Principal component-2 (PC-2) from the PCA of spectra from all donors (Figure 4.1 (b) (i)). The components are numbered according to the amount of variance they account for, i.e. PC-1 accounts for most of the variance found between the platelet samples. PCA analysis was carried out on the baseline subtracted and normalised Raman data of all samples using The Unscrambler® software.

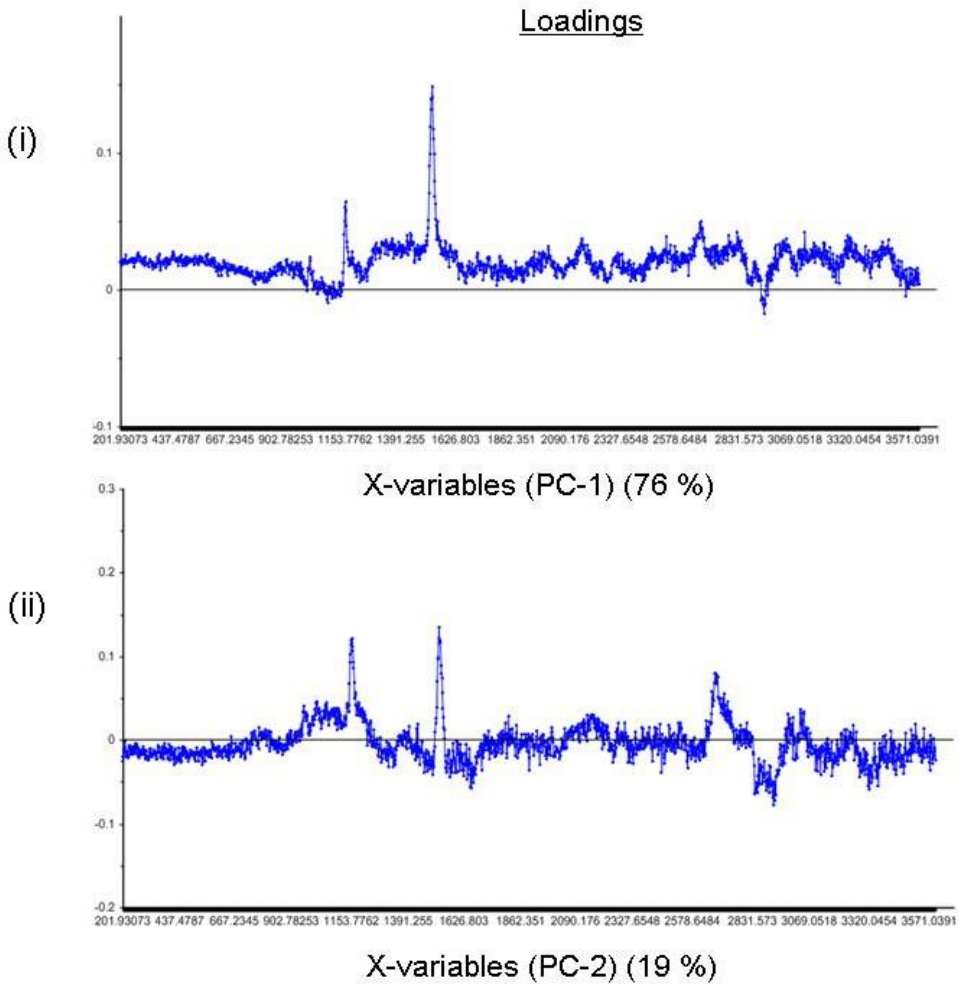

Figure 4.1 (d) The loadings of the principal components used in the Principal component analysis (PCA) scatter plot of the full spectrum of the average or signature platelet Raman spectra. (i) Principal component-1 (PC-1) and (ii) Principal component-2 (PC-2) from the PCA of the signature Raman spectra (Figure 4.1 (b) (ii) and (iii)). The components are numbered according to the amount of variance they account for, i.e. PC-1 accounts for most of the variance found between the platelet samples. PCA analysis was carried out on the baseline subtracted and normalised Raman data of all samples using The Unscrambler® software.

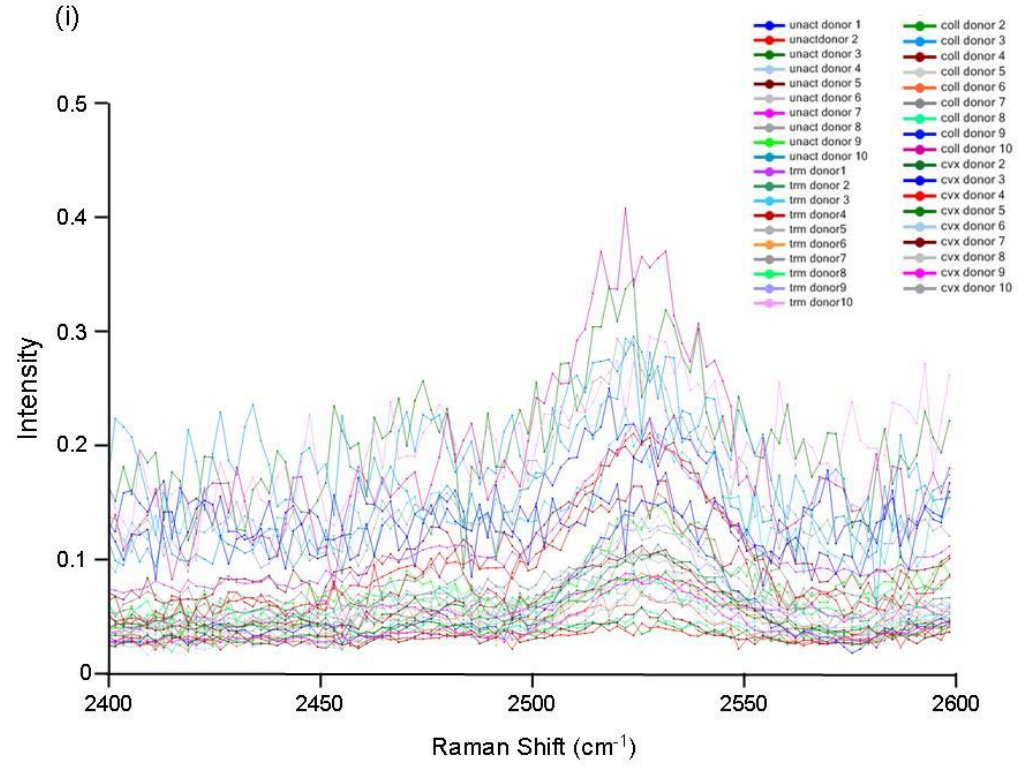
(i)
unact donor 1
unactdonor 2
unact donor 3
unact donor 4
unact donor 5
unact donor 6
unact donor 7
unact donor 8
unact donor 9
unact donor 10
trm donor1
trm donor 2
trm donor 3
trm donor4
trm donor5
trm donor6
trm donor7
trm donor8
trm donor9
trm donor10
coll donor 2
coll donor 3
coll donor 4
coll donor 5
coll donor 6
coll donor 7
coll donor 8
coll donor 9
coll donor 10
cvx donor 2
cvx donor 3
cvx donor 4
cvx donor 5
cvx donor 6
cvx donor 7
cvx donor 8
cvx donor 9
cvx donor 10
Intensity
0.5
0.4
0.3
0.2
0.1
0
2400
2450
2500
2550
2600
Raman Shift (cm-1)

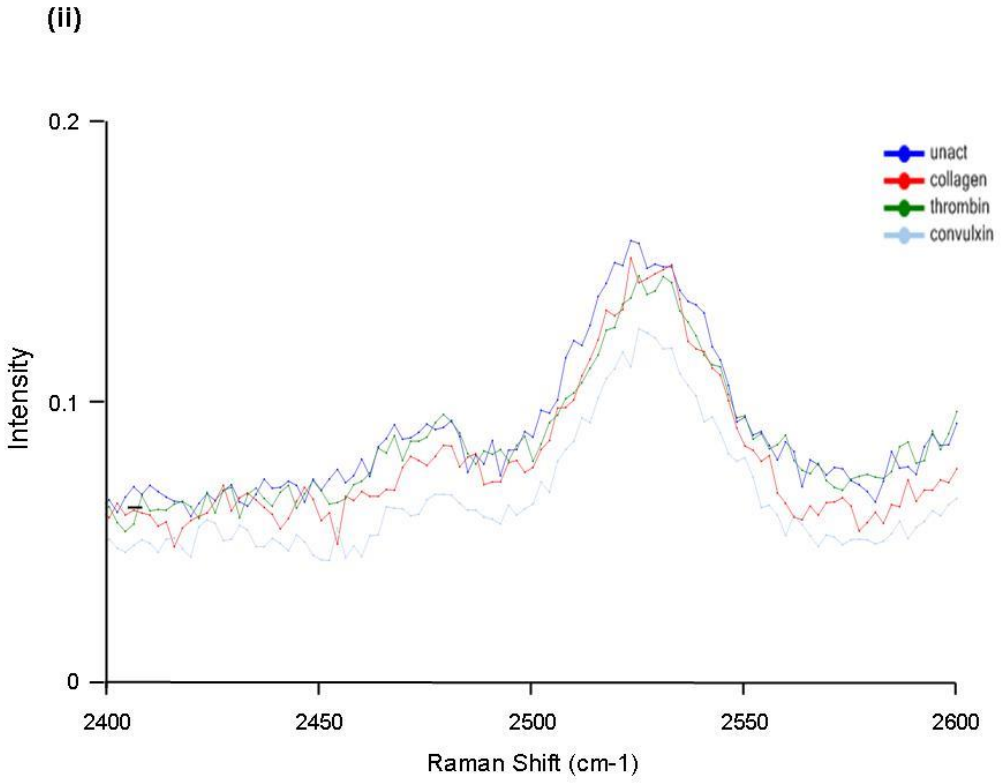
(ii)
unact
collagen
thrombin
convulxin
Intensity
0.2
0.1
0
2400
2450
2500
2550
2600
Raman Shift (cm-1)

Figure 4.2 (a) The thiol region of the Raman spectra of unactivated platelets and platelets activated with either 0.1U/ml thrombin, 38 μg/ml collagen or 50 ng/ml convulxin. Gel-filtered platelets were fixed with 1 % formaldehyde, centrifuged and supernatant removed. Raman spectra were obtained from the resulting platelet pellet. Spectra were baseline subtracted and normalised to the lipid peak at approximately 3000 cm^{-1}. (i) Three or four spectra were taken for each platelet activator and averaged, to give one spectrum per activator per donor. (ii) Signature Raman spectra of platelets generated by averaging spectra for each platelet activator from all n=10 donors.

(i)

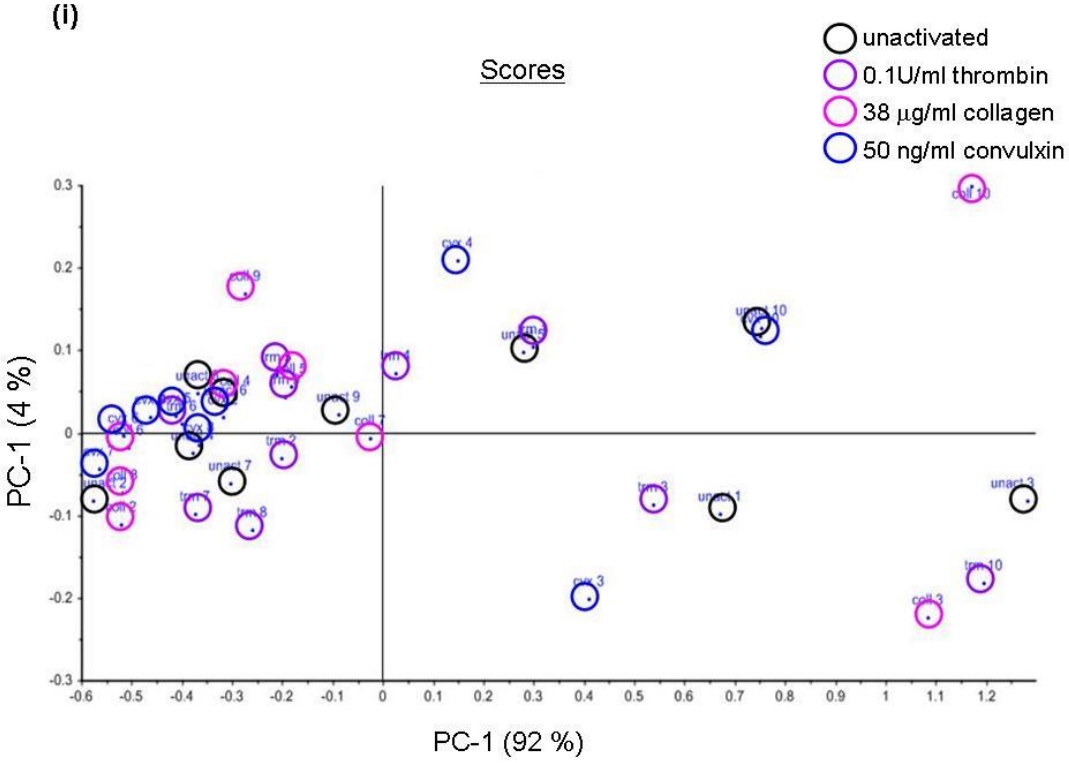
Scores
unactivated
0.1U/ml thrombin
38 μg/ml collagen
50 ng/ml convulxin
PC-1 (4 %)
PC-1 (92 %)

(ii)

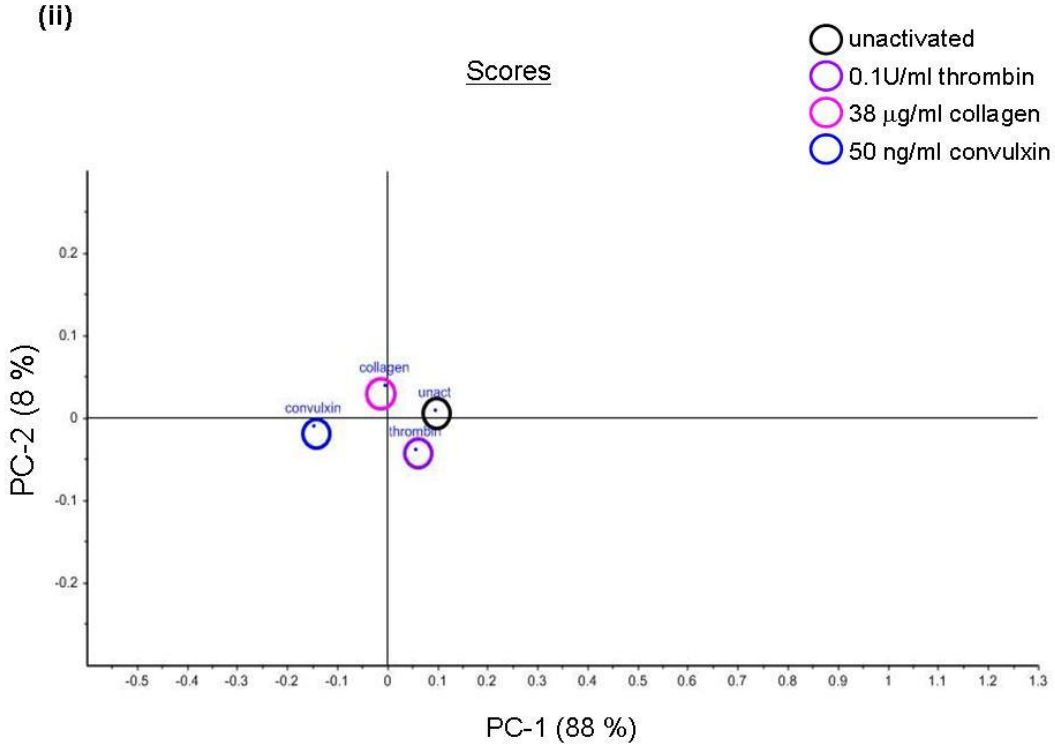
Scores
unactivated
0.1U/ml thrombin
38 μg/ml collagen
50 ng/ml convulxin
collagen
unact
convulxin
thrombin
PC-2 (8 %)
PC-1 (88 %)

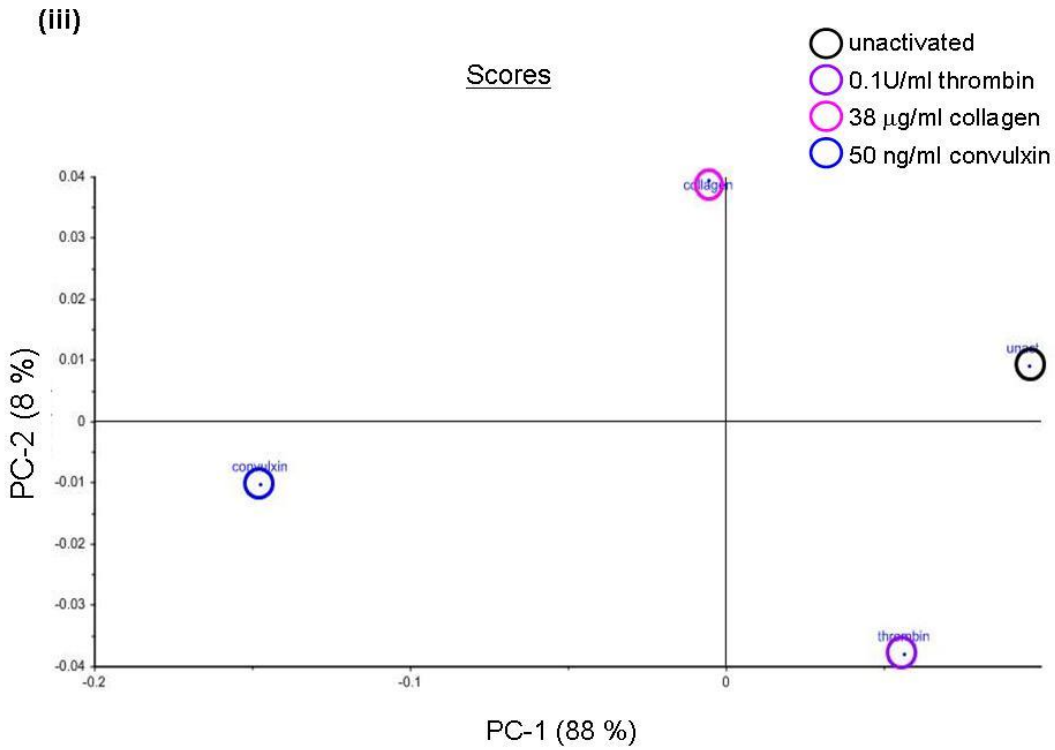

Figure 4.2 (b) Principal component analysis (PCA) of the thiol region of the Raman spectra of unactivated platelets and platelets activated with either 0.1U/ml thrombin, 38 μg/ml collagen or 50 ng/ml convulxin. PCA analysis was performed on the 2400 – 2600 cm^{-1} region of the Raman spectra. The graphs are scatter plots of the first principal component (PC-1) versus the second principal component (PC-2). (i) PCA of all donors, n=10 independent experiments. (ii) PCA of average spectra, graphed on same scale as (i). (iii) PCA of signature, average spectra on a smaller scale illustrating that the samples can be differentiated according to the platelet activator.

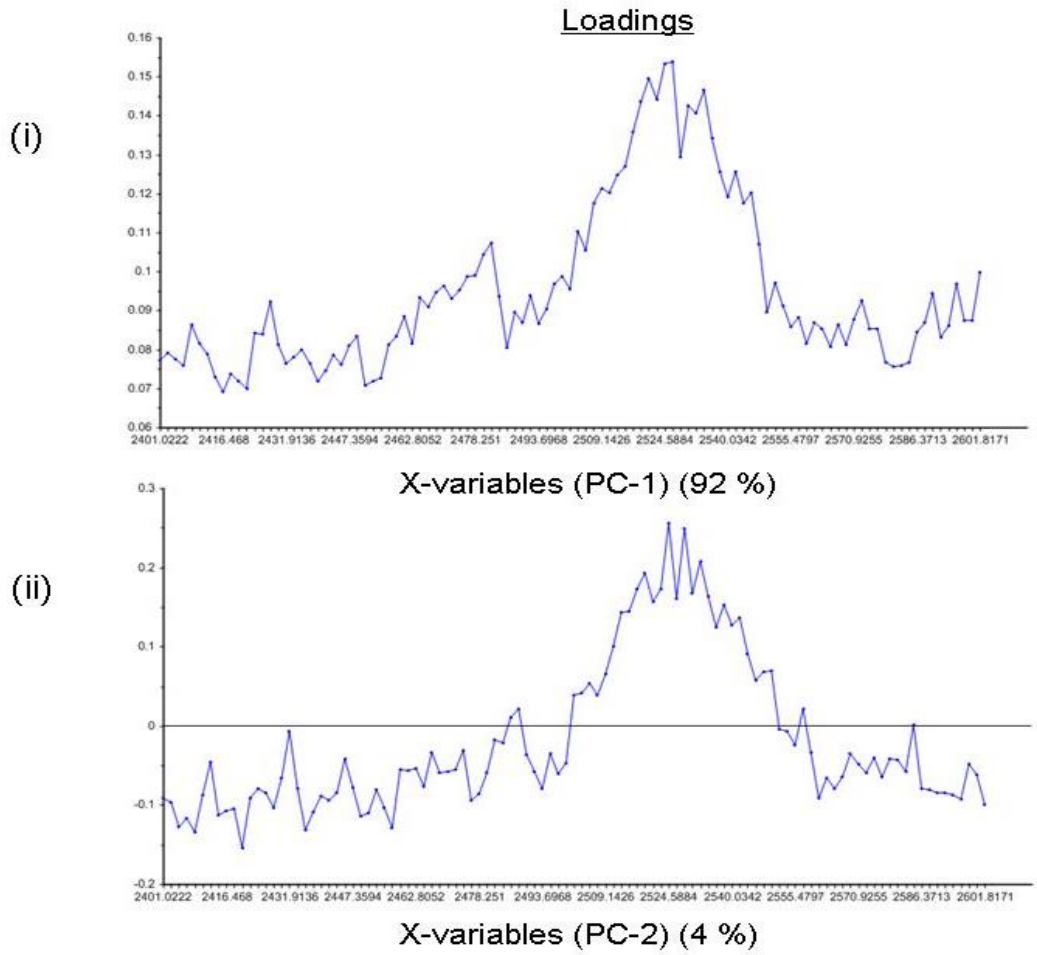

Figure 4.2 (c) The loadings of the principal components used in the Principal component analysis (PCA) scatter plot of the thiol region of all platelet Raman spectra. (i) Principal component-1 (PC-1) and (ii) Principal component-2 (PC-2) from the PCA of the spectra from all donors (Figure 4.2 (b) (i)). The components are numbered according to the amount of variance they account for, i.e. PC-1 accounts for most of the variance found between the platelet samples. PCA analysis was carried out on the baseline subtracted and normalised Raman data of all samples using The Unscrambler® software.

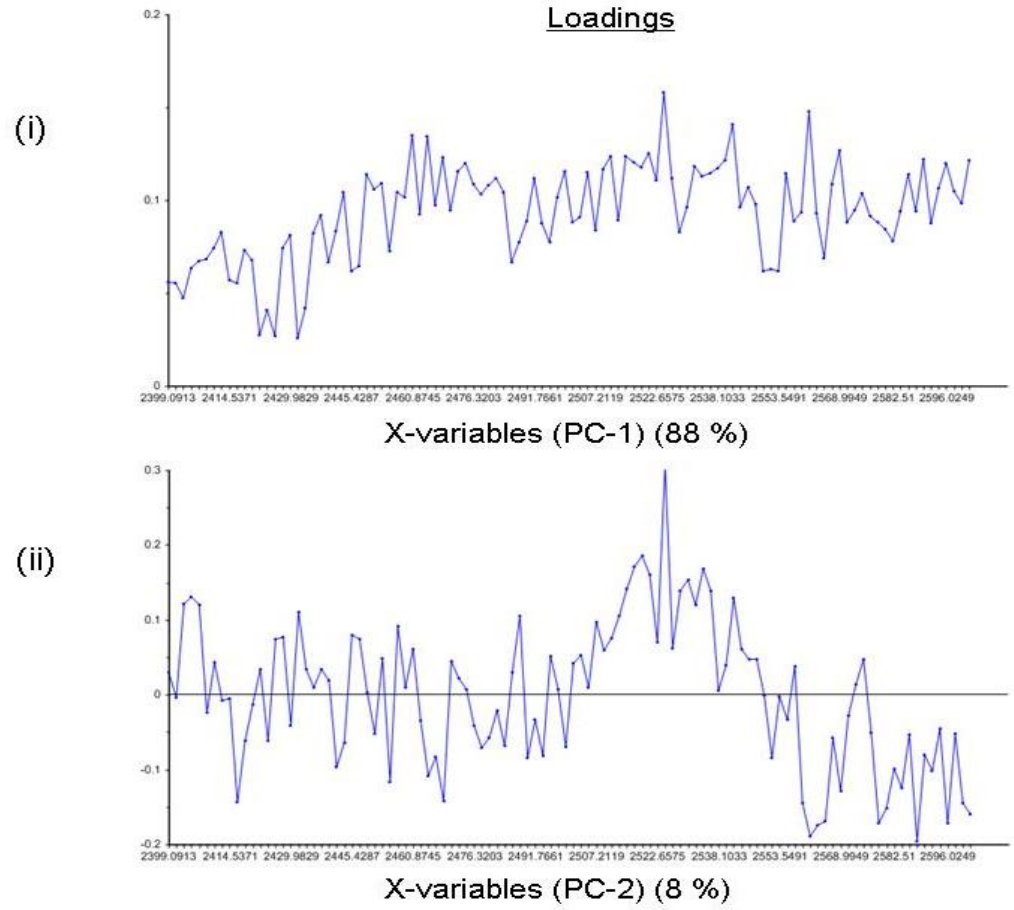

Figure 4.2 (d) The loadings of the principal components used in the Principal component analysis (PCA) scatter plot of the thiol region of the signature platelet Raman spectra. (i) Principal component-1 (PC-1) and (ii) Principal component-2 (PC-2) from the PCA of the signature spectra (Figure 4.2 (b) (ii) and (iii)). The components are numbered according to the amount of variance they account for, i.e. PC-1 accounts for most of the variance found between the platelet samples. PCA analysis was carried out on the baseline subtracted and normalised Raman data of all samples using The Unscrambler® software.

(i)

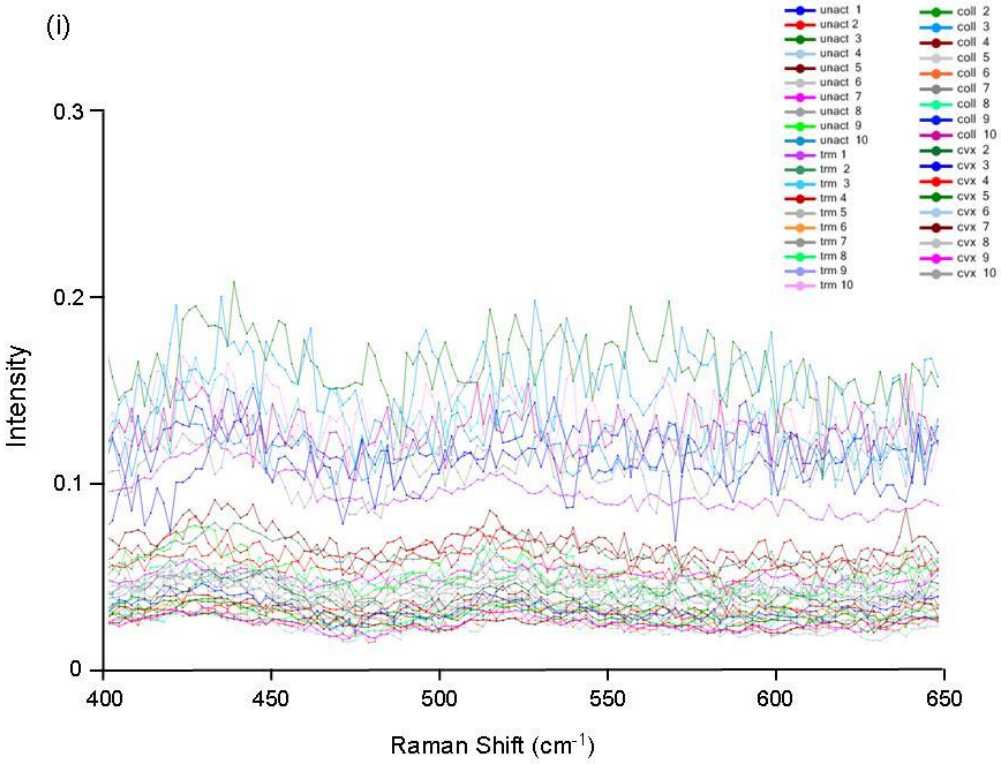
unact 1
unact 2
unact 3
unact 4
unact 5
unact 6
unact 7
unact 8
unact 9
unact 10
trm 1
trm 2
trm 3
trm 4
trm 5
trm 6
trm 7
trm 8
trm 9
trm 10
coll 2
coll 3
coll 4
coll 5
coll 6
coll 7
coll 8
coll 9
coll 10
cvx 2
cvx 3
cvx 4
cvx 5
cvx 6
cvx 7
cvx 8
cvx 9
cvx 10
Intensity
0.3
0.2
0.1
0
400
450
500
550
600
650
Raman Shift (cm-1)

(ii)

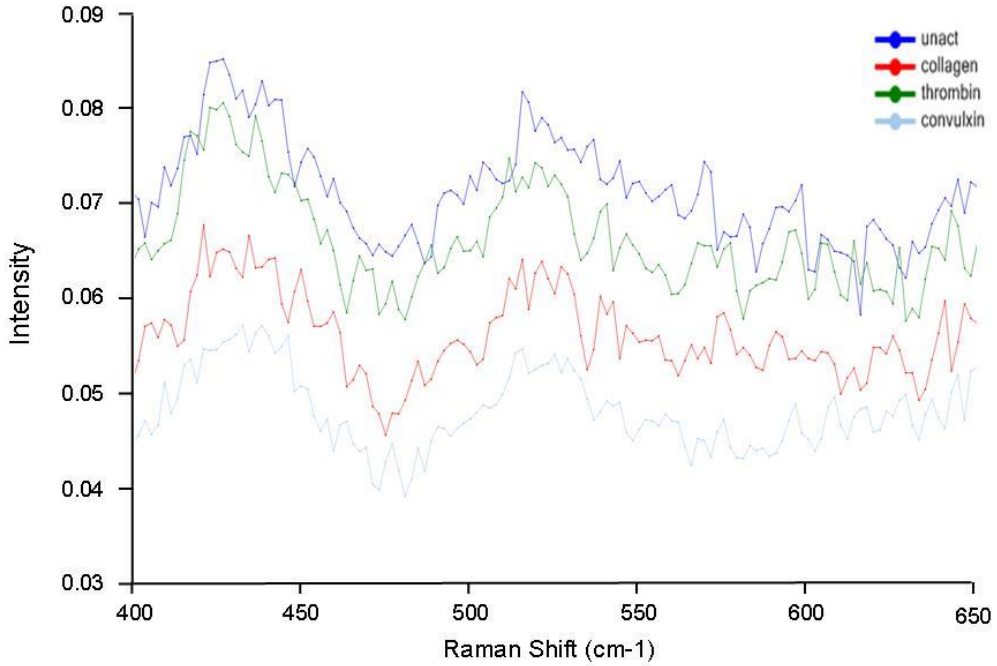
unact
collagen
thrombin
convulxin
Intensity
0.09
0.08
0.07
0.06
0.05
0.04
0.03
400
450
500
550
600
650
Raman Shift (cm-1)

Figure 4.3 (a) The disulphide region of the Raman spectra of unactivated platelets and platelets activated with either 0.1U/ml thrombin, 38 μg/ml collagen or 50 ng/ml convulxin. Gel-filtered platelets were fixed with 1 % formaldehyde, centrifuged and supernatant removed. Raman spectra were obtained from the resulting platelet pellet. Spectra were baseline subtracted and normalised to the lipid peak at approximately 3000 cm^{-1}. (i) Three or four spectra were taken for each platelet activator and averaged, to give one spectrum per activator per donor. (ii) Signature Raman spectra of platelets generated by averaging spectra for each platelet activator from all n=10 donors.

(i)

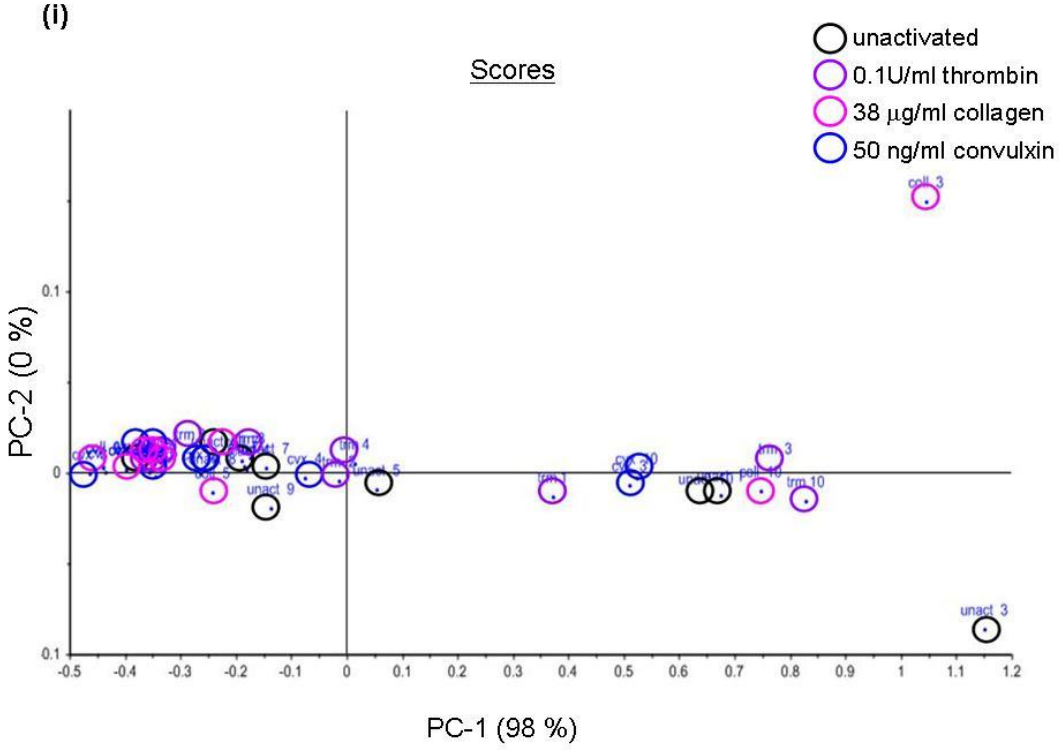
Scores
unactivated
0.1U/ml thrombin
38 μg/ml collagen
50 ng/ml convulxin
coll_3
unact_3
PC-2 (0 %)
PC-1 (98 %)

(ii)

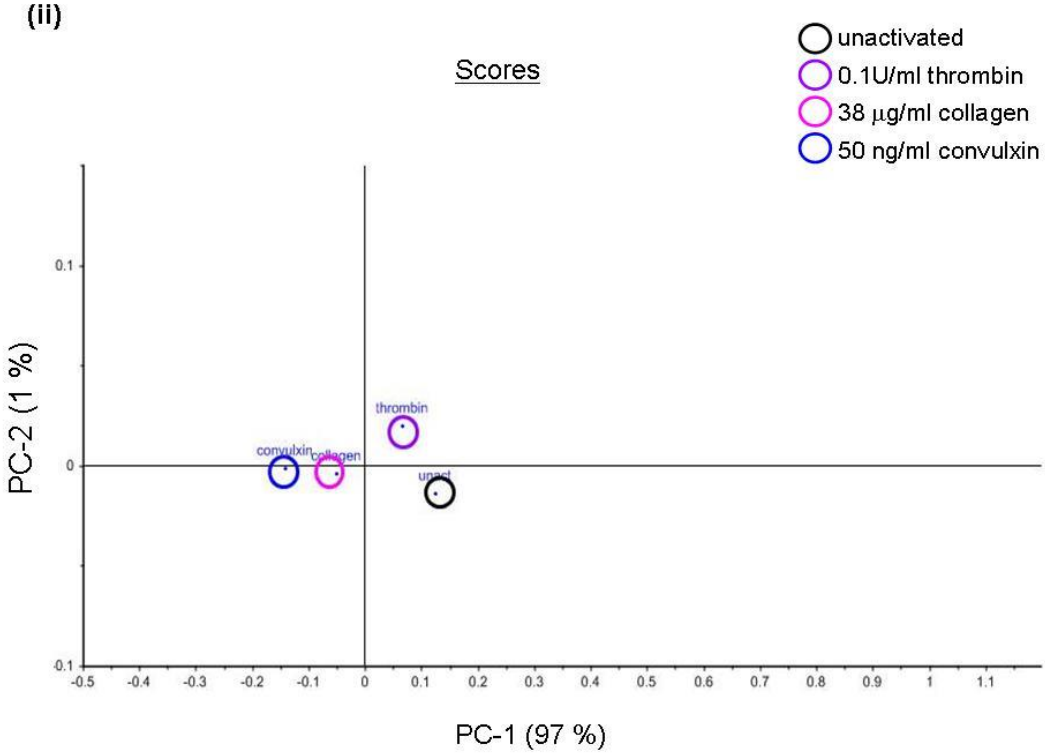
Scores
unactivated
0.1U/ml thrombin
38 μg/ml collagen
50 ng/ml convulxin
thrombin
convulxin
collagen
unact
PC-2 (1 %)
PC-1 (97 %)

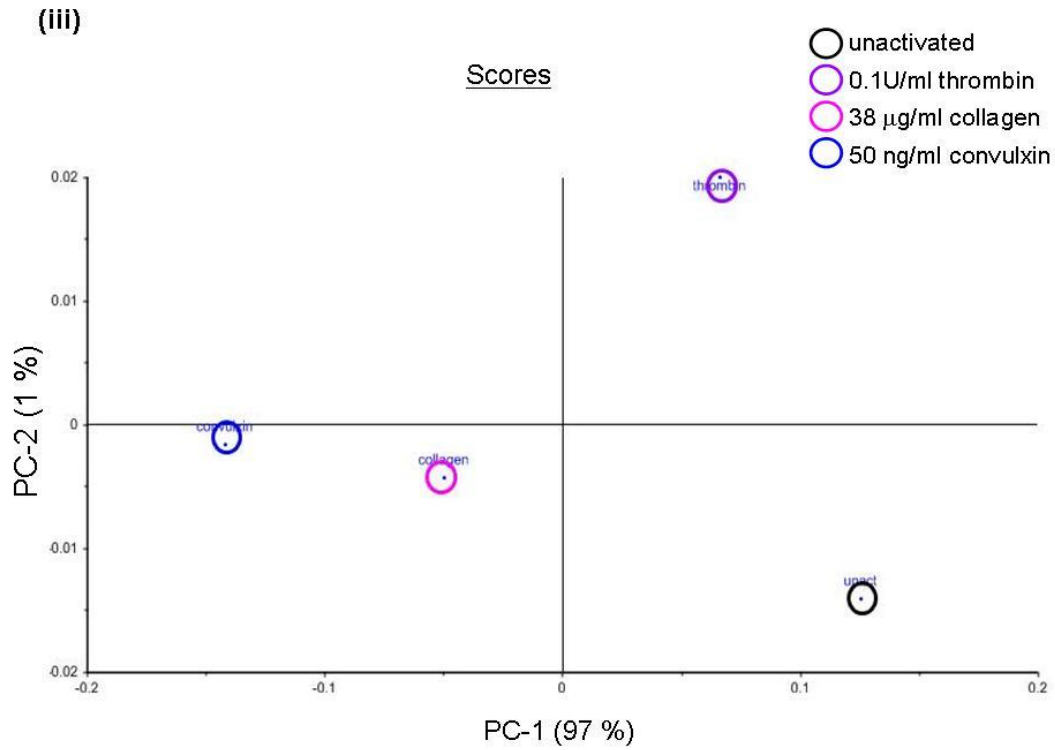

Figure 4.3 (b) Principal component analysis (PCA) of the disulphide region of the Raman spectra of unactivated platelets and platelets activated with either 0.1U/ml thrombin, 38 μg/ml collagen or 50 ng/ml convulxin. PCA analysis was performed on the 400 – 650 cm^{-1} region of the Raman spectra. The graphs are scatter plots of the first principal component (PC-1) versus the second principal component (PC-2). (i) PCA of all donors, n=10 independent experiments, (ii) PCA of average spectra, graphed on same scale as (i), (iii) PCA of signature, average spectra on a smaller scale illustrating that the samples can be differentiated according to the platelet activator.

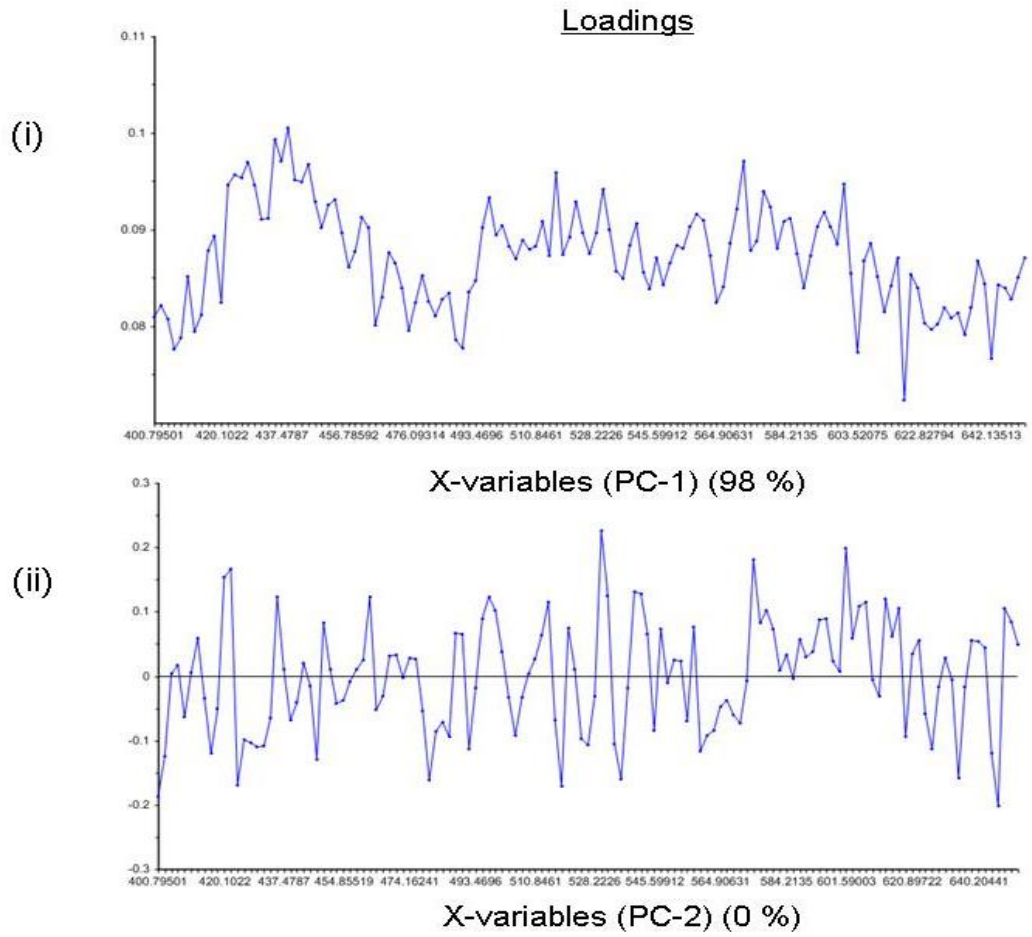

Figure 4.3 (c) The loadings of the principal components used in the Principal component analysis (PCA) scatter plot of the disulphide region of all platelet Raman spectra. (i) Principal component-1 (PC-1) and (ii) Principal component-2 (PC-2) from the PCA of spectra from all donors (Figure 4.3 (b) (i)). The components are numbered according to the amount of variance they account for, i.e. PC-1 accounts for most of the variance found between the platelet samples. PCA analysis was carried out on the baseline subtracted and normalised Raman data of all samples using The Unscrambler® software.

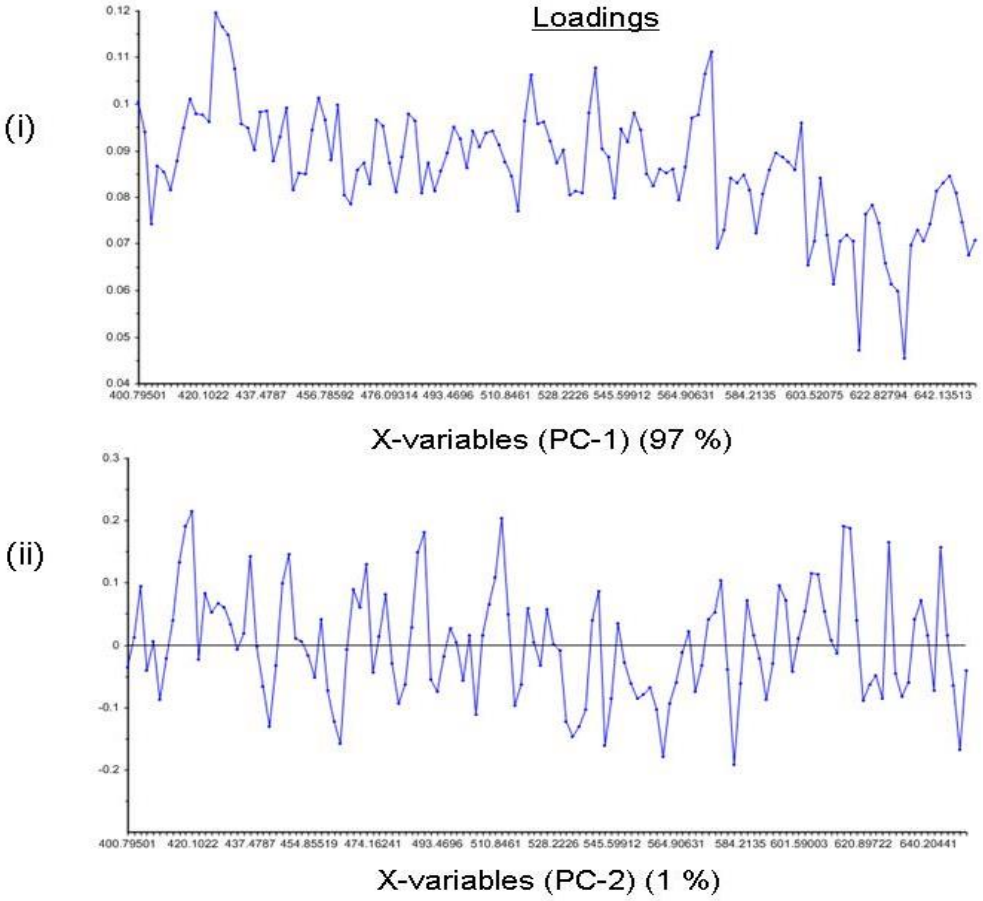

Figure 4.3 (d) The loadings of the principal components used in the Principal component analysis (PCA) scatter plot of the disulphide region of the signature platelet Raman spectra. (i) Principal component-1 (PC-1) and (ii) Principal component-2 (PC-2) from the PCA of the signature spectra (Figure 4.3 (b) (ii) and (iii)). The components are numbered according to the amount of variance they account for, i.e. PC-1 accounts for most of the variance found between the platelet samples. PCA analysis was carried out on the baseline subtracted and normalised Raman data of all samples using The Unscrambler® software.

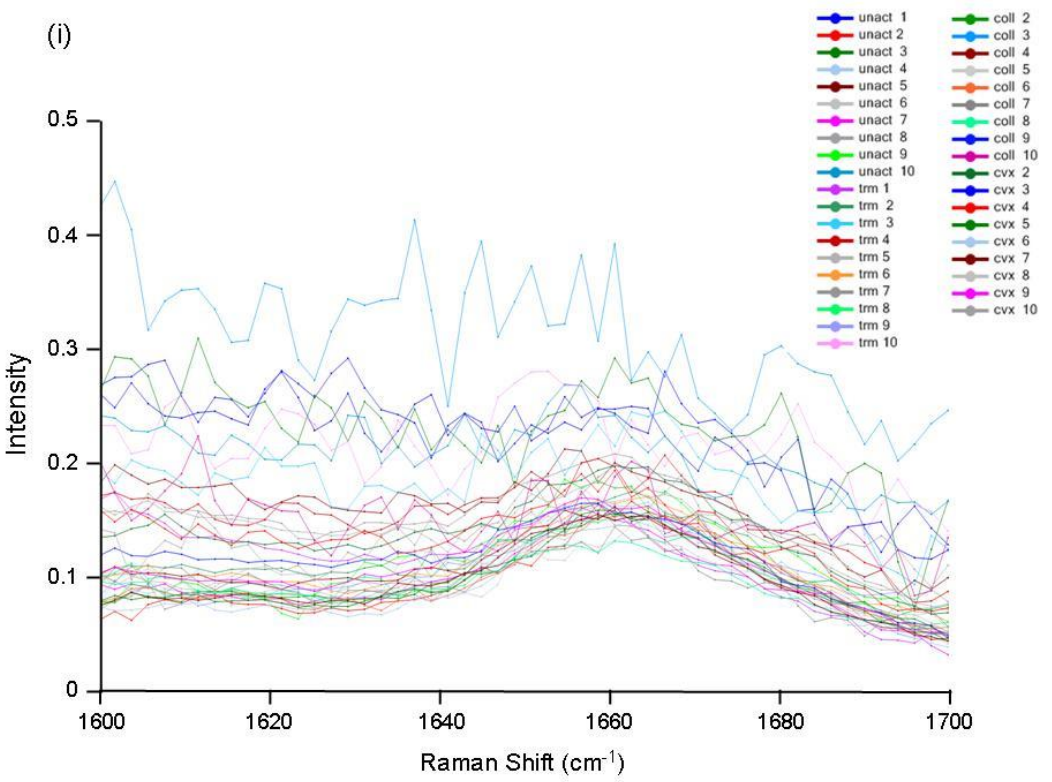
(i)
unact 1
unact 2
unact 3
unact 4
unact 5
unact 6
unact 7
unact 8
unact 9
unact 10
trm 1
trm 2
trm 3
trm 4
trm 5
trm 6
trm 7
trm 8
trm 9
trm 10
coll 2
coll 3
coll 4
coll 5
coll 6
coll 7
coll 8
coll 9
coll 10
cvx 2
cvx 3
cvx 4
cvx 5
cvx 6
cvx 7
cvx 8
cvx 9
cvx 10
Intensity
0.5
0.4
0.3
0.2
0.1
0
1600
1620
1640
1660
1680
1700
Raman Shift (cm-1)

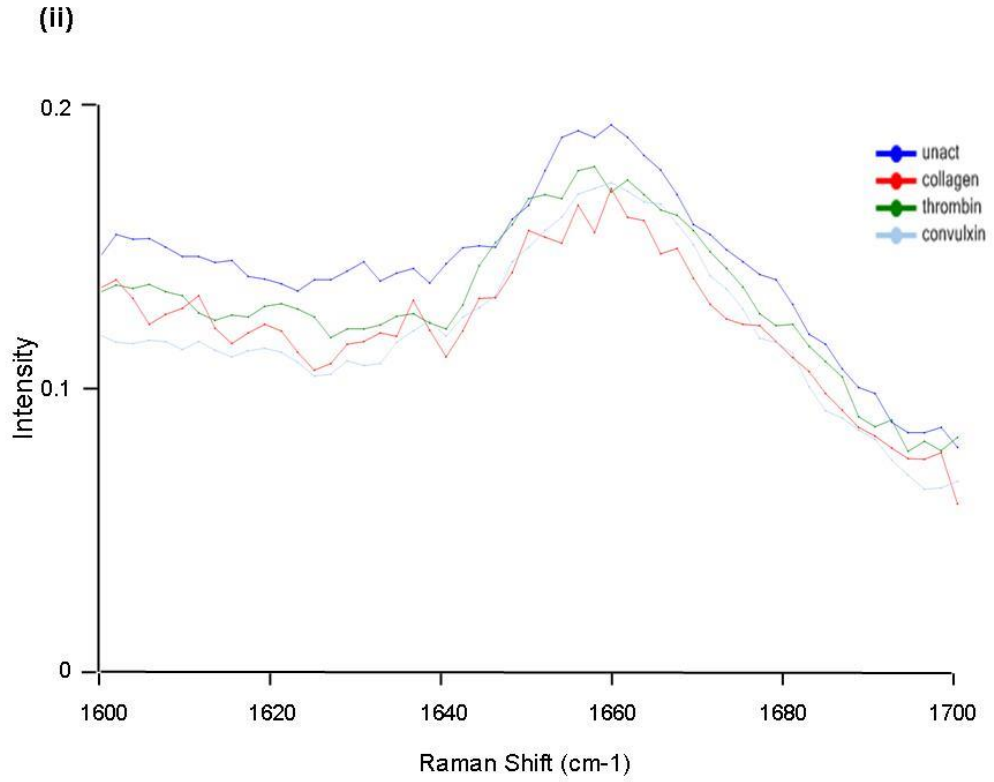
(ii)
unact
collagen
thrombin
convulxin
Intensity
0.2
0.1
0
1600
1620
1640
1660
1680
1700
Raman Shift (cm-1)

Figure 4.4 (a) The amide I region of the Raman spectra of unactivated platelets and platelets activated with either 0.1U/ml thrombin, 38 μg/ml collagen or 50 ng/ml convulxin. Gel-filtered platelets were fixed with 1 % formaldehyde, centrifuged and supernatant removed. Raman spectra were obtained from the resulting platelet pellet. Spectra were baseline subtracted and normalised to the lipid peak at approximately 3000 cm^{-1}. (i) Three or four spectra were taken for each platelet activator and averaged, to give one spectrum per activator per donor. (ii) Signature Raman spectra of platelets generated by averaging spectra for each platelet activator from all n=10 donors.

(i)

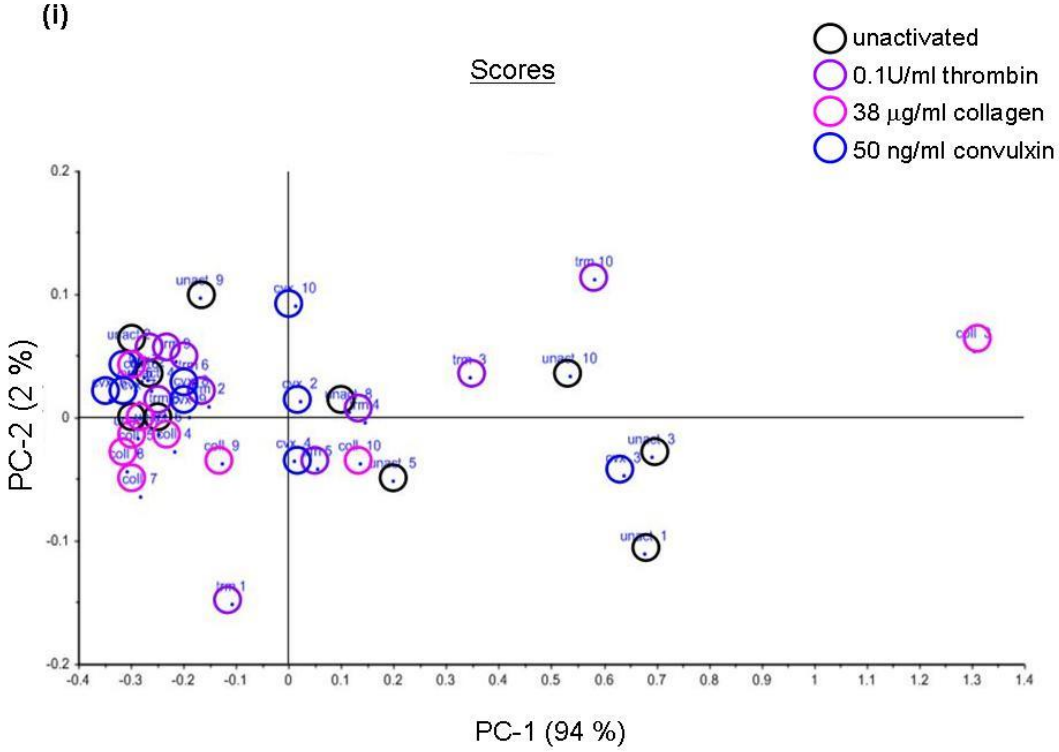
Scores
unactivated
0.1U/ml thrombin
38 μg/ml collagen
50 ng/ml convulxin
PC-2 (2 %)
PC-1 (94 %)

(ii)

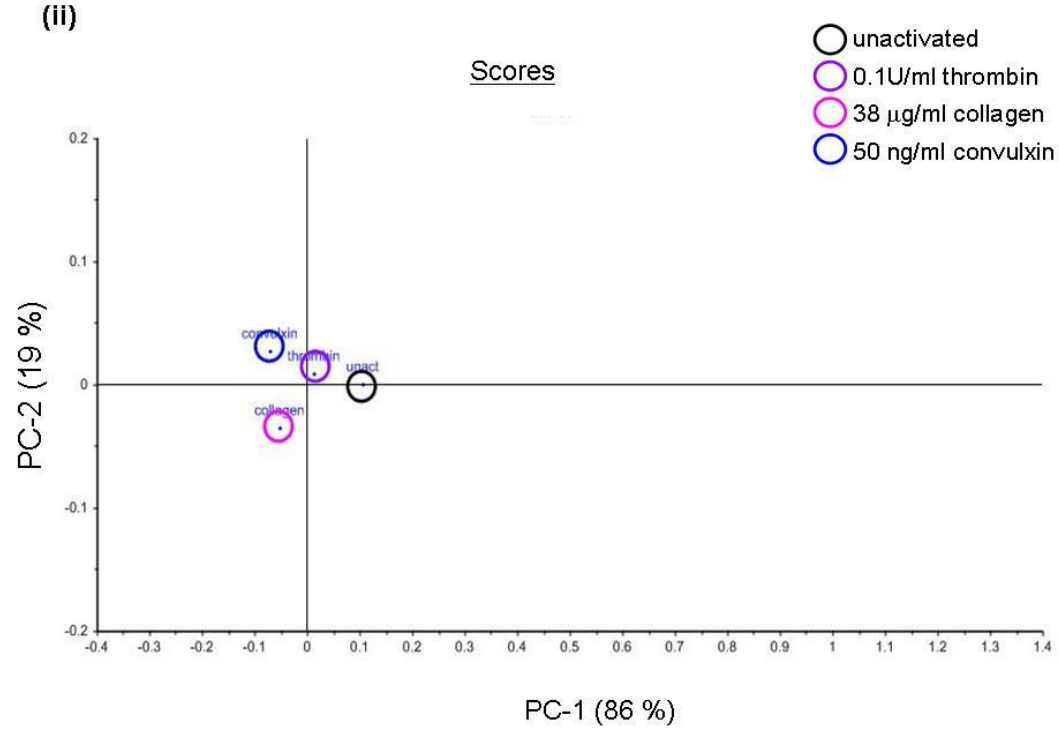
Scores
unactivated
0.1U/ml thrombin
38 μg/ml collagen
50 ng/ml convulxin
PC-2 (19 %)
PC-1 (86 %)
collagen
unact

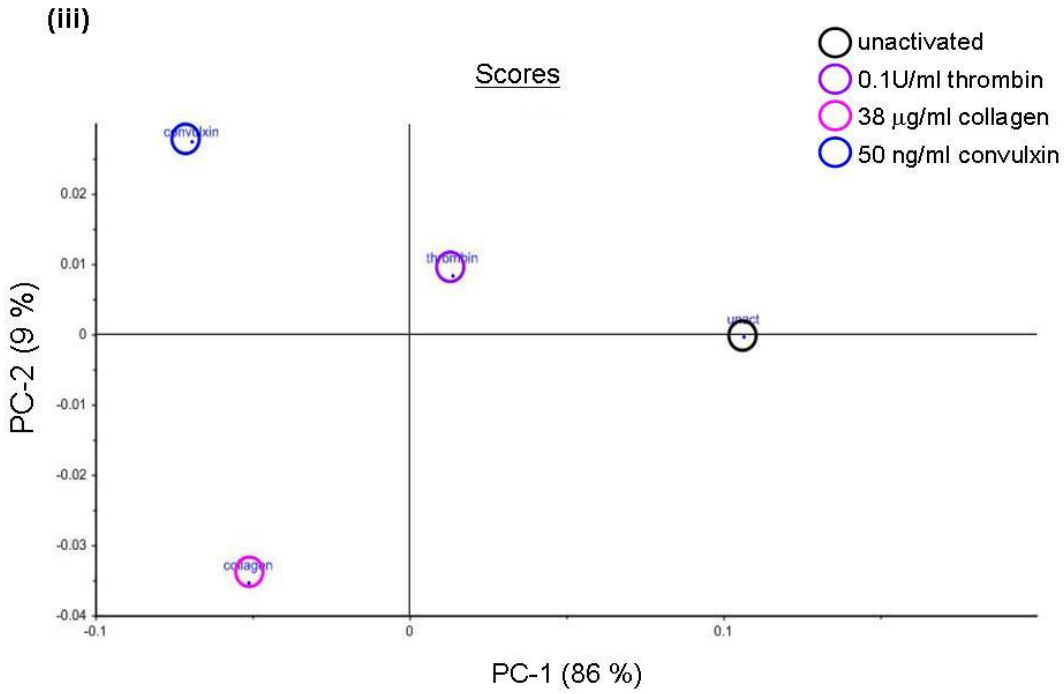

Figure 4.4 (b) Principal component analysis (PCA) of the amide I region of the Raman spectra of unactivated platelets and platelets activated with either 0.1U/ml thrombin, 38 μg/ml collagen or 50 ng/ml convulxin. PCA analysis was performed on the 1600 – 1700 cm^{-1} region of the Raman spectra. The graphs are scatter plots of the first principal component (PC-1) versus the second principal component (PC-2). (i) PCA of all donors, n=10 independent experiments, (ii) PCA of average spectra, graphed on same scale as (i), (iii) PCA of signature, average spectra on a smaller scale illustrating that the samples can be differentiated according to the platelet activator.

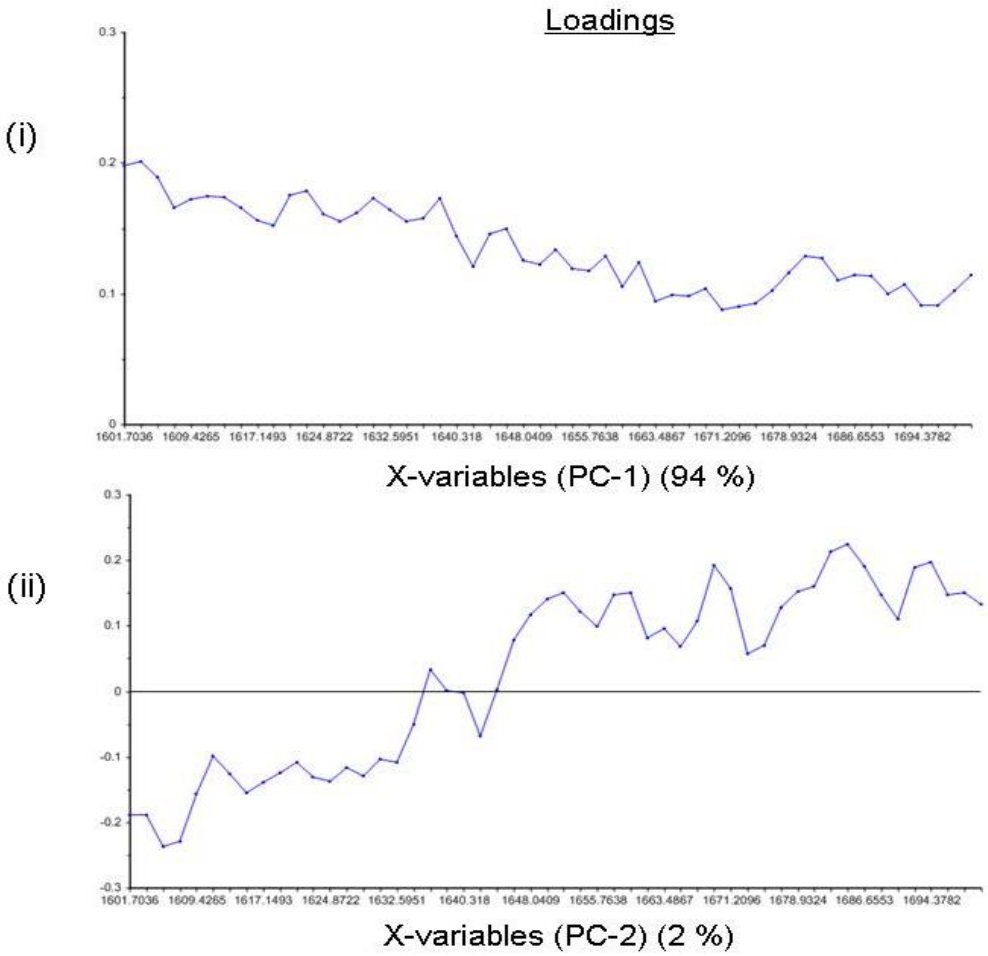

Figure 4.4 (c) The loadings of the principal components used in the Principal component analysis (PCA) scatter plot of the amide I region of the spectrum of all samples. (i) Principal component-1 (PC-1) and (ii) Principal component-2 (PC-2) from the PCA of spectra from all donors (Figure 4.4 (b) (i)). The components are numbered according to the amount of variance they account for, i.e. PC-1 accounts for most of the variance found between the platelet samples. PCA analysis was carried out on the baseline subtracted and normalised Raman data of all samples using The Unscrambler® software.

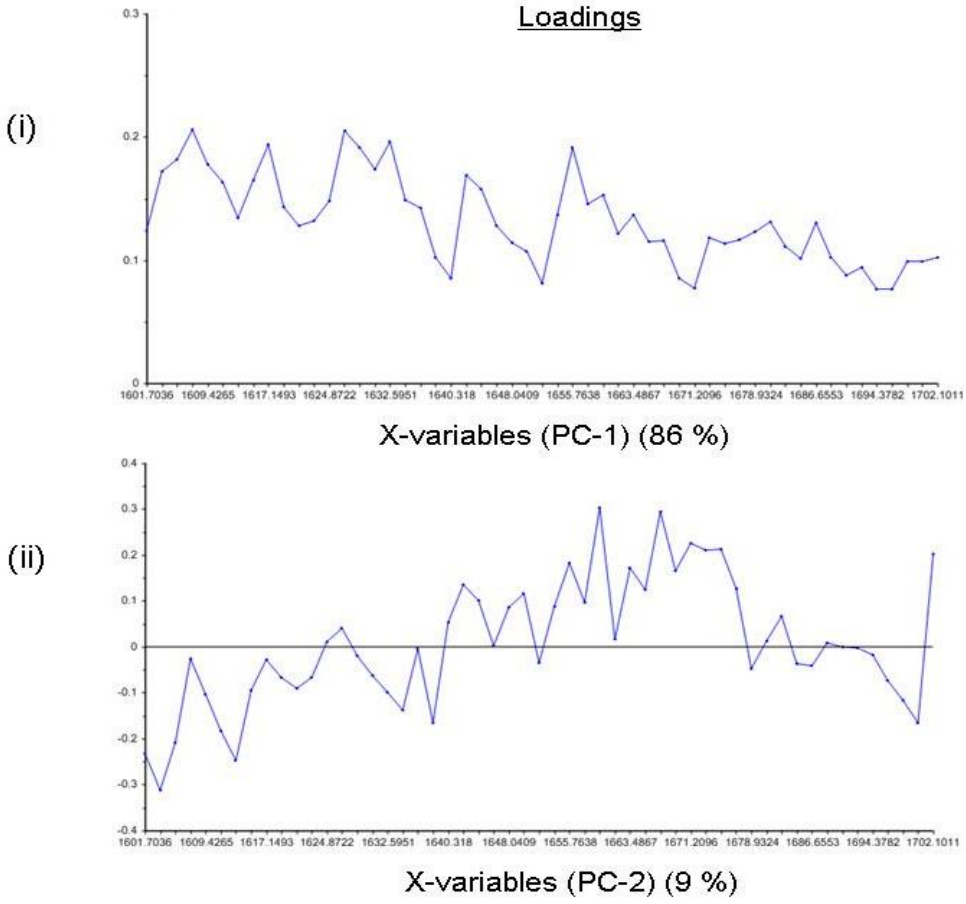

Figure 4.4 (d) The loadings of the principal components used in the Principal component analysis (PCA) scatter plot of the amide I region of the signature Raman spectra. (i) Principal component-1 (PC-1) and (ii) Principal component-2 (PC-2) from the PCA of the signature spectra (Figure 4.4 (b) (ii) and (iii)). The components are numbered according to the amount of variance they account for, i.e. PC-1 accounts for most of the variance found between the platelet samples. PCA analysis was carried out on the baseline subtracted and normalised Raman data of all samples using The Unscrambler® software.

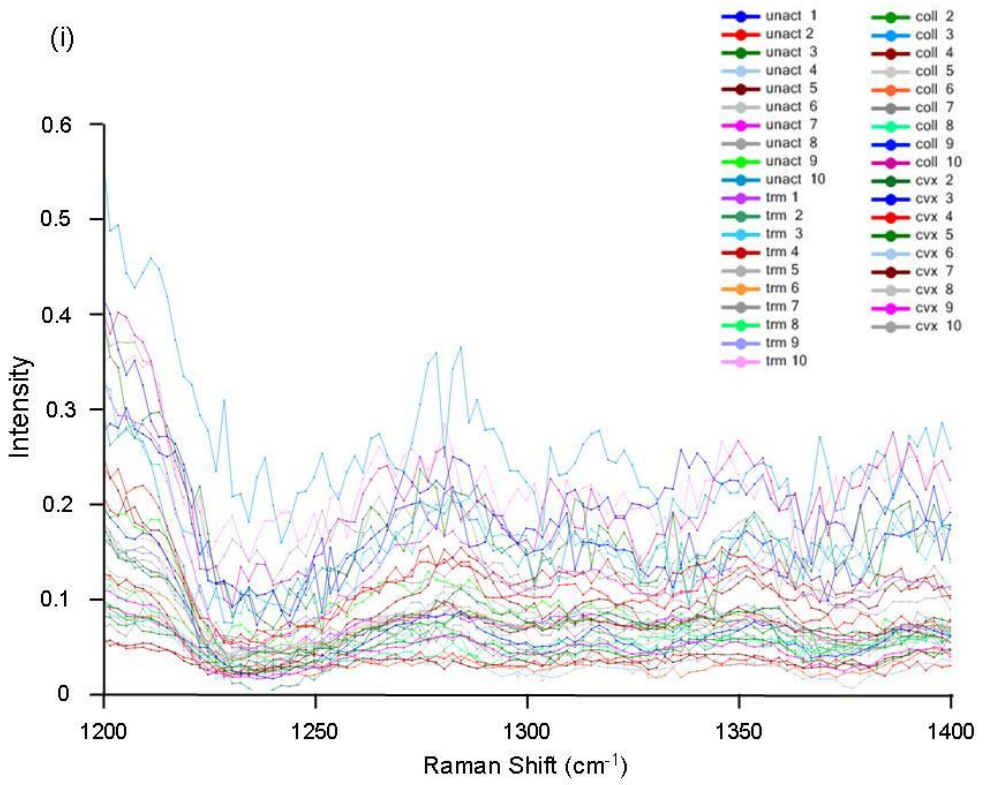
(i)
unact 1
unact 2
unact 3
unact 4
unact 5
unact 6
unact 7
unact 8
unact 9
unact 10
trm 1
trm 2
trm 3
trm 4
trm 5
trm 6
trm 7
trm 8
trm 9
trm 10
coll 2
coll 3
coll 4
coll 5
coll 6
coll 7
coll 8
coll 9
coll 10
cvx 2
cvx 3
cvx 4
cvx 5
cvx 6
cvx 7
cvx 8
cvx 9
cvx 10
Intensity
0.6
0.5
0.4
0.3
0.2
0.1
0
1200
1250
1300
1350
1400
Raman Shift (cm-1)

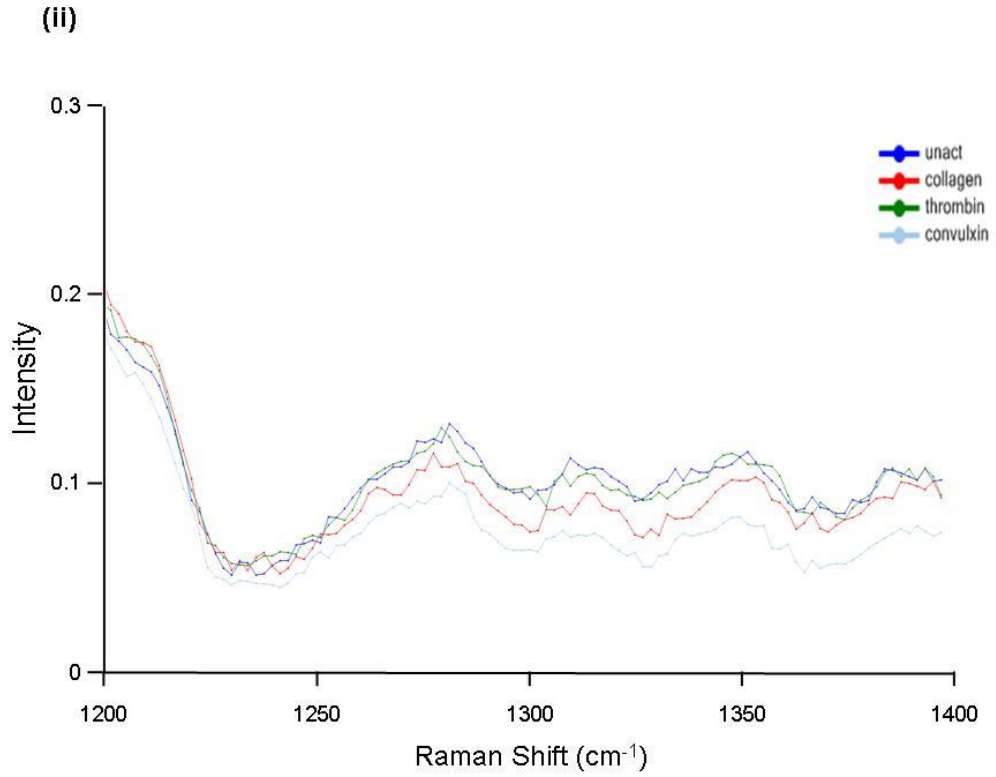
(ii)
unact
collagen
thrombin
convulxin
Intensity
0.3
0.2
0.1
0
1200
1250
1300
1350
1400
Raman Shift (cm-1)

Figure 4.5 (a) The amide III region of the Raman spectra of unactivated platelets and platelets activated with either 0.1U/ml thrombin, 38 μg/ml collagen or 50 ng/ml convulxin. Gel-filtered platelets were fixed with 1 % formaldehyde, centrifuged and supernatant removed. Raman spectra were obtained from the resulting platelet pellet. Spectra were baseline subtracted and normalised to the lipid peak at approximately 3000 cm^{-1}. (i) Three or four spectra were taken for each platelet activator and averaged, to give one spectrum per activator per donor. (ii) Signature Raman spectra of platelets generated by averaging spectra for each platelet activator from all n=10 donors.

(i)

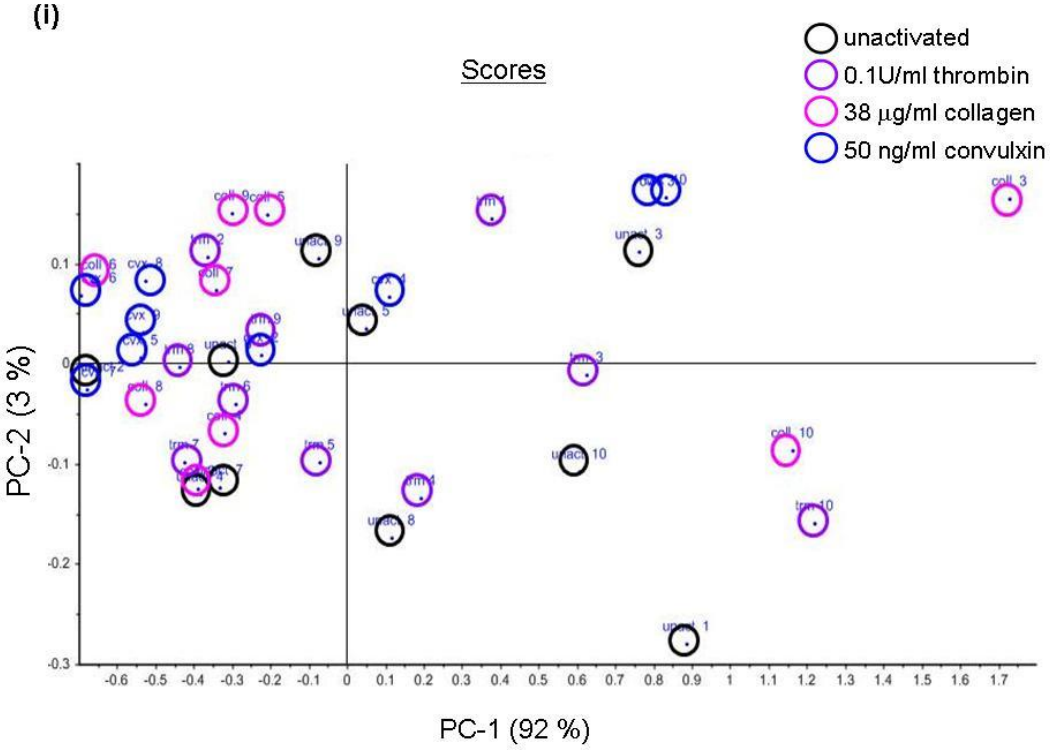
Scores
unactivated
0.1U/ml thrombin
38 μg/ml collagen
50 ng/ml convulxin
PC-2 (3 %)
PC-1 (92 %)

(ii)

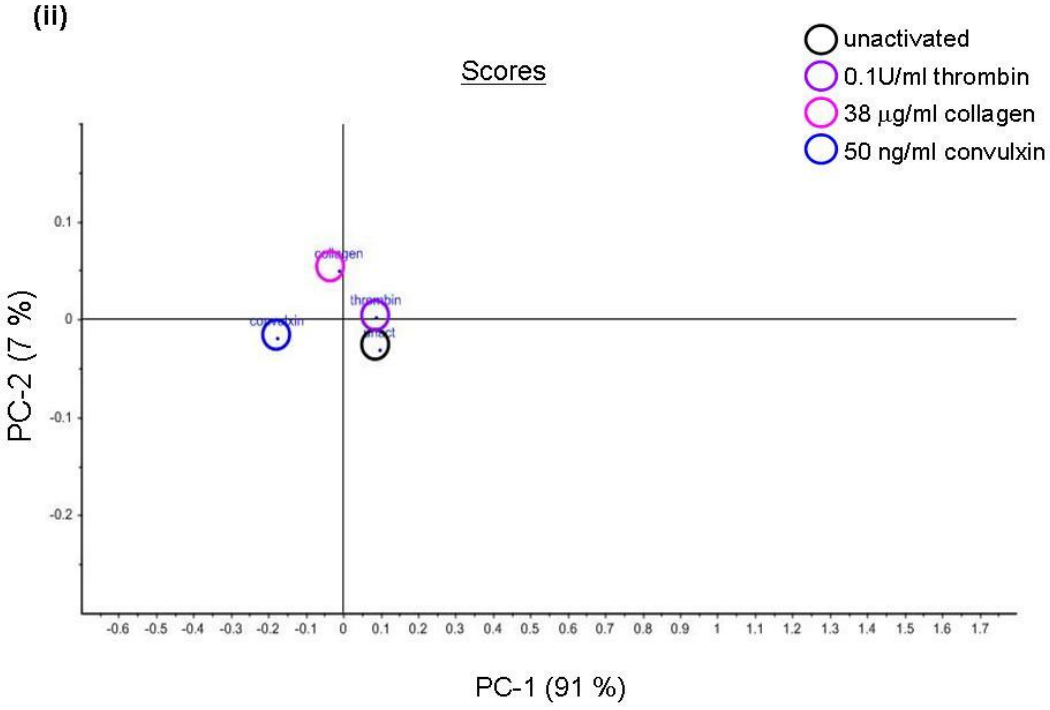
Scores
unactivated
0.1U/ml thrombin
38 μg/ml collagen
50 ng/ml convulxin
collagen
thrombin
PC-2 (7 %)
PC-1 (91 %)

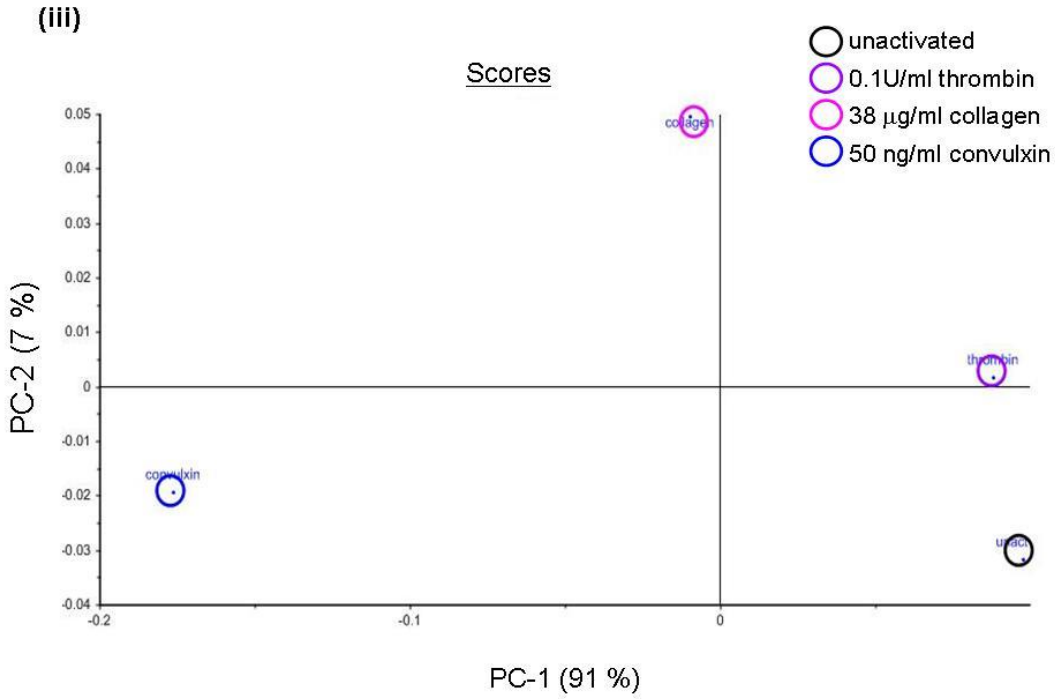

Figure 4.5 (b) Principal component analysis (PCA) of the amide III region of the Raman spectra of unactivated platelets and platelets activated with either 0.1U/ml thrombin, 38 μg/ml collagen or 50 ng/ml convulxin. PCA analysis was performed on the 1200 - 1400 cm^{-1} region of the Raman spectra. The graphs are scatter plots of the first principal component (PC-1) versus the second principal component (PC-2). (i) PCA of all donors, n=10 independent experiments, (ii) PCA of average spectra, graphed on same scale as (i), (iii) PCA of signature, average spectra on a smaller scale illustrating that the samples can be differentiated according to the platelet activator.

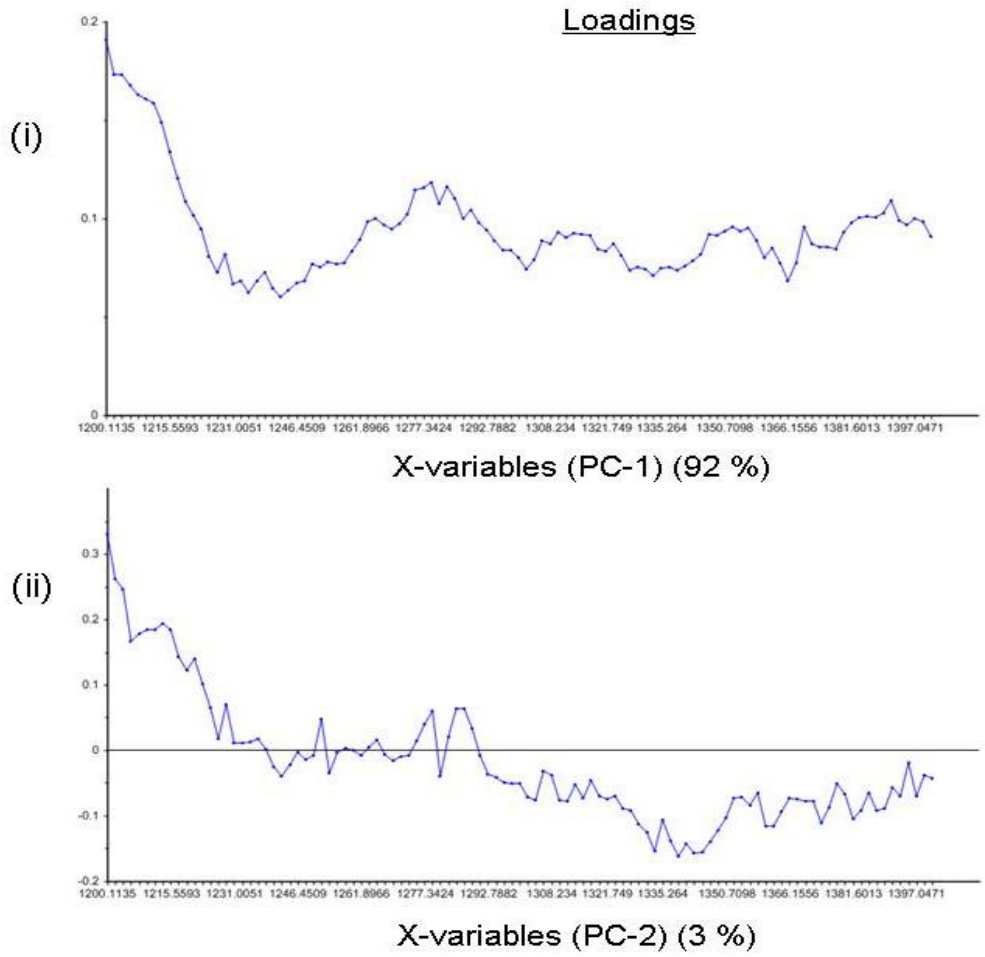

Figure 4.5 (c) The loadings of the principal components used in the Principal component analysis (PCA) scatter plot of the amide III region of all platelet Raman spectra. (i) Principal component-1 (PC-1) and (ii) Principal component-2 (PC-2) from the PCA of all spectra (Figure 4.5 (b) (i)). The components are numbered according to the amount of variance they account for, i.e. PC-1 accounts for most of the variance found between the platelet samples. PCA analysis was carried out on the baseline subtracted and normalised Raman data of all samples using The Unscrambler® software.

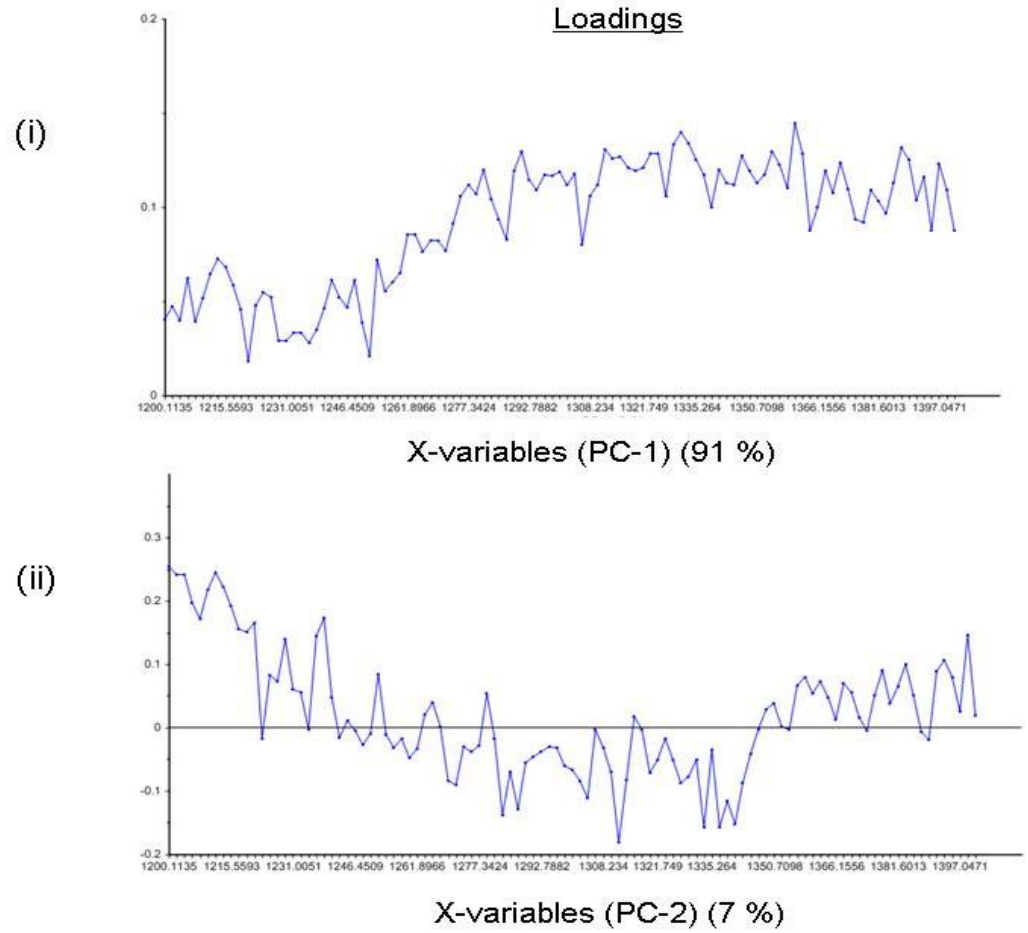

Figure 4.5 (d) The loadings of the principal components used in the Principal component analysis (PCA) scatter plot of the amide III region of the signature platelet Raman spectra. (i) Principal component-1 (PC-1) and (ii) Principal component-2 (PC-2) from the PCA of the signature Raman spectra (Figure 4.5 (b) (ii) and (iii)). The components are numbered according to the amount of variance they account for, i.e. PC-1 accounts for most of the variance found between the platelet samples. PCA analysis was carried out on the baseline subtracted and normalised Raman data of all samples using The Unscrambler® software.

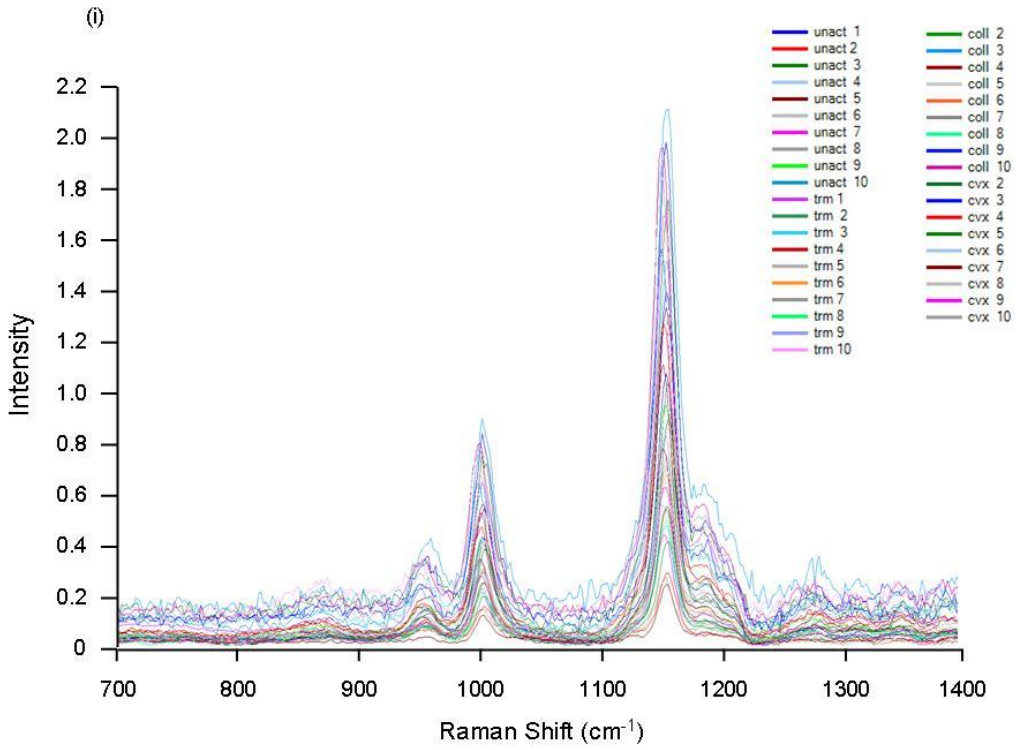
(i)
unact 1
unact 2
unact 3
unact 4
unact 5
unact 6
unact 7
unact 8
unact 9
unact 10
trm 1
trm 2
trm 3
trm 4
trm 5
trm 6
trm 7
trm 8
trm 9
trm 10
coll 2
coll 3
coll 4
coll 5
coll 6
coll 7
coll 8
coll 9
coll 10
cvx 2
cvx 3
cvx 4
cvx 5
cvx 6
cvx 7
cvx 8
cvx 9
cvx 10
Intensity
Raman Shift (cm-1)

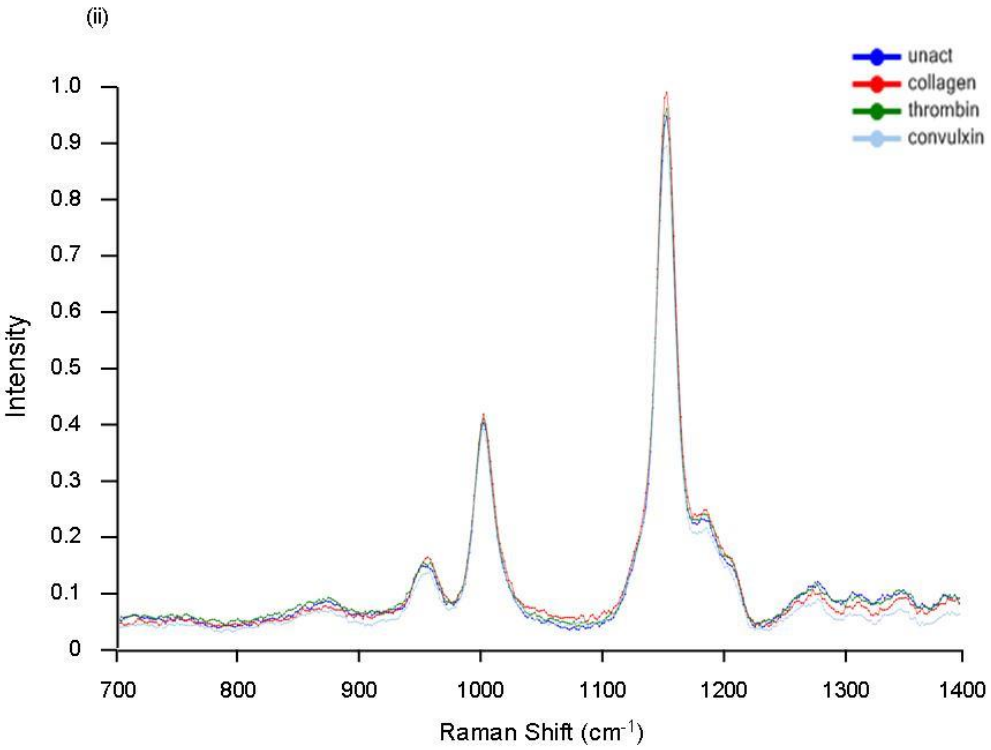
(ii)
unact
collagen
thrombin
convulxin
Intensity
Raman Shift (cm-1)

Figure 4.6 (a) The 700 – 1400 cm^{-1} region of the Raman spectra of unactivated platelets and platelets activated with either 0.1U/ml thrombin, 38 μg/ml collagen or 50 ng/ml convulxin. Gel-filtered platelets were fixed with 1 % formaldehyde, centrifuged and supernatant removed. Raman spectra were obtained from the resulting platelet pellet. Spectra were baseline subtracted and normalised to the lipid peak at approximately 3000 cm^{-1}. (i) Three or four spectra were taken for each platelet activator and averaged, to give one spectrum per activator per donor. (ii) Signature Raman spectra of platelets generated by averaging spectra for each platelet activator from all n=10 donors.

(i)

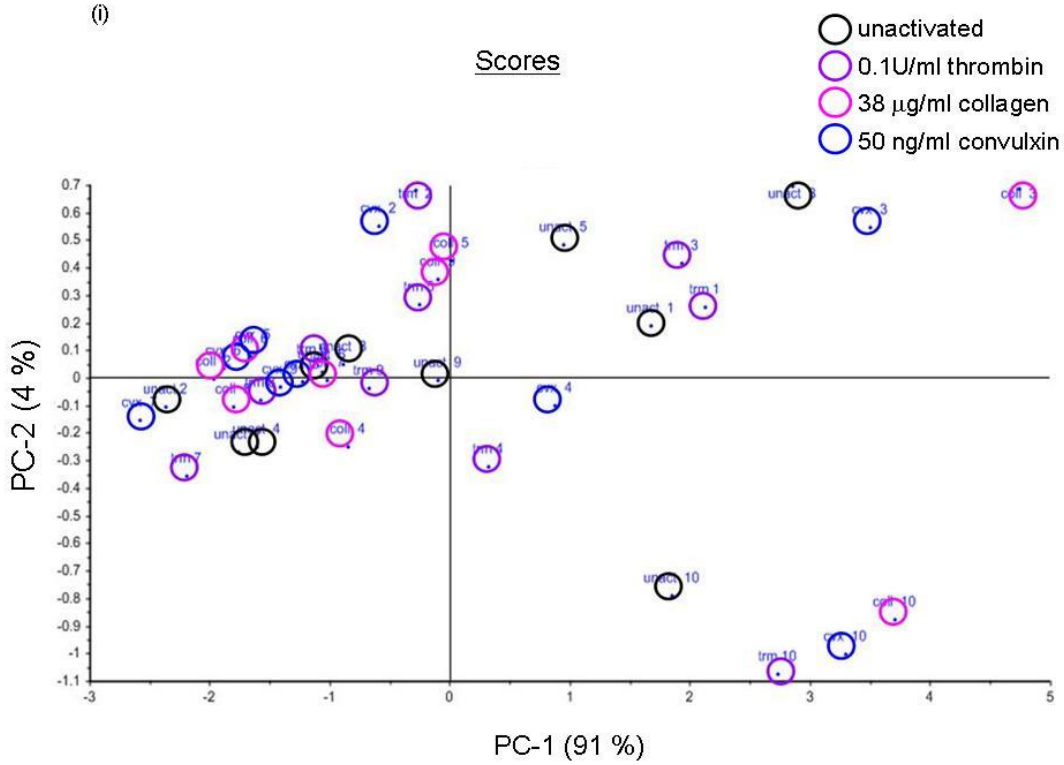
Scores
unactivated
0.1U/ml thrombin
38 μg/ml collagen
50 ng/ml convulxin
PC-2 (4 %)
PC-1 (91 %)

(ii)

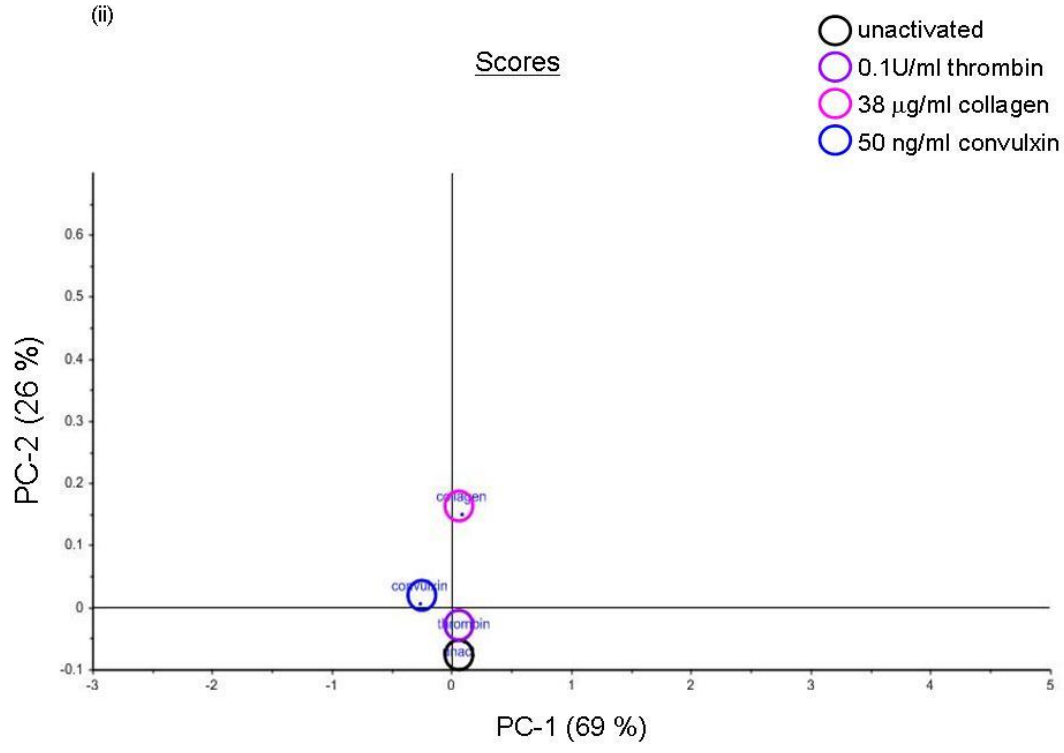
Scores
unactivated
0.1U/ml thrombin
38 μg/ml collagen
50 ng/ml convulxin
PC-2 (26 %)
PC-1 (69 %)
collagen
convulxin
thrombin

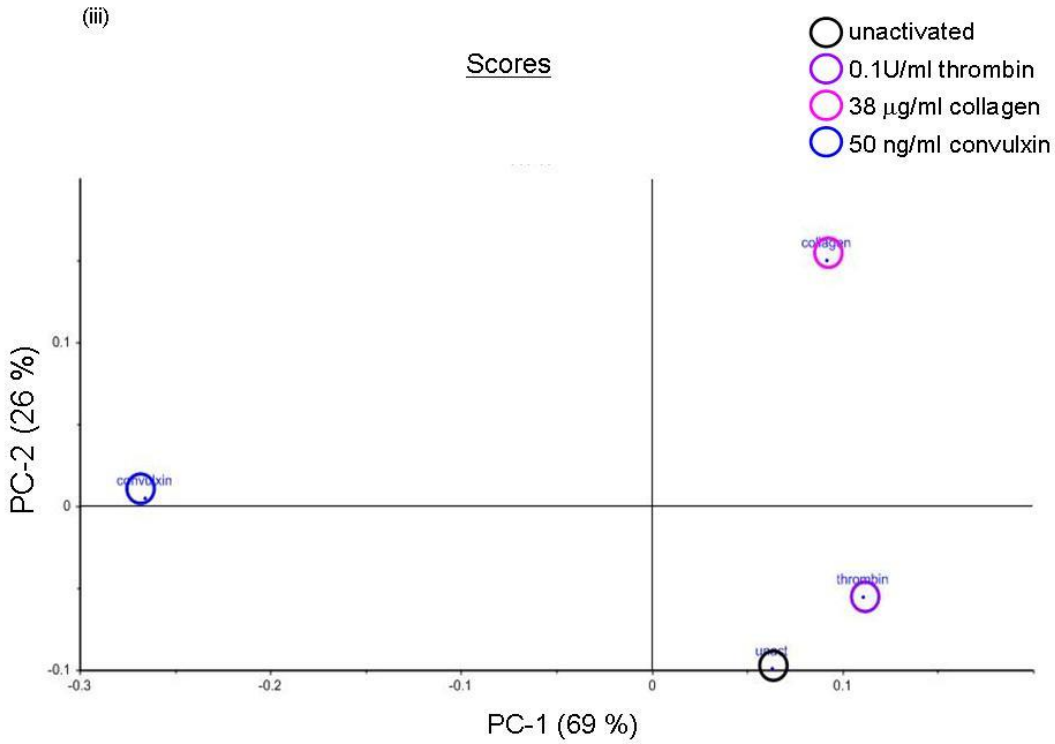

Figure 4.6 (b) Principal component analysis (PCA) of the 700 – 1400 cm^{-1} region of the Raman spectra of unactivated platelets and platelets activated with either 0.1U/ml thrombin, 38 μg/ml collagen or 50 ng/ml convulxin. PCA analysis was performed on the 700 – 1400 cm^{-1} region of the Raman spectra. The graphs are scatter plots of the first principal component (PC-1) versus the second principal component (PC-2). (i) PCA of all donors, n=10 independent experiments, (ii) PCA of average spectra, graphed on same scale as (i), (iii) PCA of signature, average spectra on a smaller scale illustrating that the samples can be differentiated according to the platelet activator.

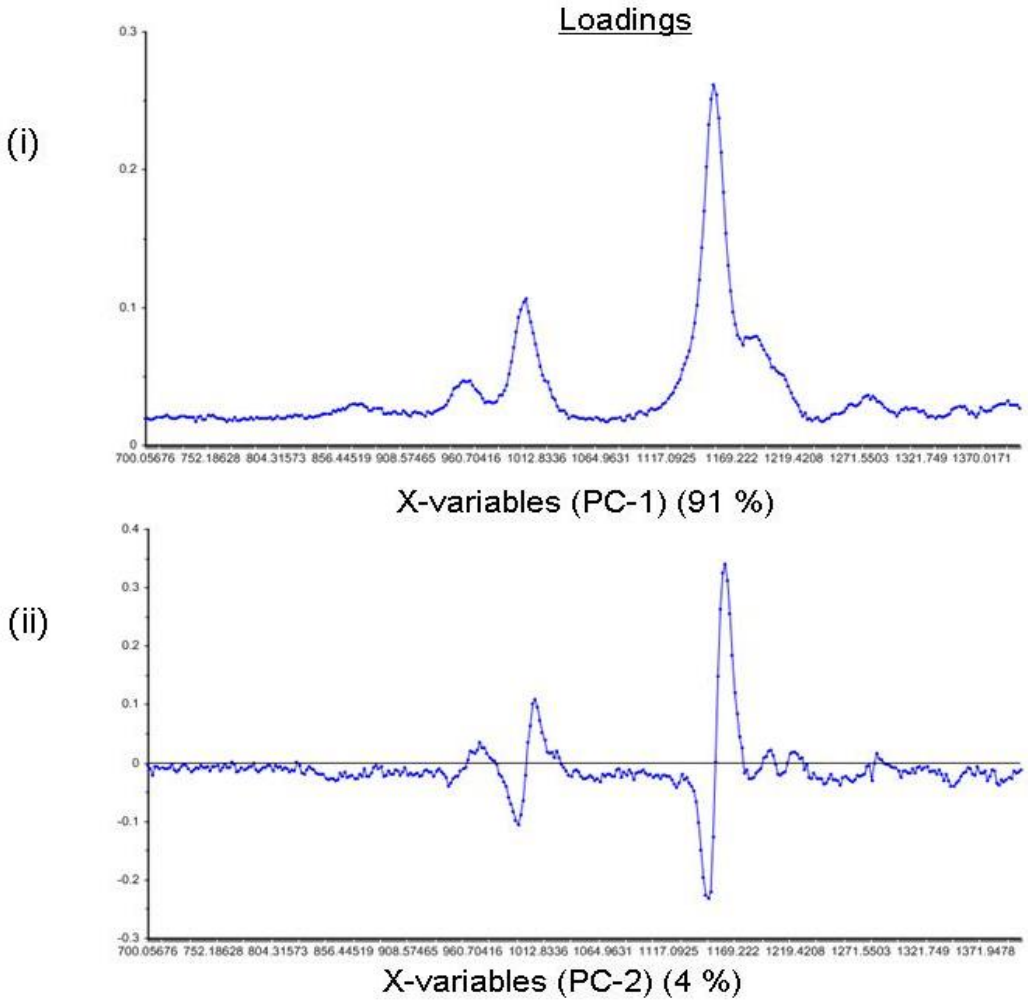

Figure 4.6 (c) The loadings of the principal components used in the Principal component analysis (PCA) scatter plot of the 700 – 1400 cm^{-1} region of the spectrum of all samples. (i) Principal component-1 (PC-1) and (ii) Principal component-2 (PC-2) from the PCA of spectra from all donors (Figure 4.6 (b) (i)). The components are numbered according to the amount of variance they account for, i.e. PC-1 accounts for most of the variance found between the platelet samples. PCA analysis was carried out on the baseline subtracted and normalised Raman data of all samples using The Unscrambler® software.

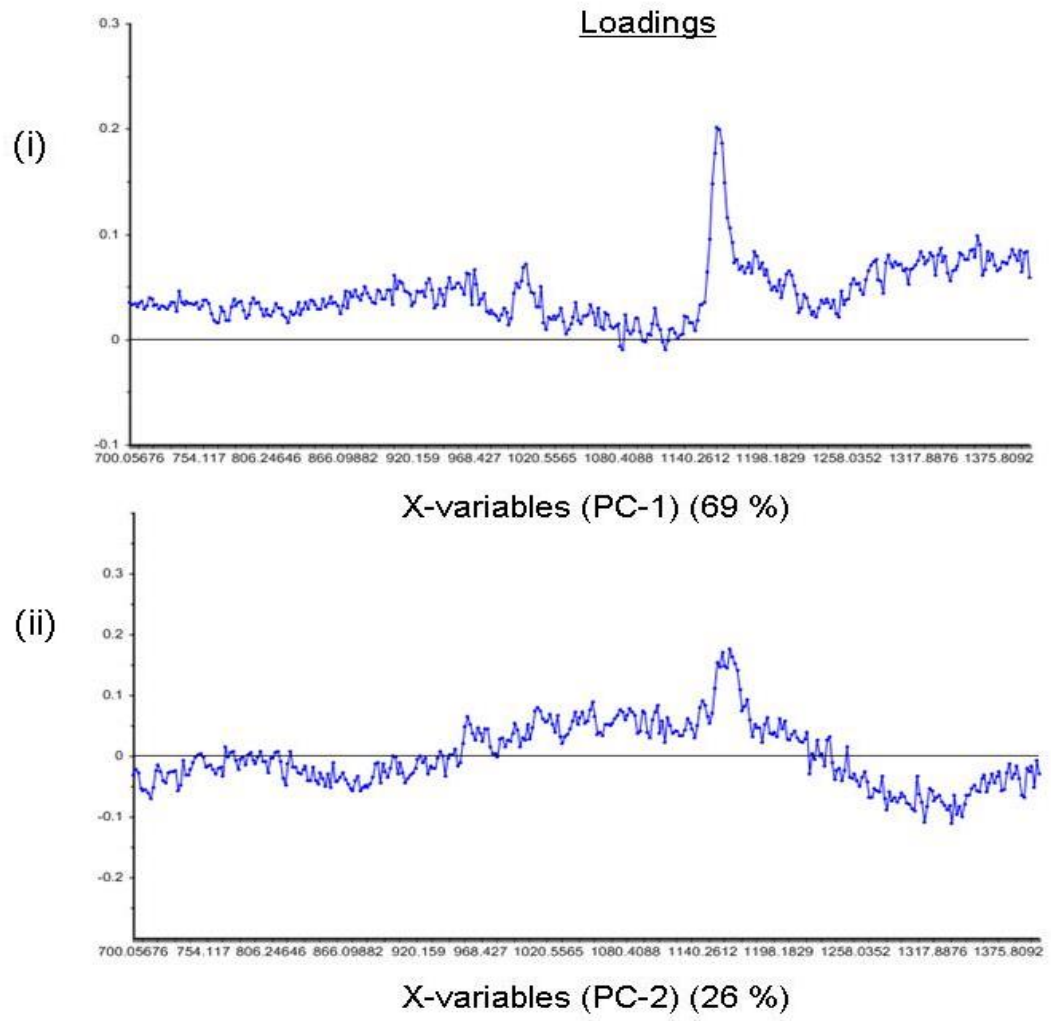

Figure 4.6 (d) The loadings of the principal components used in the Principal component analysis (PCA) scatter plot of the 700 – 1400 cm^{-1} region of the signature Raman spectra. (i) Principal component-1 (PC-1) and (ii) Principal component-2 (PC-2) from the PCA of the signature spectra (Figure 4.6 (b) (ii) and (iii)). The components are numbered according to the amount of variance they account for, i.e. PC-1 accounts for most of the variance found between the platelet samples. PCA analysis was carried out on the baseline subtracted and normalised Raman data of all samples using The Unscrambler® software.

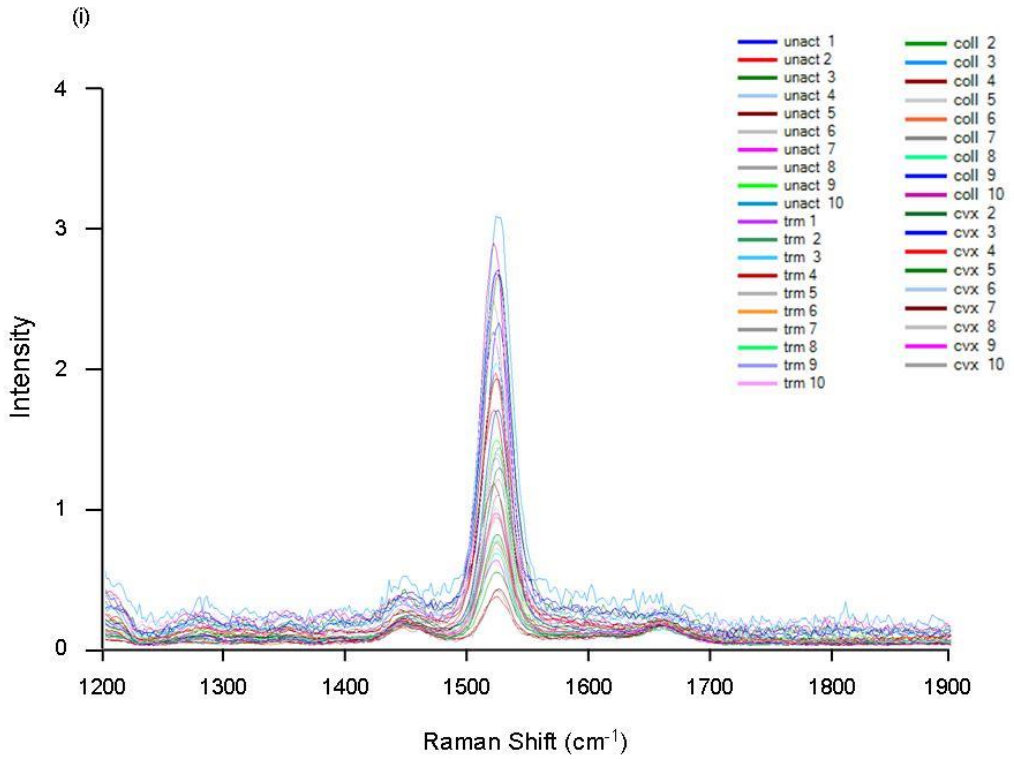
(i)
unact 1
unact 2
unact 3
unact 4
unact 5
unact 6
unact 7
unact 8
unact 9
unact 10
trm 1
trm 2
trm 3
trm 4
trm 5
trm 6
trm 7
trm 8
trm 9
trm 10
coll 2
coll 3
coll 4
coll 5
coll 6
coll 7
coll 8
coll 9
coll 10
cvx 2
cvx 3
cvx 4
cvx 5
cvx 6
cvx 7
cvx 8
cvx 9
cvx 10
Intensity
0
1
2
3
4
1200
1300
1400
1500
1600
1700
1800
1900
Raman Shift (cm-1)

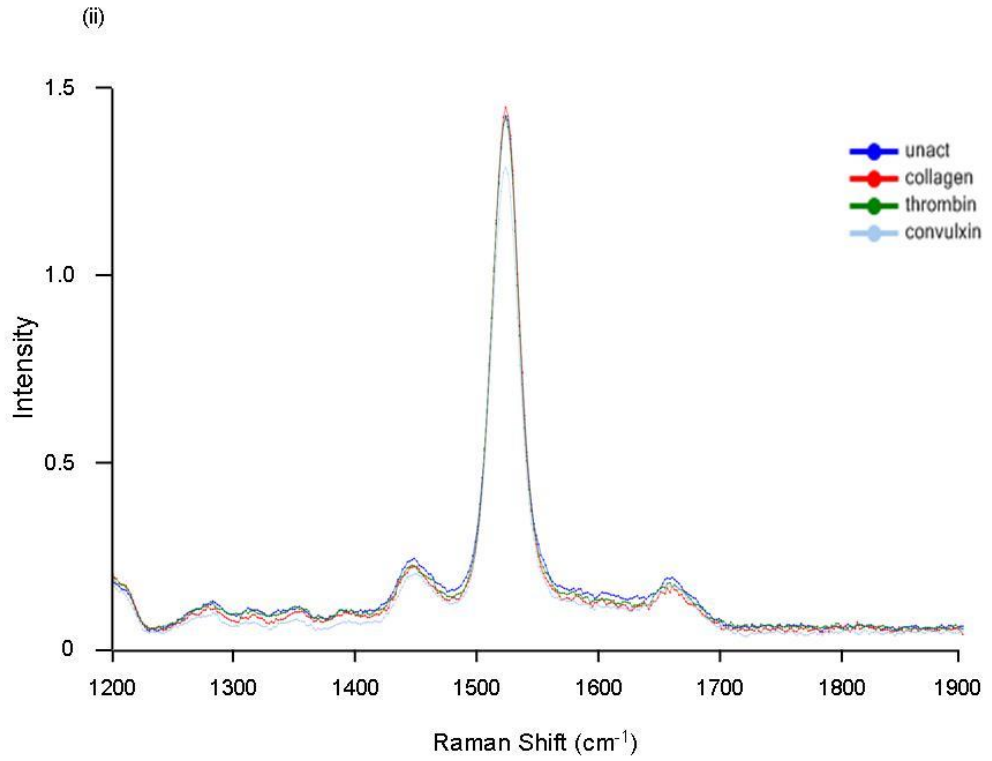
(ii)
unact
collagen
thrombin
convulxin
Intensity
0
0.5
1.0
1.5
1200
1300
1400
1500
1600
1700
1800
1900
Raman Shift (cm-1)

Figure 4.7 (a) The 1200 – 1900 cm^{-1} region of the Raman spectra of unactivated platelets and platelets activated with either 0.1U/ml thrombin, 38 μg/ml collagen or 50 ng/ml convulxin. Gel-filtered platelets were fixed with 1 % formaldehyde, centrifuged and supernatant removed. Raman spectra were obtained from the resulting platelet pellet. Spectra were baseline subtracted and normalised to the lipid peak at approximately 3000 cm^{-1}. (i) Three or four spectra were taken for each platelet activator and averaged, to give one spectrum per activator per donor. (ii) Signature Raman spectra of platelets generated by averaging spectra for each platelet activator from all n=10 donors.

(i)

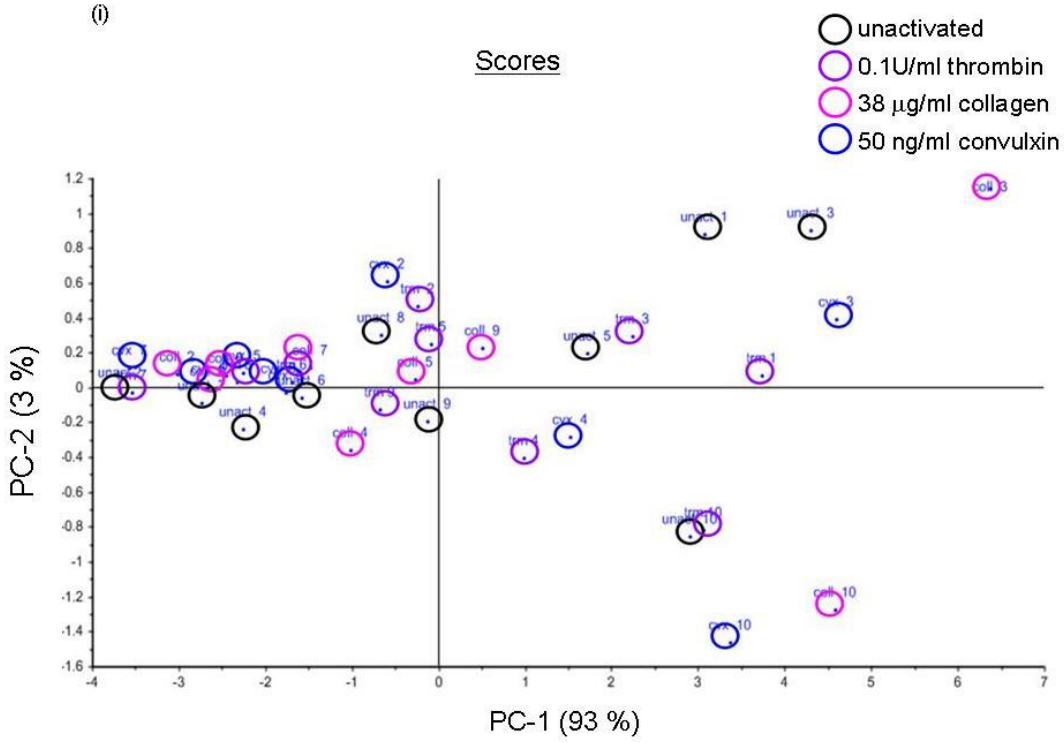
Scores
unactivated
0.1U/ml thrombin
38 μg/ml collagen
50 ng/ml convulxin
PC-2 (3 %)
PC-1 (93 %)

(ii)

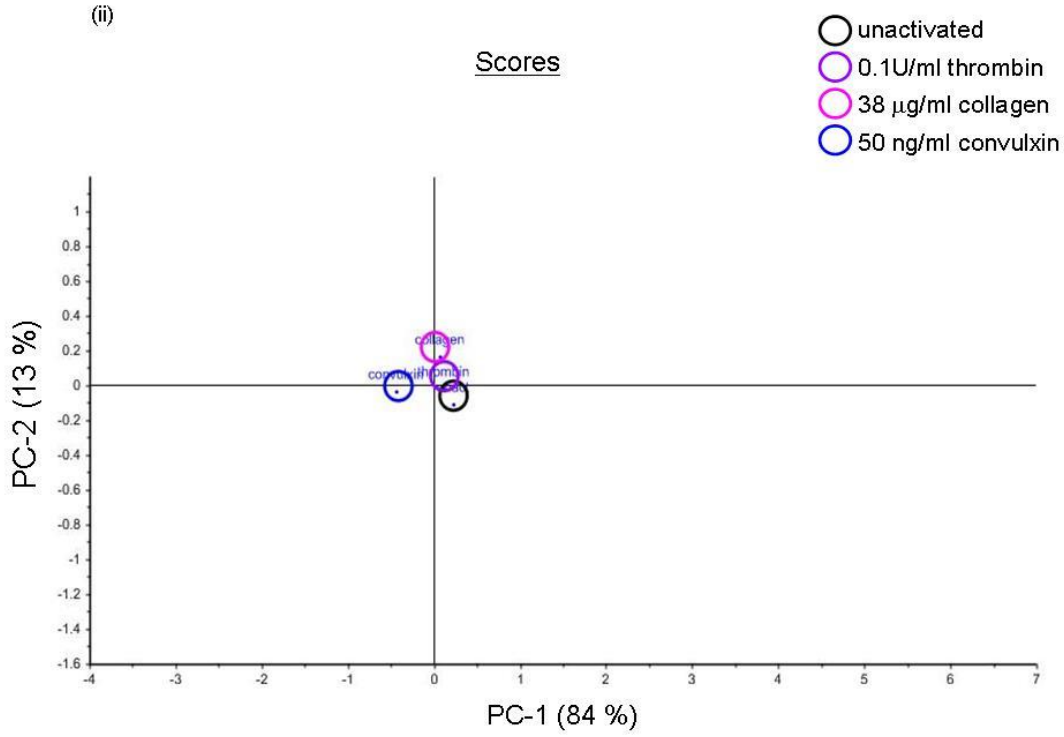
Scores
unactivated
0.1U/ml thrombin
38 μg/ml collagen
50 ng/ml convulxin
PC-2 (13 %)
PC-1 (84 %)

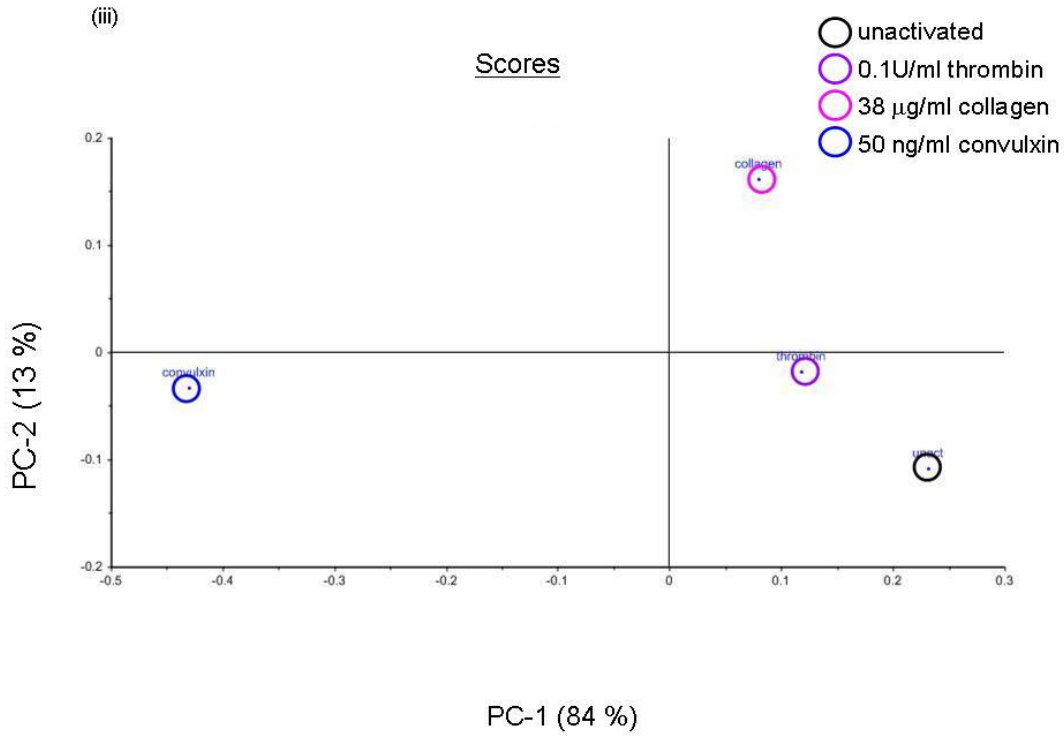

Figure 4.7 (b) Principal component analysis (PCA) of the 1200 – 1900 cm^{-1} region of the Raman spectra of unactivated platelets and platelets activated with either 0.1U/ml thrombin, 38 μg/ml collagen or 50 ng/ml convulxin. PCA analysis was performed on the 1200 – 1900 cm^{-1} region of the Raman spectra. The graphs are scatter plots of the first principal component (PC-1) versus the second principal component (PC-2). (i) PCA of all donors, n=10 independent experiments, (ii) PCA of average spectra, graphed on same scale as (i), (iii) PCA of signature, average spectra on a smaller scale illustrating that the samples can be differentiated according to the platelet activator.

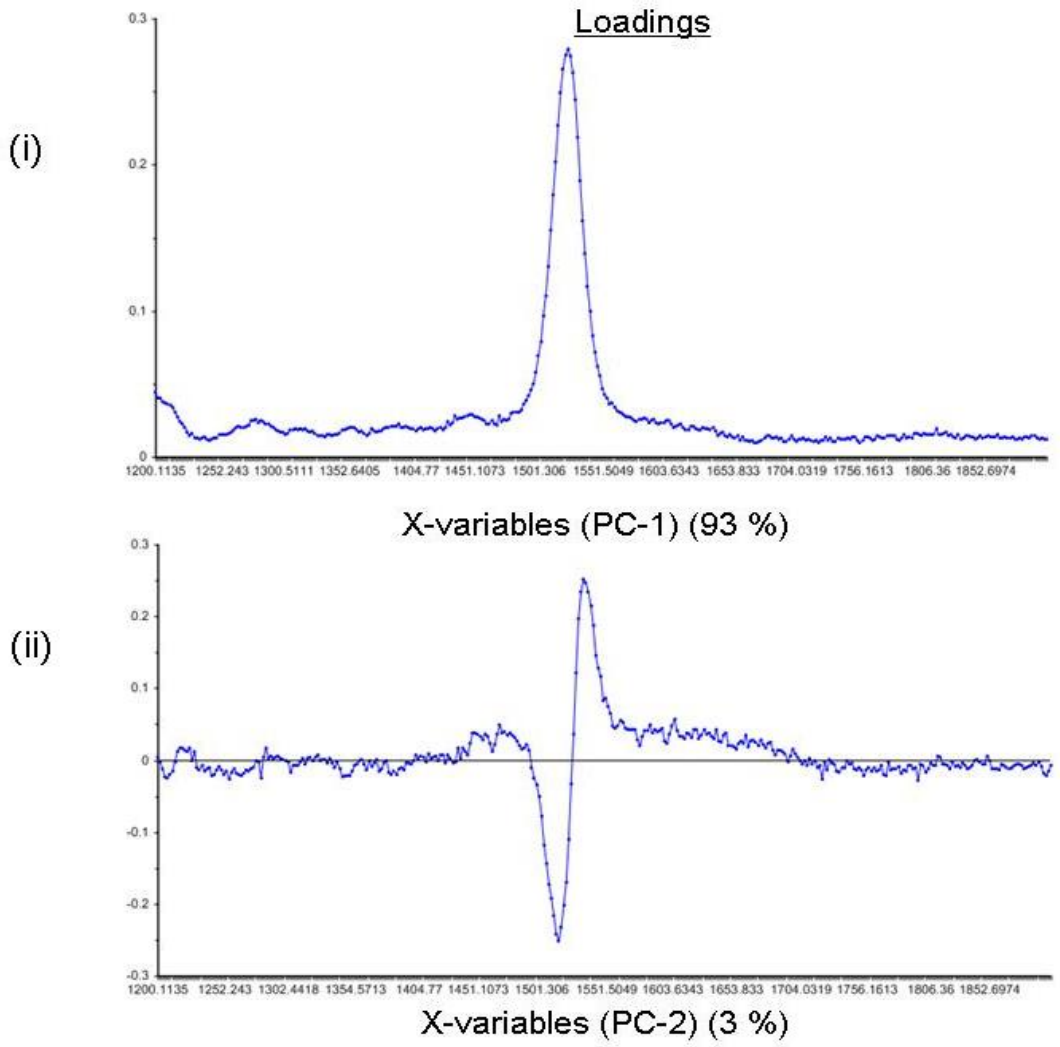

Figure 4.7 (c) The loadings of the principal components used in the Principal component analysis (PCA) scatter plot of the 1200 – 1900 cm^{-1} region of the spectrum of all samples. (i) Principal component-1 (PC-1) and (ii) Principal component-2 (PC-2) from the PCA of spectra from all donors (Figure 4.7 (b) (i)). The components are numbered according to the amount of variance they account for, i.e. PC-1 accounts for most of the variance found between the platelet samples. PCA analysis was carried out on the baseline subtracted and normalised Raman data of all samples using The Unscrambler® software.

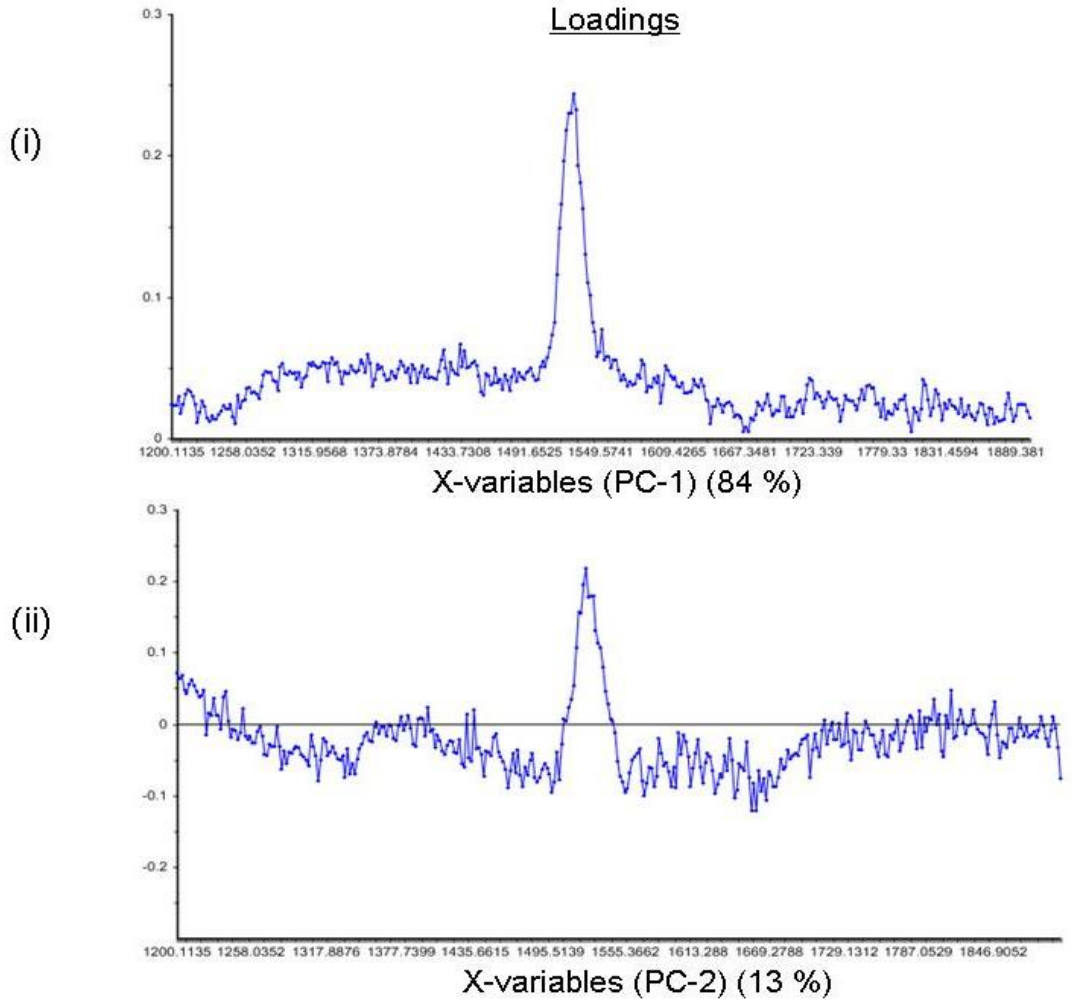

Figure 4.7 (d) The loadings of the principal components used in the Principal component analysis (PCA) scatter plot of the 1200 – 1900 cm^{-1} region of the signature Raman spectra. (i) Principal component-1 (PC-1) and (ii) Principal component-2 (PC-2) from the PCA of the signature spectra (Figure 4.7 (b) (ii) and (iii)). The components are numbered according to the amount of variance they account for, i.e. PC-1 accounts for most of the variance found between the platelet samples. PCA analysis was carried out on the baseline subtracted and normalised Raman data of all samples using The Unscrambler® software.

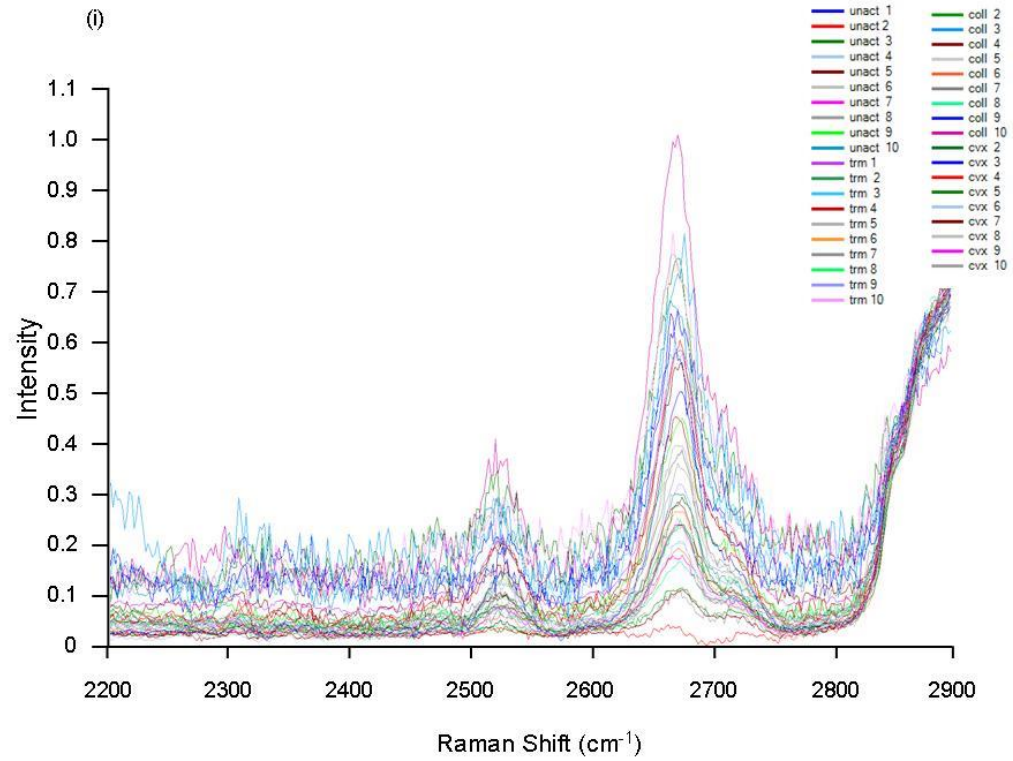
(i)
unact 1
unact 2
unact 3
unact 4
unact 5
unact 6
unact 7
unact 8
unact 9
unact 10
trm 1
trm 2
trm 3
trm 4
trm 5
trm 6
trm 7
trm 8
trm 9
trm 10
coll 2
coll 3
coll 4
coll 5
coll 6
coll 7
coll 8
coll 9
coll 10
cvx 2
cvx 3
cvx 4
cvx 5
cvx 6
cvx 7
cvx 8
cvx 9
cvx 10
Intensity
Raman Shift (cm-1)

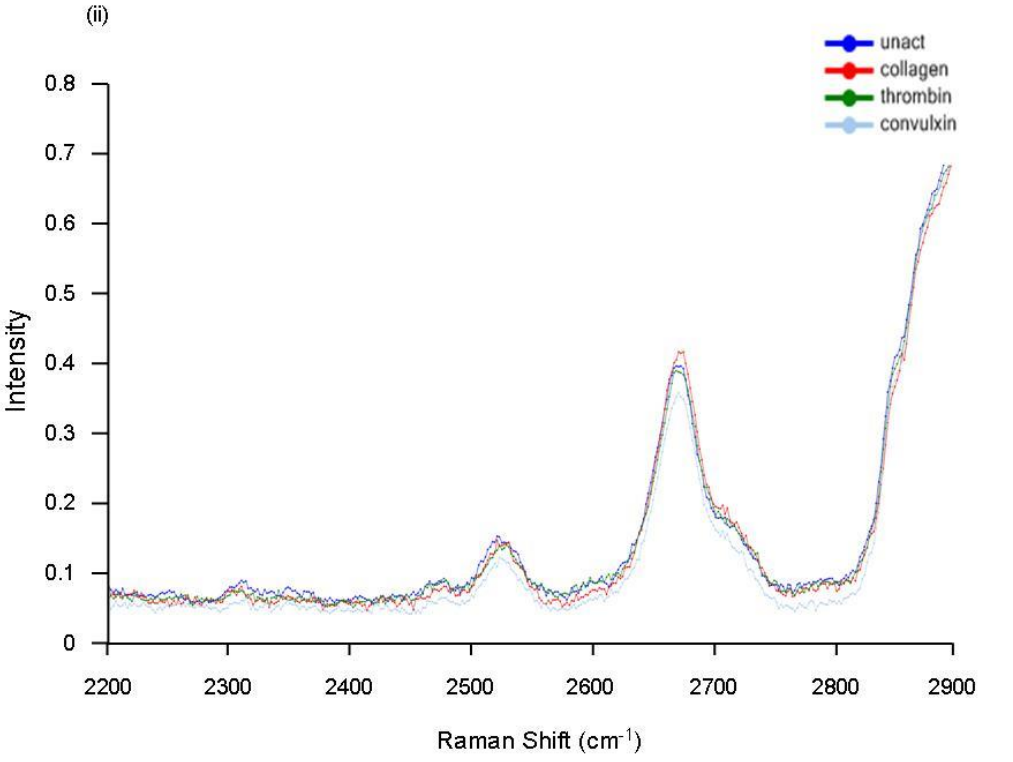
(ii)
unact
collagen
thrombin
convulxin
Intensity
Raman Shift (cm-1)

Figure 4.8 (a) The 2200 – 2900 cm^{-1} region of the Raman spectra of unactivated platelets and platelets activated with either 0.1U/ml thrombin, 38 μg/ml collagen or 50 ng/ml convulxin. Gel-filtered platelets were fixed with 1 % formaldehyde, centrifuged and supernatant removed. Raman spectra were obtained from the resulting platelet pellet. Spectra were baseline subtracted and normalised to the lipid peak at approximately 3000 cm^{-1}. (i) Three or four spectra were taken for each platelet activator and averaged, to give one spectrum per activator per donor. (ii) Signature Raman spectra of platelets generated by averaging spectra for each platelet activator from all n=10 donors.

(i)

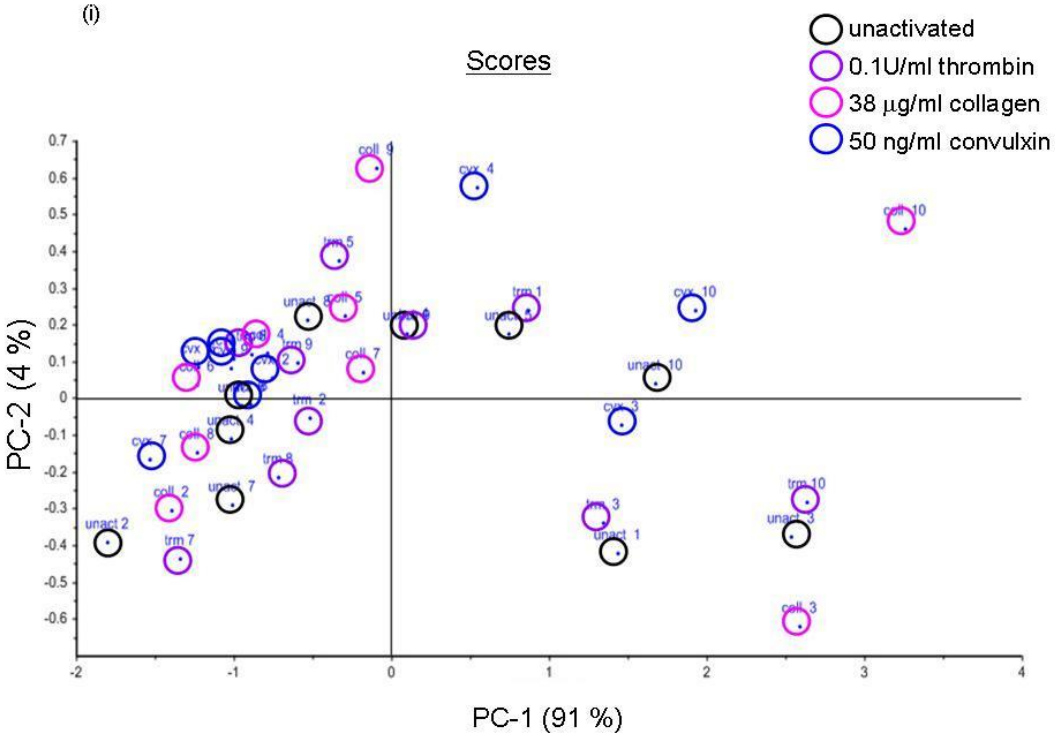
Scores
unactivated
0.1U/ml thrombin
38 μg/ml collagen
50 ng/ml convulxin
PC-2 (4 %)
PC-1 (91 %)

(ii)

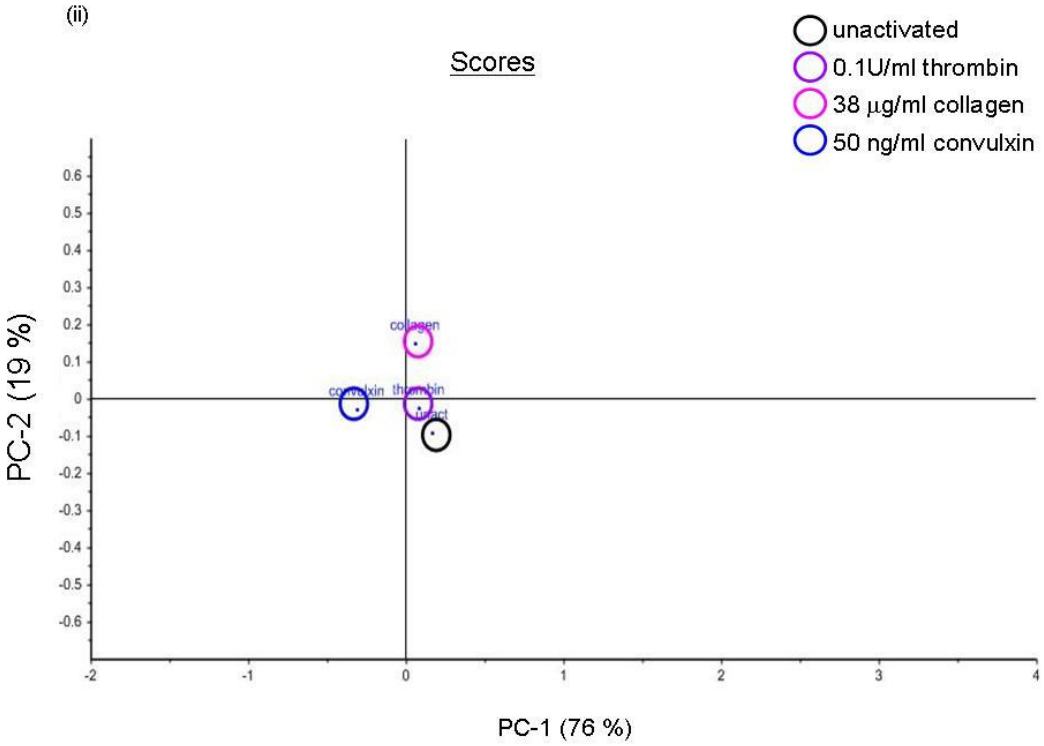
Scores
unactivated
0.1U/ml thrombin
38 μg/ml collagen
50 ng/ml convulxin
PC-2 (19 %)
PC-1 (76 %)
collagen
convulxin
thrombin
unact

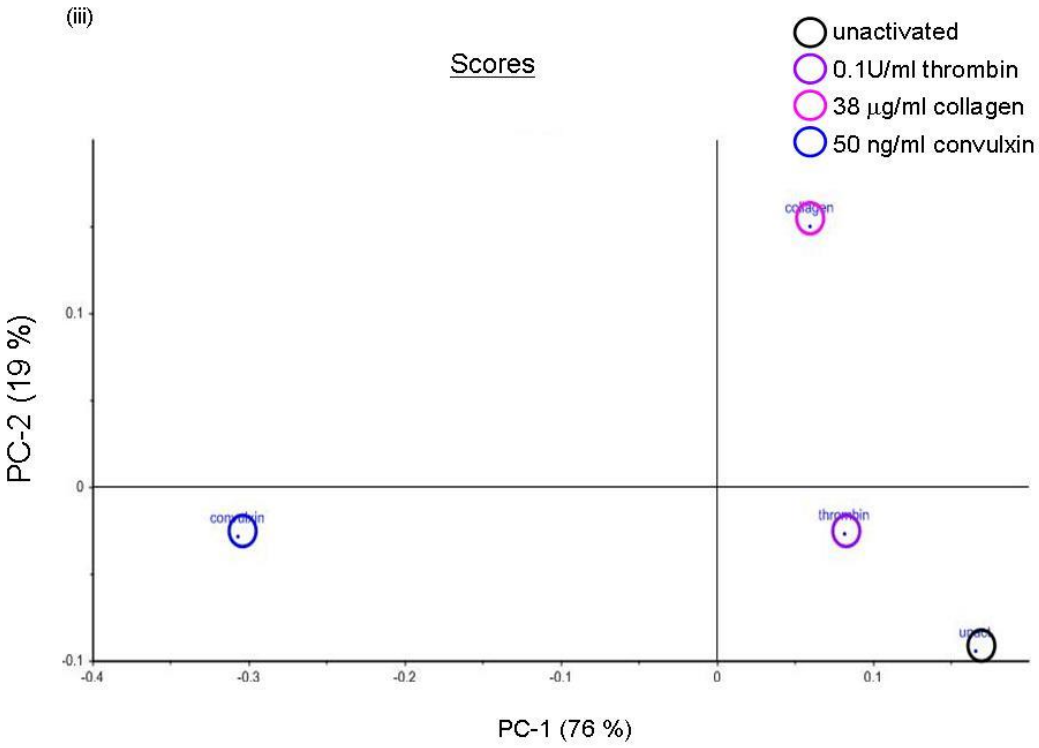

Figure 4.8 (b) Principal component analysis (PCA) of the 2200 – 2900 cm^{-1} region of the Raman spectra of unactivated platelets and platelets activated with either 0.1U/ml thrombin, 38 μg/ml collagen or 50 ng/ml convulxin. PCA analysis was performed on the 2200 – 2900 cm^{-1} region of the Raman spectra. The graphs are scatter plots of the first principal component (PC-1) versus the second principal component (PC-2). (i) PCA of all donors, n=10 independent experiments, (ii) PCA of average spectra, graphed on same scale as (i), (iii) PCA of signature, average spectra on a smaller scale illustrating that the samples can be differentiated according to the platelet activator.

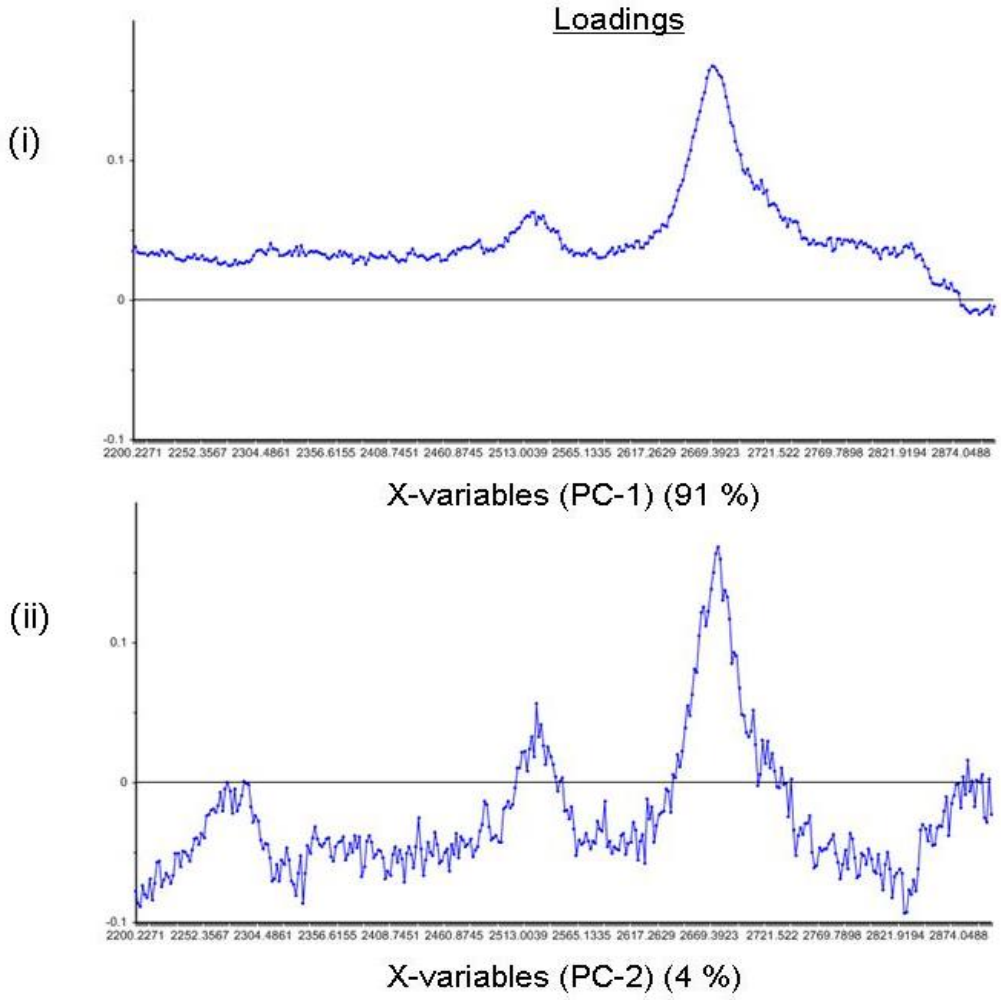

Figure 4.8 (c) The loadings of the principal components used in the Principal component analysis (PCA) scatter plot of the 2200 – 2900 cm^{-1} region of the spectrum of all samples. (i) Principal component-1 (PC-1) and (ii) Principal component-2 (PC-2) from the PCA of spectra from all donors (Figure 4.8 (b) (i)). The components are numbered according to the amount of variance they account for, i.e. PC-1 accounts for most of the variance found between the platelet samples. PCA analysis was carried out on the baseline subtracted and normalised Raman data of all samples using The Unscrambler® software.

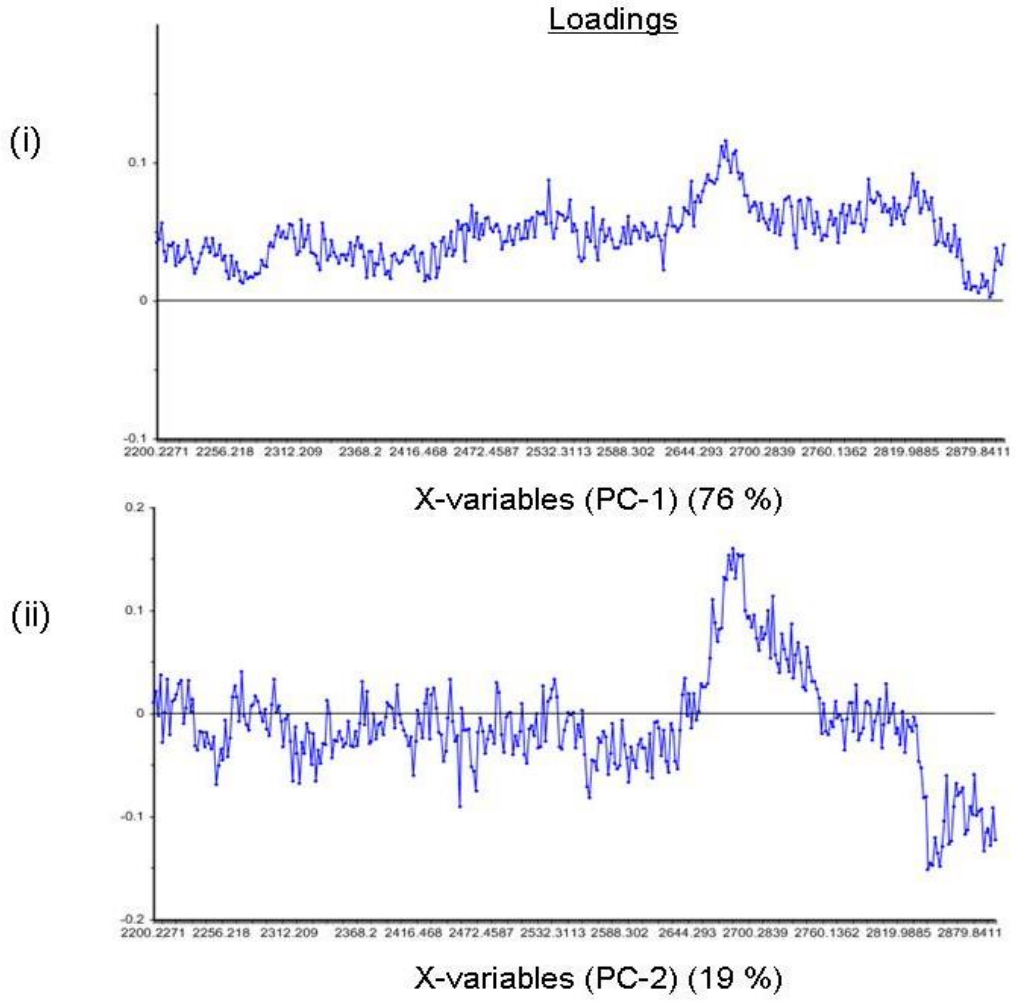

Figure 4.8 (d) The loadings of the principal components used in the Principal component analysis (PCA) scatter plot of the 2200 – 2900 cm^{-1} region of the signature Raman spectra. (i) Principal component-1 (PC-1) and (ii) Principal component-2 (PC-2) from the PCA of the signature spectra (Figure 4.8 (b) (ii) and (iii)). The components are numbered according to the amount of variance they account for, i.e. PC-1 accounts for most of the variance found between the platelet samples. PCA analysis was carried out on the baseline subtracted and normalised Raman data of all samples using The Unscrambler® software.

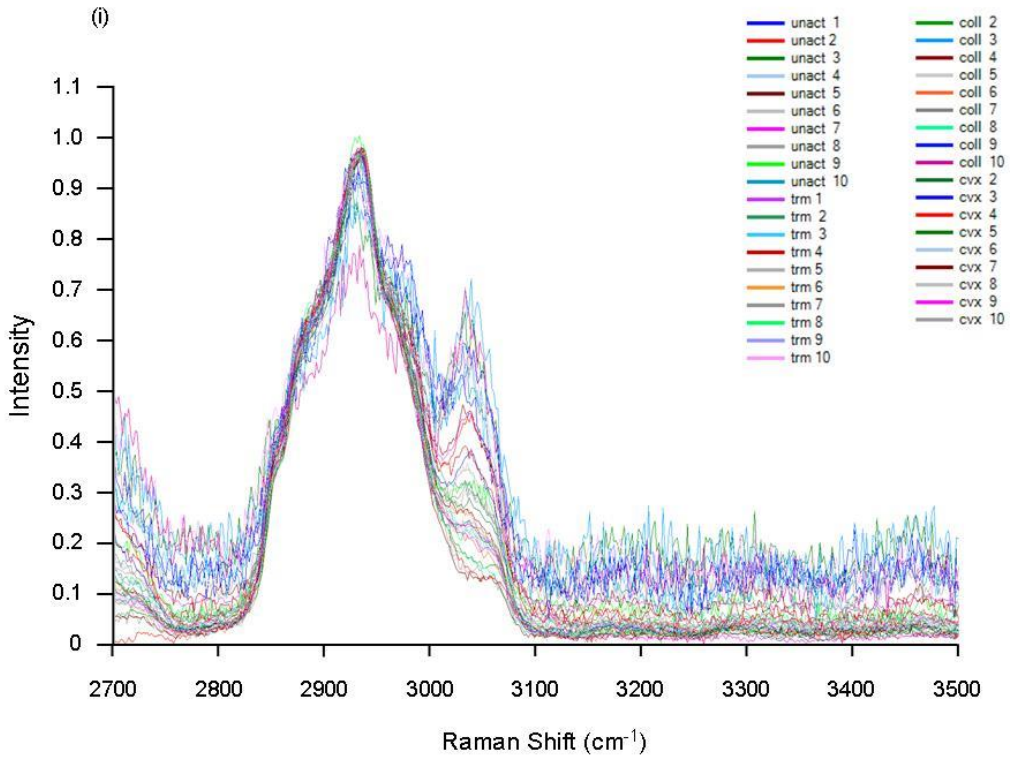
(i)
unact 1
unact 2
unact 3
unact 4
unact 5
unact 6
unact 7
unact 8
unact 9
unact 10
trm 1
trm 2
trm 3
trm 4
trm 5
trm 6
trm 7
trm 8
trm 9
trm 10
coll 2
coll 3
coll 4
coll 5
coll 6
coll 7
coll 8
coll 9
coll 10
cvx 2
cvx 3
cvx 4
cvx 5
cvx 6
cvx 7
cvx 8
cvx 9
cvx 10
Intensity
Raman Shift (cm-1)

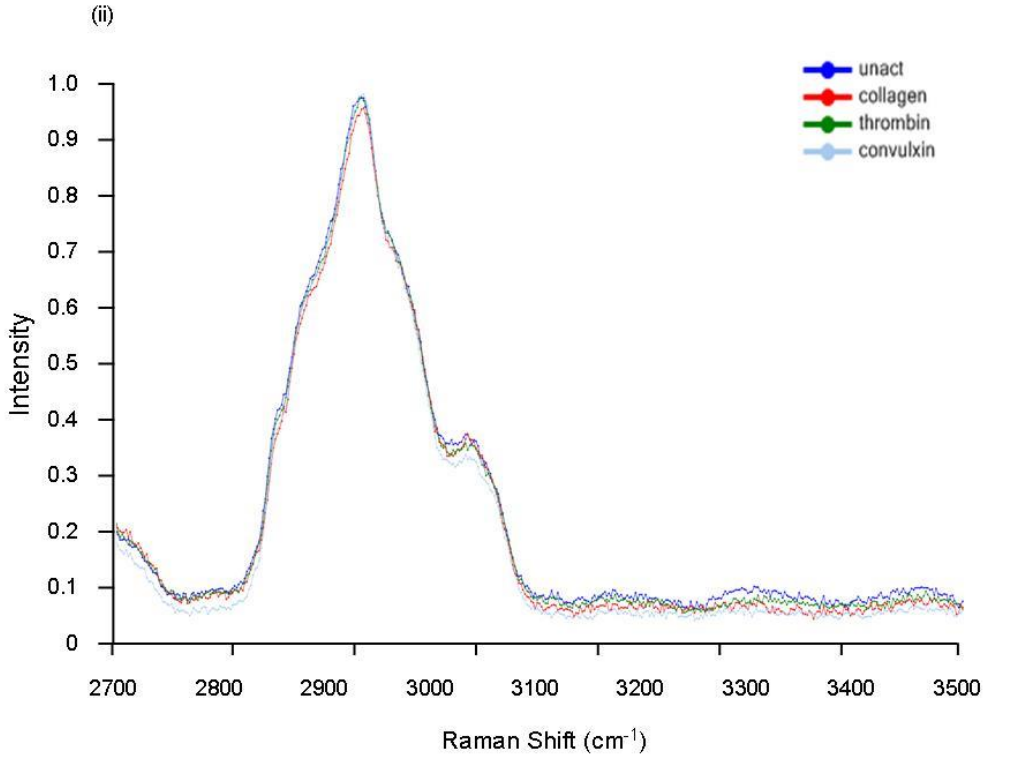
(ii)
unact
collagen
thrombin
convulxin
Intensity
Raman Shift (cm-1)

Figure 4.9 (a) The 2700 – 3500 cm^{-1} region of the Raman spectra of unactivated platelets and platelets activated with either 0.1U/ml thrombin, 38 μg/ml collagen or 50 ng/ml convulxin. Gel-filtered platelets were fixed with 1 % formaldehyde, centrifuged and supernatant removed. Raman spectra were obtained from the resulting platelet pellet. Spectra were baseline subtracted and normalised to the lipid peak at approximately 3000 cm^{-1}. (i) Three or four spectra were taken for each platelet activator and averaged, to give one spectrum per activator per donor. (ii) Signature Raman spectra of platelets generated by averaging spectra for each platelet activator from all n=10 donors.

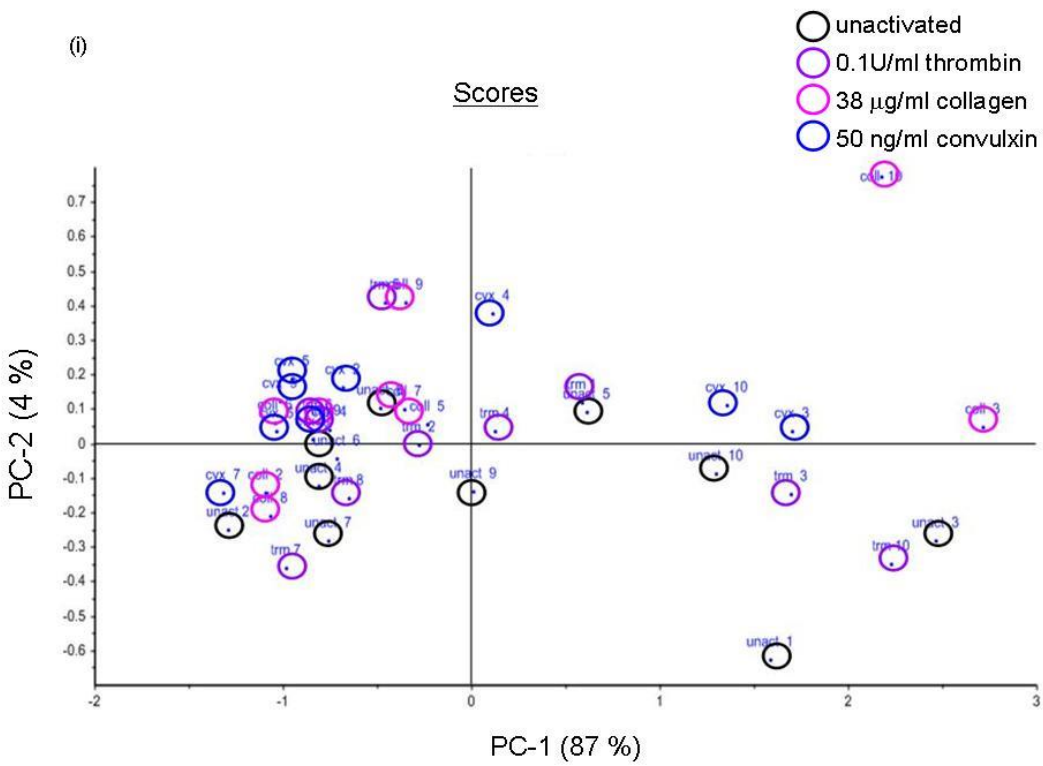
(i)
Scores
unactivated
0.1U/ml thrombin
38 μg/ml collagen
50 ng/ml convulxin
PC-2 (4 %)
PC-1 (87 %)

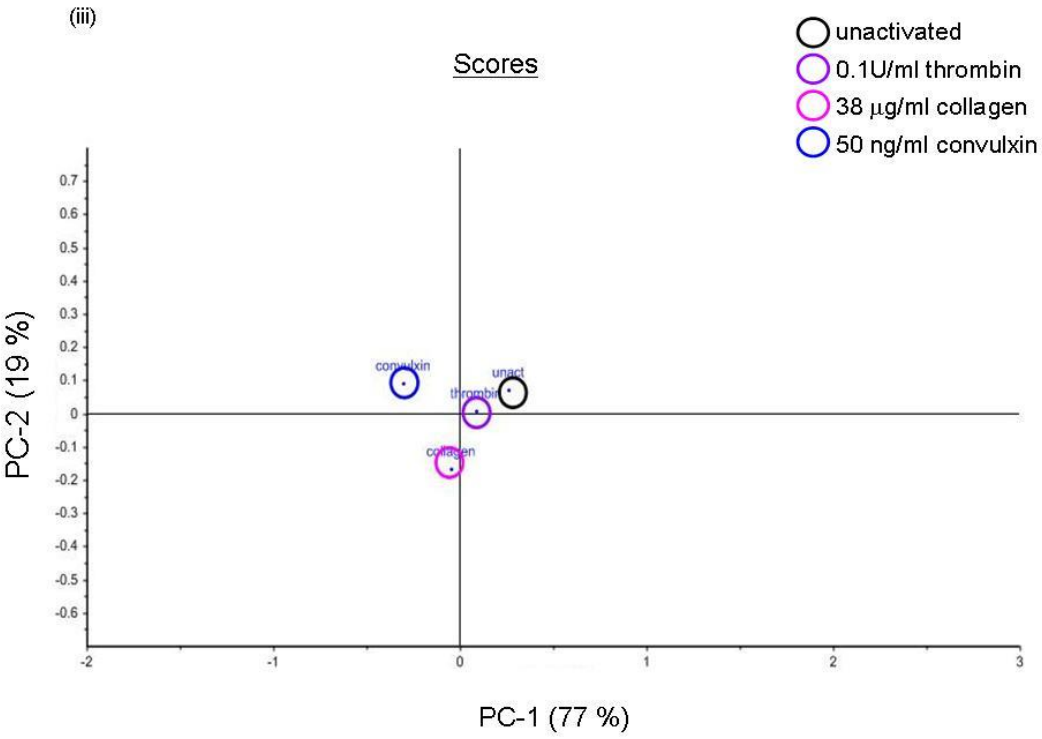
(iii)
Scores
unactivated
0.1U/ml thrombin
38 μg/ml collagen
50 ng/ml convulxin
PC-2 (19 %)
PC-1 (77 %)
convulxin
unact
thrombin
collagen

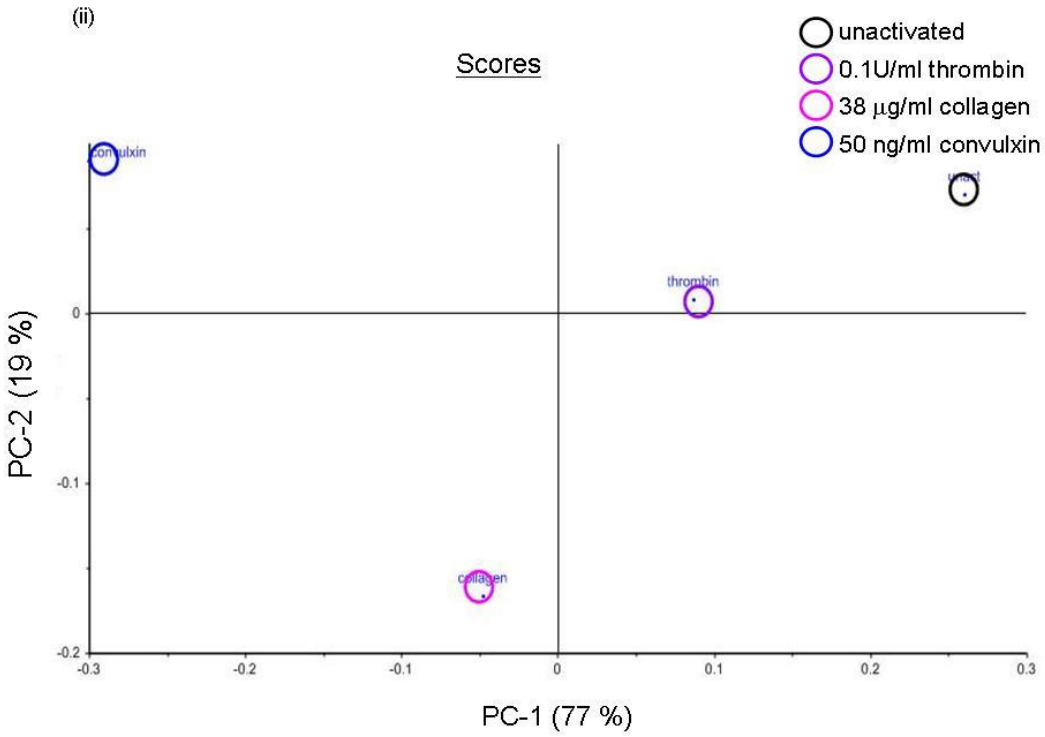

Figure 4.9 (b) Principal component analysis (PCA) of the 2700 –3500 cm^{-1} region of the Raman spectra of unactivated platelets and platelets activated with either 0.1U/ml thrombin, 38 μg/ml collagen or 50 ng/ml convulxin. PCA analysis was performed on the 2700 – 3500 cm^{-1} region of the Raman spectra. The graphs are scatter plots of the first principal component (PC-1) versus the second principal component (PC-2). (i) PCA of all donors, n=10 independent experiments, (ii) PCA of average spectra, graphed on same scale as (i), (iii) PCA of signature, average spectra on a smaller scale illustrating that the samples can be differentiated according to the platelet activator.

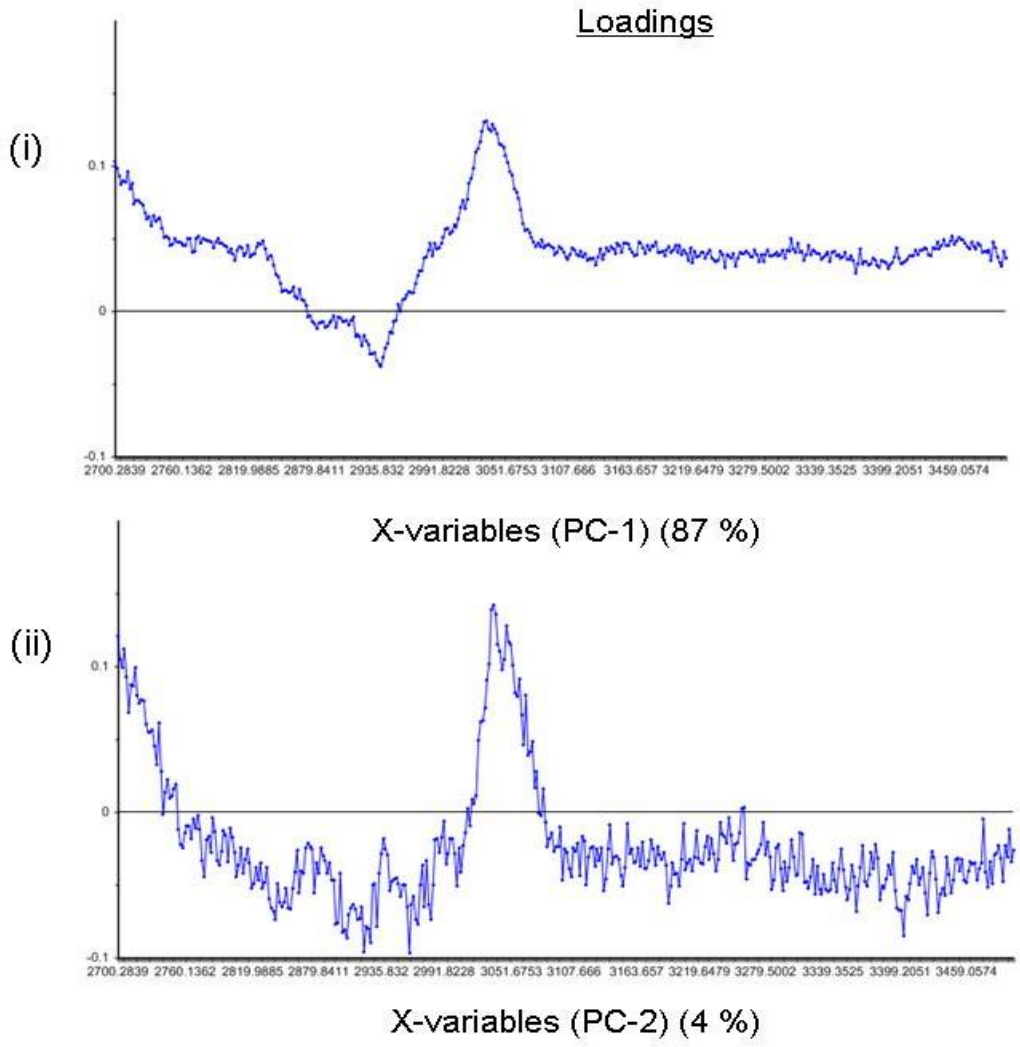

Figure 4.9 (c) The loadings of the principal components used in the Principal component analysis (PCA) scatter plot of the 2700 – 3500 cm^{-1} region of the spectrum of all samples. (i) Principal component-1 (PC-1) and (ii) Principal component-2 (PC-2) from the PCA of spectra from all donors (Figure 4.9 (b) (i)). The components are numbered according to the amount of variance they account for, i.e. PC-1 accounts for most of the variance found between the platelet samples. PCA analysis was carried out on the baseline subtracted and normalised Raman data of all samples using The Unscrambler® software.

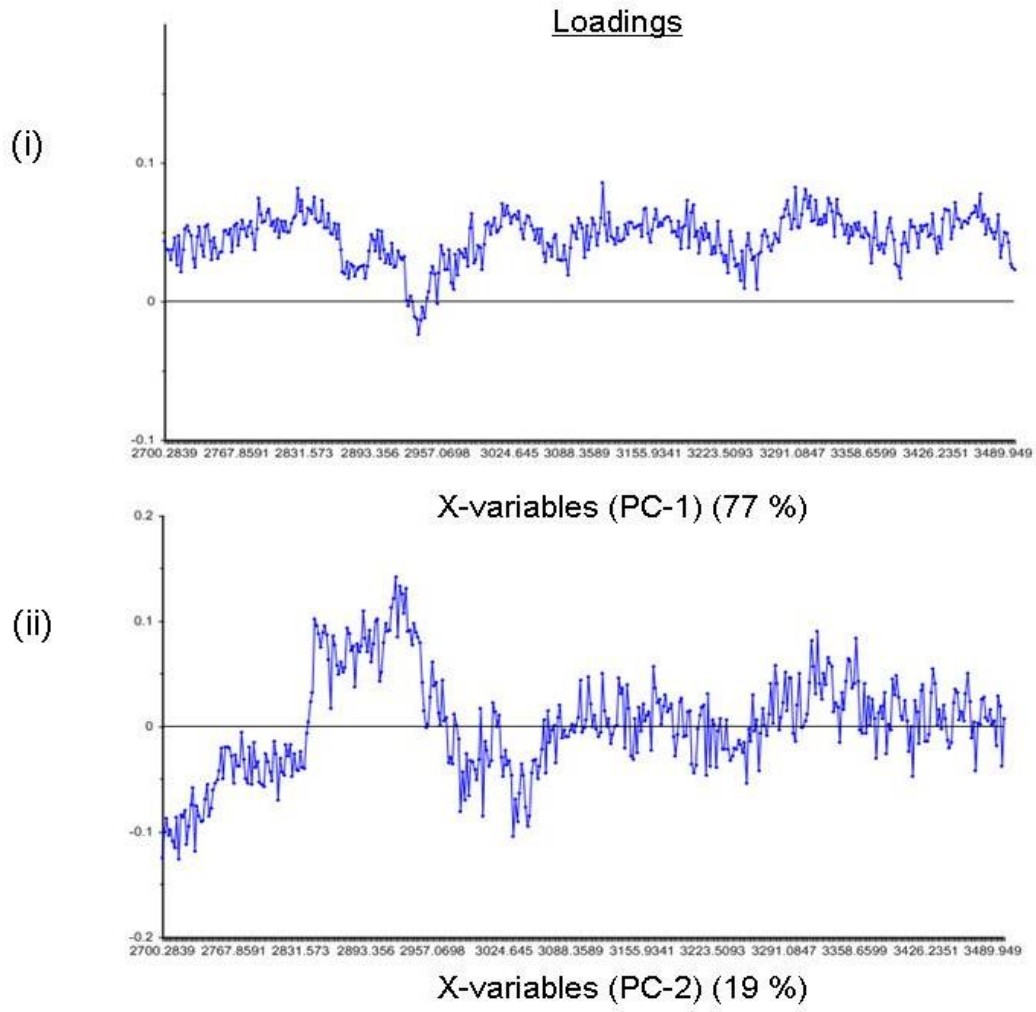

Figure 4.9 (d) The loadings of the principal components used in the Principal component analysis (PCA) scatter plot of the 2700 – 3500 cm^{-1} region of the signature Raman spectra. (i) Principal component-1 (PC-1) and (ii) Principal component-2 (PC-2) from the PCA of the signature spectra (Figure 4.9 (b) (ii) and (iii)). The components are numbered according to the amount of variance they account for, i.e. PC-1 accounts for most of the variance found between the platelet samples. PCA analysis was carried out on the baseline subtracted and normalised Raman data of all samples using The Unscrambler® software.

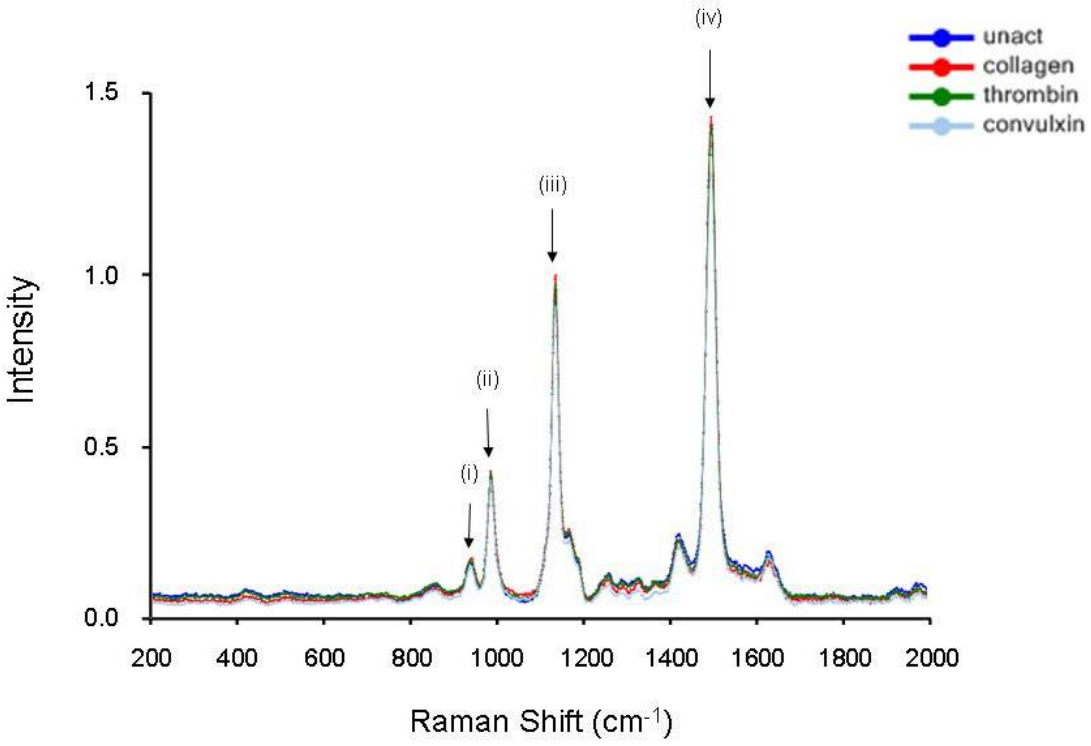

Figure 4.10 (a) Signature carotenoid peaks observed in the Raman spectra of unactivated platelets and platelets activated with either 0.1U/ml thrombin, 38 μg/ml collagen or 50 ng/ml convulxin. Characteristic carotenoid peaks are labelled (i) 968 cm^{-1}, (ii) 1006 cm^{-1}, (iii) 1160 cm^{-1} and (iv) 1525 cm^{-1}. Gel-filtered platelets were fixed with 1 % formaldehyde, centrifuged and supernatant removed. Raman spectra were obtained from the resulting platelet pellet. Spectra were baseline subtracted and normalised to the lipid peak at approximately 3000 cm^{-1}. Spectra shown are the average spectra of n=10 independent experiments.

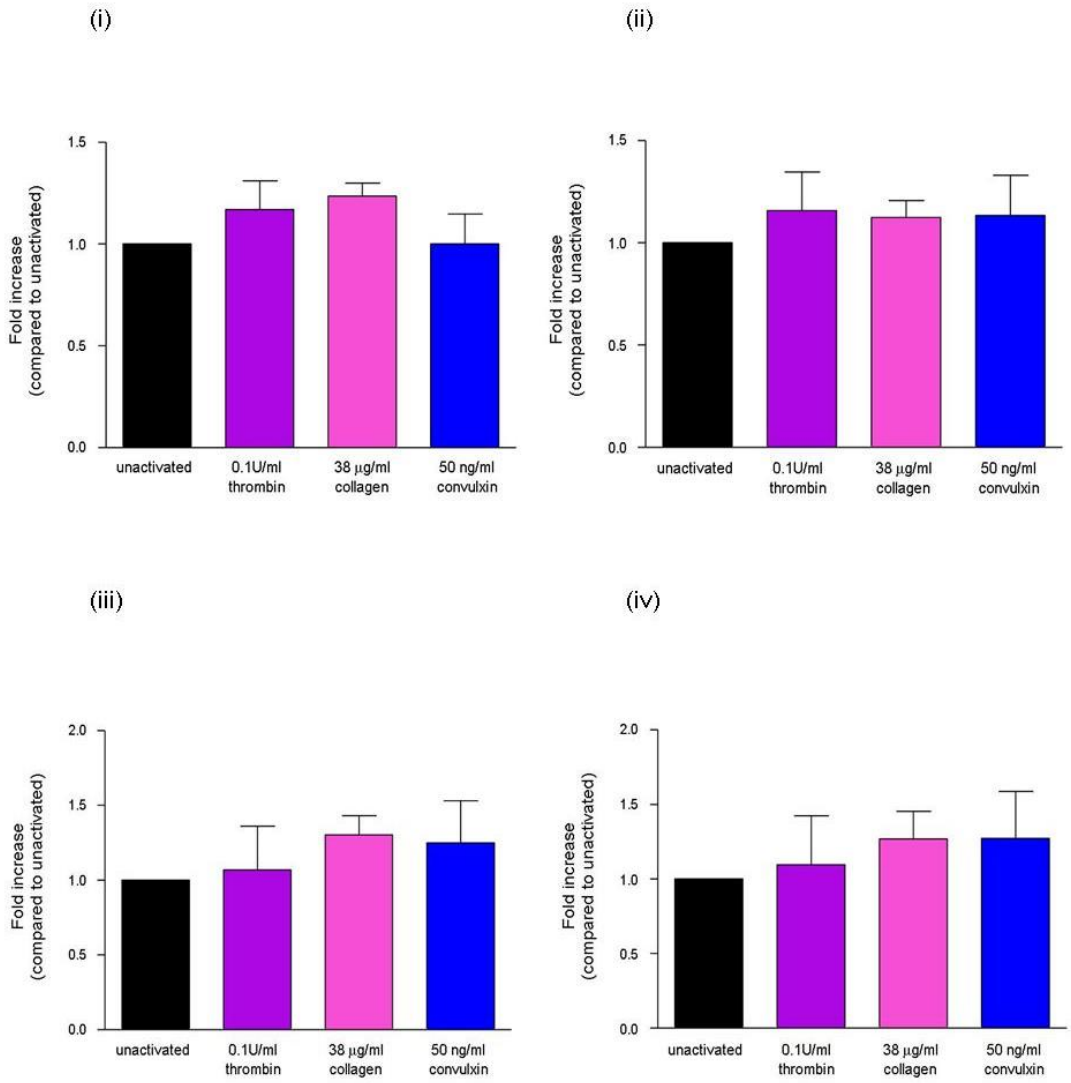

Figure 4.10 (b) There is a trend towards an increase in intensity of carotenoid peaks in the Raman spectrum of platelets activated with 0.1U/ml thrombin, 38 µg/ml collagen or 50 ng/ml convulxin to unactivated platelets. Characteristic carotenoid peaks in the Raman spectra of platelets were analysed: (i) 968 cm^{-1}, (ii) 1006 cm^{-1}, (iii) 1160 cm^{-1} and (iv) 1525 cm^{-1}. Gel-filtered platelets were fixed with 1 % formaldehyde, centrifuged and supernatant removed. Raman spectra were obtained from the resulting platelet pellet. Spectra were baseline subtracted and normalised to the lipid peak at approximately 3000 cm^{-1}. The fold increase was determined by recording the intensity values for all conditions, assigning unactivated a value of one and calculating the increase in intensity of the activated platelets relative to this. Data is presented as the mean ± SEM, n=10 independent experiments.

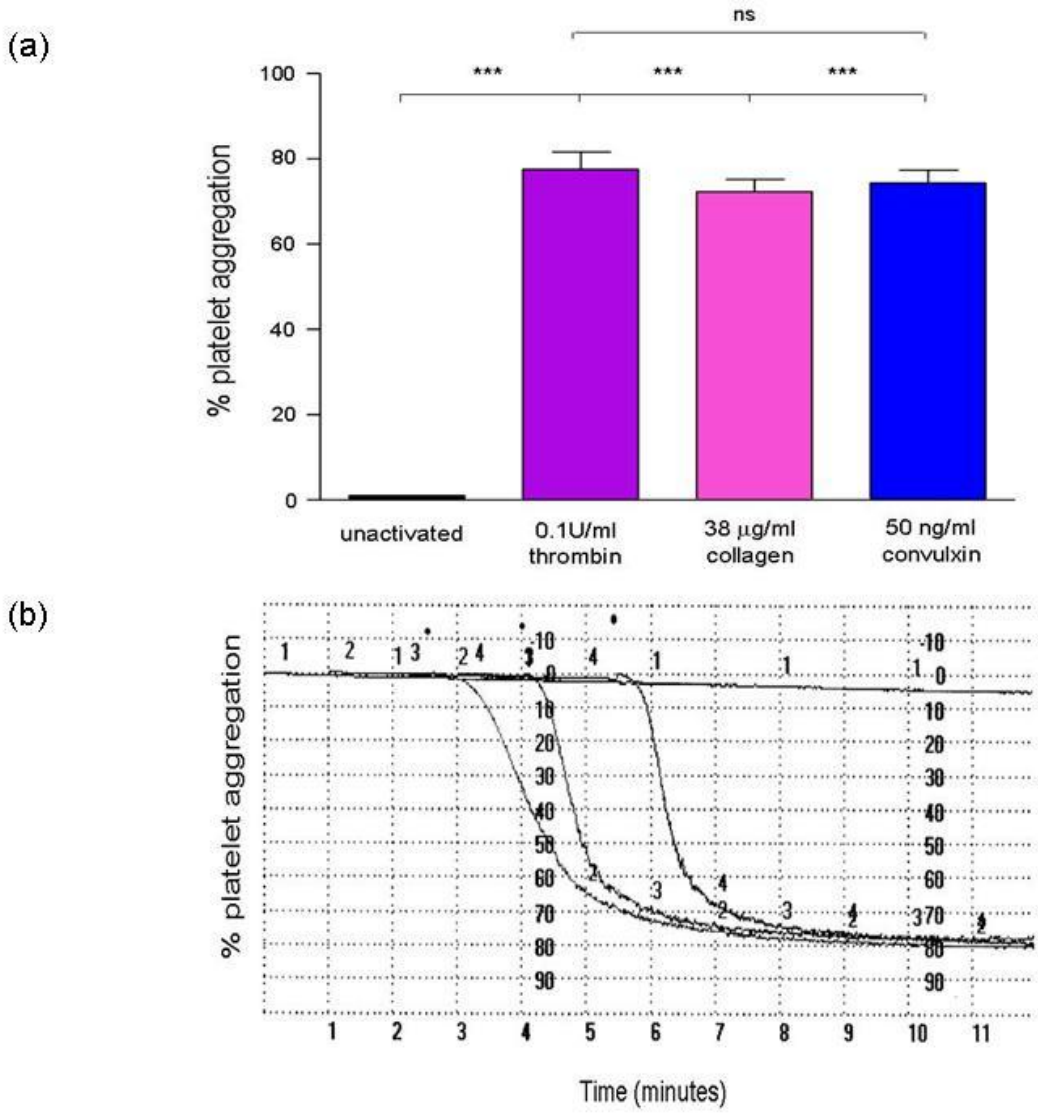

Figure 4.11 Thrombin (0.1U/ml), collagen (38 μg/ml) and convulxin (50 ng/ml) induce comparable levels of platelet aggregation. (a) Gel-filtered platelets were either unactivated or activated with 0.1U/ml thrombin, 38 μg/ml collagen or 50 ng/ml convulxin for 10 minutes at 37 °C with constant stirring at 1100 rpm. Each agonist was found to induce approximately 80 % platelet aggregation, with no statistically significant difference between each agonist. Data is presented as the mean ± SEM, n=4 independent experiments, ***p < 0.001. (b) A platelet aggregation tracing illustrating the levels of platelet aggregation of (1) unactivated gel-filtered platelets; (2) gel-filtered platelets activated with 0.1U/ml thrombin; (3) 38 μg/ml collagen; (4) 50 ng/ml convulxin. This tracing is representative of n=4 independent experiments.

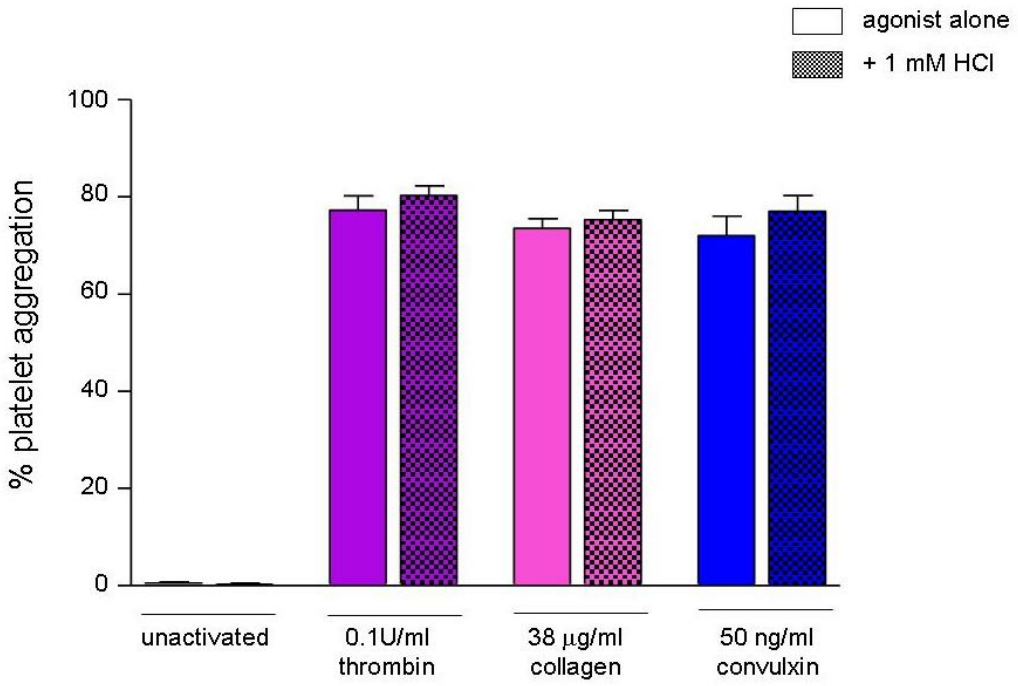

Figure 4.12 Hydrochloric acid (HCl) does not affect unactivated platelets or platelets activated with either thrombin, collagen or convulxin. Gel-filtered platelets were incubated with 1 mM HCl for 10 minutes at 37 °C with constant stirring at 1100 rpm. Platelets remained unactivated or were then activated with either 0.1U/ml thrombin, 38 μg/ml collagen or 50 ng/ml convulxin for at least 10 minutes. Data is presented as the mean ± SEM, n=4 independent experiments.

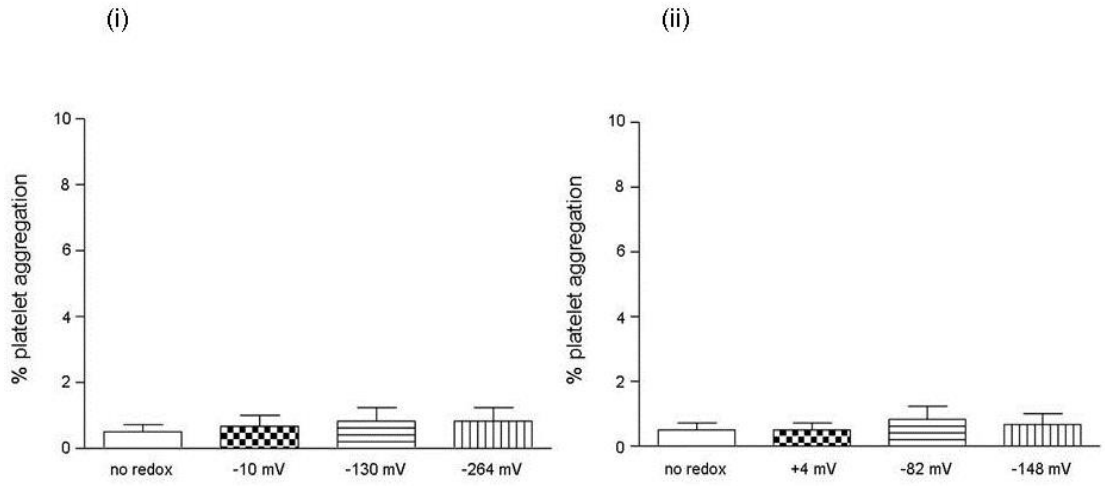

Figure 4.13 Altering the external redox environment has no impact on the activation status of unactivated platelets. The level of platelet aggregation of unactivated gel-filtered platelets in the presence of (i) GSH/GSSG redox potentials: oxidising (-10 mV), mean (-130 mV) or reducing (-264 mV) or (ii) Cys/CySS redox potentials: oxidising (+4 mV), mean (-82 mV) or reducing (-148 mV) was measured. Platelet aggregations were carried out for at least 10 minutes at 37 °C with constant stirring at 1100 rpm. Data is presented as the mean ± SEM, n=6 independent experiments.

(a)

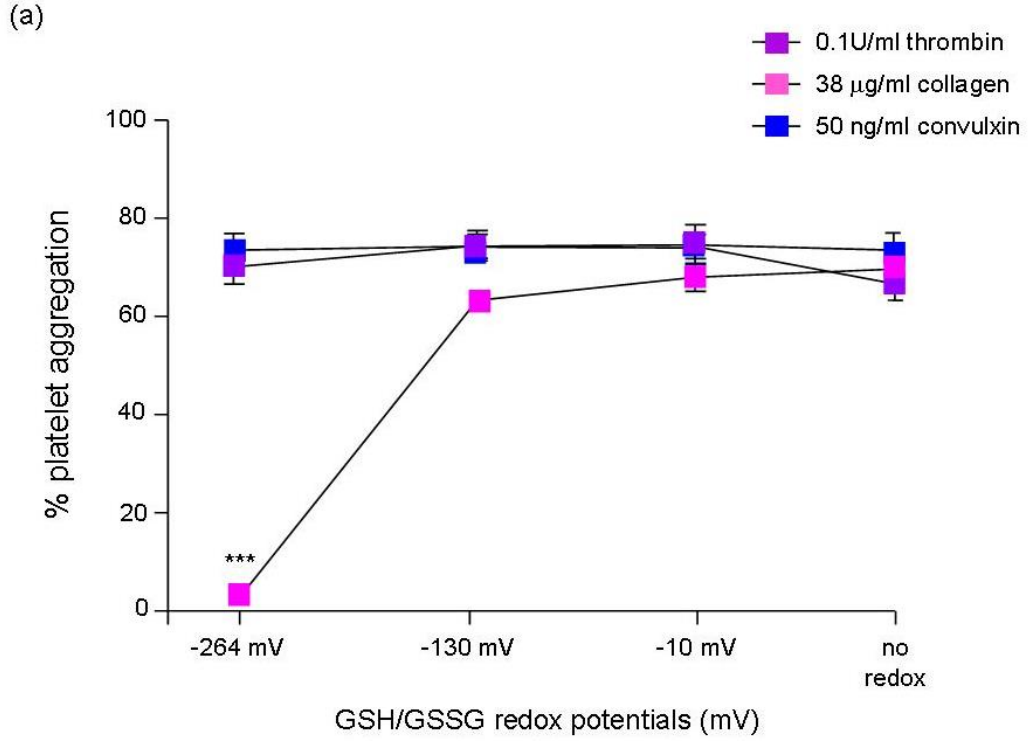
0.1U/ml thrombin
38 μg/ml collagen
50 ng/ml convulxin
% platelet aggregation
100
80
60
40
20
0
***
-264 mV
-130 mV
-10 mV
no redox
GSH/GSSG redox potentials (mV)

(b)

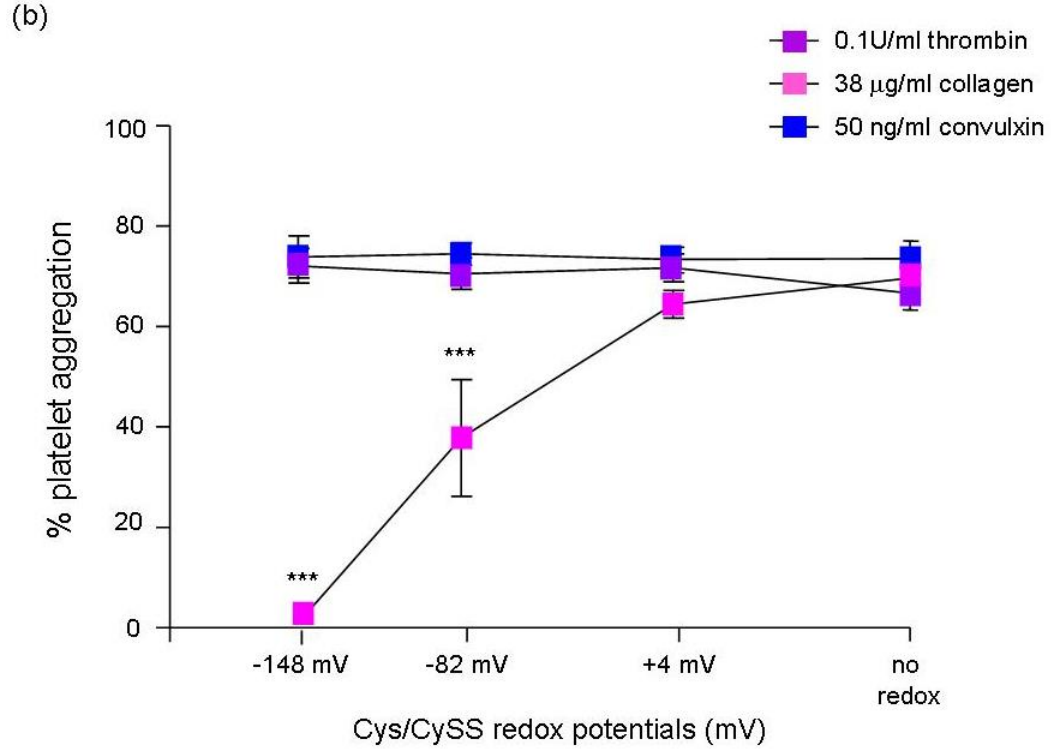
0.1U/ml thrombin
38 μg/ml collagen
50 ng/ml convulxin
% platelet aggregation
100
80
60
40
20
0
***
***
-148 mV
-82 mV
+4 mV
no redox
Cys/CySS redox potentials (mV)

Figure 4.14 A reducing external redox environment inhibits platelet aggregation to collagen but has no impact on unactivated platelets or platelet aggregation induced by thrombin or convulxin. The level of platelet aggregation of unactivated gel-filtered platelets or gel-filtered platelets activated with 0.1U/ml thrombin, 38 μg/ml collagen or convulxin in the presence of (a) GSH/GSSG redox potentials (-10 mV, -130 mV or -264 mV) or (b) Cys/CySS redox potentials (+4 mV, -82 mV or -148 mV) was measured. Platelet aggregations were carried out for at least 10 minutes at 37 °C with constant stirring at 1100 rpm. Data is presented as the mean ± SEM, n=6 independent experiments, ***$p < 0.001$. (As demonstrated by (Murphy et al, 2010).

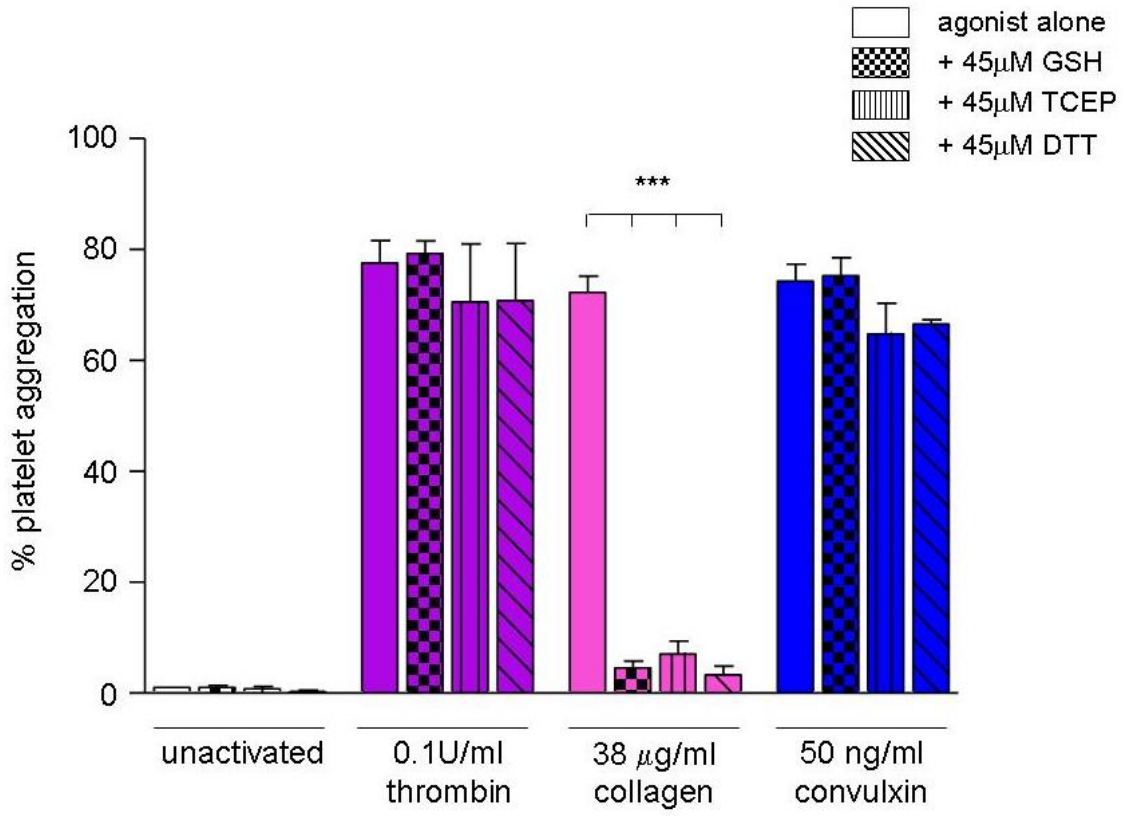

Figure 4.15 (a) A reducing external redox environment generated by the reducing agents glutathione (GSH), *tris*(2-carboxyethyl)phosphine (TCEP) and dithiothreitol (DTT) inhibits platelet aggregation to collagen but has no significant impact on unactivated platelets or platelet aggregation induced by thrombin or convulxin. The level of platelet aggregation of unactivated gel-filtered platelets or gel-filtered platelets activated with 0.1U/ml thrombin, 38 μg/ml collagen or convulxin in the presence of 45 μM GSH, 45 μM TCEP or 45 μM DTT was measured. Platelet aggregations were carried out for at least 10 minutes at 37 °C with constant stirring at 1100 rpm. Data is presented as the mean ± SEM, n=4 independent experiments, ***$p < 0.001$.

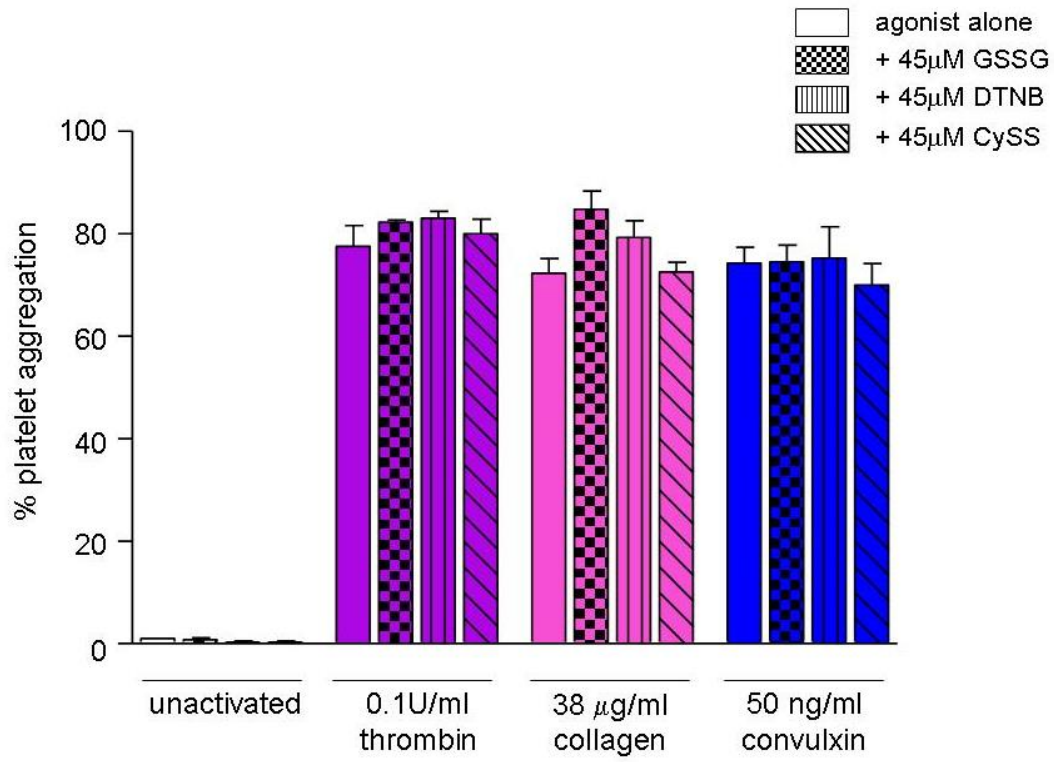

Figure 4.15 (b) An oxidising external redox environment generated by the oxidising agents glutathione (GSSG), 5,5'-dithiobis-(2-nitrobenzoic acid) (DTNB) and cystine (CySS) has no impact on unactivated platelets or platelet aggregation induced by thrombin, collagen or convulxin. The level of platelet aggregation of unactivated gel-filtered platelets or gel-filtered platelets activated with 0.1U/ml thrombin, 38 μg/ml collagen or convulxin in the presence of 45 μM GSSG, 45 μM DTNB or 45 μM CySS was measured. Platelet aggregations were carried out for at least 10 minutes at 37 °C with constant stirring at 1100 rpm. Data is presented as the mean ± SEM, n=4 independent experiments.

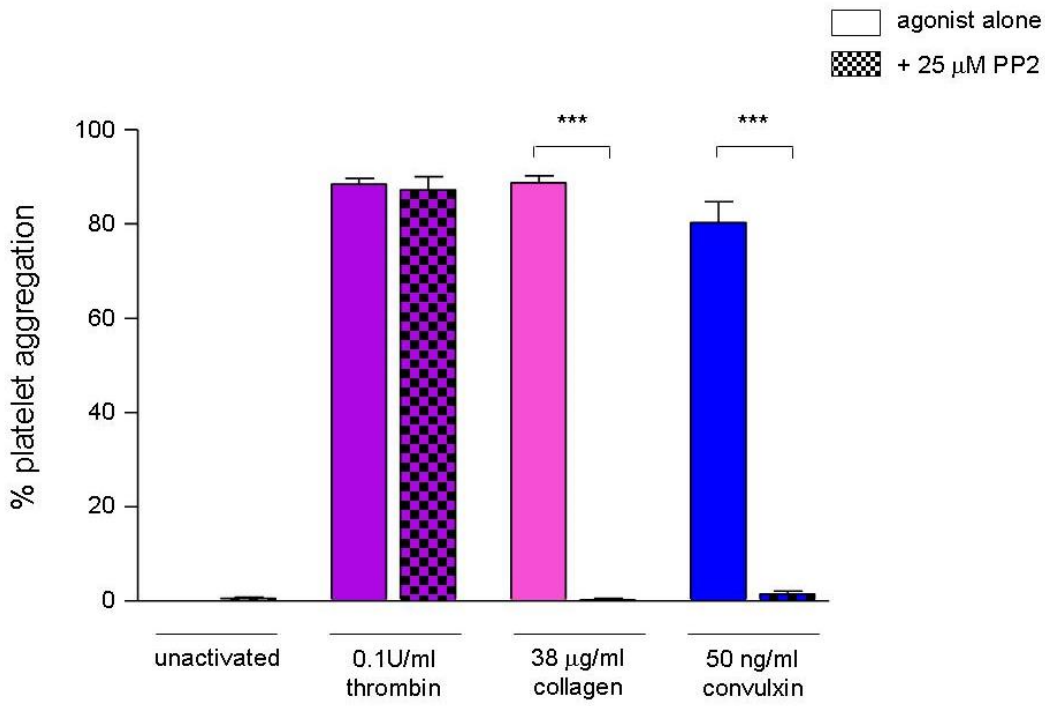

Figure 4.16 (a) The broad Src family kinase inhibitor, PP2, inhibits platelet aggregation induced by collagen and convulxin. There is no impact on the level of platelet aggregation induced by thrombin. Gel-filtered platelets were incubated with PP2 (25 μM) for 15 minutes at 37 °C, with stirring (1100 rpm). Platelets remained unactivated or activated with either 0.1U/ml thrombin, 38 μg/ml collagen or 50 ng/ml convulxin. Platelet aggregations were followed for at least 10 minutes at 37 °C, with constant stirring at 1100 rpm. Data is presented as the mean ± SEM, n=4 independent experiments, ***$p < 0.001$.

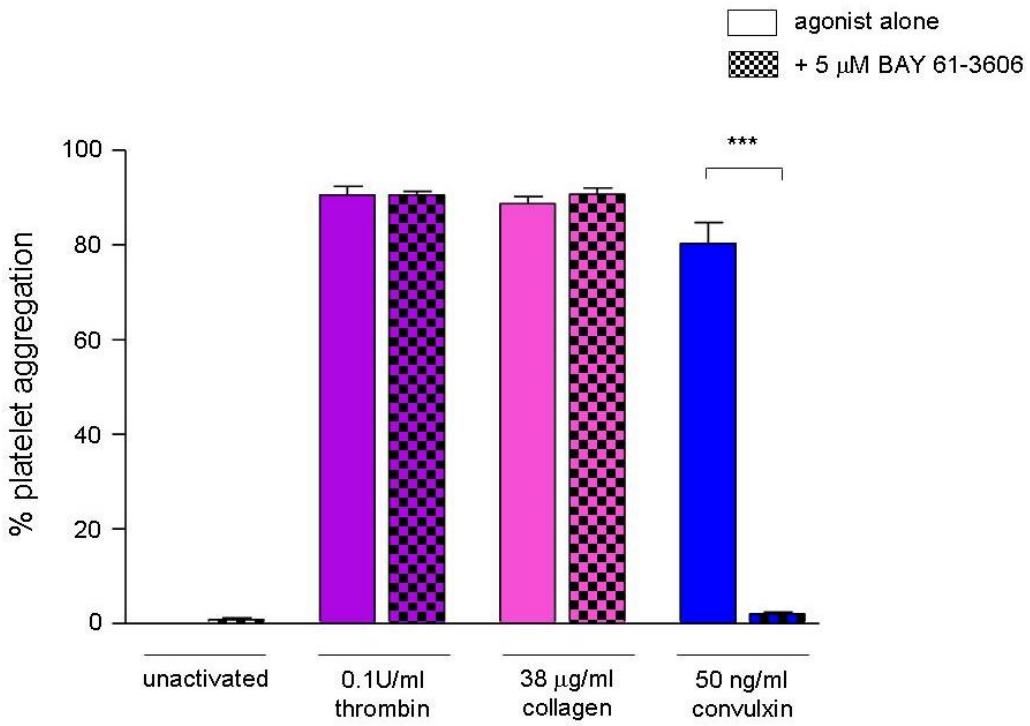

Figure 4.16 (b) The Syk kinase inhibitor, BAY 61-3606, inhibits convulxin induced platelet aggregation only. There is no impact on the level of platelet aggregation induced by thrombin or collagen. Gel-filtered platelets were incubated with BAY 61-3606 (5 μM) for 10 minutes at 37 °C, with stirring (1100 rpm). Platelets remained unactivated or activated with either 0.1U/ml thrombin, 38 μg/ml collagen or 50 ng/ml convulxin. Platelet aggregations were followed for at least 10 minutes at 37 °C, with constant stirring at 1100 rpm. Data is presented as the mean ± SEM, n=4 independent experiments, ***$p < 0.001$.

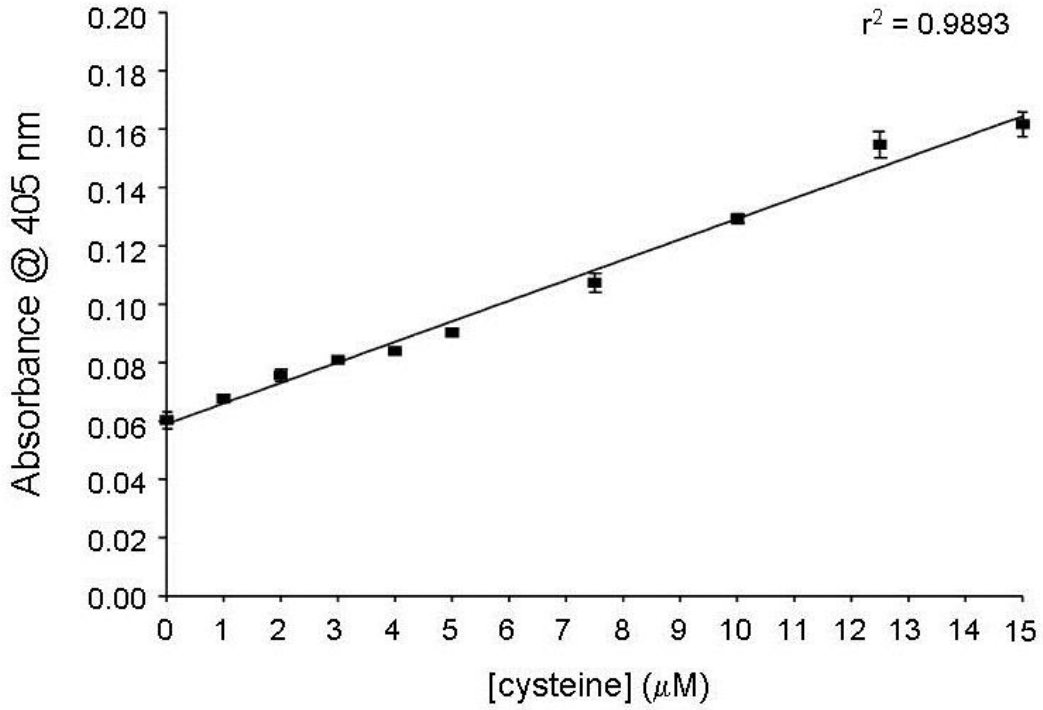

Figure 4.17 A standard curve generated with cysteine in the presence of 5,5'-dithiobis-(2-nitrobenzoic acid) (DTNB). Cysteine (Cys), a thiol containing compound, at a number of concentrations ranging from 0 - 15 μM, was incubated with DTNB (100 μM) for 1 minute at room temperature. The absorbance of the samples was read in a clear, flat bottom 96-well plate at 405 nm in the Wallac plate reader. Data is presented as the mean ± SEM, n=3 independent experiments, with each performed in triplicate. The concentration of thiols was calculated using the equation of the line: $y = 0.007x + 0.059$, $r^2 = 0.9893$.

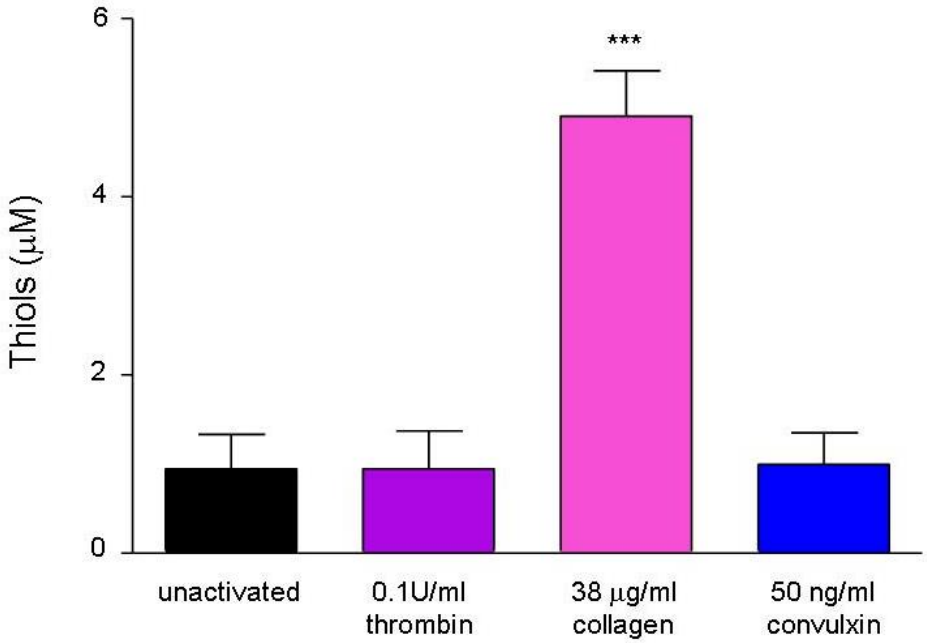

Figure 4.18 (a) There is a significant increase in the surface free thiol population of platelets activated with collagen compared to unactivated platelets and platelets activated by thrombin or convulxin. Gel-filtered platelets were either unactivated or activated with 0.1U/ml thrombin, 38 μg/ml collagen or 50 ng/ml convulxin for 10 minutes at 37 °C, in the absence of stirring. 5,5'-dithiobis-(2-nitrobenzoic acid) (DTNB) (100 μM) was added and incubated for 1 minute at room temperature. Samples were centrifuged and the supernatant was removed and transferred to a clear, flat-bottom 96-well plate. Absorbance was measured at 405 nm, using a Wallac plate reader. The thiol concentration was calculated from the cysteine standard curve. Data is presented as the mean ± SEM, n=6 independent experiments, ***$p < 0.001$.

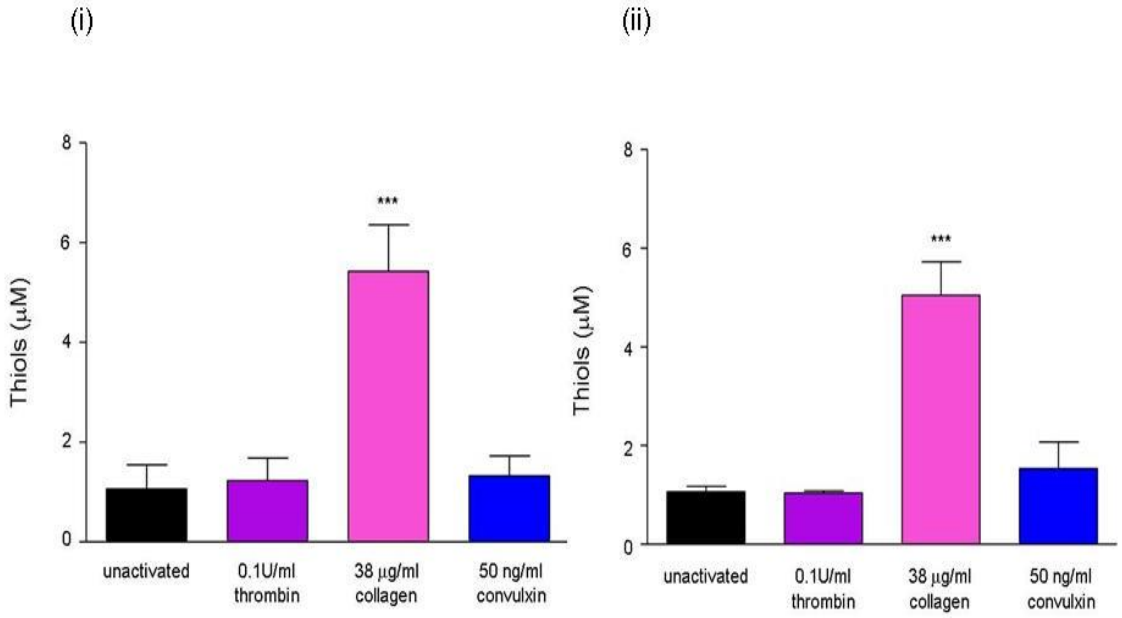

Figure 4.18 (b) In the presence of an oxidising external redox environment, there is a significant increase in the surface free thiol population of platelets activated with collagen compared to unactivated platelets and platelets activated with thrombin or convulxin. Gel-filtered platelets remained unactivated or activated with either 0.1U/ml thrombin, 38 μg/ml collagen or 50 ng/ml convulxin in presence of (i) a GSH/GSSG oxidising redox potential (-10 mV) or (ii) a Cys/CySS oxidising redox potential (+4 mV). Gel-filtered platelets were incubated with agonists and redox for 10 minutes at 37 °C, in the absence of stirring. 5,5'-dithiobis-(2-nitrobenzoic acid) (DTNB) (100 μM) was added and incubated for 1 minute at room temperature. Samples were centrifuged and the supernatant was removed and transferred to a clear, flat-bottom 96-well plate. Absorbance was measured at 405 nm, using a Wallac plate reader. The thiol concentration was calculated from the cysteine standard curve. Data is presented as the mean ± SEM, n=6 independent experiments, ***$p < 0.001$.

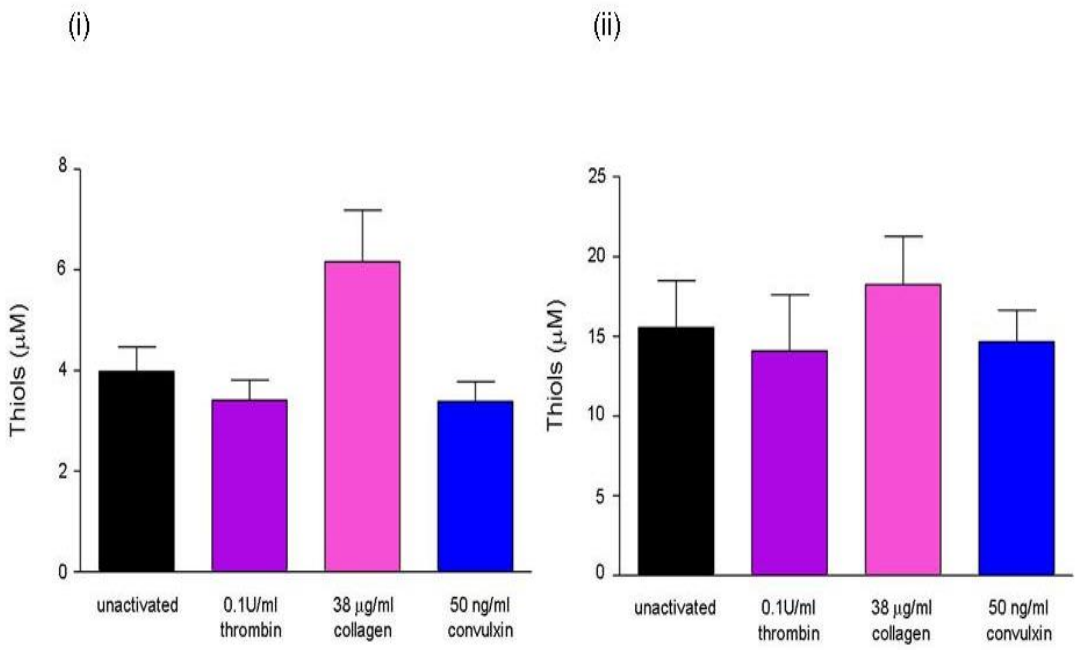

Figure 4.18 (c) In the presence of a mean external redox environment, there is a trend towards an increase in the surface free thiol population of platelets activated with collagen compared to unactivated platelets and platelets activated with thrombin or convulxin. Gel-filtered platelets were unactivated or activated with either 0.1U/ml thrombin, 38 μg/ml collagen or 50 ng/ml convulxin in presence of (i) a GSH/GSSG mean redox potential (-130 mV) or (ii) a Cys/CySS mean redox potential (-82 mV). Gel-filtered platelets were incubated with agonists and redox for 10 minutes at 37 °C, in the absence of stirring. 5,5'-dithiobis-(2-nitrobenzoic acid) (DTNB) (100 μM) was added and incubated for 1 minute at room temperature. Samples were centrifuged and the supernatant was removed and transferred to a clear, flat-bottom 96-well plate. Absorbance was measured at 405 nm, using a Wallac plate reader. The thiol concentration was calculated from the cysteine standard curve. Data is presented as the mean ± SEM, n=6 independent experiments.

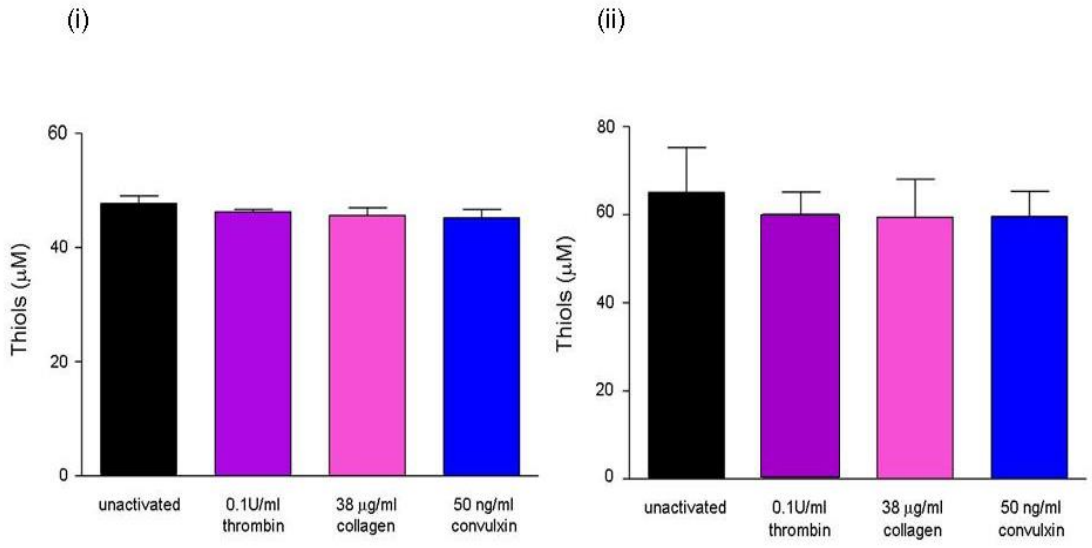

Figure 4.18 (d) In the presence of a reducing external redox environment, there is no difference between the surface thiol population of unactivated platelets and platelets activated with either thrombin, collagen or convulxin. Gel-filtered platelets were either unactivated or activated with 0.1U/ml thrombin, 38 μg/ml collagen or 50 ng/ml convulxin in presence of (i) a GSH/GSSG reducing redox potential (-264 mV) or (ii) a Cys/CySS reducing redox potential (-148 mV). Gel-filtered platelets were incubated with agonists and redox for 10 minutes at 37 °C, in the absence of stirring. 5,5'-dithiobis-(2-nitrobenzoic acid) (DTNB) (100 μM) was added and incubated for 1 minute at room temperature. Samples were centrifuged and the supernatant was removed and transferred to a clear, flat-bottom 96-well plate. Absorbance was measured at 405 nm, using a Wallac plate reader. The thiol concentration was calculated from the cysteine standard curve. Data is presented as the mean ± SEM, n=6 independent experiments.

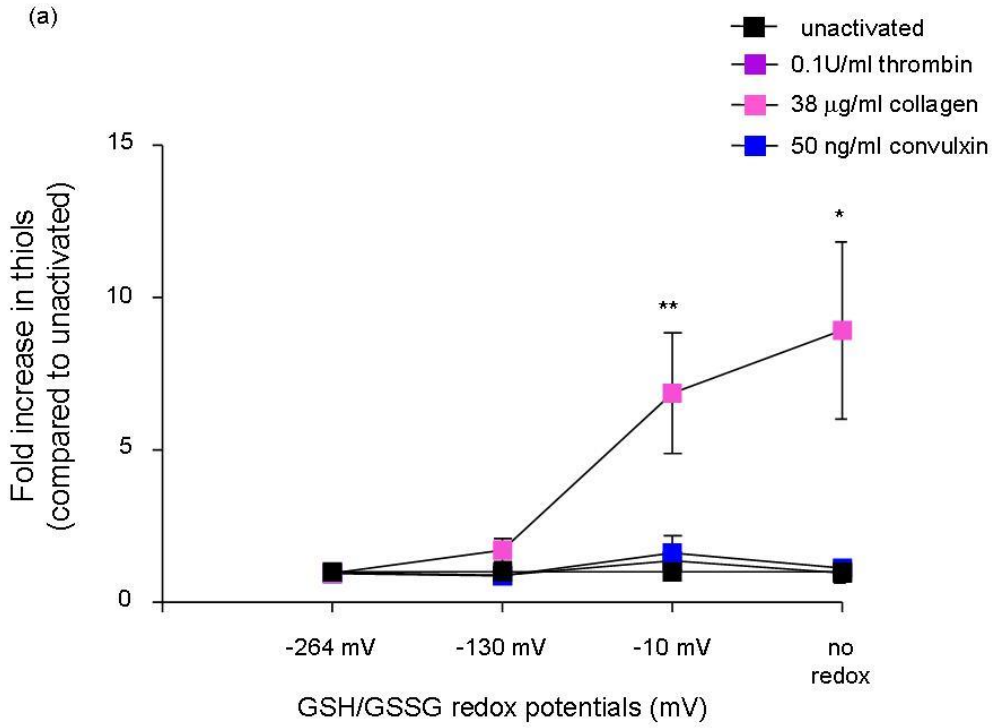
(a)
unactivated
0.1U/ml thrombin
38 μg/ml collagen
50 ng/ml convulxin
Fold increase in thiols (compared to unactivated)
15
10
5
0
**
*
-264 mV
-130 mV
-10 mV
no redox
GSH/GSSG redox potentials (mV)

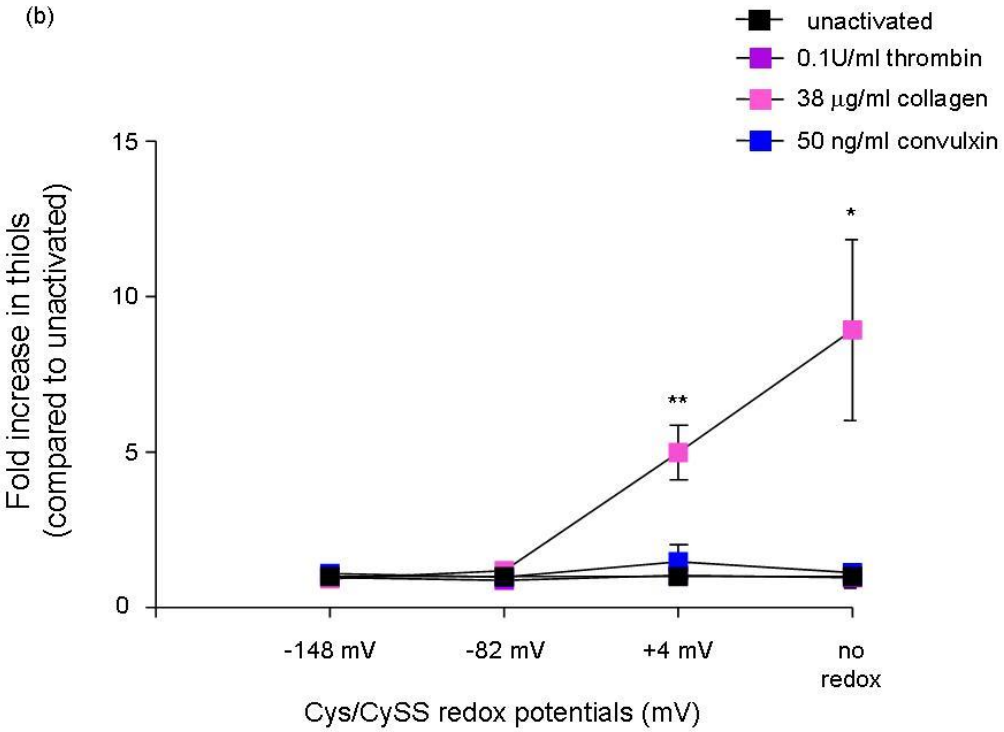
(b)
unactivated
0.1U/ml thrombin
38 μg/ml collagen
50 ng/ml convulxin
Fold increase in thiols (compared to unactivated)
15
10
5
0
**
*
-148 mV
-82 mV
+4 mV
no redox
Cys/CySS redox potentials (mV)

Figure 4.19 There is an approximately 8-fold increase in the surface thiol population of platelets activated with collagen compared to unactivated platelets and platelets activated with thrombin or convulxin. This increase diminishes as the external redox environment becomes more reducing in nature. There is no change in the surface thiol population of platelets activated with thrombin or collagen compared to unactivated platelets. Gel-filtered platelets were unactivated (no redox) or activated with either 0.1U/ml thrombin, 38 μg/ml collagen or 50 ng/ml convulxin for 10 minutes at 37 °C (without stirring) in the presence of (a) GSH/GSSG redox potentials or (b) Cys/CySS redox potentials. 5,5'-dithiobis-(2-nitrobenzoic acid) (DTNB) (100 μM) was added and incubated for 1 minute at room temperature. Samples were centrifuged and the supernatant was removed and transferred to a clear, flat-bottom 96-well plate. Absorbance was measured at 405 nm, using a Wallac plate reader. The thiol concentration was calculated from the cysteine standard curve. Fold increase was determined by assigning a value of 1 to unactivated platelets and calculating the change in platelet surface thiol population relative to this value. Data is presented as the mean ± SEM, n=6 independent experiments, *$p < 0.05$, **$p < 0.01$.

Table 4.1 The average number of moles of thiols present on the surface of unactivated platelets or platelets activated with either thrombin, collagen or convulxin in the presence of (a) GSH/GSSG redox potentials or (b) Cys/CySS redox potentials.

(a)

	No redox	-264 mV	-130 mV	-10 mV
Unactivated	3.784×10^{-18}	1.909×10^{-16}	1.592×10^{-17}	4.256×10^{-18}
0.1U/ml thrombin	3.784×10^{-18}	1.850×10^{-16}	1.365×10^{-17}	4.92×10^{-18}
38 μg/ml collagen	19.62×10^{-18}	1.825×10^{-16}	2.465×10^{-17}	21.708×10^{-18}
50 ng/ml convulxin	3.972×10^{-18}	1.808×10^{-16}	1.355×10^{-17}	5.3×10^{-18}

(b)

	No redox	-148 mV	-82 mV	+4 mV
Unactivated	3.784×10^{-18}	2.601×10^{-16}	6.221×10^{-17}	4.256×10^{-18}
0.1U/ml thrombin	3.784×10^{-18}	2.405×10^{-16}	5.633×10^{-17}	4.16×10^{-18}
38 μg/ml collagen	19.62×10^{-18}	2.378×10^{-16}	7.302×10^{-17}	20.192×10^{-18}
50 ng/ml convulxin	3.972×10^{-18}	2.383×10^{-16}	5.860×10^{-17}	6.156×10^{-18}

(a)

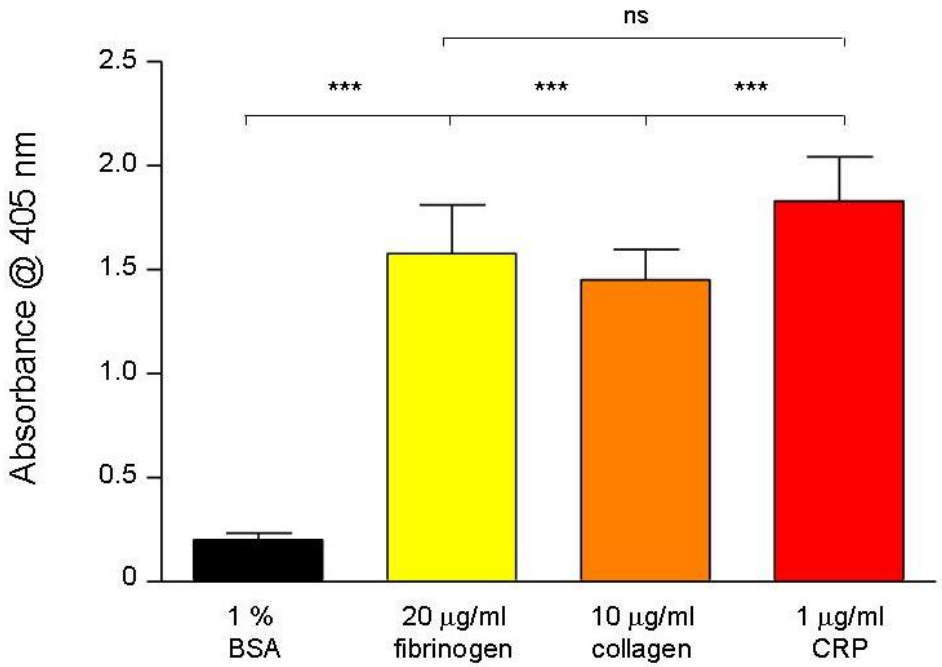
ns
***
***
***
Absorbance @ 405 nm
2.5
2.0
1.5
1.0
0.5
0
1 %
BSA
20 μg/ml
fibrinogen
10 μg/ml
collagen
1 μg/ml
CRP

(b)

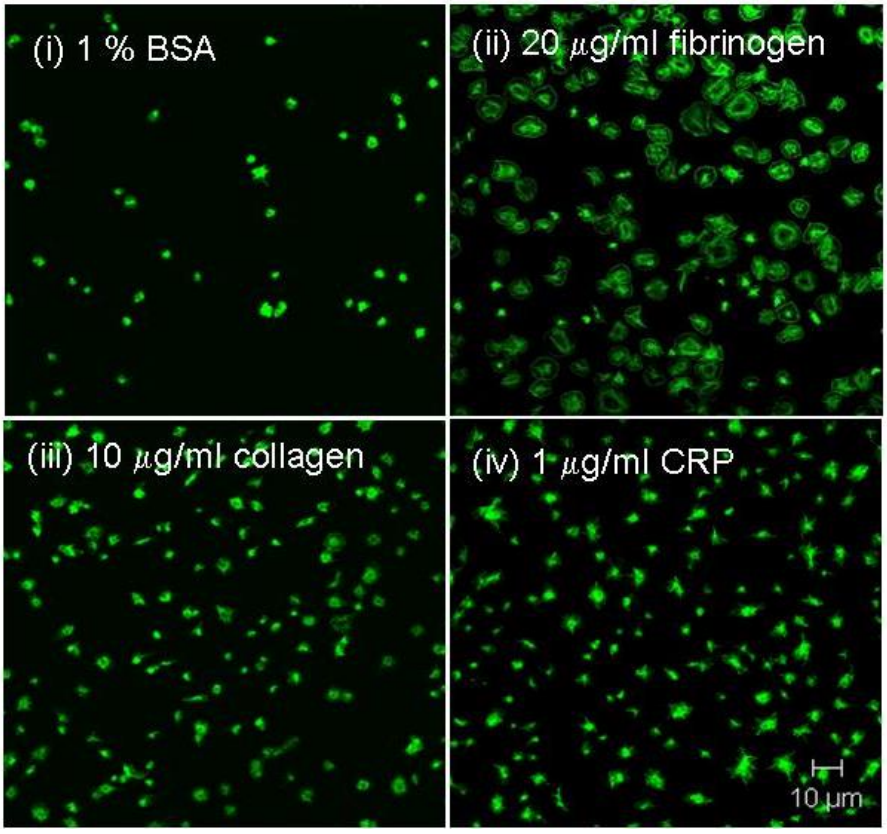
(i) 1 % BSA
(ii) 20 μg/ml fibrinogen
(iii) 10 μg/ml collagen
(iv) 1 μg/ml CRP
10 μm

Figure 4.20 The extent of platelet adhesion to fibrinogen (20 μg/ml), collagen (10 μg/ml) or collagen related peptide (CRP) (1 μg/ml) is similar. (a) Washed platelets were allowed to adhere to clear, flat bottom 96-well plates coated with either BSA, fibrinogen, collagen or CRP. Adhered platelets were incubated with a lysis buffer containing *para*-nitrophenyl phosphate (*p*NPP) for 1 hour at room temperature. The reaction was stopped by the addition of 2 M NaOH. Absorbance was measured using a Wallac plate reader. Data is presented as the mean ± SEM, n=6 independent experiments, ***$p < 0.001$. (b) Washed platelets adhered to poly-L-lysine slides coated with (i) 1 % BSA, (ii) 20 μg/ml fibrinogen, (iii) 10 μg/ml collagen or (iv) 1 μg/ml CRP for 45 minutes at 37 °C. Samples were fixed with 1 % formaldehyde for 10 minutes at room temperature and permeabilised with 0.1 % Triton-X-100 for 10 minutes at room temperature. Platelets were stained with Alexa Fluor® 488 phalloidin. Samples were imaged using a Zeiss LSM510 Meta confocal microscope with a 63X oil-immersion lens. A laser wavelength of 488 nm, at an intensity of 1 % was employed.

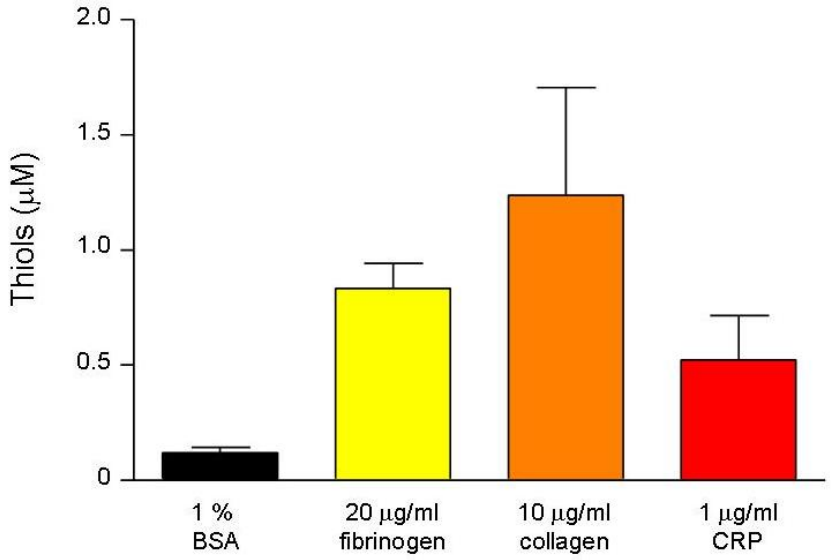

Figure 4.21 While not statistically significant, there is an increase observed in the surface free thiol population of platelets adhered to collagen compared to that of platelets adhered to fibrinogen or collagen related peptide (CRP). Washed platelets were allowed to adhere to clear, flat bottom 96-well plates coated with either 1 % BSA, 20 μg/ml fibrinogen, 10 μg/ml collagen or 1 μg/ml CRP for 45 minutes at 37 °C. 5,5'-dithiobis-(2-nitrobenzoic acid) (DTNB) (100 μM) was added and incubated for 1 minute at room temperature. The absorbance was measured at 405 nm using a Wallac plate reader. Data is presented as the mean ± SEM, n=6 independent experiments.

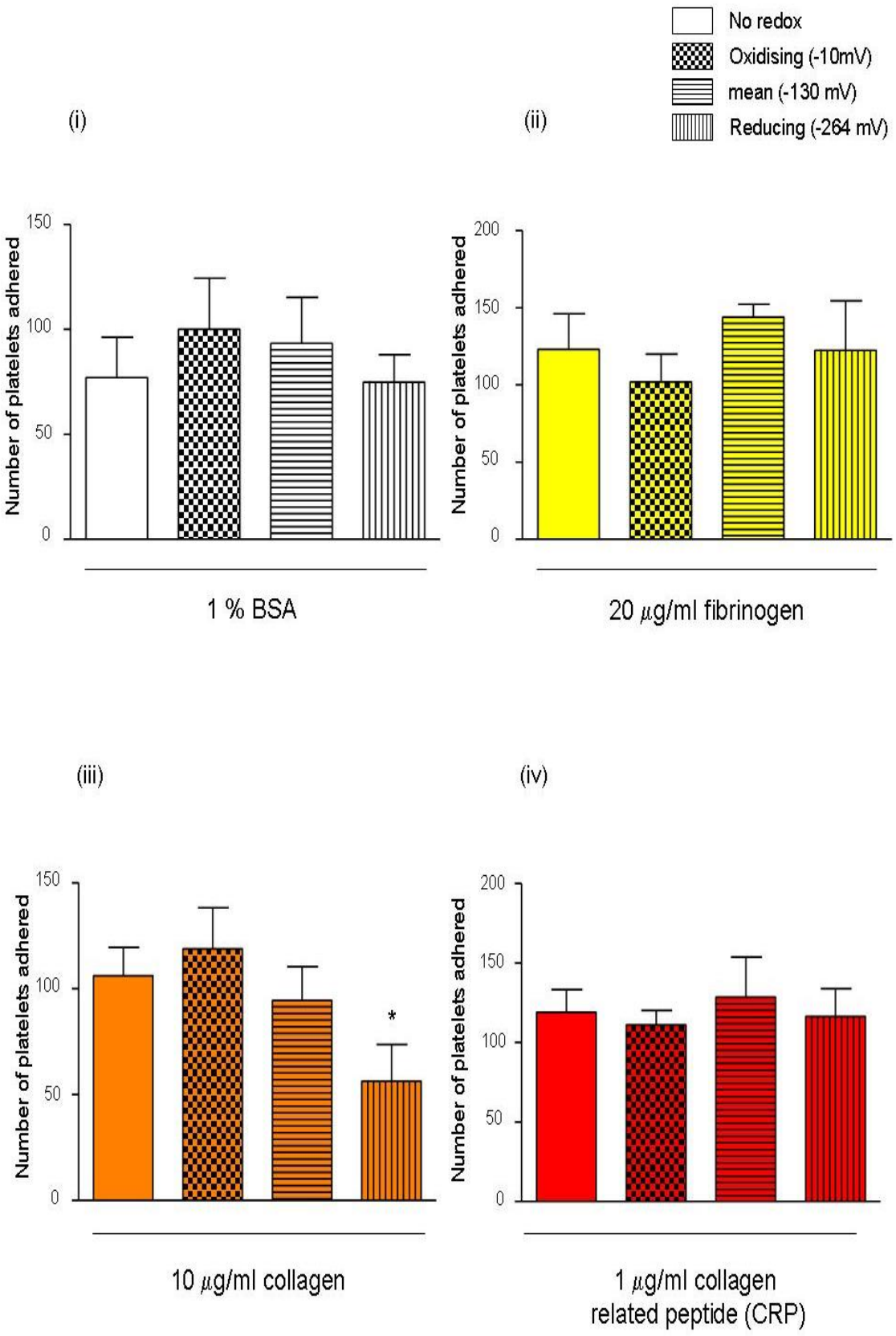
No redox
Oxidising (-10mV)
mean (-130 mV)
Reducing (-264 mV)
(i)
(ii)
Number of platelets adhered
150
100
50
0
200
150
100
50
0
1 % BSA
20 μg/ml fibrinogen
(iii)
(iv)
*
10 μg/ml collagen
1 μg/ml collagen
related peptide (CRP)

Figure 4.22 (a) Platelet adhesion to collagen is significantly decreased in a reducing external redox environment. Washed platelets were either untreated or incubated with GSH/GSSG redox potentials. Platelets were adhered to poly-L-lysine slides coated with (i) 1 % BSA, (ii) 20 μg/ml fibrinogen, (iii) 10 μg/ml collagen or (iv) 1 μg/ml CRP for 45 minutes at 37 °C. Samples were fixed with 1 % formaldehyde for 10 minutes at room temperature and permeabilised with 0.1 % Triton-X-100 for 10 minutes at room temperature. Platelets were stained with Alexa Fluor® 488 phalloidin and imaged using a Zeiss LSM510 Meta confocal microscope with a 63X oil-immersion lens. A laser wavelength of 488 nm, at an intensity of 1 % was employed. Data was analysed using the 'Cell Counter' plugin in the ImageJ software package. Date is presented as the mean ± SEM, n=4 independent experiments, *$p < 0.05$.

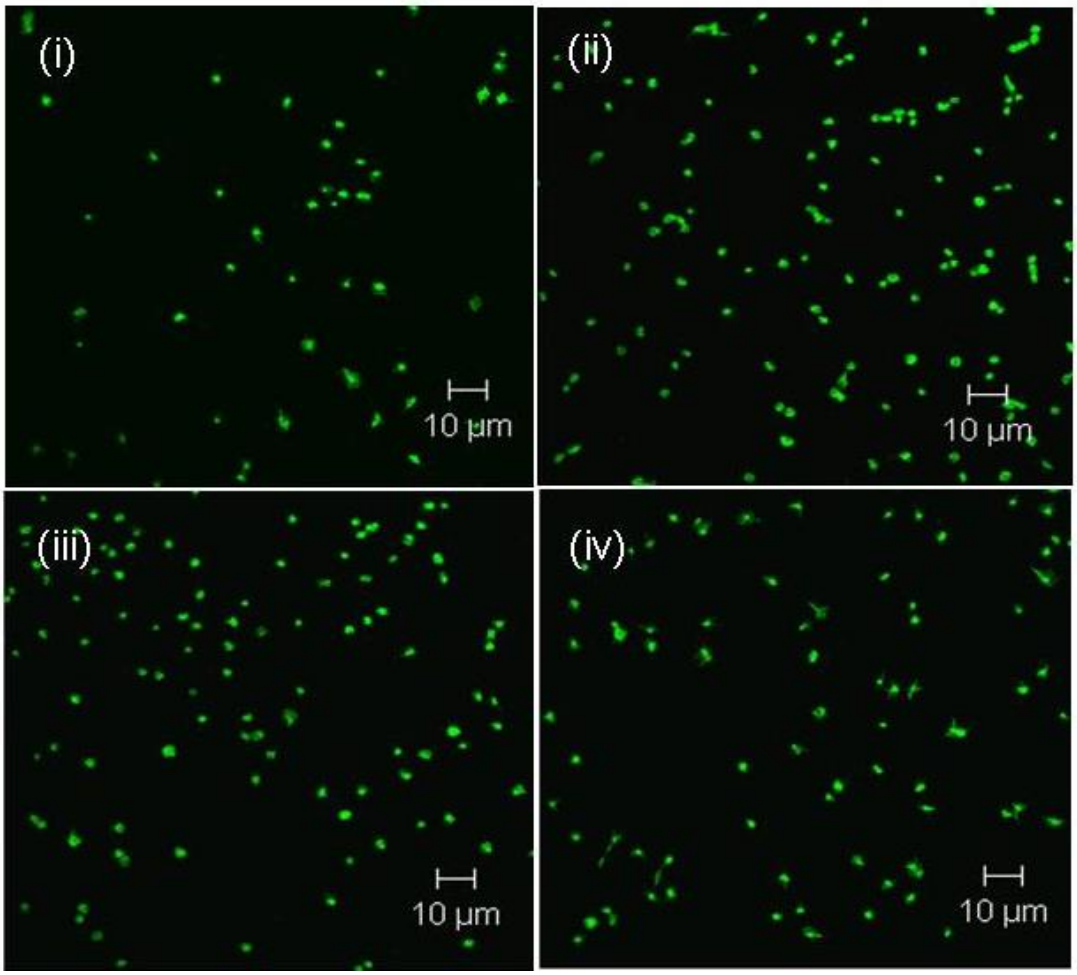

Figure 4.22 (b) An altered external redox environment has no impact on platelets adhered to bovine serum albumin (BSA). Washed platelets were either untreated or incubated with GSH/GSSG redox potentials for 10 minutes at 37 °C: (i) no redox, (ii) oxidising (-10 mV), (iii) mean (-130 mV) and (iv) reducing (-264 mV). Platelets adhered to poly-L-lysine slides coated with 1 % BSA for 45 minutes at 37 °C. Samples were fixed with 1 % formaldehyde for 10 minutes at room temperature and permeabilised with 0.1 % Triton-X-100 for 10 minutes at room temperature. Platelets were stained with Alexa Fluor® 488 phalloidin and imaged using a Zeiss LSM510 Meta confocal microscope with a 63X oil-immersion lens. A laser wavelength of 488 nm, at an intensity of 1 % was employed. Images are representative of n=4 independent experiments.

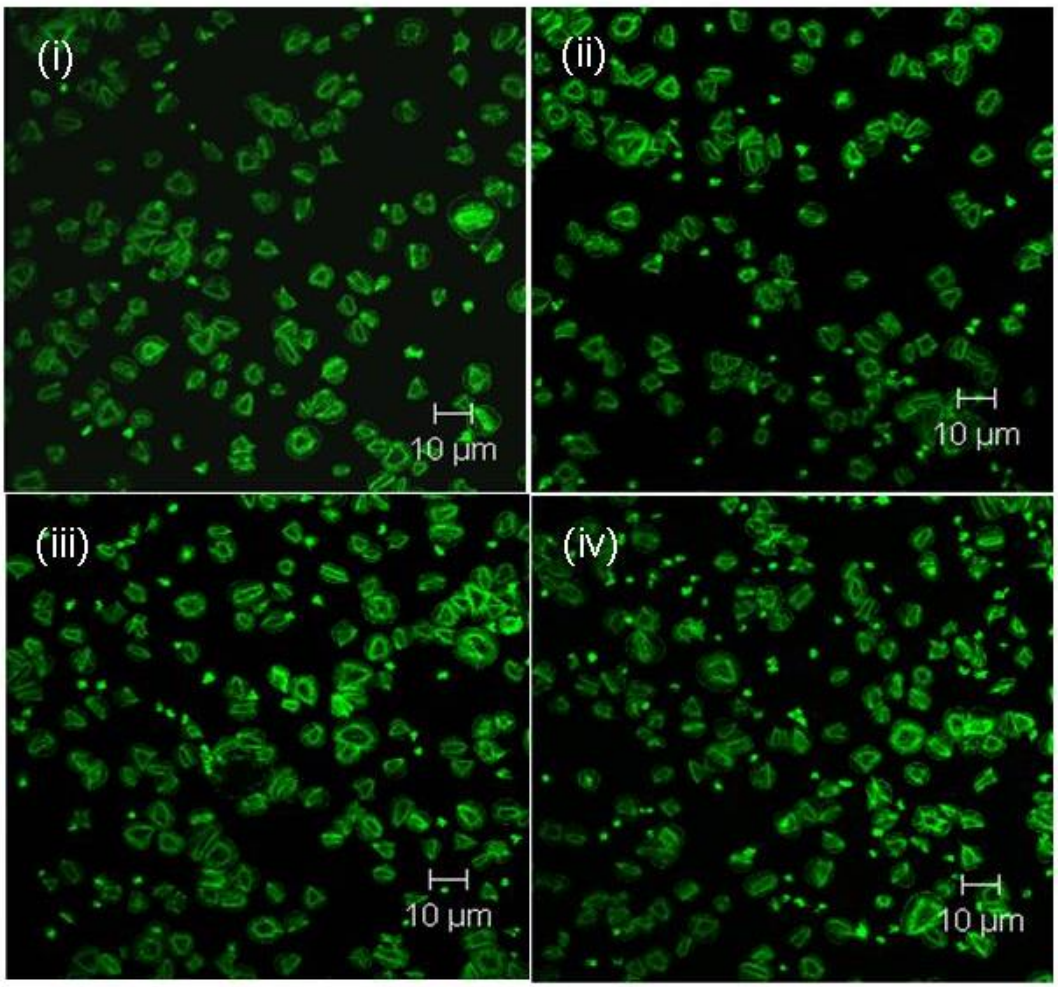

Figure 4.22 (c) An altered external redox environment has no impact on platelets adhered to fibrinogen. Washed platelets were either untreated or incubated with GSH/GSSG redox potentials for 10 minutes at 37 °C: (i) no redox, (ii) oxidising (-10 mV), (iii) mean (-130 mV) and (iv) reducing (-264 mV). Platelets adhered to poly-L-lysine slides coated with 20 µg/ml fibrinogen for 45 minutes at 37 °C. Samples were fixed with 1 % formaldehyde for 10 minutes at room temperature and permeabilised with 0.1 % Triton-X-100 for 10 minutes at room temperature. Platelets were stained with Alexa Fluor® 488 phalloidin and imaged using a Zeiss LSM510 Meta confocal microscope with a 63X oil-immersion lens. A laser wavelength of 488 nm, at an intensity of 1 % was employed. Images are representative of n=4 independent experiments.

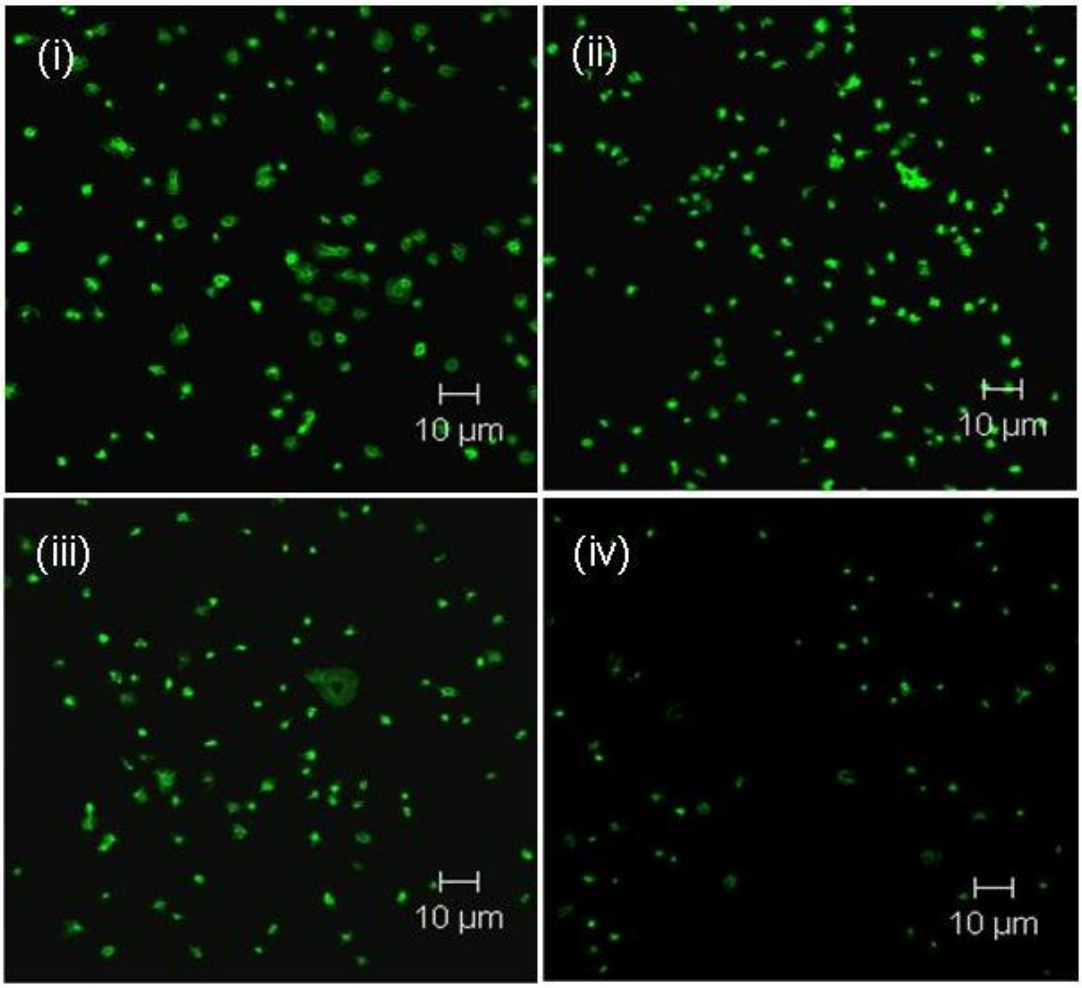

Figure 4.22 (d) Platelet adhesion to collagen is decreased in a reducing external redox environment. Washed platelets were either untreated or incubated with GSH/GSSG redox potentials for 10 minutes at 37 °C: (i) no redox, (ii) oxidising (-10 mV), (iii) mean (-130 mV) and (iv) reducing (-264 mV). Platelets adhered to poly-L-lysine slides 10 µg/ml collagen for 45 minutes at 37 °C. Samples were fixed with 1 % formaldehyde for 10 minutes at room temperature and permeabilised with 0.1 % Triton-X-100 for 10 minutes at room temperature. Platelets were stained with Alexa Fluor® 488 phalloidin for 20 minutes at room temperature. Samples were imaged using a Zeiss LSM510 Meta confocal microscope with a 63X oil-immersion lens. A laser wavelength of 488 nm, at an intensity of 1 % was employed. Images are representative of n=4 independent experiments.

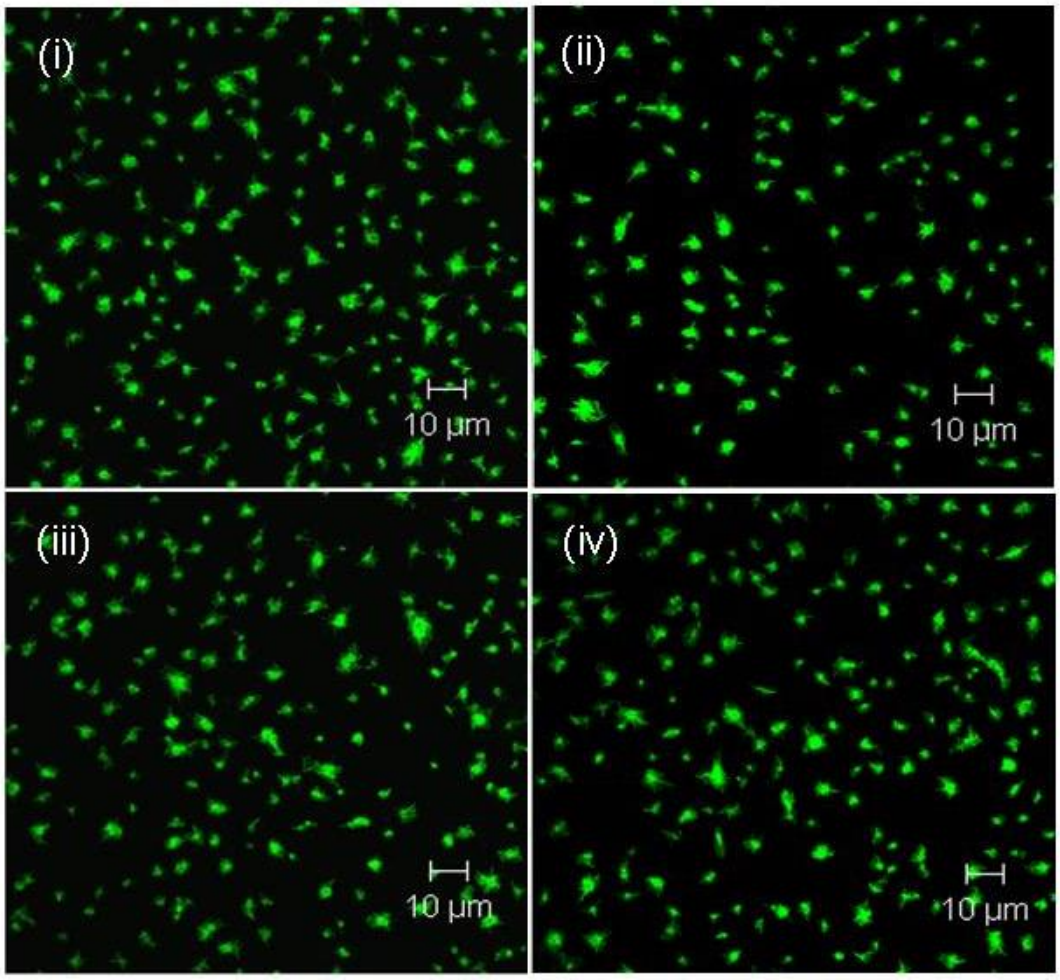

Figure 4.22 (e) An altered external redox environment has no significant impact on platelets adhered to collagen related peptide (CRP). Washed platelets were either untreated or incubated with GSH/GSSG redox potentials for 10 minutes at 37 °C: (i) no redox, (ii) oxidising (-10 mV), (iii) mean (-130 mV) and (iv) reducing (-264 mV). Platelets were adhered to poly-L-lysine slides coated with 1 µg/ml CRP for 45 minutes at 37 °C. Samples were fixed with 1 % formaldehyde for 10 minutes at room temperature and permeabilised with 0.1 % Triton-X-100 for 10 minutes at room temperature. Platelets were stained with Alexa Fluor® 488 phalloidin for 20 minutes at room temperature. Samples were imaged using a Zeiss LSM510 Meta confocal microscope with a 63X oil-emersion lens. A laser wavelength of 488 nm, at an intensity of 1 % was employed. Images are representative of n=4 independent experiments.

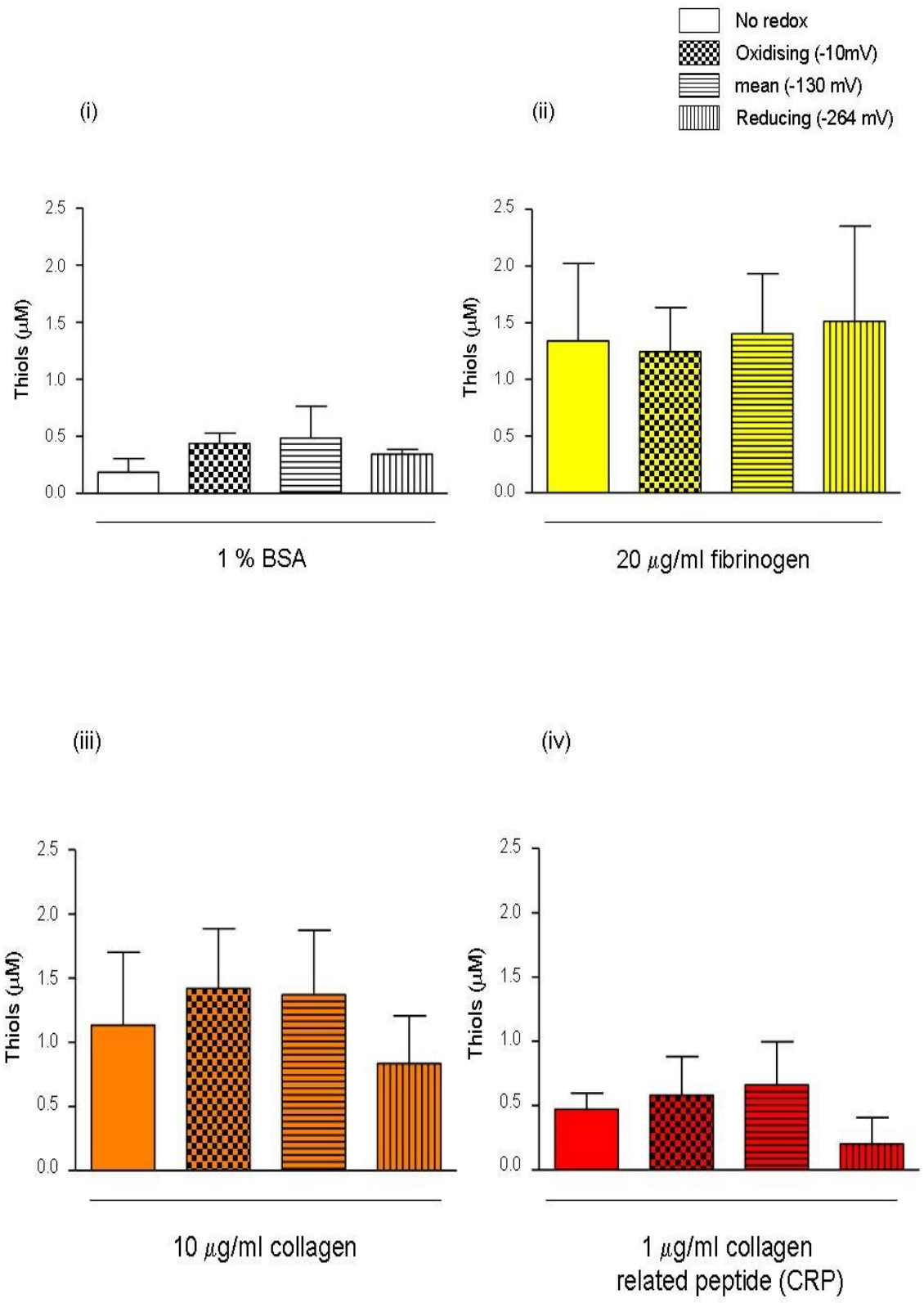
No redox
Oxidising (-10mV)
mean (-130 mV)
Reducing (-264 mV)
(i)
(ii)
(iii)
(iv)
Thiols (μM)
2.5
2.0
1.5
1.0
0.5
0.0
1 % BSA
20 μg/ml fibrinogen
10 μg/ml collagen
1 μg/ml collagen related peptide (CRP)

Figure 4.23 In the presence of a reducing external redox environment, the thiol population of platelet adhered to collagen is decreased, though not significantly. This finding is consistent with a decreased level of platelet adhesion to collagen observed in a reducing environment. The external redox environment has no impact on the thiol population of platelets adhered to BSA, fibrinogen or collagen related peptide (CRP). Washed platelets were either untreated or incubated with GSH/GSSG redox potentials: oxidising (-10 mV), mean (-130 mV) and reducing (-264 mV) for 10 minutes at 37 °C. Platelets were then allowed to adhere to clear, flat bottom 96-well plates coated with 1 % BSA, 20 μg/ml fibrinogen, 10 μg/ml collagen or 1 μg/ml CRP for 45 minutes at 37 °C. 5,5'-dithiobis-(2-nitrobenzoic acid) (DTNB) (100 μM) was added and incubated for 1 minute at room temperature. Absorbance was measured, using a Wallac plate reader, at 405 nm. Data is presented as the mean ± SEM, n=3 independent experiments.

(a) 1 % BSA

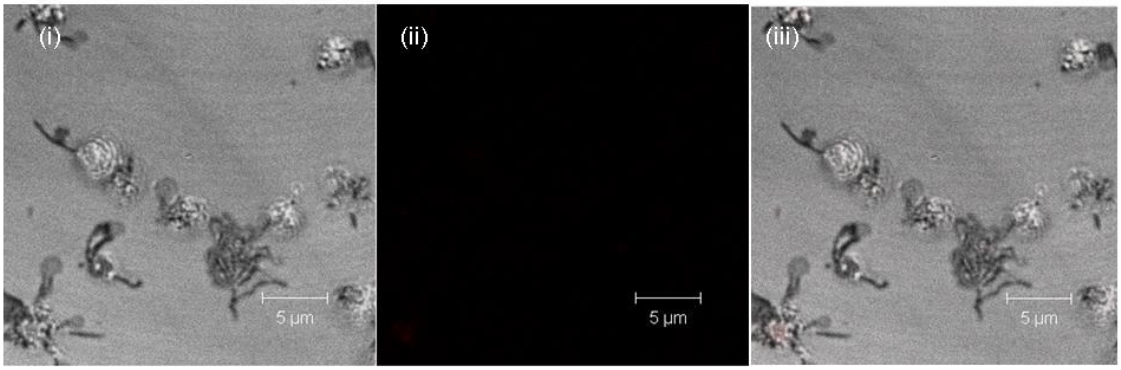

(b) 20 µg/ml fibrinogen

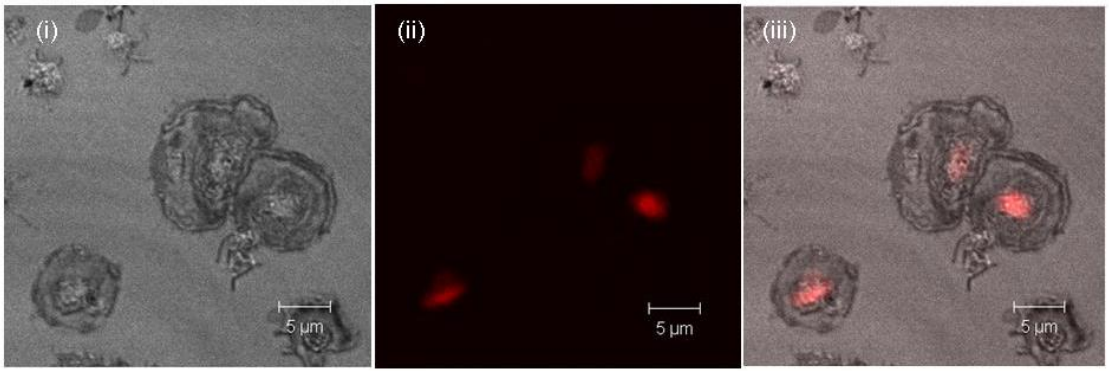

(c) 10 µg/ml collagen

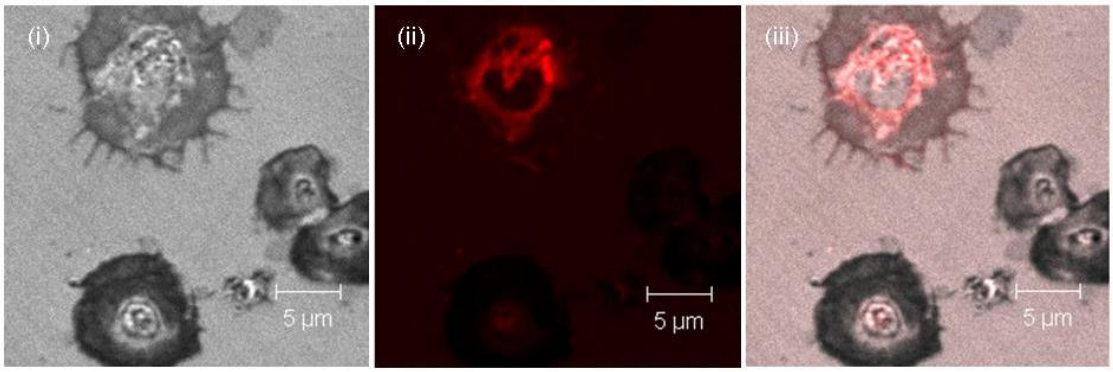

(d) 1 µg/ml collagen related peptide (CRP)

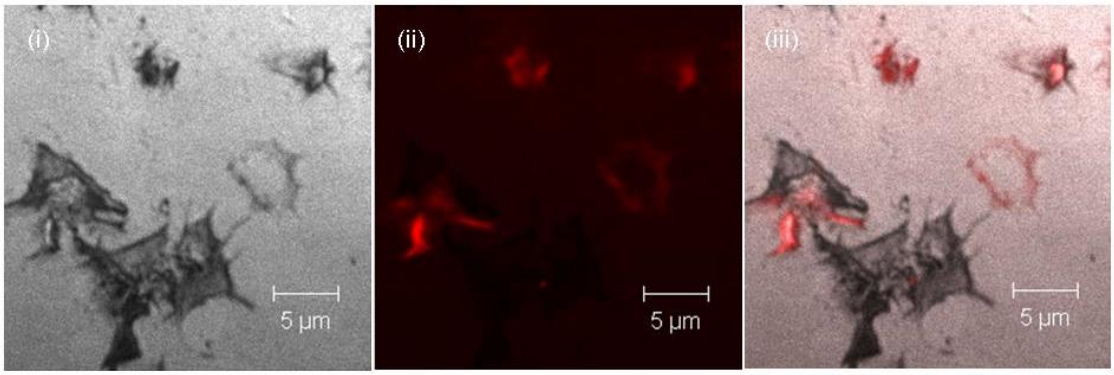

Figure 4.24 The surface thiol population of platelets adhered to BSA, fibrinogen, collagen and collagen related peptide (CRP) labelled with the thiol probe Atto 655 maleimide. Washed platelets adhered to poly-L-lysine slides coated with (a) 1 % BSA, (b) 20 μg/ml fibrinogen, (c) 10 μg/ml collagen or (d) 1 μg/ml CRP for 45 minutes at 37 °C. Platelets were stained with Atto 655 maleimide (100 nM) for 10 minutes at room temperature and fixed with 1 % formaldehyde for 10 minutes at room temperature Samples were imaged using a Zeiss LSM510 Meta confocal microscope with a 63X oil-immersion lens. A laser wavelength of 633 nm, at an intensity of 30 % was employed. (i) Back-scatter image (light reflected from the sample), (ii) fluorescent image (fluorescence from Atto 655 maleimide), (iii) backscatter and fluorescence images merged. Images are representative of n=4 independent experiments.

4.3 Discussion

Raman spectroscopy is a powerful, non-invasive technique useful for the analysis of the structure and composition of chemical and, more recently, biological samples at a molecular level. In Chapter 3, it was demonstrated that Raman could be used as a novel method to examine platelet membrane structure and to differentiate platelets stimulated with various platelet activators. In light of these findings, it was decided to employ Raman to further investigate the impact of the activation of platelets with more physiologically relevant platelet agonists. This study aimed to reveal the structural subtleties brought about by platelet activation and confirm that platelets can be distinguished from each other irrespective of the nature or potency of the platelet activator.

Raman spectroscopy has been successfully employed in a number of recent studies to analyse and distinguish biological samples based on characteristic properties which were examined at a molecular level (Bensalah et al, 2010; Crow et al, 2005; Lyng et al, 2007). Here, it was again demonstrated that a combination of Raman spectroscopy and PCA analysis could be used to separate platelet samples based on whether they are in an unactivated or activated state. Significantly, activated platelets could also be separated from each other based on whether they were activated with the platelet agonists: thrombin, collagen or convulxin.

A more rigorous analysis of regions corresponding to different molecular structures, such as thiol, disulphide, amide I and amide III regions, revealed there were modifications in all of these regions which contributed to the

discrimination of platelet Raman spectra. It was also discovered during this analysis that lipid groups, and in particular carotenoids, appeared to play a key role in the separation of platelet Raman spectra by PCA.

Carotenoids are a group of organic pigments, lipid in nature, which, unusually, are not produced by humans but are found in most cell membranes including platelets (Stefanini et al, 1957). Humans obtain carotenoids through their diet from foods such as fruit and vegetables which are rich in carotenoids. The exact role of carotenoids in cell membranes has yet to be fully elucidated but it is thought they act to minimise membrane damage and protect lipids. Carotenoids are tetraterpenoids, i.e. they contain 40 carbon atoms in their structure. Their basic structure consists of a long polyene hydrocarbon chain that can be modified, at one or both ends, by cyclisation, changes in hydrogenation level or by addition of oxygen-containing functional groups (Britton, 1995). Carotenoids can be divided into two classes: xanthophylls (oxygen containing) or carotenes (parent hydrocarbon). It is these variations in structure that give rise to more than 600 different carotenoids. The polyene chain which consists of a long system of alternating single and double carbon bonds is the main feature responsible for the chemical reactivity of carotenoids (Figure 4.21).

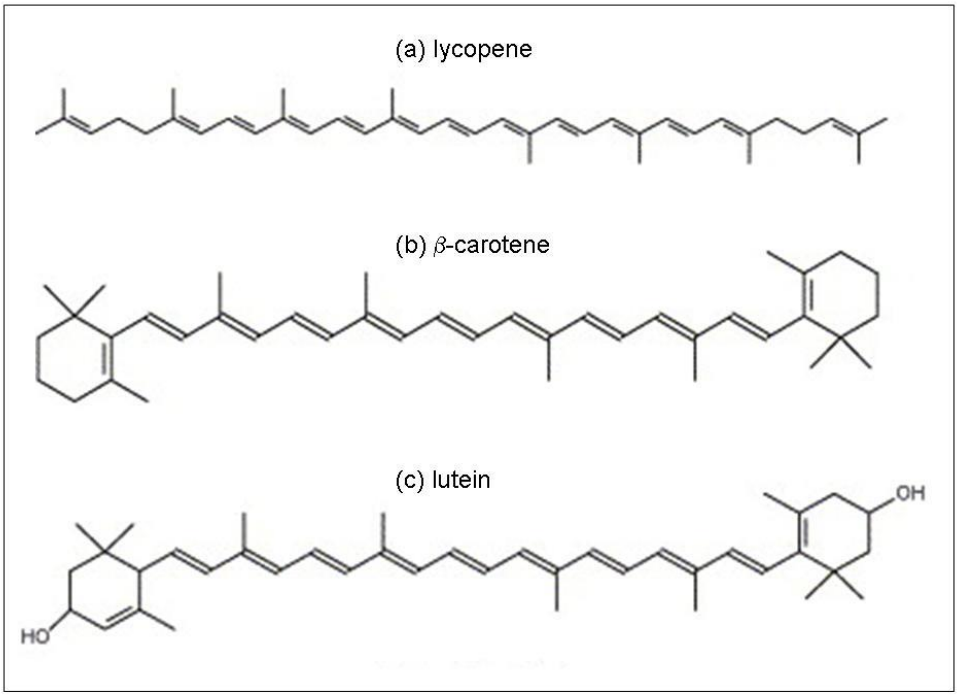

Figure 4.25 Basic structure of some common carotenoids. (a) Lycopene, an acyclic carotenoid; (b) β-carotene, a dicyclic carotenoid, (c) lutein, a xanthophyll (oxygen containing carotenoid). Adapted from (Melendez-Martineza et al, 2007).

In the characteristic Raman spectrum of carotenoids, the intense band at 1160 cm^{-1} is usually attributed to the C-C stretching mode and the very strong band near 1520 cm^{-1} is assigned to the C=C stretching vibration (Merlin, 1985). In the Raman spectra of platelets (Figure 4.6 (a)), these peaks are very prominent. There is also an intense peak at approximately 1006 cm^{-1}, which is assigned to the rocking motion of the molecules methyl components, and a peak at 968 cm^{-1} (Koyama et al, 1988).

The antioxidant properties of carotenoids and the proposal that they are efficient scavengers of free radicals are particularly interesting with regard to their potential role in platelets (Di Mascio et al, 1989). The polyene chain in the basic

structure of carotenoid is highly reactive and rich in electrons. This forms the basis for carotenoids susceptibility to attack by electrophilic reagents and their instability towards oxidation (Britton, 1995). Carotenoids appear to have a direct effect on the structural and dynamic properties of lipid membranes, along with modulating the fluidity of the membrane, thereby, protecting the membrane from susceptibility to degradation as a result of oxidative stress (Gruszecki & Strzalka, 2005). Many human diseases, including cardiovascular disease, involve oxidation processes mediated by free radicals and it has been suggested in the literature that carotenoids may play a key role in the prevention of cardiovascular disease (Voutilainen et al, 2006).

The absolute signal intensity of Raman spectra can be quite unreliable, as a result of variability from experiment to experiment due to environmental factors. However, normalisation of the spectra to the same peak across the board ensures the intensity (measured in arbitrary units) can be taken into consideration. Examination of the intensity of the carotenoid peaks present in the signature Raman spectra of unactivated platelets or platelets activated with thrombin, collagen or convulxin found that carotenoids may well play an important part in the reorganisation of the platelet membrane upon activation. The relative intensity of a Raman peak is a quantitative measure. Therefore, a trend towards an enhanced intensity of the carotenoid peaks in platelets as a result of activation is suggestive of an increase in the quantity of these particular carotenoids present in the platelet membrane.

Similar to other biological membranes, platelets possess an asymmetrical phospholipid bilayer membrane. The lipid bilayer consists of an outer and an

inner leaf. The outer leaf is composed mainly of choline-phospholipids, while there is an abundance of amino-phospholipids in the inner layer. It is well established that upon activation there is a rearrangement of the platelet membrane lipid bilayer, whereby some phospholipids from the inner membrane become translocated to the outer surface. This phenomenon leads to the exposure of phospholipids such as phosphatidylserine (PS) on the outer surface of platelets (Bevers et al, 1983; Heemskerk et al, 2002).

It is known that due to their hydrophobic nature carotenoids are generally localised to inner membranes (Britton, 1995). Consequently, it is quite plausible that the increase in the carotenoid peak intensity observed in the Raman spectra of activated platelets compared to unactivated platelets may be due to the exposure of additional carotenoid groups on the platelet membrane upon platelet activation. Prominent peaks in the platelet Raman spectra, at approximately 2670 cm^{-1} and 3040 cm^{-1}, also indicate that the platelet lipid profile is an important factor in PCA distinguishing platelets stimulated with various activators. Lipid features at this higher end of the spectrum are generally thought to be less useful for identifying lipids and their conformation. This is due to the CH bond being highly localised and, therefore, rather insensitive to chain configuration or environment (Wallach et al, 1979). Nonetheless, the finding that these peaks are involved in the discrimination of platelet samples into distinct clusters associated with activation state indicates that these lipids are more important than previously thought. Studies have shown the presence of cholesterol-rich lipid islands in the resting platelet surface membrane. Following platelet activation, these lipid islands become

associated with the outer layer of the membrane (Del Conde et al, 2005). Additionally, the rearrangement of the platelet membrane and the subsequent exposure of PS on the surface of platelets is associated with the formation of membrane blebs which are eventually shed as pro-coagulant platelet-derived microparticles (Heemskerk et al, 2002). This phenomenon may be the link to the variances we observed in the lipid profile in the Raman spectra of unactivated and activated platelets. More in depth analysis may be required before any definitive conclusions relating to the role of lipids and carotenoids in platelet membrane can be reached.

Similarly, PCA analysis of the thiol and disulphide containing regions of the Raman spectra of platelets revealed that there were differences in these regions that could potentially be associated with thiol/disulphide modifications as a result of platelet activation. As discussed in Chapter 3, the exact nature of these modifications is difficult to pinpoint due to the complex composition of platelets. However, differences in this region can be attributed to a change in the absolute number of thiol groups present or may also be indicative of shuffling or rearrangement of the bonds or changes in the strain on the cysteine bonds.

Based on these interesting findings, further examination of the role of thiol populations in platelet function was performed. Previous studies in our laboratory, found the external redox environment impacted significantly on platelet activity, in particular in response to platelet stimulation by collagen. A reducing redox environment generated by glutathione (GSH/GSSG) and

cysteine (Cys/CySS) redox potentials inhibits platelet aggregation to collagen only (Murphy et al, 2010). Similarly, in my study reducing environments generated using the reducing agents, DTT, TCEP and GSH also inhibited platelet aggregation to collagen. A reducing environment has no effect on platelet aggregation to thrombin or convulxin. Oxidising redox potentials and other oxidising conditions have no effect on collagen, thrombin or convulxin induced aggregation. While others have found that reducing conditions can inhibit platelet activation, using concentrations of the reducing agents in millimolar (mM) concentrations, I show here that lower, physiologically relevant concentrations, in the micromolar range (μM), have significant effects on platelet function (Pacchiarini et al, 1996). The results obtained from these combined studies point specifically to the collagen receptor, integrin $\alpha_2\beta_1$, as a redox sensitive receptor. This is corroborated from the fact that neither thrombin nor convulxin induced platelet aggregation is affected by changing the external redox environment. The finding that platelet aggregation induced by convulxin, a GPVI specific agonist, implies this receptor is not implicated in the redox sensitive collagen pathway. In order to categorically confirm that type I collagen and convulxin in these studies were signalling through different receptors and intracellular pathways, two established tyrosine kinase inhibitors were employed. PP2 is a broad Src family kinase inhibitor, while BAY 61-3606 is a Syk specific inhibitor. Protein-tyrosine phosphorylation is a key signalling event associated with platelet activation (Clark et al, 1994). Platelet activation through collagen is known to stimulate activation of a number of protein-tyrosine kinases, including Src family kinases and Syk, which is downstream of Src kinases, and promote the rapid phosphorylation of a number of proteins. It was

found that PP2 inhibited platelet aggregation to both collagen and convulxin, implicating Src family kinases in the signalling cascade of both platelet agonists. However, BAY 61-3606 inhibited convulxin induced platelet aggregation only. BAY 61-3606 had no impact on the platelet aggregation response to collagen, indicating a divergence in the signalling pathways of the two agonists. These results confirmed the type I collagen was targeting integrin $\alpha_2\beta_1$, and not GPVI. These findings are consistent with previous findings, whereby Src family kinases have been shown to be implicated in signalling through both GPVI and integrin $\alpha_2\beta_1$, whereas collagen induced activation of Syk is specific to GPVI (Asselin et al, 1997; Dangelmaier et al, 2005; Ichinohe et al, 1997; Inoue et al, 2003).

The membrane-impermeable thiol blocker 5, 5'-Dithio-bis-(2-nitrobenzoic acid) (DTNB) was used to detect platelet surface thiols through Ellman's test, a well established thiol detection assay. It was found that there are, on average, approximately 3.78×10^{-18} moles of thiols present on the surface of an unactivated platelet. Although it is well known that thiols are present on the surface of platelets, the actual number of free thiols present has not been well documented. One of few studies found 3.1×10^{-18} moles of thiol per platelet, a finding similar to ours (Harbury & Schrier, 1974). However, the study by Harbury and Schrier looked solely at the thiol population of unactivated platelets, while this study examined the thiol population of unactivated platelets along with the effects of platelet activation with a number of activators on this population.

The surface thiol population of platelets activated by collagen in suspension was found to be significantly increased compared to unactivated platelets, from 3.78×10^{-18} to 19.62×10^{-18} moles of thiol per platelet. Platelet activation by

thrombin or convulxin had no impact on the thiol population. In a parallel study examining the thiol population of adhered platelets, it was again observed that there was a trend towards an increase in the surface thiol population of platelets adhered to collagen, compared to those adhered to BSA, fibrinogen or CRP. This increase in the thiol population induced by collagen was abolished as the external redox environment became more reducing. All of the findings thus far highlight the importance of thiols in the collagen activation pathway of platelets, specifically suggesting a particular significance of the thiol groups in integrin $\alpha_2\beta_1$. The presence of a reducing redox environment inhibited platelet aggregation to collagen only. This is suggestive of an integrin $\alpha_{IIb}\beta_3$ independent effect, due to the final common pathway in platelet aggregation to thrombin or convulxin being integrin $\alpha_{IIb}\beta_3$ mediated. These findings were unexpected as it was demonstrated in Chapter 3 that an altered redox environment impacts on integrin $\alpha_{IIb}\beta_3$ in a purified system and in a CHO-K1 cell model. However, this finding therefore highlights the sensitivity of integrin $\alpha_2\beta_1$ even compared to other integrins such as integrin $\alpha_{IIb}\beta_3$. This increased sensitivity may be due to a greater number of reactive cysteine residues present in the β_1-subunit in comparison to that of the β_3-subunit. In an analysis of the cysteine rich region of these two β-subunits, it was found there are almost twice as many potentially reactive cysteines in the β_1-subunit as there are in the β_3-subunit (personal communication, Dr. Desmond Murphy, RCSI). The reactivity of a cysteine residue is defined by its pK_a value, which is inversely related to reactivity, i.e. a cysteine with a low pK_a value is more reactive. The reactivity of a cysteine residue is influenced by the amino acid surrounding it. In particular, the pK_a values of cysteine thiols may be decreased by charge interactions with

positively charged, basic amino acids adjacent to the cysteine thiol (Vukelić et al, 2012; Wakabayashi et al, 2004). There are 18 cysteines with at least one adjacent basic amino acid in the β_1-subunit while there are only 10 in the β_3-subunit. The reactivity of the thiols in the cysteines of integrin $\alpha_2\beta_1$ makes them prime targets for thiol modifications such as S-glutathionylation or S-cysteinylation. S-glutathionylation is a reversible process in which mixed disulphide bonds are formed between the thiol group of the protein itself and glutathione (Dalle-Donne et al, 2007). S-cysteinylation is a similar process and both are potential mechanisms for the post-translational regulation of proteins. The inhibition of the collagen activation pathway of platelets by reducing redox environments is suggestive of some such external modification of the receptor, whereby it may become locked into a particular conformation thereby unable to induce further intra-platelet signals which usually culminate in full platelet activation.

The generation of thiols on the surface of platelets activated with collagen only is a very interesting observation. It is established that conversion of integrin $\alpha_{IIb}\beta_3$ to an activated, ligand-binding conformation is associated with conformational changes and a subsequent increase in the free thiol population (Yan & Smith, 2000). It is somewhat surprising that there was such a significant increase in the thiol population of platelets activated by collagen, especially due to the smaller copy number of integrin $\alpha_2\beta_1$ compared to integrin $\alpha_{IIb}\beta_3$, the most abundant protein on platelets. However, the persistence of this new thiol population even in the presence of an oxidising environment, confirms the generation of these thiols in the collagen activation pathway is a robust and real event. These results suggest that activation of platelets by collagen induces a

reduction of disulphide bonds within the integrin or a thiol/disulphide exchange mechanism exists whereby thiols that were previously buried within the integrin become exposed upon stimulation with collagen. A reducing redox environment prevents the generation of this new thiol population on the surface of platelets activated with collagen, by potentially modifying or locking the integrin into a particular conformation.

When the values corresponding to the redox background were subtracted from the values of platelets in the presence of redox, a negative value was found, indicating the thiols from the reduced form of the redox couples (GSH and Cys) were reacting with the thiols on the surface of platelets. Therefore, the absolute number of thiols in the system available for detection in the Ellman's test is decreased. This is further evidence supporting the interaction of the external redox environment with the thiol population of integrin and thus demonstrates that S-glutathionylation or S-cysteinylation of thiols in a reducing redox environment is a plausible hypothesis.

It is clear that we have uncovered a redox sensitive element of the collagen activation pathway in platelets and further elucidated a role for thiols in integrin activation. Further investigation of the collagen signalling pathway and downstream events is warranted and outlined in Chapter 5.

Chapter 5

External modification of the platelet surface thiol population impacts on intra-platelet signalling events

5.1 Introduction

Platelet activation leads to a series of morphological and biochemical changes to the platelet. Upon activation, the platelet membrane undergoes a substantial transformation with the expression of a number of proteins which are not found on the surface of unactivated platelets. The characteristic discoid shape of unactivated platelets is maintained by a main microtubule arranged in a coil. This is associated with multiple short, highly dynamic microtubules, located beneath the plasma membrane (Patel-Hett et al, 2008). In addition to major membrane changes, platelets also undergo dramatic shape change as a result of activation. The underlying cause of this shape change is platelet cytoskeleton rearrangement. The platelet cytoskeleton contains two main actin filament-based components. They are the actin filament network of the cytoplasm and the membrane skeleton, which is composed of a latticework of short cross-linked actin filaments (Fox, 1993a). Actin is the most abundant protein present in platelets and is estimated to make up approximately 15 - 20 % of the total platelet protein content. The role of the cytoplasmic cytoskeleton is to mediate contractile events and to direct rapid platelet shape change upon activation. The platelet membrane cytoskeleton, which coats the plasma membrane, regulates membrane contours and stability along with the lateral distribution of membrane glycoproteins (Fox, 1993b). Reorganisation of the actin cytoskeleton is an essential part of platelet morphological modifications and functions (Hartwig, 2006).

In unactivated platelets, 30 - 40 % of actin is polymerised into filaments and is termed F-actin. The remaining actin is thought to be prevented from

polymerisation by the association of thymosin-β4 with monomeric actin and by the association of gelsolin with the barbed ends of pre-existing actin filaments. Activation of platelets greatly increases the percentage of F-actin (Hartwig & DeSisto, 1991). New filaments form to fill extended filopodia and an actin network is formed at the periphery of the platelet. In addition to controlling shape changing events, the platelet cytoskeleton is also involved in the regulation of spatial organisations and, thus, in the integration of platelet activities. The cytoskeleton binds signalling molecules resulting in their localisation to specific regions, along with binding the plasma membrane and modulating membrane proteins (Fox, 2001).

Proteins involved in signalling may become associated with actin in a direct interaction whereby the proteins specifically bind to actin or actin may be the link to other signalling proteins. Heat shock protein 27 (HSP27) is an example of a signalling protein that upon platelet activation becomes phosphorylated and bound to assembling actin (Zhu et al, 1994). HSP27 has been shown to not only interact with actin but also to regulate the actin cytoskeleton of platelets (Butt et al, 2001). The redox environment has been shown to play a significant role in the regulation of the actin cytoskeleton of cells. HSP27 is one of the proteins implicated in this process. In endothelial cells, hydrogen peroxide (H_2O_2), a critical player in the initiation of oxidative stress, potentiates activation of p38 mitogen-activated protein kinase (p38 MAP kinase), which leads to the activation of MAP kinase-activated protein kinase-2/3 and the phosphorylation of HSP27 (Huot et al, 1997). In these cells, H_2O_2 also caused major reorganisation of the actin cytoskeleton (Huot et al, 1998). A similar signalling

pathway exists in platelets suggesting the role of intra-platelet redox environment may be just as significant.

Membrane glycoproteins such as integrin $\alpha_{IIb}\beta_3$ are also strongly associated with the actin cytoskeleton of platelets. Integrin activating inside-out signals are mediated by actin filament turnover, rearrangement of the platelet cytoskeleton and integrin regulatory proteins. A number of regulatory proteins involved with the linkage between integrins and the actin cytoskeleton have been identified and include talin-1, kindlin-2 and kindlin-3 (Montanez et al, 2008; Moser et al, 2008). Talin-1 binds the cytoplasmic tails of the β-subunits of integrins thereby connecting the actin cytoskeleton through its actin binding site. This links the cytoskeletal network to the extra-cellular matrix (ECM) (Tadokoro et al, 2003; Wegener et al, 2007). Indeed, a mutation of the β_3-subunit (β_3(L746A)) of integrin $\alpha_{IIb}\beta_3$ specifically abolishes talin-1 binding and impairs inside-out signalling associated with the integrin (Petrich et al, 2007). In a separate study, the platelets of talin-1 deficient mice displayed an inability to activate integrin $\alpha_{IIb}\beta_3$ in response to platelet agonists. Furthermore, integrin $\alpha_2\beta_1$ was also found to be impaired due to a defective response in adhesion of these platelets to collagen (Nieswandt et al, 2007).

Vasodilator-stimulated phosphoprotein (VASP) is another protein capable of affecting and regulating actin polymerisation and filament bundling (Reinhard et al, 2001). VASP is a key regulatory protein found in platelets in particularly high concentrations (Eigenthaler et al, 1992). It is a substrate of both cAMP- and cGMP- dependent kinases (PKA and PKG) (Comerford et al, 2002). VASP

possesses three phosphorylation sites: Ser157, Ser239 and Thr278. Each of these sites is phosphorylated with different affinities by PKA or PKG. Approximately 90 % of VASP is present in the platelet membrane (Reinhard et al, 1992) and is also found in focal contacts (Jockusch et al, 1995). Focal contacts are protein rich structures which link the actin cytoskeleton to the ECM via integrins. These observations suggest a role for VASP in integrin activation and regulation. VASP plays a role in the binding of fibrinogen to integrin $\alpha_{IIb}\beta_3$ and the phosphorylation of VASP results in inhibition of platelet aggregation, thereby supporting an important role for VASP in the regulation of integrin function (Horstrup et al, 1994); (Aszodi et al, 1999). Additionally, previous work in our laboratory demonstrated integrin $\alpha_{IIb}\beta_3$ exists in an activated conformation in the presence of increasing concentrations of homocysteine and similarly platelets obtained from patients presenting with clinical hyperhomocysteinemia displayed integrin $\alpha_{IIb}\beta_3$ in a greater state of activation than healthy controls (McGarrigle et al, 2011). Subsequently, a link between the presence of homocysteine and the phosphorylation state of VASP in platelets was also demonstrated (unpublished data).

It is clear platelet spreading, membrane alterations and the reorganisation of the cytoskeleton are critical events associated with the activation of platelets. A number of signalling molecules and regulatory proteins are involved in the process. The aim of this chapter is to examine receptor-ligand interactions and their impact on the dynamics of platelet shape change. Furthermore, the impact of an altered external redox environment on platelet spreading and actin cytoskeleton rearrangement in response to adhesion to a number of surfaces

will also be investigated. In order to further elucidate the critical role of thiols in the regulation of platelet function and specifically platelet intracellular signalling pathways and based on previous work carried out in our laboratory in relation to VASP, the effects of platelet activation and an altered external redox environment on the expression of VASP and its phosphorylation state will be explored.

5.2 Results

5.2.1 The effects of platelet adhesion on platelet morphology and actin cytoskeleton rearrangement

5.2.1.1 Platelet imaging by scanning electron microscopy

Scanning electron microscopy (SEM) was employed to investigate the morphology of platelets adhered to various substrates (with the assistance of Dr. Úna Prendergast (DCU)). SEM is a powerful imaging method superior to other imaging techniques due to its high resolution and degree of magnification control, which is independent of the power of an objective lens. The depth of field of SEM also produces high quality images displaying features on specimens that may not be visible with alternatives such as light microscopy.

Unactivated platelets adhered to 1 % BSA, 20 μg/ml fibrinogen, 10 μg/ml collagen or 1 μg/ml collagen related peptide (CRP) were prepared for SEM and imaged. The resulting SEM images revealed distinct and separate morphological changes of platelets adhered to these substrates (Figure 5.1). As expected, few platelets adhered to BSA. In general, those present were in a

typical unactivated state, with a round, discoid shape. Some platelets had a small number of tiny filopodia emerging from them indicating that these platelets may not be in a fully resting state. This may have resulted from the length of time the platelets were in contact with the BSA surface. Platelets adhered to fibrinogen displayed the distinct characteristic 'fried-egg-like' appearance associated with activated, spread platelets. The platelets became flattened with the organelles forced into the centre and the cytoplasm spread out to fill all spaces created by original filopodia. The ruffling of the membrane around the edges and the lack of interaction between individual platelets is interesting to note. In contrast, while many of the platelets adhered to collagen became flattened and spread, there appeared to be a clear interaction between platelets. The platelets adhered to CRP were most definitely interacting with each other although not quite to the same extent as those adhered to collagen. However, their appearance was strikingly dissimilar to platelets adhered to the other substrates. They formed a unique web-like pattern, created by numerous filopodia extensions from the platelets.

5.2.1.2 Platelet imaging by confocal microscopy

The major morphological differences in platelets observed by SEM suggested there may be a variation in the rearrangement of the cytoskeleton of platelets based on the substrate they are adhered to. Therefore, further examination of the actin cytoskeleton of adhered platelets was carried out.

Unactivated platelets adhered to 1 % BSA, 20 μg/ml fibrinogen, 10 μg/ml collagen or 1 μg/ml collagen related peptide (CRP) were permeabilised and stained with Alexa Fluor® 488 phalloidin and imaged using confocal microscopy.

Phalloidin is a high-affinity probe that specifically binds to filamentous actin (F-actin).

Analysis of the samples, at a high magnification (63X objective, ScanZoom 5.0), revealed the actin cytoskeleton rearrangement was primarily dictated by the surface to which the platelets had adhered (Figure 5.2). Platelets adhered to BSA were small and mostly in a discoid shape. Platelets adhered to fibrinogen were large in terms of diameter, and spread with the actin mainly around the perimeter of the platelets, with very little, if any, present in the centre of the platelets. Platelets adhered to collagen were slightly similar in appearance than those adhered to fibrinogen with the actin mainly localised around the outer surface of the platelets adhered to collagen. However, in contrast to platelets adhered to fibrinogen, collagen adhered platelets were found to be interacting and linking each other through their actin cytoskeletons. Platelets adhered to CRP displayed a ‘spindly’ appearance, whereby the platelets had formed a number of actin containing filopodia reaching out in all directions. Full spreading of the membrane and redistribution of all actin to the outer regions had not occurred within these platelets adhered to CRP.

5.2.2 Examination of the surface coverage and spreading of platelets adhered to various surfaces

Platelet spreading is an essential element of platelet plug formation and, ultimately, blood clot development. Following the observations of the morphological changes in platelets as a result of adhesion platelet spreading and actin cytoskeleton rearrangement was further investigated.

Unactivated platelets were allowed to adhere to 1 % BSA, 20 μg/ml fibrinogen, 10 μg/ml collagen or 1 μg/ml collagen related peptide (CRP), stained with Alexa Fluor® 488 phalloidin and examined by confocal microscopy. The percentage surface coverage was calculated based on a total surface area of 20408.98 μm^2 (based on an image size: 142.86 μm X 142.86 μm).

The percentage surface coverage of platelets adhered to fibrinogen was significantly higher than platelets adhered to BSA, collagen or CRP, in the absence of a redox environment (n=4, *p < 0.05, **p < 0.01) (Figure 5.3 (a) (i)). In reducing (-264 mV) and mean (-130 mV) GSH/GSSG redox environments, the percentage surface coverage by platelets adhered to fibrinogen was significantly greater than platelets adhered to BSA, collagen, or CRP. There was no significant difference observed between the level of platelet adhesion to their substrates in an oxidising environment (n=4, **p < 0.01, ***p < 0.001) (Figure 5.3 (a) (ii-iv)).

Platelets adhered to fibrinogen were found to have a significantly larger area than platelets adhered to BSA, collagen or CRP. This was observed in the absence of an altered redox environment and in the presence of reducing (-264 mV) and mean (-130 mV) GSH/GSSG redox environments (n=4, **p < 0.01, ***p < 0.001) (Figure 5.3 (b) (i-iii)). In the presence of an oxidising environment, platelets adhered to fibrinogen were significantly larger than platelets adhered to BSA. There was no significant difference between platelets

adhered to fibrinogen and those adhered to collagen or CRP (n=4, *p < 0.05) (Figure 5.3 (b) (iv)).

5.2.3 The effects of an altered external redox environment on surface coverage and spreading of statically adhered platelets

It was found that a reducing (-264 mV), mean (-130 mV) or oxidising (-10 mV) redox environment had no significant effect on the percentage surface coverage by platelets adhered to BSA, fibrinogen or CRP, compared to platelets adhered to their respective surfaces in the absence of an altered external redox environment (n=4) (Figure 5.4). However, the percentage surface coverage by platelets adhered to collagen was significantly decreased in an external reducing environment, compared to platelets adhered to collagen in the absence of an altered redox environment (n=4, *p < 0.05) (Figure 5.4 (a)).

Furthermore, the impact of an altered external redox environment on the average size of a platelet adhered to each of the surfaces was investigated. There was no significant effect of any of the altered redox environments on the average size of platelets adhered to BSA, fibrinogen or CRP compared to in the absence of an altered external redox environment (n=4) (Figure 5.4 (b)). Interestingly though, while it did not quite reach statistical significance, there was an obvious trend towards a decreased average area of platelets adhered to collagen in the presence of a reducing environment compared to platelets adhered to collagen in the absence of an altered redox environment (n=4) (Figure 5.4 (b)).

5.2.4 Examination of an intra-platelet signalling molecule: vasodilator-stimulated phosphoprotein (VASP)

5.2.4.1 Measuring total vasodilator-stimulated phosphoprotein (VASP) expression in platelets

The levels of vasodilator-stimulated phosphoprotein (VASP) expression and phosphorylation in platelets were examined through Western blot analysis in order to investigate the effects of changing redox external environment on intra-platelet signalling events.

Platelets were unactivated or activated with either 0.1U/ml thrombin, 38 μg/ml collagen or 50 ng/ml convulxin in the absence of an altered redox environment or in the presence of reducing (-264 mV), mean (-130 mV) or oxidising (-10 mV) GSH/GSSG redox potentials. Platelet aggregations were performed and subsequently the samples were lysed. Initially, platelet lysates were separated on 10 % polyacrylamide gels and stained with Coomassie Blue in order to confirm the platelets had been lysed correctly and the platelet protein profile was found to be intact (Figure 5.5).

For Western blot analysis platelet lysates were separated on 10 % polyacrylamide gels, transferred to polyvinyl difluoride (PVDF) membrane and probed with a rabbit polyclonal anti-VASP (A290) antibody, which detects total VASP expression. The levels of total VASP in platelets regardless of whether the platelets were unactivated or activated, in the presence or absence of an altered redox environment were similar as assessed by densitometry analysis using ImageJ software. Additionally, membranes were probed with an anti-α-actinin antibody in order to assess sample loading. There was no significant

difference between the α-actinin content across all conditions indicating equal loading of all samples (n=4) (Figure 5.6 (a) and (b)).

5.2.4.2 The impact of platelet activation and altering the external redox environment on the phosphorylation status of vasodilator-stimulated phosphoprotein (VASP) at Serine 157 (Ser157)

One of the sites at which vasodilator-stimulated phosphoprotein (VASP) can be phosphorylated is Serine 157 (Ser157). In order to investigate the impact of platelet activation and an altered external redox environment on the phosphorylation status of VASP an antibody to detect VASP phosphorylation at Ser157 through Western blotting was employed.

Platelets were unactivated or activated with either 0.1U/ml thrombin, 38 μg/ml collagen or 50 ng/ml convulxin in the absence of an altered redox environment or in the presence of reducing (-264 mV), mean (-130 mV) or oxidising (-10 mV) GSH/GSSG redox potentials. Platelet aggregations were performed and subsequently the samples were lysed. Platelet lysates were run on 10 % polyacrylamide gels, transferred to polyvinyl difluoride (PVDF) membrane and probed with a rabbit polyclonal anti-VASP-P (Ser157) antibody.

Analysis of the Western blots was carried out through densitometry. VASP phosphorylation at Ser157 was minimal in unactivated platelets in the presence of all redox environments. VASP was found to be phosphorylated at Ser157 in platelets activated with thrombin, convulxin and collagen, which was significantly greater than unactivated platelets. An altered redox environment had no significant impact on VASP phosphorylation at Ser157 in platelets activated with thrombin or convulxin, when compared to that of platelets

activated in the absence of an external redox environment. Activation of platelets with collagen, in the absence of an altered redox environment and in the presence of a mean or oxidising environment, led to the phosphorylation of VASP at Ser157. However, interestingly, in the presence of a reducing external redox environment there was a significant decrease in the level of VASP phosphorylation at Ser157 to a level comparable to that observed in unactivated platelets (n=4, *p < 0.05) (Figure 5.7 (a) and (b) (i)). Sample loading was also examined to ensure confirm there was equal loading in all lanes. This was carried out by reprobing the blots with anti-α-actinin antibody. Statistical analysis of the densitometry data associated with the α-actinin bands found no significant difference between the loading of the platelet samples (n=4) (Figure 5.7 (b) (ii)).

5.2.4.3 The impact of platelet activation and altering the external redox environment on the phosphorylation status of vasodilator-stimulated phosphoprotein (VASP) at Serine 239 (Ser239)

In addition to vasodilator-stimulated phosphoprotein (VASP) being phosphorylated at Ser157, it can also be phosphorylated at Serine 239 (Ser239). The effects of platelet activation and GSH/GSSG redox potentials on VASP phosphorylation at Ser239 were investigated by Western blotting.

Platelets were either unactivated or activated with either 0.1U/ml thrombin, 38 μg/ml collagen or 50 ng/ml convulxin in the absence of an altered redox environment or in the presence of reducing (-264 mV), mean (-130 mV) or oxidising (-10 mV) GSH/GSSG redox potentials. Platelet aggregations were performed and subsequently the samples were lysed. Platelet lysates were separated on 10 % polyacrylamide gels, transferred to polyvinyl difluoride

(PVDF) membrane and probed with a rabbit polyclonal anti-VASP-P (Ser239) antibody.

Densitometry was employed to analyse the resulting Western blots. VASP phosphorylation was found to occur at Ser239 in unactivated platelets and platelets activated with thrombin in the absence and presence of all redox environments, with the redox environment having no significant impact on the phosphorylated VASP expression. There was a similar finding in platelets activated with convulxin. Although the overall levels appeared to be lower than that observed in unactivated or thrombin activated platelets, the redox environment did not impact on the level of VASP phosphorylation at Ser239. The level of VASP phosphorylation at Ser239 in platelets activated with collagen in the absence of an altered redox environment, or in the presence of a mean or oxidising environment, was comparable to that observed in unactivated and thrombin activated platelets. However, there was a significant increase in VASP phosphorylation at Ser239 in platelets activated with collagen in the presence of a reducing external environment ($n=4$, $*p < 0.05$) (Figure 5.8 (a) and (b) (i)). The loading of platelet lysate samples was found to be consistent by reprobing the blots with an anti-α-actinin antibody and carrying out densitometry on the resulting α-actinin bands ($n=4$) (Figure 5.8 (b) (ii)).

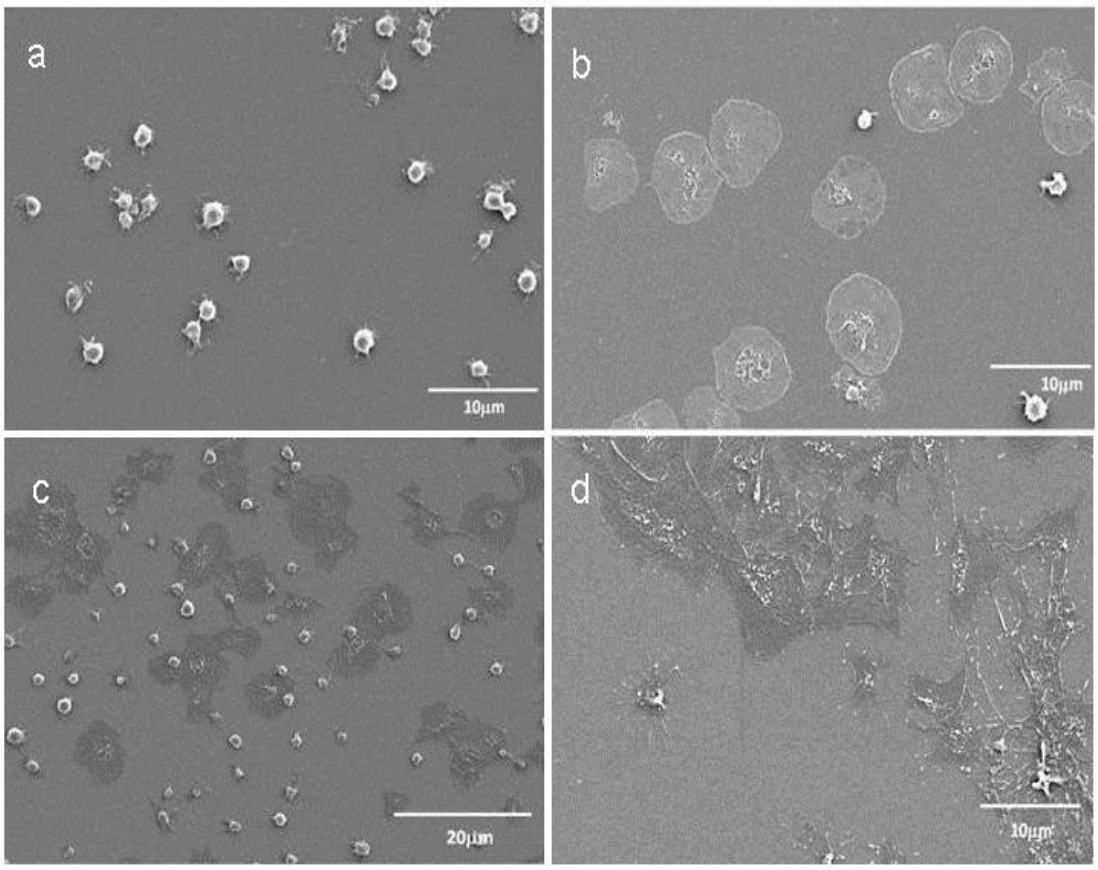

Figure 5.1 The morphology of adhered platelets varies greatly depending on the nature of the substrate to which they are adhered. Washed platelets adhered to round, glass cover slips pre-coated with poly-L-lysine, then coated with (a) 1 % BSA, (b) 20 μg/ml fibrinogen, (c) 10 μg/ml collagen or (d) 1 μg/ml CRP, for 45 minutes at 37 °C. Samples were fixed with 1 % formaldehyde for 10 minutes at room temperature with subsequent dehydration through a series of acetone concentrations. Samples were sputter coated with approximately 20 nm gold and mounted for SEM imaging. Images were obtained using a Hitachi S3400n SEM operating at 5 kV. Images are representative of n=2 independent experiments.

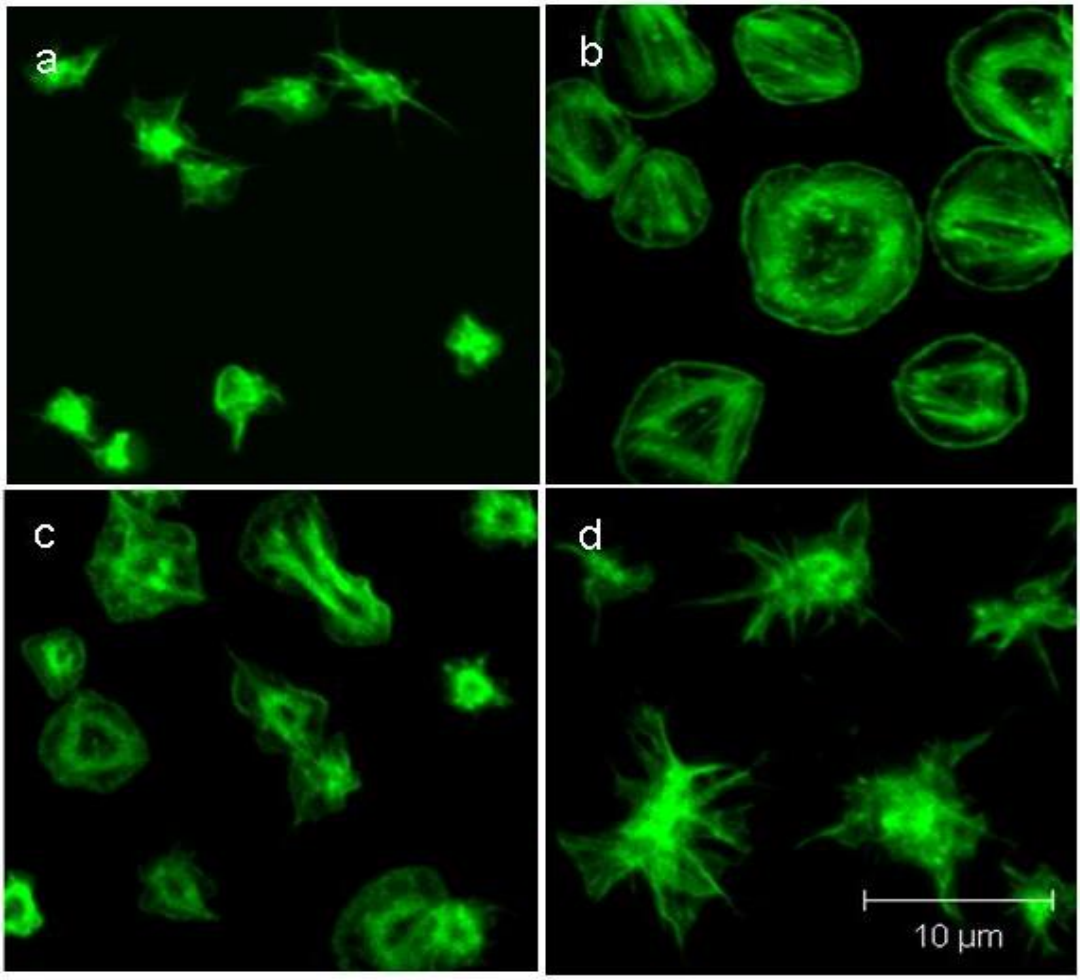

Figure 5.2 The actin cytoskeleton rearrangement of adhered platelets is dependent on the substrate to which the platelets are adhered. Washed platelets were allowed to adhere to poly-L-lysine slides coated with (a) 1 % BSA, (b) 20 µg/ml fibrinogen, (c) 10 µg/ml collagen or (d) 1 µg/ml collagen related peptide (CRP) for 45 minutes at 37 °C. Samples were fixed with 1 % formaldehyde for 10 minutes at room temperature and permeabilised with 0.1 % Triton-X-100 for 10 minutes at room temperature. Platelets were then stained with Alexa Fluor® 488 phalloidin for 20 minutes at room temperature. Samples were imaged using a Zeiss LSM510 Meta confocal microscope with a 63X oil-immersion lens. A laser wavelength of 488 nm, at an intensity of 1 % was employed. Images are representative of n=4 independent experiments.

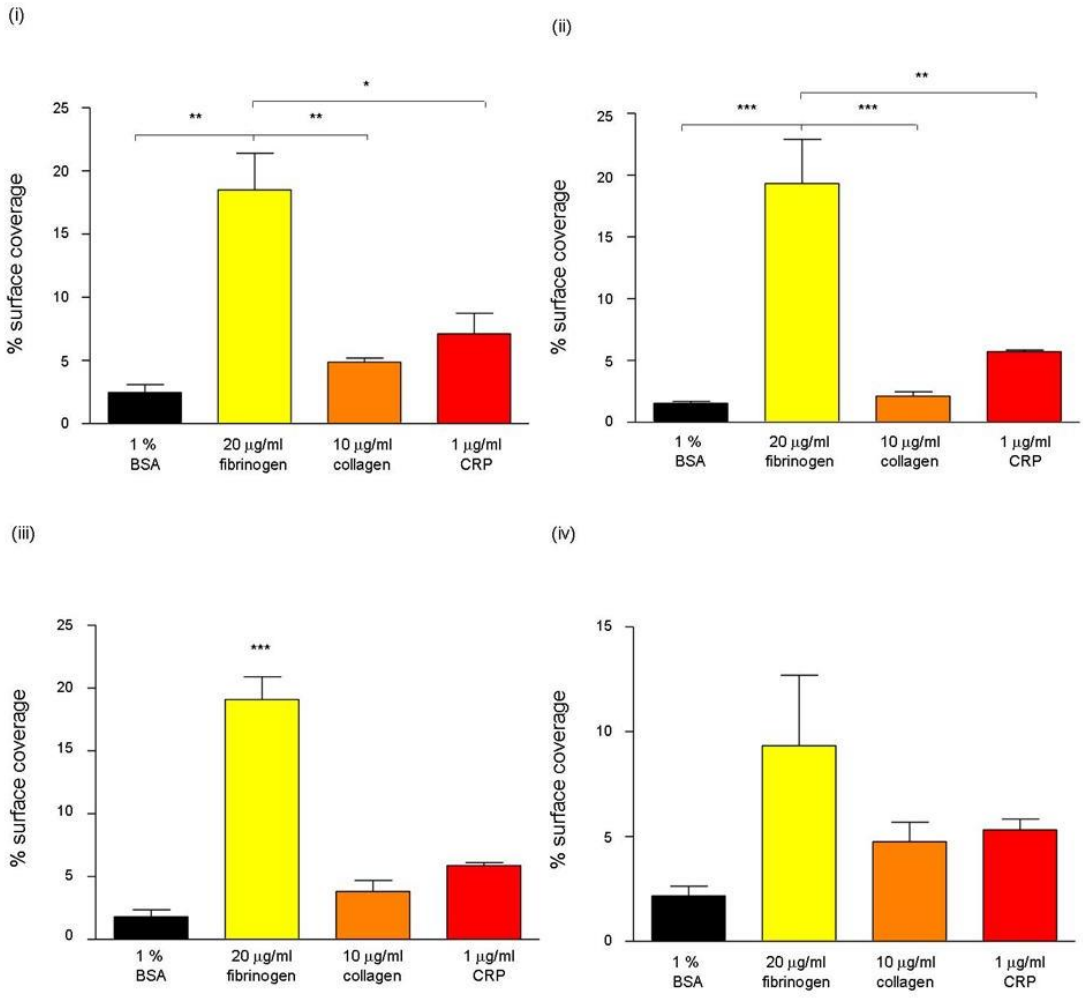

Figure 5.3 (a) Percentage surface coverage by platelets adhered to fibrinogen is significantly higher than the percentage coverage by platelets adhered to BSA, collagen or collagen related peptide (CRP) in all external redox environments. Washed platelets were either (i) untreated (no redox) or incubated with the following GSH/GSSG redox potentials: (ii) reducing (-264 mV), (iii) mean (-130 mV) or (iv) oxidising (-10 mV) for 10 minutes at 37 °C. Platelets adhered to poly-L-lysine slides coated with 1 % BSA, 20 μg/ml fibrinogen, 10 μg/ml collagen or 1 μg/ml CRP for 45 minutes at 37 °C. Samples were fixed first with 1 % formaldehyde and then permeabilised with 0.1 % Triton-X-100 for 10 minutes at room temperature. Platelets were stained with Alexa Fluor® 488 phalloidin for 20 minutes at room temperature. Samples were imaged using a Zeiss LSM510 Meta confocal microscope with a 63X oil-immersion lens. A laser wavelength of 488 nm, at an intensity of 1 % was employed. Data was analysed using the ImageJ software package. Percentage surface coverage was calculated based on a total surface area of 20408.98 μm^2. Date is presented as the mean ± SEM, n=4 independent experiments, **$p < 0.01$, *** $p < 0.001$.

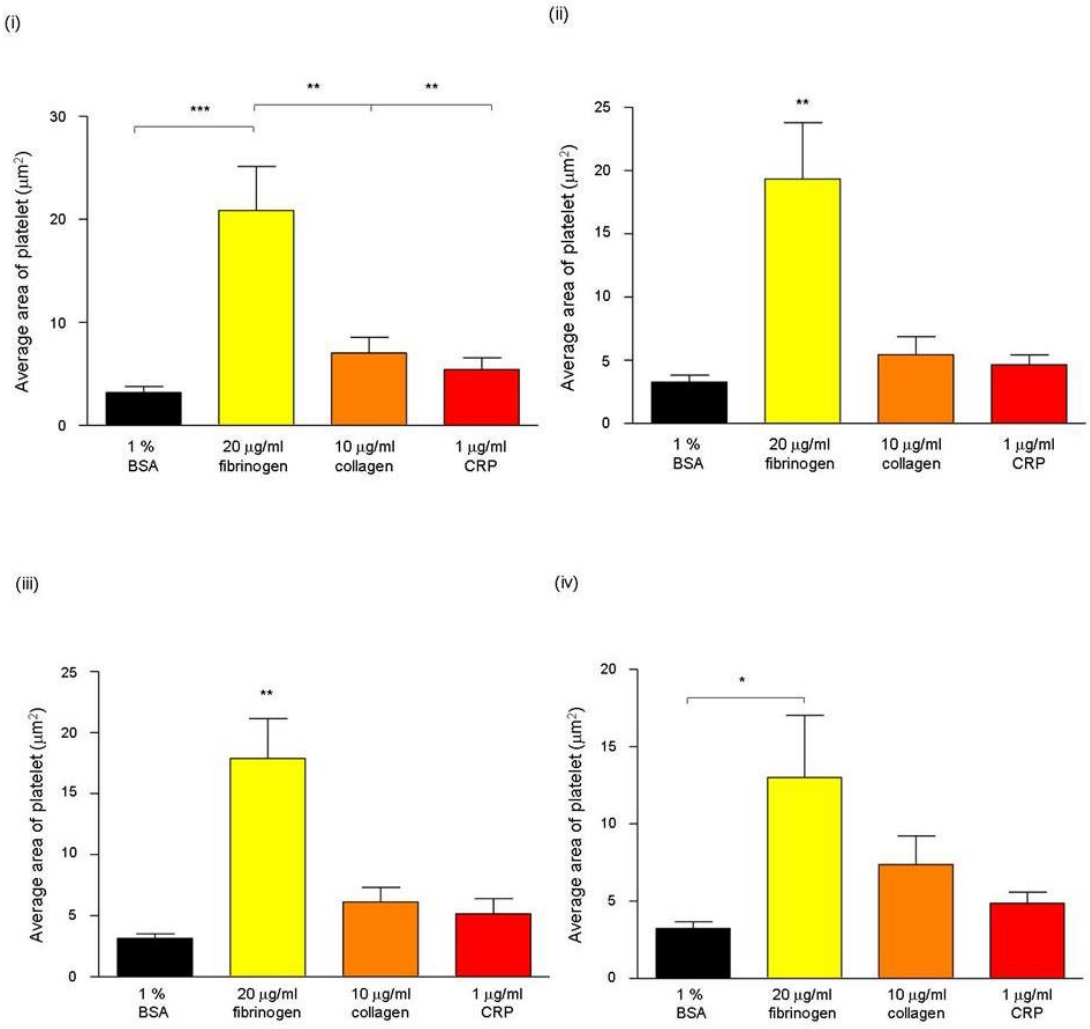

Figure 5.3 (b) The average area of platelets adhered to fibrinogen is significantly greater than the average area of platelets adhered to BSA, collagen or collagen related peptide (CRP). Washed platelets were either (i) untreated (no redox) or incubated with the following GSH/GSSG redox potentials: (ii) reducing (-264 mV), (iii) mean (-130 mV) or (iv) oxidising (-10 mV) for 10 minutes at 37 °C. Platelets adhered to poly-L-lysine slides coated with either 1 % BSA, 20 μg/ml fibrinogen, 10 μg/ml collagen or 1 μg/ml CRP for 45 minutes at 37 °C. Samples were fixed with 1 % formaldehyde and then permeabilised with 0.1 % Triton-X-100 for 10 minutes at room temperature. Platelets were stained with Alexa Fluor® 488 phalloidin for 20 minutes at room temperature. Samples were imaged using a Zeiss LSM510 Meta confocal microscope with a 63X oil-immersion lens. A laser wavelength of 488 nm, at an intensity of 1 % was employed. Data was analysed using the ImageJ software package. Date is presented as the mean ± SEM, n=4 independent experiments, *$p < 0.05$, **$p < 0.01$, ***$p < 0.001$.

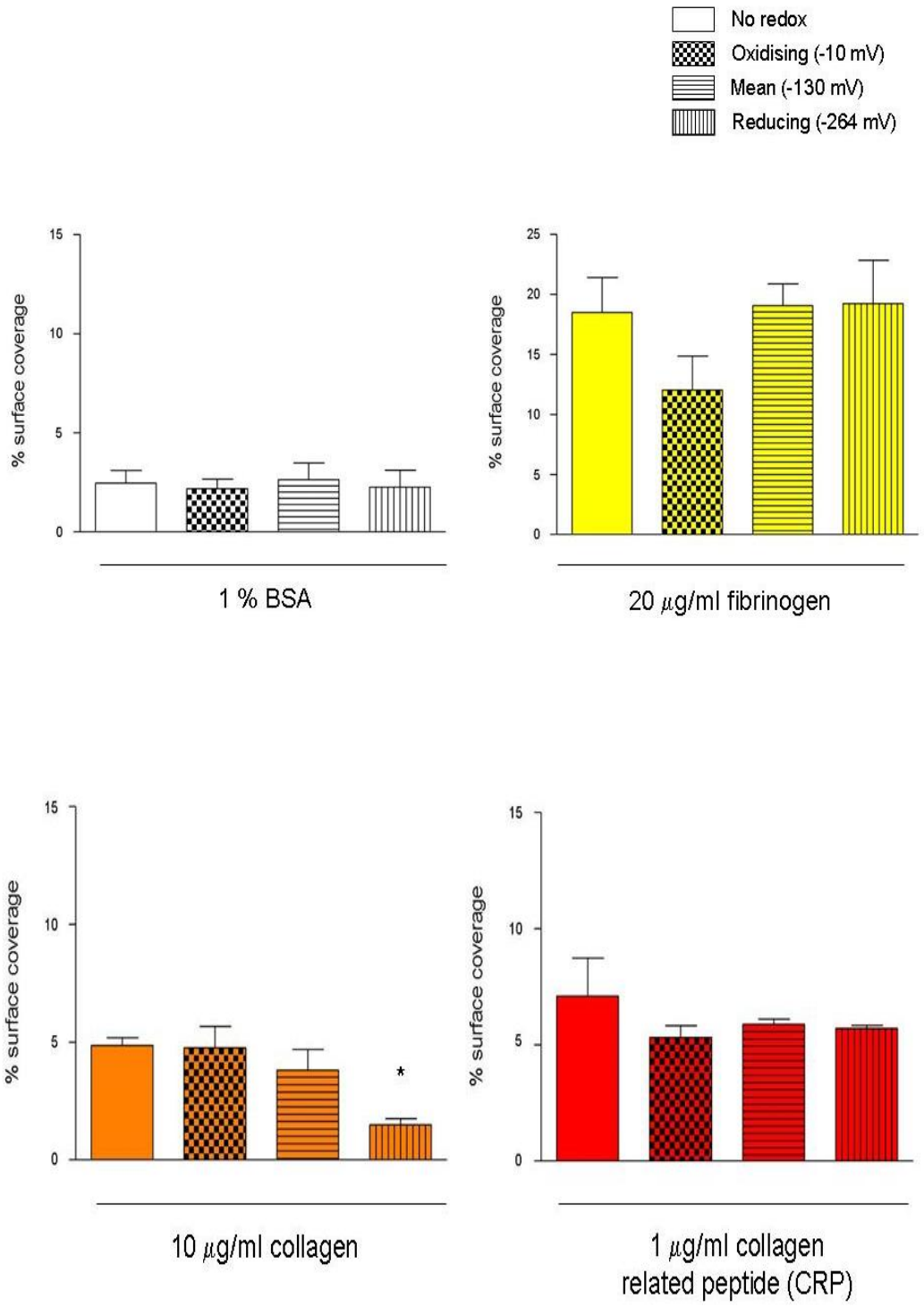
No redox
Oxidising (-10 mV)
Mean (-130 mV)
Reducing (-264 mV)
% surface coverage
15
10
5
0
1 % BSA
% surface coverage
25
20
15
10
5
0
20 μg/ml fibrinogen
% surface coverage
15
10
5
0
*
10 μg/ml collagen
% surface coverage
15
10
5
0
1 μg/ml collagen
related peptide (CRP)

Figure 5.4 (a) The percentage surface coverage by platelets adhered to collagen in the presence of an external reducing redox environment is significantly decreased compared to the total surface coverage by platelets adhered to collagen in the absence of an altered external redox environment. There is no impact of an altered redox environment on the total surface coverage by platelets adhered to BSA, fibrinogen or collagen related peptide (CRP). Washed platelets were allowed to adhere to poly-L-lysine slides coated with (a) 1 % BSA, (b) 20 μg/ml fibrinogen, (c) 10 μg/ml collagen or (d) 1 μg/ml CRP for 45 minutes at 37 °C. Samples were fixed with 1 % formaldehyde for 10 minutes at room temperature and permeabilised with 0.1 % Triton-X-100 for 10 minutes at room temperature. Platelets were then stained with Alexa Fluor® 488 phalloidin for 20 minutes at room temperature. Samples were imaged using a Zeiss LSM510 Meta confocal microscope with a 63X oil-immersion lens. A laser wavelength of 488 nm, at an intensity of 1 % was employed. Total surface coverage was determined using ImageJ software. Data is presented as the mean ± SEM, n=4 independent experiments, *$p < 0.05$.

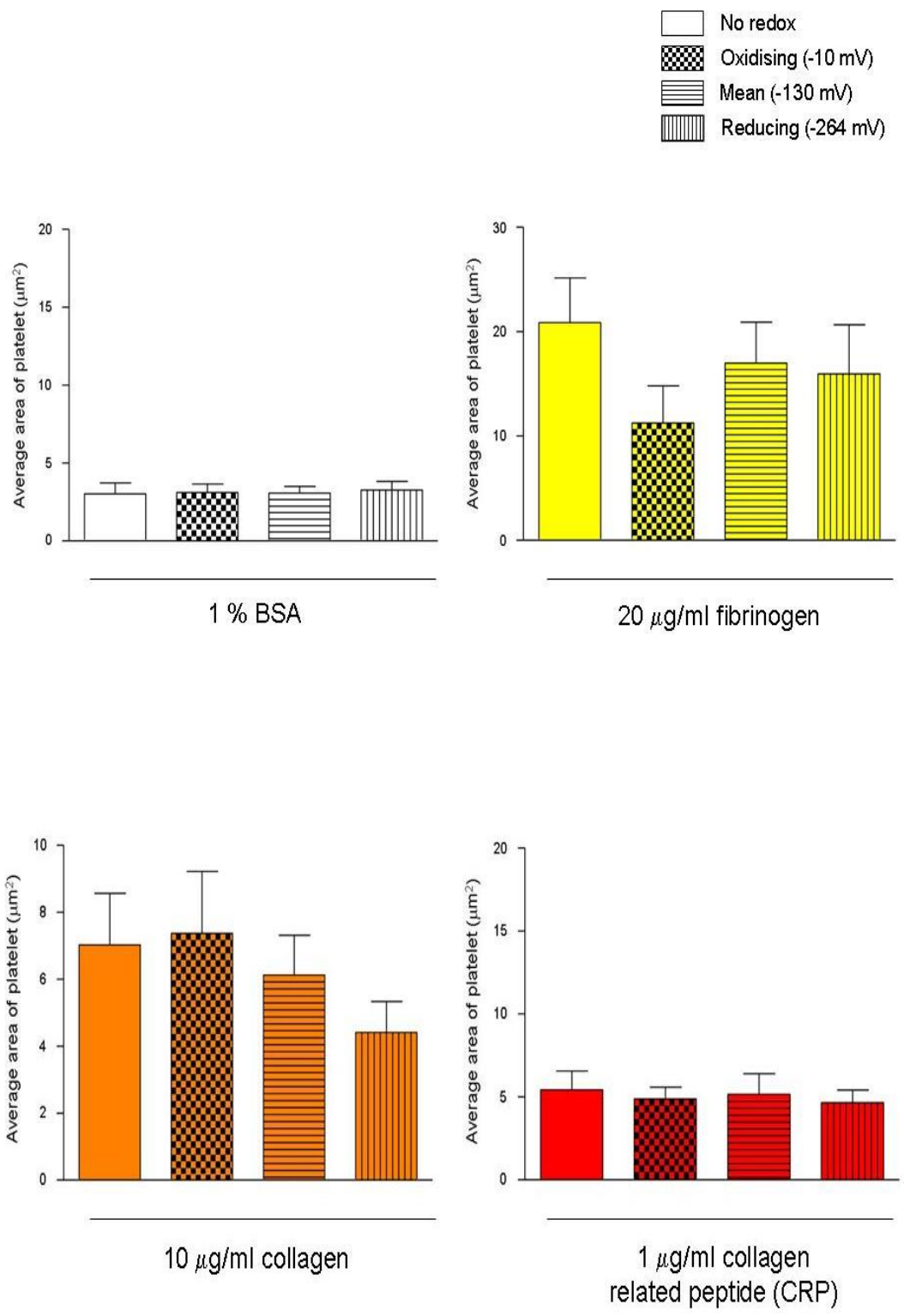
No redox
Oxidising (-10 mV)
Mean (-130 mV)
Reducing (-264 mV)
Average area of platelet (μm²)
1 % BSA
20 μg/ml fibrinogen
10 μg/ml collagen
1 μg/ml collagen related peptide (CRP)

Figure 5.4 (b) The average area of platelets adhered to collagen decreases as the external redox environment becomes more reducing, while the average area of platelets adhered to BSA, fibrinogen or collagen related peptide (CRP) remains consistent irrespective of an altered external redox environment. Washed platelets were allowed to adhere to poly-L-lysine slides coated with (a) 1 % BSA, (b) 20 μg/ml fibrinogen, (c) 10 μg/ml collagen or (d) 1 μg/ml CRP for 45 minutes at 37 °C. Samples were fixed with 1 % formaldehyde for 10 minutes at room temperature and permeabilised with 0.1 % Triton-X-100 for 10 minutes at room temperature. Platelets were then stained with Alexa Fluor® 488 phalloidin for 20 minutes at room temperature. Samples were imaged using a Zeiss LSM510 Meta confocal microscope with a 63X oil-immersion lens. A laser wavelength of 488 nm, at an intensity of 1 % was employed. Total surface coverage was determined using ImageJ software. Data is presented as the mean ± SEM, n=4 independent experiments.

(i)

1. No redox
2. Reducing (-264 mV)
3. Mean (-130 mV)
4. Oxidising (-10 mV)

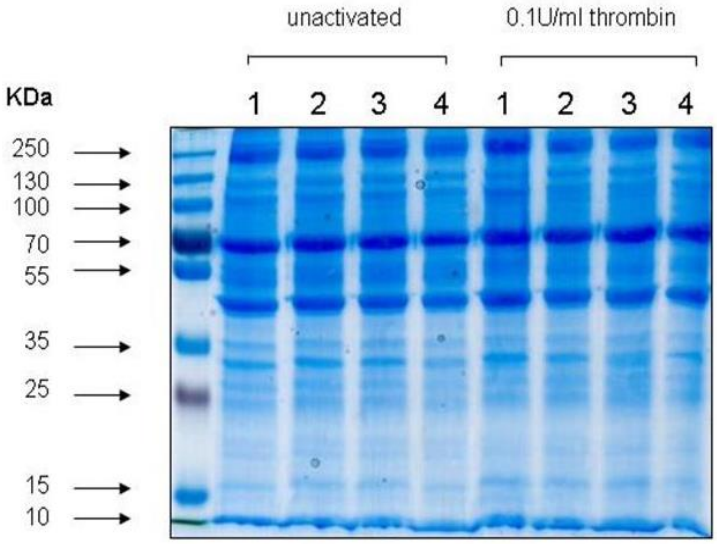

(ii)

1. No redox
2. Reducing (-264 mV)
3. Mean (-130 mV)
4. Oxidising (-10 mV)

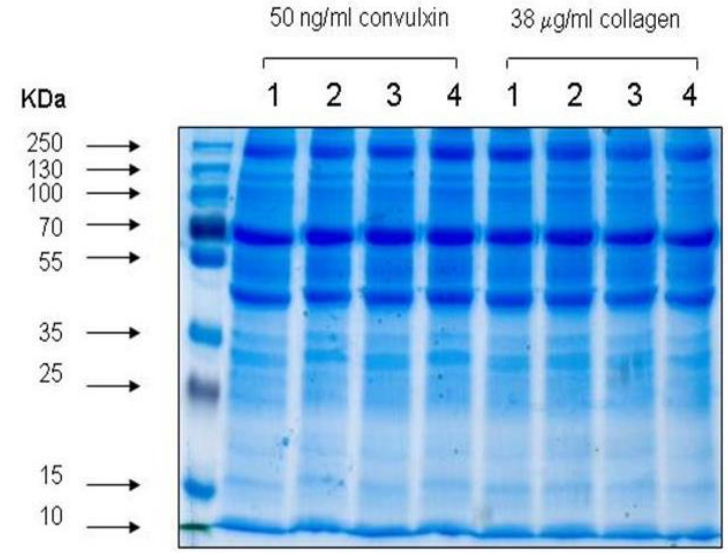

Figure 5.5 Coomassie Blue stained gels demonstrating the protein profile of unactivated and activated platelets in the absence and presence of an altered external redox environment. Gel filtered platelets were (i) unactivated or were activated with either 0.1U/ml thrombin (ii) 38 μg/ml collagen or 50 ng/ml convulxin in the absence or presence of an altered redox environment generated by GSH/GSSG redox potentials: reducing (-264 mV), mean (-130 mV) or oxidising (-10 mV). Platelet lysates were run on 10 % polyacrylamide gels for 1 hour at a constant voltage of 100 V. Gels were then stained with a sensitive Coomassie Blue stain overnight at room temperature with gently rocking. In order to visualise the protein bands clearly, excess Coomassie Blue stain was removed in a destaining process. The gels were then stored in dH_2O and imaged.

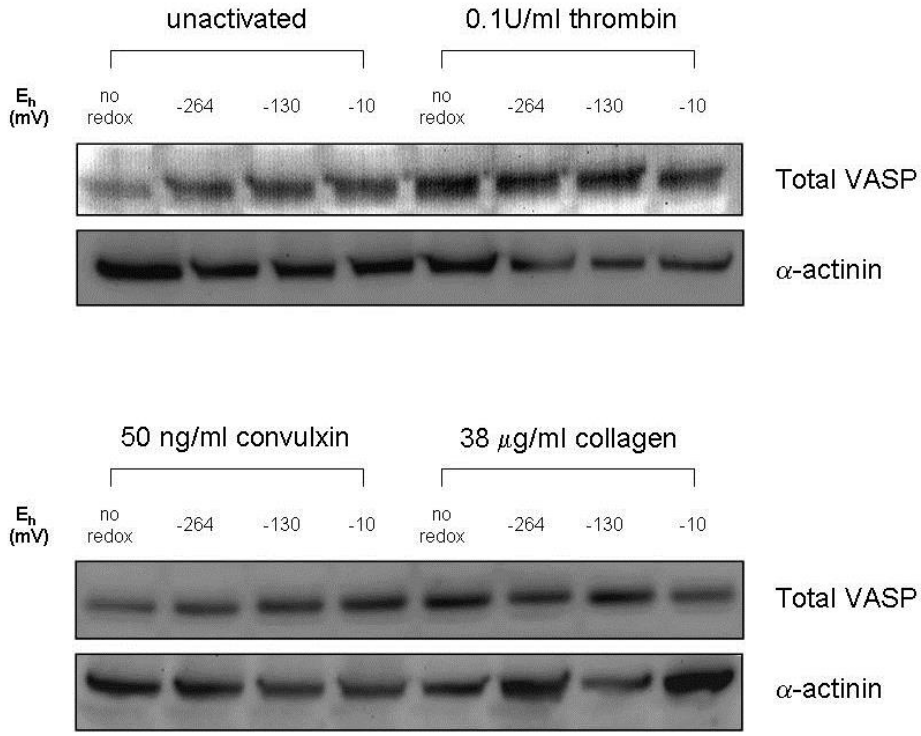

Figure 5.6 (a) Vasodilator-stimulated phosphoprotein (VASP) is present in equal quantities in all platelets, irrespective of the activation state of the platelets or their external redox environment. Gel filtered platelets remained unactivated or were activated with either 0.1U/ml thrombin, 38 μg/ml collagen or 50 ng/ml convulxin in the absence or presence of an altered redox environment generated by GSH/GSSG redox potentials: reducing (-264 mV), mean (-130 mV) or oxidising (-10 mV). Platelet lysates were separated on 10 % polyacrylamide gels and proteins were transferred from the gel to PVDF membrane. Membrane was probed with rabbit polyclonal anti-VASP A290 or monoclonal anti-α-actinin (loading control) antibodies. Blots are representative of n=4 independent experiments.

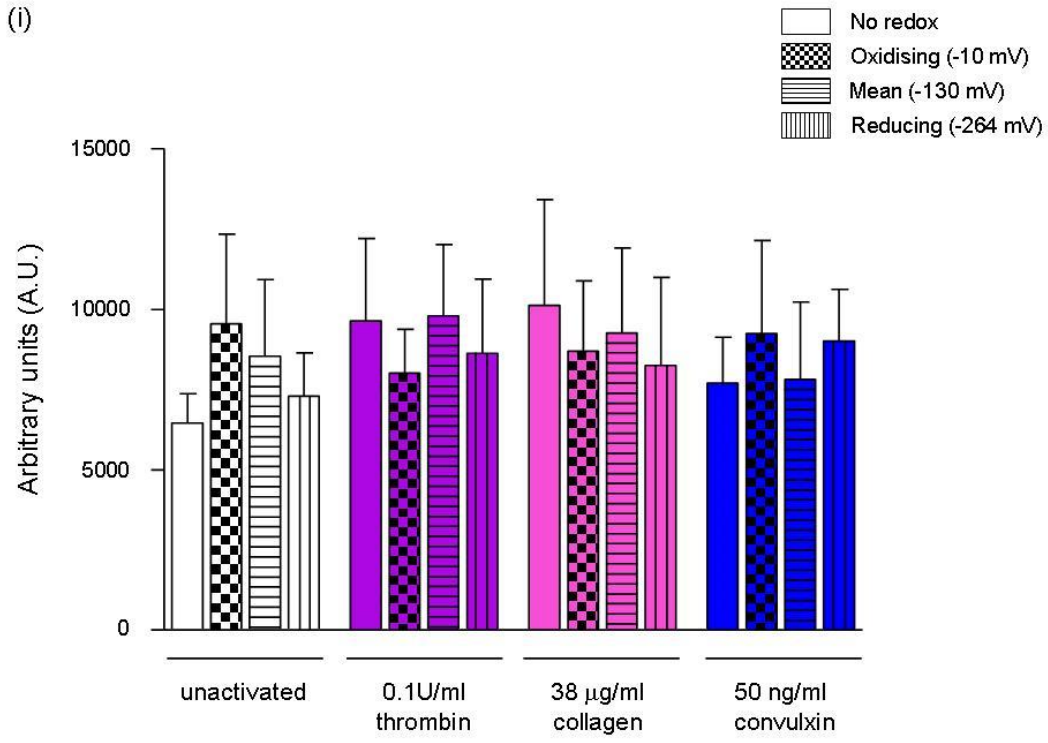
(i)
No redox
Oxidising (-10 mV)
Mean (-130 mV)
Reducing (-264 mV)
Arbitrary units (A.U.)
15000
10000
5000
0
unactivated
0.1U/ml thrombin
38 μg/ml collagen
50 ng/ml convulxin

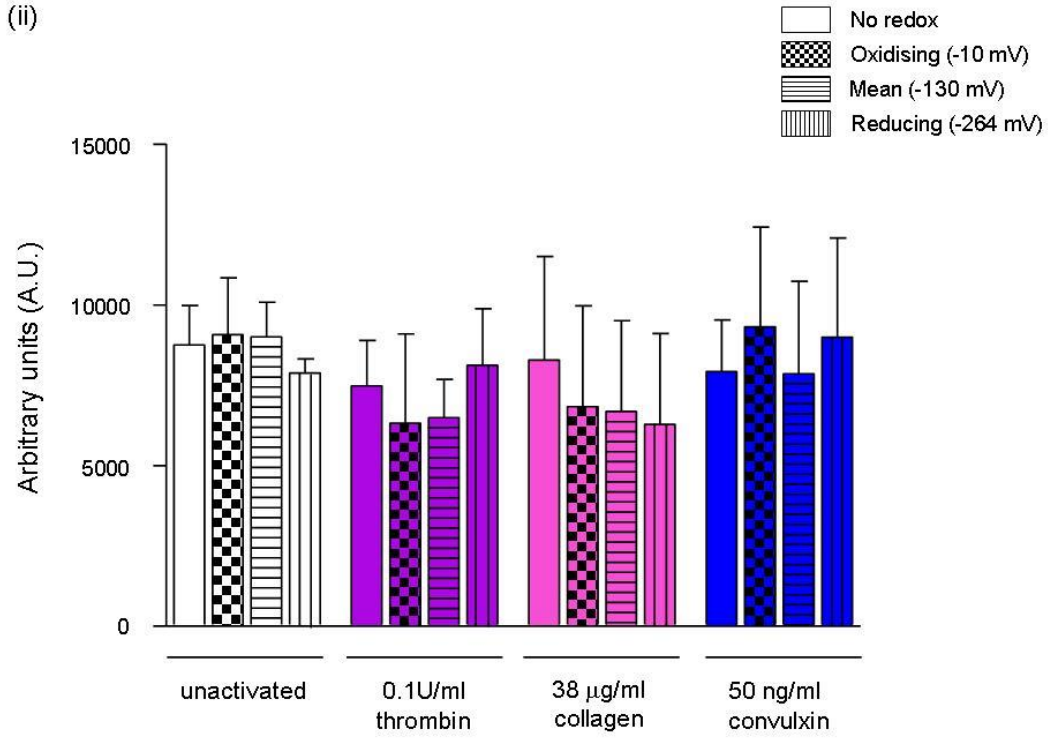
(ii)
No redox
Oxidising (-10 mV)
Mean (-130 mV)
Reducing (-264 mV)
Arbitrary units (A.U.)
15000
10000
5000
0
unactivated
0.1U/ml thrombin
38 μg/ml collagen
50 ng/ml convulxin

Figure 5.6 (b) Analysis by densitometry confirmed that vasodilator-stimulated phosphoprotein (VASP) is present at comparable levels in unactivated platelets and platelets activated with thrombin, collagen or convulxin in all external redox environments. Gel filtered platelets remained unactivated or were activated with either 0.1U/ml thrombin, 38 μg/ml collagen or 50 ng/ml convulxin in the absence or presence of an altered redox environment generated by GSH/GSSG redox potentials: reducing (-264 mV), mean (-130 mV) or oxidising (-10 mV). Platelet lysates were separated on 10 % polyacrylamide gels and proteins were transferred from the gel to PVDF membrane. Membrane was probed with (i) rabbit polyclonal anti-VASP A290 or (ii) monoclonal anti-α-actinin (loading control) antibodies. Densitometry analysis was performed using ImageJ software. Data is presented as the mean ± SEM, n=4 independent experiments.

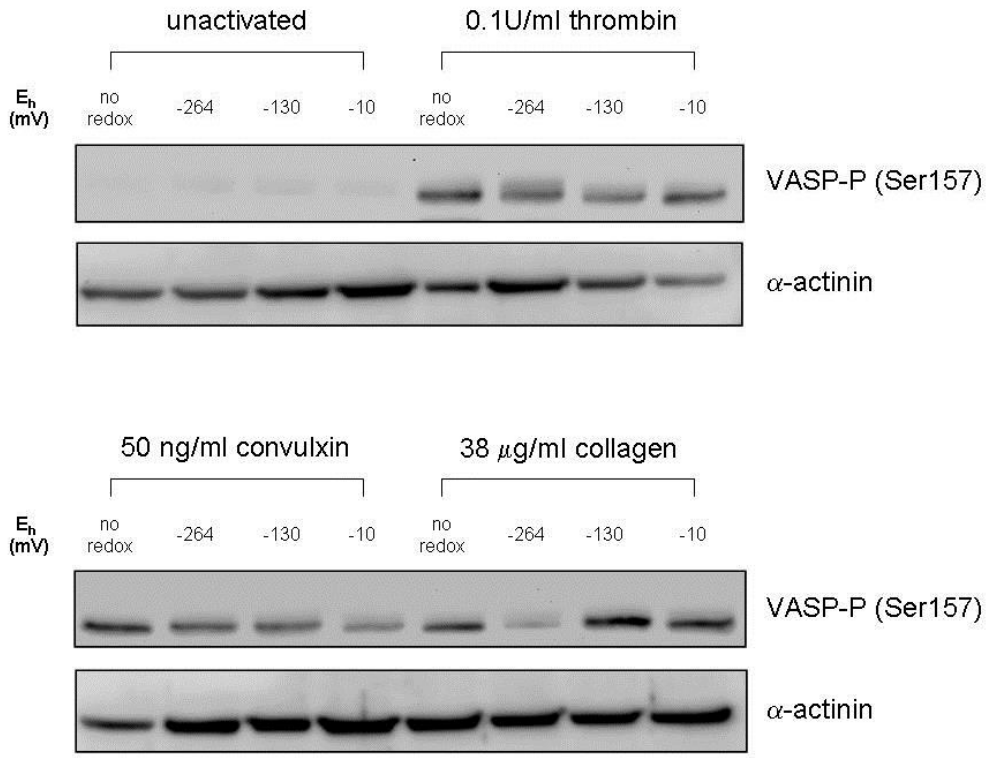

Figure 5.7 (a) Vasodilator-stimulated phosphoprotein (VASP) phosphorylation at Serine 157 (VASP-P (Ser157)) in platelets activated with collagen in the presence of a reducing environment is decreased to levels comparable to that of unactivated platelets. There is an increase in VASP phosphorylation at Ser157 in platelets activated with thrombin or convulxin compared to unactivated platelets, and the levels are not impacted on by an altered external redox environment. Gel-filtered platelets remained unactivated or were activated with either 0.1U/ml thrombin, 38 μg/ml collagen or 50 ng/ml convulxin in the absence or presence of an altered redox environment generated by GSH/GSSG redox potentials: reducing (-264 mV), mean (-130 mV) or oxidising (-10 mV. Platelet lysates were separated on 10 % polyacrylamide and proteins were transferred from the gel to PVDF membrane. Membranes were probed with a rabbit polyclonal anti-VASP-P Ser157 or anti-α-actinin (loading control) antibody. Blots are representative of n=4 independent experiments.

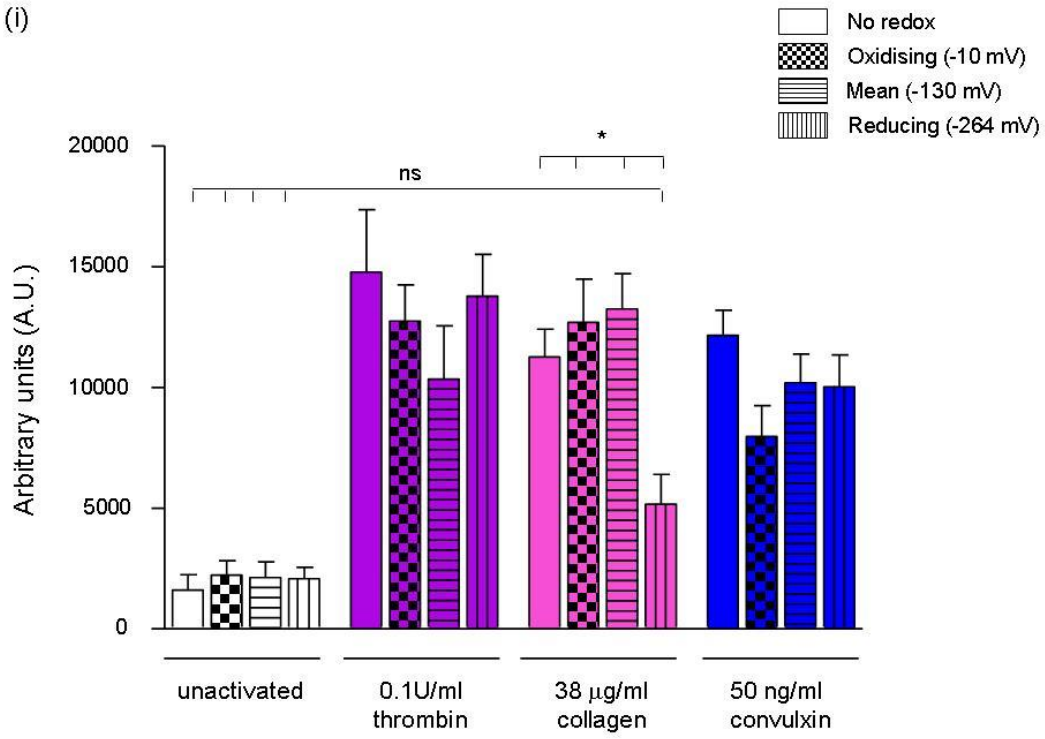
(i)
No redox
Oxidising (-10 mV)
Mean (-130 mV)
Reducing (-264 mV)
ns
*
20000
15000
10000
5000
0
Arbitrary units (A.U.)
unactivated
0.1U/ml thrombin
38 μg/ml collagen
50 ng/ml convulxin

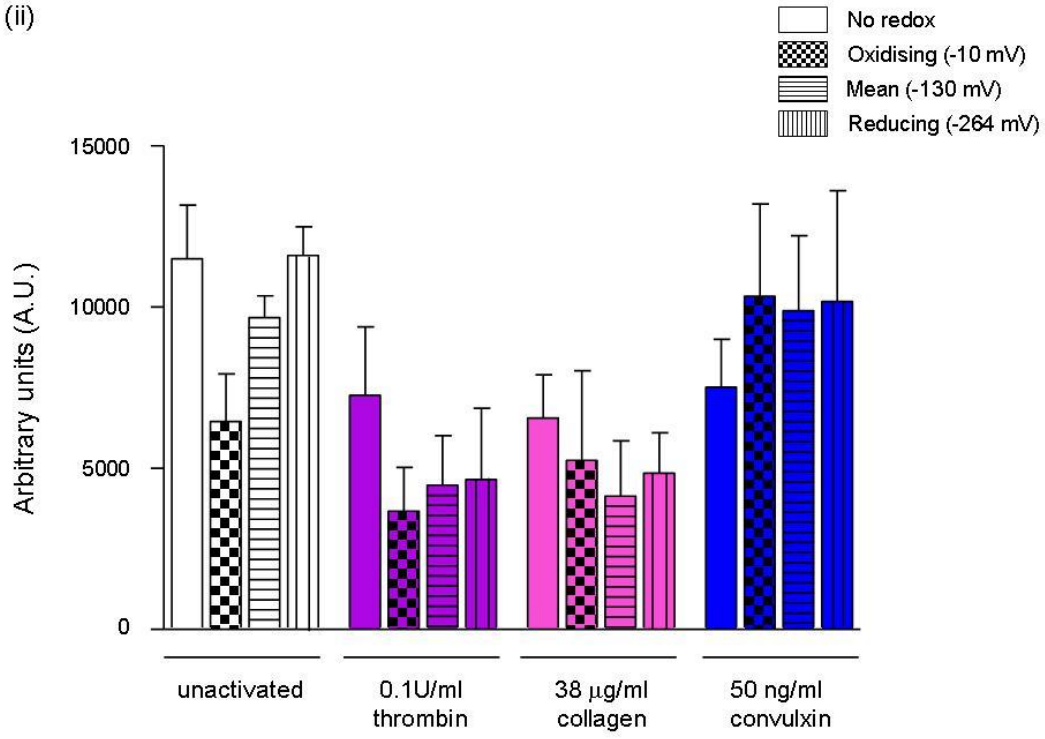
(ii)
No redox
Oxidising (-10 mV)
Mean (-130 mV)
Reducing (-264 mV)
15000
10000
5000
0
Arbitrary units (A.U.)
unactivated
0.1U/ml thrombin
38 μg/ml collagen
50 ng/ml convulxin

Figure 5.7 (b) Analysis by densitometry confirmed that phosphorylation of vasodilator-stimulated phosphoprotein (VASP) at Serine 157 (Ser157) is significantly decreased in platelets activated with collagen in a reducing external redox environment, compared to platelets activated with collagen in the absence of an altered external redox environment. There was increased phosphorylation of VASP at Ser157 in platelets activated with thrombin or convulxin. An altered external redox environment had no significant effect on this level of VASP phosphorylation at Ser157 observed in platelets activated with thrombin or convulxin. Gel filtered platelets remained unactivated or were activated with either 0.1U/ml thrombin, 38 μg/ml collagen or 50 ng/ml convulxin in the absence or presence of an altered redox environment generated by GSH/GSSG redox potentials: reducing (-264 mV), mean (-130 mV) or oxidising (-10 mV). Platelet lysates were separated on 10 % polyacrylamide gels and proteins were transferred from the gel to PVDF membrane. Membrane was probed with (i) rabbit polyclonal anti-VASP-P Ser157 or (ii) monoclonal anti-α-actinin (loading control) antibodies. Densitometry analysis was performed using ImageJ software. Data is presented as the mean ± SEM, n=4 independent experiments, *$p < 0.05$.

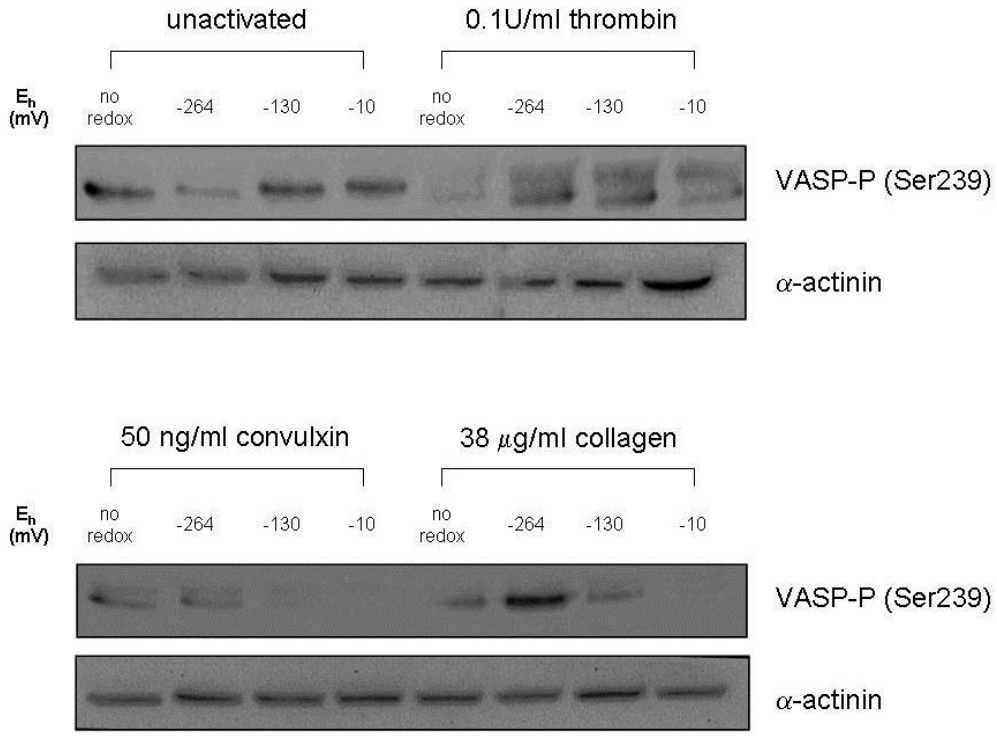

Figure 5.8 (a) Vasodilator-stimulated phosphoprotein (VASP) phosphorylation at Serine 239 (VASP-P (Ser239)) is significantly increased in platelets activated with collagen in the presence of a reducing redox environment. Gel filtered platelets remained unactivated or were activated with 0.1U/ml thrombin, 38 μg/ml collagen or 50 ng/ml convulxin in the absence or presence of an altered redox environment generated by GSH/GSSG redox potentials: reducing (-264 mV), mean (-130 mV) or oxidising (-10 mV). Platelet lysates were separated on 10 % polyacrylamide gels and proteins were transferred from the gel to PVDF membrane. The membranes were probed with a rabbit polyclonal anti-VASP-P Ser239 or a monoclonal anti-α-actinin (loading control) antibody. Blots are representative of n=4 independent experiments.

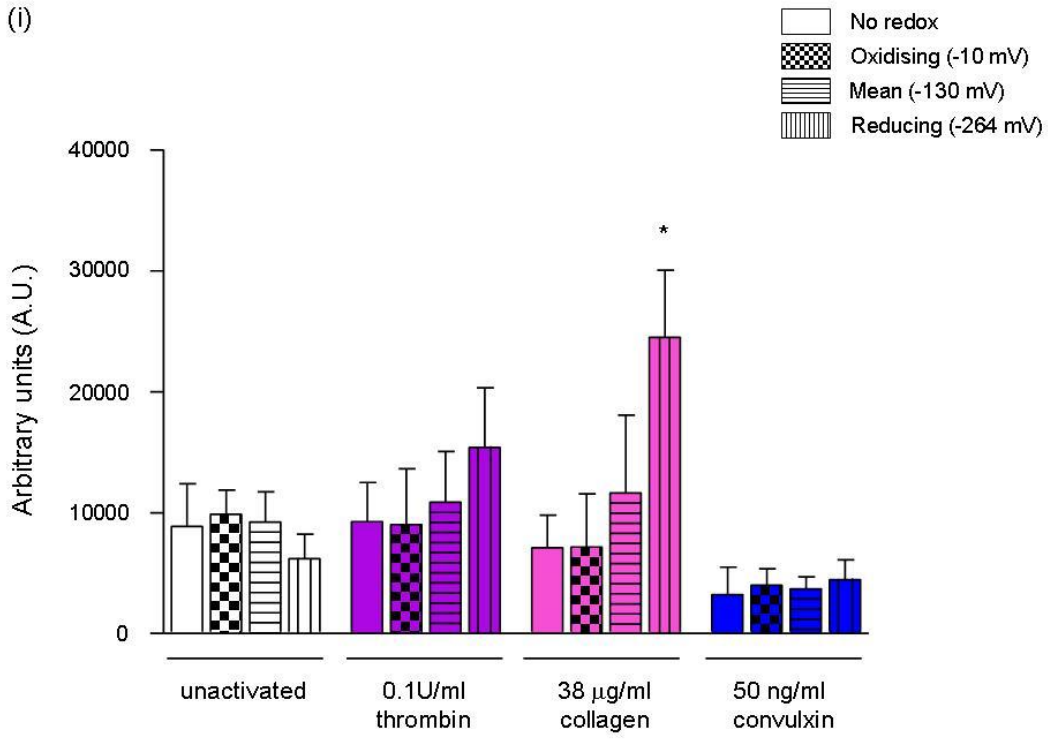
(i)
No redox
Oxidising (-10 mV)
Mean (-130 mV)
Reducing (-264 mV)
Arbitrary units (A.U.)
40000
30000
20000
10000
0
*
unactivated
0.1U/ml thrombin
38 μg/ml collagen
50 ng/ml convulxin

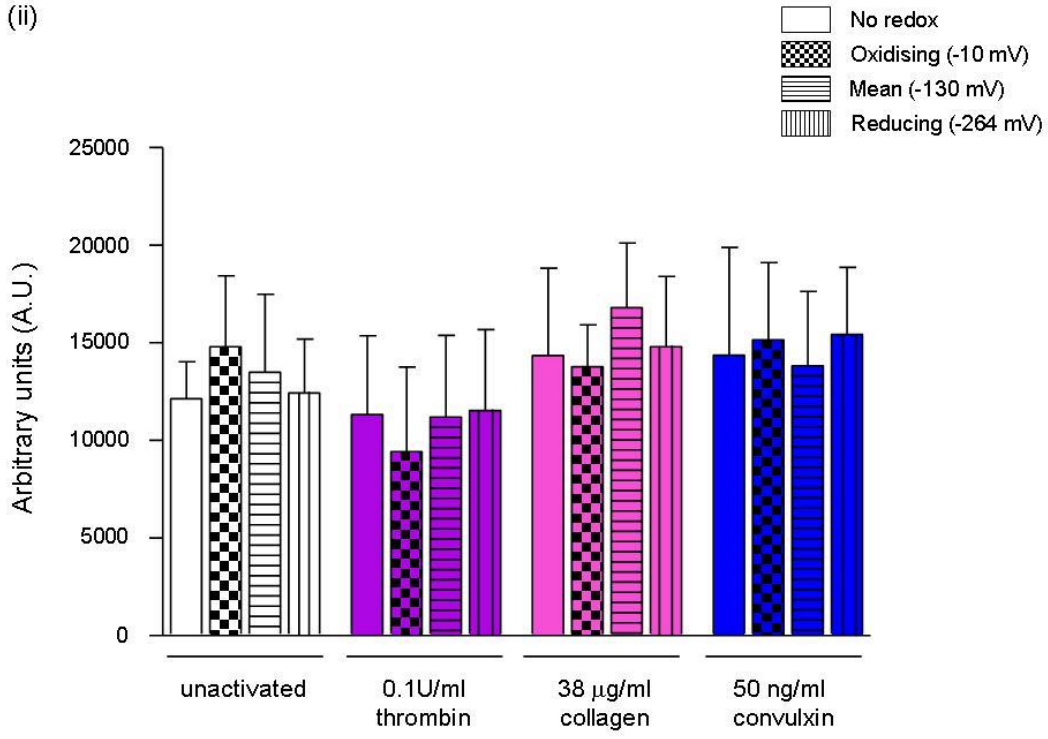
(ii)
No redox
Oxidising (-10 mV)
Mean (-130 mV)
Reducing (-264 mV)
Arbitrary units (A.U.)
25000
20000
15000
10000
5000
0
unactivated
0.1U/ml thrombin
38 μg/ml collagen
50 ng/ml convulxin

Figure 5.8 (b) Analysis by densitometry confirmed there was a significant increase in the level of vasodilator-stimulated phosphoprotein (VASP) phosphorylation at Serine 239 (Ser239) in platelets activated with collagen in the presence of a reducing external redox environment. There is no significant change in the levels of VASP Ser239 phosphorylation of platelets activated with thrombin or convulxin compared to unactivated platelets, in the presence of any of the external redox environments. Gel filtered platelets remained unactivated or were activated with either 0.1U/ml thrombin, 38 μg/ml collagen or 50 ng/ml convulxin in the absence or presence of an altered redox environment generated by GSH/GSSG redox potentials: reducing (-264 mV), mean (-130 mV) or oxidising (-10 mV). Platelet lysates were separated on 10 % polyacrylamide gels and proteins were transferred from the gel to PVDF membrane. Membrane was probed with (i) rabbit polyclonal anti-VASP-P Ser239 or (ii) monoclonal anti-α-actinin (loading control) antibodies. Densitometry analysis was performed using ImageJ software. Data is presented as the mean ± SEM, n=4 independent experiments, *$p < 0.05$.

5.3 Discussion

Platelet shape change, directed by membrane and cytoskeleton rearrangement, is a key event in the process of platelet activation. From my studies here it was revealed the substrate to which platelets adhere plays a significant role in determining not only the extent to which the platelets spread and the overall surface coverage but also the manner in which the actin cytoskeleton is rearranged, which leads to the a characteristic shape for platelets adhered to each substrate. These findings emphasise that the platelet response is directly linked to the activator and its specific signalling pathway. The platelet response is entirely dictated by the stimulus. The understanding of the impact of signalling pathways and regulatory proteins on changes in the cytoskeleton structure is still somewhat limited. While some signalling pathways overlap, such as the involvement of phospholipase Cγ2 (PLCγ-2) in platelet signalling through both integrin $\alpha_{IIb}\beta_3$ and GPVI, there are also distinct differences between these signalling cascades (Wonerow et al, 2003).

Having established the external redox environment plays a significant role in the response of platelets to various stimuli the impact of an altered redox environment on platelet spreading and actin cytoskeleton rearrangement was examined. Consistent with the findings so far, the platelet response to collagen exclusively was significantly affected. There was no impact on the degree of platelet spreading or the average size of platelets adhered to BSA, fibrinogen or collagen related peptide (CRP) in altered external redox environments. The average area of the platelets adhered to collagen in the presence of a reducing GSH/GSSG redox potential was less than that of platelets adhered to collagen

in the absence of any altered redox environment. This indicated that although these platelets were capable of binding to collagen, the signalling pathways leading to platelet spreading were disrupted. This finding is complementary to that shown in our laboratory previously (by Dr. Desmond Murphy, RCSI) where it was demonstrated, by flow cytometry, that a FITC-labelled collagen could still bind to platelets to some degree in the presence of a reducing redox environment though platelet activation could not be initiated.

VASP is one of a number of proteins implicated in the regulation of actin rearrangement in platelets upon platelet activation (Reinhard et al, 2001). VASP and VASP-like proteins contain conserved N-terminal (EVH1) and C-terminal domains (EVH2). EVH2 is known to mediate tetramerisation of VASP (which enhances F-actin interactions), F-actin binding and bundle formation (Bachmann et al, 1999). The regions in which VASP proteins are found further support an important role for VASP in relation to actin remodelling and polymerisation. VASP is mainly localised to sites of actin assembly such as focal adhesions and membrane ruffles along with the tips of lamellipodia (Jockusch et al, 1995; Reinhard et al, 1992; Rottner et al, 1999). Focal adhesions are protein rich structures which link the actin cytoskeleton to the ECM via integrins, therefore also implicating VASP in integrin activation and regulation. Moreover, a link between integrin $\alpha_{IIb}\beta_3$ has been suggested, in which VASP is a negative regulator of integrin $\alpha_{IIb}\beta_3$ and consequently platelet aggregation (Horstrup et al, 1994). VASP null mice display increased agonist-induced P-selectin expression along with enhanced fibrinogen binding to

integrin $\alpha_{IIb}\beta_3$ (Aszodi et al, 1999; Hauser et al, 1999). To date there has yet to be any studies connecting VASP to integrin $\alpha_2\beta_1$ activity.

VASP is phosphorylated at three different sites: serine 157 (Ser157), serine 239 (Ser239) and threonine 278 (Thr278) (Butt et al, 1994) (Figure 5.9). Ser239 is the VASP phosphorylation site preferred by cGMP-dependent protein kinase (PKG) (Smolenski et al, 1998), while Ser157 has a preference to be phosphorylated by cAMP-dependent protein kinase (PKA). Thr278 appears to come into play once the phosphorylation at the other two sites has essentially been completed (Butt et al, 1994). Along with visually analysing the Western blots illustrating VASP and its phosphorylation state in platelets, densitometry analysis was also employed. Densitometry provides a means of demonstrating the observations of a number of Western blots and summarising the findings in one graphical illustration.

VASP is expressed at comparable levels in platelets, irrespective of the activation state or redox environment, as was expected. However, the phosphorylation of VASP at Ser157 was significantly decreased in collagen activated platelets in the presence of a reducing redox environment compared to collagen activated platelets in the absence of an altered external redox environment. A mean or oxidising external redox environment had no significant impact on this phosphorylation event. Ser157 was phosphorylated in platelets activated with thrombin and convulxin. The redox environment had no significant effect on the level of this phosphorylation event. There was no phosphorylation of VASP at Ser157 observed in unactivated platelets in any of

the redox environments. This finding suggests, contrary to some reports in the literature, activation of platelets induces phosphorylation of VASP. The phosphorylation state of VASP in platelets activated with collagen in the presence of a reducing environment were comparable to unactivated platelets indicating that collagen was incapable of inducing any response in platelet under these conditions.

Platelets are known to contain significant levels of PKA and PKG, which are regulated by cAMP and cGMP, respectively (Waldmann et al, 1986; Waldmann et al, 1987). cAMP elevation leads to PKA stimulation, while an increase in cGMP leads to stimulation of PKG. Regulation of protein kinases alters the phosphorylation state of specific key protein substrates associated with a biological function. Indeed, it is well established that cAMP elevating substances (PGE_1, PGI_2, forskolin) and cGMP elevating substances, such as the endothelium-derived relaxing factor, sodium nitroprusside, which releases nitric oxide (NO), inhibit the platelet aggregation (Waldmann et al, 1987; Walter, 1989).

The increase in VASP phosphorylation at Ser239 in platelets activated with collagen in the presence of a reducing environment is a particularly interesting revelation, especially as the levels were significantly higher than that observed in unactivated platelets. This result suggests that the reducing redox environment is not just preventing the activation of platelets by collagen but is in fact inducing an inhibitory response within the platelets. There is a significant difference between these states: unactivated implies that there has been no

stimulus applied to the platelets therefore they are in a resting state, whereas inhibited implies that a signalling pathway within the platelets has been initiated which prevents platelets becoming activated despite the presence of a platelet agonist. The findings suggest an external modification of the collagen receptor integrin $\alpha_2\beta_1$ generates intra-platelet signals resulting in an increase in cGMP which leads to activation of PKG, ultimately, leading to phosphorylation of VASP at Ser239. The increase in Ser239 phosphorylation is a somewhat surprising as there is a high concentration of PKG found in platelets which would require significant increases in cGMP levels in order to activate PKG sufficiently to cause phosphorylation of VASP (Eigenthaler et al, 1992). However, the finding that the increase in phosphorylation at Ser239 correlates with a significant decrease in phosphorylation at Ser157 is also a fascinating discovery and demonstrates that the phosphorylation of VASP at different sites is related to distinct functions. Phosphorylation at one site may be associated with an initial stimulatory response which promotes platelet activation and aggregation by regulating integrin function and this may be followed by phosphorylation at the other site which induces an inhibitory response that may play a role in limiting the size of the thrombus formed and keeping the process under control. Such a mechanism has been alluded to in the literature for PKG implicating Ser239 (Li et al, 2003). Similarly, thrombin stimulation of platelets leads to phosphorylation of Ser157 in a PKC- and Rho-kinase-dependent mechanism (Wentworth et al, 2006). However, our findings implicate both phosphorylation sites and are suggestive of synergy between these two molecules regulating VASP and its activities.

The differences that were observed in platelet morphology and cytoskeleton rearrangement in platelets which were dictated by the surface to which they were adhered may be related to variation in the levels of VASP phosphorylation. It would be interesting to further investigate this relationship by examining the expression and localisation of VASP within platelets adhered to different surfaces in the absence and presence of an altered external redox environment. Again, these findings imply that platelet activity and the activation end point reached is very much dependent on the stimulus and the signalling pathways activated thereafter.

Future work on this study would entail measuring the levels of cAMP and cGMP in platelets following platelet activation with each of the platelet agonists and examining the impact of an altered external redox environment on these two cyclic nucleotides. Based on the findings to date, it is anticipated there would be elevated levels of one with a concomitant decrease in the other modulated by the platelet activator and external redox environment. Furthermore, an investigation into the exact location of VASP within the signalling pathway induced upon platelet activation by collagen could potentially further elucidate the role of VASP and its significance within this particular signalling cascade. An association between integrin $\alpha_{IIb}\beta_3$ and VASP has been hypothesised, through a link with signalling proteins such as vinculin and zyxin providing a linkage to the actin and thereby controlling actin cytoskeleton rearrangement (Figure 5.9). The findings of my study suggest perhaps VASP may be found further upstream and closer to integrin $\alpha_2\beta_1$ in terms of signalling events that previously thought.

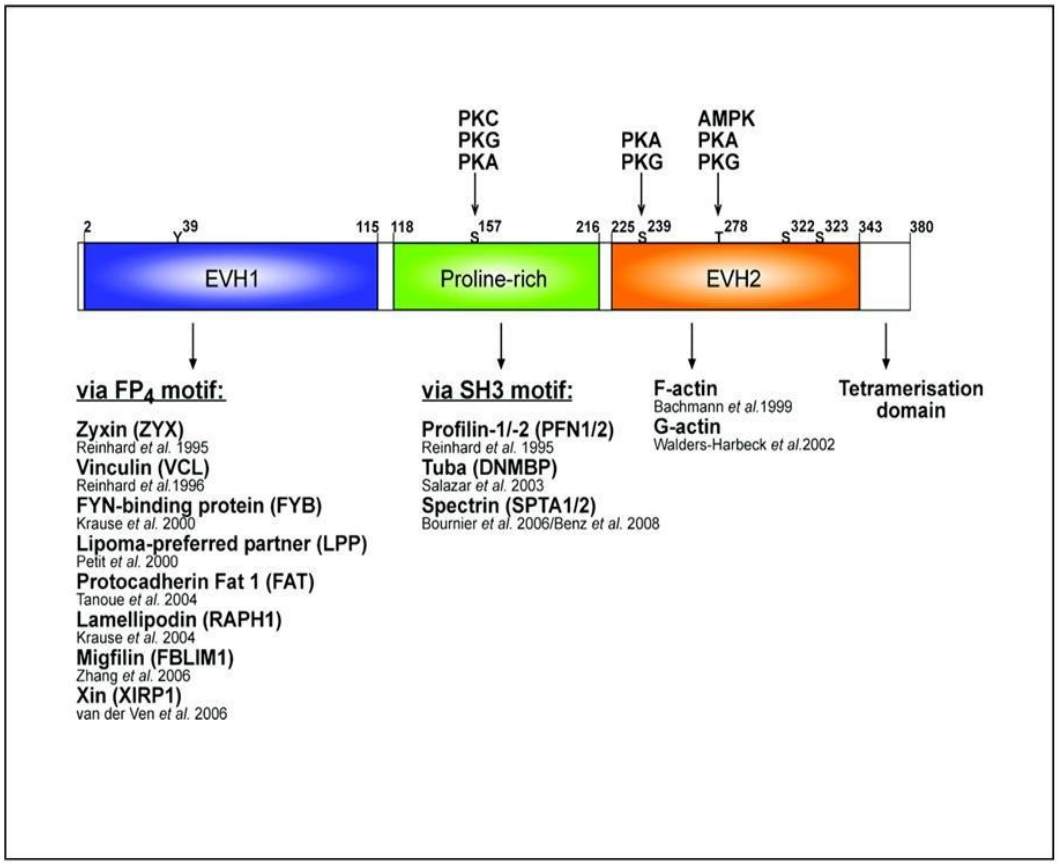

Figure 5.9 The structure of vasodilator-stimulated phosphoprotein (VASP) and its direct interaction partners. VASP contains three phosphorylation sites: Serine 157 (proline-rich domain) and Serine 239 and Threonine 278 (both located in the EVH2 domain). The interaction partners of VASP and the domains through which they interact are shown in this schematic (adapted from (Dittrich et al, 2010)).

Consistent with results in the previous chapter, these findings in relation to the collagen activation pathway again highlight integrin $\alpha_2\beta_1$ as a particularly redox sensitive receptor. We have demonstrated that a reducing redox environment does not entirely inhibit the binding of collagen to the platelet. Therefore, it is hypothesised that the effects of a reducing redox environment on the collagen mediated signalling cascade are due to an external modification of the integrin $\alpha_2\beta_1$. This may in turn lead to disruption of signalling events involving intra-platelet regulatory proteins thereby inhibiting normal platelet function.

Chapter 6

The impact of bile acids on platelets: a novel insight into the role of platelets in inflammatory bowel disease

6.1 Introduction

Although first proposed in 1936, a link between the two major biological processes, coagulation and inflammation, has only become a major focus of research in recent years (Bargen & Barker, 1936). Inflammatory bowel disease (IBD) is one such condition in which platelet activity may play a key role (Yoshida & Granger, 2009). IBD is the collective name for Crohn's disease and ulcerative colitis, two pathologically different conditions but with similar symptoms. Crohn's disease can affect the entire gastrointestinal tract while ulcerative colitis is limited to the colon region.

There have been a number of discoveries in IBD which serve to enhance the proposed role of platelets in this debilitating, idiopathic disease. Thrombocytosis, characterised by a large number of smaller sized platelets, is known to be associated with IBD, although the underlying causes remain unknown (Harries et al, 1991). Additionally, platelets in IBD patients have been found to circulate in an active-like state which could be linked to the increased risk of thromboembolic events associated with IBD patients. Platelet hyperactivity and dysfunction in IBD is manifested as increased platelet surface expression of P-selectin, CD40-ligand (CD40L) and GP53 (Collins et al, 1994; Danese et al, 2003a; Danese et al, 2003b). Plasma levels of CD40L, β-thromboglobulin and platelet factor-4 (PF4), released from the α-granules of platelets upon activation, have also been found to be increased in IBD patients (Collins & Rampton, 1997; Danese et al, 2003b; Vrij et al, 2000). *In vitro* studies have demonstrated spontaneous platelet aggregation occurs in platelets from active IBD patients along with patients in remission. An increased sensitivity to platelet agonists such as ADP, arachidonic acid, ristocetin, collagen and

thrombin is also described (Collins et al, 1994; Mori et al, 1980; van Wersch et al, 1990). Platelet aggregates have been found circulating *in vivo* in venous blood of active IBD patients (Collins et al, 1994; Dhillon et al, 1992). Furthermore, higher numbers of platelet-leukocyte aggregates (PLA) mediated through the interaction of P-selectin on activated platelets with P-selectin glycoprotein ligand-1 (PSGL-1) expressed on leukocytes have been found in IBD patients compared to healthy controls and inflammatory controls (rheumatology patients) (Irving et al, 2004).

Bile acids are commonly known for their role in facilitating the digestion and absorption of lipids. However, bile acids are becoming increasingly recognised as important signalling molecules regulating epithelial homeostasis, transport and barrier function, thereby modulating intestinal function (Keating & Keely, 2009).

Cholic acid (CA) and chenodeoxycholic acid (CDCA), the primary bile acids, are synthesised from cholesterol, conjugated to glycine and taurine in the hepatocytes and stored in the gallbladder. They are the primary constituents of bile which is secreted into the duodenum following ingestion of a meal. Approximately 95 % of bile acids are reabsorbed from the intestine and transported back to the liver while a small percentage (2 – 5 %) pass into the large intestine where they are converted to secondary bile acids (Figure 6.1).

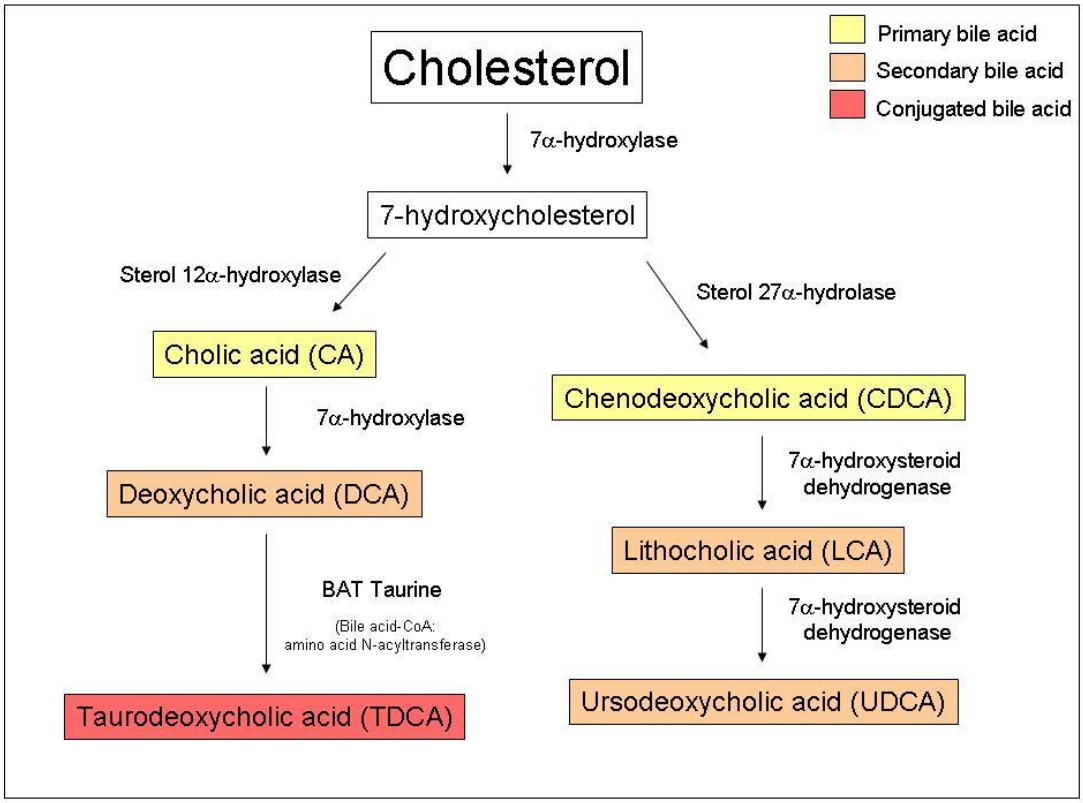

Figure 6.1 The biosynthesis of bile acids from cholesterol. The biosynthesis of bile acids is a complex process involving at least 16 enzymes that catalyse as many as 17 reactions (Russell, 2009). For purposes of clarity, this diagram only illustrates the synthesis of the bile acids used in this study – ursodeoxycholic acid (UDCA), deoxycholic acid (DCA) and taurodeoxycholic acid (TDCA). Cholesterol is hydroxylated at the 7 position, via the cytochrome P450 enzyme 7α-hydrolase, to form 7-hydroxycholesterol. 7α-hydrolase is the rate limiting step in the biosynthesis of bile acids. The synthesis process is then divided into two branches, the 'classic pathway', which leads to the formation of the primary bile acid, cholic acid (CA), or the 'acidic pathway', which results in an alternative primary bile acid, chenodeoxycholic acid (CDCA). CA and CDCA, when secreted into the intestine, are converted to the secondary bile acids, deoxycholic acid (DCA) and lithocholic acid (LCA), respectively. DCA may be conjugated to the amino acid taurine to form TDCA, while LCA can be further converted to UDCA. (The bile acid biosynthesis pathway is adapted from (Beilke et al, 2009)).

One of the main functions of the intestinal epithelium is fluid and electrolyte transport to and from the gut lumen. Fluid transport is dictated by secretion or absorption of ions, predominantly chloride (Cl^-) controlled by an active ion transport mechanism (Barrett & Keely, 2000). Disruption of the balance between fluid absorption and secretion can lead to problems such as constipation or diarrhoea. An altered concentration of bile acids in the system can impact on this fluid balance. Indeed, bile acid malabsorption (BAM) has long been linked to the onset of diarrhoea. Bile acids have also been implicated in the regulation of the enteric nervous system and the mucosal immune systems, disruptions in which are linked to the development of IBD.

The central role bile acids play in regulating intestinal function makes them a potentially significant player in the pathogenesis of IBD. Similarly, there is an ever growing body of evidence implicating platelet activity in IBD also. In this study the impact of bile acids on platelet function was investigated based on the hypothesis that there may be a link between these two key players in this chronic disease.

6.2 Results

6.2.1 The effects of bile acids on platelet aggregation

The impact of bile acids on platelet function was investigated by examining the effects of three commercially available bile acids, ursodeoxycholic acid (UDCA), deoxycholic acid (DCA) and taurodeoxycholic acid (TDCA), on platelet aggregation.

An MTT (3-(4,5-Dimethylthiazol-2-yl)-2,5-diphenyltetrazolium bromide) colorimetric assay demonstrated that even the highest concentration (500 μM) used of each of the bile acids had no significant effect on platelet viability (personal communication from Ms. Joanna Tan, RCSI).

Gel filtered platelets were incubated with each bile acid at concentrations of 10 μM, 100 μM or 500 μM. The levels of platelet aggregation of unactivated platelets or platelets activated with 0.1U/ml thrombin, 50 ng/ml convulxin, 38 μg/ml collagen or 19 μg/ml collagen following pre-treatment with the bile acid were measured.

There was no significant difference between the levels of platelet aggregation of unactivated platelets treated with each of the bile acids compared to the level of platelet aggregation observed in unactivated platelets in the absence of any bile acid treatment (n=6) (Figure 6.2).

UDCA was found only to impact on the levels of platelet aggregation in response to platelet activation by collagen. There was a trend towards a decrease in the level of platelet aggregation of platelets activated with 38 μg/ml collagen following treatment with 500 μM, while this decrease became

statistically significant in platelets activated with 19 μg/ml collagen. UDCA had no impact on platelet aggregation in response to thrombin or convulxin (n=6, (n=3 convulxin) **p < 0.01) (Figure 6.3).

The bile acid, DCA, decreased platelet aggregation to thrombin, convulxin and collagen in a concentration dependent manner (n=5 (n=3 convulxin), **p < 0.01, ***p < 0.001) (Figure 6.4).

Likewise, TDCA impacted on the platelet aggregation response to all agonists. There was a significant decrease in platelet aggregation observed in platelets pre-treated with 500 μM TDCA then activated with either 0.1U/ml thrombin or 19 μg/ml collagen. A similar trend was observed with platelets activated with 38 μg/ml collagen or 50 ng/ml convulxin, while not quite reaching statistical significance (n=3, *p < 0.05, **p < 0.01, ***p < 0.001) (Figure 6.5).

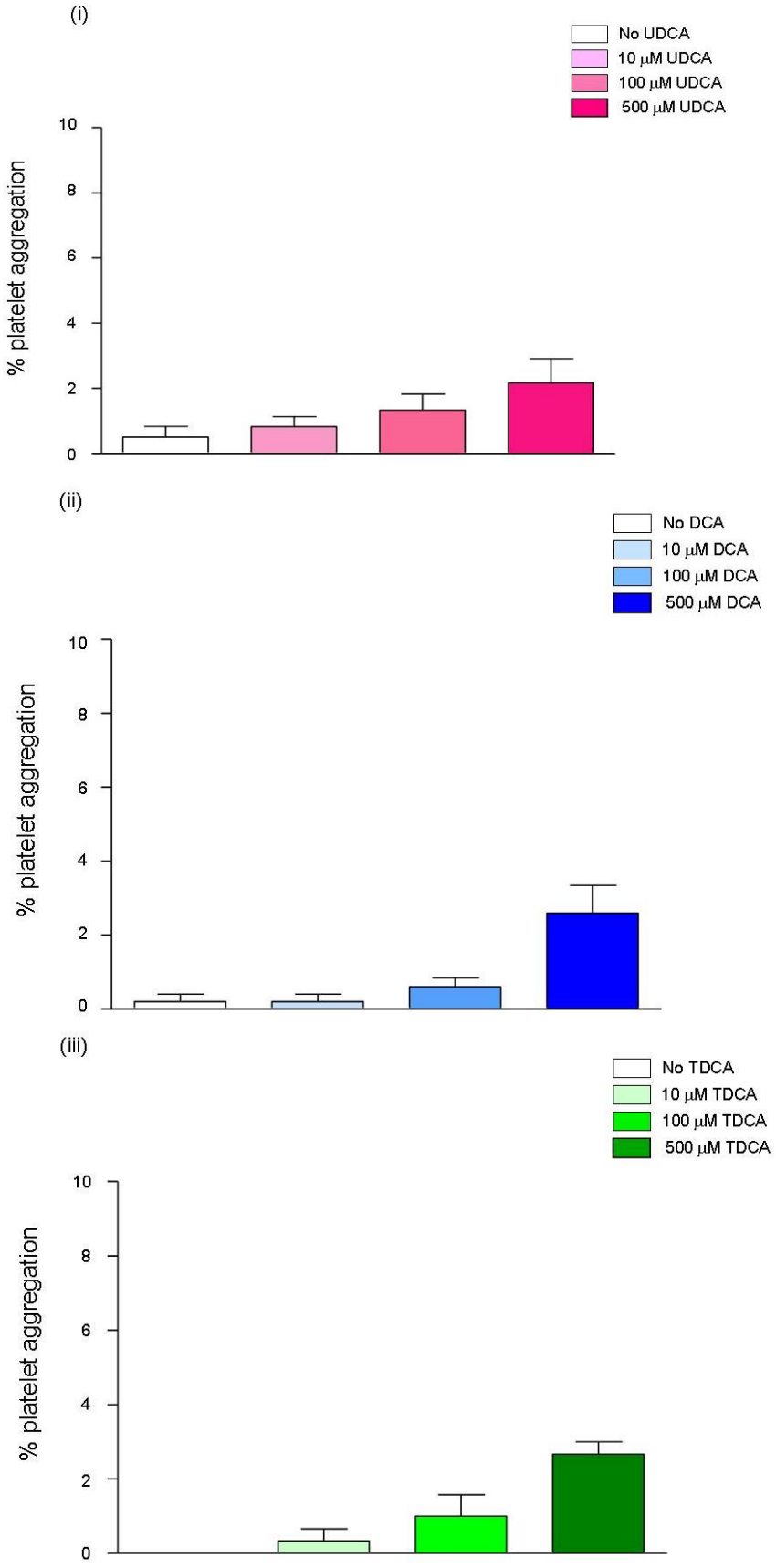
(i)
No UDCA
10 μM UDCA
100 μM UDCA
500 μM UDCA
% platelet aggregation
0
2
4
6
8
10
(ii)
No DCA
10 μM DCA
100 μM DCA
500 μM DCA
% platelet aggregation
0
2
4
6
8
10
(iii)
No TDCA
10 μM TDCA
100 μM TDCA
500 μM TDCA
% platelet aggregation
0
2
4
6
8
10

Figure 6.2 Bile acids alone do not induce platelet aggregation at any of the chosen concentrations. Gel filtered platelets were either untreated or incubated with bile acids: ursodeoxycholic acid (UDCA), deoxycholic acid (DCA) or taurodeoxycholic acid (TDCA) at concentrations of 10 μM, 100 μM or 500 μM for 10 minutes at 37 °C with constant stirring at 1100 rpm. The levels of platelet aggregation were recorded. Data is presented as the mean ± SEM, n=6 independent experiments.

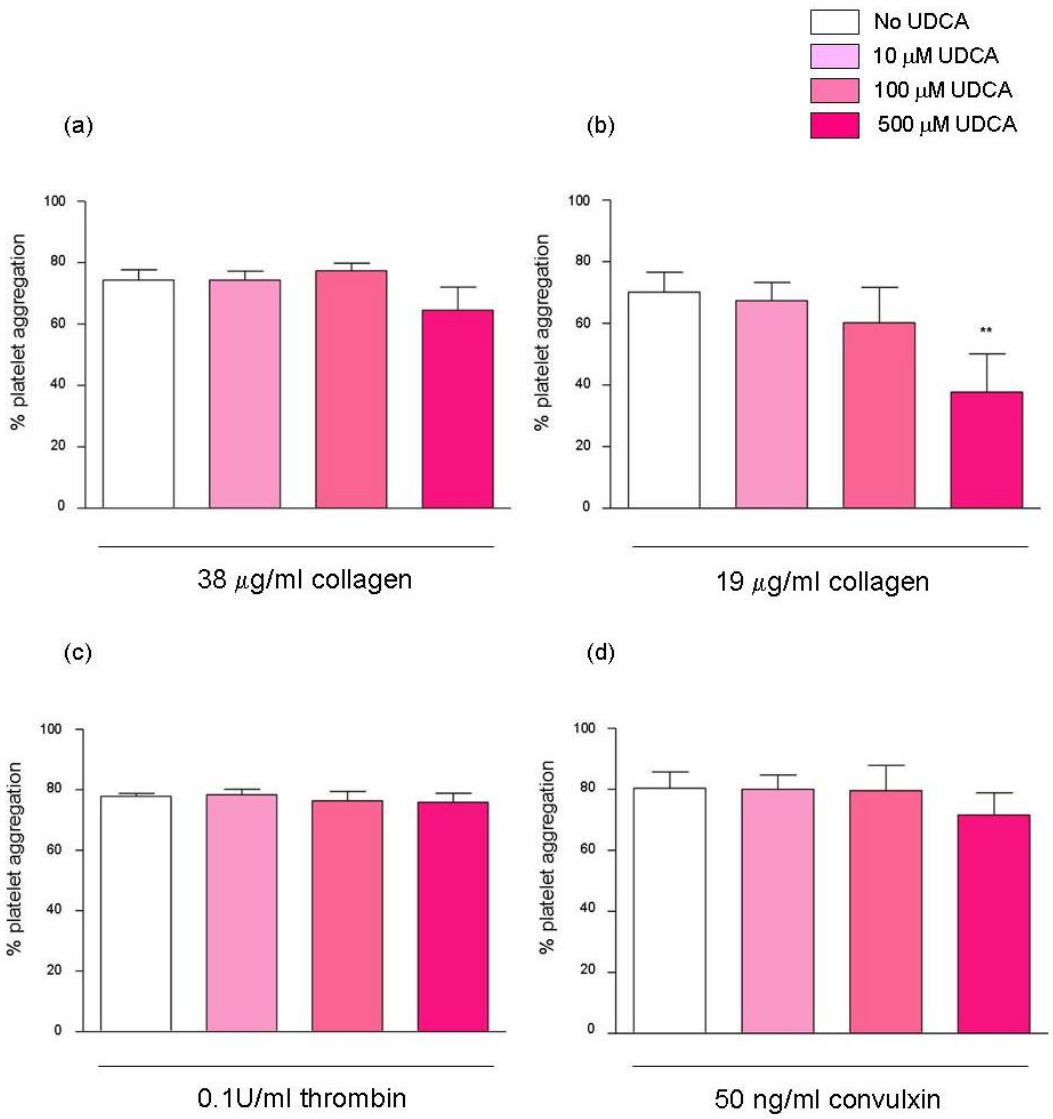

Figure 6.3 Ursodeoxycholic acid (UDCA) decreases platelet aggregation in response to collagen but has no impact on platelet aggregation induced by thrombin or convulxin. Gel filtered platelets were either untreated or incubated with 10 μM, 100 μM or 500 μM UDCA for 10 minutes at 37 °C with constant stirring at 1100 rpm. Platelets were left unactivated or were activated with either 0.1U/ml thrombin, 50 ng/ml convulxin, 38 μg/ml collagen or 19 μg/ml collagen. Platelet aggregations were carried out for 10 minutes at 37 °C with constant stirring at 1100 rpm. Data is presented as the mean ± SEM, n=6 (n=3 for convulxin) independent experiments, **p < 0.01.

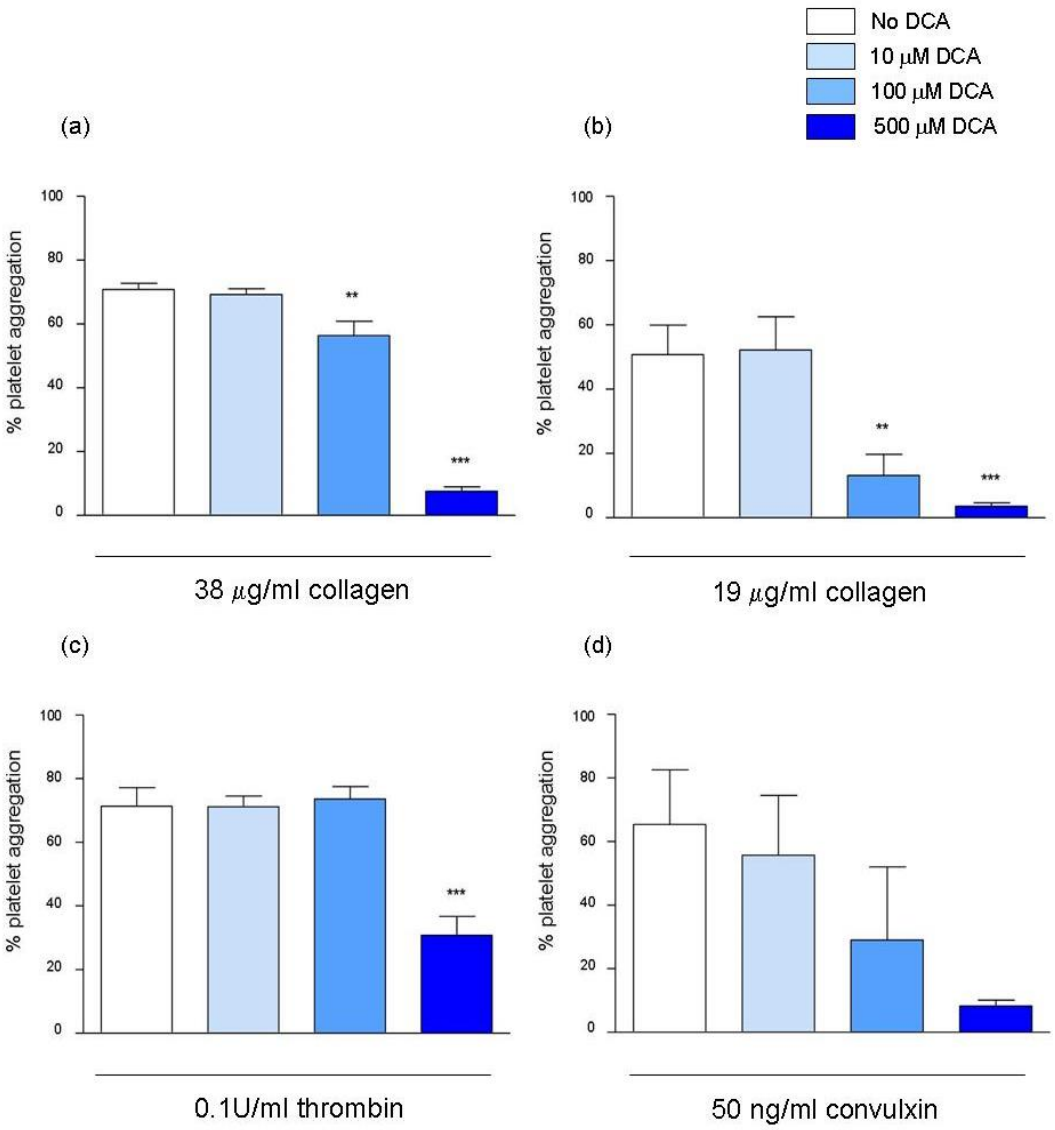

Figure 6.4 Deoxycholic acid (DCA) affects platelet aggregation to thrombin, collagen and convulxin. Gel filtered platelets were either untreated or incubated with 10 μM, 100 μM or 500 μM DCA for 10 minutes at 37 °C with constant stirring at 1100 rpm. Platelets were left unactivated or were activated with either 0.1U/ml thrombin, 50 ng/ml convulxin, 38 μg/ml collagen or 19 μg/ml collagen. Platelet aggregations were carried out for 10 minutes at 37 °C with constant stirring at 1100 rpm. Data is presented as the mean ± SEM, n=5 (n=3 for convulxin) independent experiments, **p < 0.01, ***p < 0.001.

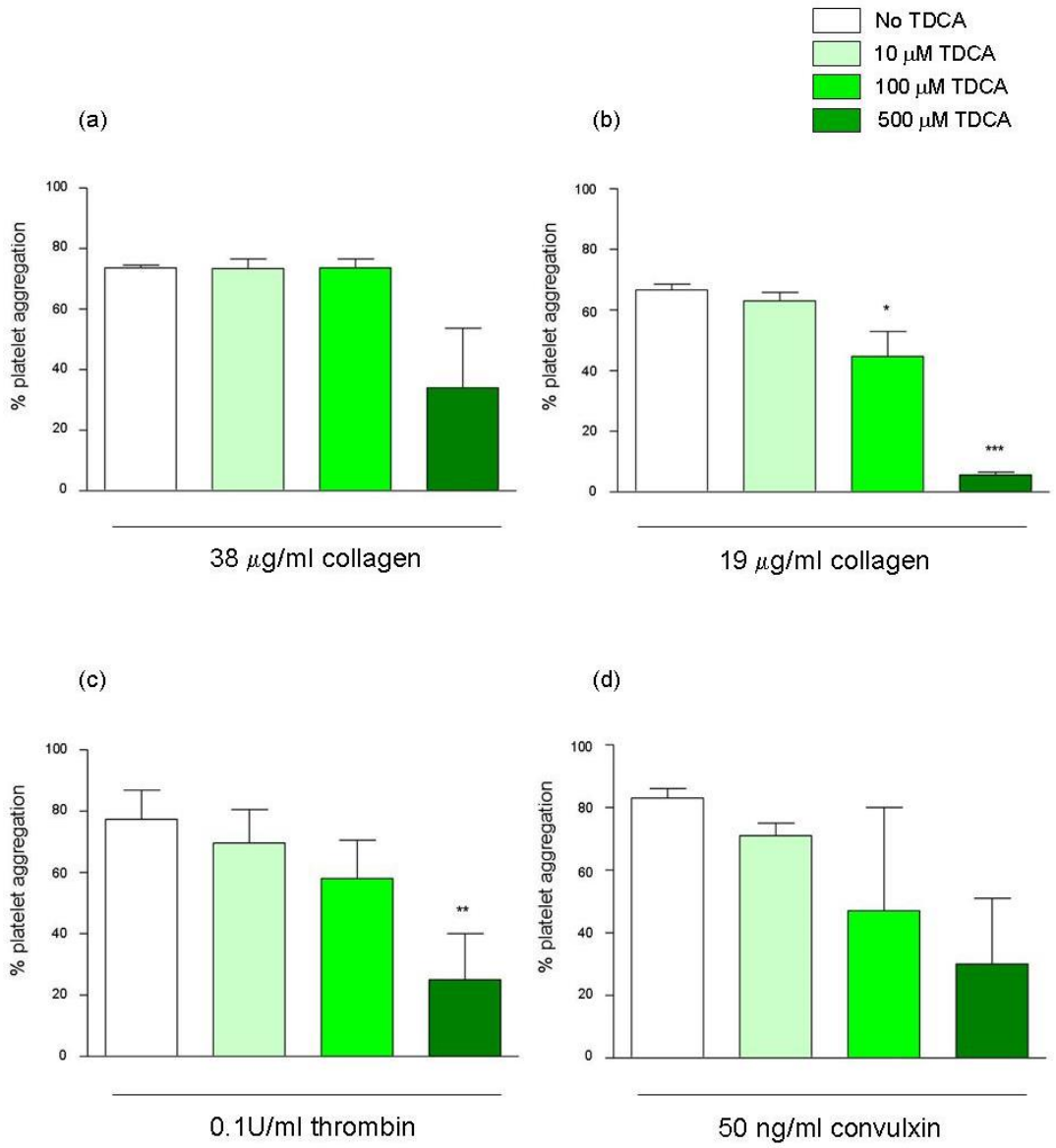

Figure 6.5 Taurodeoxycholic acid (TDCA) affects platelet aggregation to thrombin, collagen and convulxin. Gel filtered platelets were either untreated or incubated with 10 μM, 100 μM or 500 μM TDCA for 10 minutes at 37 °C with constant stirring at 1100 rpm. Platelets were left unactivated or were activated with either 0.1U/ml thrombin, 50 ng/ml convulxin, 38 μg/ml collagen or 19 μg/ml collagen. Platelet aggregations were carried out for 10 minutes at 37 °C with constant stirring at 1100 rpm. Data is presented as the mean ± SEM, n=3 independent experiments, *$p < 0.05$, **$p < 0.01$, ***$p < 0.001$.

6.3 Discussion

Recent studies have suggested a role for platelets in a variety of clinical conditions such as atherosclerosis, sepsis, rheumatoid arthritis and IBD, thus linking the complex processes of inflammation and haemostasis. Inflammatory bowel disease (IBD) is a condition which affects approximately 15,000 people in Ireland and over 2 million across Europe. Subclinical thrombosis is common in IBD and is a major source of morbidity in approximately 25 % of IBD deaths (Tabibian & Roth, 2009). Therefore, a greater understanding of the underlying causes of IBD and the development of therapy for the condition is crucial.

Platelet dysfunction in IBD patients has been demonstrated with the expression of activation surface markers (P-selectin, GP53 and CDL40) on platelets along with platelet secretory products (β-thromboglobulin and PF4) in the plasma of IBD patients (Collins et al, 1994; Danese et al, 2003a). Furthermore, experimental IBD studies in which dextran sodium sulphate (DSS)-induced colitis mice were examined, showed a significant role for platelets interacting with leukocytes through the PSGL-1 receptor (Mori et al, 2005; Vowinkel et al, 2007). Additional studies found antibody immuno-blockade of either P-selectin or PSGL-1 significantly attenuates the inflammatory response and histological tissue injury in a DSS-induced colitis mouse model, further evidence for the importance of platelets in IBD (Gironella et al, 2002; Rijcken et al, 2004).

There is increased levels of circulating vWF in both active and inactive Crohn's disease patients which is indicative of vascular cell damage (Stevens et al, 1992). Platelets encounter inflamed or damaged endothelial cells in the vast

intestinal microvascular bed in IBD patients. Endothelial cell damage exposes basement membrane to which platelets are exquisitely sensitive. Exposure of substances such as collagen leads to platelet adhesion, activation and recruitment of further platelets. Additionally, platelet activation in IBD patients may be caused by virus-induced changes in the endothelium promoting platelet adhesion and activation prior to damage. Similarly, platelets could be activated by platelet activating factors, such as TXA_2 and PAF (platelet-activating factor), released from neutrophils into the mesenteric circulation at the site of intestinal disease (Eliakim et al, 1988; Visser et al, 1988; Webberley et al, 1993). Platelet activation in turn leads to the release of a number of pro-inflammatory cytokines, such as CD40L and interleukin-1β (IL-β1), which can activate leukocytes and monocytes. Upon activation, these cells secrete more platelet activators such as ADP, arachidonic acid and PAF. All of these events, ultimately, demonstrate a vicious cycle wherein each activation process fuels and intensifies the other. It remains to be seen whether platelet activation is a cause or consequence of the inflammatory response.

Bile acids, synthesised from cholesterol, are primarily involved in the digestion and absorption of dietary lipids. However, bile acids have been implicated in the pathogenesis of IBD due to their central role in the regulation of intestinal function. Bile acids contribute to the control of intestinal function by regulating a number of major functions of the intestine, namely epithelial proliferation and death, the epithelial barrier function and fluid and electrolyte transport. Bile acids also regulate the enteric nervous system, which innervates the mucosa, along with the mucosal immune systems (Keating & Keely, 2009). Bile acids are known to interact with G-protein-coupled receptors (GPCR) (TGR5),

receptor tyrosine kinases (RTK), nuclear receptors (farnesoid X receptor – FXR) and membrane perturbations (Akare & Martinez, 2005; Cheng & Raufman, 2005; Maruyama et al, 2002; Merchant et al, 2005; Schmidt & Mangelsdorf, 2008). This vast number of interactions indicates that bile acids can potentially exert an effect on almost any cell they encounter.

Preliminary findings from this study examining the effects of bile acids on platelet function proved interesting. It was demonstrated that deoxycholic acid (DCA) and taurodeoxycholic acid (TDCA) disrupted platelet aggregation responses to platelets activated with thrombin, convulxin and collagen. However, ursodeoxycholic acid (UDCA) displayed a specific inhibitory effect on the platelet collagen activation pathway only. Similar results were observed in a platelet secretion assay measuring the levels of ADP released from the dense granules of platelets upon activation. It was found that while DCA and TDCA significantly decreased the quantity of ADP released from platelets activated by all platelet agonists, UDCA again demonstrated an inhibitory effect on platelets activated by collagen only (personal communication from Ms. Joanna Tan, RCSI). The greater potency of DCA and TDCA may be due to their membrane permeability, whereas UDCA is known to have less affinity for membranes.

These findings indicate that there may be a direct interaction between platelets and bile acids. As the inhibitory effects of the bile acids appear to be concentration dependent, the results suggest that higher concentrations of bile acids may have a protective function through maintaining platelets in an unactivated state, thereby disrupting or inhibiting the coagulation/inflammation cycle in IBD. The specificity of UDCA for the collagen activation pathway of platelets is a particularly interesting discovery. The observation that UDCA has

no impact on platelet activation induced by the GPVI specific agonist convulxin, suggests that UDCA is specifically targeting the collagen receptor integrin $\alpha_2\beta_1$. In the previous chapters, a unique redox sensitivity of integrin $\alpha_2\beta_1$ was revealed. These results provide further evidence to support a sensitivity of this particular platelet receptor to its external environment and indicate that it may play a significant role in the regulation of platelet activity in disease states where there is a major imbalance in the homeostasis of the platelet external environment.

These findings, though preliminary, are quite promising with regard to novel insights into the interactions between platelets and bile acids. Further work in this study will entail examining the membrane permeability of the bile acids in greater detail, and the exact mechanisms involved in the interaction including investigating the presence of a bile acid receptor on the surface of platelets and examining the effects of bile acids on intra-platelet signalling cascades. Furthermore, the impact of bile acid supplements on the platelet function of DSS colitis-induced mice will be explored.

These studies will lead to a greater understanding of the intimacies of platelet activity and inflammation. Improved knowledge of the exact mechanisms may lead to novel targeted therapies working at the interface of both processes, thus providing a new treatment for IBD which is currently without a medical cure.

Chapter 7

General Discussion

Platelets are small, versatile megakaryocyte-derived cell fragments that are primarily involved in haemostasis and thrombosis but have also been implicated in cancer progression and inflammatory conditions. The capabilities of platelets may have been underestimated in the past due to their 'simple' structure which lacks a nucleus and genetic material. However, the sheer volume of studies and literature relating to platelet activity and function demonstrates the significance and complex role of platelets in a variety of biological processes. Despite this ongoing research, the understanding of the fundamental mechanisms of platelet activity remains limited, thus restricting the development of advanced pro- and anti-platelet therapies. Further studies, such as this one, will enhance our understanding of platelet activation and the pathogenesis of platelet related diseases, potentially leading to the development of novel targeted therapies.

Integrins, such as integrin $\alpha_{IIb}\beta_3$ and integrin $\alpha_2\beta_1$, are key players in stable platelet adhesion, aggregation and thrombus formation. Therefore, elucidation of the intricate mechanisms of integrin activation is essential to enhance knowledge of the processes of platelet activation. Integrins possess a cysteine-rich structure which is critical in the regulation of integrin function and activity. It is well established the conformational rearrangement of integrins as they 'switch' from an unactivated state to an activated state is mediated by a thiol/disulphide shuffling or exchange mechanism. In Chapter 3, purified integrin $\alpha_{IIb}\beta_3$ and a CHO-K1 cell model, expressing integrin $\alpha_{IIb}\beta_3$, were employed to examine the thiol population of integrin $\alpha_{IIb}\beta_3$. It was demonstrated, consistent with reports in the literature, activation of integrin $\alpha_{IIb}\beta_3$ by $MnCl_2$, the universal integrin activator, leads to conformational changes in the integrin, resulting in an

increased thiol population. Furthermore, it was demonstrated that $MnCl_2$ and dithiothreitol (DTT), a reducing agent, induced platelet aggregation and PAC-1 binding to the activated conformation of integrin $\alpha_{IIb}\beta_3$ on platelets. However, neither $MnCl_2$ nor DTT induced platelet secretion. These findings indicate external modification of integrin $\alpha_{IIb}\beta_3$ is insufficient to initiate outside-in signalling, leading to platelet secretion and, eventually, full platelet activation. Interestingly, Raman spectroscopy, in conjunction with principal component analysis (PCA), successfully separated platelet spectra into distinct clusters due to changes in the thiol/disulphide regions of the spectra, based on the platelet activator. These findings imply $MnCl_2$, DTT and thrombin exert unique effects on the surface thiol population of platelets and suggest the thiol groups may play an important role not only in the regulation of integrin function but also the function of platelets as a whole.

Based on the findings of Chapter 3, the remainder of this thesis was aimed at further investigating the role of thiols in platelet activity and examining the impact of modifying these thiol groups on platelet function. In contrast to the initial studies in Chapter 3, more physiologically relevant platelet agonists were used throughout the rest of the thesis. It was revealed the platelet surface thiol population was increased upon platelet activation by collagen only. Furthermore, this thiol increase was specifically associated with collagen activation through integrin $\alpha_2\beta_1$ and not GPVI, the other collagen receptor. This is a novel and significant finding in relation to the mechanisms of integrin $\alpha_2\beta_1$ activation and, ultimately, the platelet activation pathways of collagen.

I hypothesise this new thiol population is as a result of conformational rearrangements of integrin $\alpha_2\beta_1$, in which a shuffling of thiol/disulphide groups or a reduction in disulphide bonds results in the exposure of more external free thiols. Due to the relatively low copy number of integrin $\alpha_2\beta_1$ expressed on platelets, compared to integrin $\alpha_{IIb}\beta_3$, the significant increase in the surface thiol population of platelets activated with collagen is somewhat surprising. In Chapter 3, it was confirmed that activation of integrin $\alpha_{IIb}\beta_3$ led to an increase in the thiol population, thus integrin $\alpha_{IIb}\beta_3$ could potentially contribute to this elevated platelet surface thiol population in response to collagen activation. Thrombin and convulxin, two potent platelet agonists, both induced platelet aggregation similar to that induced by collagen, indicating these agonists converted platelet integrin $\alpha_{IIb}\beta_3$ to an activated, ligand-binding conformation. However, the surface thiol population of platelets activated with thrombin or convulxin remained similar to that of unactivated platelets. Likewise, while the level of platelet adhesion to collagen, fibrinogen and collagen related peptide (CRP) was comparable, there was again an increase in the thiol population of platelets adhered to collagen only. Though, it was noted the thiol population of platelets adhered to fibrinogen was higher than that of platelets adhered to CRP. Nonetheless, this indicates integrin $\alpha_{IIb}\beta_3$ is not the major source of the increased platelet surface thiol population and, therefore, hypothetically the thiols may originate from another source that is specifically associated with integrin $\alpha_2\beta_1$ stimulation.

Thiol isomerase enzymes have been implicated in receptor regulation, activation and substrate processing when expressed on the surface of cells.

Such enzymes, for example protein disulphide isomerase (PDI), have been found on the surface of platelets following activation. Modification of the activity of these enzymes impacts on platelet function, with a decrease in platelet aggregation, secretion and integrin $\alpha_{IIb}\beta_3$ activation (Essex & Li, 1999). Additionally, it has been revealed that integrin $\alpha_{IIb}\beta_3$ has an endogenous thiol isomerase activity (O'Neill et al, 2000). An attractive proposition is the increased surface thiol population of platelets activated with collagen may, therefore, be due to the translocation of one or more thiol isomerase enzymes to the surface of platelets upon stimulation of integrin $\alpha_2\beta_1$ specifically. Indeed, PDI activity has been associated with integrin $\alpha_2\beta_1$ whereby bacitracin, an inhibitor of disulphide exchange, abrogated platelet aggregation to collagen (Lahav et al, 2003). Similarly, a monoclonal antibody raised against PDI inhibited platelet adhesion to the integrin $\alpha_2\beta_1$ specific peptide GFOGER-GPP but not CRP.

A parallel, novel, redox sensitivity, exclusive to the collagen activation pathway of platelets was also revealed in Chapter 5. This redox sensitivity was assigned specifically to the collagen receptor, integrin $\alpha_2\beta_1$. An external reducing redox environment inhibited platelet aggregation and adhesion, along with affecting the phosphorylation state of an intra-cellular signalling protein, VASP, in response to stimulation by collagen only. Additionally, the increased surface thiol population associated with platelet activation by collagen was also abolished. This confirms the importance of thiols in integrin $\alpha_2\beta_1$ function and demonstrates that, unlike integrin $\alpha_{IIb}\beta_3$, external modification of these thiol groups can trigger downstream intra-platelet effects, ultimately, impacting on

the activation state of platelets through the modification of outside-in signalling mechanisms.

As previously alluded to, the sensitivity of integrin $\alpha_2\beta_1$ compared to that of integrin $\alpha_{IIb}\beta_3$ may be due to the presence of a greater number of reactive cysteines in the β-subunit of the integrin. This greater sensitivity of integrin $\alpha_2\beta_1$ is supported by the study of Lahav *et al*. In their study they demonstrate that bacitracin completely abolished platelet aggregation to collagen, while only decreasing the platelet aggregation response to CRP. Subsequently, higher concentrations of bacitracin were found to completely inhibit platelet aggregation to CRP (Lahav et al, 2003). This finding was attributed to the higher concentration of bacitracin blocking conformational changes and activation of integrin $\alpha_{IIb}\beta_3$, thereby inhibiting platelet aggregation. The fact that this phenomenon was only observed with a high concentration of bactrican, while a low concentration of bactracin impeded integrin $\alpha_2\beta_1$, again highlights a greater sensitivity of integrin $\alpha_2\beta_1$ compared in integrin $\alpha_{IIb}\beta_3$.

Reactive cysteines, with a lower pK_a value than others, are more likely to interact with other thiol containing agents. I hypothesise the inhibition of platelets response to collagen in the presence of a reducing external redox environment may be as a result of the modification of the reactive cysteines present in integrin $\alpha_2\beta_1$. Such modifications, due to an interaction with glutathione or cysteine, could result in S-glutathionylation or S-cysteinylation of the thiol groups. These thiol modifications may potentially lock integrin $\alpha_2\beta_1$ into a conformation, whereby the mechanism which results in the generation of an

increased thiol population is prevented from occurring and thus further signalling from integrin $\alpha_2\beta_1$ is also altered.

An alternative hypothesis is one based on the push-pull mechanism proposed for the regulation of integrin $\alpha_{IIb}\beta_3$ function. Li et al suggest that a resting α_{IIb}/β_3 transmembrane domain heterodimer may be destabilised and activated by stabilising the resulting α_{IIb} and β_3 transmembrane domain homodimers (Li et al, 2005). This push-pull mechanism is based on the concept of association and dissociation of receptor subunits. A heterodimeric association of subunits to form a receptor complex is also demonstrated in the GPIb-IX complex in which the GPIbα and GPIbβ subunits are in fact linked via disulphide bridges between their respective Cys residues (Luo & Li, 2008; Luo et al, 2007; Mo et al, 2008). A similar mechanism may exist in integrin $\alpha_2\beta_1$ whereby dissociation of the subunits upon activation leads to exposure of free thiols extracellularly. An altered external redox environment could potentially inhibit this mechanism from occurring, thereby inhibiting the exposure of the free thiol population and resulting in the integrin being fixed into a conformation that leads to altered downstream signalling. This modulation of integrin $\alpha_2\beta_1$ by the external redox environment would impact on the interaction between the integrin and its ligand, collagen, ultimately, impacting on platelet activity induced by collagen.

The significance of the balance of the components of the physiological redox environment is well established. However, the results observed in this thesis suggest the converse, lesser known condition, reductive stress, could be a real player in the regulation of platelet activity. It would be interesting to investigate

the redox potential of the plasma from patients with disease states associated with bleeding disorders and examine whether the balance of the redox environment is tipped in favour of a more reducing one, thereby, affecting integrin $\alpha_2\beta_1$ function and impacting on platelet adhesion at sites of injury.

Clinically, the implications of these findings may be significant. Alterations of the redox environment, to a more oxidising environment, are common in disease states such as in atherosclerosis, rheumatoid arthritis, IBD and diabetes. Likewise, thromboembolic events, linked to platelet hyperactivity, are frequent in patients suffering from these conditions. Antioxidant management is a potential therapy to alleviate such events. Reducing agents could be employed to specifically target the collagen receptor integrin $\alpha_2\beta_1$, without completely shutting down platelet activity. Platelet adhesion to collagen is one of the primary events in platelet plug formation. By inhibiting this process, abnormal thrombus formation, potentially resulting in events such as heart attack or stroke, could be prevented. Altering the redox environment and quenching platelet activity will inevitably not cure the original disease but will work to the limit the complications that arise thereafter.

The findings of this thesis suggest the redox environment is critical in the regulation of platelet activity and an imbalance in the system may have significant consequences. A noteworthy observation throughout the study was that platelet activity in the absence of an altered redox environment was comparable to that of platelets in the presence of an oxidising environment, while a mean redox potential was consistently lower. These findings highlight

the importance of the redox environment of plasma in the regulation of platelet activity. Furthermore, normal platelet behaviour is more reminiscent of that observed in a mean redox environment. This, rather controversially, suggests that perhaps all platelet studies, across the board, should be carried out in the presence of a mean redox environment rather than an unaltered external redox environment.

The final section of the study investigating a link between bile acids and platelets in IBD produced some interesting results. Preliminary findings suggest there is undoubtedly an interaction between bile acids and platelets, which may be significant in relation to these two key players in the pathogenesis of IBD. While, the nature of this interaction remains to be seen, the impact of UDCA specifically on the collagen activation pathway of platelets, calls for further investigation, particularly based on other findings of this thesis with regard to the collagen receptor, integrin $\alpha_2\beta_1$.

Additionally, not only has work in this thesis helped further elucidate the role of thiols in platelet function but also demonstrates Raman spectroscopy as a potentially novel technique for the analysis of platelets. Raman spectroscopy was successfully employed to discriminate platelet Raman spectra based on the platelet activation state and, even more significantly, on the platelet activator. The separation of platelet Raman spectra was due to molecular variances in the platelet membrane arising as a result of the treatment or activation of platelets. The sensitivity of the technique indicates it could be employed to predict the onset of platelet dysfunction leading to disease, by the identification of specific

platelet surface biomarkers. A study using Raman to examine platelets from patients suffering from cardiovascular disease (CVD), compared to healthy controls, could detect such biomarkers or biochemical changes associated with CVD onset. Patients presenting with IBD, in addition to a cardiovascular-related event, would be ideal candidates to take part in such a study. The significance of thiol/disulphide groups in platelet function has been demonstrated throughout this thesis, and based on the serious implications of modification of thiol groups, i.e. inhibition of the platelet response to collagen, I propose them as a platelet surface marker worthy of examination. The clinical potential of Raman spectroscopy as a novel non-invasive diagnostic tool could be assessed based on the findings of such a study.

In conclusion, this thesis has not only highlighted the significant role of the external redox environment of platelets but has also succeeded in furthering our knowledge of the role of thiols in the regulation of platelet function. It has demonstrated the lesser recognised platelet integrin $\alpha_2\beta_1$ displays a superior sensitivity to integrin $\alpha_{IIb}\beta_3$ and furthermore, modification of its function can impact greatly on the platelet response to collagen, one of the primary physiological agonists of platelets. The exclusive redox sensitivity of this platelet receptor to its external environment signifies its potentially crucial role in dictating the platelet response to variations in external conditions. The impact of an altered redox environment on platelet aggregation and adhesion implies that integrin $\alpha_2\beta_1$ could be a significant platelet regulator, whereby the platelet is switched ‘on’ or ‘off’ depending on the nature of the external redox imbalance. I propose integrin $\alpha_2\beta_1$ as a novel target for improved pro- and anti-platelet

therapies, whereby redox reagents could be exploited to modify integrin $\alpha_2\beta_1$ and thereby regulate platelet activity. Administration of redox reagents could also work in a complimentary manner to combat the original imbalance in the redox environment which is ultimately responsible for the abnormal platelet activity. A therapeutic intervention such as this could alleviate the complication of thromboembolic events associated with a number of conditions including IBD, diabetes and rheumatoid arthritis.

References

Akare S, Martinez JD (2005) Bile acid induces hydrophobicity-dependent membrane alterations. *Biochim Biophys Acta* **1735:** 59-67

Andrews RK, Lopez JA, Berndt MC (1997) Molecular mechanisms of platelet adhesion and activation. *The international journal of biochemistry & cell biology* **29:** 91-105

Argyrou A, Blanchard JS (2004) Flavoprotein disulfide reductases: advances in chemistry and function. *Progress in nucleic acid research and molecular biology* **78:** 89-142

Asselin J, Gibbins JM, Achison M, Lee YH, Morton LF, Farndale RW, Barnes MJ, Watson SP (1997) A collagen-like peptide stimulates tyrosine phosphorylation of syk and phospholipase C gamma2 in platelets independent of the integrin alpha2beta1. *Blood* **89:** 1235-1242

Aszodi A, Pfeifer A, Ahmad M, Glauner M, Zhou XH, Ny L, Andersson KE, Kehrel B, Offermanns S, Fassler R (1999) The vasodilator-stimulated phosphoprotein (VASP) is involved in cGMP- and cAMP-mediated inhibition of agonist-induced platelet aggregation, but is dispensable for smooth muscle function. *The EMBO journal* **18:** 37-48

Aylward K, Meade G, Ahrens I, Devocelle M, Moran N (2006) A novel functional role for the highly conserved alpha-subunit KVGFFKR motif distinct from integrin alphaIIbbeta3 activation processes. *J Thromb Haemost* **4:** 1804-1812

Bachmann C, Fischer L, Walter U, Reinhard M (1999) The EVH2 domain of the vasodilator-stimulated phosphoprotein mediates tetramerization, F-actin binding, and actin bundle formation. *J Biol Chem* **274:** 23549-23557

Ball DW (2001) Theory of Raman Spectroscopy. *Spectroscopy* **16:** 32-34

Bargen JA, Barker NW (1936) Extensive arterial and venous thrombosis complicating chronic ulcerative colitis. *Archives of Internal Medicine* **58:** 17-31

Barnes MJ, Knight CG, Farndale RW (1998) The collagen-platelet interaction. *Current opinion in hematology* **5:** 314-320

Barrett KE, Keely SJ (2000) Chloride secretion by the intestinal epithelium: molecular basis and regulatory aspects. *Annual review of physiology* **62:** 535-572

Baumgartner HR, Haudenschild C (1972) Adhesion of platelets to subendothelium. *Annals of the New York Academy of Sciences* **201:** 22-36

Bayir H (2005) Reactive oxygen species. *Crit Care Med* **33:** S498-501

Baynes JW, Thorpe SR (1999) Role of oxidative stress in diabetic complications: a new perspective on an old paradigm. *Diabetes* **48:** 1-9

Bazzoni G, Hemler ME (1998) Are changes in integrin affinity and conformation overemphasized? *Trends in biochemical sciences* **23:** 30-34

Beckman KB, Ames BN (1998) The free radical theory of aging matures. *Physiological reviews* **78:** 547-581

Beilke LD, Aleksunes LM, Holland RD, Besselsen DG, Beger RD, Klaassen CD, Cherrington NJ (2009) Constitutive androstane receptor-mediated changes in bile acid composition contributes to hepatoprotection from lithocholic acid-induced liver injury in mice. *Drug metabolism and disposition: the biological fate of chemicals* **37:** 1035-1045

Bennett JS, Berger BW, Billings PC (2009) The structure and function of platelet integrins. *J Thromb Haemost* **7 Suppl 1:** 200-205

Bennett MR (2001) Reactive oxygen species and death: oxidative DNA damage in atherosclerosis. *Circulation research* **88:** 648-650

Bensalah K, Fleureau J, Rolland D, Lavastre O, Rioux-Leclercq N, Guille F, Patard JJ, Senhadji L, de Crevoisier R (2010) Raman spectroscopy: a novel experimental approach to evaluating renal tumours. *Eur Urol* **58:** 602-608

Berndt MC, Shen Y, Dopheide SM, Gardiner EE, Andrews RK (2001) The vascular biology of the glycoprotein Ib-IX-V complex. *Thrombosis and haemostasis* **86:** 178-188

Bevers EM, Comfurius P, Zwaal RF (1983) Changes in membrane phospholipid distribution during platelet activation. *Biochimica et biophysica acta* **736:** 57-66

Bilotta JJ, Waye JD (1989) Hydrogen peroxide enteritis: the "snow white" sign. *Gastrointest Endosc* **35:** 428-430

Blomback B (2001) Fibrinogen: evolution of the structure-function concept. Keynote address at fibrinogen 2000 congress. *Annals of the New York Academy of Sciences* **936:** 1-10

Born GV (1962) Aggregation of blood platelets by adenosine diphosphate and its reversal. *Nature* **194:** 927-929

Brass LF, Vassallo RR, Jr., Belmonte E, Ahuja M, Cichowski K, Hoxie JA (1992) Structure and function of the human platelet thrombin receptor. Studies using monoclonal antibodies directed against a defined domain within the receptor N terminus. *J Biol Chem* **267:** 13795-13798

Brinckmann J (2005) Collagens at a glance. *Top Curr Chem* **247:** 1-6

Britton G (1995) Structure and properties of carotenoids in relation to function. *FASEB journal : official publication of the Federation of American Societies for Experimental Biology* **9:** 1551-1558

Burgess JK, Hotchkiss, K.A., Suter, C., Dudman, N.P., Szollosi, J., Chesterman, C.N., Chong, B.H., and Hogg, P.J. (2000) Physical Proximity and Functional Association of Glycoprotein 1ba and Protein-disulphide Isomerase on the Platelet Plasma Membrane. *The Journal of Biological Chemistry* **275:** 9758-9766

Butt E, Abel K, Krieger M, Palm D, Hoppe V, Hoppe J, Walter U (1994) cAMP- and cGMP-dependent protein kinase phosphorylation sites of the focal adhesion vasodilator-stimulated phosphoprotein (VASP) in vitro and in intact human platelets. *J Biol Chem* **269:** 14509-14517

Butt E, Immler D, Meyer HE, Kotlyarov A, Laass K, Gaestel M (2001) Heat shock protein 27 is a substrate of cGMP-dependent protein kinase in intact human platelets: phosphorylation-induced actin polymerization caused by HSP27 mutants. *J Biol Chem* **276:** 7108-7113

Calvete JJ (1999) Platelet integrin GPIIb/IIIa: structure-function correlations. An update and lessons from other integrins. *Proc Soc Exp Biol Med* **222:** 29-38

Calvete JJ, Henschen A, Gonzalez-Rodriguez J (1991) Assignment of disulphide bonds in human platelet GPIIIa. A disulphide pattern for the beta-subunits of the integrin family. *Biochem J* **274 (Pt 1):** 63-71

Campion A, Kambhampati, P. (1998) Surface-enhanced Raman scattering *Chem Soc Reviews* **27:** 241-250

Candiano G, Bruschi M, Musante L, Santucci L, Ghiggeri GM, Carnemolla B, Orecchia P, Zardi L, Righetti PG (2004) Blue silver: a very sensitive colloidal Coomassie G-250 staining for proteome analysis. *Electrophoresis* **25:** 1327-1333

Carlsson LE, Santoso S, Spitzer C, Kessler C, Greinacher A (1999) The alpha2 gene coding sequence T807/A873 of the platelet collagen receptor integrin

alpha2beta1 might be a genetic risk factor for the development of stroke in younger patients. *Blood* **93:** 3583-3586

Ceriello A (2000) Oxidative stress and glycemic regulation. *Metabolism* **49:** 27-29

Chawla RK, Lewis FW, Kutner MH, Bate DM, Roy RG, Rudman D (1984) Plasma cysteine, cystine, and glutathione in cirrhosis. *Gastroenterology* **87:** 770-776

Chen XG, Schweitzer-Stenner R, Krimm S, Mirkin NG, Asher SA (1994) N-methylacetamide and its hydrogen-bonded water molecules are vibrationally coupled. *J Am Chem Soc* **116:** 11141-11142

Cheng K, Raufman JP (2005) Bile acid-induced proliferation of a human colon cancer cell line is mediated by transactivation of epidermal growth factor receptors. *Biochemical pharmacology* **70:** 1035-1047

Cheresh DA (1992) Structural and biologic properties of integrin-mediated cell adhesion. *Clinics in laboratory medicine* **12:** 217-236

Clark EA, Shattil SJ, Brugge JS (1994) Regulation of protein tyrosine kinases in platelets. *Trends in biochemical sciences* **19:** 464-469

Clemetson KJ, Clemetson JM (1994) Molecular abnormalities in Glanzmann's thrombasthenia, Bernard-Soulier syndrome, and platelet-type von Willebrand's disease. *Current opinion in hematology* **1:** 388-393

Collins CE, Cahill MR, Newland AC, Rampton DS (1994) Platelets circulate in an activated state in inflammatory bowel disease. *Gastroenterology* **106:** 840-845

Collins CE, Rampton DS (1997) Review article: platelets in inflammatory bowel disease--pathogenetic role and therapeutic implications. *Alimentary pharmacology & therapeutics* **11:** 237-247

Comerford KM, Lawrence DW, Synnestvedt K, Levi BP, Colgan SP (2002) Role of vasodilator-stimulated phosphoprotein in PKA-induced changes in endothelial junctional permeability. *FASEB journal : official publication of the Federation of American Societies for Experimental Biology* **16:** 583-585

Coughlin SR (2000) Thrombin signalling and protease-activated receptors. *Nature* **407:** 258-264

Coyle JT, Puttfarcken P (1993) Oxidative stress, glutamate, and neurodegenerative disorders. *Science* **262:** 689-695

Crow P, Molckovsky A, Stone N, Uff J, Wilson B, WongKeeSong LM (2005) Assessment of fiberoptic near-infrared raman spectroscopy for diagnosis of bladder and prostate cancer. *Urology* **65:** 1126-1130

Cupit LD, Schmidt VA, Bahou WF (1999) Proteolytically activated receptor-3. A member of an emerging gene family of protease receptors expressed on vascular endothelial cells and platelets. *Trends in cardiovascular medicine* **9:** 42-48

D'Andrea MR, Derian CK, Leturcq D, Baker SM, Brunmark A, Ling P, Darrow AL, Santulli RJ, Brass LF, Andrade-Gordon P (1998) Characterization of protease-activated receptor-2 immunoreactivity in normal human tissues. *The journal of histochemistry and cytochemistry : official journal of the Histochemistry Society* **46:** 157-164

Dalle-Donne I, Rossi R, Giustarini D, Colombo R, Milzani A (2007) S-glutathionylation in protein redox regulation. *Free radical biology & medicine* **43:** 883-898

Dalle-Donne I, Scaloni A, Giustarini D, Cavarra E, Tell G, Lungarella G, Colombo R, Rossi R, Milzani A (2005) Proteins as biomarkers of oxidative/nitrosative stress in diseases: the contribution of redox proteomics. *Mass spectrometry reviews* **24:** 55-99

Danese S, de la Motte C, Sturm A, Vogel JD, West GA, Strong SA, Katz JA, Fiocchi C (2003a) Platelets trigger a CD40-dependent inflammatory response in the microvasculature of inflammatory bowel disease patients. *Gastroenterology* **124:** 1249-1264

Danese S, Katz JA, Saibeni S, Papa A, Gasbarrini A, Vecchi M, Fiocchi C (2003b) Activated platelets are the source of elevated levels of soluble CD40 ligand in the circulation of inflammatory bowel disease patients. *Gut* **52:** 1435-1441

Dangelmaier CA, Quinter PG, Jin J, Tsygankov AY, Kunapuli SP, Daniel JL (2005) Rapid ubiquitination of Syk following GPVI activation in platelets. *Blood* **105:** 3918-3924

De Botton S, Sabri S, Daugas E, Zermati Y, Guidotti JE, Hermine O, Kroemer G, Vainchenker W, Debili N (2002) Platelet formation is the consequence of caspase activation within megakaryocytes. *Blood* **100:** 1310-1317

de Groot PG, Sixma JJ (1997) Role of glycoprotein IIb:IIIa in the adhesion of platelets to collagen under flow conditions. *Blood* **89:** 1837

Del Conde I, Shrimpton CN, Thiagarajan P, Lopez JA (2005) Tissue-factor-bearing microvesicles arise from lipid rafts and fuse with activated platelets to initiate coagulation. *Blood* **106:** 1604-1611

Depraetere H, Wille C, Gansemans Y, Stanssens P, Lauwereys M, Baruch D, De Reys S, Deckmyn H (1997) The integrin alpha 2 beta 1 (GPIa/IIa)-I-domain inhibits platelet-collagen interaction. *Thrombosis and haemostasis* **77:** 981-985

Dhillon AP, Anthony A, Sim R, Wakefield AJ, Sankey EA, Hudson M, Allison MC, Pounder RE (1992) Mucosal capillary thrombi in rectal biopsies. *Histopathology* **21:** 127-133

Di Mascio P, Kaiser S, Sies H (1989) Lycopene as the most efficient biological carotenoid singlet oxygen quencher. *Arch Biochem Biophys* **274:** 532-538

Ding Z, Kim, S., Dorsam, R.T., Jin, J., Kunapuli, S.P. (2003) Inactivation of the human P2Y12 receptor by thiol reagents requires interaction with both extracellular cysteine residues, Cys17 and Cys270. *Blood* **101:** 3908-3914

Dittrich M, Strassberger V, Fackler M, Tas P, Lewandrowski U, Sickmann A, Walter U, Dandekar T, Birschmann I (2010) Characterization of a novel interaction between vasodilator-stimulated phosphoprotein and Abelson interactor 1 in human platelets: a concerted computational and experimental approach. *Arteriosclerosis, thrombosis, and vascular biology* **30:** 843-850

Dormann D, Clemetson KJ, Kehrel BE (2000) The GPIb thrombin-binding site is essential for thrombin-induced platelet procoagulant activity. *Blood* **96:** 2469-2478

Duman BS, Ozturk M, Yilmazeri S, Hatemi H (2003) Thiols, malonaldehyde and total antioxidant status in the Turkish patients with type 2 diabetes mellitus. *The Tohoku journal of experimental medicine* **201:** 147-155

Dumas JJ, Kumar R, Seehra J, Somers WS, Mosyak L (2003) Crystal structure of the GpIbalpha-thrombin complex essential for platelet aggregation. *Science* **301:** 222-226

Eigenthaler M, Nolte C, Halbrugge M, Walter U (1992) Concentration and regulation of cyclic nucleotides, cyclic-nucleotide-dependent protein kinases and one of their major substrates in human platelets. Estimating the rate of cAMP-regulated and cGMP-regulated protein phosphorylation in intact cells. *European journal of biochemistry / FEBS* **205:** 471-481

Eliakim R, Karmeli F, Razin E, Rachmilewitz D (1988) Role of platelet-activating factor in ulcerative colitis. Enhanced production during active disease and inhibition by sulfasalazine and prednisolone. *Gastroenterology* **95:** 1167-1172

Ellman GL (1959) Tissue sulfhydryl groups. *Arch Biochem Biophys* **82:** 70-77

Emsley J, Knight CG, Farndale RW, Barnes MJ, Liddington RC (2000) Structural basis of collagen recognition by integrin alpha2beta1. *Cell* **101:** 47-56

Essex DW, Li J (1999) Protein disulphide isomerase mediates platelet aggregation and secretion. *British Journal of Haematology* **104:** 448-454

Essex DW, Li M (2006) Redox modification of platelet glycoproteins. *Curr Drug Targets* **7:** 1233-1241

Essex DW, Li M, Miller A, Feinman RD (2001) Protein disulfide isomerase and sulfhydryl-dependent pathways in platelet activation. *Biochemistry* **40:** 6070-6075

Esworthy RS, Aranda R, Martin MG, Doroshow JH, Binder SW, Chu FF (2001) Mice with combined disruption of Gpx1 and Gpx2 genes have colitis. *Am J Physiol Gastrointest Liver Physiol* **281:** G848-855

Ferraro JR, Nakamoto, K., Brown, C.W. (2003) *Introductory Raman Spectroscopy, Second Edition*.

Finkelstein JD (1990) Methionine metabolism in mammals. *The Journal of nutritional biochemistry* **1:** 228-237

Finkelstein JD, Martin JJ (2000) Homocysteine. *The international journal of biochemistry & cell biology* **32:** 385-389

Flaumenhaft R, Dilks JR, Rozenvayn N, Monahan-Earley RA, Feng D, Dvorak AM (2005) The actin cytoskeleton differentially regulates platelet alpha-granule and dense-granule secretion. *Blood* **105:** 3879-3887

Fox JE (1993a) The platelet cytoskeleton. *Thrombosis and haemostasis* **70:** 884-893

Fox JE (1993b) Regulation of platelet function by the cytoskeleton. *Advances in experimental medicine and biology* **344:** 175-185

Fox JE (2001) Cytoskeletal proteins and platelet signaling. *Thrombosis and haemostasis* **86:** 198-213

Ghyczy M, Boros M (2001) Electrophilic methyl groups present in the diet ameliorate pathological states induced by reductive and oxidative stress: a hypothesis. *The British journal of nutrition* **85:** 409-414

Gironella M, Molla M, Salas A, Soriano A, Sans M, Closa D, Engel P, Pique JM, Panes J (2002) The role of P-selectin in experimental colitis as determined by antibody immunoblockade and genetically deficient mice. *Journal of leukocyte biology* **72:** 56-64

Go YM, Jones DP (2005) Intracellular proatherogenic events and cell adhesion modulated by extracellular thiol/disulfide redox state. *Circulation* **111:** 2973-2980

Go YM, Jones DP (2011) Cysteine/cystine redox signaling in cardiovascular disease. *Free radical biology & medicine* **50:** 495-509

Gofer-Dadosh N, Klepfish, A., Schmilowitz, H., Shaklai, M., Lahav, J. (1997) Affinity modulation in a2b1 following ligand binding. *Biochem Biophys Res Commun* **232:** 724-727

Griffith OW (1999) Biologic and pharmacologic regulation of mammalian glutathione synthesis. *Free radical biology & medicine* **27:** 922-935

Griffith OW, Mulcahy RT (1999) The enzymes of glutathione synthesis: gamma-glutamylcysteine synthetase. *Advances in enzymology and related areas of molecular biology* **73:** 209-267, xii

Gruszecki WI, Strzalka K (2005) Carotenoids as modulators of lipid membrane physical properties. *Biochim Biophys Acta* **1740:** 108-115

Halliwell B (1989) Free radicals, reactive oxygen species and human disease: a critical evaluation with special reference to atherosclerosis. *British journal of experimental pathology* **70:** 737-757

Harbury CB, Schrier SL (1974) Modification of platelet sulfhydryl groups. *Thromb Diath Haemorrh* **31:** 469-484

Harries AD, Beeching NJ, Rogerson SJ, Nye FJ (1991) The platelet count as a simple measure to distinguish inflammatory bowel disease from infective diarrhoea. *J Infect* **22:** 247-250

Harrison D, Griendling KK, Landmesser U, Hornig B, Drexler H (2003) Role of oxidative stress in atherosclerosis. *The American journal of cardiology* **91:** 7A-11A

Hartwig JH (2006) The platelet: form and function. *Seminars in hematology* **43:** S94-100

Hartwig JH (2007) The Platelet Cytoskeleton. In *Platelets, Second Edition*, Michelson AD (ed), 4, pp 75-97.

Hartwig JH, DeSisto M (1991) The cytoskeleton of the resting human blood platelet: structure of the membrane skeleton and its attachment to actin filaments. *The Journal of cell biology* **112:** 407-425

Hauser W, Knobeloch KP, Eigenthaler M, Gambaryan S, Krenn V, Geiger J, Glazova M, Rohde E, Horak I, Walter U, Zimmer M (1999) Megakaryocyte hyperplasia and enhanced agonist-induced platelet activation in vasodilator-stimulated phosphoprotein knockout mice. *Proc Natl Acad Sci U S A* **96:** 8120-8125

Heemskerk JW, Bevers EM, Lindhout T (2002) Platelet activation and blood coagulation. *Thrombosis and haemostasis* **88:** 186-193

Henn V, Slupsky JR, Grafe M, Anagnostopoulos I, Forster R, Muller-Berghaus G, Kroczek RA (1998) CD40 ligand on activated platelets triggers an inflammatory reaction of endothelial cells. *Nature* **391:** 591-594

Holmes EW, Yong SL, Eiznhamer D, Keshavarzian A (1998) Glutathione content of colonic mucosa: evidence for oxidative damage in active ulcerative colitis. *Digestive diseases and sciences* **43:** 1088-1095

Horstrup K, Jablonka B, Honig-Liedl P, Just M, Kochsiek K, Walter U (1994) Phosphorylation of focal adhesion vasodilator-stimulated phosphoprotein at Ser157 in intact human platelets correlates with fibrinogen receptor inhibition. *European journal of biochemistry / FEBS* **225:** 21-27

Humphries MJ (2000) Integrin structure. *Biochemical Society transactions* **28:** 311-339

Humphries MJ, McEwan PA, Barton SJ, Buckley PA, Bella J, Mould AP (2003) Integrin structure: heady advances in ligand binding, but activation still makes the knees wobble. *Trends in biochemical sciences* **28:** 313-320

Huot J, Houle F, Marceau F, Landry J (1997) Oxidative stress-induced actin reorganization mediated by the p38 mitogen-activated protein kinase/heat shock protein 27 pathway in vascular endothelial cells. *Circulation research* **80:** 383-392

Huot J, Houle F, Rousseau S, Deschesnes RG, Shah GM, Landry J (1998) SAPK2/p38-dependent F-actin reorganization regulates early membrane blebbing during stress-induced apoptosis. *The Journal of cell biology* **143:** 1361-1373

Hwang C, Sinskey AJ, Lodish HF (1992) Oxidized redox state of glutathione in the endoplasmic reticulum. *Science* **257:** 1496-1502

Hynes RO (1992) Integrins: versatility, modulation, and signaling in cell adhesion. *Cell* **69:** 11-25

Hynes RO (2002) Integrins: bidirectional, allosteric signaling machines. *Cell* **110:** 673-687

Ichinohe T, Takayama H, Ezumi Y, Arai M, Yamamoto N, Takahashi H, Okuma M (1997) Collagen-stimulated activation of Syk but not c-Src is severely compromised in human platelets lacking membrane glycoprotein VI. *J Biol Chem* **272:** 63-68

Ikeda Y, Handa M, Kawano K, Kamata T, Murata M, Araki Y, Anbo H, Kawai Y, Watanabe K, Itagaki I, et al. (1991) The role of von Willebrand factor and fibrinogen in platelet aggregation under varying shear stress. *The Journal of clinical investigation* **87:** 1234-1240

Inoue O, Suzuki-Inoue K, Dean WL, Frampton J, Watson SP (2003) Integrin alpha2beta1 mediates outside-in regulation of platelet spreading on collagen through activation of Src kinases and PLCgamma2. *The Journal of cell biology* **160:** 769-780

Irving PM, Macey MG, Shah U, Webb L, Langmead L, Rampton DS (2004) Formation of platelet-leukocyte aggregates in inflammatory bowel disease. *Inflammatory bowel diseases* **10:** 361-372

Ishihara H, Connolly AJ, Zeng D, Kahn ML, Zheng YW, Timmons C, Tram T, Coughlin SR (1997) Protease-activated receptor 3 is a second thrombin receptor in humans. *Nature* **386:** 502-506

Israels SJ, McNicol A, Robertson C, Gerrard JM (1990) Platelet storage pool deficiency: diagnosis in patients with prolonged bleeding times and normal platelet aggregation. *Br J Haematol* **75:** 118-121

Jin J, Daniel JL, Kunapuli SP (1998) Molecular basis for ADP-induced platelet activation. II. The P2Y1 receptor mediates ADP-induced intracellular calcium mobilization and shape change in platelets. *J Biol Chem* **273:** 2030-2034

Jockusch BM, Bubeck P, Giehl K, Kroemker M, Moschner J, Rothkegel M, Rudiger M, Schluter K, Stanke G, Winkler J (1995) The molecular architecture of focal adhesions. *Annual review of cell and developmental biology* **11:** 379-416

Jones DP, Carlson JL, Mody VC, Cai J, Lynn MJ, Sternberg P (2000) Redox state of glutathione in human plasma. *Free radical biology & medicine* **28:** 625-635

Jones DP, Go YM, Anderson CL, Ziegler TR, Kinkade JM, Jr., Kirlin WG (2004) Cysteine/cystine couple is a newly recognized node in the circuitry for biologic redox signaling and control. *FASEB journal : official publication of the Federation of American Societies for Experimental Biology* **18:** 1246-1248

Jordan T, Spiro TG (1994) Enhancement of Ca hydrogen vibrations in the resonance Raman spectra of amides. *Journal of Raman Spectroscopy* **25:** 537-543

Jose B, Steffen R, Neugebauer U, Sheridan E, Marthi R, Forster RJ, Keyes TE (2009) Emission enhancement within gold spherical nanocavity arrays. *Phys Chem Chem Phys* **11:** 10923-10933

Jurk K, Kehrel BE (2005) Platelets: physiology and biochemistry. *Seminars in thrombosis and hemostasis* **31:** 381-392

Kahn ML, Nakanishi-Matsui M, Shapiro MJ, Ishihara H, Coughlin SR (1999) Protease-activated receptors 1 and 4 mediate activation of human platelets by thrombin. *The Journal of clinical investigation* **103:** 879-887

Keating N, Keely SJ (2009) Bile acids in regulation of intestinal physiology. *Current gastroenterology reports* **11:** 375-382

Kloczewiak M, Timmons S, Lukas TJ, Hawiger J (1984) Platelet receptor recognition site on human fibrinogen. Synthesis and structure-function relationship of peptides corresponding to the carboxy-terminal segment of the gamma chain. *Biochemistry* **23:** 1767-1774

Knight CG, Morton LF, Onley DJ, Peachey AR, Ichinohe T, Okuma M, Farndale RW, Barnes MJ (1999) Collagen-platelet interaction: Gly-Pro-Hyp is uniquely specific for platelet Gp VI and mediates platelet activation by collagen. *Cardiovasc Res* **41:** 450-457

Knight CG, Morton LF, Onley DJ, Peachey AR, Messent AJ, Smethurst PA, Tuckwell DS, Farndale RW, Barnes MJ (1998) Identification in collagen type I of an integrin alpha2 beta1-binding site containing an essential GER sequence. *J Biol Chem* **273:** 33287-33294

Knight CG, Morton LF, Peachey AR, Tuckwell DS, Farndale RW, Barnes MJ (2000) The collagen-binding A-domains of integrins alpha(1)beta(1) and alpha(2)beta(1) recognize the same specific amino acid sequence, GFOGER, in native (triple-helical) collagens. *J Biol Chem* **275:** 35-40

Koyama Y, Takatsuka I, Nakata M, Tasumi M (1988) Raman and infrared spectra of the all-*trans*, 7-*cis*, 9-*cis*, 13-*cis* and 15-*cis* isomers of b-carotene: Key bands distinguishing stretched or terminal-bent configurations from central-bent configurations. *Journal of Raman Spectroscopy* **19:** 37-49

Krafft C, Knetschke, T., Siegner, A., Funk, R.H.W., Salzer, R. (2003) Mapping of single cells by near infrared Raman microspectroscpy. *Vibrational Spectroscopy***:** 75-83

Kretzschmar M (1996) Regulation of hepatic glutathione metabolism and its role in hepatotoxicity. *Experimental and toxicologic pathology : official journal of the Gesellschaft fur Toxikologische Pathologie* **48:** 439-446

Kurth MC, Bryan J (1984) Platelet activation induces the formation of a stable gelsolin-actin complex from monomeric gelsolin. *J Biol Chem* **259:** 7473-7479

Lahav J, Gofer-Dadosh N, Luboshitz J, Hess O, Shaklai M (2000) Protein disulfide isomerase mediates integrin-dependent adhesion. *FEBS Lett* **475:** 89-92

Lahav J, Wijnen EM, Hess O, Hamaia SW, Griffiths D, Makris M, Knight CG, Essex DW, Farndale RW (2003) Enzymatically catalyzed disulfide exchange is required for platelet adhesion to collagen via integrin alpha2beta1. *Blood* **102:** 2085-2092

Landis RC, McDowall A, Holness CL, Littler AJ, Simmons DL, Hogg N (1994) Involvement of the "I" domain of LFA-1 in selective binding to ligands ICAM-1 and ICAM-3. *The Journal of cell biology* **126:** 529-537

Leisner TM, Wencel-Drake JD, Wang W, Lam SC (1999) Bidirectional transmembrane modulation of integrin alphaIIbbeta3 conformations. *J Biol Chem* **274:** 12945-12949

Li W, Metcalf DG, Gorelik R, Li R, Mitra N, Nanda V, Law PB, Lear JD, Degrado WF, Bennett JS (2005) A push-pull mechanism for regulating integrin function. *Proc Natl Acad Sci U S A* **102:** 1424-1429

Li Z, Xi X, Gu M, Feil R, Ye RD, Eigenthaler M, Hofmann F, Du X (2003) A stimulatory role for cGMP-dependent protein kinase in platelet activation. *Cell* **112:** 77-86

Lind SE, Yin HL, Stossel TP (1982) Human platelets contain gelsolin. A regulator of actin filament length. *The Journal of clinical investigation* **69:** 1384-1387

Lindemann S, Tolley ND, Dixon DA, McIntyre TM, Prescott SM, Zimmerman GA, Weyrich AS (2001) Activated platelets mediate inflammatory signaling by regulated interleukin 1beta synthesis. *The Journal of cell biology* **154:** 485-490

Lopez JA, Leung B, Reynolds CC, Li CQ, Fox JE (1992) Efficient plasma membrane expression of a functional platelet glycoprotein Ib-IX complex requires the presence of its three subunits. *J Biol Chem* **267:** 12851-12859

Lowry OH, Rosebrough NJ, Farr AL, Randall RJ (1951) Protein measurement with the Folin phenol reagent. *J Biol Chem* **193:** 265-275

Lu SC (2009) Regulation of glutathione synthesis. *Molecular aspects of medicine* **30:** 42-59

Luo SZ, Li R (2008) Specific heteromeric association of four transmembrane peptides derived from platelet glycoprotein Ib-IX complex. *Journal of molecular biology* **382:** 448-457

Luo SZ, Mo X, Afshar-Kharghan V, Srinivasan S, Lopez JA, Li R (2007) Glycoprotein Ibalpha forms disulfide bonds with 2 glycoprotein Ibbeta subunits in the resting platelet. *Blood* **109:** 603-609

Lyng FM, Faolain EO, Conroy J, Meade AD, Knief P, Duffy B, Hunter MB, Byrne JM, Kelehan P, Byrne HJ (2007) Vibrational spectroscopy for cervical cancer pathology, from biochemical analysis to diagnostic tool. *Exp Mol Pathol* **82:** 121-129

MacIntyre DE, Gordon, J.L. (1974) Evidence for two populations of disulfide bonds on blood platelets. *Biochemical Society transactions* **2:** 1265-1269

Manickam N, Ahmad SS, Essex DW (2011) Vicinal thiols are required for activation of the alphaIIbbeta3 platelet integrin. *J Thromb Haemost* **9:** 1207-1215

Manickam N, Sun X, Hakala KW, Weintraub ST, Essex DW (2008) Thiols in the alphaIIbbeta3 integrin are necessary for platelet aggregation. *Br J Haematol* **142:** 457-465

Margaritis A, Priora R., Frosali S., Di Guiseppe, D., Summa, D., Coppo, L., Di Stefano, A., Di Simplicio, P. (2011) The role of protein sulfhydryl groups and protein disulfides of the platelet surface in aggregation processes involving thiol exchange reactions. *Pharmacological Research***:** 77-84

Maruyama T, Miyamoto Y, Nakamura T, Tamai Y, Okada H, Sugiyama E, Itadani H, Tanaka K (2002) Identification of membrane-type receptor for bile acids (M-BAR). *Biochem Biophys Res Commun* **298:** 714-719

McDowall A, Leitinger B, Stanley P, Bates PA, Randi AM, Hogg N (1998) The I domain of integrin leukocyte function-associated antigen-1 is involved in a conformational change leading to high affinity binding to ligand intercellular adhesion molecule 1 (ICAM-1). *J Biol Chem* **273:** 27396-27403

McGarrigle SA, O'Neill S, Walsh GM, Moran N, Graham IM, Cooney MT, Monavari A, Mayne P, Collins P (2011) Integrin alpha(IIb)beta(3) exists in an activated state in subjects with elevated plasma homocysteine levels. *Platelets* **22:** 65-73

McNicol A, Gerrard JM (1993) Post-receptor events associated with thrombin-induced platelet activation. *Blood Coagul Fibrinolysis* **4:** 975-991

Meister A (1988) Glutathione metabolism and its selective modification. *J Biol Chem* **263:** 17205-17208

Melendez-Martineza AJ, Britton G, Vicarioa IM, Heredia FJ (2007) Relationship between the colour and the chemical structure of carotenoid pigments. *Food Chemistry* **101:** 1145-1150

Merchant NB, Rogers CM, Trivedi B, Morrow J, Coffey RJ (2005) Ligand-dependent activation of the epidermal growth factor receptor by secondary bile acids in polarizing colon cancer cells. *Surgery* **138:** 415-421

Meredith MJ, Reed DJ (1982) Status of the mitochondrial pool of glutathione in the isolated hepatocyte. *J Biol Chem* **257:** 3747-3753

Merlin JC (1985) Resonance Raman spectroscopy of carotenoids and carotenoid-containing systems *Pure & Applied Chemistry* **57:** 785-792

Meyer CT, Brand M, DeLuca VA, Spiro HM (1981) Hydrogen peroxide colitis: a report of three patients. *J Clin Gastroenterol* **3:** 31-35

Minsky M (1988) Memoir on Inventing the Confocal Scanning Microscope. *SCANNING* **10:** 128-138

Mo X, Luo SZ, Lopez JA, Li R (2008) Juxtamembrane basic residues in glycoprotein Ibbeta cytoplasmic domain are required for assembly and surface expression of glycoprotein Ib-IX complex. *FEBS Lett* **582:** 3270-3274

Modderman PW, Admiraal LG, Sonnenberg A, von dem Borne AE (1992) Glycoproteins V and Ib-IX form a noncovalent complex in the platelet membrane. *J Biol Chem* **267:** 364-369

Montanez E, Ussar S, Schifferer M, Bosl M, Zent R, Moser M, Fassler R (2008) Kindlin-2 controls bidirectional signaling of integrins. *Genes & development* **22:** 1325-1330

Mori K, Watanabe H, Hiwatashi N, Sugai K, Goto Y (1980) Studies on blood coagulation in ulcerative colitis and Crohn's disease. *The Tohoku journal of experimental medicine* **132:** 93-101

Mori M, Salter JW, Vowinkel T, Krieglstein CF, Stokes KY, Granger DN (2005) Molecular determinants of the prothrombogenic phenotype assumed by inflamed colonic venules. *Am J Physiol Gastrointest Liver Physiol* **288:** G920-926

Moriarty SE, Shah JH, Lynn M, Jiang S, Openo K, Jones DP, Sternberg P (2003) Oxidation of glutathione and cysteine in human plasma associated with smoking. *Free radical biology & medicine* **35:** 1582-1588

Moroi M, Jung SM (2004) Platelet glycoprotein VI: its structure and function. *Thrombosis research* **114:** 221-233

Moser M, Nieswandt B, Ussar S, Pozgajova M, Fassler R (2008) Kindlin-3 is essential for integrin activation and platelet aggregation. *Nature medicine* **14:** 325-330

Moshfegh K, Wuillemin WA, Redondo M, Lammle B, Beer JH, Liechti-Gallati S, Meyer BJ (1999) Association of two silent polymorphisms of platelet glycoprotein Ia/IIa receptor with risk of myocardial infarction: a case-control study. *Lancet* **353:** 351-354

Murphy D, Reddy E, Forster R, O'Neill S (2010) Platelet reactivity to collagen is diminished in an external reducing environment. *Platelets* **21:** 393-419

Nachmias VT, Yoshida, k. (1988) The cytoskeleton of the blood platelet: a dynamic structure. *Adv Cell Biol* **2:** 181-211

Niedergang F, Alcover A, Knight CG, Farndale RW, Barnes MJ, Francischetti IM, Bon C, Leduc M (2000) Convulxin binding to platelet receptor GPVI:

competition with collagen related peptides. *Biochem Biophys Res Commun* **273:** 246-250

Nieswandt B, Brakebusch C, Bergmeier W, Schulte V, Bouvard D, Mokhtari-Nejad R, Lindhout T, Heemskerk JW, Zirngibl H, Fassler R (2001a) Glycoprotein VI but not alpha2beta1 integrin is essential for platelet interaction with collagen. *The EMBO journal* **20:** 2120-2130

Nieswandt B, Moser M, Pleines I, Varga-Szabo D, Monkley S, Critchley D, Fassler R (2007) Loss of talin1 in platelets abrogates integrin activation, platelet aggregation, and thrombus formation in vitro and in vivo. *The Journal of experimental medicine* **204:** 3113-3118

Nieswandt B, Schulte V, Bergmeier W, Mokhtari-Nejad R, Rackebrandt K, Cazenave JP, Ohlmann P, Gachet C, Zirngibl H (2001b) Long-term antithrombotic protection by in vivo depletion of platelet glycoprotein VI in mice. *The Journal of experimental medicine* **193:** 459-469

Nieswandt B, Watson, S.P. (2003) Platelet-collagen interaction: is GPVI the central receptor? *Blood* **102:** 449-461

Nieuwenhuis HK, Akkerman JW, Houdijk WP, Sixma JJ (1985) Human blood platelets showing no response to collagen fail to express surface glycoprotein Ia. *Nature* **318:** 470-472

Nissinen L, Koivunen J, Kapyla J, Salmela M, Nieminen J, Jokinen J, Sipila K, Pihlavisto M, Pentikainen OT, Marjamaki A, Heino J (2012) Novel alpha2beta1 integrin inhibitors reveal that integrin binding to collagen under shear stress conditions does not require receptor preactivation. *J Biol Chem* **287:** 44694-44702

Norton KJ, Scarborough RM, Kutok JL, Escobedo MA, Nannizzi L, Coller BS (1993) Immunologic analysis of the cloned platelet thrombin receptor activation mechanism: evidence supporting receptor cleavage, release of the N-terminal

peptide, and insertion of the tethered ligand into a protected environment. *Blood* **82:** 2125-2136

O'Neill S, Robinson A, Deering A, Ryan M, Fitzgerald DJ, Moran N (2000) The platelet integrin alpha IIbbeta 3 has an endogenous thiol isomerase activity. *J Biol Chem* **275:** 36984-36990

Onley DJ, Knight CG, Tuckwell DS, Barnes MJ, Farndale RW (2000) Micromolar Ca2+ concentrations are essential for Mg2+-dependent binding of collagen by the integrin alpha 2beta 1 in human platelets. *J Biol Chem* **275:** 24560-24564

Ozaki Y, Asazuma N, Suzuki-Inoue K, Berndt MC (2005) Platelet GPIb-IX-V-dependent signaling. *J Thromb Haemost* **3:** 1745-1751

Pacchiarini L, Tua A, Grignani G (1996) In vitro effect of reduced glutathione on platelet function. *Haematologica* **81:** 497-502

Packham MA, Mustard JF (2005) Platelet aggregation and adenosine diphosphate/adenosine triphosphate receptors: a historical perspective. *Seminars in thrombosis and hemostasis* **31:** 129-138

Patel-Hett S, Richardson JL, Schulze H, Drabek K, Isaac NA, Hoffmeister K, Shivdasani RA, Bulinski JC, Galjart N, Hartwig JH, Italiano JE, Jr. (2008) Visualization of microtubule growth in living platelets reveals a dynamic marginal band with multiple microtubules. *Blood* **111:** 4605-4616

Pelton JT, McLean LR (2000) Spectroscopic methods for analysis of protein secondary structure. *Analytical biochemistry* **277:** 167-176

Petersen FNR, Nielsen CH (2009) Raman Spectroscopy as a Tool for Investigating Lipid-Protein Interactions. *Spectroscopy* **24:** 1-8

Petrich BG, Fogelstrand P, Partridge AW, Yousefi N, Ablooglu AJ, Shattil SJ, Ginsberg MH (2007) The antithrombotic potential of selective blockade of talin-dependent integrin alpha IIb beta 3 (platelet GPIIb-IIIa) activation. *The Journal of clinical investigation* **117:** 2250-2259

Philippeaux MM, Vesin C, Tacchini-Cottier F, Piguet PF (1996) Activated human platelets express beta2 integrin. *Eur J Haematol* **56:** 130-137

Piotrowicz RS, Orchekowski RP, Nugent DJ, Yamada KY, Kunicki TJ (1988) Glycoprotein Ic-IIa functions as an activation-independent fibronectin receptor on human platelets. *The Journal of cell biology* **106:** 1359-1364

Plow EF, Byzova T (1999) The biology of glycoprotein IIb-IIIa. *Coron Artery Dis* **10:** 547-551

Poncz M, Eisman R, Heidenreich R, Silver SM, Vilaire G, Surrey S, Schwartz E, Bennett JS (1987) Structure of the platelet membrane glycoprotein IIb. Homology to the alpha subunits of the vitronectin and fibronectin membrane receptors. *J Biol Chem* **262:** 8476-8482

Puppels GM, Bakker, T.C., Sitjsema, N.M.. Grond, M., Maraboeuf, F., de Grauw, C.G., Greve, J. (1995) Development and Application of Raman microspectroscopic and Raman imaging techniques for cell biological studies. *Journal of Molecular Structure* **347:** 477-484

Rajasekaran NS, Connell, P., Christians, E. S., Yan, L. J. et, al. (2007) Human alpha B-crystallin mutation causes oxido-reductive
stress and protein aggregation cardiomyopathy inmice. *Cell* **130**

Raman CV (1928) A change of wave-length in light scattering. *Nature* **121:** 619

Ramshaw JAM, Shah NK, Brodsky B (1998) Gly-X-Y tripeptide freqencies in collagen: a context for host-guest triple-helical peptides. *Journal of Structural Biology* **122:** 86-91

Reinhard M, Halbrugge M, Scheer U, Wiegand C, Jockusch BM, Walter U (1992) The 46/50 kDa phosphoprotein VASP purified from human platelets is a novel protein associated with actin filaments and focal contacts. *The EMBO journal* **11:** 2063-2070

Reinhard M, Jarchau T, Walter U (2001) Actin-based motility: stop and go with Ena/VASP proteins. *Trends in biochemical sciences* **26:** 243-249

Reuter S, Gupta SC, Chaturvedi MM, Aggarwal BB (2010) Oxidative stress, inflammation, and cancer: how are they linked? *Free radical biology & medicine* **49:** 1603-1616

Rezaie A, Parker RD, Abdollahi M (2007) Oxidative stress and pathogenesis of inflammatory bowel disease: an epiphenomenon or the cause? *Digestive diseases and sciences* **52:** 2015-2021

Rhee SG, Bae YS, Lee SR, Kwon J (2000) Hydrogen peroxide: a key messenger that modulates protein phosphorylation through cysteine oxidation. *Science's STKE : signal transduction knowledge environment* **2000:** pe1

Rijcken EM, Laukoetter MG, Anthoni C, Meier S, Mennigen R, Spiegel HU, Bruewer M, Senninger N, Vestweber D, Krieglstein CF (2004) Immunoblockade of PSGL-1 attenuates established experimental murine colitis by reduction of leukocyte rolling. *Am J Physiol Gastrointest Liver Physiol* **287:** G115-124

Rocic P, Kolz C, Reed R, Potter B, Chilian WM (2007) Optimal reactive oxygen species concentration and p38 MAP kinase are required for coronary collateral growth. *Am J Physiol Heart Circ Physiol* **292:** H2729-2736

Rolf MG, Mahaut-Smith MP (2002) Effects of enhanced P2X1 receptor Ca2+ influx on functional responses in human platelets. *Thrombosis and haemostasis* **88:** 495-502

Rosenberg S, Stracher A (1982) Effect of actin-binding protein on the sedimentation properties of actin. *The Journal of cell biology* **94:** 51-55

Rosenberg S, Stracher A, Burridge K (1981a) Isolation and characterization of a calcium-sensitive alpha-actinin-like protein from human platelet cytoskeletons. *J Biol Chem* **256:** 12986-12991

Rosenberg S, Stracher A, Lucas RC (1981b) Isolation and characterization of actin and actin-binding protein from human platelets. *The Journal of cell biology* **91:** 201-211

Rottner K, Behrendt B, Small JV, Wehland J (1999) VASP dynamics during lamellipodia protrusion. *Nature cell biology* **1:** 321-322

Ruggeri ZM, Ware J (1993) von Willebrand factor. *FASEB journal : official publication of the Federation of American Societies for Experimental Biology* **7:** 308-316

Russell DW (2009) Fifty years of advances in bile acid synthesis and metabolism. *Journal of lipid research* **50 Suppl:** S120-125

Samaha FF, Hibbard C, Sacks J, Chen H, Varello MA, George T, Kahn ML (2005) Density of platelet collagen receptors glycoprotein VI and alpha2beta1 and prior myocardial infarction in human subjects, a pilot study. *Medical science monitor : international medical journal of experimental and clinical research* **11:** CR224-229

Santoro SA (1999) Platelet surface collagen receptor polymorphisms: variable receptor expression and thrombotic/hemorrhagic risk. *Blood* **93:** 3575-3577

Savage B, Saldivar E, Ruggeri ZM (1996) Initiation of platelet adhesion by arrest onto fibrinogen or translocation on von Willebrand factor. *Cell* **84:** 289-297

Savi P, Labouret C, Delesque N, Guette F, Lupker J, Herbert JM (2001) P2y(12), a new platelet ADP receptor, target of clopidogrel. *Biochem Biophys Res Commun* **283:** 379-383

Schafer FQ, Buettner GR (2001) Redox environment of the cell as viewed through the redox state of the glutathione disulfide/glutathione couple. *Free radical biology & medicine* **30:** 1191-1212

Schmidt DR, Mangelsdorf DJ (2008) Nuclear receptors of the enteric tract: guarding the frontier. *Nutrition reviews* **66:** S88-97

Semwogerere D, Weeks, E.R. (2005) Confocal Microscopy. *Encyclopedia of Biomaterials and Biomedical Engineering*. Taylor & Francis.

Sevier CS, Kaiser CA (2002) Formation and transfer of disulphide bonds in living cells. *Nature reviews Molecular cell biology* **3:** 836-847

Shatill SJ, Newman, P.J. (2004) Integrin: dynamic scaffolds for adhesion and signalling in platelets. *Blood* **104:** 1606-1615

Shattil SJ, Hoxie JA, Cunningham M, Brass LF (1985) Changes in the platelet membrane glycoprotein IIb.IIIa complex during platelet activation. *J Biol Chem* **260:** 11107-11114

Sheridan E, Hjelm, J., Forster, R.J. (2007) Electrodeposition of gold nanoparticles on fluorine-doped
tin oxide: Control of particle density and size distribution. *Journal of Electroanalytical Chemistry* **608:** 1-7

Shimaoka M, Springer TA (2003) Therapeutic antagonists and conformational regulation of integrin function. *Nat Rev Drug Discov* **2:** 703-716

Sixma JJ, Slot JW, Geuze HJ (1989) Immunocytochemical localization of platelet granule proteins. *Methods in enzymology* **169:** 301-311

Smolenski A, Bachmann C, Reinhard K, Honig-Liedl P, Jarchau T, Hoschuetzky H, Walter U (1998) Analysis and regulation of vasodilator-stimulated phosphoprotein serine 239 phosphorylation in vitro and in intact cells using a phosphospecific monoclonal antibody. *J Biol Chem* **273:** 20029-20035

Springer TA (1997) Folding of the N-terminal, ligand-binding region of integrin alpha-subunits into a beta-propeller domain. *Proc Natl Acad Sci U S A* **94:** 65-72

Stefanini M, Krinsky N, Magalini SI (1957) Studies on platelets XIX: Carotenoid pigments in human platelets. *J Lab Clin Med* **50:** 225-228

Stevens TR, James JP, Simmonds NJ, McCarthy DA, Laurenson IF, Maddison PJ, Rampton DS (1992) Circulating von Willebrand factor in inflammatory bowel disease. *Gut* **33:** 502-506

Sun QH, Liu CY, Wang R, Paddock C, Newman PJ (2002) Disruption of the long-range GPIIIa Cys(5)-Cys(435) disulfide bond results in the production of constitutively active GPIIb-IIIa (alpha(IIb)beta(3)) integrin complexes. *Blood* **100:** 2094-2101

Tabibian JH, Roth BE (2009) Local thrombolysis: a newer approach to treating inflammatory bowel disease-related thromboembolism. *J Clin Gastroenterol* **43:** 391-398

Tadokoro S, Shattil SJ, Eto K, Tai V, Liddington RC, de Pereda JM, Ginsberg MH, Calderwood DA (2003) Talin binding to integrin beta tails: a final common step in integrin activation. *Science* **302:** 103-106

Takagi J, Petre BM, Walz T, Springer TA (2002) Global conformational rearrangements in integrin extracellular domains in outside-in and inside-out signaling. *Cell* **110:** 599-511

Tarver H, Schmidt CL (1939) The conversion of methionine to cystine: experiments with radioactive sulfur. *Journal of Biological Chemistry* **130:** 67-80

Thannickal VJ, Fanburg BL (2000) Reactive oxygen species in cell signaling. *American journal of physiology Lung cellular and molecular physiology* **279:** L1005-1028

Toyokuni S, Okamoto K, Yodoi J, Hiai H (1995) Persistent oxidative stress in cancer. *FEBS Lett* **358:** 1-3

Tsunada S, Iwakiri R, Ootani H, Aw TY, Fujimoto K (2003) Redox imbalance in the colonic mucosa of ulcerative colitis. *Scandinavian journal of gastroenterology* **38:** 1002-1003

van Wersch JW, Houben P, Rijken J (1990) Platelet count, platelet function, coagulation activity and fibrinolysis in the acute phase of inflammatory bowel disease. *Journal of clinical chemistry and clinical biochemistry Zeitschrift fur klinische Chemie und klinische Biochemie* **28:** 513-517

Vial C, Rolf MG, Mahaut-Smith MP, Evans RJ (2002) A study of P2X1 receptor function in murine megakaryocytes and human platelets reveals synergy with P2Y receptors. *Br J Pharmacol* **135:** 363-372

Visser MR, Tracy PB, Vercellotti GM, Goodman JL, White JG, Jacob HS (1988) Enhanced thrombin generation and platelet binding on herpes simplex virus-infected endothelium. *Proc Natl Acad Sci U S A* **85:** 8227-8230

von Hundelshausen P, Weber KS, Huo Y, Proudfoot AE, Nelson PJ, Ley K, Weber C (2001) RANTES deposition by platelets triggers monocyte arrest on inflamed and atherosclerotic endothelium. *Circulation* **103:** 1772-1777

Voutilainen S, Nurmi T, Mursu J, Rissanen TH (2006) Carotenoids and cardiovascular health. *Am J Clin Nutr* **83:** 1265-1271

Vowinkel T, Wood KC, Stokes KY, Russell J, Tailor A, Anthoni C, Senninger N, Krieglstein CF, Granger DN (2007) Mechanisms of platelet and leukocyte recruitment in experimental colitis. *Am J Physiol Gastrointest Liver Physiol* **293:** G1054-1060

Vrij AA, Rijken J, Van Wersch JW, Stockbrugger RW (2000) Platelet factor 4 and beta-thromboglobulin in inflammatory bowel disease and giant cell arteritis. *European journal of clinical investigation* **30:** 188-194

Vukelić B, Salopek-Sondi B, Špoljarić J, Sabljić I, Meštrović N, Agić D, Abramić M. (2012) Reactive cysteine in the active-site motif of Bacteroides thetaiotaomicron dipeptidyl peptidase III is a regulatory residue for enzyme activity. *Biological Chemistry*, Vol. 393, p. 37.

Wagner CL, Mascelli MA, Neblock DS, Weisman HF, Coller BS, Jordan RE (1996) Analysis of GPIIb/IIIa receptor number by quantification of 7E3 binding to human platelets. *Blood* **88:** 907-914

Wakabayashi N, Dinkova-Kostova AT, Holtzclaw WD, Kang MI, Kobayashi A, Yamamoto M, Kensler TW, Talalay P (2004) Protection against electrophile and oxidant stress by induction of the phase 2 response: fate of cysteines of the Keap1 sensor modified by inducers. *Proc Natl Acad Sci U S A* **101:** 2040-2045

Waldmann R, Bauer S, Gobel C, Hofmann F, Jakobs KH, Walter U (1986) Demonstration of cGMP-dependent protein kinase and cGMP-dependent phosphorylation in cell-free extracts of platelets. *European journal of biochemistry / FEBS* **158:** 203-210

Waldmann R, Nieberding M, Walter U (1987) Vasodilator-stimulated protein phosphorylation in platelets is mediated by cAMP- and cGMP-dependent protein kinases. *European journal of biochemistry / FEBS* **167:** 441-448

Wallach DF, Verma SP, Fookson J (1979) Application of laser Raman and infrared spectroscopy to the analysis of membrane structure. *Biochim Biophys Acta* **559:** 153-208

Walsh GM, Leane D, Moran N, Keyes TE, Forster RJ, Kenny D, O'Neill S (2007) S-Nitrosylation of platelet alphaIIbbeta3 as revealed by Raman spectroscopy. *Biochemistry* **46:** 6429-6436

Walsh GM, Sheehan D, Kinsella A, Moran N, O'Neill S (2004) Redox modulation of integrin [correction of integin] alpha IIb beta 3 involves a novel allosteric regulation of its thiol isomerase activity. *Biochemistry* **43:** 473-480

Walter U (1989) Physiological role of cGMP and cGMP-dependent protein kinase in the cardiovascular system. *Reviews of physiology, biochemistry and pharmacology* **113:** 41-88

Watson SP, Harrison, P. (2005) The vascular function of platelets. In *Postgraduate Haematology*, Hoffbrand AV, Catovsky, D., Tuddenham, E.G.D. (ed), Fifth edn.

Webberley MJ, Hart MT, Melikian V (1993) Thromboembolism in inflammatory bowel disease: role of platelets. *Gut* **34:** 247-251

Weber T, Zemelman BV, McNew JA, Westermann B, Gmachl M, Parlati F, Sollner TH, Rothman JE (1998) SNAREpins: minimal machinery for membrane fusion. *Cell* **92:** 759-772

Wegener KL, Partridge AW, Han J, Pickford AR, Liddington RC, Ginsberg MH, Campbell ID (2007) Structural basis of integrin activation by talin. *Cell* **128:** 171-182

Wentworth JK, Pula G, Poole AW (2006) Vasodilator-stimulated phosphoprotein (VASP) is phosphorylated on Ser157 by protein kinase C-dependent and -

independent mechanisms in thrombin-stimulated human platelets. *Biochem J* **393:** 555-564

White JG (1968) Tubular elements in platelet granules. *Blood* **32:** 148-156

White JG (1969) The dense bodies of human platelets: inherent electron opacity of the seratonin storage particles. *Blood* **33:** 598-606

White JG (1974) Electron microscopic studies of platelet secretion. *Prog Hemost Thromb* **2:** 49-98

White JG (1999) Platelet glycosomes. *Platelets* **10:** 242-246

White JG (2002) Electron dense chains and clusters in human platelets. *Platelets* **13:** 317-325

White JG (2004) Medich giant platelet disorder: a unique alpha granule deficiency I. Structural abnormalities. *Platelets* **15:** 345-353

White JG (2005) Platelets are covercytes, not phagocytes: uptake of bacteria involves channels of the open canalicular system. *Platelets* **16:** 121-131

White JG (2007) Platelet Structure. In *Platelets, Second Edition*, Michelson AD (ed), 3, pp 45-73.

White JG, Escolar G (1991) The blood platelet open canalicular system: a two-way street. *Eur J Cell Biol* **56:** 233-242

Winterbourn CC, Metodiewa D (1999) Reactivity of biologically important thiol compounds with superoxide and hydrogen peroxide. *Free radical biology & medicine* **27:** 322-328

Wonerow P, Pearce AC, Vaux DJ, Watson SP (2003) A critical role for phospholipase Cgamma2 in alphaIIbbeta3-mediated platelet spreading. *J Biol Chem* **278:** 37520-37529

Yan B, Smith JW (2000) A Redox Site Involved in Integrin Activation. *Journal of Biological Chemistry* **275:** 39964-39972

Yan B, Smith JW (2001) Mechanism of integrin activation by disulfide bond reduction. *Biochemistry* **40:** 8861-8867

Yoshida H, Granger DN (2009) Inflammatory bowel disease: a paradigm for the link between coagulation and inflammation. *Inflammatory bowel diseases* **15:** 1245-1255

Zhang X, Min X, Li C, Benjamin IJ, Qian B, Ding Z, Gao X, Yao Y, Ma Y, Cheng Y, Liu L (2010) Involvement of reductive stress in the cardiomyopathy in transgenic mice with cardiac-specific overexpression of heat shock protein 27. *Hypertension* **55:** 1412-1417

Zhu Y, O'Neill S, Saklatvala J, Tassi L, Mendelsohn ME (1994) Phosphorylated HSP27 associates with the activation-dependent cytoskeleton in human platelets. *Blood* **84:** 3715-3723

Zimrin AB, Gidwitz S, Lord S, Schwartz E, Bennett JS, White GC, 2nd, Poncz M (1990) The genomic organization of platelet glycoprotein IIIa. *J Biol Chem* **265:** 8590-8595

Zitomersky NL, Verhave M, Trenor CC, 3rd (2011) Thrombosis and inflammatory bowel disease: a call for improved awareness and prevention. *Inflammatory bowel diseases* **17:** 458-470

Zucker MB, Masiello NC (1984) Platelet aggregation caused by dithiothreitol. *Thrombosis and haemostasis* **51:** 119-124

Zucker MB, Nachmias VT (1985) Platelet activation. *Arteriosclerosis* **5:** 2-18